AD

AD647665

USAAVLABS TECHNICAL REPORT 66-61

STUDY OF THE HEAVY-LIFT HELICOPTER ROTOR CONFIGURATION

By

Charles M. Wax

Rocco C. Tocci

November 1966

U. S. ARMY AVIATION MATERIEL LABORATORIES
FORT EUSTIS, VIRGINIA

CONTRACT DA 44-177-AMC-206(T)

VERTOL DIVISION
THE BOEING COMPANY
MORTON, PENNSYLVANIA

Distribution of this document is unlimited

DDC
RECEIVED
MAR 1 1967
C

ARCHIVE COPY

Disclaimers

The findings in this report are not to be construed as an official Department of the Army position unless so designated by other authorized documents.

When Government drawings, specifications, or other data are used for any purpose other than in connection with a definitely related Government procurement operation, the United States Government thereby incurs no responsibility nor any obligation whatsoever; and the fact that the Government may have formulated, furnished, or in any way supplied the said drawings, specifications, or other data is not to be regarded by implication or otherwise as in any manner licensing the holder or any other person or corporation, or conveying any rights or permission, to manufacture, use, or sell any patented invention that may in any way be related thereto.

Trade names cited in this report do not constitute an official endorsement or approval of the use of such commercial hardware or software.

Disposition Instructions

Destroy this report when no longer needed. Do not return it to the originator.

DEPARTMENT OF THE ARMY
U. S. ARMY AVIATION MATERIEL LABORATORIES
FORT EUSTIS, VIRGINIA 23604

This report has been reviewed by the U. S. Army Aviation Materiel Laboratories, and basic technical data presented herein are considered to be sound. However, assumptions dependent upon design philosophy and/or engineering judgment are those of the contractor and do not necessarily reflect the views of the U. S. Army Aviation Materiel Laboratories.

This report is published for the dissemination of information and the stimulation of ideas.

Task 1P125901A14203
Contract DA44-177-AMC-206(T)
USAAVLABS Technical Report 66-61
November 1966

STUDY OF THE HEAVY-LIFT HELICOPTER ROTOR CONFIGURATION

R-445

by
Charles M. Wax
and
Rocco C. Tocci

Prepared by
VERTOL DIVISION
THE BOEING COMPANY
Morton, Pennsylvania

for
U.S. Army Aviation Materiel Laboratories
Fort Eustis, Virginia

Distribution of this document is unlimited

ABSTRACT

The purpose of this study has been to define the optimum shaft-driven rotor system for the heavy-lift helicopter.

A parametric analysis was made for the tandem-lift rotor system and the single-lift/antitorque rotor system; mathematical models programmed for derivation by large digital machines were used for the analysis. The tandem-lift rotor system was chosen for preliminary design study.

The preliminary design study used the rotor geometry determined by the rotor system parametric analysis. Attention was given primarily to the articulated rotor and secondarily to the hingeless semirigid rotor. Study of the hingeless semirigid rotor was limited to an exploratory parametric analysis to determine its compatibility with a tandem-lift rotor system. Although the analysis does not represent an optimized hingeless semirigid rotor, it does indicate the areas of risk, the weight increment, and the areas worthy of further study.

The preliminary design study includes stability, control, and flying qualities; a static and dynamic structural analysis; preliminary design layouts; weights; and a brief evaluation of reliability. It specifically includes stall flutter, flap-lag instability, rotor hub shaking forces, and fuselage response.

A dual longitudinal control system has been developed which uses both differential collective and longitudinal cyclic pitch to provide hover attitude control. It permits the helicopter to hover parallel to an external load or terrain without its fuselage attitude being influenced by center of gravity.

It was concluded that the tandem-lift rotor system with articulated rotors and dual longitudinal control best meets the requirements of the heavy-lift helicopter.

FOREWORD

A two-part parametric analysis and design study of a shaft-driven rotor system for the heavy-lift helicopter has been conducted under U.S. Army Aviation Materiel Laboratories (USAAVLABS) contract DA44-177-AMC-206(T) with the Vertol Division of Boeing.

Part I consisted of a rotor system parametric analysis. In Part II, a preliminary design study was made of the rotor configuration selected in Part I. This report covers both parts.

USAAVLABS was represented by Mr. W. Oyler, Research Contracting Office; by Lt. N. Solow and Mr. W. Nettles, Project Engineers; and by Mr. J. Yeates, Chief of the Aeromechanics Division.

CONTENTS

	Page
Abstract	iii
Foreword	v
List of Illustrations	x
List of Tables	xix
List of Symbols	xxi
SUMMARY	1
Rotor System Performance Parametric Analysis	1
Preliminary Design Study	4
Conclusions	10
ROTOR SYSTEM PERFORMANCE PARAMETRIC ANALYSIS	18
Introduction	18
Procedure	18
Basic Data	20
Parametric Weights and Performance Computer Program	31
Mission Cargo Cubage Analysis	35
Optimization of Tandem-Lift Rotor System	40
Optimization of Single-Lift/Antitorque Rotor System	70
Final Weights and Performance	70
Configuration Selection	77
Effect of Mission Cruise Speed on Payload	77
Exploratory Dynamics Study	78
STABILITY, CONTROL, AND FLYING QUALITIES	85
Analysis of Mission Requirements	85
Static Stability	95
Longitudinal (Pitch) Control	100
Lateral and Directional (Roll and Yaw) Control	112
Cumulative Collective and Cyclic Pitch	115
Hover Attitude Control	115
Evaluation of Hingeless Semirigid Rotor	115
Analysis of Stall Flutter and Flap-Lag Instability	119
STATIC AND DYNAMIC STRUCTURAL ANALYSIS OF THE ARTICULATED ROTOR	157
Methodology and Approach to Stress Analysis of Rotor Blades	158

Page

Methodology and Approach to Stress Analysis of Rotor Hub 164
Methodology and Approach to Stress Analysis of Rotor Controls. 165
Analysis Methods -- Comparison of Theory and Test 165
Criteria for Structural Analysis 165
Structural Analysis of Fiberglass Plastic Rotor Blades 172
Structural Analysis of Metal Rotor Blades . . . 173
Structural Analysis of Rotor Hub 175
Structural Analysis of Rotor Control System . . 176
Dynamic Analysis 177

STATIC AND DYNAMIC STRUCTURAL ANALYSIS OF THE HINGELESS SEMIRIGID ROTOR 245
Background 245
Conclusions 248
Configuration 252
Method of Analysis 260
Results of Analysis 260
Evaluation of Analysis 263

PRELIMINARY DESIGN LAYOUTS 281
Rotor Blades for an Articulated Rotor System . . 281
Rotor Head for an Articulated Rotor System . . . 284
Rotor Controls for an Articulated Rotor System . 289
Hingeless Rotor Hub and Plastic Blade 290
Elastomeric Rotor Hub 290

WEIGHTS 323
Main Rotor Group (Articulated) 323
Tail Group (Single-Lift/Antitorque Rotor Helicopters) 328
Body Group 329
Alighting Gear Group 330
Flight Controls Group 330
Engine Section or Nacelle Group 330
Propulsion Group 331
Derivation of Weights for Fixed Equipment . . . 332
Auxiliary Powerplant 332
Instrument Group 332
Hydraulic and Pneumatic Group 332
Electrical Group 332

Page

Electronics Group 332
Furnishing and Equipment Group 333
Fixed Useful Load 335
Comparison Study 336
Summary Weight Statement for Tandem-Lift Rotor Transport 338
Summary Weight Statement for Tandem-Lift Rotor Crane/Personnel Carrier 344
Summary Weight Statement for Single-Lift/ Antitorque Rotor Transport 350
Summary Weight Statement for Single-Lift/ Antitorque Rotor Crane/Personnel Carrier . . . 356

RELIABILITY 362
System Reliability 362
Mission Reliability 362
Flight-Safety Reliability 362

BIBLIOGRAPHY 365

DISTRIBUTION 368

Appendix: WEIGHT-ESTIMATION METHODS 370

ILLUSTRATIONS

Figure		Page
1	Heavy-Lift Helicopter Concept	14
2	Tandem-Lift Rotor Transport	21
3	Single-Lift/Antitorque Rotor Transport	23
4	Tandem-Lift Rotor Crane/Personnel Carrier	25
5	Single-Lift/Antitorque Rotor Crane/ Personnel Carrier	27
6	Specification Missions	29
7	Analysis of Typical Mission	30
8	Configuration Analysis Flow Chart	33
9	Rotor Group Weight Trend	36
10	Drive System Weight Trend	37
11	Initial Iteration of Transport Mission	41
12	Second Iteration of Transport Mission	45
13	20-Ton Mission Weight and Performance Study for Tandem-Lift Rotor Helicopter	49
14	12-Ton Mission Weight and Performance Study for Tandem-Lift Rotor Helicopter	51
15	Selection of Blade Radius and Engine Combinations	54
16	Selection of Design $\bar{C}_L$, Tip Speed, and Solidity	55
17	Effect of Tip Speed on Speed Limitations	56
18	Selection of Number of Blades, Chord, and Twist	57

Figure		Page
19	Effect of Blade Twist on Maximum Speed Free of Blade Stall	59
20	Effect of Blade Twist on Hover Performance of the Tandem-Lift Rotor Transport	60
21	Angle-of-Attack Distribution of the Tandem-Lift Rotor at 75,700 Pounds, 5000 Feet, 120 Knots	63
22	Angle-of-Attack Distribution of the CH-47 Rotor at 28,290 Pounds, 5000 Feet, 120 Knots	67
23	Angle-of-Attack Distribution of the Tandem-Lift Rotor at 87,000 Pounds, Sea Level, 165 Knots	68
24	Projected Rotor Limits for Continuous Cruise	69
25	12-Ton Mission Weight and Performance Study for Single-Lift/Antitorque Rotor Transport	71
26	12-Ton Mission Weight and Performance Study for Single-Lift/Antitorque Rotor Crane/Personnel Carrier	73
27	12-Ton Mission Speed and Payload Capability of Tandem-Lift Rotor Helicopter	79
28	Natural Frequency Spectra of Three- and Four-Bladed Rotors	81
29	In-Plane Hub Loads	83
30	Vertical Hub Loads	84
31	Lateral-Directional Control Requirements in Sideslip Flight at 130 Knots	87
32	Collective and Differential-Collective Pitch Envelope	88

Figure		Page
33	Lateral and Differential-Lateral Cyclic Pitch Envelope	89
34	Cumulative Collective and Cyclic Pitch Envelopes	90
35	Pitch Damping and Control Sensitivity in Hover	92
36	Roll Damping and Control Sensitivity in Hover	93
37	Yaw Damping and Control Sensitivity in Hover	94
38	Longitudinal Cyclic Trim	96
39	Stick Position as a Function of Airspeed	97
40	Rotor System Static Stability in Pitch at 28.5 Inches Aft cg	99
41	Rotor System Static Stability in Pitch at 11.5 Inches Forward cg	101
42	Static Stability in Pitch of Transport With SAS Off	102
43	Directional Stability of Transport	103
44	Variation of Longitudinal Flapping With Airspeed and Gross Weight	105
45	Trimmed Stick Position (Automatic DCP Trim Off) With and Without Delta-Three on Forward Rotor	110
46	Minimum Collective Pitch Requirement	111
47	Hover Attitude Control	117
48	Pitch-Link Load at 87,000 Pounds Gross Weight	125

Figure		Page
49	Pitch-Link Load at 75,700 Pounds Gross Weight	127
50	Forward Rotor Angle-of-Attack Contours	132
51	Forward Rotor Local Aerodynamic Moment Contours	133
52	Forward Rotor Local Aerodynamic Damping Contours	134
53	CH-47A Aft Rotor Pitch-Link Load at 28,940 Pounds Gross Weight, 5000 Feet, 147 Knots	135
54	CH-47A Aft Rotor Angle-of-Attack Contours	136
55	CH-47A Aft Rotor Local Aerodynamic Moment Contours	137
56	CH-47A Aft Rotor Local Aerodynamic Damping Contours	138
57	Coupled Flap and Lag Motions at 87,000 Pounds Gross Weight	139
58	Gust Input Parallel to Shaft	143
59	Coupled Flap and Lag Motions at 75,700 Pounds Gross Weight	145
60	CH-47A Forward Rotor Coupled Flap and Lag Motions	155
61	Correlation of Theoretical and Experimental Vibratory Flapwise Bending Moment	166
62	Correlation of Theoretical and Experimental Vibratory Pitch-Link Load	167
63	Summary of Tandem-Lift Rotor Helicopter Geometry	168
64	Spanwise Weight Distribution of Plastic Blade	184

Figure		Page
65	Flapwise Stiffness Distribution of Plastic Blade	185
66	Chordwise Stiffness Distribution of Plastic Blade	186
67	Torsional Stiffness Distribution of Plastic Blade	187
68	Centrifugal Force Distribution of Plastic Blade	188
69	Static Bending and Tip Deflection of Plastic Blade	189
70	Flapwise Natural Frequency Spectrum of Plastic Blade	190
71	Chordwise and Torsional Natural Frequency Spectrum of Plastic Blade	191
72	Flapwise Bending Moments of Plastic Blade	192
73	Chordwise Bending Moments of Plastic Blade	196
74	Torsional Moments of Plastic Blade	200
75	Weight Distribution of Metal Blades	204
76	Flapwise Stiffness Distribution of Metal Blades	205
77	Chordwise Stiffness Distribution of Metal Blades	206
78	Torsional Stiffness Distribution of Metal Blades	207
79	Centrifugal Force Distribution of Metal Blades	208
80	Static Bending and Tip Deflection of High- and Low-Stiffness Metal Blades	209

Figure		Page
81	Natural Frequency Spectra of Metal Blades	210
82	Flapwise Bending Moments of Metal Blades	214
83	Chordwise Bending Moments of Metal Blades	217
84	Torsional Moments of Metal Blades	220
85	Parametric Evaluation of Tension-Torsion Assembly	223
86	Blade Pitching Moments Versus Airspeed	226
87	Blade Pitching Moments Versus Azimuth of Plastic Blade	227
88	Blade Pitching Moments Versus Azimuth of Metal Blade	230
89	Hub Shaking Force: Correlation of Tests and Analysis	233
90	Effect of Twist on Hub Shaking Forces	234
91	Effect of Airspeed on Rotor Forces	235
92	Nondimensional Shaking Forces	236
93	Geometric Similarities Between Heavy-Lift Helicopter and CH-47A	237
94	Vibration Level: Correlation of Tests and Analysis	238
95	Fuselage Response to Rotor Forces	239
96	Synthesized Cockpit Vibration Level	240
97	Predicted Cockpit Vibration Level Without Antivibration Devices	241
98	Blade Pendulum Absorber	242
99	Cockpit Absorbers	243

Figure		Page
100	Force Balancer	244
101	Yaw Schematic	249
102	Delta Weight Analysis	251
103	Basic Geometry of Airframe	253
104	Spanwise Weight Distribution of Conventional Blade	255
105	Spanwise Stiffness Distribution of Conventional Blade	256
106	Spanwise Chord-Stiffness Distribution of Conventional Blade	257
107	Spanwise Weight Distribution of Matched-Stiffness Blade	258
108	Spanwise Stiffness Distribution of Matched-Stiffness Blade	259
109	Flapwise and Chordwise Natural Frequencies of the Hingeless Rotor With Matched-Stiffness Blades	264
110	Vibratory Bending Characteristics of the Hingeless Rotor With Matched-Stiffness Blades	265
111	Speed Sweep at Constant Inboard Flap Stiffness for the Hingeless Rotor With Matched-Stiffness Blades	266
112	Flapwise Bending Moments of the Hingeless Rotor With Matched-Stiffness Blades	267
113	Chordwise Bending Moments of the Hingeless Rotor With Matched-Stiffness Blades	268
114	Steady Lateral Aerodynamic Force Output for the Hingeless Rotor With Matched-Stiffness Blades	269

Figure		Page
115	Comparison of Hub Overturning Moments for Hingeless and Articulated Rotors With Matched-Stiffness Blades	270
116	Static Deflection Characteristics of the Hingeless Rotor With Matched-Stiffness Blades	271
117	Flapwise and Chordwise Natural Frequencies of the Hingeless Rotor With Conventional Blades	272
118	Vibratory Bending Characteristics of the Hingeless Rotor With Conventional Blades	273
119	Speed Sweep at Constant Inboard Flap Stiffness for the Hingeless Rotor With Conventional Blades	274
120	Flapwise Bending Moments of the Hingeless Rotor With Conventional Blades	275
121	Chordwise Bending Moments of the Hingeless Rotor With Conventional Blades	276
122	Steady Lateral Aerodynamic Force Output for the Hingeless Rotor With Conventional Blades	277
123	Comparison of Hub Overturning Moments for Hingeless and Articulated Rotors With Conventional Blades	278
124	Static Deflection Characteristics of the Hingeless Rotor With Conventional Blades	279
125	Pylon Structure for Forward and Aft Rotors	293
126	Powerplant and Drive System	295
127	Metal D-Spar Nonsymmetrical Rotor Blade	297
128	Steel Hexagonal-Spar Rotor Blade	299
129	Fiberglass Plastic C-Spar Rotor Blade	301

Figure		Page
130	Articulated Forward Rotor Hub	303
131	Forward Rotor Upper Controls	307
132	Flight Controls	311
133	Collective-Pitch Bungee	313
134	Hingeless Forward Rotor Hub	315
135	Plastic Rotor Blade for Hingeless Rotor	317
136	Coincident-Hinge Elastomeric Bearing Rotor Hub	319
137	Rotor Group Weight Trend	372
138	Body Group - Transport Helicopters	380
139	Body Group - Basic Structure	381
140	Flight Controls Group - Cockpit Controls Weight Trend for Helicopter Dual Cockpit Controls	392
141	Flight Controls Group Upper Controls Weight Trend, Including Upper Boost Actuators	393
142	Flight Controls Group System Controls Weight Trend	394
143	Drive System Weight Trend for Turbine-Powered Helicopters	400

TABLES

Table		Page
I	Mission Requirements per Contract	2
II	Parameters	3
III	Weights and Performance Summary	5
IV	Summary of Blade Load Distributions and Bearing Life Derived from Static and Dynamic Structural Analysis	9
V	Mission Fuel in Pounds	10
VI	Engine Characteristics	32
VII	Payload Capability for TO&E Equipment Weighing Over 500 Pounds	38
VIII	Payload Capability for TO&E Equipment Over 500 Pounds	38
IX	Engineer Equipment	39
X	Air-Transportability of Missile Systems	39
XI	High-Priority Equipment	39
XII	Integration of Weights for Transport and Heavy-Lift Missions -- Tandem-Lift Rotor Helicopter	53
XIII	DCP Control Requirements in Degress of Blade Pitch Travel	107
XIV	Lateral Cyclic Pitch Requirements in Degrees of Blade Pitch Travel	113
XV	Configuration Details	124
XVI	Rotor Blade Structural Design Conditions	159
XVII	Mission Profile	170

Tables		Page
XVIII	Coning Angles	171
XIX	Cubic Mean Load on Horizontal Hinge Pin Roller Bearings	224
XX	B_{10} Life of Horizontal Hinge Pin Roller Bearings	225
XXI	Bearing Loads and B_{10} Life of Swashplate Bearings	232
XXII	Design Features of Conventional and Matched-Stiffness Blades for the Hingeless Semirigid Rotor	280
XXIII	Weight Comparison of the Hingeless Matched-Stiffness Rotor System and the Articulated Rotor System	337
XXIV	Weight Increases (Δ) in Body Group and Drive System Required by Increased Overturning Moment in Hingeless Hub	337

SYMBOLS

NOTE: The symbols used in STATIC AND DYNAMIC STRUCTURAL ANALYSIS OF THE ARTICULATED ROTOR applicable to metallic materials and elements for flight vehicle structures are listed in MIL-HDBK-5.

A	Multiplying constant for standard weight trend
alt	Subscript indicating alternating load
A_{1c}	Blade lateral cyclic pitch in degrees
A_{1f}	Flap angle in degrees
B	Basic structure weight constant (WEIGHTS) Multiplying constant for advanced-technology weight trend (WEIGHTS)
b	Number of blades per rotor
B_{1c}	Blade longitudinal cyclic pitch in degrees
B_{10} Life	Minimum life in hours that 90 percent of the ball and rolling element bearings will achieve before first evidence of failure will be perceptible
c	Blade chord in feet (ROTOR SYSTEM PERFORMANCE PARAMETRIC ANALYSIS and WEIGHTS) Blade chord in inches (STATIC AND DYNAMIC STRUCTURAL ANALYSIS OF THE ARTICULATED ROTOR) Basic oscillating capacity of bearing in pounds (STATIC AND DYNAMIC STRUCTURAL ANALYSIS OF THE ARTICULATED ROTOR)

c	Distance of stressed fiber to neutral axis in inches (STATIC AND DYNAMIC STRUCTURAL ANALYSIS OF THE HINGELESS SEMIRIGID ROTOR)
CBR	California Bearing Ratio
C.F.	Centrifugal force in pounds (STATIC AND DYNAMIC STRUCTURAL ANALYSIS OF THE HINGELESS SEMIRIGID ROTOR)
$\overline{C}_F$	Centrifugal force in pounds (STATIC AND DYNAMIC STRUCTURAL ANALYSIS OF THE ARTICULATED ROTOR)
C_L	Coefficient of lift
$\overline{C}_L$	Mean blade lift coefficient
Comp CF	Component part of centrifugal force in pounds
C_T	Rotor thrust coefficient
C_T'	Vertical component of rotor thrust coefficient
d	Roller element diameter of bearing in inches (STATIC AND DYNAMIC STRUCTURAL ANALYSIS OF THE ARTICULATED ROTOR)
	Rotor diameter in feet (STATIC AND DYNAMIC STRUCTURAL ANALYSIS OF THE ARTICULATED ROTOR)
	Lateral distance of center of gravity from roll axis in inches (STATIC AND DYNAMIC STRUCTURAL ANALYSIS OF THE HINGELESS SEMIRIGID ROTOR)
	Flapping hinge offset in feet (WEIGHTS)
D_{pitch}	Roller bearing pitch diameter in inches
D_{shaft}	Roller bearing shaft diameter in inches

e	Rotor flap hinge offset in inches or feet (STATIC AND DYNAMIC STRUCTURAL ANALYSIS OF THE HINGELESS SEMIRIGID ROTOR)
fe	Equivalent flat-plate drag in square feet
F_{CF}	Tension stress due to centrifugal force in pounds per square inch
F_x	Relative longitudinal load
F_y	Relative lateral load (ROTOR SYSTEM PERFORMANCE PARAMETRIC ANALYSIS)
	Lateral force in pounds (STATIC AND DYNAMIC STRUCTURAL ANALYSIS OF THE HINGELESS SEMIRIGID ROTOR)
F_{y_o}	Lateral aerodynamic force in pounds
$F_{y_{o_A}}$	Lateral aerodynamic force (aft rotor) in pounds
$F_{y_{o_F}}$	Lateral aerodynamic force (forward rotor) in pounds
F_z	Relative vertical load
F_{z_3}	Vertical force in pounds
$f(F_{yo}, \theta_i)$	Yaw control power
GW	Gross weight in pounds
h	Couple distance in feet
H_D	Density altitude in feet

H_F	Height of forward rotor above horizontal reference in feet (STATIC AND DYNAMIC STRUCTURAL ANALYSIS OF THE ARTICULATED ROTOR)
h_f	Height of forward rotor above horizontal reference in feet (STATIC AND DYNAMIC STRUCTURAL ANALYSIS OF THE HINGELESS SEMIRIGID ROTOR)
H_p	Pressure altitude in feet
HP_r	Horsepower required per rotor
HP_x	Transmission design horsepower
H_R	Height of aft rotor above horizontal reference in feet (STATIC AND DYNAMIC STRUCTURAL ANALYSIS OF THE ARTICULATED ROTOR)
h_r	Height of aft rotor above horizontal reference in feet (STATIC AND DYNAMIC STRUCTURAL ANAIYSIS OF THE HINGELESS SEMIRIGID ROTOR)
i	Identifying subscript for flap
I_f	Blade flapping inertia in foot pounds per second squared
i_F	Inclination of forward rotor shaft in degrees
i_R	Inclination of aft rotor shaft in degrees
I_{ZZ}	Mass moment of inertia about Z axis in slug feet squared
j	Identifying subscript for chord
K	Group weight factor

k	Ratio of shaft ID to OD (STATIC AND DYNAMIC STRUCTURAL ANALYSIS OF THE HINGELESS SEMIRIGID ROTOR)
	Blade flapping inertia proportionality factor (WEIGHTS)
	Droop constant (WEIGHT ESTIMATION METHODS)
K_D	Drive system weight factor
K_d	Nondimensional drag factor (ROTOR SYSTEM PERFORMANCE PARAMETRIC ANALYSIS)
	Nondimensional blade droop factor (WEIGHTS)
KE Cap	Kinetic energy capacity in foot pounds
K_r	Rotor system weight factor
k_θ	Blade torsional spring rate in inch-pounds per radian
L	Horizontal distance between rotors in feet (STATIC AND DYNAMIC STRUCTURAL ANALYSIS OF THE ARTICULATED ROTOR and STATIC AND DYNAMIC STRUCTURAL ANALYSIS OF THE HINGELESS SEMIRIGID ROTOR)
	Length of flapping portion of blade in feet, or R-d (WEIGHTS)
L_c or l_c	Length of cabin in feet
L_{eff}	Effective length of roller bearing in inches
L_{rw} or l_{rw}	Length of ramp well in feet
L_l	Length of cargo floor in feet
M	Rotor blade pitch moment in inch pounds

M	Blade static moment in foot pounds (WEIGHTS)
$M_{allowable}$	Allowable moment in inch pounds
M_{hub_A}	Aft hub roll moment in inch pounds
M_{hub_F}	Forward hub roll moment in inch pounds
M_i	Generalized hub moment in inch pounds
M_{pitch}	Rotor shaft pitching moment in inch pounds
M_{sp}	Swashplate moment in inch pounds
M_x	Longitudinal effective fuselage mass at hub in slugs
M_y	Lateral effective fuselage mass at hub in slugs
M_z	Vertical effective fuselage mass at hub in slugs
M_1	Average vibratory moment in inch pounds
M_β	Rotor blade static moment about flap pin in foot pounds
N	Rotor speed in rpm
(N)	Number of rolling elements in bearing
n	Ultimate load factor (WEIGHTS)
	Number of rotors (STATIC AND DYNAMIC STRUCTURAL ANALYSIS OF THE ARTICULATED ROTOR)
N_E	Number of engines
N_L	Number of litters
N_N	Normal rotor speed in rpm
N_r	Rotor hover speed in rpm
n_r	Number of rotors (WEIGHTS)

N_T	Number of troops
N_β	Rate of change in yawing moment with sideslip angle in foot pounds per radian
OLF	Oil lubrication factor
OPM	Bearing speed in oscillations per minute
P	Pitch-link load in pounds (STATIC AND DYNAMIC STRUCTURAL ANALYSIS OF THE ARTICULATED ROTOR)
	Radial load on bearing in pounds (STATIC AND DYNAMIC STRUCTURAL ANALYSIS OF THE HINGELESS SEMIRIGID ROTOR)
P_m	Bearing cubic mean load in pounds
P_n	Bearing load in pounds for rotor speed N_n
PV	Bearing pressure-velocity parameter in pounds per square inch x feet per minute
$qd^2\sigma$	Rotor performance parameter in pounds
R	Rotor radius in feet
	Outside radius of tubular shaft in inches (STATIC AND DYNAMIC STRUCTURAL ANALYSIS OF THE HINGELESS SEMIRIGID ROTOR)
$\overline{R}$	Radial blade center of gravity from centerline of flapping hinge in feet
r	Distance from centerline of rotation to point of blade attachment in feet
R_o	Inside radius of tubular shaft in inches
R_{pa}	Radius of the pitch arm in inches

R_{sp}	Radius of the swashplate arm in inches
s	Subscript indicating steady load
SF	Bearing size factor
S_f	Wetted area of fuselage (including pylons) in square feet
SHF	Shaft hardness factor
SSF	Stationary shaft factor
t	Time in minutes (STATIC AND DYNAMIC STRUCTURAL ANALYSIS OF THE ARTICULATED ROTOR)
	Blade thickness at 25-percent radius in feet (WEIGHT ESTIMATION METHODS)
T_{sp}	Swashplate thrust in pounds
UCI	Unit construction index
V_{cr}	Cruise speed in knots
$V_{forward}$	Forward speed of the helicopter in knots
V_H	Forward speed of the helicopter in knots (STATIC AND DYNAMIC STRUCTURAL ANALYSIS OF THE ARTICULATED ROTOR)
V_{max}	Maximum forward flight speed in knots
V_t	Blade tip speed in feet per second
V_{t_l}	Blade design-limit tip speed in feet per second

W	Design gross weight (STABILITY, CONTROL, AND FLYING QUALITIES)
W_{AC}	Weight of airconditioning and anti-icing group in pounds
W_b	Blade weight in pounds
W_{BG}	Weight of body group in pounds
W_{BS}	Weight of basis structure in pounds
W_{cc}	Weight of cockpit controls in pounds
W_D or W_{DS}	Weight of drive system in pounds
W_e	Engine weight in pounds
W_{EE}	Weight of emergency equipment in pounds
W_{ES}	Engine section weight in pounds
$(W_{ES})_A$	Engine section weight by advanced technology in pounds
W_F	Weight of root-end fitting in pounds
W_f	Flapping weight of one blade in pounds
W_{FC}	Total flight controls weight in pounds
W_{FUL}	Weight of fixed useful load in pounds
W_g	Design gross weight in pounds (WEIGHTS)
W_H	Weight of hinge and blade retention in pounds
W_I	Weight of instrument group in pounds
W_{LC}	Weight of loadmaster's hover controls in pounds
W_M	Weight of engine mounts in pounds
W_{ME}	Weight of miscellaneous equipment in pounds
W_{PA}	Weight of personnel accommodations in pounds

W_R	Total rotor group weight in pounds
W_r	Weight of one rotor in pounds
W_S	Weight of structure for landing gear in pounds
W_{SAS}	Weight of stability augmentation system in pounds
W_{sc}	Weight of system controls (including hydraulic boost system) in pounds
W_{uc}	Weight of upper controls in pounds
W_l	Weight of cargo floor in pounds
x	Exponential power factor for K
X_C	Inboard airfoil blade cutout (r/R)
Y	Lateral force in pounds
y	Exponential power factor for K
Z	Vertical force in pounds
$\frac{1/2\rho aoCoR^4}{I_{flap}}$	Locke number
β	Coning angle in degrees
	Angular separation in degrees between rolling elements of a bearing
$\beta_{(radians)}$	Coning angle in radians
ΔCG	Allowable center-of-gravity travel in feet
Δfe	Change in equivalent flat-plate area in square feet
$\delta T/\delta \alpha$	Rate of change of rotor thrust with respect to fuselage angle of attack in pounds per radian

$\%\Delta WT$	Percent change in weight between hingeless and articulated rotor
δ_3	Delta three
η	Ultimate load factor
η_{CR}	Crash load factor
θ_F	Inclination of the forward rotor shaft in degrees
θ_R	Inclination of the aft rotor shaft in degrees
θ_{TW} or θ_t	Total linear blade twist in degrees
θ_1	Lateral cyclic control input in degrees
$\theta_{0,75}$	Blade collective pitch in degrees at 75-percent radius
λ	Inflow ratio
μ	Rotor advance ratio
ρ	Air density in slugs per cubic foot
σ	Solidity (bc/ R)
ψ	Blade azimuth position
Ω	Rotor rotational speed in radians per second
ω/Ω	Exciting frequency (multiple of rotor speed)
ω_n	Natural frequency associated with the th bending mode of the blade in cycles per minute
ω_o	Blade fundamental mode frequency in cycles per second

SUMMARY

The purpose of this investigation is to define the optimum configuration and physical characteristics for a shaft-driven heavy-lift helicopter rotor system (this includes the number of rotors, the rotor blade geometry, hub articulation and control requirements) and a general functional and structural description of the aircraft for which the selected rotor design is applicable.

ROTOR SYSTEM PERFORMANCE PARAMETRIC ANALYSIS

The objective of the parametric analysis is the selection of a rotor system for the heavy-lift helicopter missions from within the limited field of two shaft-driven systems: the tandem-lift rotor system and the single-lift/antitorque rotor system. Calculation of propulsion, performance, and weight parameters for each rotor configuration was iterated for a set of mission ground rules; successive iterations were continued until the assumed and derived parameters converged. The missions and parameters are categorized in Tables I and II.

> NOTE: The use of the word "parametric" in this report has been limited to its mathematical connotation: assignment of successive arbitrary values to variables for the purpose of obtaining discrete solutions which approximate the closed-form solutions of real, physical models. As with many mathematical models of a hypergeometric nature, the independent variables become parameters especially when they are used with convergence techniques involving successive iterations by digital computer.

To evaluate the results from the mathematical models, selection criteria were postulated in two categories: necessary conditions for selection and sufficient conditions for selection. The use of the words "sufficient conditions" here implies that once the necessary conditions are met by both the tandem-lift rotor system and the single-lift/antitorque rotor system, any residual conditions constitute an area for tradeoff analysis. The resultant selected subset conditions then become adequate and commensurate reasons for choosing one configuration over the other. In this context, these are termed "sufficient conditions."

Necessary conditions are those which must be met without compromise:

TABLE I

MISSION REQUIREMENTS PER CONTRACT

Requirement	Transport Mission	Heavy-Lift Mission	Ferry Mission
Payload out	12 tons*	20 tons**	None
Minimum design load factor	2.5	2.5	2.0
Radius	100 n.mi.	20 n.mi.	1500 n.mi. (STOL takeoff)
Cruise speed:			
W/payload	110 kt	95 kt	-
W/o payload	130 kt	130 kt	For best range
Hover time:			
At takeoff	3 min	5 min	-
At midpoint w/ payload	2 min	10 min	-
Hover OGE	6000 ft 95°F	Sea level 59°F	-
Mission altitude	Sea level standard	Sea level standard	For best range
Reserve fuel (% initial fuel)	10%	10%	10%
Fuel allowance @ MIL-C-5011A	Ref	Ref	Ref

* Payload considered to be carried internally. For crane/personnel carrier, a pod was assumed to enclose the load, and a flat-plate-area increment of 10 square feet was assumed for extra drag. Pod weight was considered part of payload.

**Payload considered to be carried externally. A flat-plate-area increment of 100 square feet was assumed for extra drag on both the transport and the crane/personnel carrier.

TABLE II
PARAMETERS

Length of cargo compartment*	540 inches
Width x height of cargo compartment*	144 x 108 inches for transport 120 x 78 inches for crane
Percent of Inf. Div. transportable with 12-ton payload*	91 percent of items; 59 percent of weight**
Ground-to-fuselage clearance*	4.25 feet for transport 13.5 feet for crane
Tip speed (V_t)	600 to 800 feet per second
Mean blade lift coefficient ($\bar{C}_l$)	0.60 to 0.80
Blade twist	-12 to -6 degrees
Airfoil section	NACA 0012 and 23012
Rotor blade overlap	0 to 35 percent for tandem Not applicable for single
Rotor blade coning angle	4.3 to 7.4 degrees
Solidity	0.05 to 0.25 for tandem 0.06 to 0.21 for single
Number of blades per rotor	3, 4, and 5 for tandem 4, 5, and 6 lift blades for single 4, 5, and 6 antitorque blades for single
Power required (transmission rating)	11,000 to 17,200 shp for tandem 12,400 to 15,200 shp for single
Rotor radius	30 to 50 feet for tandem 46 to 64 feet for single
Cruising speed	100 to 170 knots for tandem 80 to 160 knots for single

*These parameters were defined by estimates; they were not specified in the contract, but they are necessary to the study. All other parameters listed here were defined by helicopter aerodynamic science, history, configurations, and by iteration.
**Payload considered to be carried internally by transport, internally and externally by crane/personnel carrier.

1. Mission requirements

2. Inherently good flying qualities

3. Acceptable vibration levels

4. A high safety index, as reflected in structural integrity and reliability

Sufficient conditions are those which become the basis for choice between configurations:

1. A competitively low producibility, maintainability, and availability cost/effectiveness index, as reflected in weight empty

2. A competitively low fuel requirement

3. Margins of superiority beyond mission requirements, provided that these margins do not increase cost.

4. Because the airframe has not been defined, the selected rotor configuration must be compatible with the forms the aircraft may eventually take.

Both the analysis and historical confidence indicate that both the tandem-lift and single-lift/antitorque rotor systems can meet the necessary conditions for selection. (The ability to meet all mission requirements is implicit in the mathematical models.) The details on flying qualities, airframe vibration, structural integrity, and reliability are found in the STABILITY, CONTROL, AND FLYING QUALITIES; STATIC AND DYNAMIC STRUCTURAL ANALYSIS; and RELIABILITY chapters of this report.

A summary of heavy-lift helicopter weights and performance is given in Table III. Based on a review of the computer-generated results, which show differences in optimized weights between configurations, the tandem-lift rotor system was selected for the preliminary design study because it best satisfies those conditions defined above as sufficient conditions for selection.

PRELIMINARY DESIGN STUDY

The objective of the preliminary design study is to define the rotor system in detail. At an early stage in the study, it

TABLE III
WEIGHTS AND PERFORMANCE SUMMARY

Item	Single-Lift/Antitorque Rotor Helicopter Four 501-M26				Three 501-M26		
	Transport		Crane		Transport		Cr
	Req'd Cruise Speed	Max Cruise Speed	Req'd Cruise Speed	Max Cruise Speed	Req'd Cruise Speed	Max Cruise Speed	Req' Crui Spee
Blade radius (ft)	48.0		48.0		43.0		4
Chord (ft)	4.0		4.0		3.5		
Airfoil section	NACA 23012		NACA 23012		NACA 23012		NACA
Solidity	0.133		0.133		0.07772		0.0
Tip speed (fps)	700		700		700		
Blade twist (deg)	-12		-12		-9		
Number of blades	5		5		3		
Transmission rating (shp)	15500		15500		12000		12
Cabin size (cu ft)	45x12x9		-		45x12x9		
Basic flat plate area (sq ft)	96.6		142.2		93.5		13
Design gross weight (lb) (load factor 2.5)	91600		91600		87000		87
Empty weight (lb)	47173		45949		42027		39
Transport Mission [8]							
Fixed useful load (lb)	880	880	880	880	880	880	88
Payload	24000	24000	24000[1]	24000	24000	24000	2400
Mission fuel	9890	9747	10816	10801	8250	9050	892
Takeoff gross weight	81973[6]	81800	81645[6]	81630[6]	75157	75957	7337
Maximum hover gross weight @6000 ft, 95°F (lb)	81800	81800	81120	81120	78500	78500	7830
V outbound (kt)	110	149	110	120	110	167	1
Vmax (kt) not exceeding NRP	169	169	155	155	-	167	-
Heavy-Lift Mission [8]							
Fixed useful load (lb)	880		880		880	880	8
Payload [2]	40000		40000		40000	40000	400
Mission fuel	4670		4735		3660	3640	38
Takeoff gross weight	92723[6 7]		91564		86567	86547	842
Maximum hover gross weight (lb) @ SL Std	92400		92000		89930	89930	897
V outbound (kt) [2]	95		95		95	139	
Vmax (kt) not exceeding NRP [2]	146		139		-	139	-
Ferry Mission [8]							
Fixed useful load (lb)	880		880		880		
Auxiliary tanks (lb)	4779		4805		4829		4
Mission fuel (lb)	61668		62866		61105		6
Takeoff gross weight (lb) based on L.F.=2	114500		114500		108750		108
Average cruise speed (kt)	130		126		134		
Ferry range (n.mi.) [3]	1782 [5]		1595 [5]		1930 [4]		1

NOTES:
1. Payload carried internally for crane type. Δfe = 10 square feet. To account for pod to enclosure payload, pod weight is included as payload.
2. Payload carried externally. Δfe = 100 square feet to account for drag of payload.
3. Based on flying at optimum altitude but not higher than 10,000 feet.
4. One engine
5. Two engines
6. Total overl hover weigh
7. Total overl gross weigh
8. Missions ar

TABLE III

IGHTS AND PERFORMANCE SUMMARY

ift/Antitorque licopter)1-M26	Tandem-Lift Rotor Helicopter											
	Three 501-M26				Four T55-L-11				Four T64 S/4			
	Crane		Transport		Crane		Transport		Crane		Transport	
	Req'd Cruise Speed	Max Cruise Speed	Req'd Cruise Speed	Max Cruise Speed	Req'd Cruise Speed	Max Cruise Speed	Req'd Cruise Speed	Max Cruise Speed	Req'd Cruise Speed	Max Cruise Speed	Req'd Cruise Speed	Max Cruise Speed
	48.0		43.0		43.0		43.0		43.0		43.0	
	4.0		3.5		3.5		3.5		3.5		3.5	
	NACA 23012		NACA 23012		NACA 23012		NACA 23012		NACA 23012		NACA 23012	
	0.133		0.07772		0.07772		0.07772		0.07772		0.07772	
	700		700		700		700		700		700	
	-12		-9		-9		-9		-9		-9	
	5		3		3		3		3		3	
	15500		12000		12000		12000		12000		12000	
	-		45x12x9		-		45x12x9		-		45x12x9	
	142.2		93.5		136.5		95.6		138.6		95.6	
	91600		87000		87000		87000		87000		87000	
	45949		42027		39571		42224		39769		42877	
0	880	880	880	880	880	880	880	880	880	880	880	880
0	24000[1]	24000	24000	24000	24000[1]	24000[1]	24000	24000	24000[1]	24000[1]	24000	24000
7	10816	10801	8250	9050	8920	9550	8750	9792	9600	10260	7700	7743
0	81645[6]	81630[6]	75157	75957	73371	74001	75854	76896	74249	74909	75457	75500
0	81120	81120	78500	78500	78300	78300	77300	77300	77100	77100	75500	75500
9	110	120	110	167	110	150	110	167	110	150	110	145
9	155	155	-	167	-	150	-	167	-	150	-	167
	880		880	880	880	880	880	880	880	880	880	880
	40000		40000	40000	40000	40000	40000	40000	40000	40000	40000	40000
	4735		3660	3640	3800	3770	3900	3870	4080	4010	3550	3470
7	91564		86567	86547	84251	84221	87004[7]	86974	84729	84659	87307[7]	87227
	92000		89930	89930	89700	89700	89930	89930	89700	89700	89930	89930
	95		95	139	95	131	95	139	95	131	95	139
	139		-	139	-	13[1]	-	139	-	131	-	139
	880		880		880		880		880		880	
	4805		4829		4961		4808		4944		4753	
	62866		61105		63338		60838		63157		60240	
	114500		108750		108750		108750		108750		108750	
	126		134		126		131		122		132	
	1595 [5]		1930 [4]		1810 [4]		1755 [4]		1645 [4]		1921 [4]	

Δfe = 10
ure payload,

are feet to

t higher than

4. One engine shut down.
5. Two engines shut down.
6. Total overload gross weight is higher than maximum hover weight.
7. Total overload gross weight is higher than design gross weight.
8. Missions are defined in Table I.

B

became evident that the field of contending rotor types should be limited. The primary concentration was placed on the articulated rotor. An exploratory parametric study of the hingeless semirigid rotor was limited to areas of risk, the weight increment, and areas worthy of further study. The articulated rotor preliminary design study progressed as follows:

1. The following parameters were derived from the rotor system parametric study:

   a. Rotor configuration: tandem-lift

   b. Number of lift rotor heads: 2

   c. Number of antitorque rotor heads: 0

   d. Number of blades per head: 3

   e. Rotor radius: 43 feet

   f. Blade chord: 3.5 feet

   g. Blade airfoil: NACA 23012, constant

   h. Blade twist: -9 degrees

   i. Rotor rpm: 155.5 (tip speed 700 feet per second)

   j. Powerplant-transmission configuration: 4 engines (see Figure 126)

2. Flap pin position and control motions were determined from stability and control requirements. The flap pin is at station 12 inches, or 2.3 percent of radius. The total cyclic-versus-collective envelope limits are shown in Figure 34.

3. Coning angle historical criteria are given in Table XVIII.

4. Computer-derived convergence of blade and hub parameters included the tuning of blade natural frequencies away from operating frequencies. The fiberglass plastic blade permits tuning to desired natural frequencies because it allows freedom to orient structural fibers, and thus to vary strength and elasticity

independently. The metal blade is tuned by antinodal placement of masses on a D-spar.

5. Stress levels were determined, and allowable loads were mapped against expected loads for several conditions. The fiberglass plastic blade provides a considerable margin between blade loads and allowables for speeds up to 160 knots in any flight regime (see Figures 72, 73, and 74). The metal high-stiffness blade has adequate load margins for speeds up to 140 knots. The metal low-stiffness blade has adequate load margins up to 160 knots, but not as large as those of the fiberglass plastic blade (see Figures 82, 83, and 84).

   NOTE: The contract-mission maximum speed of 130 knots is far below the maximum performance of 167 knots attainable in the tandem-lift rotor transport or 150 knots in the crane/personnel carrier. Since the technological disciplines have investigated conditions peculiar to them, some mismatch of speeds appears hereafter. All of the speeds, however, fall within 5 percent of, or are greater than, the 167-knot performance speed limit and they are not to be considered a limitation on performance. The existence of considerable margins in these static and dynamic structural analyses validates the adequacy of the designs to meet the 167-knot performance speed.

6. Design layouts of blade, hub, and controls were made consistent with the loads expected, blade-folding capability, the materials studied, and updated manufacturing methods. The stress margins are adequate, and the bearing elements are designed for 3600 hours' service life and 1200 hours between major overhaul. Table IV summarizes blade load distributions and bearing life derived from static and dynamic structural analysis.

7. The design weights were compared against the trend weights derived in the parametric study. A 466-pound weight increase (Δ) was found. This reiteration of the rotor system weight as well as other subsystem weights gives an aircraft design weight decrement 973 pounds below the parametric weight estimate. The weight-empty estimate was revised to 39,769 pounds, to

TABLE IV

SUMMARY OF BLADE LOAD DISTRIBUTIONS AND BEARING LIFE DERIVED FROM STATIC AND DYNAMIC STRUCTURAL ANALYSIS

Blade for Transport with -12° Twist	Condition	Steady Loads (10^4 in.-lb)	Alternating Loads (10^4 in.-lb)	Allowable Loads* (10^4 in.-lb)
Plastic	788 pounds	-	-	-
Flapwise, sta 10%	100 knots	2.2	±12.0	±21.5
Chordwise, sta 42%	140 knots	13.8	± 9.4	±16.8
Torsion, sta 42%	160 knots	-	± 2.15	± 6.7
Static bending, sta 35%	4g	37.0	-	127.0 ult
Metal High-Stiffness	874 pounds	-	-	-
Flapwise, sta 62%	140 knots	-	±12.8	±13.0
Chordwise, sta 50%	140 knots	3.0	± 6.5	±15.0
Torsion, sta 62%	160 knots	-	± 2.0	±21.2
Static bending, sta 21%	4g	59.0	-	72.0 ult
Metal Low-Stiffness	824 pounds	-	-	-
Flapwise, sta 50%	100 knots	1.0	± 8.9	±12.7
Chordwise, sta 50%	140 knots	0.5	± 8.4	±15.0
Torsion, sta 62%	140 knots	0.5	± 1.8	±13.0
Static bending, sta 24%	4g	52.0	-	65.0 ult

Bearing B_{10} Life: Swashplate upper bearing 5650 hours
Swashplate lower bearing 2646 hours
Horizontal pin bearing 1390 hours

*Allowable alternating moments are obtained by using the mean and alternating stresses from a modified Goodman diagram.

include the rotor design weight estimate. The weight increase (Δ) estimates for a hingeless semirigid system are shown in Table XXIV.

8. A reliability estimate was made of the aircraft dynamic system.

9. Preliminary designs were conceived for two tandem-lift rotor helicopters: the crane/personnel carrier and the transport.

10. Based on the transport, a dynamic analysis including fuselage response to vibratory rotor loads was made. The vibration levels are based on induced rotor loads applied to fuselage response characteristics. The predicted cockpit vibration levels indicate a proximity to existing pure helicopter vibration data scatter (see Figure 97).

11. A dynamic analysis of rotor stability was made. The stall-flutter analysis showed that stall flutter limits are well beyond mission cruise speeds. At the maximum-performance speed of 165 knots, moderate stall phenomena (stall flutter) are expected.

CONCLUSIONS

Both the tandem-lift and the single-lift/antitorque rotor systems can be made to meet the necessary conditions of missions, flying qualities, stability and control, acceptable fuselage response vibration levels, and inherent reliability. However, based upon findings of this preliminary design study, the following comparisons can be made of tandem-lift and single-lift/antitorque rotor heavy-lift helicopters:

1. The weight empty of the tandem-lift rotor helicopter is 11-percent lower than that of the single-lift/antitorque rotor helicopter: transport, 42,224 versus 47,173 pounds; crane/personnel carrier, 39,769 versus 45,949 pounds.

2. The tandem requires less fuel for mission completion (refer to Table V).

TABLE V
MISSION FUEL IN POUNDS

Mission	Tandem-Lift Rotor System	Single-Lift/Antitorque Rotor System
12-Ton Mission:		
Transport	8750	9890
Crane	9600	10816
20-Ton Mission:		
Transport	3900	4670
Crane	4020	4735

3. The tandem requires less shaft horsepower: the tandem helicopter required transmission rating is 12,000 horsepower for the critical condition of hover OGE at 6000 feet, 95°F. The single-lift/antitorque rotor helicopter requires a transmission rating of 15,500 shaft horsepower.

4. The tandem has inherent large cubage, with beam span for internal loading at no increase in weight empty.

5. The tandem has a greater center of gravity range with equal flapping-hinge offsets, and greater longitudinal control power.

6. The tandem has hover attitude control independent of center of gravity positions. While the dual longitudinal control system (including the hover attitude control described in Figure 47) is now categorized as a sufficient condition for configuration selection, a more refined analysis of helicopter load-acquisition techniques may well indicate it to be a necessary condition for a heavy-lift helicopter. The tandem-lift rotor helicopter is unique in this capability.

7. The vibration level in helicopters is a phenomenon involving the loads induced at the rotor heads and the tuning of airframe frequencies to them as a response. Neither configuration has essentially superior vibration characteristics.

8. Using NASA-Langley and USAAVLABS investigations as guidelines, Vertol Division has analyzed the mission of the heavy-lift helicopter and has developed control power and sensitivity requirements that exceed the requirements of specification MIL-H-8501A about all axes. The static stability provided will ensure a more natural feel of aircraft motions and thus increase pilot confidence. For pilot comfort, fuselage attitude will be controlled by longitudinal cyclic pitch. The neutral speed stability and directional stability provided in the tandem-lift rotor helicopter, with the feature of dual longitudinal control, makes it the ideal load platform for the spot hovering requirements of the heavy-lift mission.

9. Except for an additional requirement for yaw restraint, single-point cargo suspension systems favor the single-lift/antitorque rotor helicopter because the attachment is a direct shear point to the stiff rotor frame and does not create moments. For similar reasons, a fore and aft multiple-point suspension system favors the tandem-lift rotor helicopter.

Based on these advantages and disadvantages, the heavy-lift helicopter requirements would be best met with the tandem-lift rotor system, with the detail design features described in the paragraphs which follow.

Rotor Radius 43 Feet

The 43-foot blade radius results in disc loading for which the 6000-foot, 95°F hover requirement is adequately met with four TC43-11 or T64/S4A engines. A slightly smaller blade radius would be permissible with three 501-M26 or four T64/S5A engines. However, for the cabin length selected, there is no significant saving in gross weight for reducing radius.

Constant-Thickness Blades

A universally applicable design of a rotor system with constant-thickness blades can efficiently fulfill the heavy-lift requirements for a variety of fuselage types and mission cruise speeds.

Blade Twist -9 Degrees

The rotor is optimized at a blade twist of -9 degrees. A blade

twist between -12 and -9 degrees can be accepted from a performance point of view. With respect to rotor stability, stall flutter limits are well beyond mission speed requirements. Using a twist of -9 degrees rather than -12 degrees increases the margin for allowable stress loads in both the plastic and metal blades, and extends the applicability of the metal blade from a 140-knot limit to the 165-knot target. Finally, a twist of -9 degrees would lower vibration levels. Therefore, a blade twist of -9 degrees is recommended.

Articulated Rotor

While the hingeless semirigid rotor is applicable to the tandem-lift rotor system, it produces high pure hub-fuselage twisting moments when yaw control is applied, and this results, to the extent of this study, in weight penalties in the rotor drive shaft, bearings, and supports, and in the airframe. Therefore the articulated rotor is recommended for the tandem-lift rotor heavy-lift helicopter.

Dual Longitudinal Control

The dual longitudinal control system provides hover attitude control independent of center of gravity with no increase in complexity, and the weight increase in the cockpit controls is negligible.

C-Spar Plastic Rotor Blade

The C-spar plastic rotor blade is best suited for selection in this study because of its greater margin between actual loads and allowable loads. The D-spar steel blade, which is a conventional design at Vertol Division, should also be pursued as a second selection.

Helicopter Concepts

This study developed the systems and missions which can be anticipated at this time, beyond requirements of the contract under which the study was conducted. Artist's concepts of two heavy-lift helicopters -- the transport and the crane/personnel carrier -- are shown in Figure 1; they use a common rotor-propulsion dynamic system with articulated rotor hubs and upper controls. Both are shown with tricycle landing gear, but a quadricycle gear can be used on the crane/personnel carrier if full straddle mounting of external load is required.

TANDEM-LIFT ROTOR TRANSPORT

Figure 1. Heavy-Lift Helicopter Concept. (Sheet 1 of 4)

TANDEM-LIFT ROTOR CRANE/PERSONNEL CARRIER

Figure 1. Heavy-Lift Helicopter Concept. (Sheet 2 of 4)

ARTICULATED ROTOR HUB

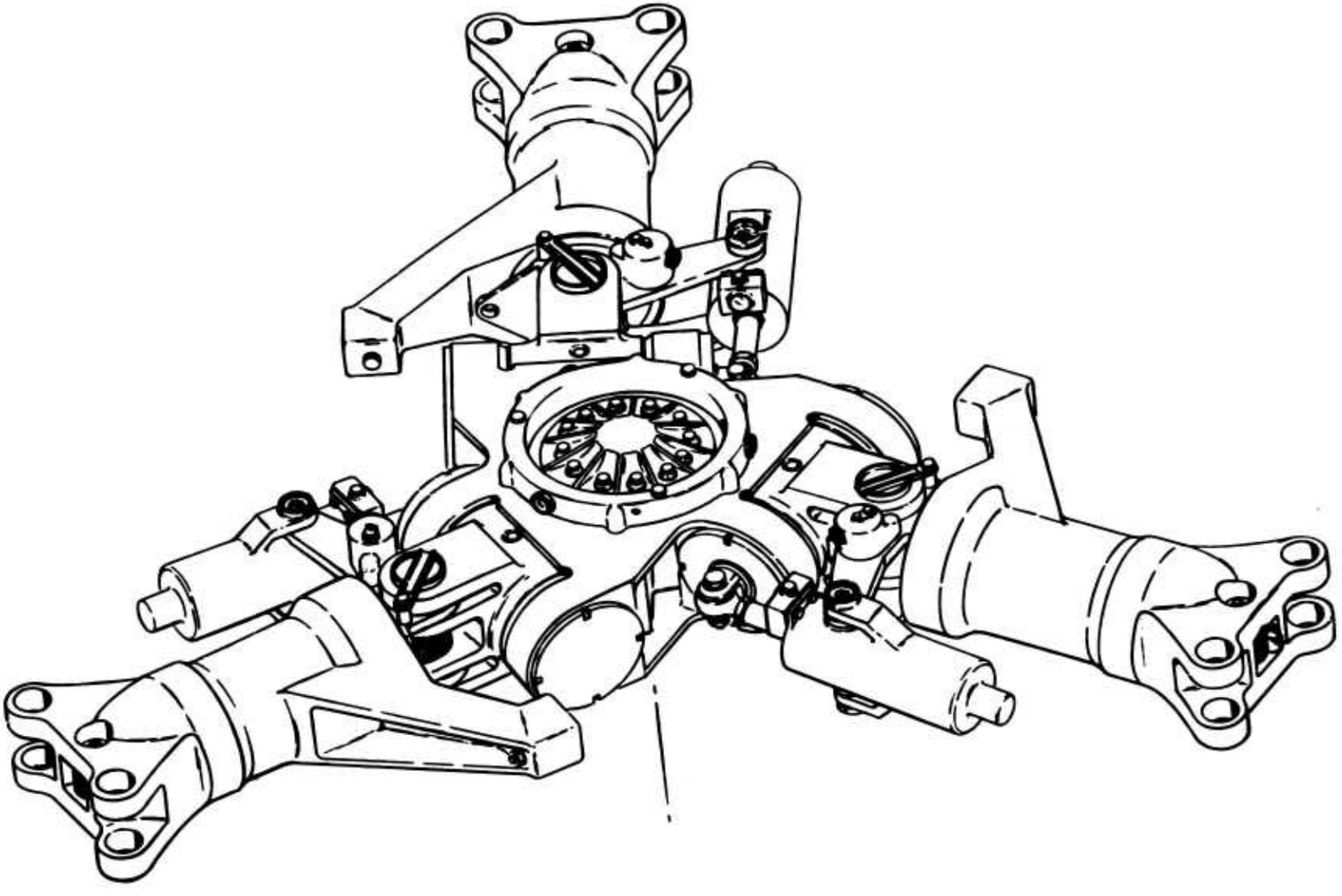

Figure 1. Heavy-Lift Helicopter Concept. (Sheet 3 of 4)

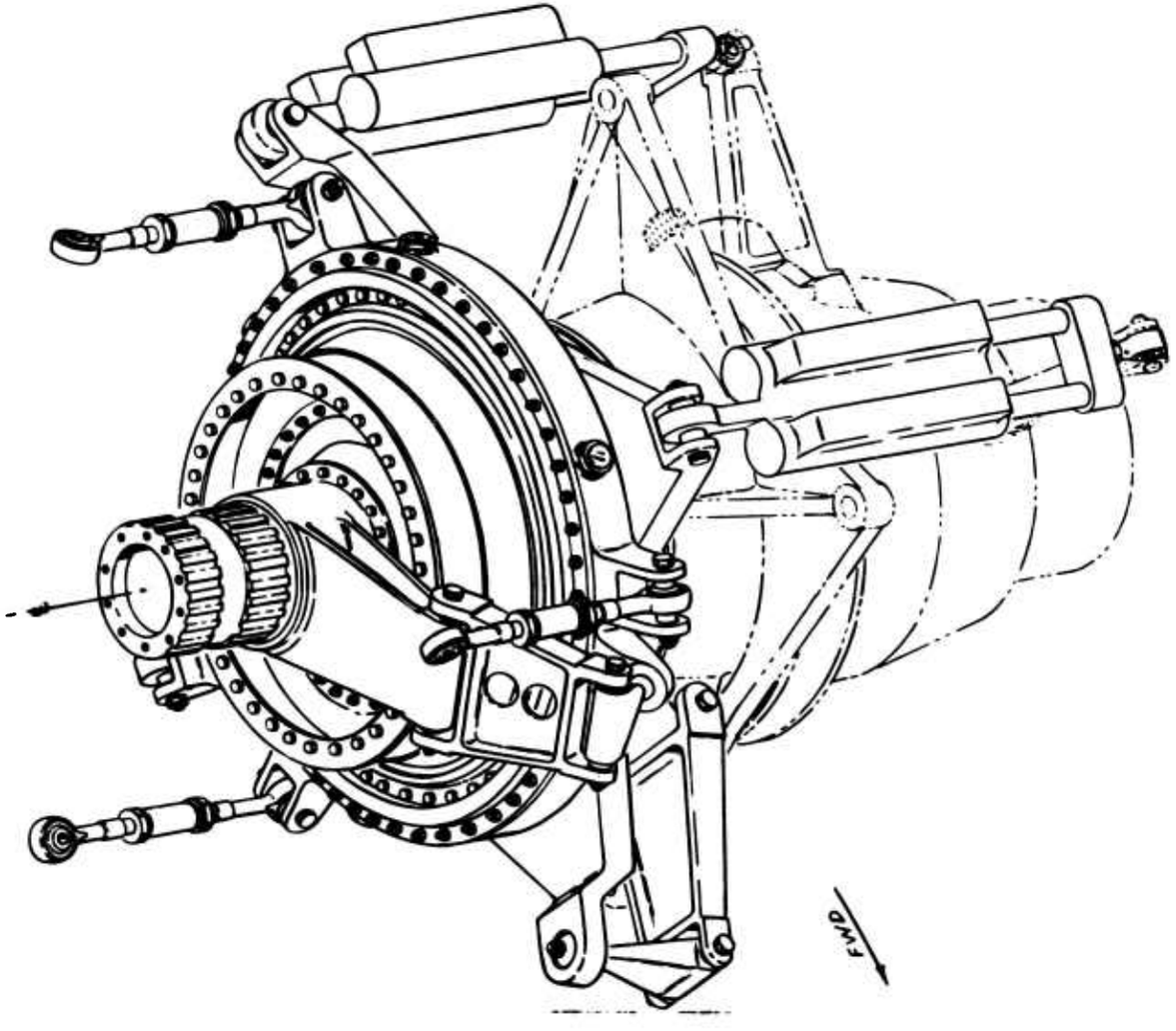

Figure 1. Heavy-Lift Helicopter Concept. (Sheet 4 of 4)

ROTOR SYSTEM PERFORMANCE PARAMETRIC ANALYSIS

INTRODUCTION

Objective

This section defines the rotor geometry for an optimized heavy-lift helicopter. It describes the selection of the number of lifting rotors and the number of rotor blades, the determination of the blade geometry, and a general description of the aircraft for which the rotor design is selected.

Basis for Optimization

The mission requirements for the aircraft are defined by the contract. The rotor system to perform the missions should be derived from all pertinent factors, such as the costs of development and manufacturing, operation, and training, the development time period, powerplants available, aircraft dynamic stability and control considerations, aircraft performance and design flexibility, acceptable vibration levels, and safety. Two of the most important of these factors may be associated with the weight of the aircraft: manufacturing costs with empty weight, and operational costs with gross weight and fuel weight. The remaining factors either are indeterminate in a study of this scope or may be considered qualitatively if they are felt to be significant. Since gross weight includes the effects of changes in fuel weight and empty weight, it is used in this study as the primary optimization index. That is, the aircraft is considered to be optimized when it performs the required missions at a minimum gross weight.

PROCEDURE

In order to ensure adequate cargo size capability, a cubage analysis was conducted first, and the minimum cabin dimensions determined from it were used throughout the parametric study.

The parametric study was conducted by the use of a parametric weights and performance computer program. The computer program calculates hover and cruise performance to define the mission power and fuel requirements, and it uses generalized group weight trend data to determine the empty weight for any given rotor geometry. By varying the rotor geometry input, variations in empty weight, mission fuel weight, and mission

gross weight were determined. The effect of each geometric variable on configuration weight established a basis for optimization. The primary, or independent, variables considered were:

1. Number of rotors
2. Blade radius
3. Number of blades
4. Mean blade lift coefficient for hover
5. Tip speed
6. Blade twist
7. Airfoil section

The secondary, or dependent, variables result from the choice of the primary variables:

1. Parasite drag area (calculated by the parametric computer program)
2. Blade chord (calculated by the parametric computer program)
3. Engine model (selected from review of power requirements calculated by the parametric computer program)

A parametric study conducted with rubberized engine characteristics resulted in a tentative selection of rotor geometry and power requirements which permitted the selection of actual powerplant combinations. The weights and performance were then recalculated for engine characteristics, and the tentative rotor selection was confirmed. The optimization process considered both the 12-ton transport mission (which was critical with respect to rotor geometry) and the 20-ton heavy-lift mission (which was critical with respect to transmission power capabilities and design gross weight). The ferry mission was not critical, and ferry performance was calculated for the optimized configurations to indicate the margin of capability over the requirement.

A parametric study was conducted for both a tandem-lift rotor

system and a single-lift/antitorque rotor system. A selection was made, then, between these optimized types, and the rotor system geometry for the tandem-lift configuration was chosen for the preliminary design portion of the study.

BASIC DATA

Mission Requirements

The contract mission requirements listed in Table I are interpreted in Figures 6 and 7.

General Aircraft Characteristics

1. Turbine-powered
2. Safe autorotation at design gross weight
3. Design load factor 2.5 at design gross weight
4. Crew minimum of one pilot, one copilot, and one crew chief. All studies have included a load master as well.
5. All components designed for 1200 hours between major overhaul and 3600 hours' service life.

Vehicle Description

Two heavy-lift helicopter fuselage versions each were considered for the tandem-lift rotor system and the single-lift/antitorque rotor system.

1. The transport (see Figures 2 and 3) can carry vehicles, cargo, or personnel internally. A five-winch system permits external loads to be carried.
2. The crane/personnel carrier (see Figures 4 and 5) is designed to carry personnel and small cargo units internally, and the landing gear design will permit partial straddle pickup.

The transport fuselage was used for the parametric study and the application of the resulting rotor system to the crane/personnel carrier was established by additional mission calculations and weight estimates.

ROTOR DATA.

ROTOR DIA ____ 86'-0"

NO. OF BLADES/ROTOR ____ 3

BLADE CHORD ____ 3'5

BLADE AIRFOIL SECTION NACA 23012

DISTANCE BETWEEN ROTOR CRS ____ 59'5

ROTOR SPEED (NORMAL POWER) ____ 155·5 RPM.

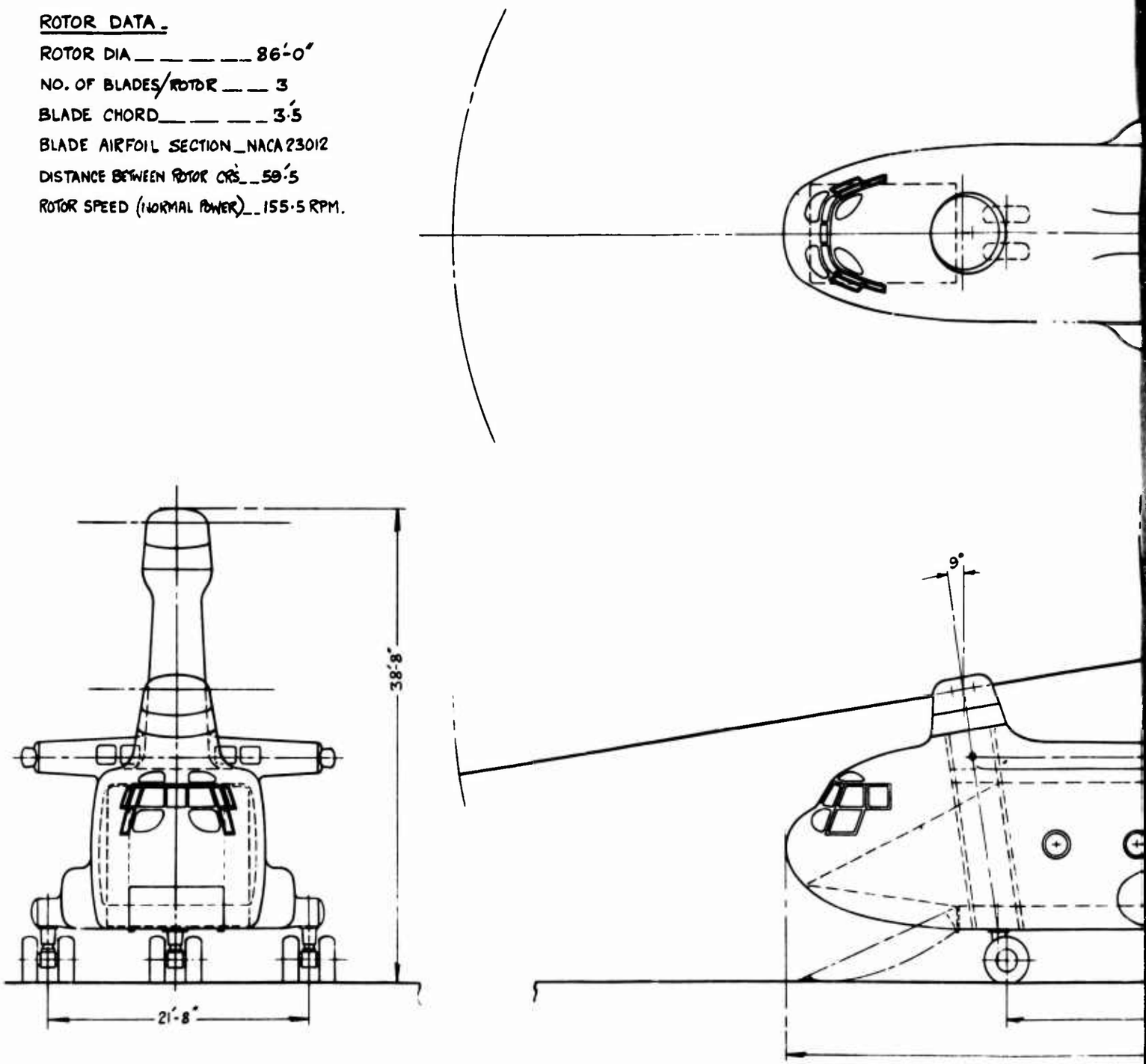

Figure 2. Tandem-Lift Rotor Transport

A

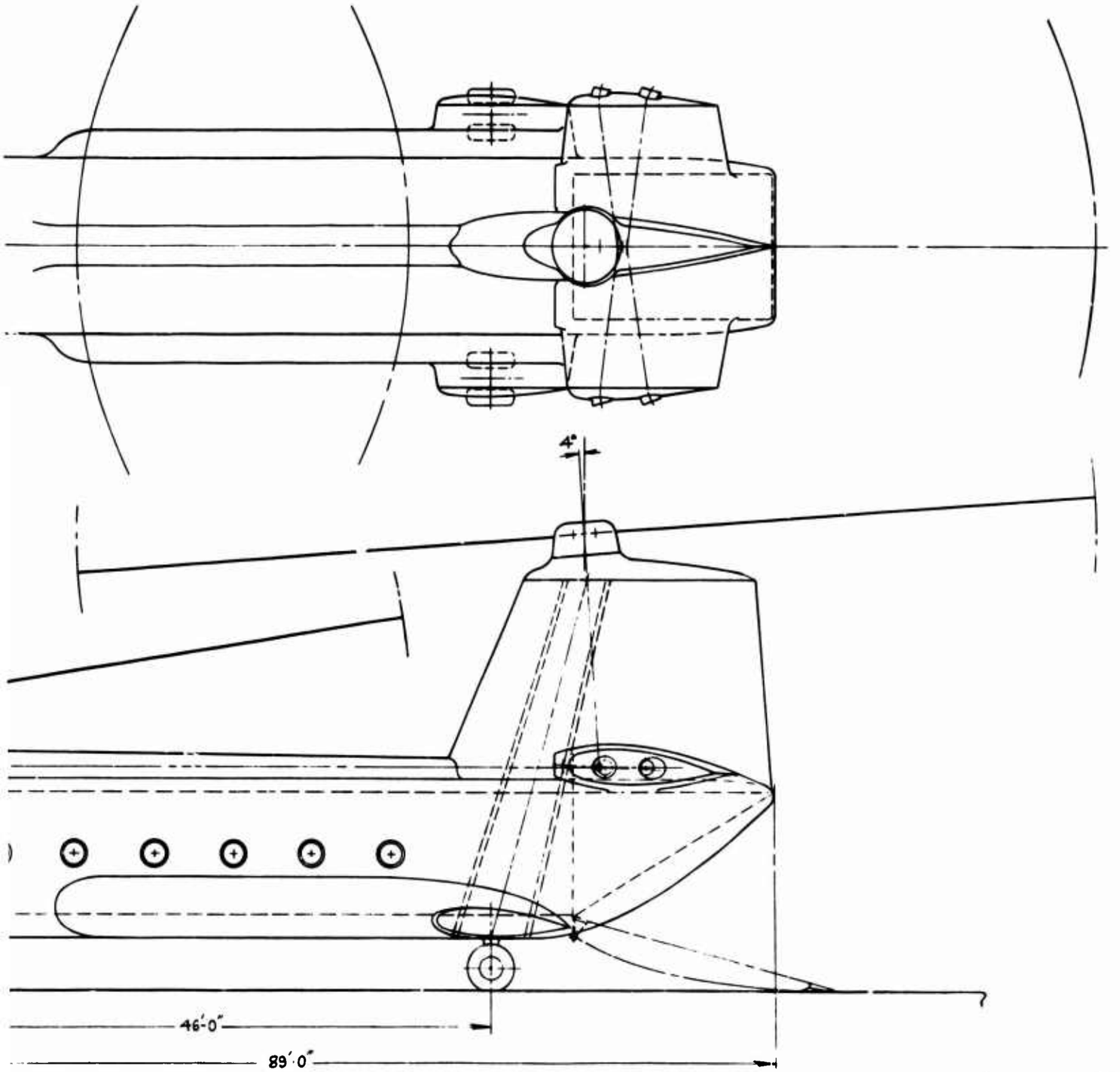

0 10 20

SCALE IN FEET.

B

ROTOR DATA.

MAIN ROTOR DIA. _____ 96'-0"

NO. OF BLADES PER ROTOR ____ 5.

TAIL ROTOR DIA. _____ 25'-0"

NO. OF BLADES PER ROTOR ___ 2.

DISTANCE BETWEEN ROTORS ___ 61'-6".

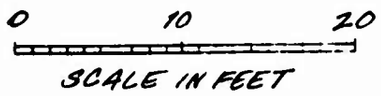

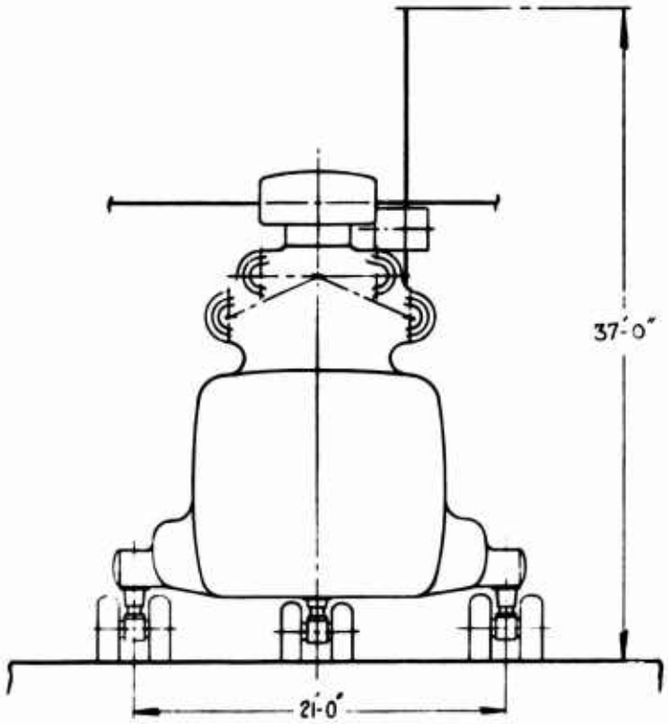

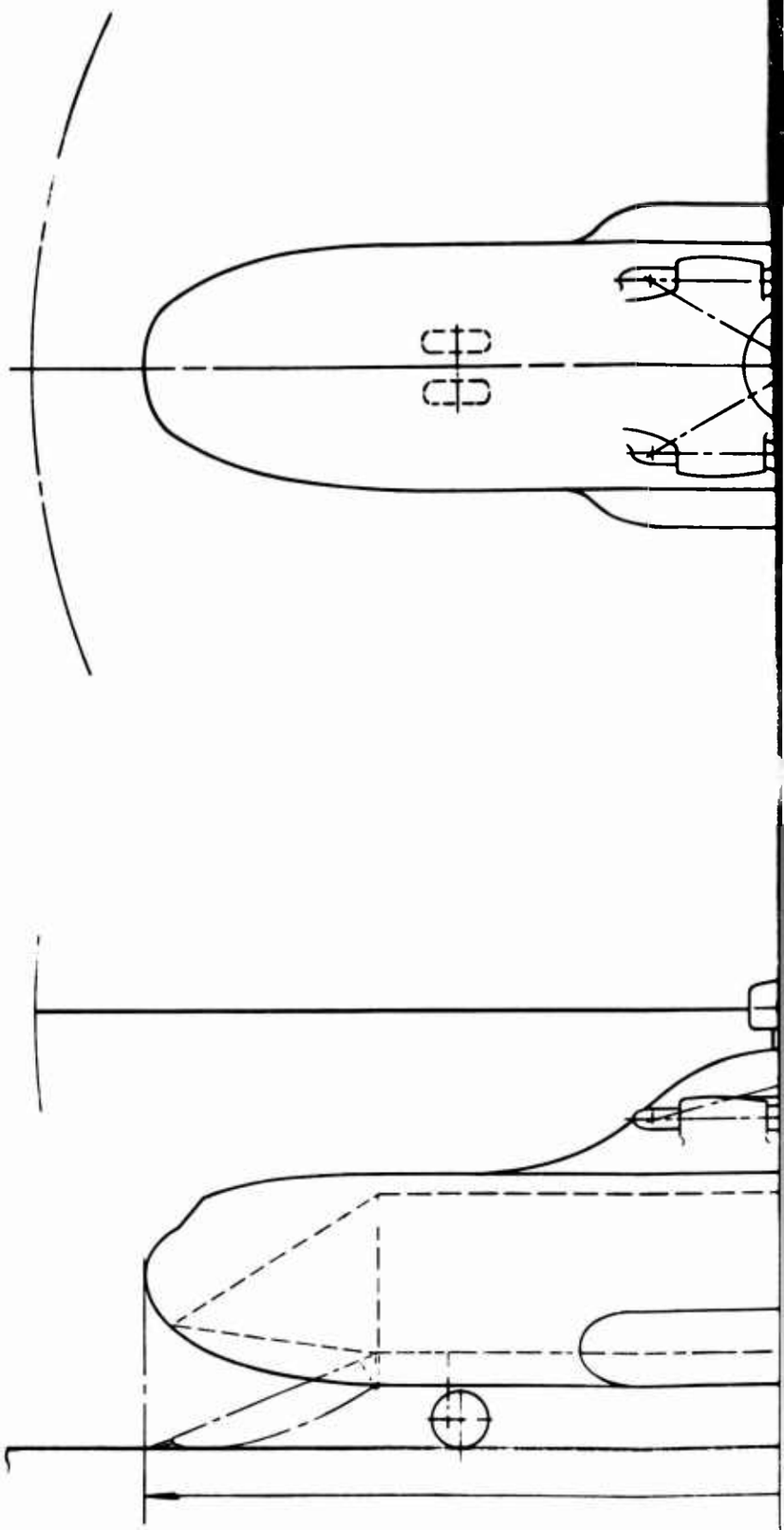

Figure 3. Single-Lift/Antitorque Rotor Transport

A

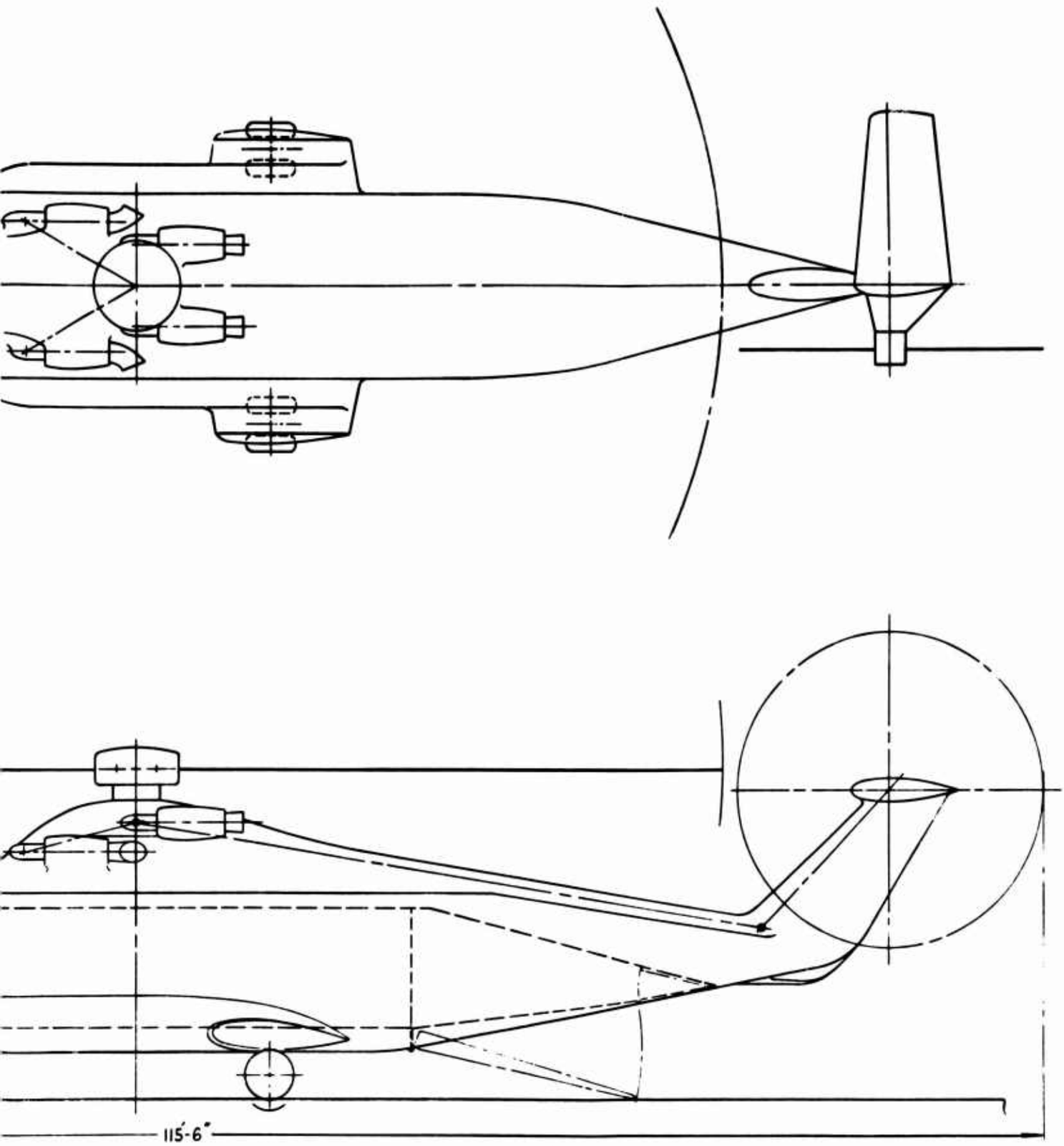

B

ROTOR DATA.

ROTOR DIA ____ 86'-0"

NO. OF BLADES/ROTOR ____ 3

BLADE CHORD ____ 3'5

BLADE AIRFOIL SECTION ____ NACA 23012

DISTANCE BETWEEN ROTOR CR'S ____ 59'.5

ROTOR SPEED (NORMAL POWER) ____ 155.5 RPM.

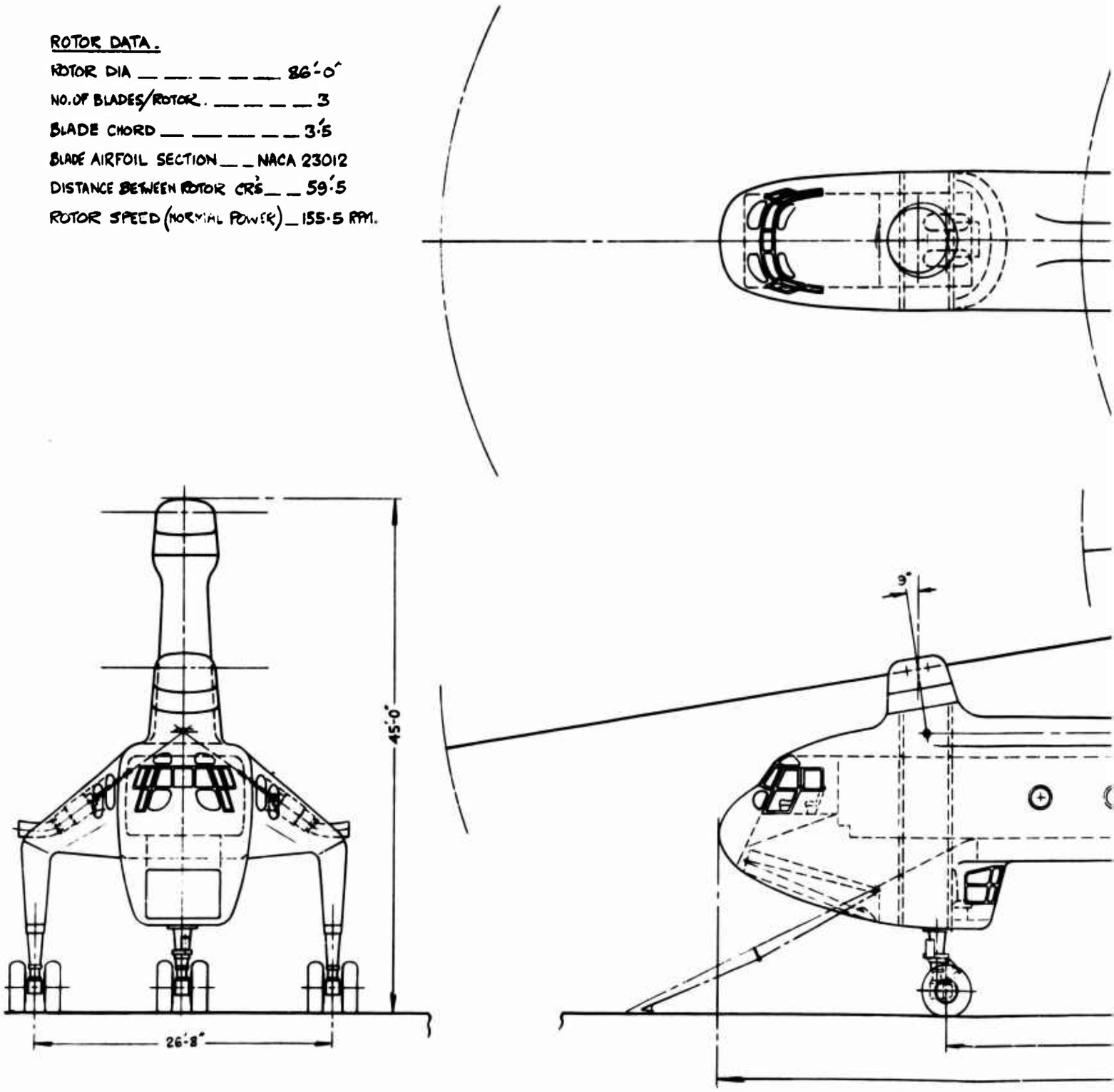

Figure 4. Tandem-Lift Rotor Crane/Personnel Carrier

A

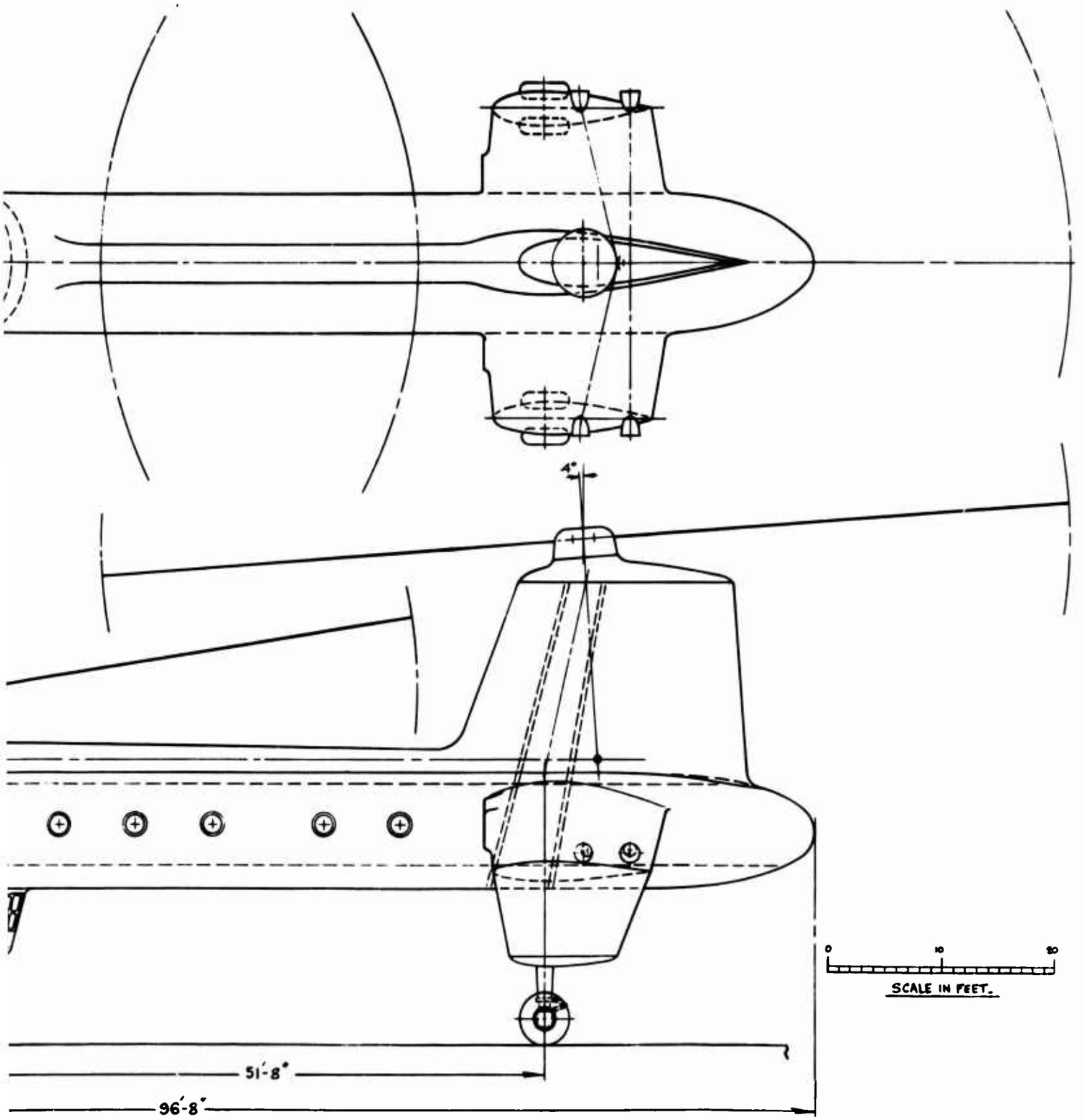

B

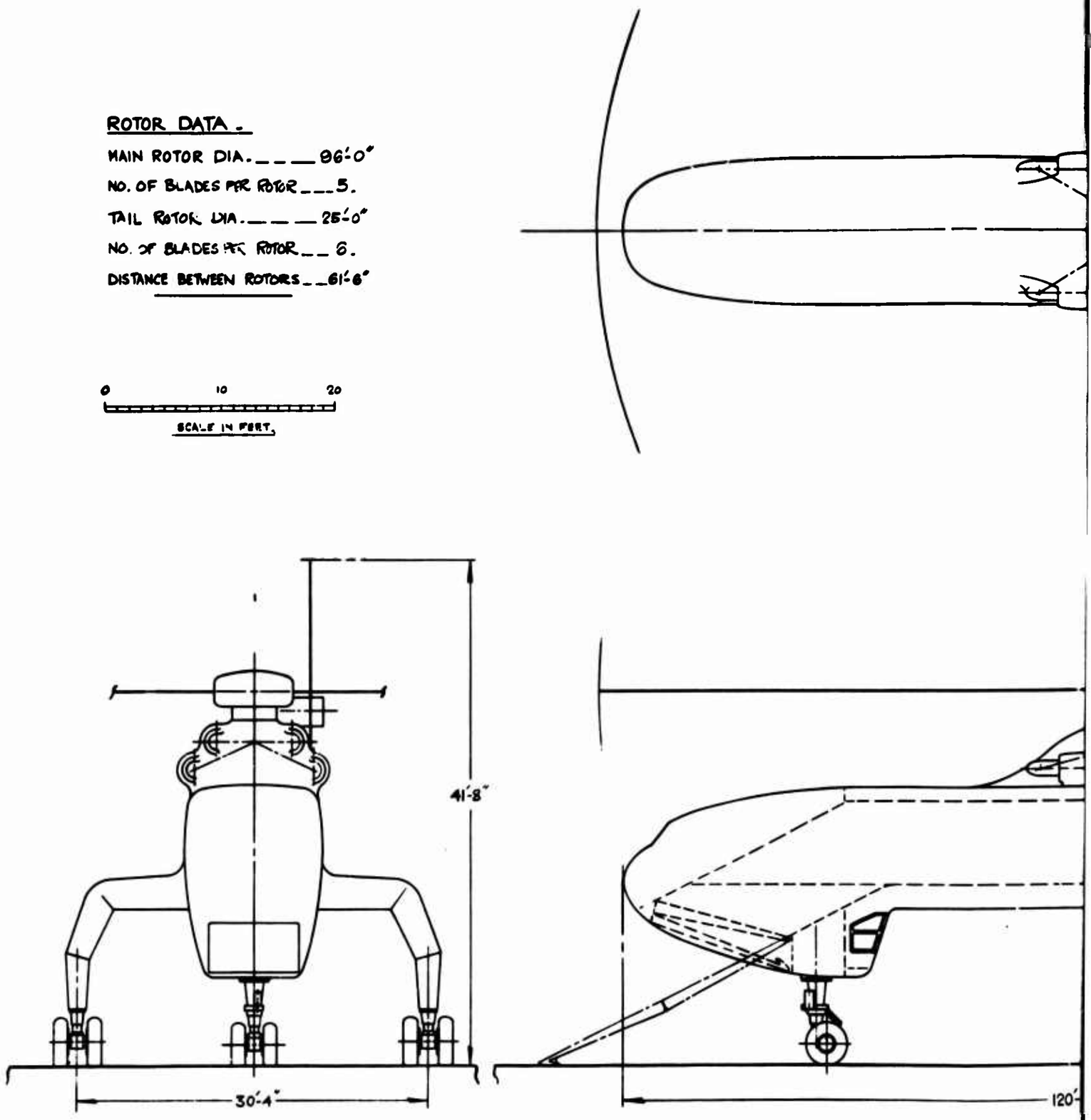

Figure 5. Single-Lift/Antitorque Rotor Crane/Personnel Carrier

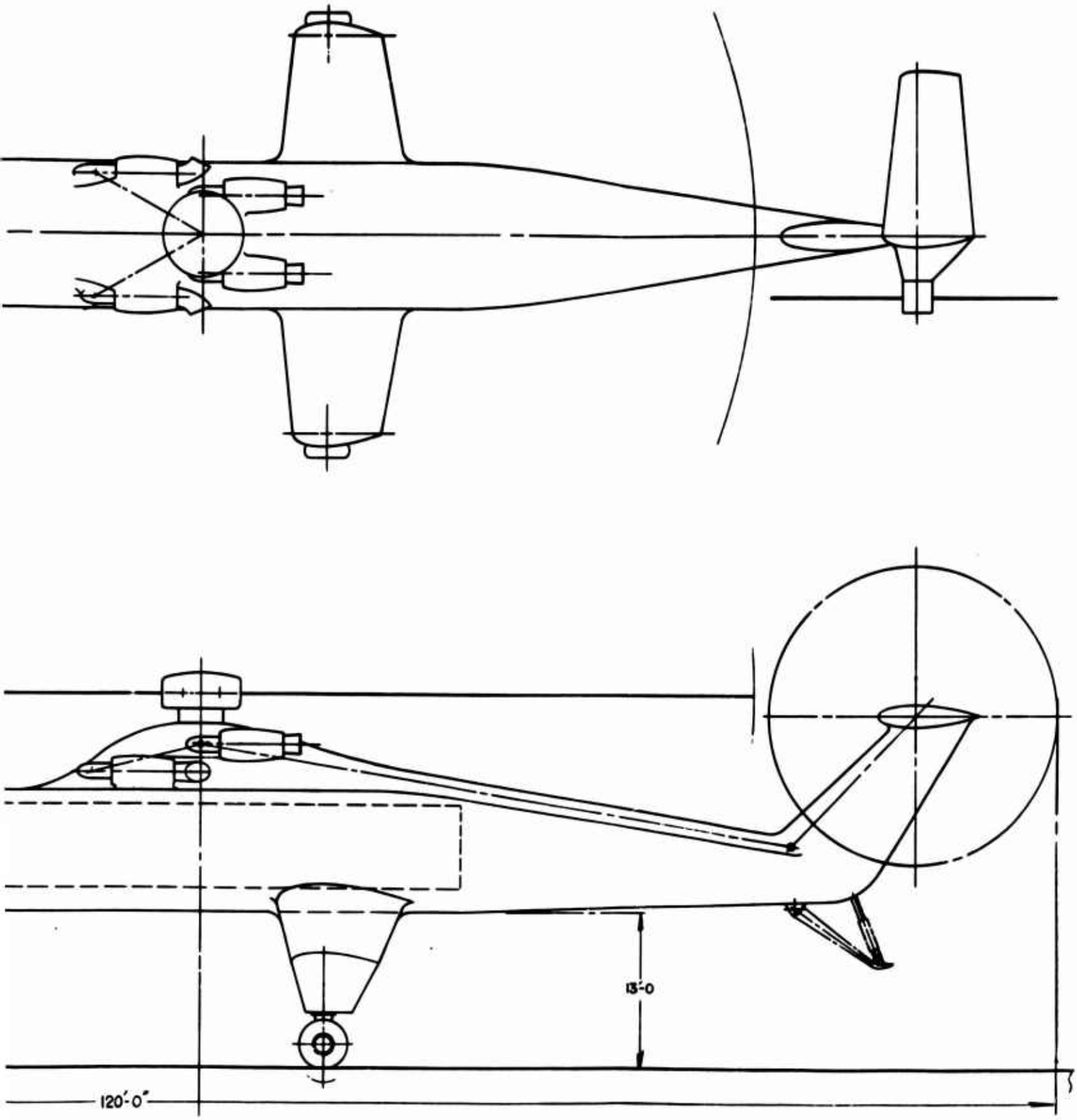

B

Transport Mission

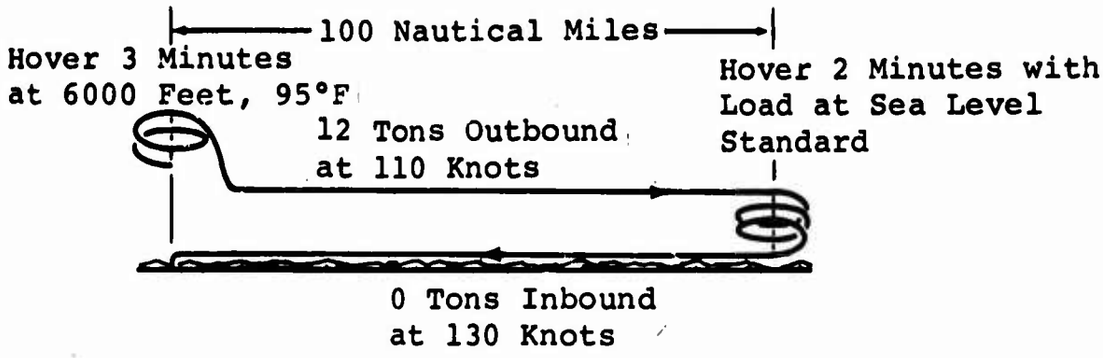

Heavy-Lift Mission

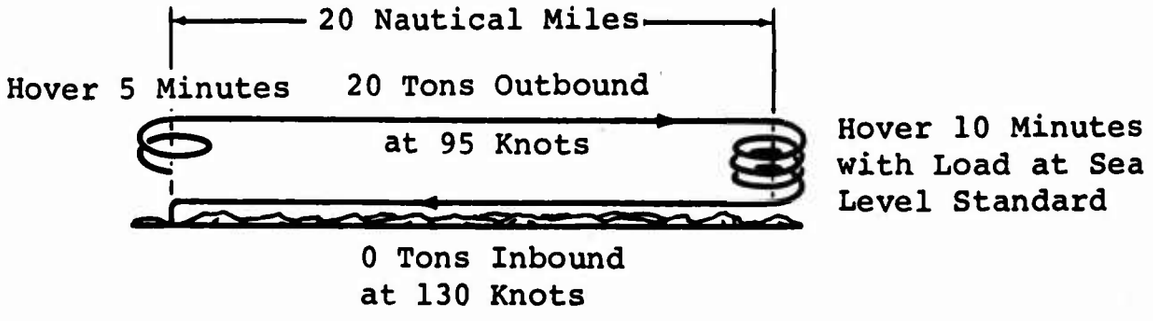

Ferry Mission

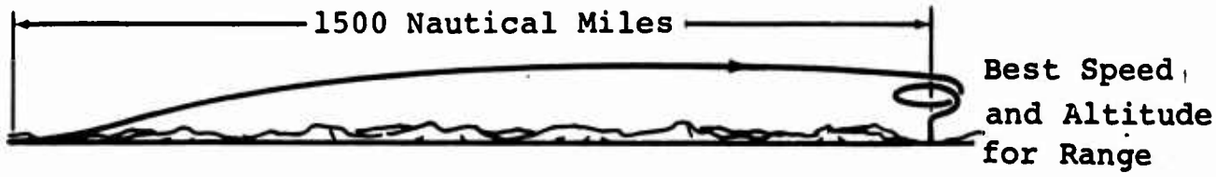

Figure 6. Specification Missions.

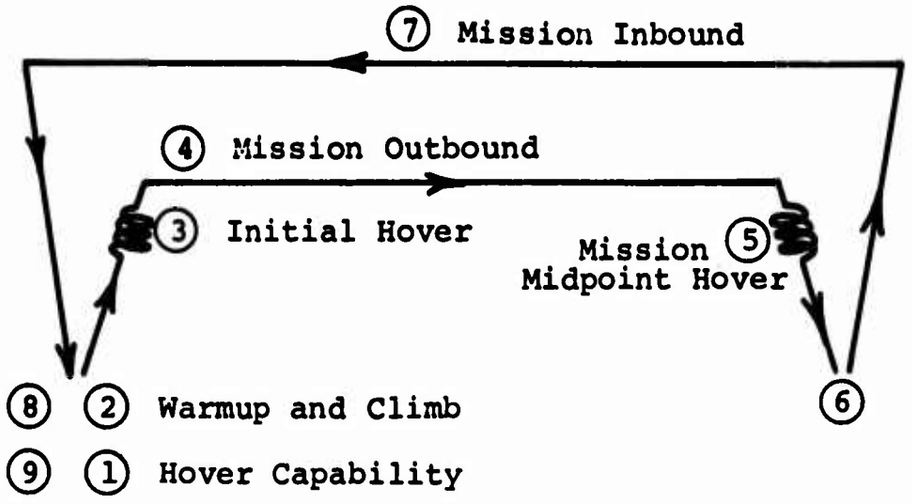

① With full payload and fuel have OGE hover capability

② Provide fuel for warmup and climb per MIL-C-5011A

③ Hover initially for (C) minutes

④ Fly at speed (D), altitude (E), and temperature (F) during mission range out, with provision for outbound external cargo drag

⑤ Hover at mission midpoint with cargo, for (G) minutes

⑥ Unload cargo outbound and load cargo inbound, with provision for inbound external cargo drag

⑦ Fly at speed (H), altitude (J), and temperature (K) during mission range in (not necessarily equal to mission range out)

⑧ Have 10 percent of initial fuel as reserve

⑨ Increase fuel flow 5 percent per MIL-C-5011A

Figure 7. Analysis of Typical Mission.

Engine Data

The engine data given in Table VI were used throughout the study. These data were obtained from specifications and brochures. No attempt has been made at this stage to judge the engine's prospects for full development.

Installed engines are rubberized on the basis of a presently available engine with growth potential. The installed weight and specific fuel consumption are based on a present model at its current power rating; logical growth trend curves are used to extrapolate the engine weight and specific fuel consumption to values required by any specific configuration.

Rubberized engine characteristics based upon the LTC4B-11 engine were used throughout the optimization. Actual engine characteristics for several engine combinations were then used to calculate the final weights and performance.

PARAMETRIC WEIGHTS AND PERFORMANCE COMPUTER PROGRAM

The parametric analysis computer program iterates to a mutually consistent set of component weights and drags, power required, blade chord, and mission fuel for a given set of independent geometric variables and a given mission. The cargo compartment dimensions derived from the cubage analysis defined the lower limit for sizing the fuselage. In this indirect way, the lower limit of rotor radius was determined for a given tip overlap and the initial conditions were established for iterational sequences of the performance computer program. Aircraft trim, cruise and hover power required, and fuel flow are computed directly for the mission and integrated to yield mission fuel weights so that the computer output reflects all the imposed criteria, and changes in input can be compared on an overall basis.

Program Flow

The basic units and flow diagram of the parametric computer program are shown in Figure 8. From the input values, which include an initial approximation of design gross weight, the helicopter geometry can be defined, and the fuel, power, blade chord, weight empty, and drag can be computed.

From the initial approximations of design gross weight and mission fuel, a weight empty and a design gross weight are

TABLE VI
ENGINE CHARACTERISTICS

Engine Data	NRP Sea Level Standard	Mil Power Sea Level Standard	Max Power 6000 ft, 95°F	Max Power Sea Level Standard	S.F.C at Max Sea Level Power
T64/S4A (T64-GE-12) "Model Spec E1102-E T64/S4A (T64-GE-12)", 23 Oct. 1964	3225	3400	2650	3435	0.483
T64/S5A "T64 Growth Engines", May 1964	4000	4500	3060	4500	0.478
T55-L-11 (LTC4B-11A) "Lycoming T55-L-11 Engine", Spec No. 12427, 15 Feb. 1965	3000	3400	2740	3750	0.519
T55-L-7 Model Spec No. 124.20-A, "T55-L-7 Shaft-Turbine Engine, Lycoming Model LTC4B-8", 21 Sept. 1962	2200	2500	1803	2650	0.615
501-M26 "Allison 501-M26 Turboshaft Engine", TDR No. AR 0000-059A, 21 Sept. 1964	4765	5450	3715	5450	0.479

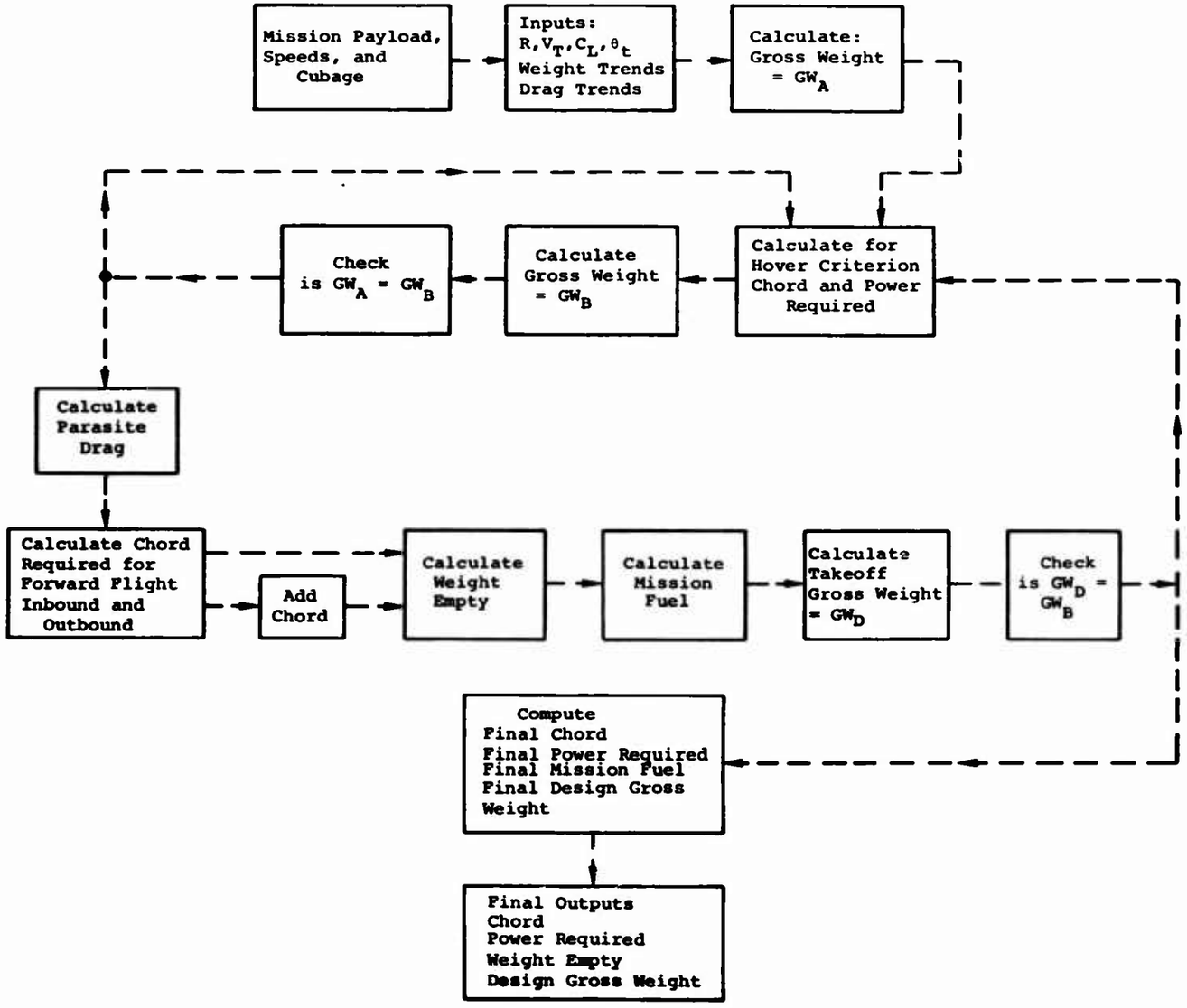

Figure 8. Configuration Analysis Flow Chart.

calculated. The hover criterion is then satisfied and the blade chord is determined by the solidity required. A new gross weight is now calculated, consistent with the hover criterion. This process is repeated until the initial and final design weights are identical.

Fuselage attitude and blade stall are checked on the two forward-flight portions of the mission: at the start of the mission, and at midpoint just before the inbound portion. If fuselage attitude is outside the boundaries, cyclic pitch is added; if retreating blade stall is encountered, chord is added. When both criteria have been met, a new weight empty is computed, the computation is made for mission fuel, and a new design gross weight results. This weight is compared with that calculated from the hover criterion, and the computation is repeated until convergence occurs.

When overall convergence is achieved, the computation is carried through all the checks on imposed criteria. The final numbers will therefore be consistent with the imposed criteria; also, design gross weight, weight empty, chord, installed power, and fuel for the mission will be compatible.

Drag Trends

The helicopter total parasite drag is calculated by use of the specified dimensions and component drag trend data. The drag trends are established from existing helicopters for the following drag components: fuselage, pylons, landing gear, hubs, engine installation, roughness and leakage, miscellaneous, and external payload drag.

Weight Trends

Component weights have been derived from Vertol-developed weight trends, statistical data on existing aircraft, preliminary design layouts, and from vendors. The components considered in the parametric study are: rotor group (see Figure 9), body group, flight controls, powerplant, drive system (see Figure 10), landing gear, fixed equipment, fixed useful load, variable useful load, and fuel tanks. By adding the mission fuel and payload to the above items, the mission gross weight is obtained. The WEIGHTS section of this report outlines the parameters used for estimating weights.

Hover Power Required

The hover criterion and fuel flow in hover were calculated by using a hover-analysis electronic data processing program. The profile and induced powers are computed separately and the induced portion is corrected for the nonuniform inflow and overlap applicable to each configuration. Download is represented as a ratio of thrust to gross weight and is computed internally; the size of the fuselage and an average drag coefficient are used as variables.

Forward Flight Trim and Power Required

The power-required analysis was used to predict fuel required and blade stall in forward flight. Trim and control positions are derived using the Wheatly-Bailey equations for rotor thrust, horizontal force, and blade motion. When the helicopter is in trim, power is computed with corrections for overlap, compressibility, stall, and reverse flow.

MISSION CARGO CUBAGE ANALYSIS

Since the contract missions did not define cubage, Vertol Division has initiated a mission cargo cubage analysis program to identify the number, size, and weight of all equipment organic to Army units and combinations of units. The program optimizes the distribution of the equipment by net weight, cross-country weight, or highway weight, and distribution of length, width, height, and reduced height. The analysis provided the data required to determine the size of the cargo compartment for the transport -- 540 inches long, 144 inches wide, and 108 inches high -- and the equivalent ground-to-fuselage clearances necessary for the crane/personnel carrier.

Tables VII and VIII summarize some of the computer program output. Table IX shows the distribution of the ROAD division's engineer equipment by net weight. As can be seen, a 12- to 20-ton payload helicopter has a significant capability to move divisional equipment from ships offshore, across obstacles, or from airheads to the combat area. Table VII shows the percentage of equipment air transportable when the equipment's dimensions are considered. Table VIII shows the percent of equipment within a given net weight that will fit within the dimensions chosen by Vertol Division for a heavy-lift helicopter: 540 inches long, 144 inches wide, and 108 inches high. Table VIII shows that, with a payload of 12 tons and the cargo

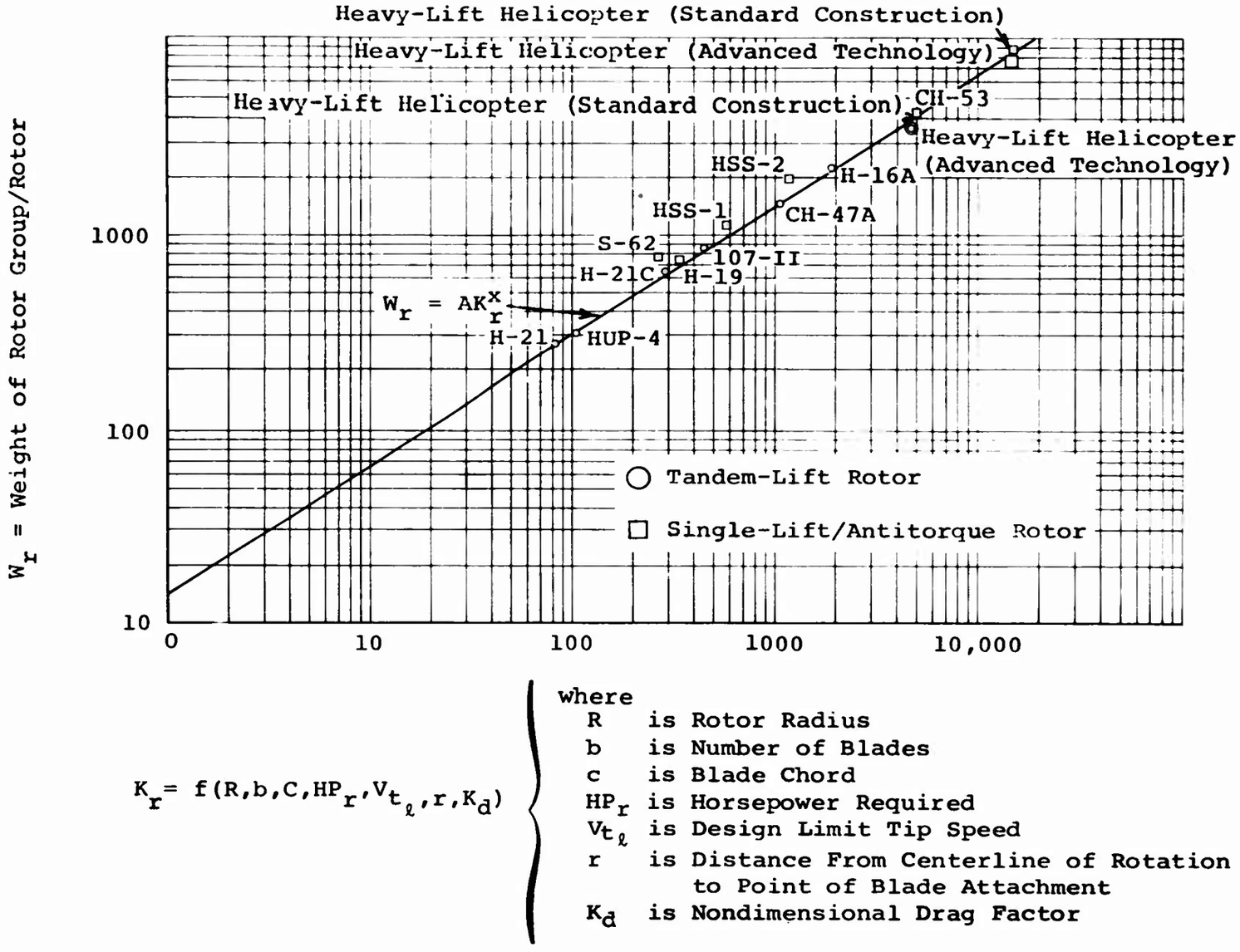

Figure 9. Rotor Group Weight Trend.

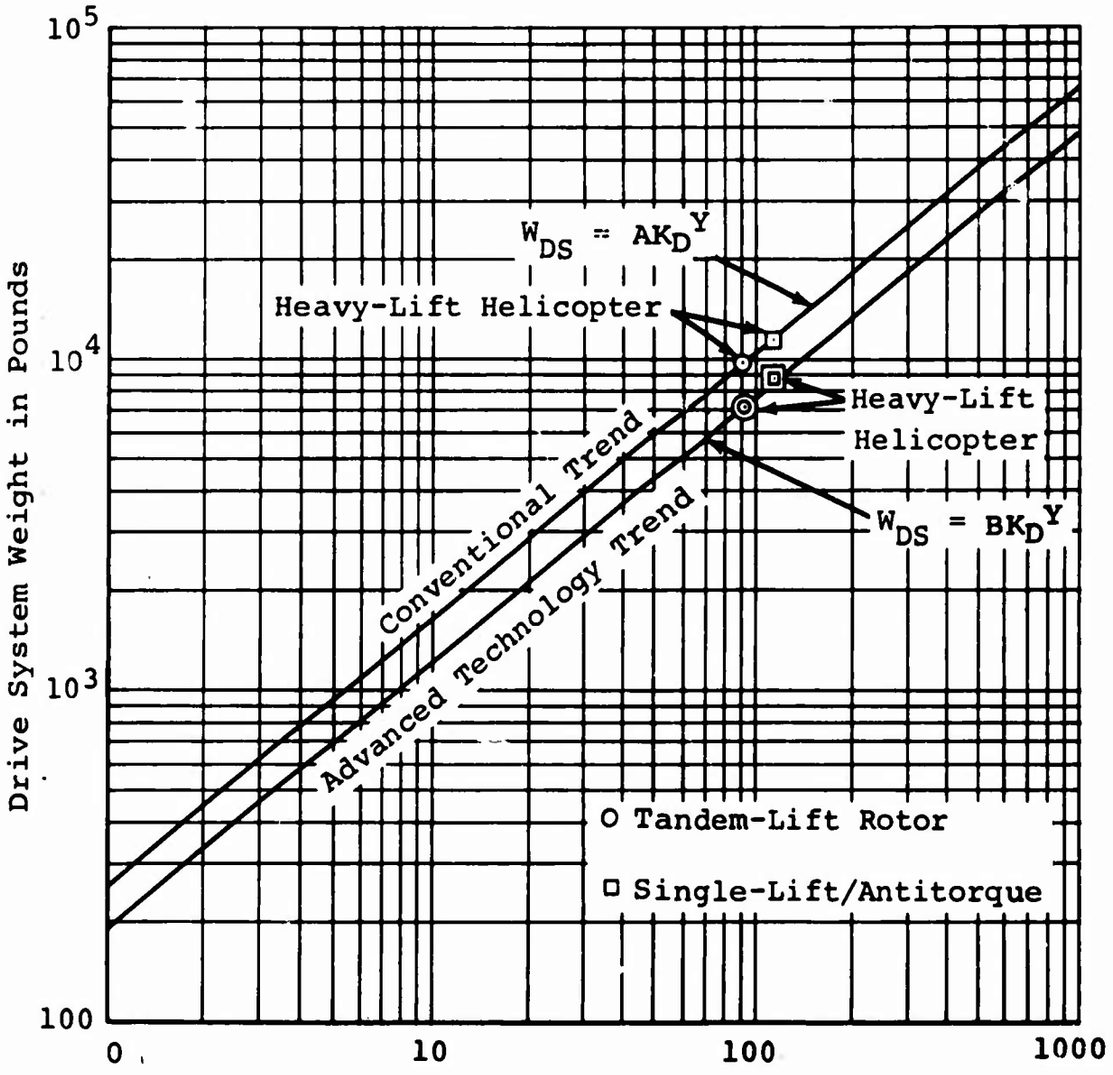

where

- HP_x is Transmission Design Horsepower
- N_r is Rotor Hover RPM
- K is Drive System Weight Factor
- A is Multiplying Constant for Standard Trend
- B is Multiplying Constant for Advanced Technology Trend
- y is Exponential Power Factor for K

Figure 10. Drive System Weight Trend.

TABLE VII

PAYLOAD CAPABILITY FOR TO&E EQUIPMENT WEIGHING OVER 500 POUNDS

Payload Tons	Airborne Div. Items %	Airborne Div. Weight %	Infantry Div. Items %	Infantry Div. Weight %	Mech. Div. Items %	Mech. Div. Weight %	Armored Div. Items %	Armored Div. Weight %
10	99.1	93.3	93.7	59.3	89.5	52.4	87.6	43.4
11	99.2	93.9	93.8	59.4	89.6	52.5	87.6	43.5
12	99.8	98.5	94.9	62.9	91.7	56.9	89.8	47.3
13	99.8	98.5	95.1	63.4	91.9	57.3	90.0	47.6
14	99.9	98.8	95.9	66.1	92.6	59.0	90.7	49.1
15	99.9	98.8	96.5	68.5	93.2	60.5	91.3	50.5
16	99.9	99.1	96.9	68.7	93.3	60.8	91.4	50.8
17	99.9	99.2	97.4	72.3	93.9	62.7	93.1	52.5
18	99.9	99.2	97.6	72.5	94.0	62.9	92.1	52.6
19	99.9	99.2	97.6	72.5	94.0	62.9	92.1	52.6
20	100.0	100.0	97.6	72.5	94.0	62.9	92.1	52.6

TABLE VIII

PAYLOAD CAPABILITY FOR TO&E EQUIPMENT WEIGHING OVER 500 POUNDS

Payload Tons	Airborne Div. Items %	Airborne Div. Weight %	Infantry Div. Items %	Infantry Div. Weight %	Mech. Div. Items %	Mech. Div. Weight %	Armored Div. Items %	Armored Div. Weight %
10	97.46	90.3	90.48	55.5	89.6	50.8	84.3	41.3
11	97.49	90.4	90.56	55.6	89.52	50.9	84.3	41.4
12	98.13	94.7	91.38	58.9	91.69	54.6	84.4	45.1
13	98.13	94.7	91.81	59.4	91.86	55.0	86.6	45.4
14	98.13	94.7	91.81	59.4	91.86	55.0	86.6	45.4
15	98.13	94.7	92.31	61.8	92.26	56.0	87.2	46.8
16	98.16	95.1	92.54	62.7	92.37	56.3	87.3	47.1
17	98.18	95.2	93.19	65.4	93.0	58.2	88.0	48.8
18	98.18	95.2	95.24	65.7	93.15	58.4	88.1	49.0
19	98.18	95.2	95.24	65.7	93.15	58.4	88.1	49.0
20	98.25	96.0	95.24	65.7	93.15	58.4	88.1	49.0

TABLE IX
ENGINEER EQUIPMENT

Item	Weight (tons)
Dump truck, 2½ ton WWN	7.80
Air compressor, 210 CFM	8.20
Roller, gas driven	10.10
Bridge, fixed, highway, aluminum 38 ft	10.75
Bituminous distributor, 800 gal	11.00
Dump truck, 5-ton WWN	11.30
Crane shovel, 20 tons, 3/4 Yd^3	13.60
Grader, road motorized	13.60
AVLB bridge, CL 60	14.30
Loader, scoop type, 2½ Yd^3	14.80
Universal engineer tractor	14.00

TABLE X
AIR-TRANSPORTABILITY OF MISSILE SYSTEMS

Missile System	Heaviest Item of Equipment	Weight (tons)
Hawk	M36 Truck cargo	6.9
Sergeant	M52 Truck tractor	9.2
Lance	Transporter - Loader	11.5
Pershing	Transporter - Launcher	12.0
Mauler*	Transporter - Launcher	15.0+

*Since the Mauler system is still in development, the exact weight of equipment has not been set.

TABLE XI
HIGH-PRIORITY EQUIPMENT

Equipment	Weight (tons)
CH-47*	9.150
OV-1*	5.497
CV-2*	11.275
Pershing missile	5.000
F-105 D	14.000
F-4B	14.000
F-5A	3.980
F-111	21.000

*Empty weight + fixed useful load (weight of crew)

compartment size described, the heavy-lift helicopter can carry 91.38 percent of the infantry division's organic equipment items; these items represent 58.9 percent of the total net weight of the infantry division's organic equipment; payload capabilities for the airborne, mechanized, and armored divisions are shown as well.

By comparing Tables VII and VIII, it can also be seen that the percentage of equipment transportable changes only slightly when a dimension change is made, which indicates that the size chosen for the cargo compartment is satisfactory.

Tab runs from Vertol Division's Tactical Loads Computer Program (on which Tables VII and VIII are based) show the equipment items weighing 500 pounds or more organic to an infantry battalion of an infantry division, and the distribution of this equipment is shown by net weight. There is similar data for all ROAD divisions and the air assault division, sorted by division and by battalion. Other distributions are made by cross-country weight, length, width, height, and reduced height; they include all equipment, and equipment weighing 500 pounds or more.

Table IX shows some of the engineer equipment to be moved to repair, construct or maintain roads, airfields, railroads, seaports, and pipelines on bridges. As can be seen in Table IX, most of the required engineer equipment is too heavy for today's existing helicopters.

Tables X and XI pertain to a mission for movement of high-priority loads such as aircraft, missiles, or missile systems.

A mission for movement of specialized pods, such as maintenance, hospital and command pods, does not necessarily affect the design of a heavy-lift helicopter, since today's pods are restricted to today's payloads and cargo compartment dimensions. A helicopter designed for high payload would allow heavier pods.

OPTIMIZATION OF TANDEM-LIFT ROTOR SYSTEM

Iterations for Transport Mission

The transport mission with a 12-ton payload and a 6000-foot, 95°F hover requirement is the critical mission with regard to installed power and rotor radius. Therefore, the transport mission was analyzed first. Figure 11 illustrates the results

Figure 11. Initial Iteration of Transport Mission

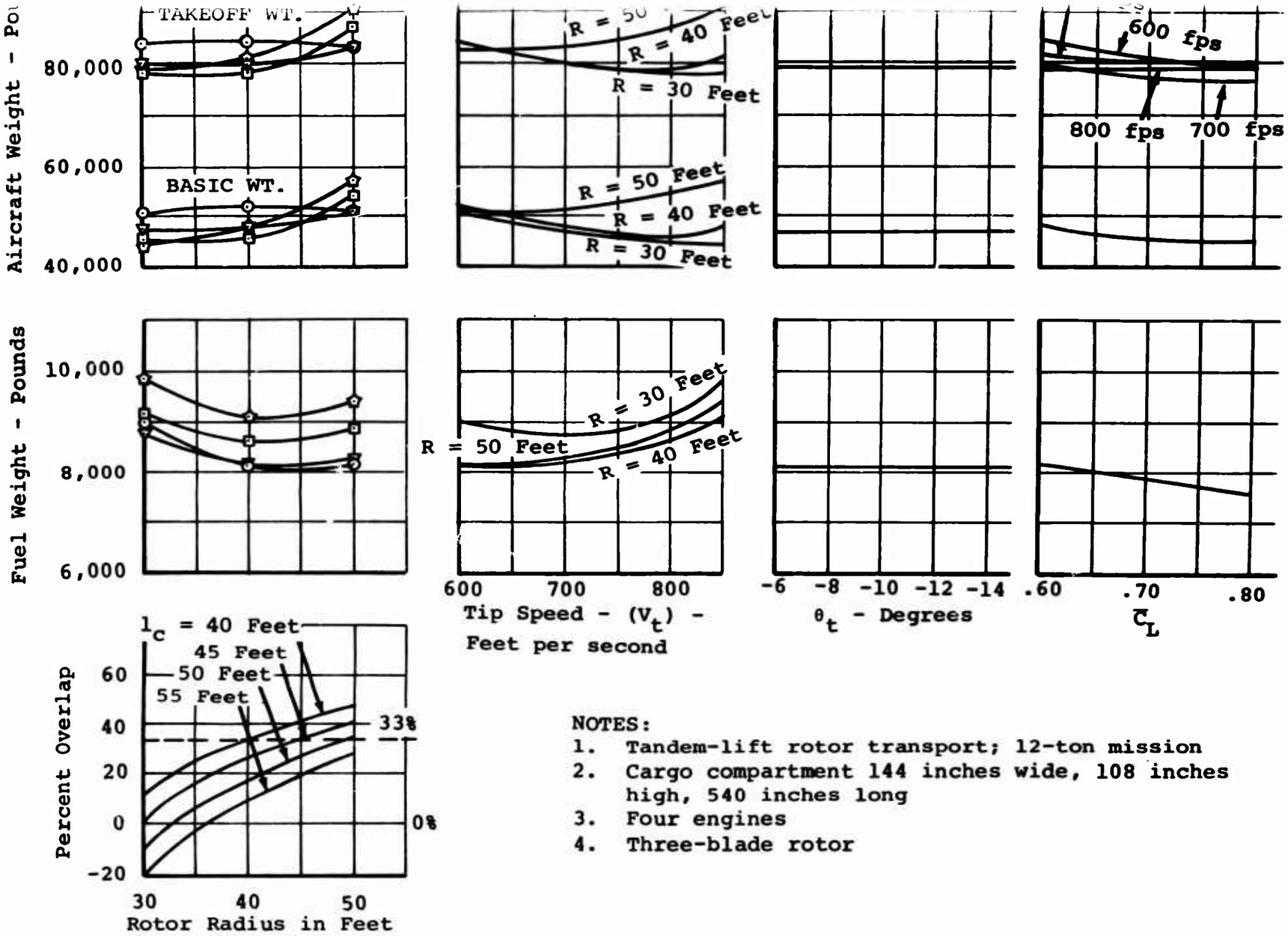

NOTES:

1. Tandem-lift rotor transport; 12-ton mission
2. Cargo compartment 144 inches wide, 108 inches high, 540 inches long
3. Four engines
4. Three-blade rotor

of the computer program's initial iterations for the transport mission. It shows the trends of gross weight, basic weight, fuel weight, and installed power required at 6000 feet, 95°F, with variations in rotor radius, tip speed, blade twist, and mean blade-lift coefficient. It is seen that for minimizing power required, takeoff weight, basic weight, and fuel weight, rotor radii of 40 to 45 feet and a tip speed of about 700 feet per second are indicated. Blade twist and mean lift coefficient do not affect the weight or power very much. The drive system was sized and weighed to absorb the sea level standard day installed power necessary to produce the power required at 6000 feet, 95°F.

(The data shown on Figure 11 should be used to evaluate trends only. The derived values or dependent variables are based on a full-rated drive system and on the normal-construction weight trends which were used in the beginning of this study while weight trends reflecting advanced materials and design techniques were being completed.)

A mean blade-lift coefficient of 0.60 was selected. This value is conservative to ensure adequate hovering control. Somewhat lower weights would result from a higher design $\bar{C}_L$, but with a risk of deteriorating hover control, and the smaller blade area would increase the difficulty of obtaining a power-limited maximum speed free of blade stall. No decision on blade twist was made at this point, although -9 degrees was chosen to be carried through the next iteration.

A second iterational analysis was conducted, as shown in Figure 12. At this point, the advanced-construction weight trends were used. For comparison, the normal-construction weight trends are also shown. A radius of 40 to 45 feet and a tip speed of 700 feet per second are again indicated. In order to apply further empty weight and flat-plate-area corrections to the results shown, a series of correction curves for them is also indicated.

Analysis of Heavy-Lift Mission and Integration of Mission Weights

The heavy-lift (20-ton) mission was next analyzed for 40- and 45-foot blade radii (see Figure 13). Blade radius and the group weights required for the heavy-lift (20-ton) mission were compared with those for the transport (12-ton) mission. The heaviest group weight required of either mission was used,

and the total of these weights results in the integrated mission weights. Table XII describes the integration of weights. Exceptions to taking the heaviest of the transport and heavy-lift mission weights were those weights that were based on installed, rather than actual, power requirements. Although installed power gives a measure of growth potential, optimization for the missions dictates the use of actual hover power requirements. The transport mission analysis overdesigned the drive system to absorb the sea level engine power rating corresponding to the 6000-foot, 95°F, power requirement. The transport mission was then recalculated for both radii with integrated weights. Figure 14 illustrates this for the tandem.

Rotor Radius

Figure 12 indicates that the trend of gross weight with radius is very flat between 40 and 45 feet. The radius was therefore selected to minimize the power required; the blade tip clearance required by the fixed distance between rotors was kept in mind. A 33-percent maximum overlap has historically been found to ensure good blade clearance for a three-bladed rotor; this would indicate a maximum blade radius of 43 feet. The 43-foot radius has a low enough value of hover power required that four T55-L-11 or T64/S4A engines may be used (see Figure 15). A reduction in blade radius would be permissible with three 501-M26 engines (to 41 feet), or four T64/S5 engines (to 36.5 feet), but there would be no significant weight saving, and the reduction in size is not enough compensation for the loss of flexibility and growth potential available with a 43-foot rotor.

Tip Speed

The tip speed of 700 feet per second and resulting solidity of 0.0777 for the selected design $\bar{C}_L$ of 0.6 were chosen to minimize the gross weight and hover power required (see Figure 16). Also, 700 feet per second is a desirable tip speed to provide a maximum speed potential of about 180 knots (for an assumed low drag configuration) with the power, stall, and compressibility limit speeds all well matched (see Figure 17).

Number of Blades

The number of blades (three) and the blade chord (3.5 feet) were chosen for minimum gross weight. A four-bladed rotor

NOTES:

1. Tandem-lift rotor transport; advanced airframe construction unless noted otherwise; 12-ton mission
2. Cargo compartment 144 inches wide, 108 inches high, 540 inches long
3. Four engines
4. Three-bladed rotor; θ_t = -9 degrees, C_L = 0.6
5. Tip speeds in feet per second (700 unless noted otherwise):
   - ⊙ = 600
   - ▽ = 700
   - ▽ = 700 (normal airframe construction)
   - ⊡ = 800
6. 30-foot rotor radius:
   4046 shaft horsepower per engine
   5.61-foot chord
   80,224 pound takeoff weight
   47,483 pound basic weight
   8742 pound fuel weight
7. 40-foot rotor radius:
   3033 shaft horsepower per engine
   4.03-foot chord
   79,694 pound takeoff weight
   47,478 pound basic weight
   8216 pound fuel weight
8. 50-foot rotor radius:
   2702 shaft horsepower per engine
   3.33-foot chord
   83,596 pound takeoff weight
   51,287 pound basic weight
   8309 pound fuel weight

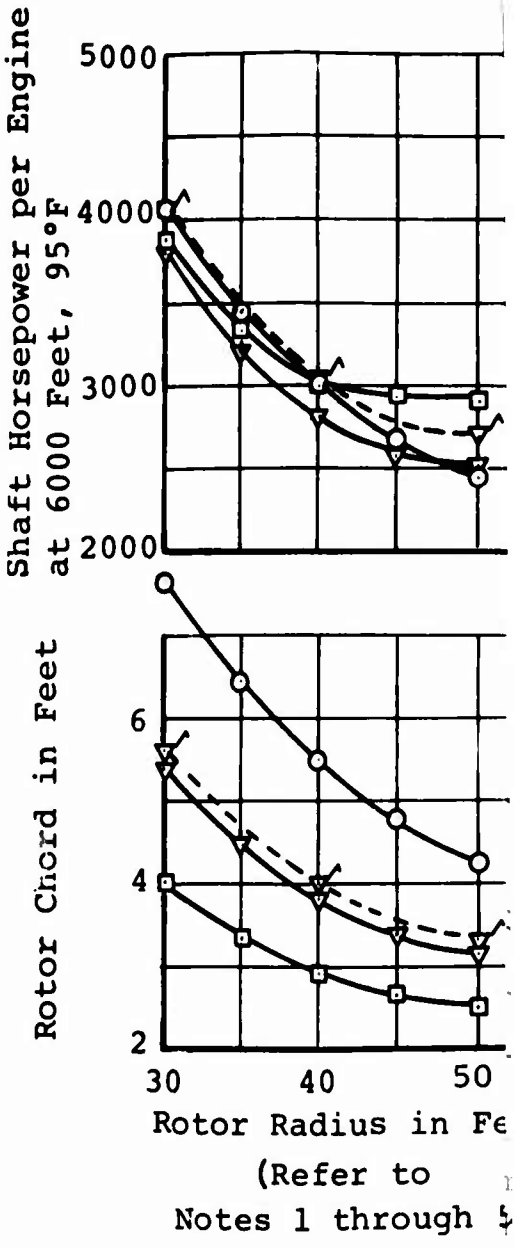

Figure 12. Second Iteration of Transport Mission.
(Sheet 1 of 2)

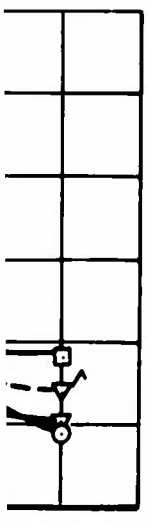

50

n Feet

gh 5)

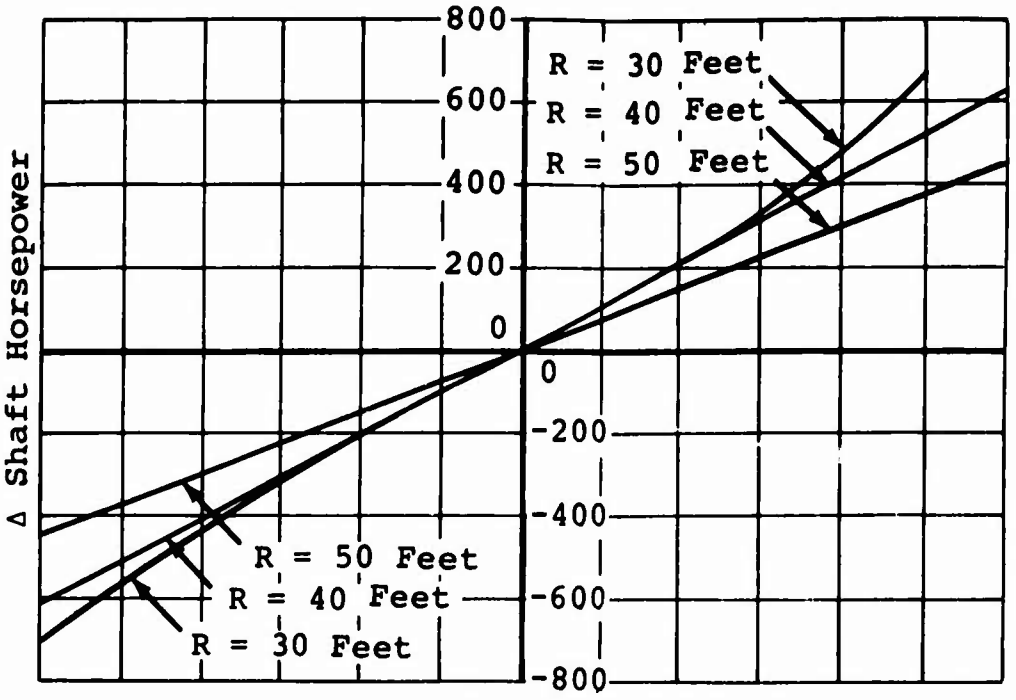

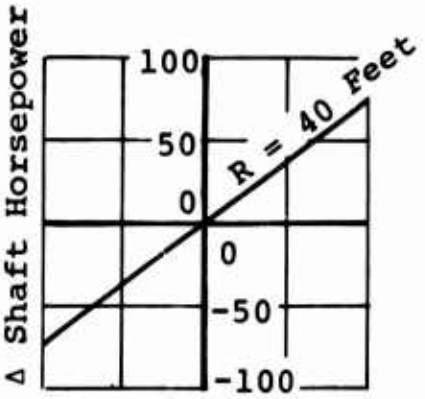

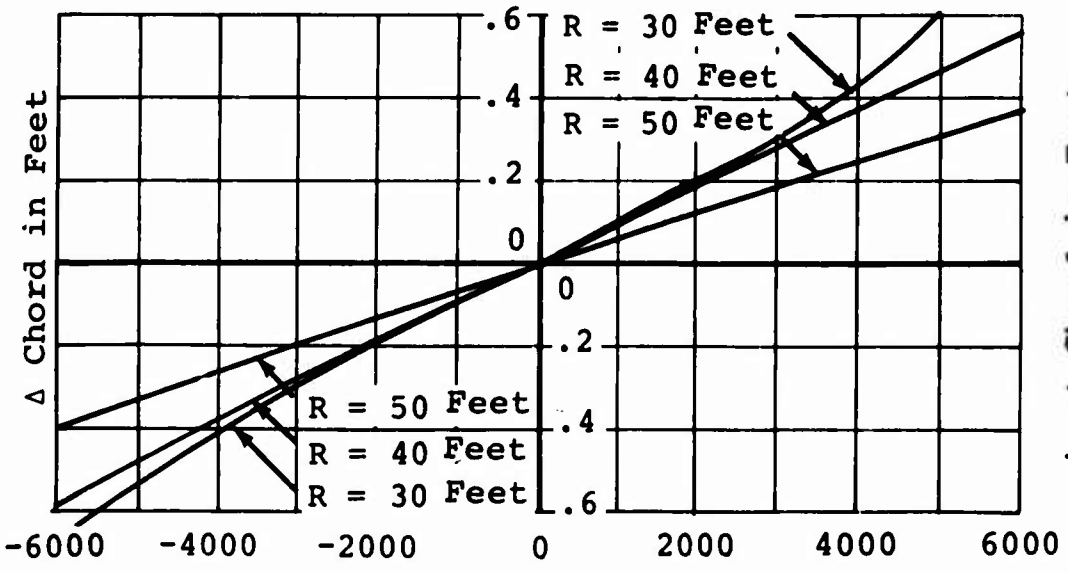

Δ Weight in Pounds
(Refer to Notes 1 through 8)

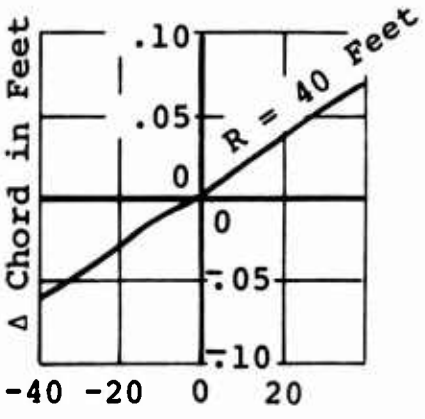

Δ fe
(Refer to Notes
1 through 5)

B

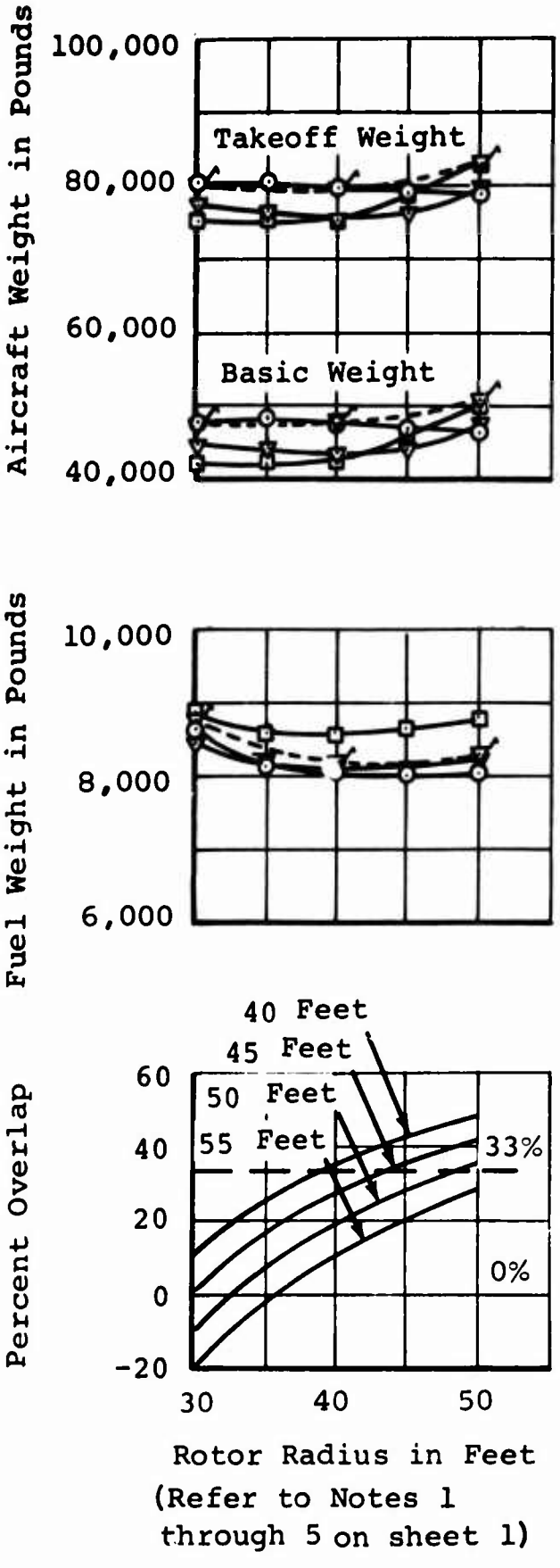

Figure 12. Second Iteration of Transport Mission.
(Sheet 2 of 2)

A

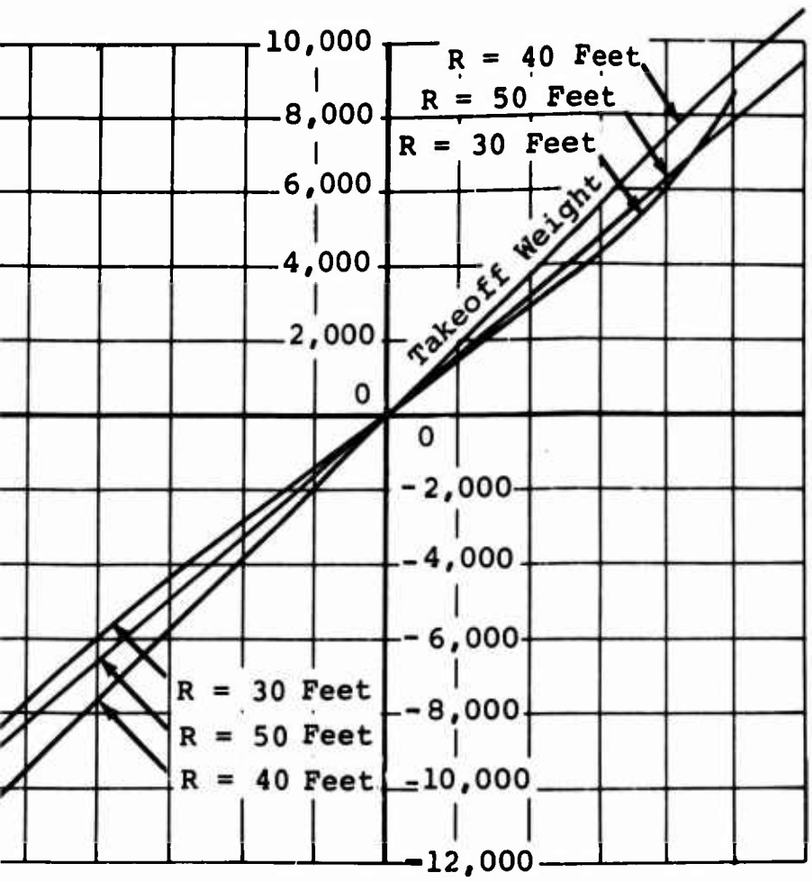

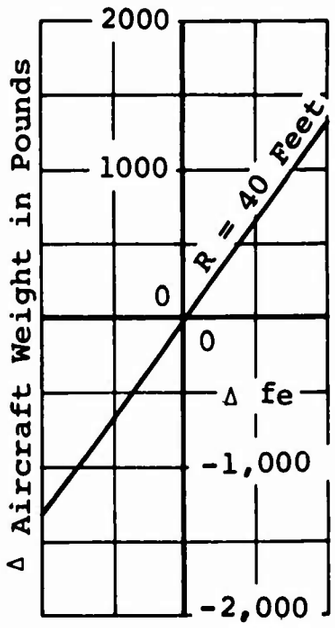

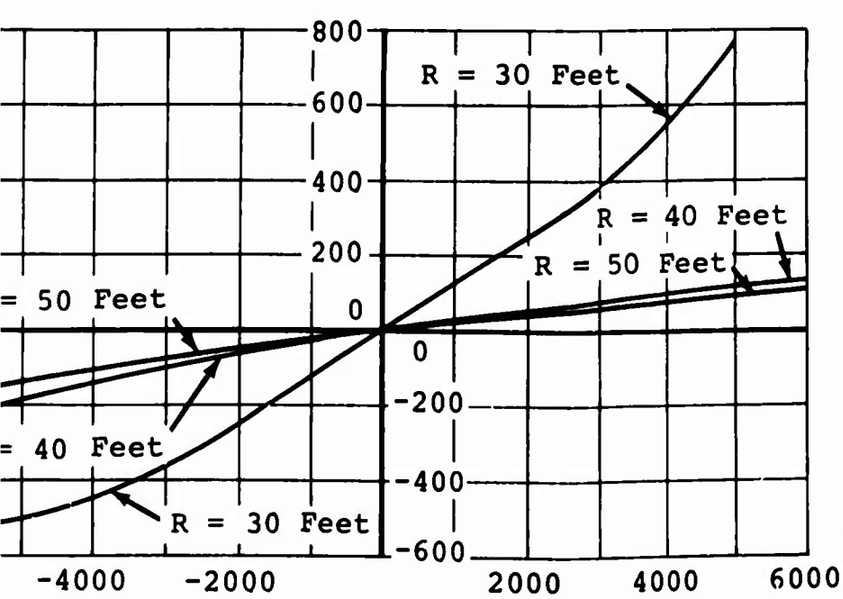

Δ Weight in Pounds
(Refer to Notes 1 through 8 on Sheet 1)

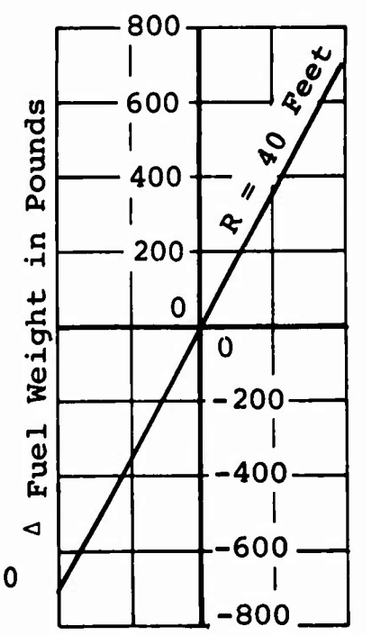

(Refer to Notes 1 through 5 on Sheet 1)

f Transport Mission.

B

Figure 13. 20-Ton Mission Weight and Performance Study for Tandem-Lift Rotor Helicopter.

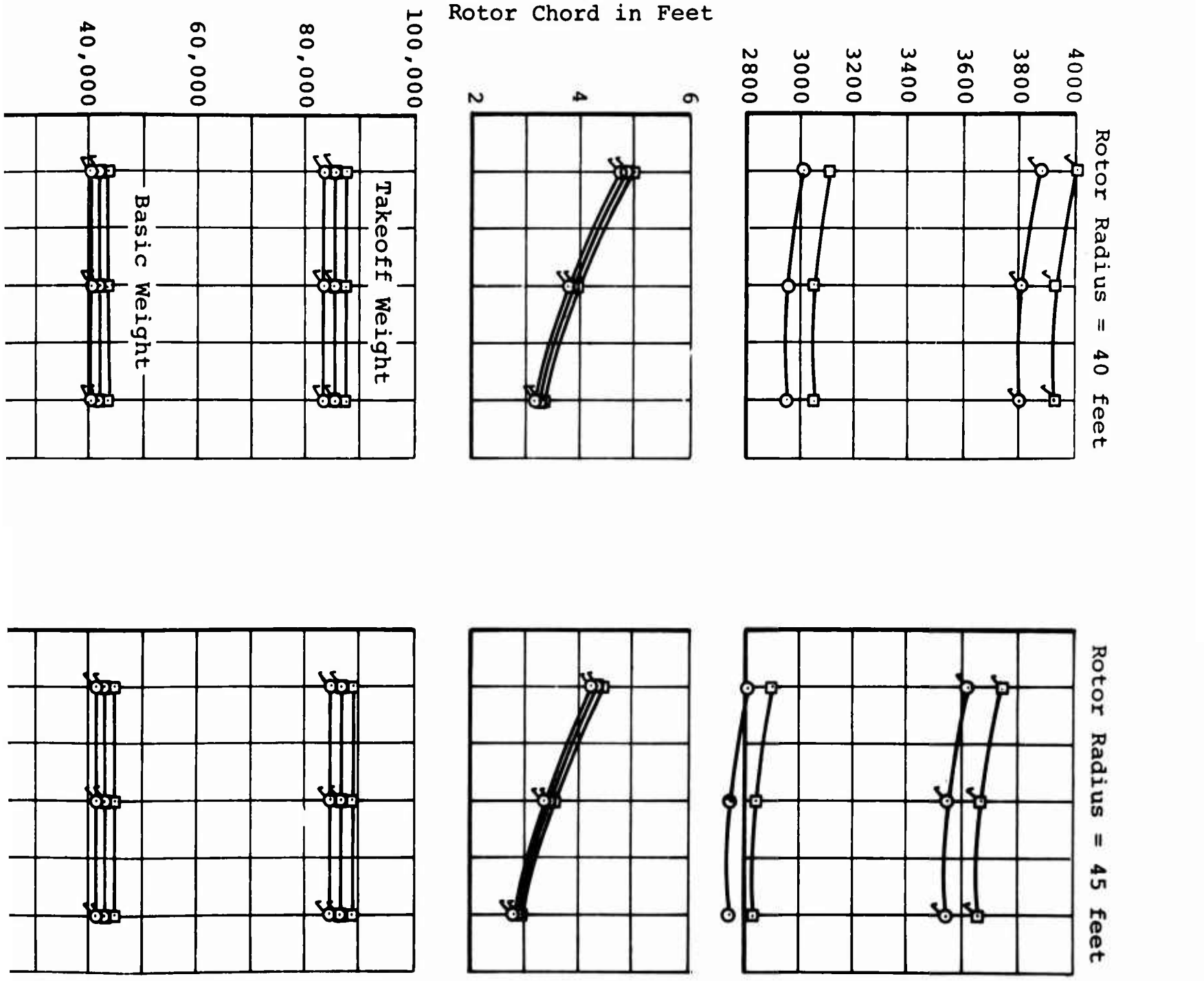

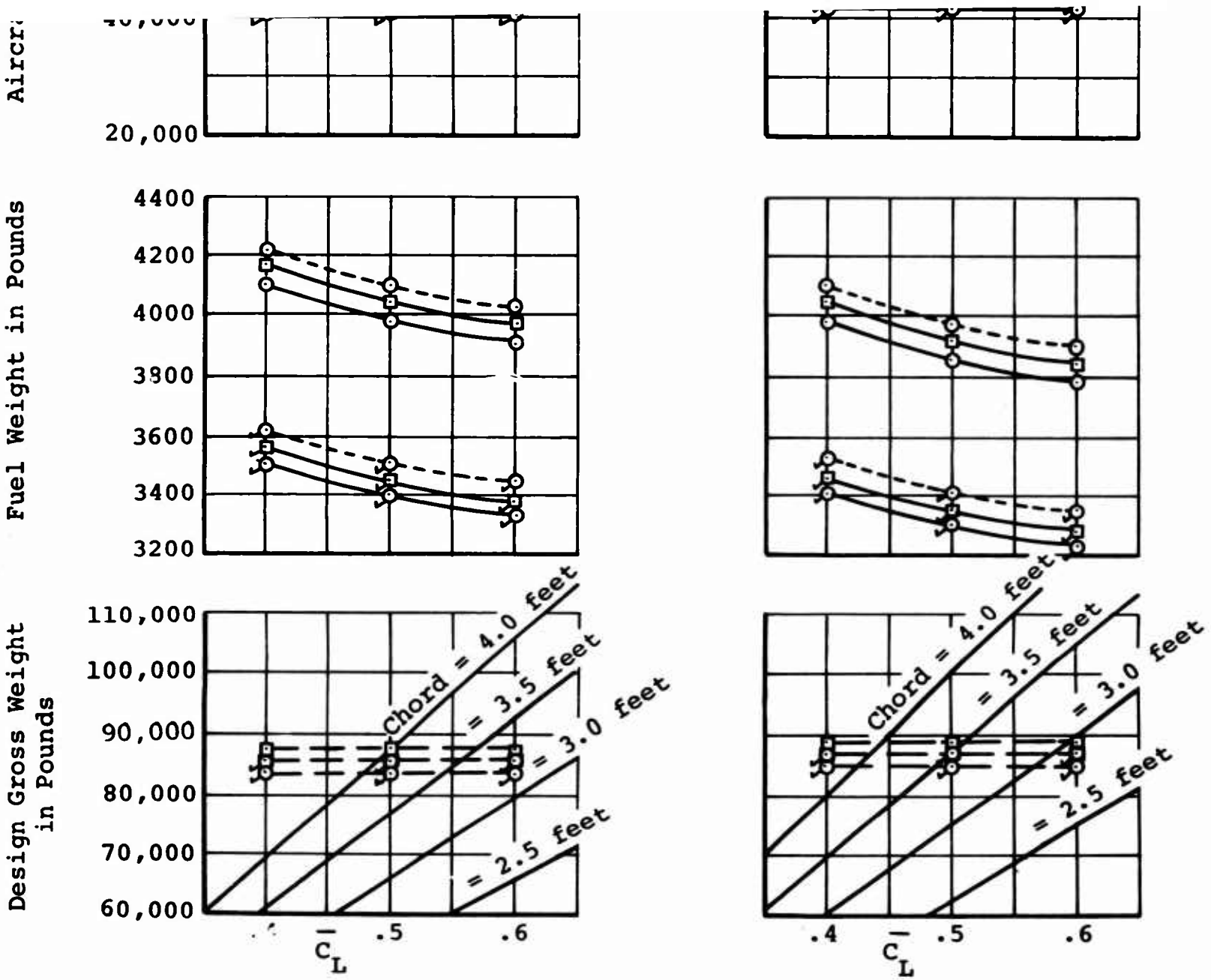

NOTES:

1. Tandem-lift rotor transport; 20-ton mission
2. Cargo compartment 144 inches wide, 108 inches high, 540 inches long
3. Three-bladed rotor:
   θ_t = -9 degrees
   tip speed = 700 feet per second
4. Symbols:
   ⊙ = advanced airframe construction and four engines
   ⊙ = advanced airframe construction and three engines
   ⊡ = conventional airframe construction and four engines
   ⊡ = conventional airframe construction and three engines
   ---- 100 pounds external drag outbound

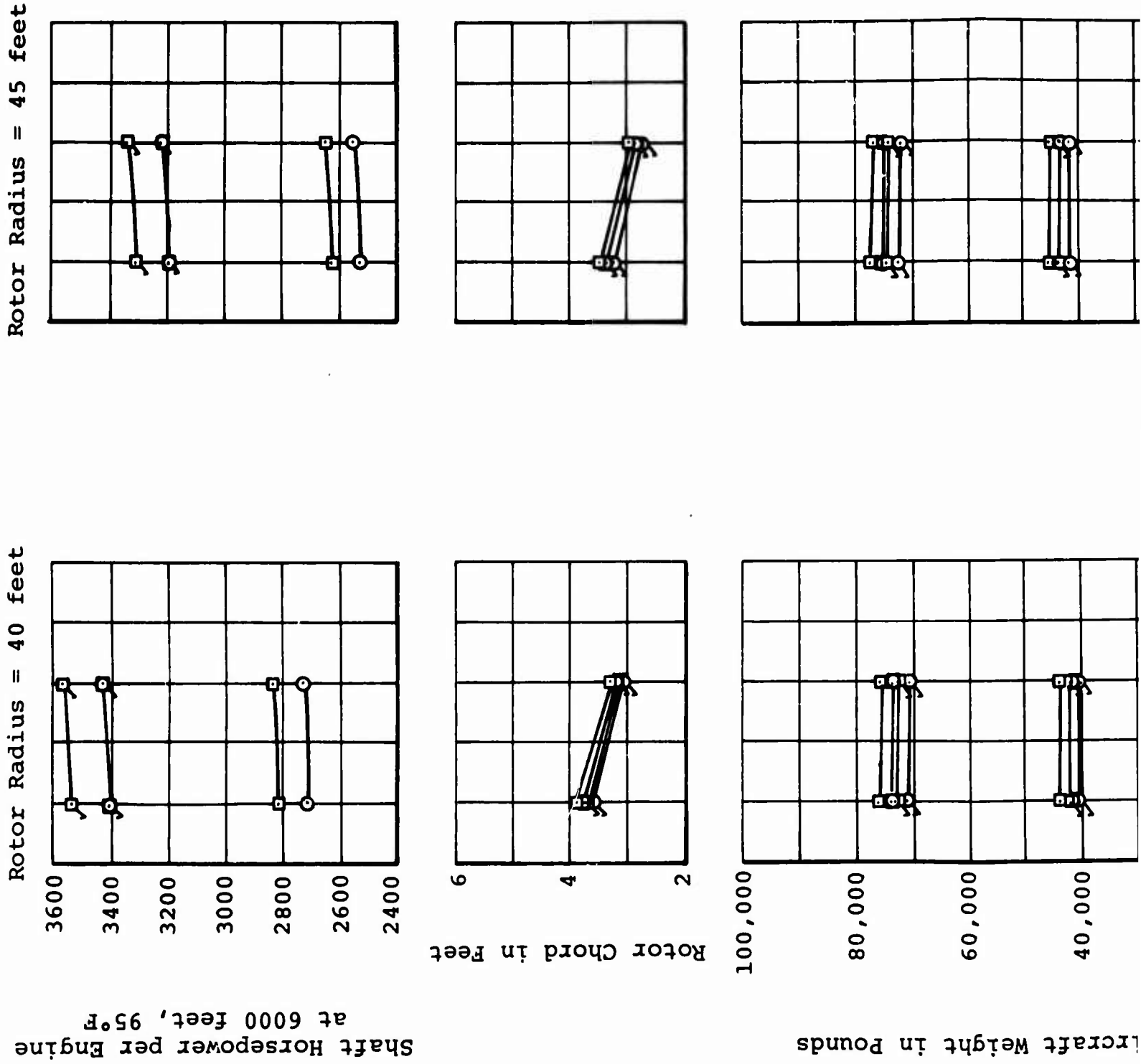

Figure 14. 12-Ton Mission Weight and Performance Study for Tandem-Lift Rotor Helicopter.

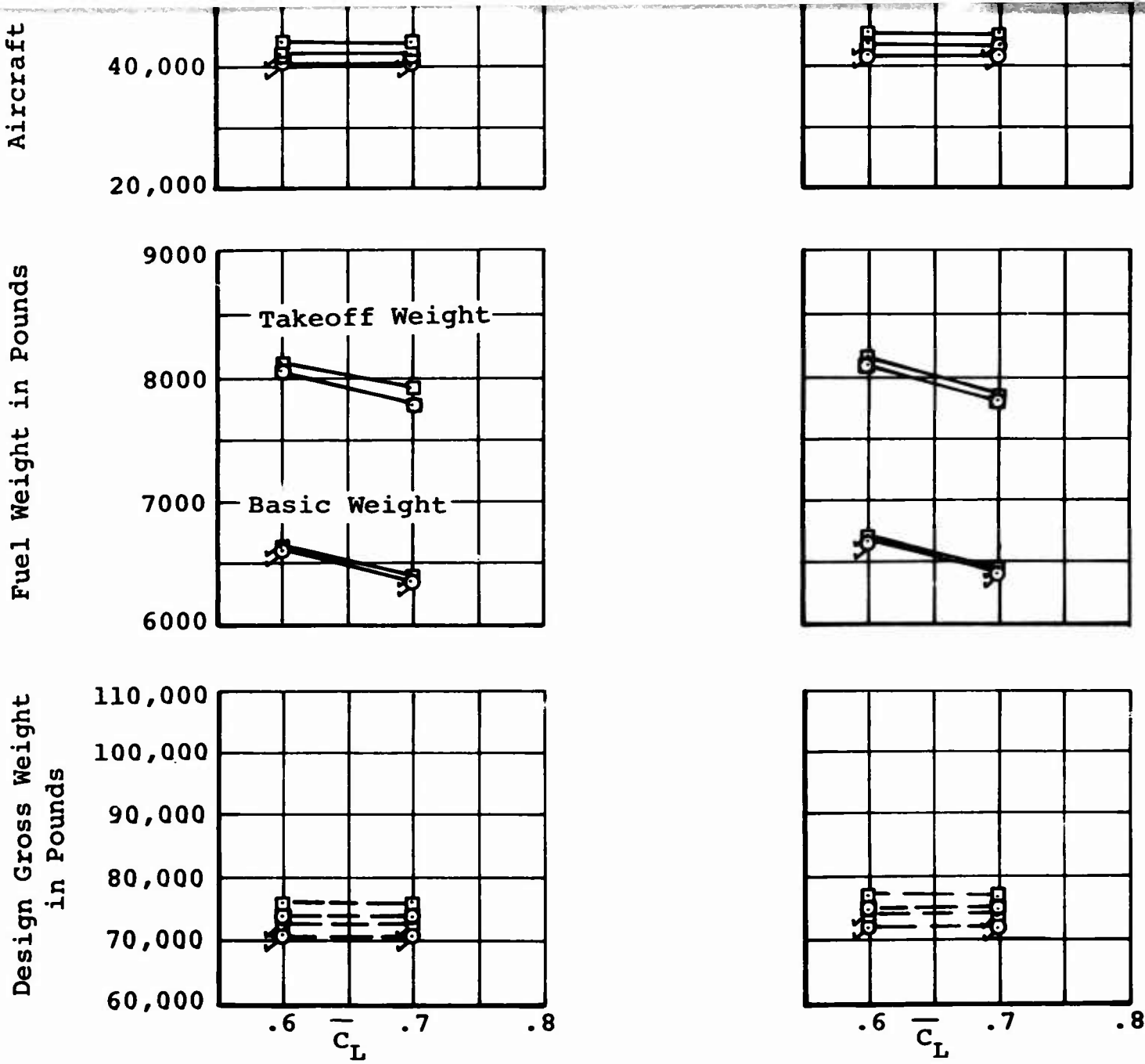

NOTES:

1. Tandem-lift rotor transport; 12-ton mission
2. Cargo compartment 144 inches wide, 108 inches high, 540 inches long
3. Three-bladed rotor:
   θ_t = -9 degrees
   tip speed = 700 feet per second
4. Symbols:
   ⊙ = advanced airframe construction and four engines
   ⊙ = advanced airframe construction and three engines
   ⊡ = conventional airframe construction and four engines
   ⊡ = conventional airframe construction and three engines

TABLE XII
INTEGRATION OF WEIGHTS FOR TRANSPORT AND HEAVY-LIFT MISSIONS -- TANDEM-LIFT ROTOR HELICOPTER

Item	12-Ton Mission	20-Ton Mission	Integrated Weights (Present Trend)	Weight Savings from Advanced Constr.	Integrated Weights @ Weight Savings
Rotor Group	9679*	7235**	7235	843	6392
Body Group	9170	9416	9416	377	9039
Landing Gear	4661	4969	4969	149	4820
Flight Controls (Cockpit)	290	296	296	0	296
Flight Controls (Upper)	1443*	1076**	1076	117	959
Flight Controls (Vertical)	1553*	1214**	1214	116	1098
Powerplant	4640	3758**	4640	232	4408
Fuel Tanks	316	150	316	0	316
Drive System	9579*	6808**	6808	0	6808
Fixed Equipment	5301	5301	5301	0	5301
Fixed Useful Load	880	880	880	0	880
Basic Weight	47512	41103	42095	1778	40317
Fuel Weight	8214	3890	8214	0	8217

* Weight based on sea level installed power rating required to hover at 6000 feet, 95°F and therefore considered as overdesigned.
**Weight based on sea level installed power rating required to hover at sea level, 59°F.

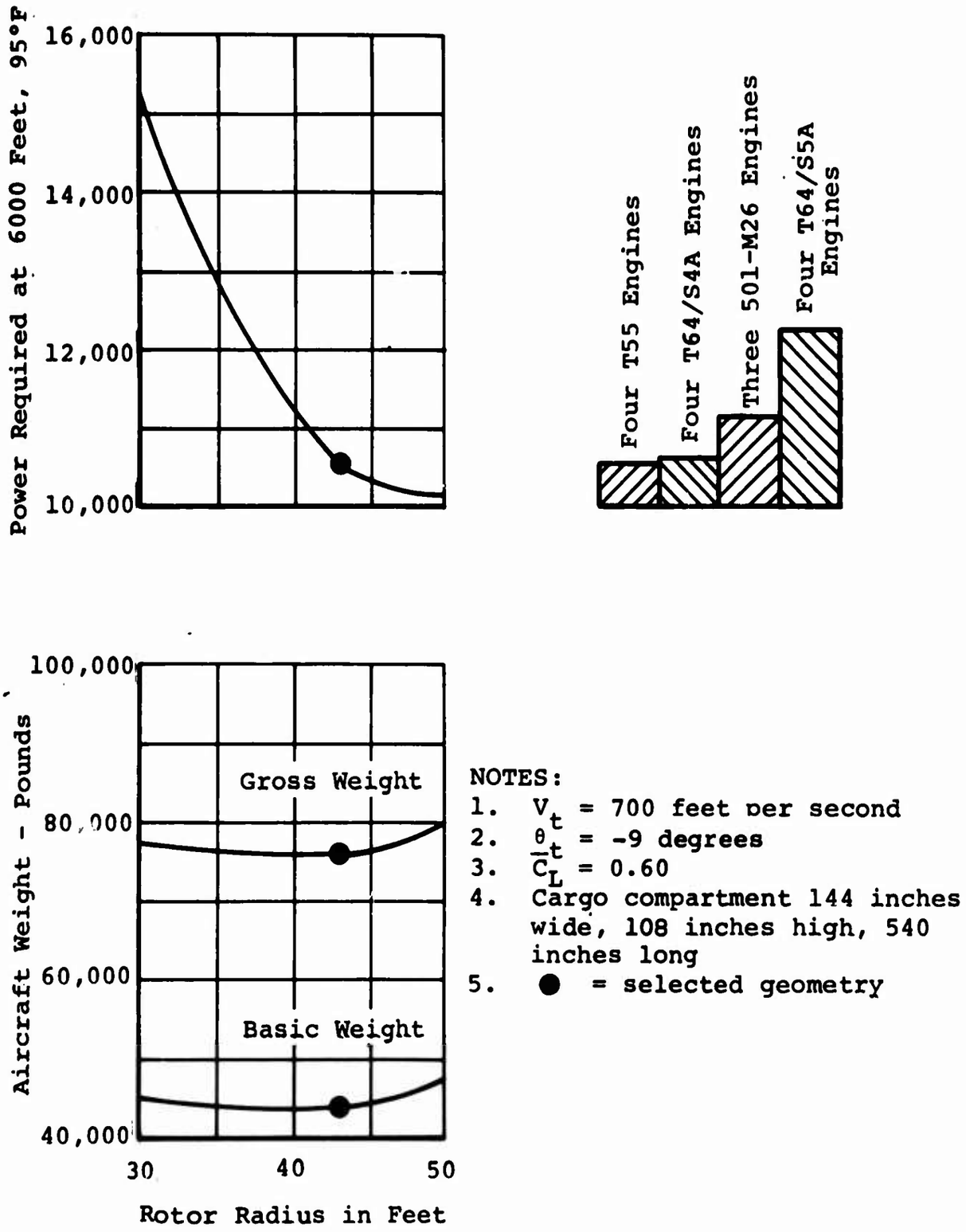

Figure 15. Selection of Blade Radius and Engine Combinations.

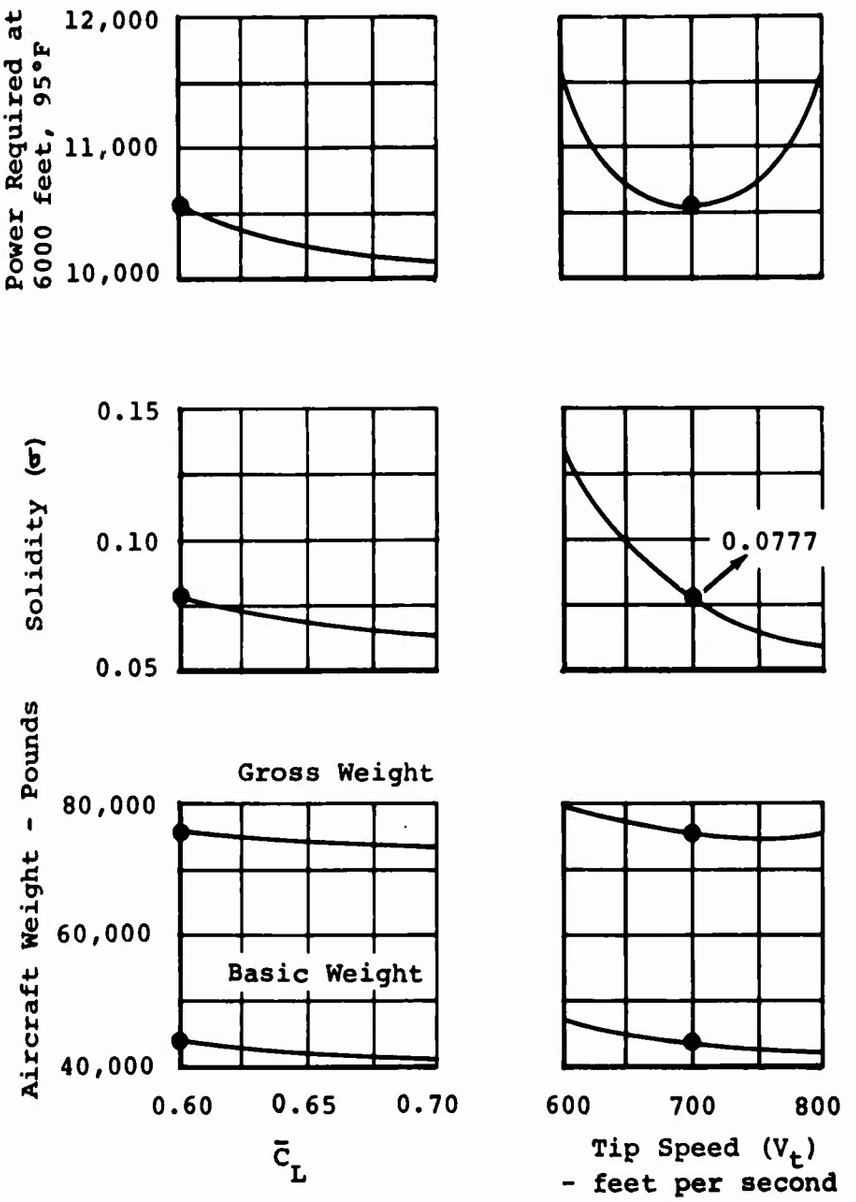

NOTES:

1. Cargo compartment 144 inches wide, 108 inches high, 540 inches long
2. Rotor radius = 43 feet
3. Twist (θ_t) = -9 degrees
4. Assume tip speed = 700 feet per second to select $\bar{C}_L$
5. Assume $\bar{C}_L$ = 0.6 to select tip speed
6. ● = selected geometry

Figure 16. Selection of Design $\bar{C}_L$, Tip Speed, and Solidity.

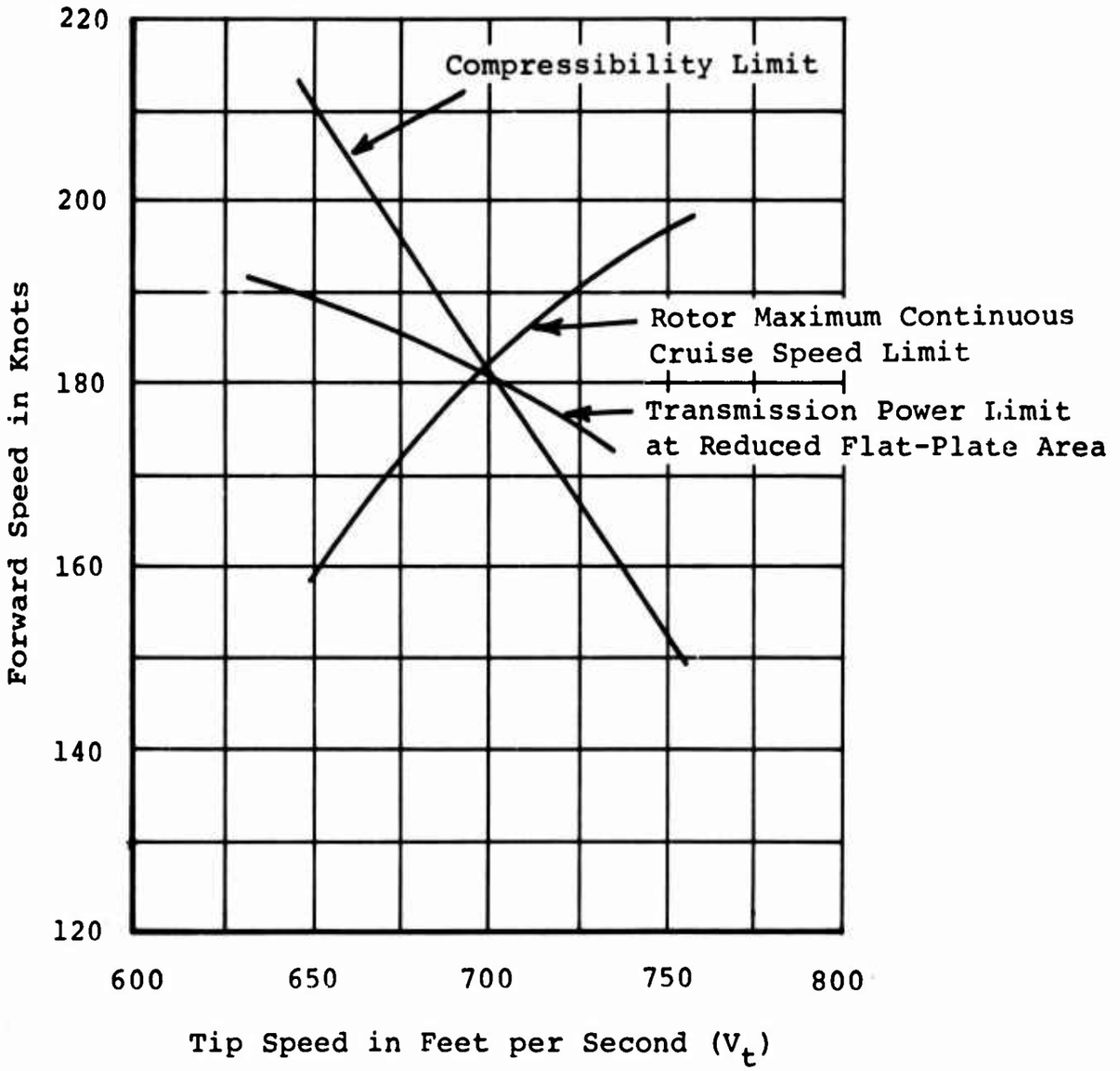

NOTES:
1. Gross weight = 75,000 pounds
2. Altitude = 2500 feet

Figure 17. Effect of Tip Speed on Speed Limitations.

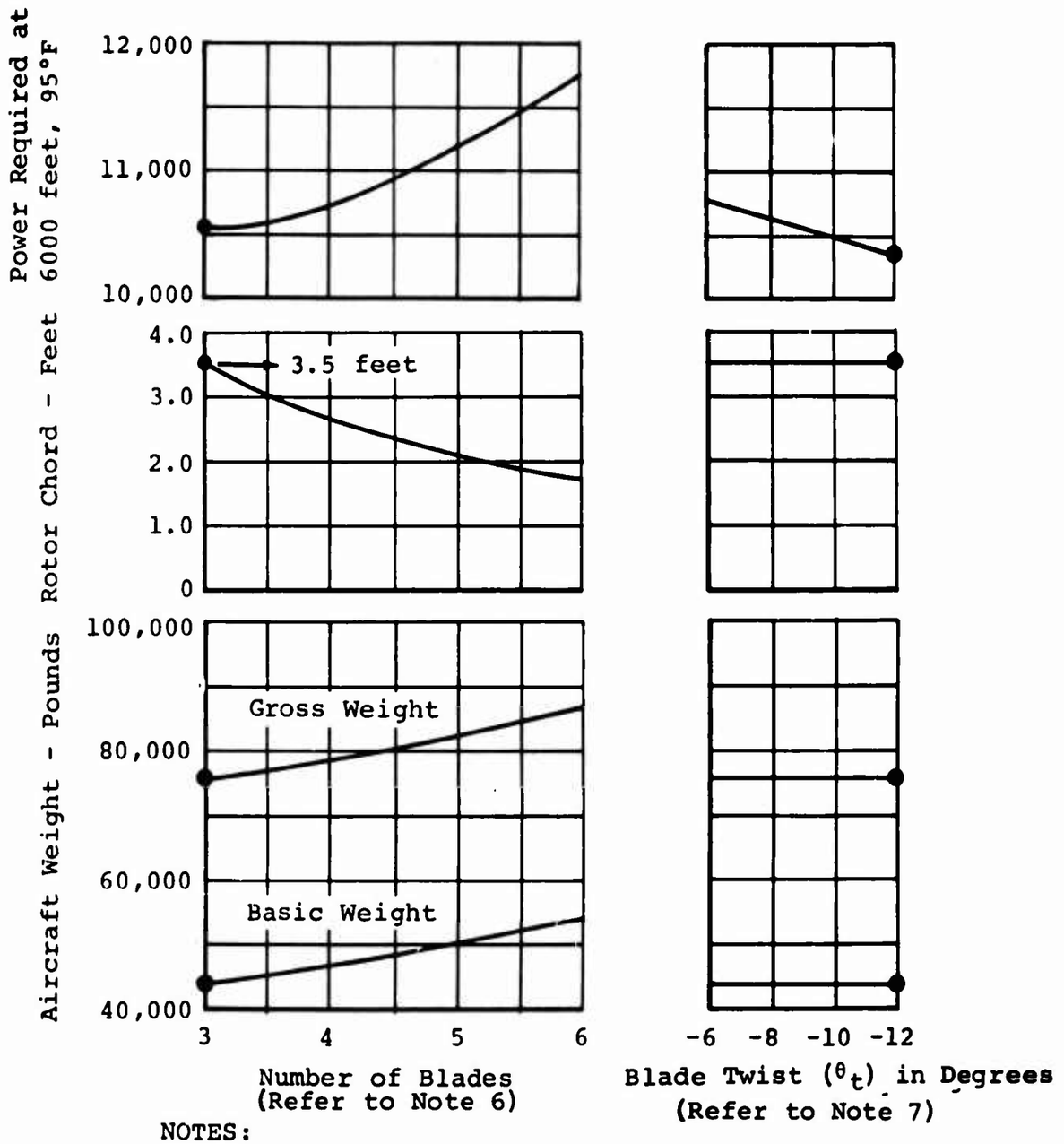

NOTES:

1. Cargo compartment 144 inches wide, 108 inches high, 540 inches long
2. Distance between rotors increased as required for blade clearance
3. Rotor radius = 43 feet
4. Tip speed = 700 feet per second
5. Solidity = 0.0777
6. To select number of blades, assume twist (θ_t) = -9 degrees
7. To select twist, assume three blades
8. ● = selected geometry

Figure 18. Selection of Number of Blades, Chord, and Twist.

system requires a gross weight approximately 3000 pounds heavier: 2000 pounds for the severe static-droop weight penalty of the higher aspect-ratio blades, and 1000 pounds for the increase in fuselage length to provide intermeshing blade clearance. Five or six blades would increase these weights even more (see Figure 18).

A brief dynamics study showed that four blades would produce lower rotor vibratory forces than three blades. However, response characteristics considered in design of the fuselage would minimize the response levels of any desired frequency, and the net benefit in vibration level of a four-bladed system would not compensate for the 3000-pound weight penalty. Proven devices to reduce vibration are available.

Airfoil Section

The constant spanwise thickness distribution and NACA 23012 airfoil section were selected for ease of manufacture and quick development time, and for inherent droop-stiffness and blade-stall characteristics.

Blade Twist

A blade twist of -12 degrees was originally selected to prevent blade stall at the potential 180-knot V_{max} of a cleaned-up configuration with retracted landing gear (see Figure 19). In addition, the hovering performance is somewhat improved over that obtainable with lesser amounts of twist (see Figure 18). Much of the rotor design study was conducted using this original value of -12 degrees. A review of blade twist was subsequently conducted, however, and the results indicate that a value of -9 degrees is acceptable from a performance standpoint, and may be more desirable from a stress standpoint. The originally selected value of -12 degrees would still be desirable from a performance standpoint, but all the mission requirements will be met with a twist of -9 degrees, and a power-limited forward speed of 163 knots can be obtained without exceeding rotor aerodynamic limits and with no increase in blade area.

The initial selection of a twist of -12 degrees was based on a relatively simple analysis of a streamlined growth configuration with retractable landing gear, for which the angle of attack at the retreating blade tip was kept below the stall value (see Figure 19) at the power-limited forward speed.

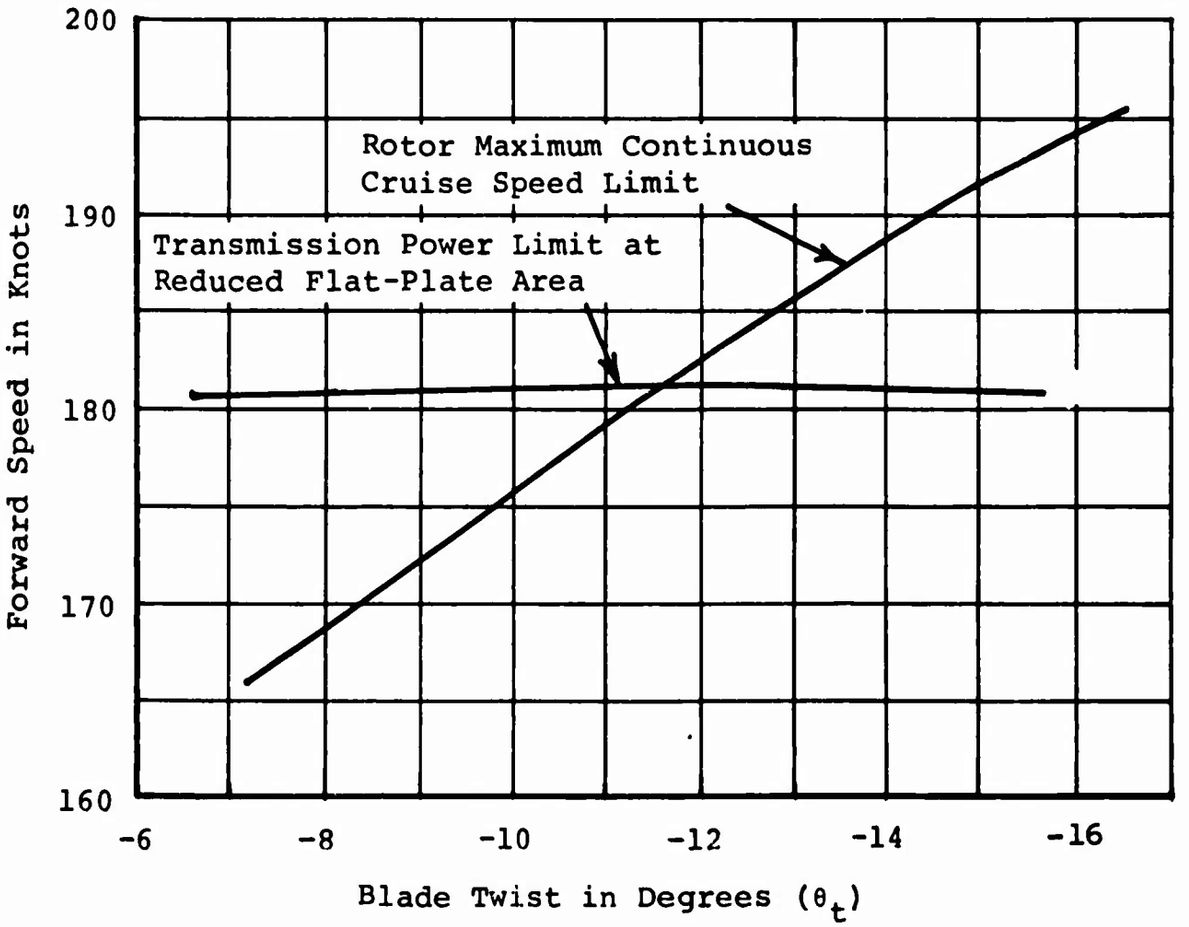

NOTES:
1. Gross weight = 75,000 pounds
2. Altitude = 2500 feet

Figure 19. Effect of Blade Twist on Maximum Speed Free of Blade Stall.

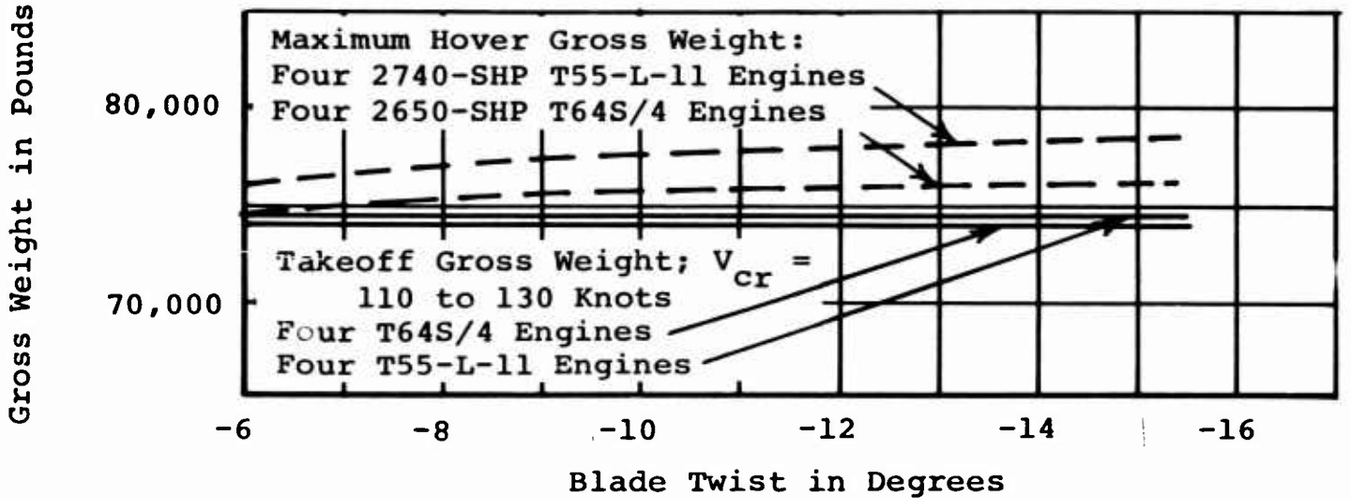

NOTES:
1. NACA 23012 airfoil
2. Radius = 43 feet
3. Chord = 3.5 feet
4. Tip speed = 700 feet per second
5. Hover OGE 6000 feet, 95°F

Figure 20. Effect of Blade Twist on Hover Performance of the Tandem-Lift Rotor Transport.

This selection was to be reviewed for the rotor design phase, especially with regard to the structural and dynamic effects. The aerodynamic effects have also been reviewed with more advanced theoretical considerations; the effect of twist on hover performance and blade stall was considered.

Effect of Blade Twist on Hover Performance

The hover performance was compared at the 6000-foot, 95°F gross weight for the transport mission. Figure 20 shows the effect of twist on the transport's maximum hover gross weight at 6000 feet, 95°F, for both the T55-L-11 and T64/S4 engines; takeoff gross weight is also shown for each engine installation. The hover performance margin increases with blade twist, from 500 pounds at -6 degrees with T64/S4 engines to 3500 pounds at -12 degrees with T55-L-11 engines. On this basis alone, it would be obviously desirable to design the blade for -12 degrees or even more.

Effect of Blade Twist on Blade Stall

The conditions at which the rotor aerodynamic speed limit (blade stall) was investigated were based upon the Vertol-imposed requirement that the aircraft be free of rotor aerodynamic limits at all speeds less than normal-rated-power V_{max} at the following conditions:

1. Hover gross weight (6000 feet, 95°F) at an altitude of 5000 feet, standard conditions. This is the 12-ton mission weight.

2. Design gross weight at sea level standard conditions. This is the 20-ton mission weight.

This requirement that the aircraft reach power limit before rotor aerodynamic limit is appropriate for the heavy-lift helicopter because it provides some measure of power-limited speed capability without compromising the mission hover requirements.

The local blade angle of attack was computed using Vertol Division EDP programs, and contour plots (Figure 21) were constructed. For comparison, the CH-47 contour map (Figure 22) shows an acceptable flight condition demonstrated in flight test. The crosshatched areas on each plot indicate possible stalled areas: angles above 14 degrees for the Chinook

symmetrical airfoil (NACA 0012), and angles above 16 degrees for the heavy-lift helicopter drooped airfoil (NACA 23012). It can be seen that as the twist increases, the stalled areas diminish in severity. At the twist of -10 degrees, the heavy-lift helicopter rotor has approximately the same character as the acceptable Chinook rotor condition.

Figure 23 shows the rotor angle-of-attack contour for the heavy-lift helicopter at the design gross weight of 87,000 pounds and a speed of 165 knots at sea level, which is in excess of the normal-rated-power speed of 163 knots. At the twist of -10 degrees shown, the stalled area is less severe at design gross weight than at 75,700 pounds, 5000 feet, 170 knots.

Vertol Division has recently established a criterion for rotor aerodynamic limits based upon Chinook flight test data and has presented it in the form of C_T/σ versus μ. This is shown in Figure 24. The projected limit line for the heavy-lift helicopter is extrapolated from the Chinook data, accounting for droop airfoil section, and propulsive-force and tip-speed differences. The points shown represent the heavy-lift helicopter V_{max} conditions at normal rated power and the Chinook condition depicted in Figure 22. All these conditions are within the aforementioned rotor aerodynamic limits. Since the Chinook rotor blade with which the test points were obtained has a blade twist of -9 degrees, the same value should be acceptable for the heavy-lift helicopter.

Transmission Rating

A 12,000-shaft-horsepower transmission rating will provide enough power for both hover requirements. The 12-ton mission at 6000 feet, 95°F, requires 10,960 shaft horsepower; 20 tons at sea level requires 11,500 shaft horsepower.

Final Configuration

The aforementioned selections have been based on the transport-type fuselage and the flat-plate area associated with this type. A brief study to determine their applicability to the crane/personnel carrier-type fuselage showed that, for the 100-nautical-mile mission, the lighter structural weight of the crane/personnel carrier is partly offset by the additional fuel required. Although the transport mission takeoff weight of the crane/personnel carrier is about 1600 pounds less than

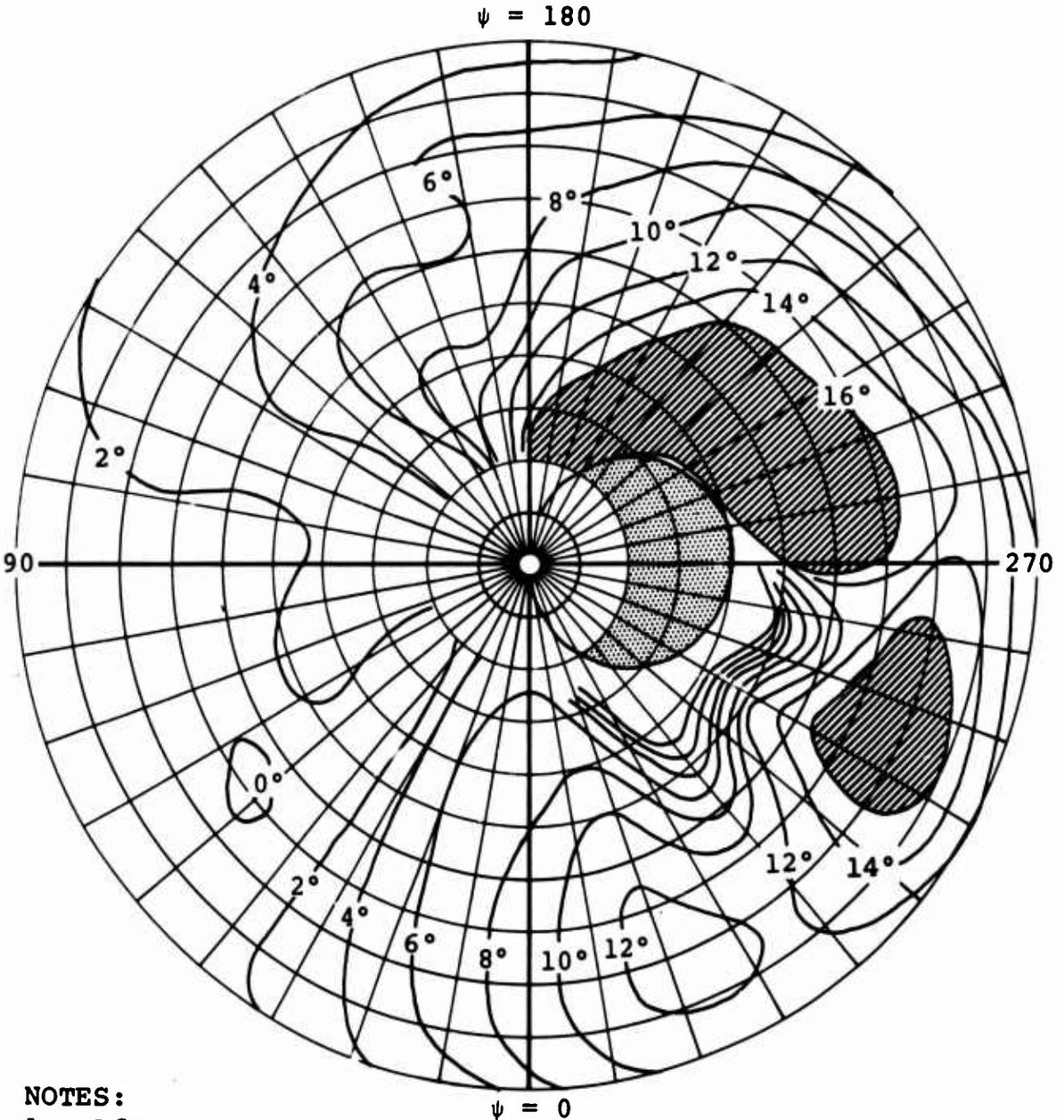

NOTES:

1. Aft rotor
2. Gross weight 75,700 pounds
3. Altitude 5000 feet, standard
4. Airspeed 170 knots
5. θ_t = -6 degrees
6. $C_T'/\sigma = 0.09204$
7. $\mu = 0.4030$

Reverse flow region

Angles of attack greater than 16 degrees

Figure 21. Angle-of-Attack Distribution of the Tandem-Lift Rotor at 75,700 Pounds, 5000 Feet, 120 Knots. (Sheet 1 of 4)

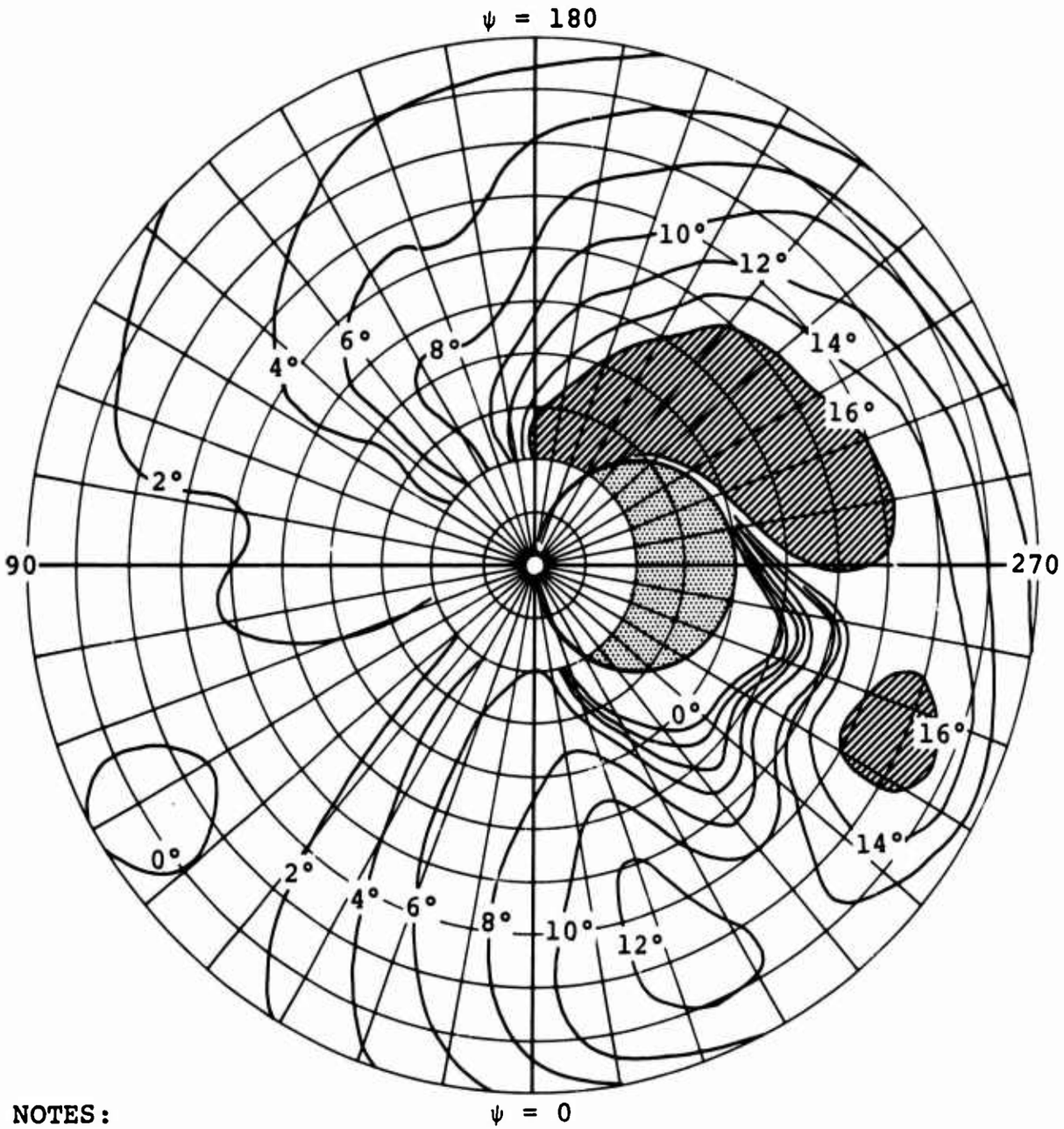

NOTES:

1. Aft rotor
2. Gross weight 75,700 pounds
3. Altitude 5000 feet, standard
4. Airspeed 170 knots
5. θ_t = -8 degrees
6. $C_T{}^1/\sigma$ = 0.09179
7. μ = 0.4032

Reverse flow region

Angles of attack greater than 16 degrees

Figure 21. Angle-of-Attack Distribution of the Tandem-Lift Rotor at 75,700 Pounds, 5000 Feet, 120 Knots. (Sheet 2 of 4)

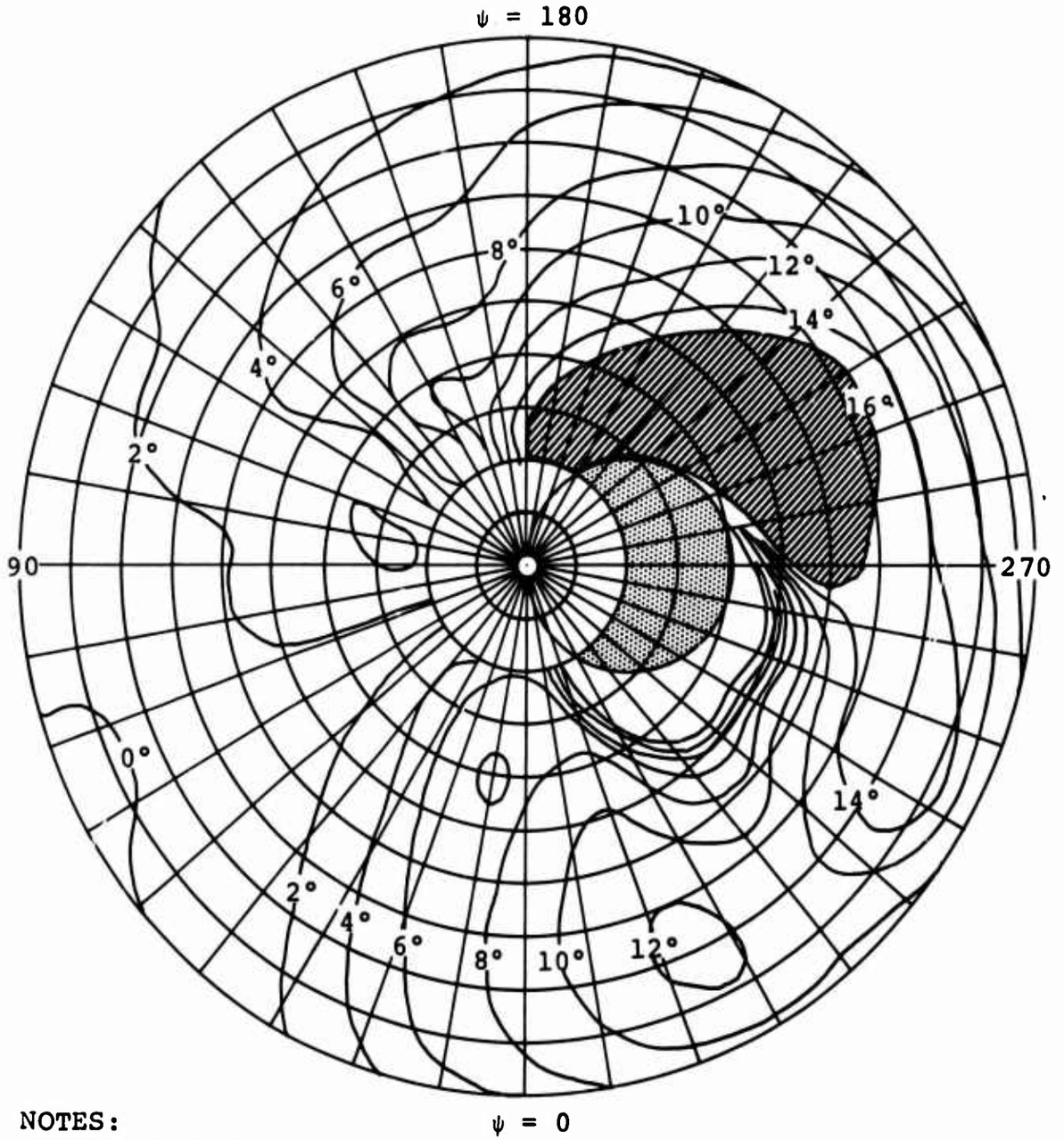

NOTES:

1. Aft rotor
2. Gross weight 75,700 pounds
3. Altitude 5000 feet, standard
4. Airspeed 170 knots
5. θ_t = -10 degrees
6. $C_T{}^1/_\sigma$ = 0.09153
7. μ = 0.4034

Angles of attack greater than 16 degrees

Reverse flow region

Figure 21. Angle-of-Attack Distribution of the Tandem-Lift Rotor at 75,700 Pounds, 5000 Feet, 120 Knots. (Sheet 3 of 4)

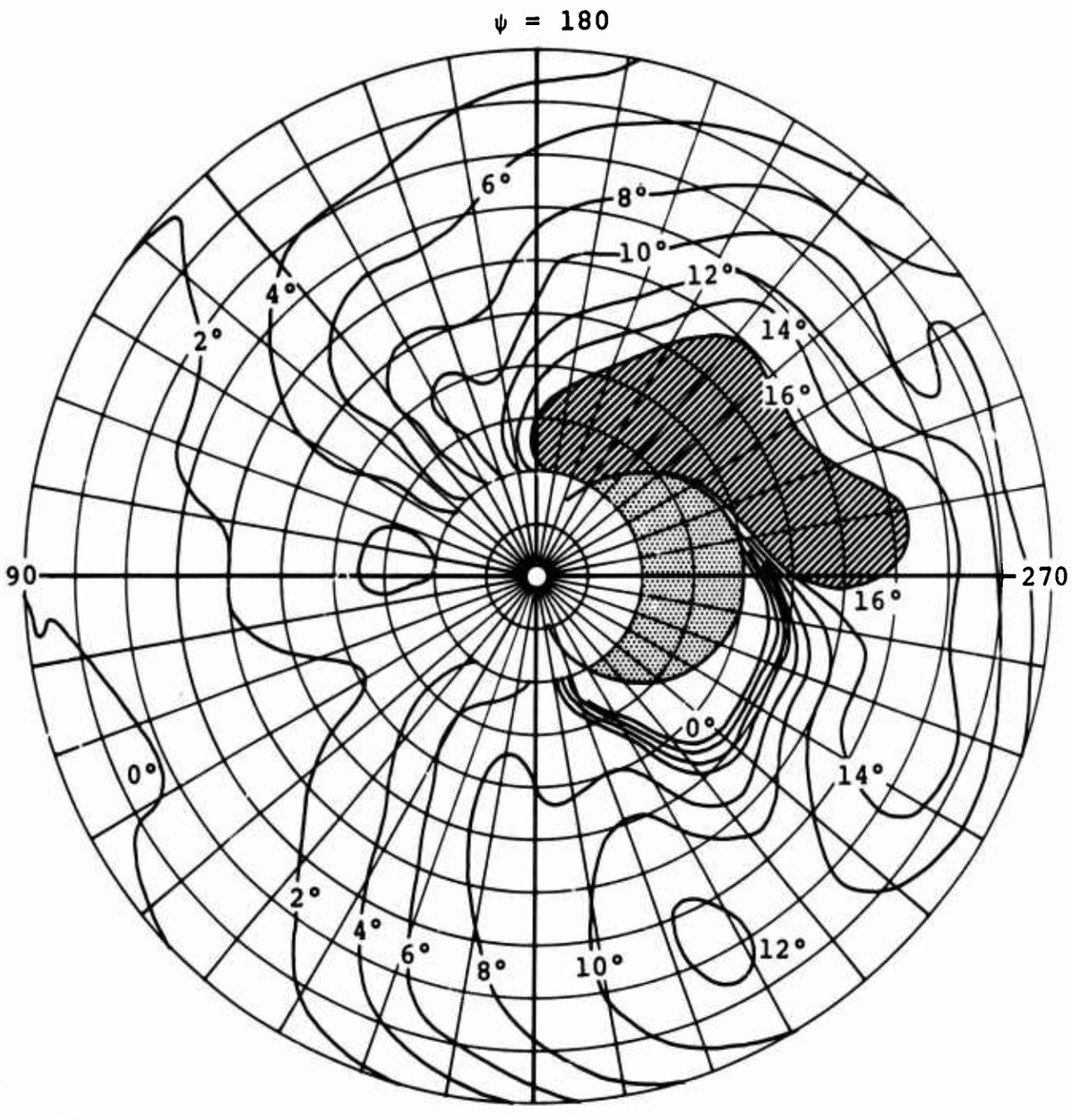

NOTES:

1. Aft rotor
2. Gross weight 75,700 pounds
3. Altitude 5000 feet, standard
4. Airspeed 170 knots
5. θ_t = -12 degrees
6. $C_T 1/\sigma$ = 0.09128
7. μ = 0.4037

Reverse flow region

Angles of attack greater than 16 degrees

Figure 21. Angle-of-Attack Distribution of the Tandem-Lift Rotor at 75,700 Pounds, 5000 Feet, 120 Knots. (Sheet 4 of 4)

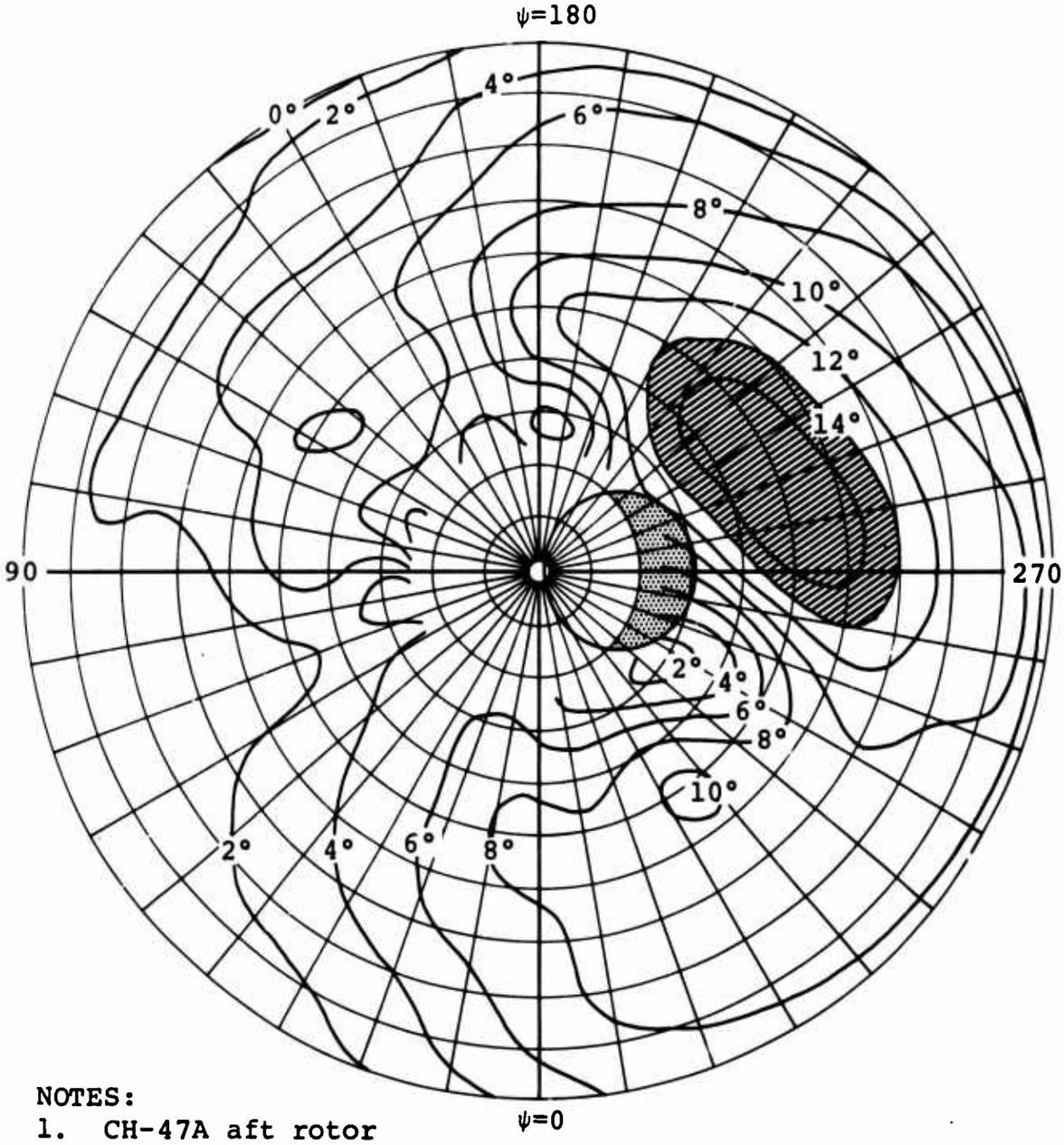

NOTES:

1. CH-47A aft rotor
2. Test weight 28,290 pounds, cg 16.7 inches aft
3. Altitude 5000 feet; trim 3/5
4. Airspeed 126 knots; 230 rotor rpm
5. θ_t = -9 degrees
6. $C_{T^1/\sigma}$ = 0.0906
7. μ = 0.2989
8. X_C = 0.195

Angles of attack greater than 14 degrees

Reverse flow region

Figure 22. Angle-of-Attack Distribution of the CH-47 Rotor at 28,290 Pounds, 5000 Feet, 120 Knots.

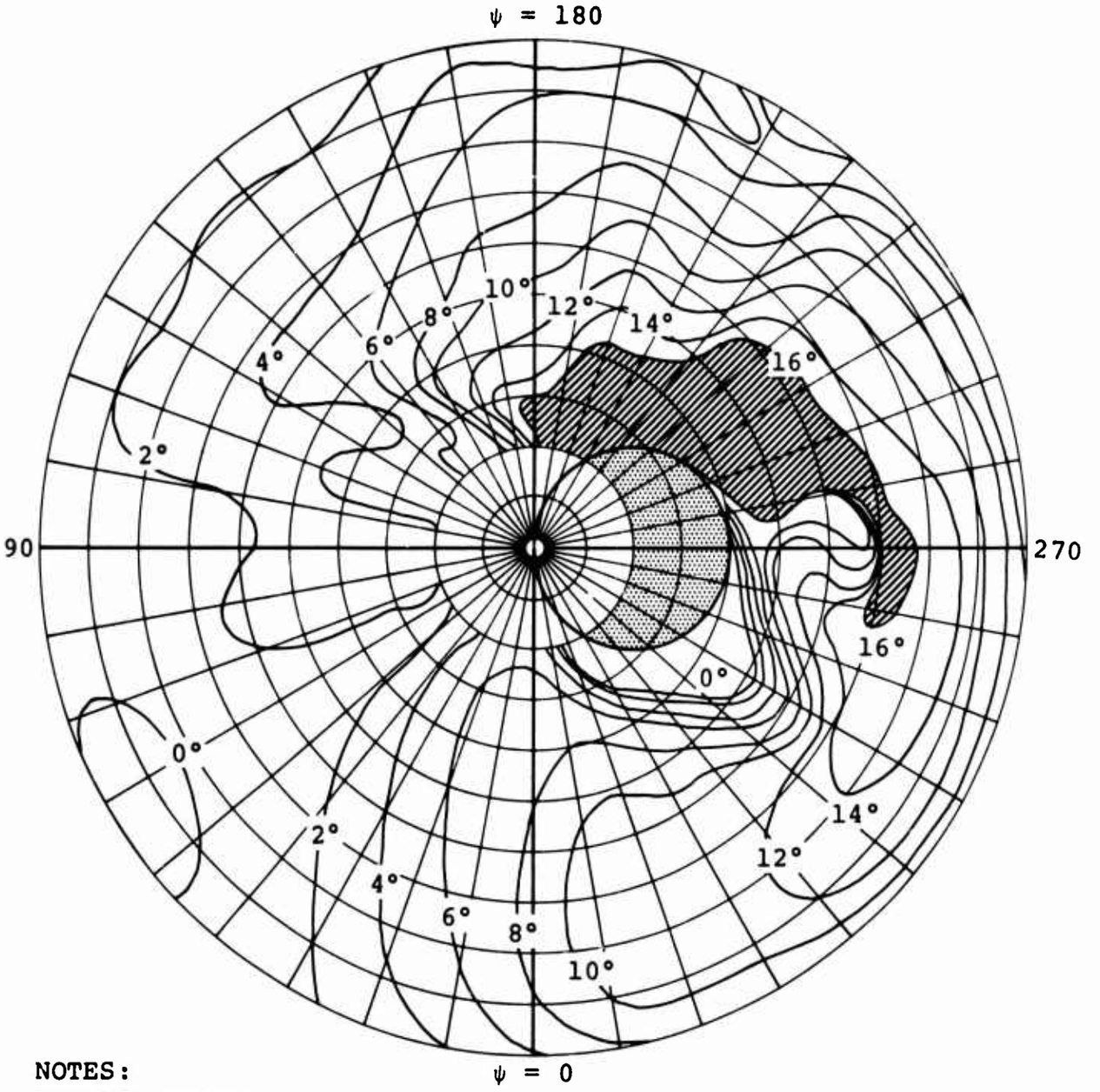

NOTES:

1. Aft rotor
2. Gross weight 87,000 pounds
3. Sea level standard
4. Airspeed 165 knots
5. θ_t = -10 degrees
6. $C_{T1}/_{\sigma}$ = 0.08932
7. $\mu \cong 0.03928$

Reverse flow region

Angles of attack greater than 16 degrees

Figure 23. Angle-of-Attack Distribution of the Tandem-Lift Rotor at 87,000 Pounds, Sea Level, 165 Knots.

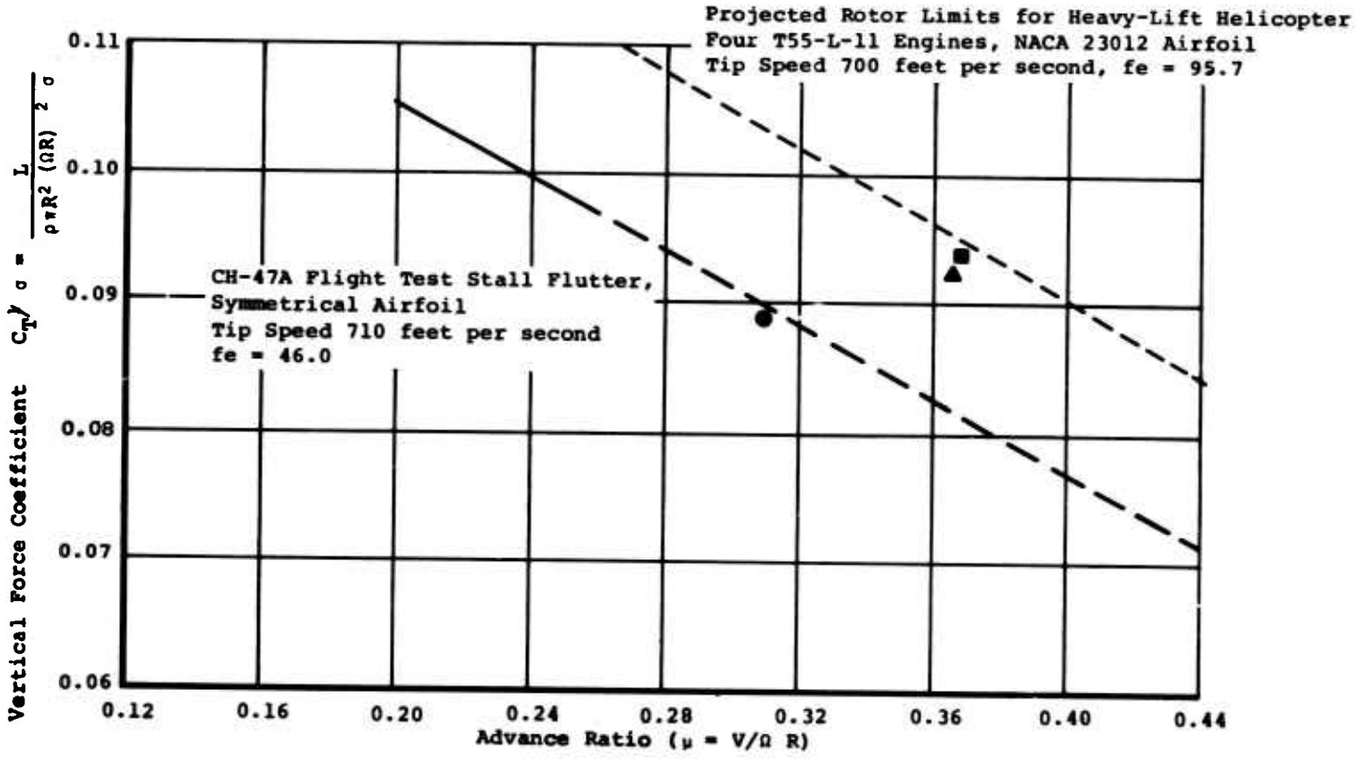

NOTES:

- ● = CH-47 aft rotor
  Gross weight 28,290 pounds
  5000 feet, standard
- ▲ = Heavy-lift helicopter aft rotor
  Gross weight 87,000 pounds
  Sea level, standard
  Normal-rated power
- ■ = Heavy-lift helicopter aft rotor
  Gross weight 75,700 pounds
  5000 feet, standard
  Normal-rated power

Figure 24. Projected Rotor Limits for Continuous Cruise.

that of the transport, the same rotor geometry is considered desirable, with resulting increases in hover capability, or payload.

As indicated in the description of rotor radius, any of several engines may be used with the selected rotor radius. The rotor system geometry is therefore applicable to different fuselage types and to several different engines. As a demonstration of this, the final weights and performance values of six tandem versions (three engine combinations for each fuselage) are derived in a subsequent section.

OPTIMIZATION OF SINGLE-LIFT/ANTITORQUE ROTOR SYSTEM

Essentially the same procedure as for the tandem-lift was used for optimizing the single-lift/antitorque rotor. On the basis of the results of the tandem-lift rotor study, a blade twist of -12 degrees, an NACA 23012 airfoil, and a hover $\bar{C}_L = 0.6$ were selected and used throughout the study. Rotor radius, tip speed, and blade chord were then selected from tradeoff studies conducted on the parametric computer program, taking into consideration the empty weight, gross weight mission fuel weight, and hover required. Figures 25 and 26 are examples of these tradeoff studies. The following rotor geometry results from the optimization:

1.	Rotor radius	48 feet
2.	Blade chord	4.0 feet
3.	Tip speed	700 feet per second
4.	Blade twist	-12 degrees
5.	Number of blades	5
6.	Transmission rating	15,500 shaft horsepower

FINAL WEIGHTS AND PERFORMANCE

Final weights and performance values were calculated for the single-lift/antitorque rotor system and the tandem-lift rotor system using several fuselage and engine combinations to demonstrate the applicability of the optimized rotor systems.

The single-lift/antitorque rotor system is shown for both the transport and the crane/personnel carrier with four 501-M26 engines. The tandem-lift rotor system is shown with both

ure 25. 12-Ton Mission Weight and Performance Study
for Single-Lift/Antitorque Rotor Transport.

A

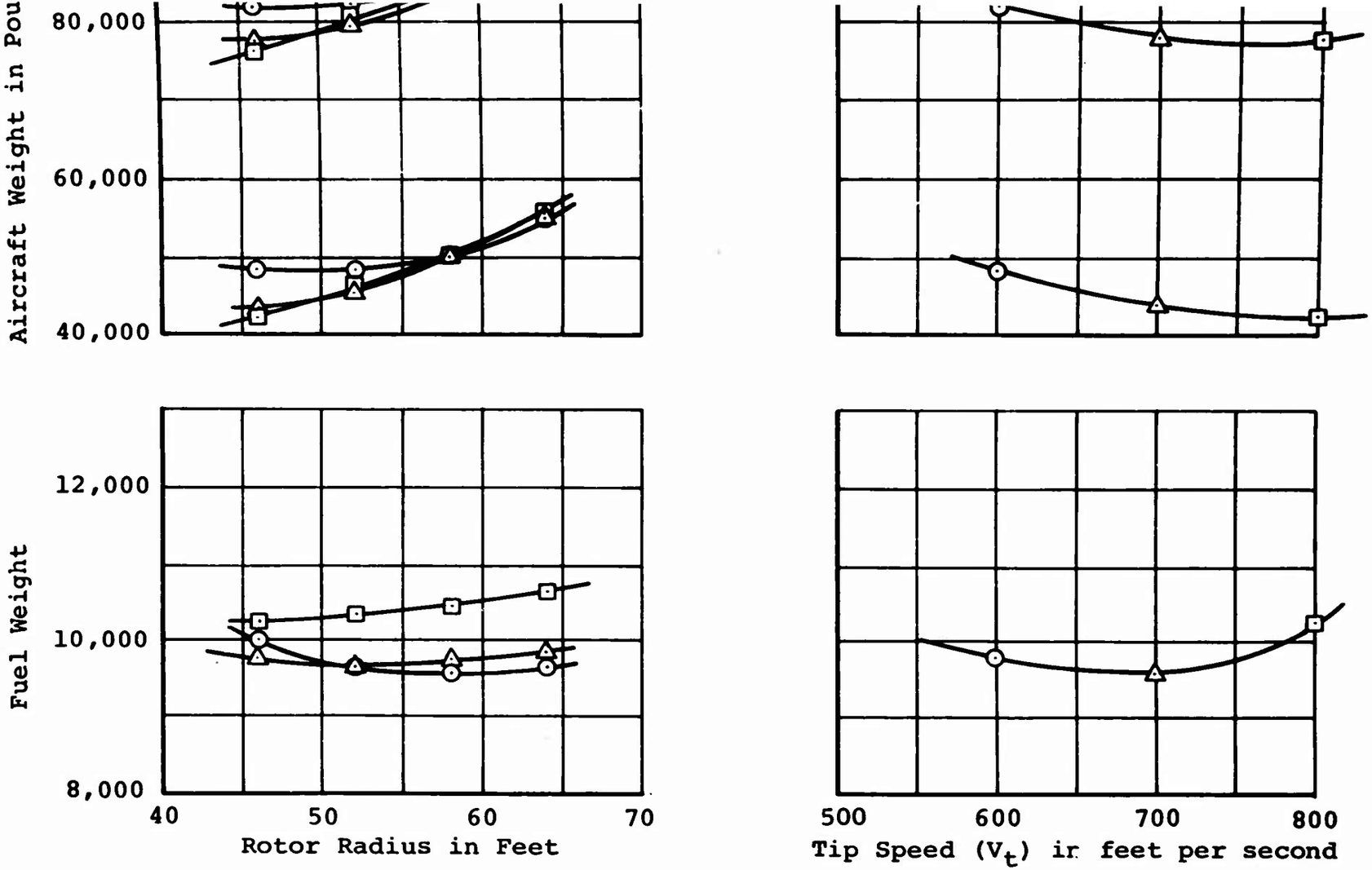

NOTES:

1. Single-lift/antitorque rotor transport; advanced construction; 12-ton mission
2. Cargo compartment 144 inches wide, 108 inches high, 540 inches long
3. Four engines
4. Five-blade rotor:
   Radius = 48 feet
   Airfoil = NACA 23012
   θ_t = -12 degrees
   $\bar{C}_L$ = 0.6
5. Tip speeds in feet per second:

   ⊙ = 600
   △ = 700
   ⊡ = 800

Figure 26. 12-Ton Mission Weight and Performance Study for Single-Lift/Antitorque Rotor Crane/ Personnel Carrier.

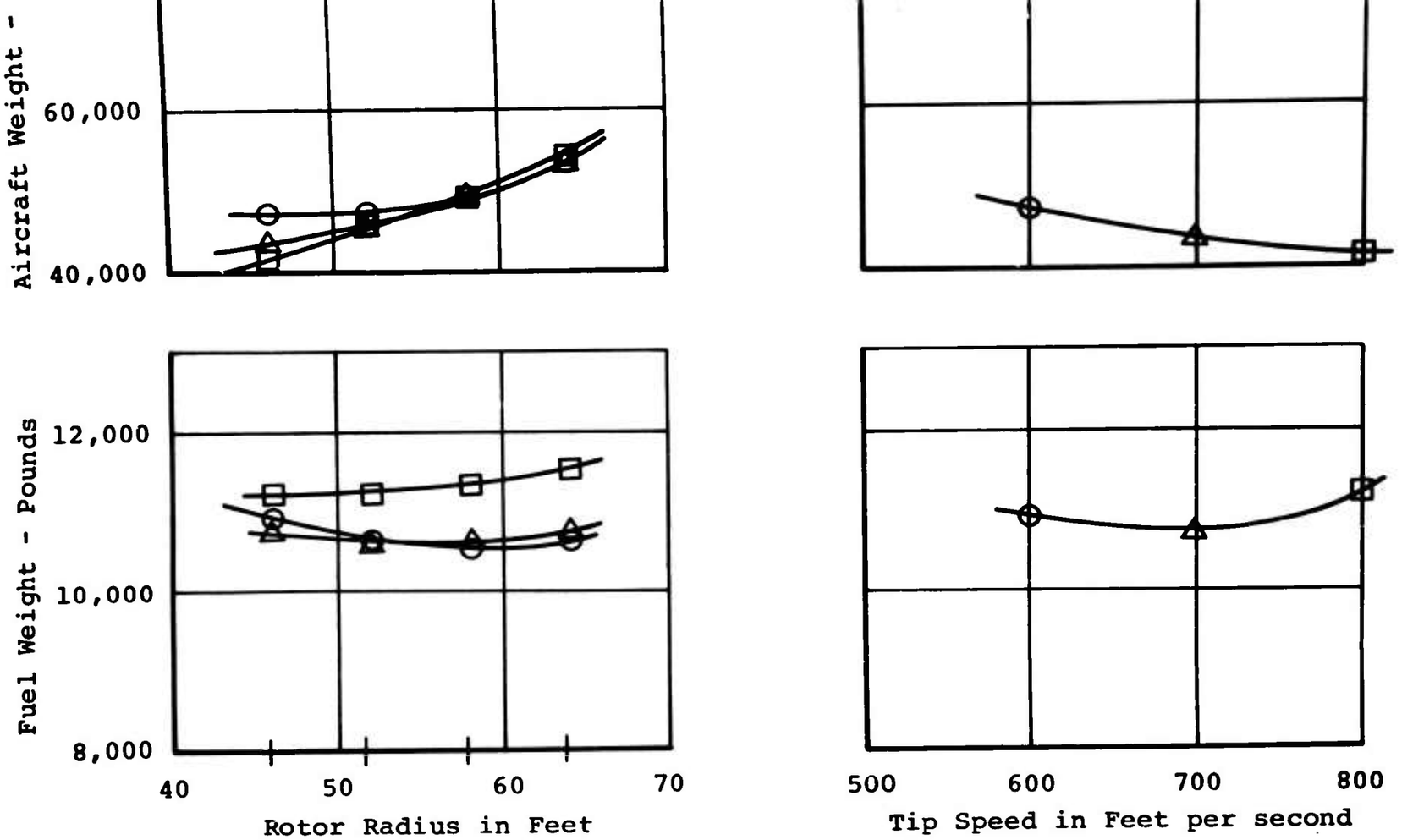

NOTES:

1. Single-lift/antitorque rotor crane/personnel Carrier; advanced construction, 12-ton mission
2. Cargo compartment 144 inches wide, 108 inches high, 540 inches long
3. Four 501-M26 engines
4. Five-bladed rotor:
   Radius = 48 feet
   Airfoil = NACA 23012
   θ_t = -12 degrees
   $\bar{C}_L$ = 0.6
5. Tip speeds in feet per second:
   ⊙ = 600
   △ = 700
   ⊡ = 800

fuselages for each of three engine combinations (three 501-M26's, four T55-L-11's, and four T64/S4A's), which results in a total of six versions.

Group Weight Estimates

Having defined the final configurations, the group weights were established using the selected transmission ratings and rotor geometry, and actual engine weights. These are shown in the summary weight statements for two single-lift/antitorque rotor configurations with four 501-M26 engines and two tandem-lift rotor configurations with four T55-L-11 engines. Overall adjustments to the tandem-lift rotor configuration's empty weight are made to reflect also the three 501-M26 engines or four T64/S4A engines, the reiterations from the rotor detail design study, and the drive system weights estimated by building-block methods.

Mission Fuel Weights

The missions were then recalculated using appropriate fuel flow for each engine, and final mission fuel weights were determined, considering each of several cruise speeds.

Ferry Range Calculations

The ferry range calculations were performed by determining the 99-percent optimum specific range versus gross weight for each of several altitudes. A 10,000-foot operational limit was conservatively assumed to allow missions without the need of oxygen or pressurization equipment. Operation with one engine shut down was also considered for the tandem-lift rotor configuration; it was found to provide superior range characteristics. For the single-lift/antitorque rotor machine, operation is shown with two engines shut down, since this is required to provide the best matching of engine fuel flow characteristics with aircraft power required.

Weights and Performance Summary

Table IV shows the results of these final weight and performance estimates; from it one may make the following observations:

1. The optimized single-lift/antitorque rotor machine has a gross weight for the transport mission 6000

pounds greater than the optimized tandem-lift rotor configuration. The required transmission rating is 3500 shaft horsepower greater, and the required fuel is 2200 to 1000 pounds greater, depending on the powerplant of the tandem-lift rotor configuration with which it is compared.

2. For the tandem-lift rotor configuration, the effect of engine selection on gross weight for the transport (12-ton) mission is small -- 700 pounds at most-- but the effect on fuel weight can vary as much as 1000 pounds.

3. The gross weight of the tandem-lift rotor transport is about 1600 pounds heavier than that for the tandem crane/personnel carrier, for the required transport mission. However, for this comparison, the pod weight was neglected and considered to be part of the 12-ton payload. Since the pod would weigh considerably more than 1600 pounds, the gross weight for the crane/personnel carrier would be more than that for the transport if the pod weight were considered to be other than payload.

4. The tandem-lift rotor configuration performs the transport mission (12-ton payload) at cruise speeds up to 167 knots with the transport type fuselage, and up to 150 knots with the crane/personnel carrier fuselage.

5. The performance reserve in hover is as much as 4900 pounds for the three-engine 501-M26 configuration at 6000 feet, 95°F. As pointed out previously, this has been achieved with no penalty in the efficiency of performing the mission.

6. The required ferry range of 1500 nautical miles can be achieved with all configurations, although the ferry range of the crane/personnel carrier is 100 nautical miles shorter than that of the transport. More than 1900 nautical miles can be achieved with both the three-engine 501-M26 installation and the four-engine T64/S4A installation.

CONFIGURATION SELECTION

A review of derived weight empty and fuel weight shows significant margins in favor of the tandem-lift rotor configuration. This and the other margins forming "sufficient conditions" for the selection of a configuration indicate that the tandem-lift rotor configuration should be chosen over the single-lift/anti-torque rotor configuration. The favorable margins forming the sufficient conditions are:

1. Weight empty
2. Fuel weight
3. Power required
4. Large cubage
5. Great center-of-gravity range
6. Hover attitude control independent of center-of-gravity positions.

Table IV summarizes some of the margins in favor of the tandem-lift rotor configurations.

EFFECT OF MISSION CRUISE SPEED ON PAYLOAD

Figure 27 shows the effect of cruise speed on the transport mission payload for three tandem-lift rotor versions of different drag values, all with T55-L-11 engines. It is assumed that the aircraft are operating at the maximum gross weight for hovering out of ground effect at 6000 feet, 95°F. It can be seen that as the outbound speed increases from the required 110 knots, the payload increases, reflecting the better specific range, until the best range speed is attained. For the transport version, the best range speed is 130 knots, at which point the payload can be 25,400 pounds. An outbound maximum cruise speed of 167 knots is possible, with a payload of over 12 tons. The maximum cruise speed of the crane/personnel carrier is limited to 150 knots, but it has a payload at that speed of over 13 tons, including the pod weight. For the transport mission, the weight penalty of retractable landing gear precludes any net benefit unless the speed requirement is increased to 160 knots or higher.

The heavy-lift helicopter inherently has high speed and ferry range potential due to the 6000-foot, 95°F hover requirement and the relatively high ratio of gross weight to flat-plate area associated with a large aircraft. Because of its long landing gear structure and the downward extension of the crew cabin for the loadmaster's station, the crane/personnel carrier has greater drag than the transport. The ferry ranges are correspondingly shorter. Speed and ferry range can be increased by the following:

1. Improve drag characteristics of hub and pylons.

2. Use regenerative engines to decrease the specific fuel consumption.

3. Shut down some engine(s) when operating at low power to decrease the specific fuel consumption.

4. Use yawed flight to increase span loading and to decrease induced power at the altitudes for best range.

EXPLORATORY DYNAMICS STUDY

A brief dynamics study investigated the effect of number of blades on hub vibratory forces for the following cases:

1.	Number of blades	3 and 4
2.	Gross weight	87,000 pounds
3.	Helicopter cg position	8 inches forward
4.	Rotor tip speed	700 feet per second (1555 rotor rpm)
5.	Airspeed	130, 150, and 170 knots

Rotor loads were determined by a comprehensive structural rotor analysis which considered nonuniform downwash effects. Blade structural properties were derived by scaling-up CH-47A blade properties.

Natural frequency spectra were obtained for both rotors to ensure dynamic similarity between the blades. The spectra presented in Figure 28 show the blades to be very similar.

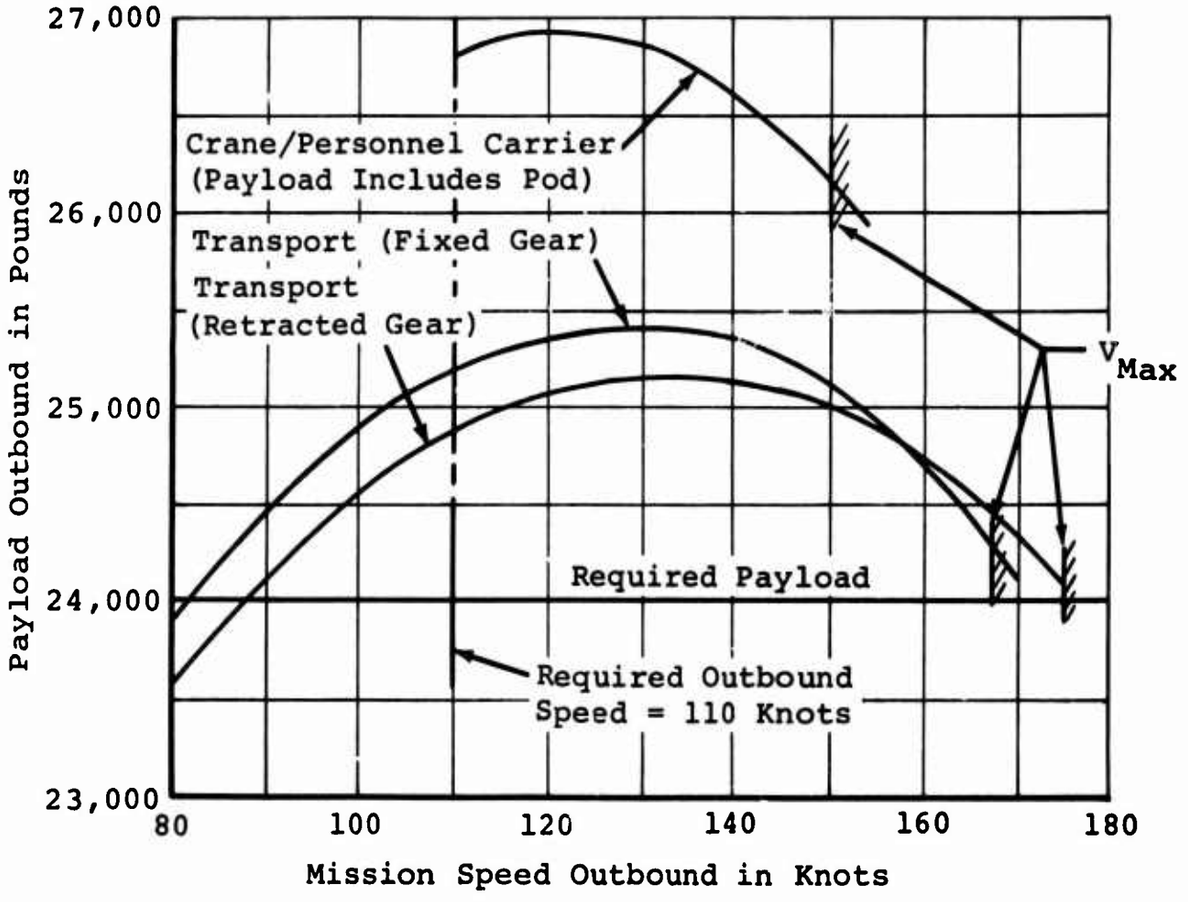

NOTES:

1. 100 nautical-mile radius 12-ton transport mission
2. Internal payload outbound only
3. Inbound cruise speed same as outbound cruise speed, but at least 130 knots
4. Load to maximum hover gross weight at 6000 feet, 95°F
5. Five minutes hover; 10-percent fuel reserve
6. Four T55-L-11 engines
7. Weight and Drag:

	Flat Plate Area (square feet)	Weight Empty (pounds)	Maximum Hover Gross Weight (pounds)
Transport (fixed gear)	95.6	42,224	77,300
Transport (retracted gear)	74.0	42,877	77,300
Crane/personnel carrier	138.6	39,769	77,100

Figure 27. 12-Ton Mission Speed and Payload Capability of Tandem-Lift Rotor Helicopter.

The first bending mode is placed between 2 and 3 per revolution, far enough below the control 3 per revolution amplification for the three-bladed rotor. The next mode, second flap bending, is placed near 5 per revolution, free from amplification of 4 per revolution for the four-bladed rotor. Third bending is between 7 and 8 per revolution, the specific location being related to the coupling occurring with the torsion mode in the same region.

Rotor hub vibratory forces (shaking forces), both vertical and in-plane, are presented in Figures 29 and 30 as 3 per revolution for the three-bladed rotor and as 4 per revolution for the four-bladed rotor. These are the predominant forces in each case. Both graphs indicate reduced forcing levels obtained for four-bladed rotors. The effects of these forcing functions on the aircraft vibration level are not indicated, since no consideration of fuselage response characteristics is possible at this stage of the design.

Although the force level is analytically reduced with the four-bladed configuration, it alone is not a guarantee of low vibration level. The fuselage response is still a key factor in obtaining the overall response. In the detail design stage, a fuselage analysis must be conducted to determine the fuselage natural modes and the forced response of the aircraft to these calculated rotor loads. The structural analysis program used at Vertol Division has proven to be more accurate than past efforts which used EI and GJ representations. Instead, the fuselage is represented by its skin and stringers, a structural matrix is formed, and then a dynamic matrix is formed from that. The natural modes and frequencies obtained have proven to be reliable when checked against ground shake tests.

As the fuselage design progresses, the analysis can be used to determine modal locations and forced amplitude. If a three-bladed rotor is used, then the stiffness properties can be designed so that the modes are located away from 3 per revolution, or similarly away from 4 per revolution for a four-bladed design. In this manner, reasonable assurance of an acceptable vibration level can be made for a new aircraft.

A more detailed dynamics analysis, including fuselage response to hub loads, is described in STATIC AND DYNAMIC STRUCTURAL ANALYSIS. The illustrations shown here (Figures 28, 29, and 30) are for comparative purposes only. This four-bladed rotor dynamics analysis has been included to project the growth of the heavy-lift helicopter.

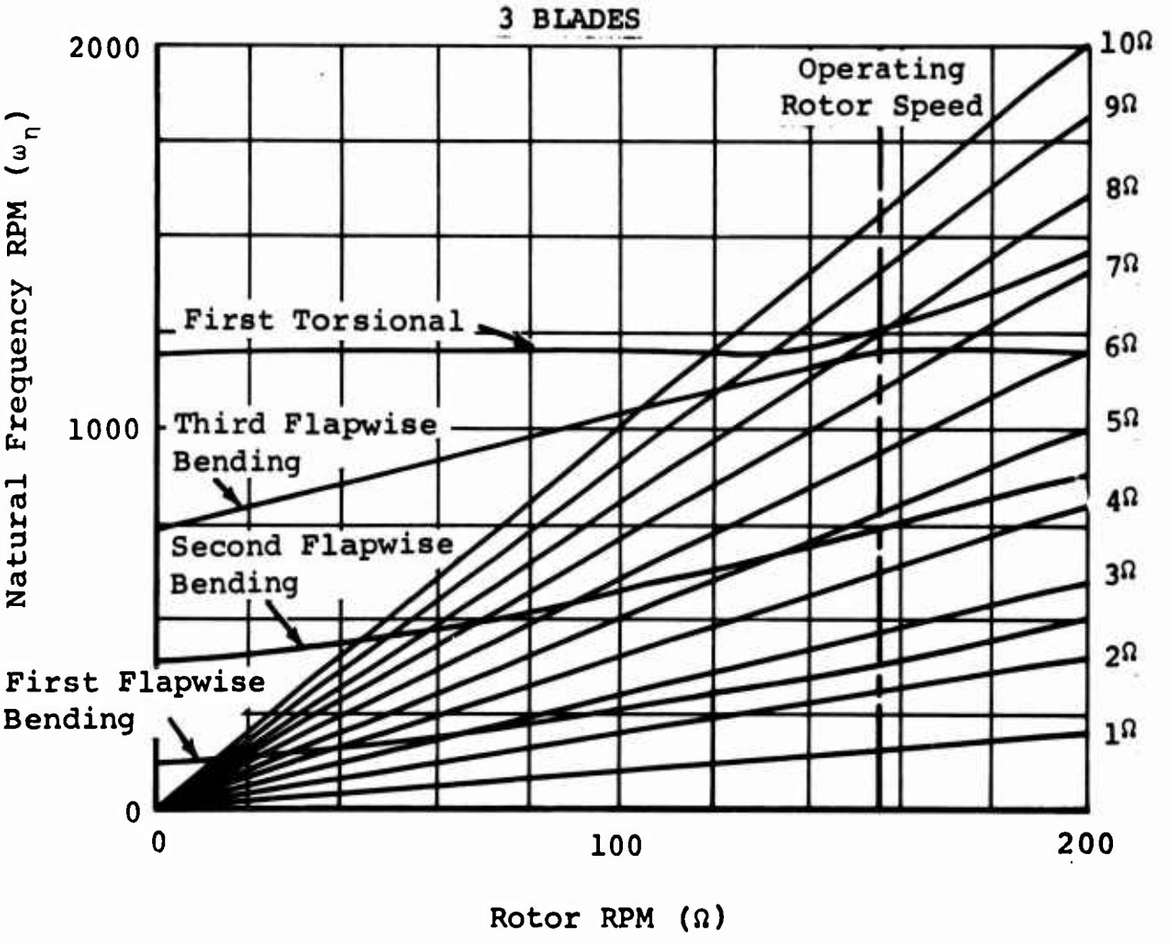

NOTES:
1. Tandem-lift rotor transport
2. Blade radius 45 feet
3. Blade chord 42 inches

Figure 28. Natural Frequency Spectra of Three- and Four-Bladed Rotors. (Sheet 1 of 2)

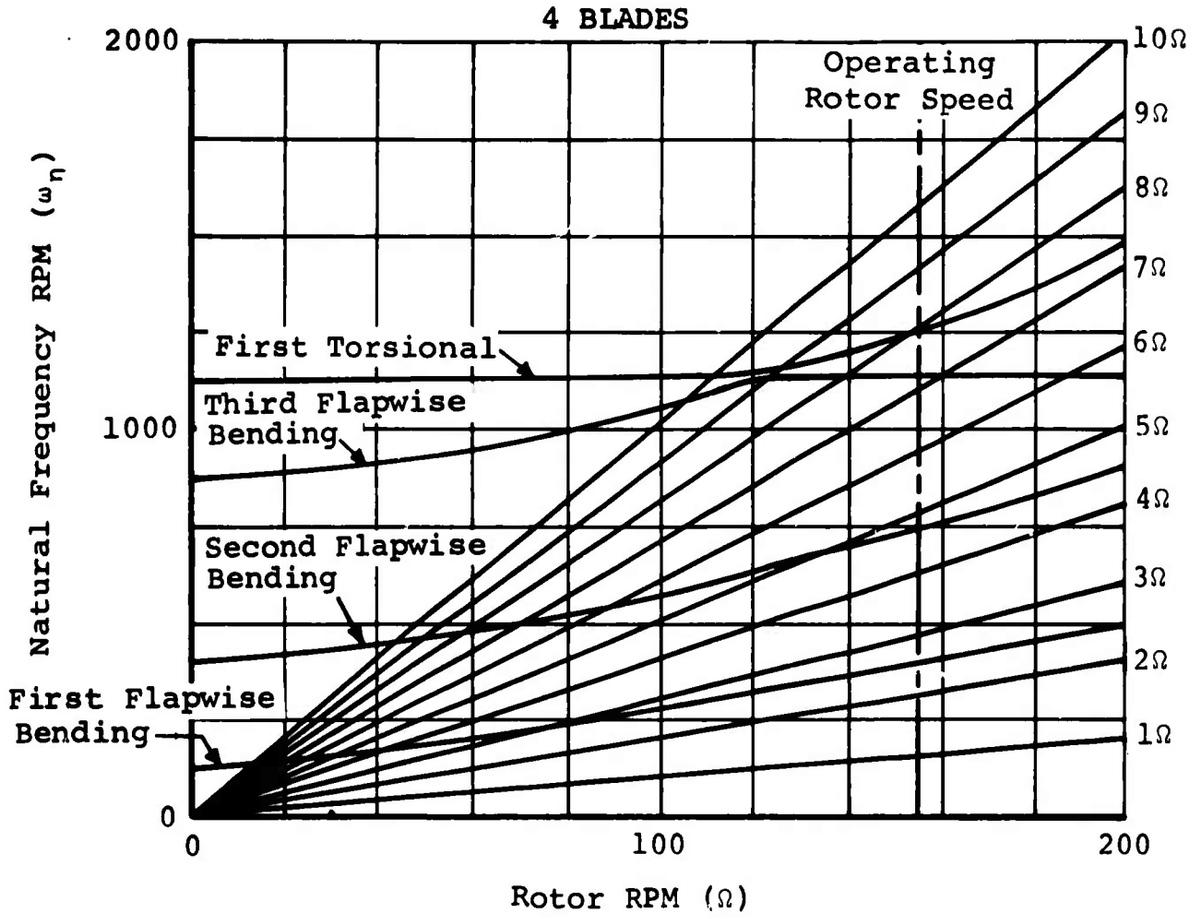

NOTES:
1. Tandem-lift rotor transport
2. Blade radius 43 feet
3. Blade chord 31.5 inches

Figure 28. Natural Frequency Spectra of Three- and Four-Bladed Rotors. (Sheet 2 of 2)

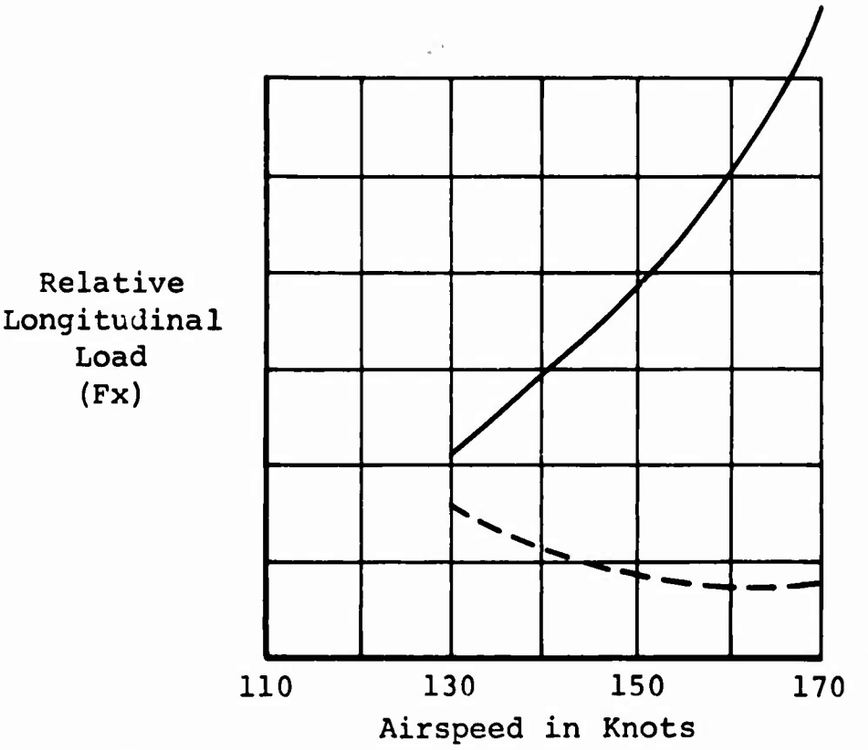

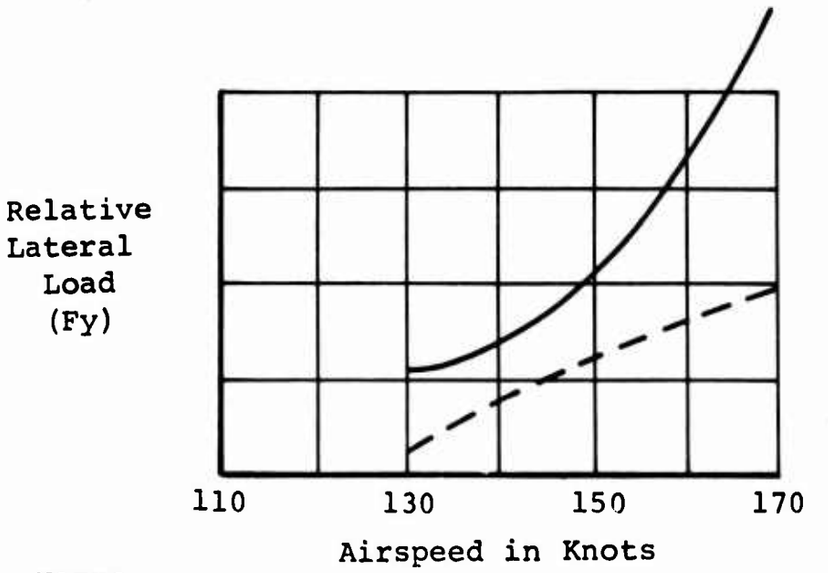

NOTES:

1. Tandem-lift rotor transport; gross weight 87,000 pounds; cg 8.01 inches forward
2. Blade radius 43 feet
3. _____ 3 blades 3Ω in-plane hub loads
   ------ 4 blades 4Ω in-plane hub loads

Figure 29. In-Plane Hub Loads.

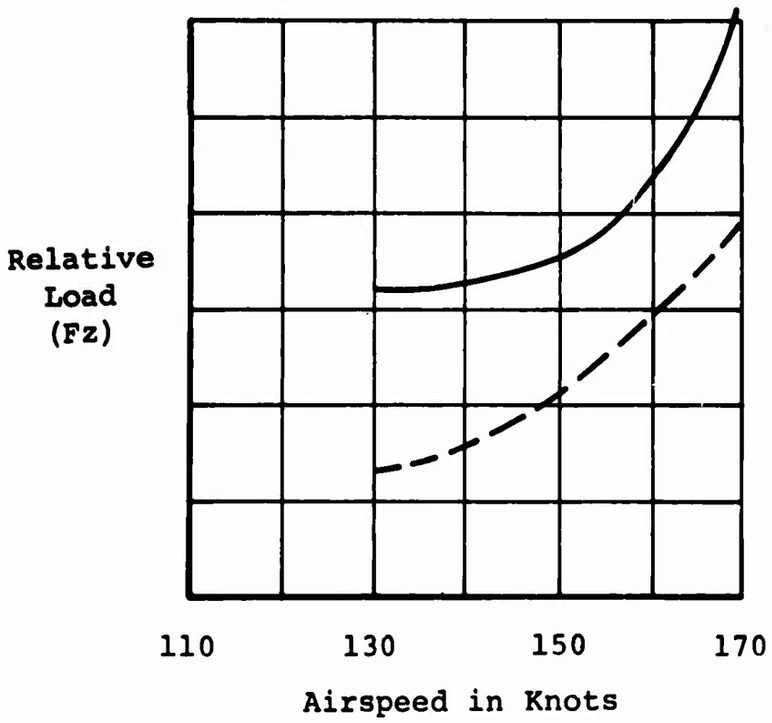

NOTES:
1. Tandem-lift rotor transport, gross weight 87,000 pounds; cg 8.01 inches forward
2. Blade radius 43 feet
3. _____ 3 blades 3Ω vertical hub loads
   ------- 4 blades 4Ω vertical hub loads

Figure 30. Vertical Hub Loads.

STABILITY, CONTROL, AND FLYING QUALITIES

Using the results of NASA-Langley and USAAVLABS investigations as guidelines (References 2, 5, 6, and 17), Vertol Division has analyzed the mission of the heavy-lift helicopter and has developed requirements on control power and sensitivity that will assist the pilot in the performance of his assigned task. The helicopter characteristics used to calculate stability and control requirements are as follows:

1. Inertia about X-axis 218,000 slug feet squared
2. Inertia about Y-axis 1,315,000 slug feet squared
3. Inertia about Z-axis 1,550,000 slug feet squared
4. Maximum gross weight 87,000 pounds
5. Minimum flying weight 40,000 pounds
6. Flat-plate drag area 96.5 square feet
7. Forward rotor shaft tilt 9 degrees
8. Aft rotor shaft tilt 4 degrees
9. Distance between rotors 59.5 feet
10. Cg 28.5 inches aft to 70.0 inches forward of centerline between rotors

ANALYSIS OF MISSION REQUIREMENTS

Longitudinal (Pitch) Control

The longitudinal (pitch) control requirement is of prime importance to the heavy-lift mission. High control power is needed to allow internal loading versatility and to provide maneuverability in operations with both internal and external loads. For this reason, in addition to the trim requirement of MIL-H-8501A, paragraph 3.2.1, sufficient control has been provided to generate a pitch attitude change in hover of $292/(W+1000)^{1/3}$ degrees in 1 second with an apparent time constant of 0.5 second. An additional margin of control equal to the moment change due to the critical cyclic trim failure is also provided.

Lateral (Roll) Control

The lateral (roll) control arises from the trim requirement of MIL-H-8501A, paragraph 3.3.9, with an additional maneuver margin. Although this provision is in excess of that required by MIL-H-8501A, it allows a roll maneuver capability with a 0.3-second time constant at all flight conditions.

Directional (Yaw) Control

The directional (yaw) control requirements are small in forward flight since coordinated turns are made with lateral and longitudinal controls, and trimmed sideslip requirements are modest (see Figure 31). The yaw control, then, arises from the necessity to provide maneuverability in hover. The total yaw control provided is 25 percent greater than that required by MIL-H-8501A, paragraph 3.3.5. In view of the tandem configuration's relative insensitivity to gust disturbance, it is felt that this excess control is sufficient.

Control Power

To ensure that aircraft response characteristics are compatible with the heavy-lift mission, the blade pitch envelopes (see Figures 32 and 33) provide greater hover control powers (radians per second squared) at maximum gross weight and with greater margins than those required by specification MIL-H-8501A:

1. Pitch: 0.14 required, 1.38 provided
2. Roll: 0.27 required, 1.25 provided
3. Yaw: 0.30 required, 0.38 provided

The combined cumulative collective and cyclic blade pitch travels will be limited to 60 degrees of total travel on each rotor as shown in Figure 34. This limit was provided so that the blade pitch travels and actuators will not be overdesigned to provide control that will never be demanded in actual flight conditions. Centrifugal droop stops will permit full freedom of blade flapping motion for full utilization of the blade pitch motions provided.

Control Sensitivity

With the pitch control power provided, the heavy-lift's control

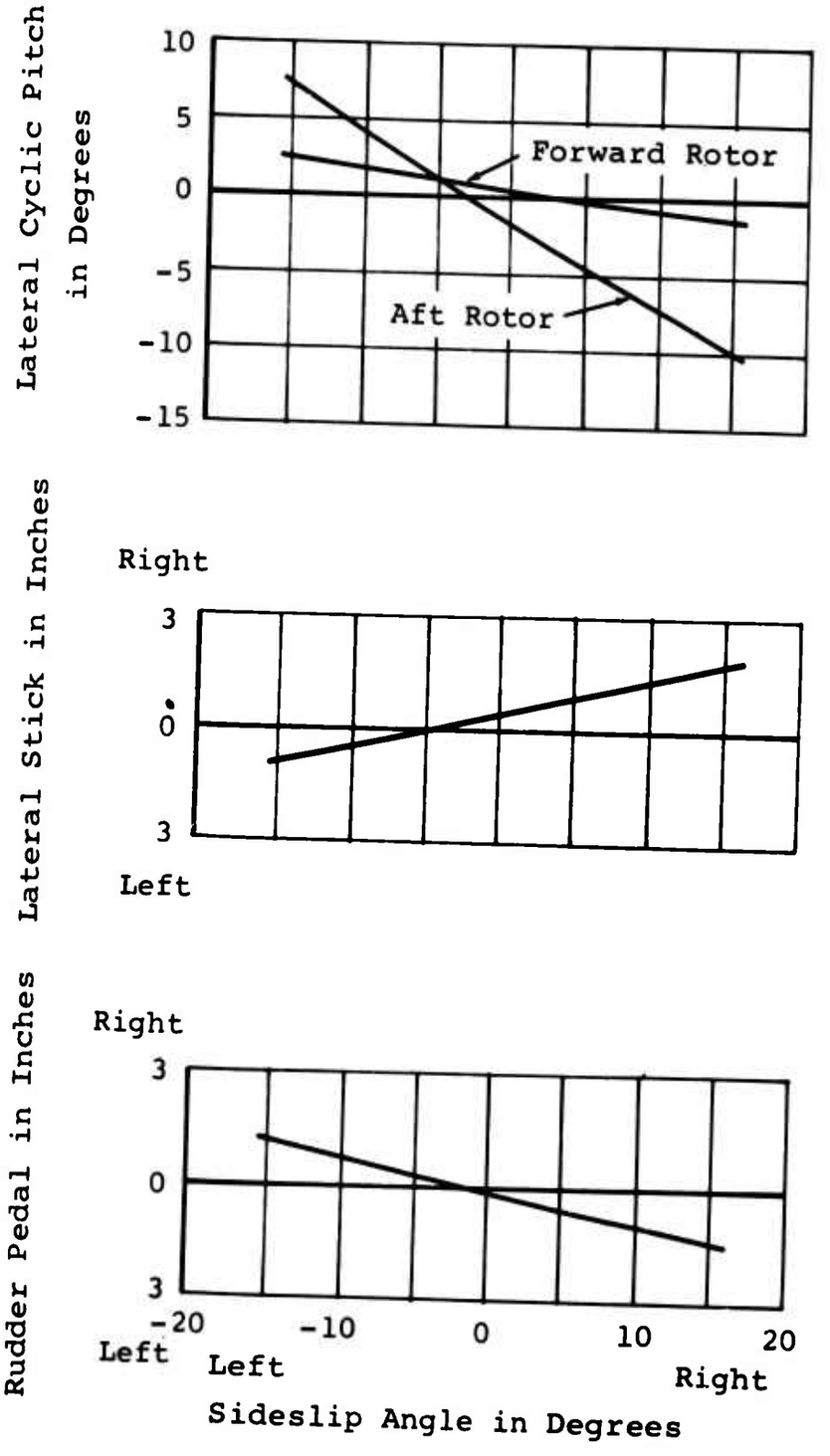

Figure 31. Lateral-Directional Control Requirements in Sideslip Flight at 130 Knots.

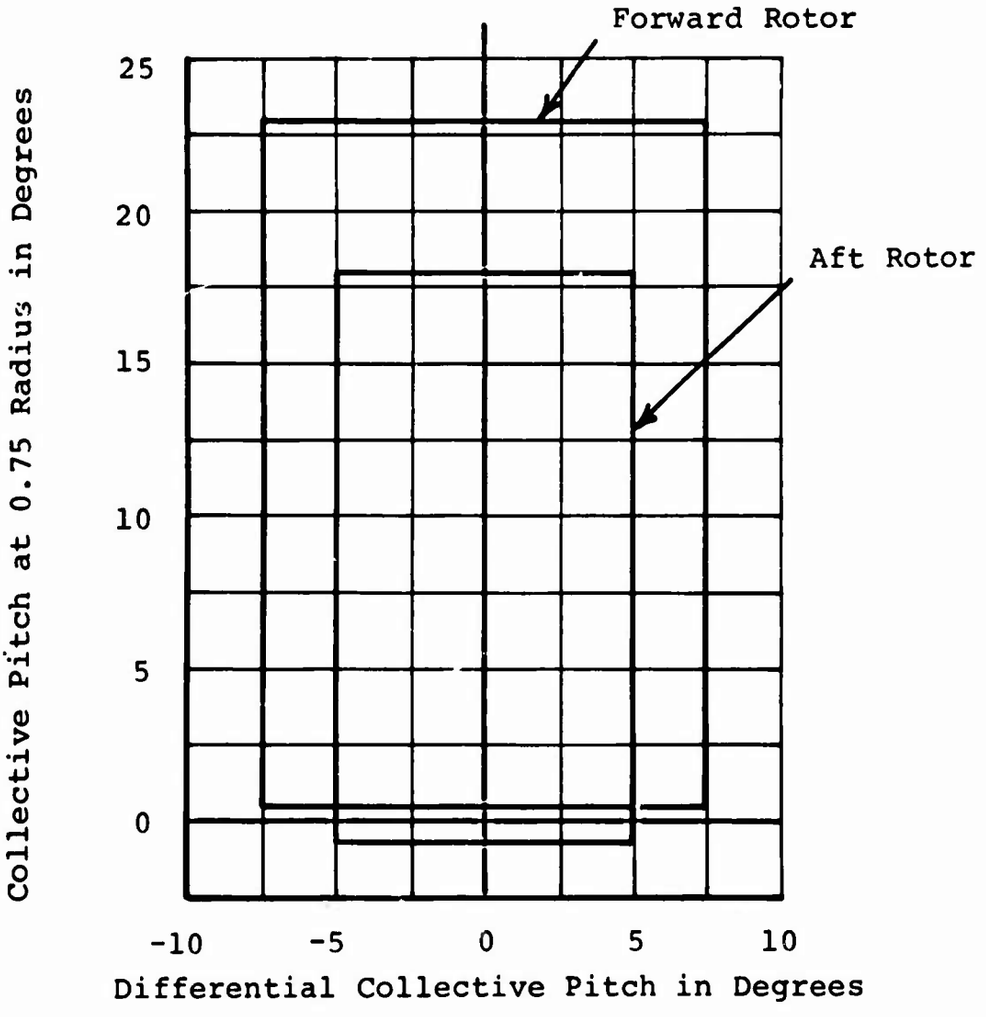

Figure 32. Collective and Differential-Collective Pitch Envelope.

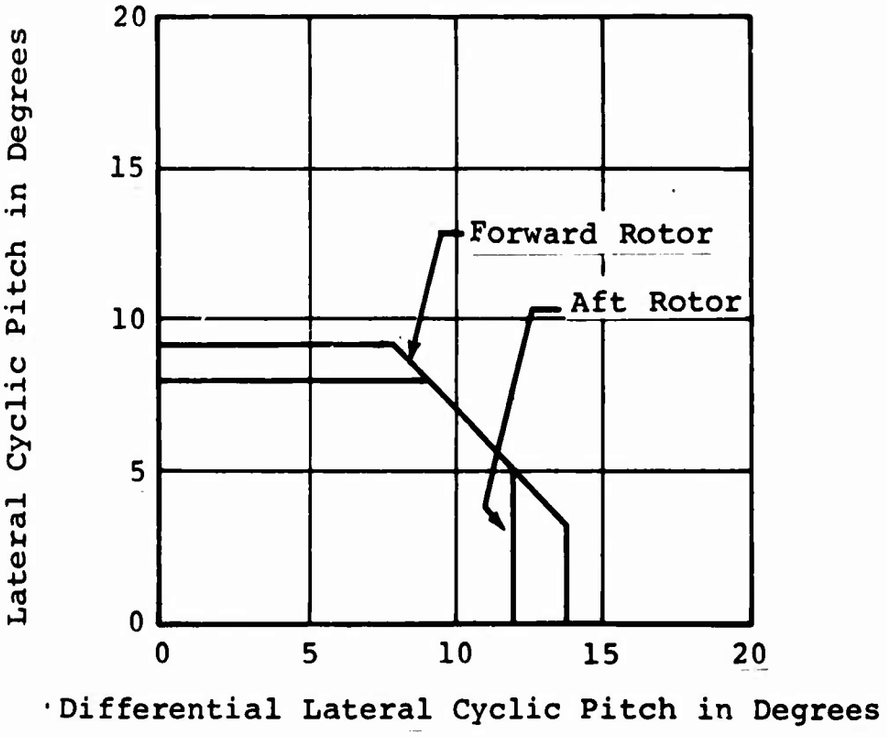

Figure 33. Lateral and Differential-Lateral Cyclic Pitch Envelope.

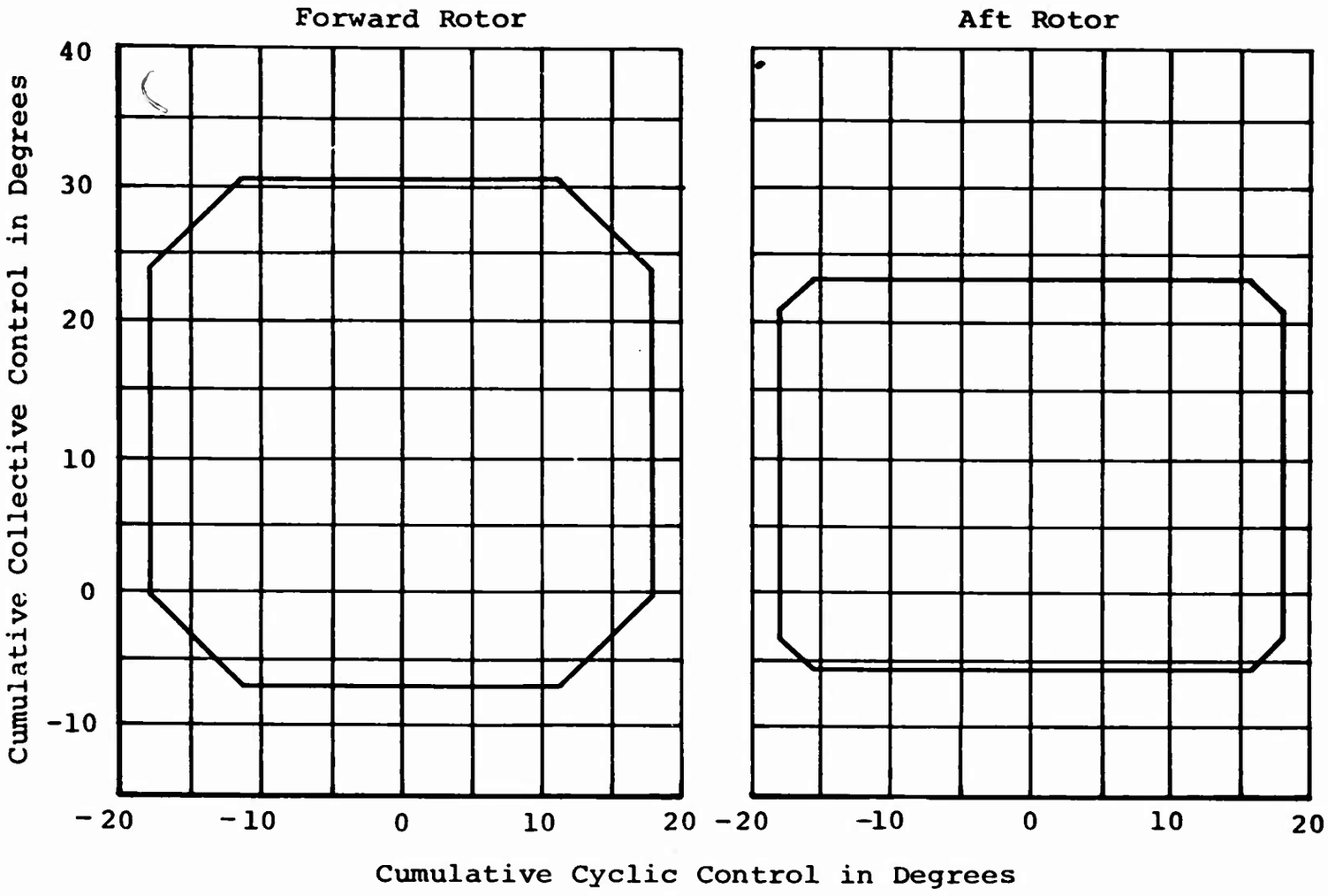

Figure 34. Cumulative Collective and Cyclic Pitch Envelopes.

sensitivity could be established at a level from that of the H-21 up to that of the CH-47 for total control travels less than the HIAD maximum limit of ±7 inches. The maximum control travel was tentatively selected to be ±5.5 inches for the following reasons:

1. The control sensitivity so provided, together with the rate damping level of 4, 1/second, provided by use of the stability augmentation system (SAS), is compatible with NASA-Langley recommendations (Reference 15) and MIL-H-8501A requirements.

2. The sensitivity and damping are compatible with the values for the other axes.

3. The control sensitivity may be increased or decreased as further study warrants.

The hover moment control sensitivities (radians per second squared per inch) at maximum gross weight exceed the maneuver requirements of specification MIL-H-8501A:

1. Pitch: 0.035 required, 0.250 provided; 5.5-inch total control movement

2. Roll: 0.090 required, 0.416 provided; 3.0-inch total control movement

3. Yaw: 0.095 required, 0.125 provided; 3.0-inch total control movement

The yaw control sensitivity listed is without quickening. Quickening used with yaw control would provide an even greater sensitivity for small inputs without increasing the total differential lateral cyclic pitch level.

The angular rate damping about all axes will be augmented with SAS to optimize short-period dynamic characteristics and provide rapid establishment of steady-state rate responses to control inputs. Figures 35, 36, and 37 indicate target levels of SAS-augmented rate damping in hover.

Stability Augmentation

Specification MIL-H-8501A (paragraphs 3.2.10 and 3.3.9) allows a helicopter to be statically unstable in pitch and yaw under

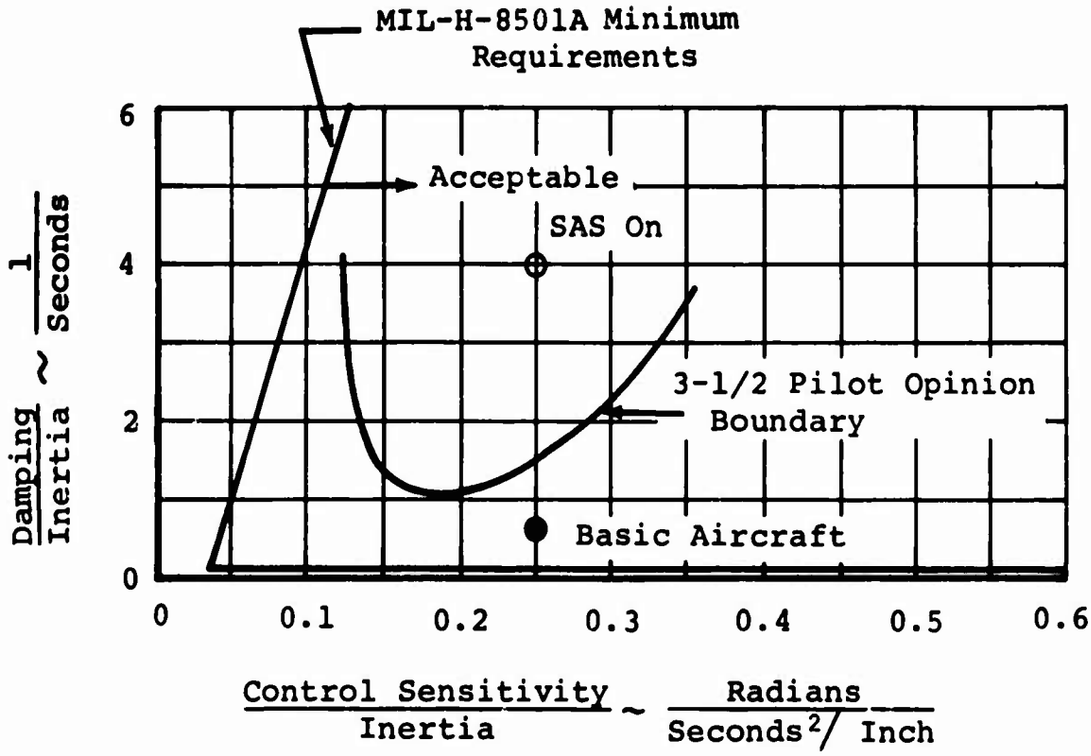

NOTE: Gross weight 87,000 pounds

Figure 35. Pitch Damping and Control Sensitivity in Hover.

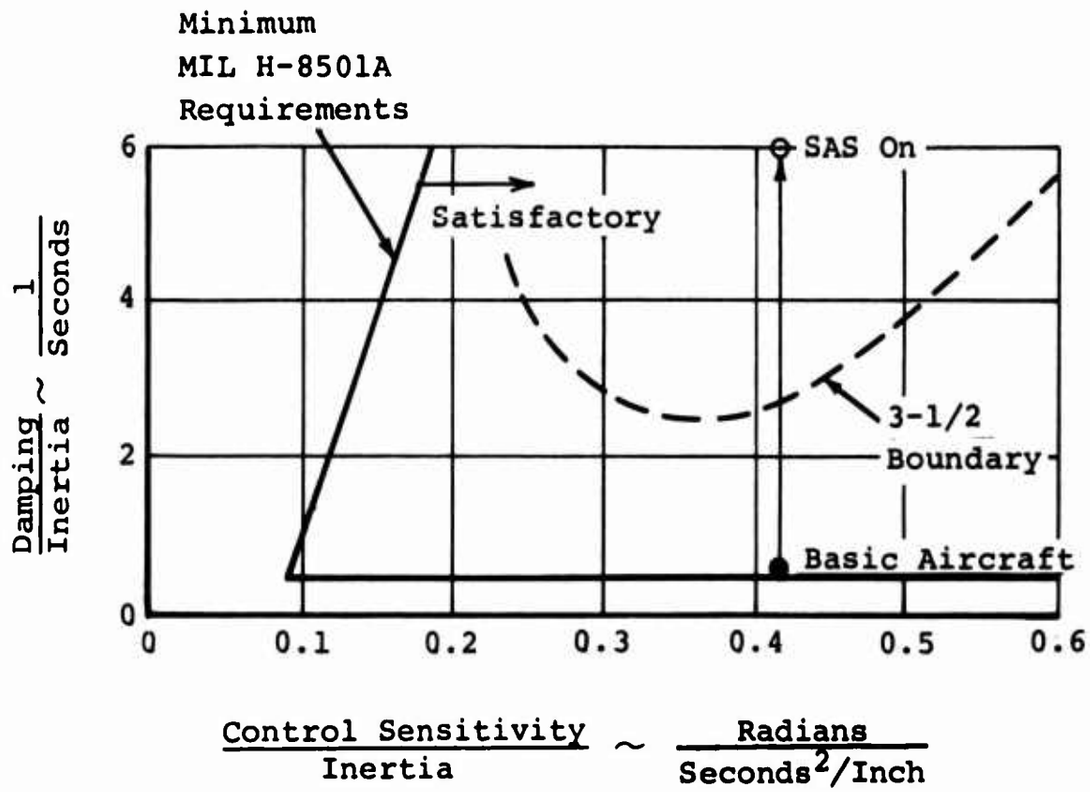

Figure 36. Roll Damping and Control Sensitivity in Hover.

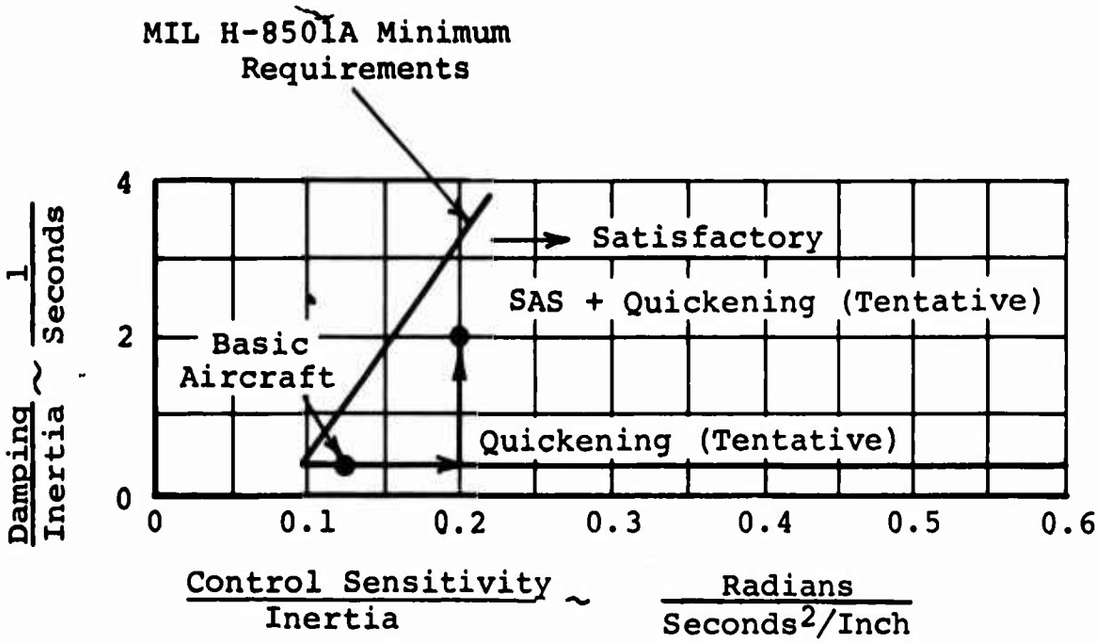

NOTE: Gross Weight 87,000 pounds

Figure 37. Yaw Damping and Control Sensitivity in Hover.

certain flight conditions. Static and dynamic stability requirements may be met through stability augmentation. It is suggested in Reference 24 that a mild degree of instability may be tolerated following a failure in the stability augmentation system. To meet this criterion with center-of-gravity 4-percent aft of the centerline between rotors, the heavy-lift helicopter will be configured with a delta-three rotor and suitable empennage. This criterion will ensure a more natural feel of the aircraft, as less reliance on the SAS will be warranted.

Longitudinal Cyclic Pitch Trim

For pilot comfort and low fuselage drag, q-programmed longitudinal cyclic pitch is used to provide a level fuselage at airspeeds greater than 100 knots. Because of the powerful independent differential collective pitch moment control, this attitude control can be achieved at any gross weight and center-of-gravity location from 30 inches aft to 70 inches forward (Figure 38). In hover, manually-selected aft cyclic pitch is provided to obtain a level attitude for improved visibility and ease in the acquisition of external cargo and straddling of loads.

Flying Qualities

The tandem configuration will not be subject to yaw disturbances in hover created by horizontal gusts. This, together with the level of longitudinal and lateral speed stability will produce desirable spot hovering capability for the heavy-lift helicopter. The high control power provided by DCP and the independent attitude control provided by longitudinal cyclic pitch allows great loading flexibility. Acquisition and off-loading of either internal or external cargo can be accomplished with negligible attitude changes.

The articulated tandem-lift rotor system is not only feasible from a stability and control standpoint (requiring no state-of-the-art advances in technology), but is also an ideal load platform for the heavy-lift mission.

STATIC STABILITY

Satisfactory flying qualities of the heavy-lift helicopter can be ensured by the provision of static stability in the basic helicopter. The benefits are improved longitudinal short-period dynamic characteristics, increased safety and pilot confidence in high-speed SAS-off flight, and a reduction in SAS authority.

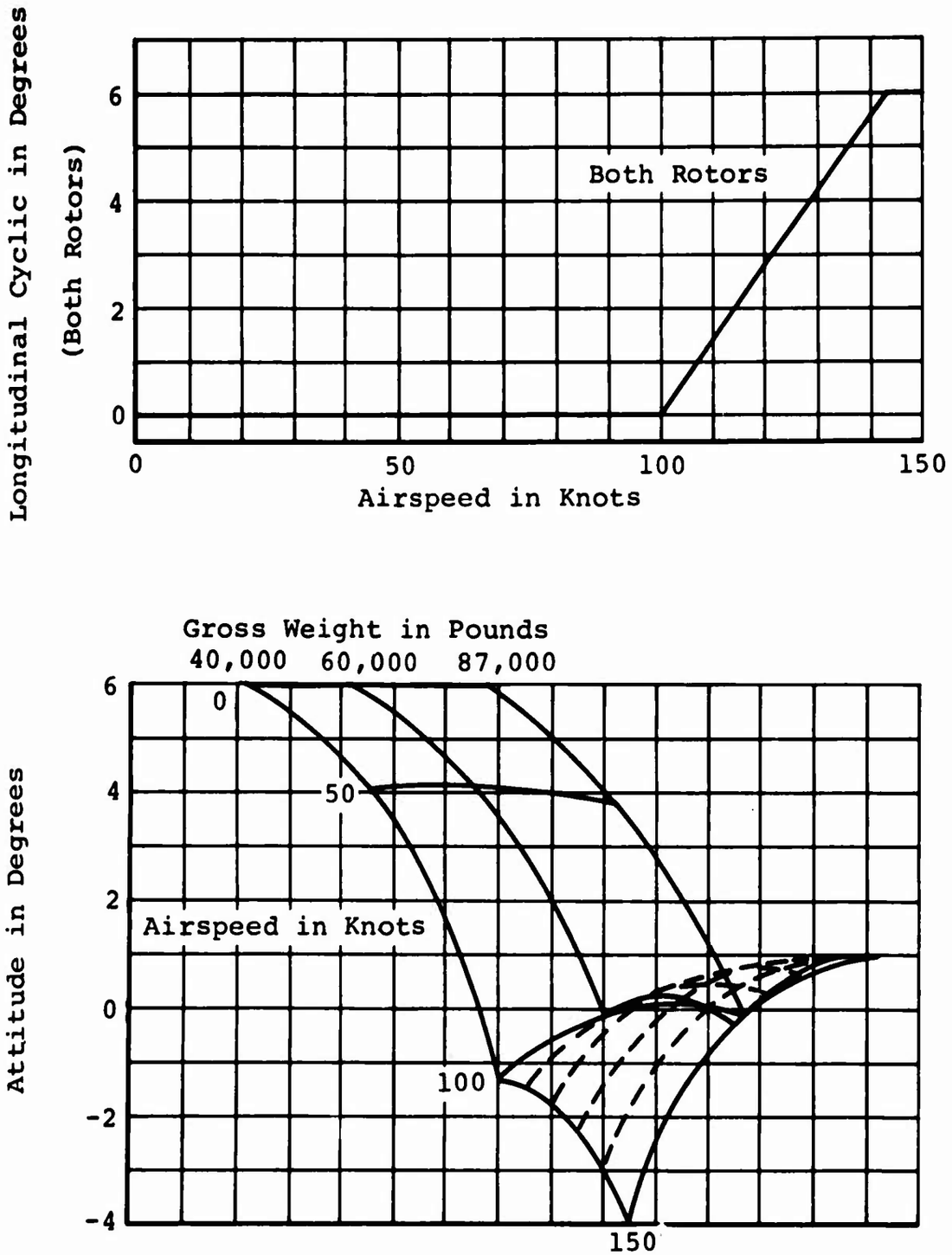

Figure 38. Longitudinal Cyclic Trim.

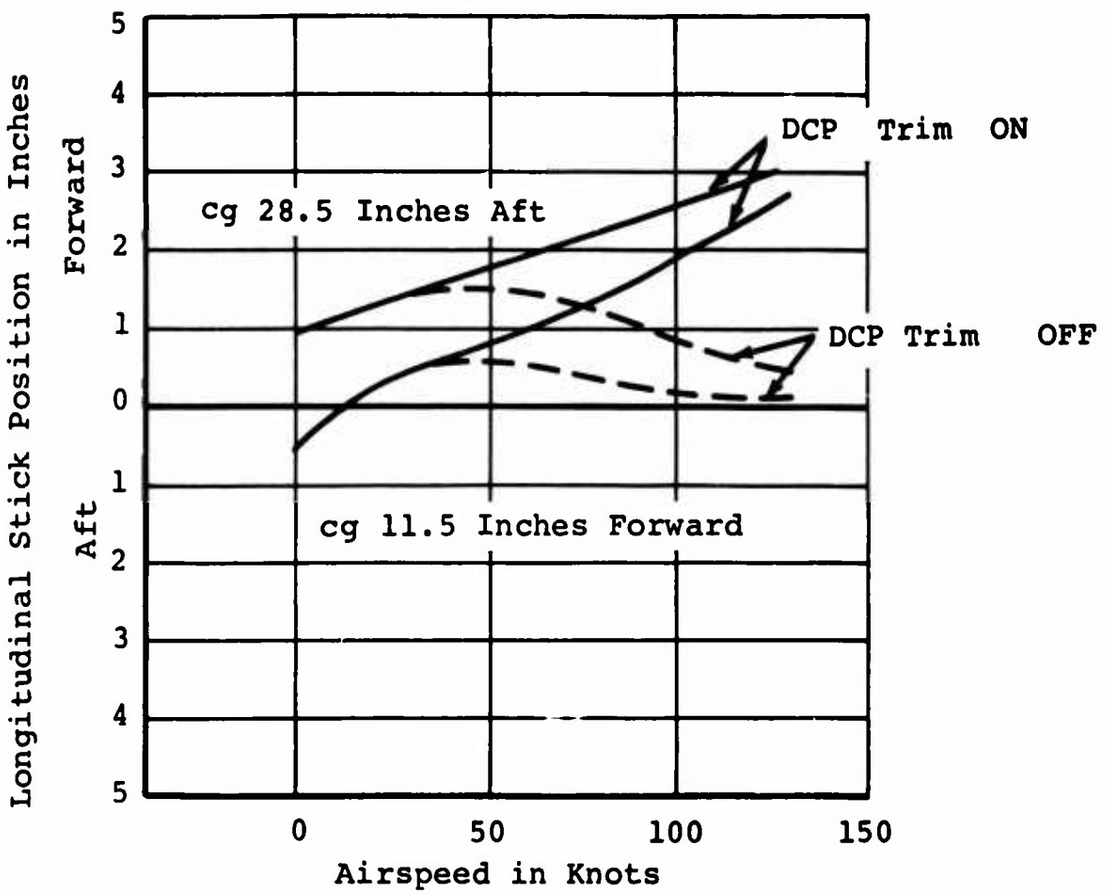

NOTE: Gross weight 87,000 pounds

Figure 39. Stick Position as a Function of Airspeed.

Longitudinal (Pitch) Stability

Three means of providing inherent pitch stability were considered: pitch-flap coupling (delta-three) on the forward rotor, location of the most aft center of gravity, and the use of horizontal stabilizers.

In hover, the angle-of-attack stability derivative is meaningless. With increasing airspeed, the rotor system tends to destabilize the aircraft in pitch because of rotor-on-rotor interference effects. Since the major source of the tandem-lift rotor helicopter's tendency to pitch instability is the rotor system, the heavy-lift will be equipped with 26.5 degrees of delta-three on the forward rotor.

The source of the tandem-lift rotor helicopter's instability with angle of attack is related to the operation of the rear rotor in the downwash field of the front rotor. When the helicopter angle of attack is increased, the rear rotor angle of attack, and hence the rear rotor thrust, increases less than the angle of attack and thrust of the front rotor, because of the increased downwash from the front rotor. The result is a nose-up, and hence unstable, movement. Differential delta-three reduces the lift curve slope of the front rotor, $C_{T\alpha}$, and thus has a stabilizing effect on the composite tandem-lift rotor system.

Delta-three (see Figure 40) is a rotor kinematic system which couples rotor blade flap to rotor blade pitch. This is accomplished by moving the attachment point of the blade pitch arm off the centerline of the flap hinge, thereby reducing changes in collective pitch with coning and in cyclic pitch with flapping.

At a fixed rotor rpm, coning is proportional to rotor thrust, so collective pitch changes with rotor thrust. Increases in rotor angle of attack will increase both the thrust and coning. Therefore, a rotor with delta-three will have a lower rate of change of thrust with angle of attack changes ($\delta T/\delta \alpha$) than a rotor without delta-three because of the reduction in collective pitch which occurs as coning increases.

The term differential δ_3 is used to describe a difference in the pitch-cone coupling characteristics of the forward and aft rotors of a tandem-lift rotor helicopter. The use of a delta-three hinge on only the forward rotor will reduce the $\delta T/\delta \alpha$ of

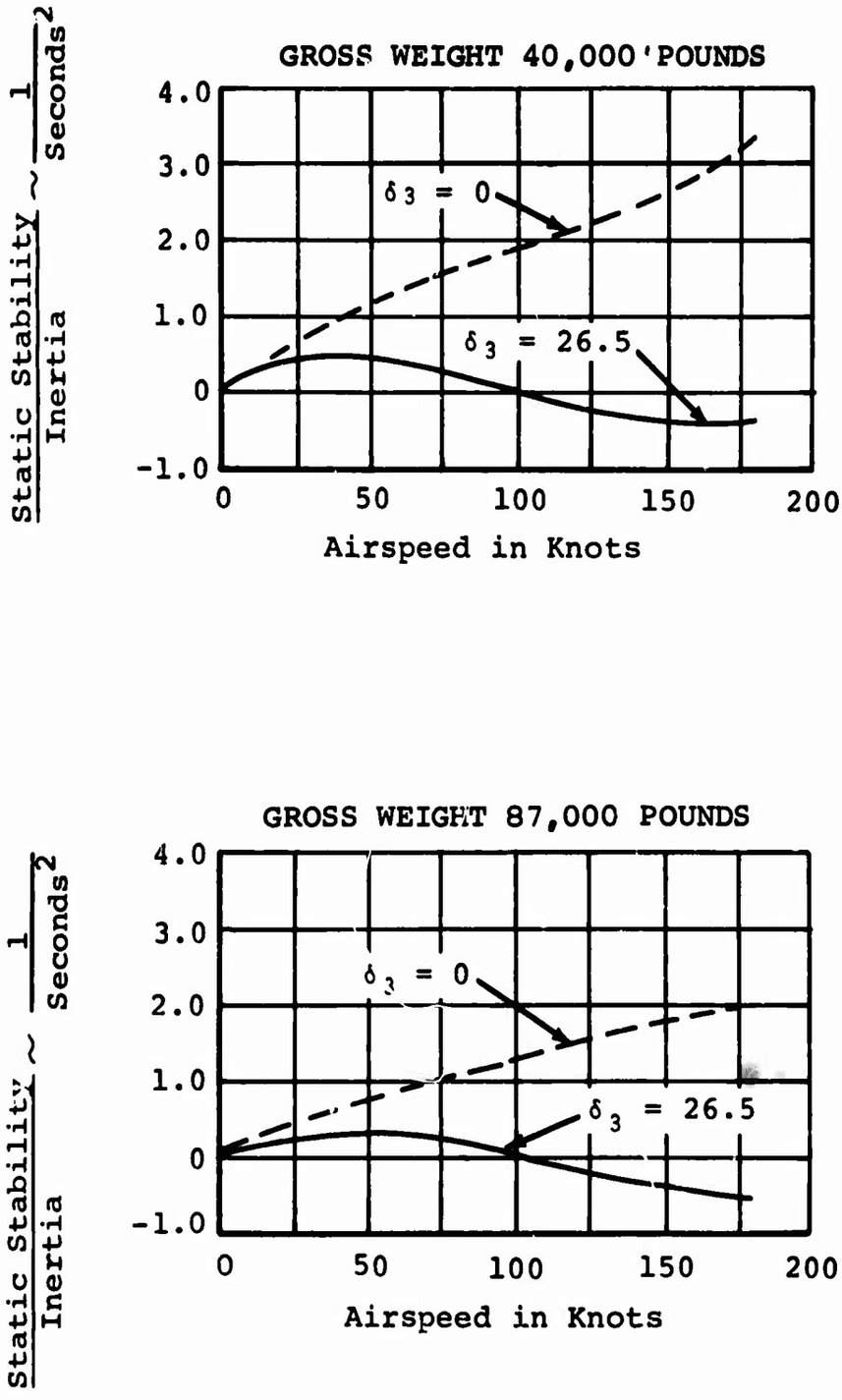

Figure 40. Rotor System Static Stability in Pitch at 28.5 Inches Aft Center of Gravity.

the forward rotor relative to the rear rotor, thereby appreciably improving the helicopter's angle-of-attack stability and gust sensitivity. Figures 40, 41, and 42 indicate the degree of stability improvement of the tandem rotor system to be gained through 26.5 degrees of differential delta-three.

Additional stability will be obtained through the use of horizontal tail surfaces and by the selection of the most aft center-of-gravity location. Here, a tradeoff must be made between the loading versatility allowed by large aft center of gravity limits and the increase in structural weight associated with tail size. The total helicopter stability shown in Figure 42 was obtained for the transport configuration, incorporating 26.5 degrees of delta-three and a horizontal tail area of approximately 300 square feet. The design aft center-of-gravity limit of 28.5 (4 percent of the distance between rotors) is proportionately about the same as existing tandem-lift helicopters. Because of the importance of interference effects, exact sizing of the necessary stabilizing surfaces must be determined from wind tunnel tests of specific configurations.

Directional (Yaw) Stability

Since the rotor disc planes are parallel to the relative wind, they can produce no tendency to yaw instability in forward flight or weathercocking in hover. Thus the aircraft can be stabilized through suitable aft center-of-gravity locations and aft pylon (vertical stabilizer) sizing. Figure 43 shows the estimated yaw static stability as a function of airspeed and center-of-gravity location for the transport configuration with an aft pylon area of approximately 500 square feet. For optimum heading stability the target level indicated in Figure 43 will be achieved with SAS. Exact sizing of the required vertical stabilizers must be determined by wind tunnel tests of specific configurations.

LONGITUDINAL (PITCH) CONTROL

Longitudinal Cyclic Trim

It is desirable for the heavy-lift mission that the helicopter attain a level fuselage attitude both at high speed and in hover. In hover, for the crane/personnel carrier or for the transport with an external cargo sling, the task of straddling a load on the ground or acquiring an external load will be simplified with level hovering capability. At cruise speed, a level attitude is desirable both from a performance (drag)

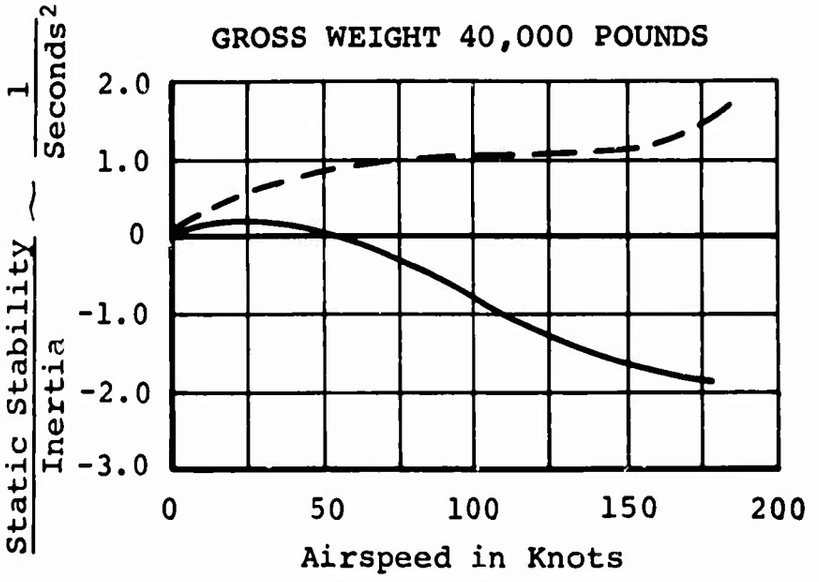

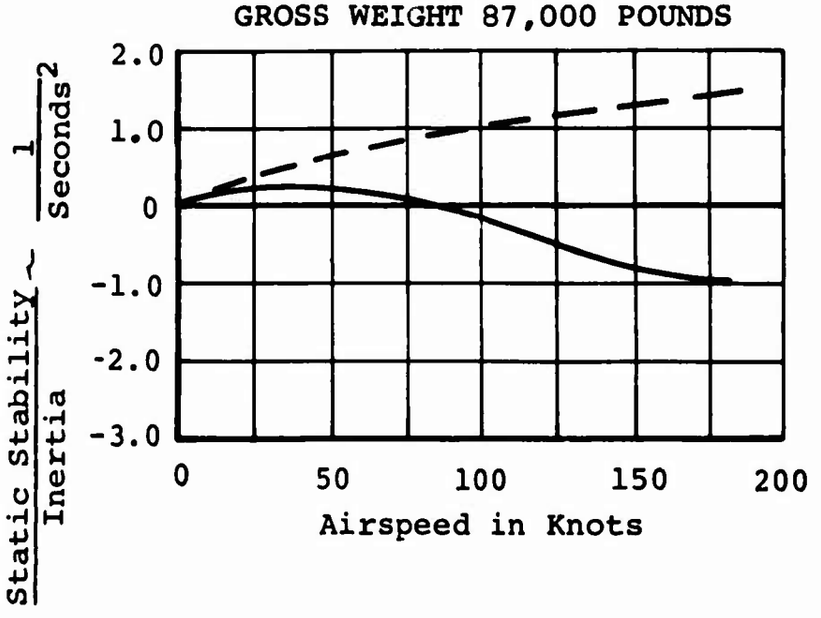

Figure 41. Rotor System Static Stability in Pitch at 11.5 Inches Forward Center of Gravity.

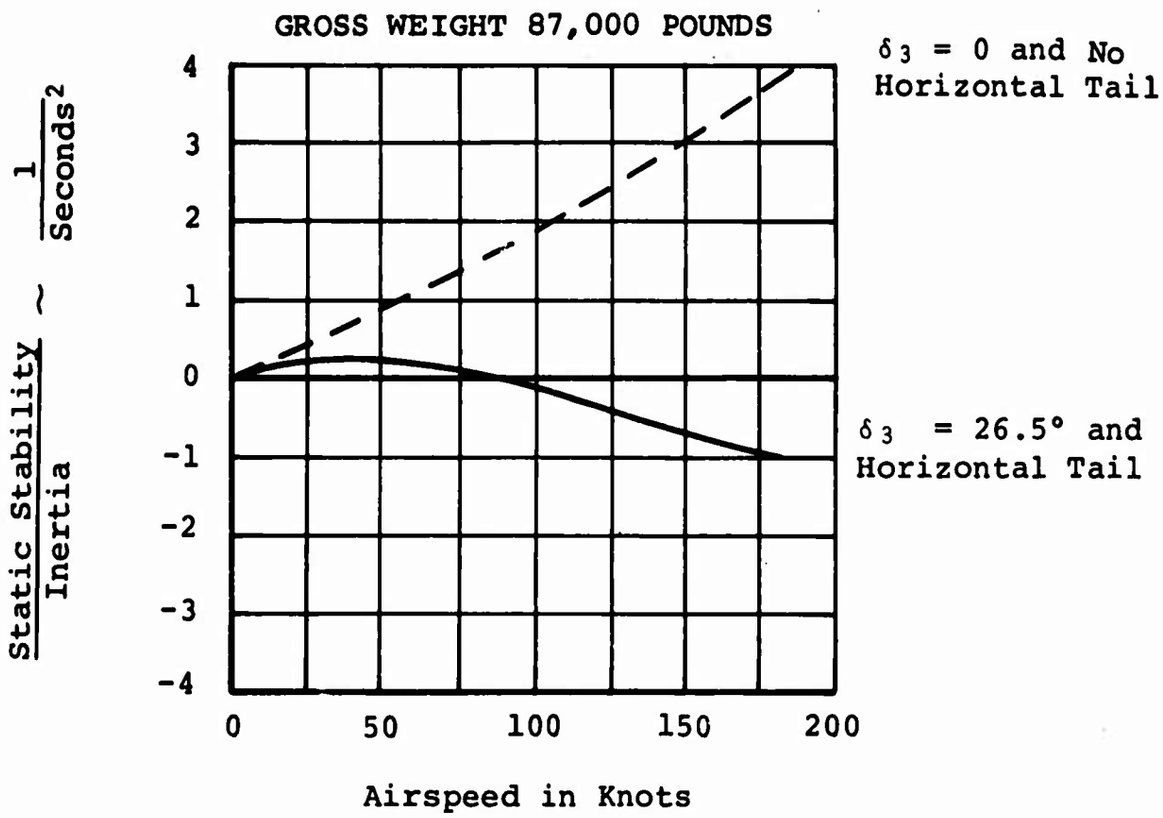

Figure 42. Static Stability in Pitch of Transport With SAS Off.

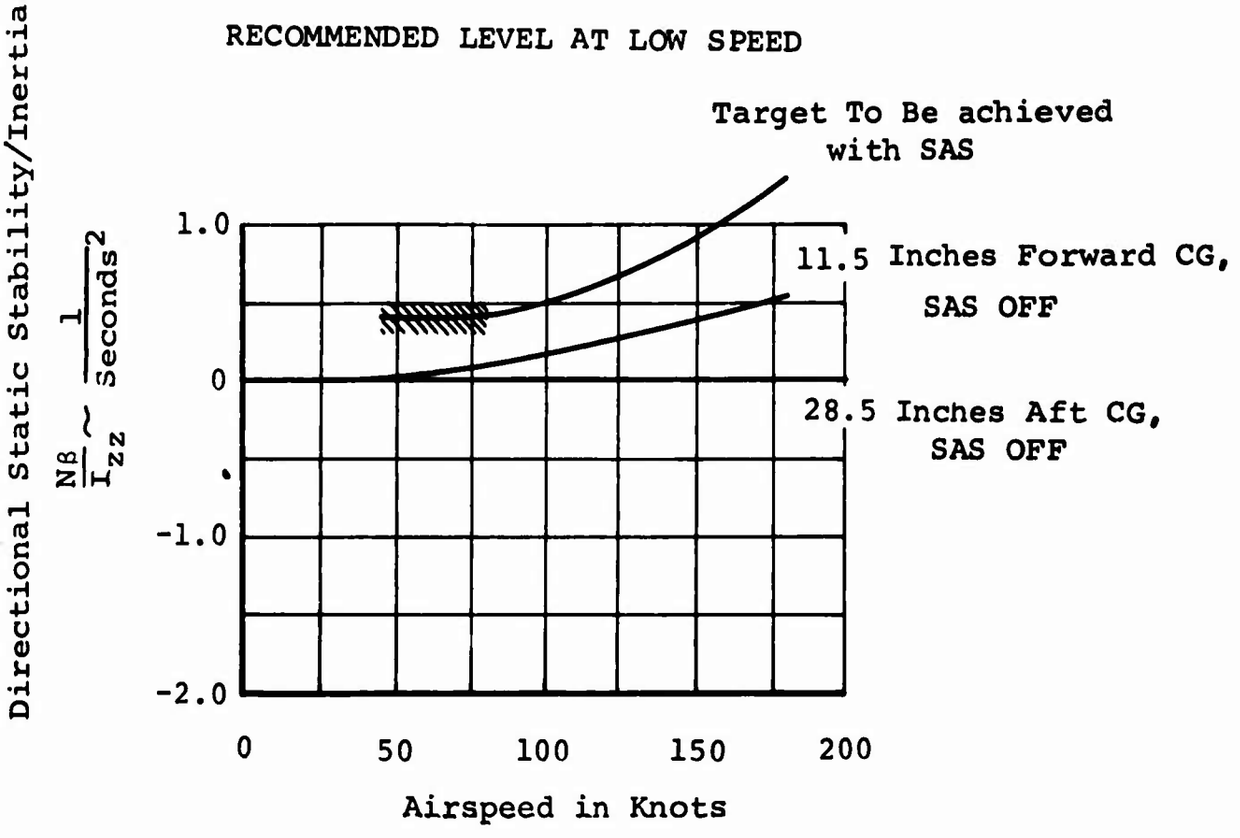

Figure 43. Directional Stability of Transport.

standpoint and for pilot comfort.

Without longitudinal cyclic control, the nose-up hover attitude equals the average of the forward and aft shaft tilts. In forward flight, forward thrust vector tilt is required to balance the increased drag. This tilt can be provided either through fuselage attitude changes or through longitudinal cyclic flapping induced by longitudinal cyclic blade pitch control.

A preliminary estimate of the shaft tilt and longitudinal cyclic control necessary to satisfy the above requirements has been made. The forward and aft shaft tilts tentatively are 9 degrees and 4 degrees respectively. Thus with no longitudinal control input, the normal hover attitude is about 6 degrees nose-up. As airspeed increases, the fuselage rotates until at about 100 knots it is approximately level. Above this speed, q-programmed forward longitudinal cyclic control is input to both rotors to maintain an approximately level fuselage (see Figure 38). Since the differential collective pitch control is used for trimming moments due to variations in center-of-gravity locations, the data shown are invariant with center-of-gravity position. In addition to providing attitude control, the programmed longitudinal cyclic reduces first-harmonic longitudinal flapping at airspeeds above 100 knots (Figure 44).

For control of hover attitude, manually selected aft cyclic settings of 6 degrees per rotor are provided to attain a level fuselage attitude. The fuselage attitude is independent of gross weight and center-of-gravity location, since thrust vector tilt is not employed to balance moments. Rather, a powerful moment control is provided by DCP. The forward shaft tilt and hub height above the fuselage provide approximately 12 degrees of blade-to-fuselage clearance in the aft cyclic mode at zero thrust (coning) to provide a large margin of fuselage clearance in ground handling.

Differential Collective Pitch

Differential collective pitch (DCP) characteristics have been allocated to longitudinal control to provide satisfactory moment control of the helicopter both in trimmed and maneuvering flight:

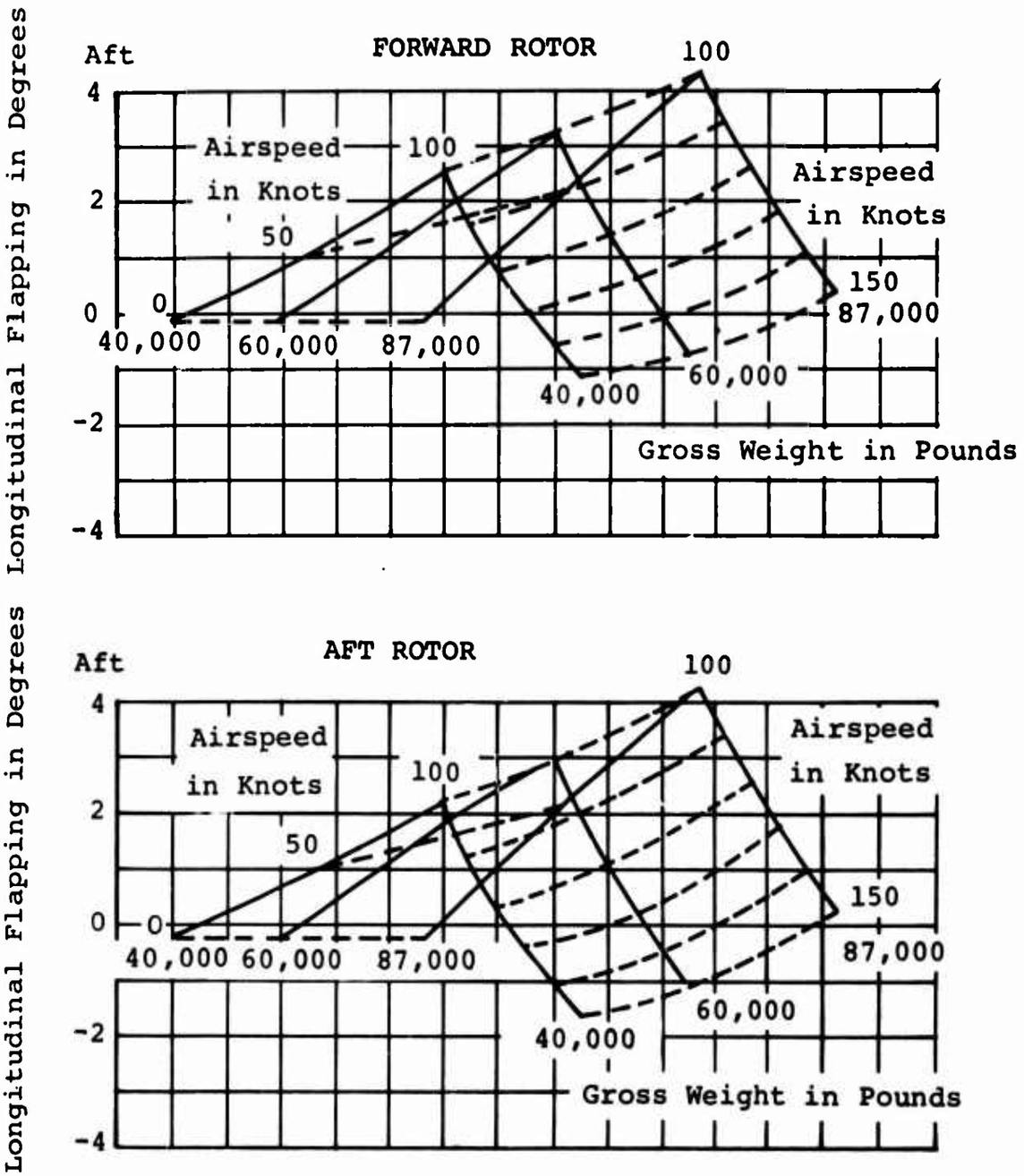

Figure 44. Variation of Longitudinal Flapping With Airspeed and Gross Weight.

1. Kinematic ratio: forward rotor 1.36, aft rotor 0.91 degree per inch

2. DCP blade travel: forward rotor ±7.5, aft rotor ±5.0 degrees

3. Total longitudinal stick travel: ±5.5 inches

Because delta-three on the forward rotor reduces its change in thrust per unit change in collective pitch with respect to the rear rotor, equal DCP kinematic ratios are not used on the forward and aft rotors due to the introduction of large Z-force coupling with longitudinal control inputs. A relative kinematic ratio increase of 50 percent on the forward rotor was found to restore the coupling to the same low level associated with the standard one-to-one kinematics used on a tandem-lift rotor helicopter without delta-three.

The differential collective blade pitch travel provided for the heavy lift is sufficient to provide the following simultaneously:

1. Trim the aircraft in the most critical trimmed flight condition as specified in MIL-H-8501A, paragraph 3.2.1.

2. Retrim the aircraft in the event of longitudinal cyclic trim failure at the most critical flight and loading condition.

3. Generate the pitch attitude change of $292/(W+1000)^{1/3}$ degrees in one second with an apparent time constant of 0.5 second, where W is the design gross weight.

The pitch attitude change described has a basis in the pilots' bias toward short time constants. It is obtained by taking the attitude change required by the IFR requirement of MIL-H-8501A and superimposing the additional requirement of 0.5-second time constant. The control required for maneuver is then made available over the entire operational envelope, not just in hover. These DCP control criteria are compared with that required by MIL-H-8501A, paragraph 3.2.1, in Table XIII.

The maneuver requirement of MIL-H-8501A, paragraph 3.2.13 is not critical for longitudinal control, so the minimum requirement of the specification arises from the critical trimmed

flight condition (rearward flight at maximum gross weight and most aft cg) plus the 10-percent margin of total hover moment control capability. Using the heavy-lift criteria given in Table XIII instead, a large margin of control above that required for critical moment trim is provided to ensure full maneuverability under conditions of extreme cg locations, as might arise with sling-carried or pod-type loads.

TABLE XIII
DCP CONTROL REQUIREMENTS IN DEGREES OF BLADE PITCH TRAVEL

	MIL-H-8501A		Heavy-Lift Criteria	
	Forward Rotor	Aft Rotor	Forward Rotor	Aft Rotor
Trim	--	--	3.36	2.24
Cyclic Failure	--	--	1.88	1.25
Subtotal Trim and Cyclic Failure	5.24	3.49	5.24	3.49
Maneuver	--	--	2.18	1.45
10-percent Margin	0.58	0.39	--	--
Total	5.82	3.88	7.42	4.94
Provided	--	--	7.50	5.00

Enough control power has been provided for the heavy-lift helicopter that control sensitivities can be adjusted over a fairly large range for total control motions within HIAD limits. The maximum total control travel has been tentatively selected to be $\pm$5.5 inches. This provides a control sensitivity of 0.25, 1/second, (at maximum gross weight) which, together with the SAS-augmented damping level of 4, 1/second, is compatible with NASA-Langley recommendations (Reference 15) and MIL-H-8501A requirements (see Figure 35).

Automatic DCP Trim

To provide positive, static longitudinal control position and control force stability with respect to speed (MIL-H-8501A, paragraph 3.6.3), automatic dynamic pressure

(q)-sensed DCP trim shall be provided. Figure 39 shows plots of stick position versus airspeed for two center-of-gravity locations with the DCP trim operative and inoperative. Above airspeeds of 40 knots, DCP programmed as a function of q will be applied to the rotors to maintain positive stick as airspeed increases.

Collective Pitch

The blade pitch and collective lever travels have been selected to provide sufficient control of the helicopter in both trimmed and maneuvering flight:

1. Forward rotor blade pitch travel at 0.75 radius: 0.45 to 22.95 degrees

2. Aft rotor blade pitch travel at 0.75 radius: 0.75 to 18.00 degrees

3. Forward rotor collective kinematic ratio: 2.50 degrees/inch

4. Aft rotor collective kinematic ratio: 2.08 degrees/inch

5. Total collective lever travel: 9.0 inches

The kinematic ratio of the forward rotor is 20 percent higher than the aft, and, in addition, there is a cuff setting, or rigging adjustment, so that at full-down collective and neutral longitudinal stick, the forward rotor has 1.2 degrees greater blade pitch angle setting than the aft. These control kinematics and cuff setting changes were found to provide reasonable trim and collective positions throughout the flight envelope. In level flight, the DCP airspeed characteristics are almost identical with those of a similar aircraft without delta-three and standard kinematics (Figure 45). Moment trim can be attained in high rates of climb and autorotation with virtually no trim changes in collective pitch setting (Figure 46). The maximum and minimum collective pitch settings were determined from critical trimmed flight conditions as follows:

Maximum Collective Pitch

High trim collective pitch settings are required for high rate of climb at low gross weight. In order that perform-

ance in these flight conditions will not be limited by control travel, the maximum blade pitch travels described previously have been selected. The corresponding maximum collective lever travel of 9.0 inches is compatible with the longitudinal and lateral-directional control motions.

Under static conditions, these maximum blade pitch settings provide a load factor capability in excess of two, which compares favorably with existing tandem helicopters. Since present vehicles have never lacked sufficient collective pitch for maneuvers such as descent-arrest in autorotation and jump takeoffs, sufficient collective pitch has been provided for maneuvers.

Minimum Collective Pitch

Sufficient down collective pitch has been provided so that the helicopter can be autorotated at rotor speeds up to normal rpm for any reasonable weight-empty center-of-gravity position (Figure 46). Thirty knots was considered to be the minimum horizontal ground speed at which a pilot would attempt to maintain trimmed autorotational flight.

The zero-thrust pitch angle for the rotor blades is estimated to be -0.24 degree. At neutral stick and full-down collective, the aft rotor would be driven to negative thrust levels, so a detent will be provided on the collective lever to ensure that negative rotor thrust is not reached during ground run-ups.

Cumulative Collective Pitch Control

Cumulative collective limits are set at the sum of full-up collective plus total DCP, and full-down collective minus total DCP. This provides full longitudinal trim and maneuver capability of the helicopter under all conditions of airspeed and loading within the flight envelope. Cumulative collective-pitch control limits at 0.75 radius are as follows:

1. Forward rotor: -7.05 to 30.45 degrees

2. Aft rotor: -5.75 to 23.00 degrees

These limits are conservative and can probably be reduced during later stages of design.

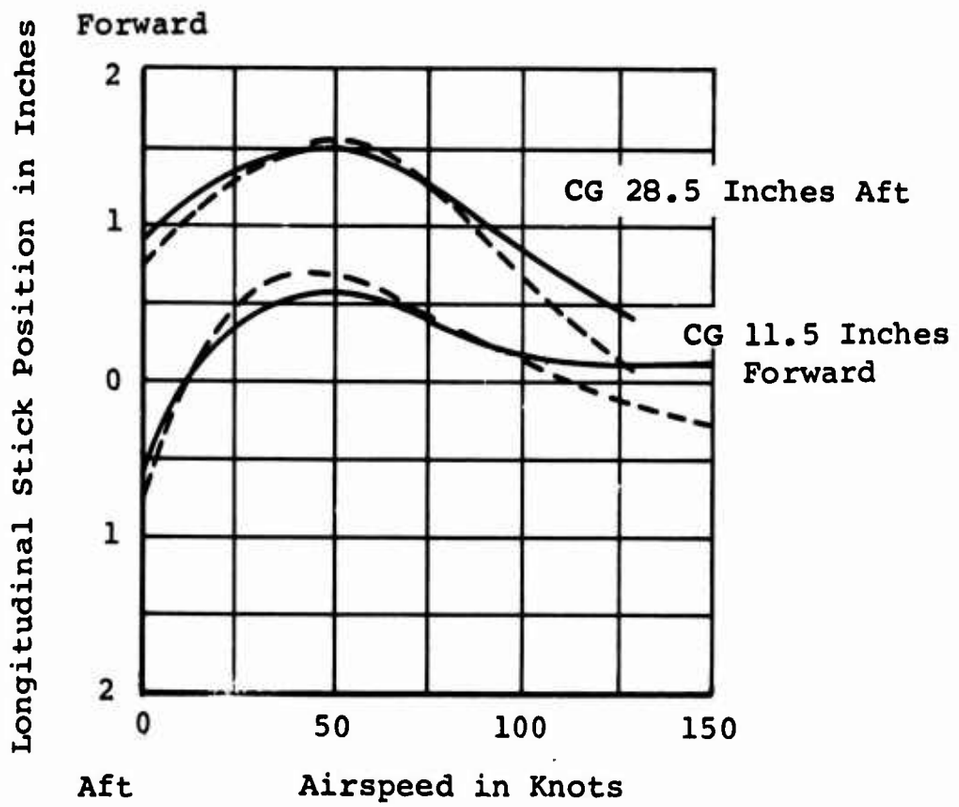

NOTES:
1. Gross weight 87,000 pounds
2. _____ δ_3 = 26.5 and revised kinematics
   ------ δ_3 = 0 and standard kinematics

Figure 45. Trimmed Stick Position (Automatic DCP Trim Off) With and Without Delta-Three on Forward Rotor.

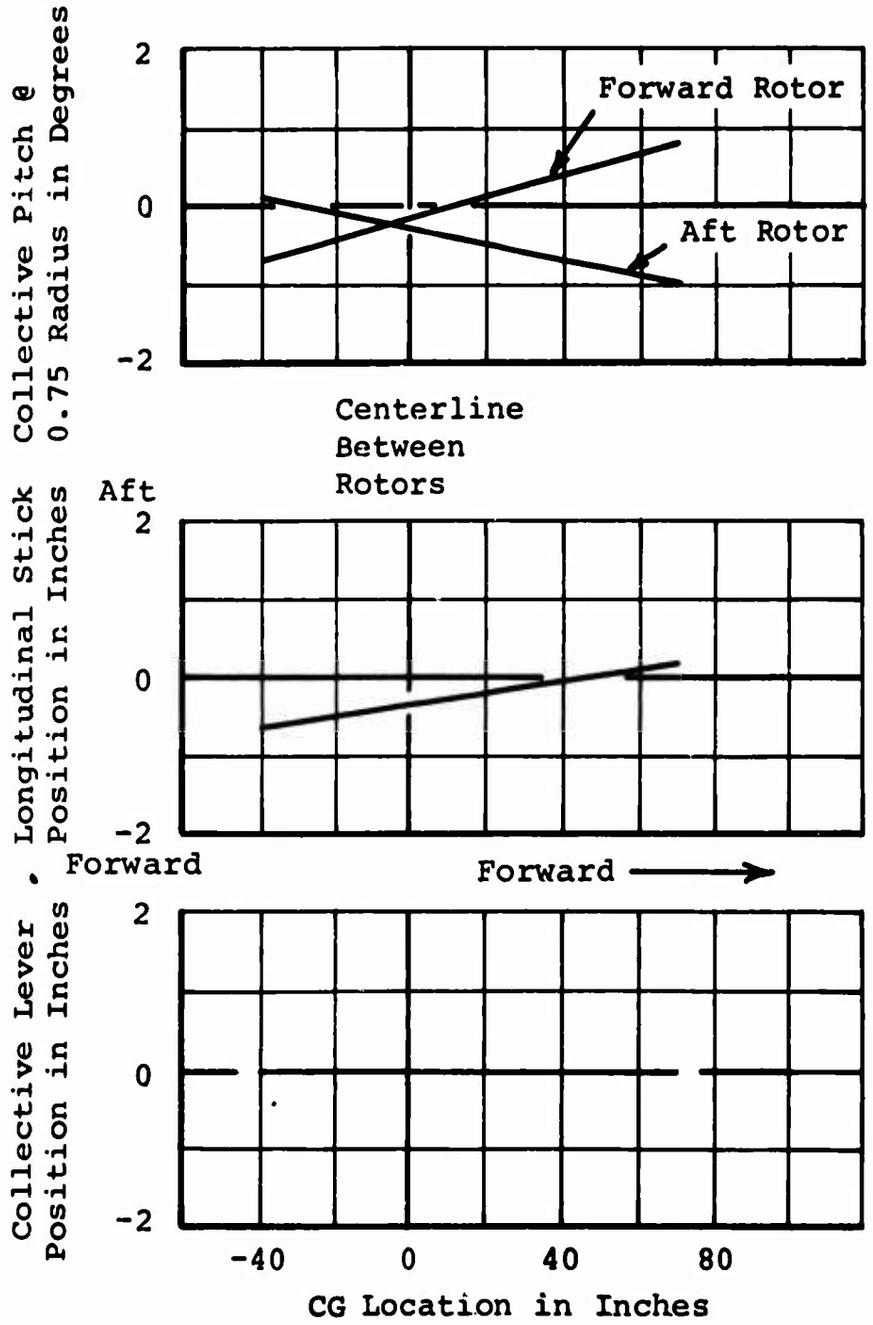

NOTES:

1. Gross weight 40,000 pounds
2. Sea level standard day
3. Autorotation at 30 knots horizontal speed
4. Tip speed 700 feet per second
5. Rotor radius 43 feet

Figure 46. Minimum Collective Pitch Requirement.

LATERAL AND DIRECTIONAL (ROLL AND YAW) CONTROL

Lateral Cyclic Pitch

The lateral cyclic blade pitch and stick travels provide trim and maneuver capability for the heavy-lift helicopter in excess of MIL-H-8501A requirements:

1. Pitch travel: forward rotor $\pm$9.2, aft rotor $\pm$8.0 degrees

2. Kinematic ratio: forward rotor 3.07, aft rotor 2.67 degrees per inch

3. Total stick travel: $\pm$3.0 inches

The use of delta-three on the forward rotor reduces lateral flapping, and hence side force and hub moments, for a given lateral cyclic control input. This effect would introduce yawing-moment coupling with lateral control inputs if it were not for the compensating 15-percent increase in kinematic ratio on the forward rotor, relative to the aft. This kinematic change reduces the coupling over the speed range from 0 to 130 knots to a level appropriate to a tandem-lift rotor helicopter with standard kinematics and no delta-three. The lateral cyclic blade pitch travels described previously represent sufficient control to satisfy the following simultaneously:

1. Trim the aircraft at minimum flying weight as required in MIL-H-8501A, paragraphs 3.3.2 and 3.3.9

2. Provide the greater of

   a. 30 percent of the lateral control requirement of item 1, above

   b. A roll attitude change of $36/(W+1000)^{1/3}$ degrees in 0.5 second with an apparent time constant of 0.3 second, where W is the design gross weight.

The control requirements arising from these specifications and from minimum MIL-H-8501A requirements (paragraph 3.3.9) are summarized in Table XIV. The maneuver requirement was not critical by the criteria of MIL-H-8501A. The critical trimmed flight condition occurred in 15 degrees sideslip at 130 knots at minimum flying weight, with center of gravity 70 inches forward.

TABLE XIV
LATERAL CYCLIC PITCH REQUIREMENTS IN
DEGREES OF BLADE PITCH TRAVEL

	MIL-H-8501A		Heavy-Lift Criteria	
	Forward Rotor	Aft Rotor	Forward Rotor	Aft Rotor
Trim	5.36	4.66	5.36	4.66
Maneuver	--	--	3.57	3.10
10-Percent Margin	0.59	0.51	--	--
Total	5.95	5.17	8.93	7.76
Provided	--	--	9.20	8.00

Because delta-three reduced the normal 90-degree phase lag between cyclic pitch input and flapping output, the controls have been rephased to provide the stick and pedal symmetry about zero sideslip shown in Figure 31. Since minimum flying weight cg actually lies near the centerline between rotors, the control provided is conservative due to the higher directional stability of the helicopter at forward cg.

The selection of a maximum lateral stick travel of ±3.00 inches provides a control sensitivity compatible with NASA-Langley recommendations (Reference 15) and MIL-H-8501A specifications, when the basic helicopter damping is augmented by SAS to the level shown in Figure 36.

Differential Lateral Cyclic Pitch

The following differential lateral cyclic blade pitch and rudder-pedal travels have been established:

1. Pitch travel: forward rotor ±13.8, aft rotor ±12.0 degrees

2. Kinematic ratio: forward rotor 4.6, aft rotor 4.0 degrees per inch

3. Total pedal travel: ±3.0 inches

For the reasons discussed under lateral cyclic pitch, the forward rotor kinematic ratio has been increased by 15 percent relative to the aft to minimize Y-force coupling with pedal control. The differential lateral cyclic pitch travels listed above may be compared to the requirements of MIL-H-8501A, paragraphs 3.3.5 and 3.3.9:

1. Maneuver: forward rotor 10.925, aft rotor 9.5 degrees

2. Trim: forward rotor 5.175, aft rotor 4.5 degrees

3. Total requirement: forward rotor 10.925, aft rotor 9.5 degrees

Although the blade pitch travel requirements are only 10.925 and 9.5 degrees for the forward and aft rotors respectively, 13.8 and 12.00 degrees are provided to allow for control quickening over a greater range of pedal travel.

Both control power and control sensitivity are sufficient to meet MIL-H-8501A requirements up to SAS-augmented rate damping levels of 1.25, 1/second, for both 1-inch and full-throw pedal inputs (Figure 37). In forward flight the directional pedal requirements are small since coordinated turns are made with lateral stick and DCP. Trimmed sideslip pedal requirements are modest, even at an airspeed of 130 knots. In hover, due to the tandem configuration's relative insensitivity to gust disturbances, the need for large pedal-control inputs is minimal. However, maneuvers such as straddling a load and acquiring external loads on cargo slings require many small, precise, corrective pedal-control inputs. The response of the helicopter to small directional-control inputs can be considerably enhanced by the use of a control quickener to effectively increase the control sensitivity. In this way higher levels of SAS-augmented damping are permissible for the rapid establishment of steady-state yaw rates without the control sluggishness that low sensitivity and high damping would produce. Tentative values of quickened control sensitivity and SAS-augmented damping which satisfy MIL-H-8501A requirements are shown in Figure 37. A more detailed investigation of the overall helicopter dynamics is required before the desired levels can be specified.

Cumulative Lateral Cyclic Pitch

Since flight conditions requiring the full limit of lateral

stick and pedal travel simultaneously do not arise, a cumulative limit is provided on the lateral directional controls to prevent overdesign of the actuators (Figure 33). The cumulative limits provide a margin of control at the critical trimmed flight condition (sideslip at 130 knots) which exceeds MIL-H-8501A requirements. Because of the inherent static stability of the airframe, the stick and pedal controls subtract on the forward head in the sideslip flight condition, thus allowing proportionately smaller cumulative limits.

CUMULATIVE COLLECTIVE AND CYCLIC PITCH

The combined cumulative collective and cyclic blade pitch travels will be limited to 60 degrees of total travel on each rotor, as shown in Figure 34, so that the blade pitch travels and actuators will not be overdesigned to provide control that will never be demanded in actual flight conditions. (The need for full pedal, lateral and longitudinal stick and lateral and longitudinal cyclic controls simultaneously is unlikely.) The cumulative limit provided is conservative and will be revised downward as further study of large perturbation maneuvers warrants.

HOVER ATTITUDE CONTROL

Figure 47 shows the hover attitude control features (independent of center-of-gravity location) of the tandem-lift rotor helicopter.

EVALUATION OF THE HINGELESS SEMIRIGID ROTOR

A preliminary study has been conducted to determine whether a hingeless semirigid rotor offers any significant control advantages over a conventional articulated system. For this purpose, estimates of the control sensitivities of each were based on the "STATIC AND DYNAMIC STRUCTURAL ANALYSIS". The geometric characteristics of both rotors are:

1. Radius 43 feet
2. Chord 3.5 feet
3. Thickness/chord ratio 0.12
4. Blade cutout 20-percent radius

The flapping stiffness variation with radius for the hingeless

semirigid rotor is shown in Figures 105 and 108. The stiffness of the inboard 20-percent radius is 13 x 10^8 pound inches squared. The articulated blade has identical physical properties but with a flapping hinge at the 8-percent radius station. No pitch-flap coupling (delta-three) was used on either configuration. The estimated control sensitivities (in radians per second squared per degree of blade pitch) for semirigid and articulated rotors at 120 knots are as follows:

1. Pitch: semirigid 0.390, articulated 0.390

2. Roll: semirigid 0.960, articulated 0.290

3. Yaw: semirigid 0.044, articulated 0.035

Longitudinal (Pitch) Control

For the purpose of this study it was assumed that both configurations obtain pitching-moment control through differential collective pitch. With this control scheme, the incremental hub moments are equal and opposite, and so are reacted within the airframe structure. Thus, both the articulated and semirigid rotor configurations possess about the same control sensitivity. Attitude control at high airspeeds is provided through q-sensed longitudinal cyclic pitch controlling the orientation of the rotor thrust vectors. Because of the large nose-down hub moments induced by the cyclic pitch, the aft differential collective pitch requirements for the semirigid rotor will be considerably higher than for an articulated rotor at high speed.

As an alternative, the large hub moments associated with the semirigid rotor could be used to generate moment control through longitudinal cyclic pitch. However, this control scheme would require the use of external movable stabilizers for attitude control at high speed.

A workable longitudinal control scheme would probably consist of DCP as well as longitudinal cyclic pitch operated by the stick, in addition to q-sensed longitudinal cyclic pitch. This dual moment control is required, not to provide an adequate level of moment control, but rather to permit both moment and attitude control at all airspeeds without the use of movable aerodynamic surfaces.

Lateral (Roll) Control

Roll control for the semirigid rotor system is provided by

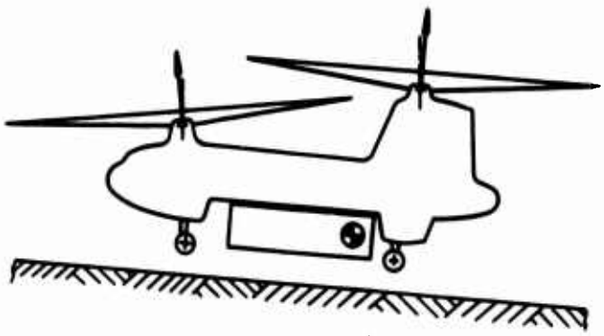

LANDING (OR LIFT-OFF) ATTITUDE.
GROUND LEVEL, POSITIVE SLOPE.

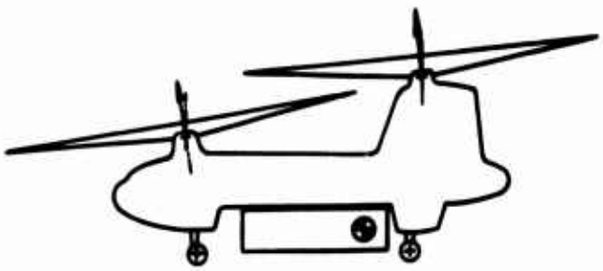

FORWARD FLIGHT ATTITUDE.

EXTERNAL CARGO C.G LOCATED AFT OF MEAN POSITION.

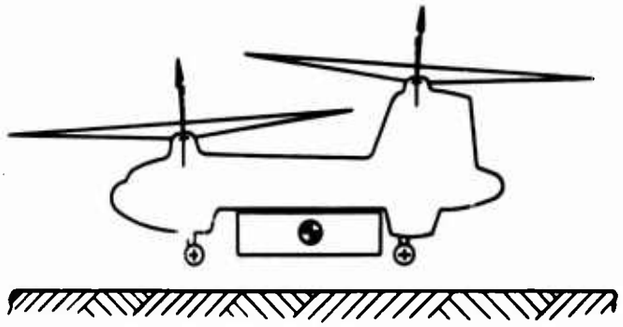

LANDING (OR LIFT-OFF) ATTITUDE.
GROUND LEVEL HORIZONTAL.

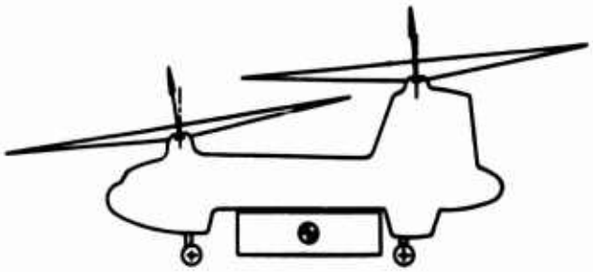

FORWARD FLIGHT ATTITUDE.

EXTERNAL CARGO CG LOCATED AT MEAN POSITION.

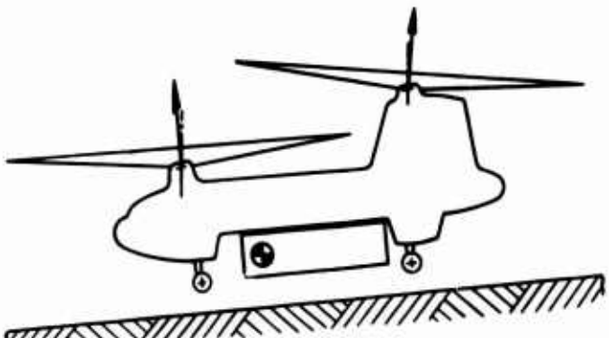

LANDING (OR LIFT-OFF) ATTITUDE.
GROUND LEVEL, NEGATIVE SLOPE.

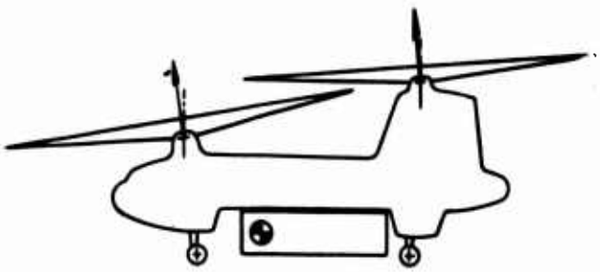

FORWARD FLIGHT ATTITUDE.

EXTERNAL CARGO C.G LOCATED FORWARD OF MEAN POSITION.

Figure 47. Hover Attitude Control.

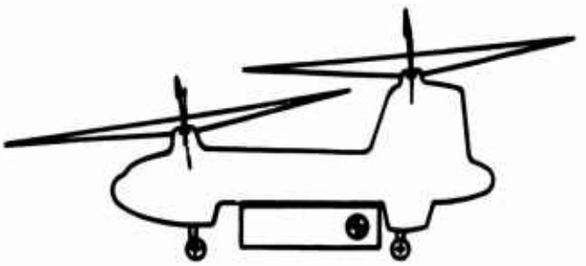

FORWARD FLIGHT ATTITUDE.

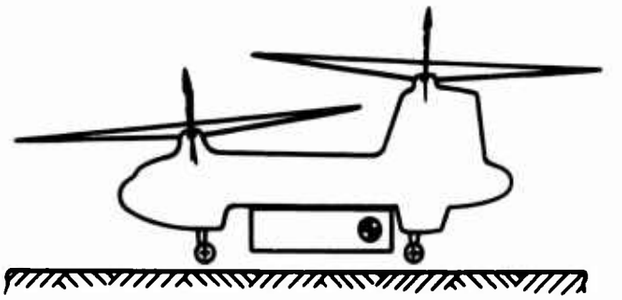

LIFT-OFF & HOVER ATTITUDE.
GROUND LEVEL HORIZONTAL.

EXTERNAL CARGO C.G LOCATED AFT OF MEAN POSITION.

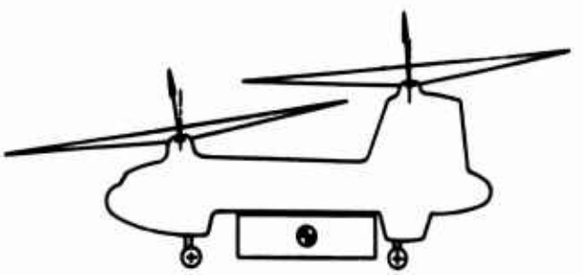

FORWARD FLIGHT ATTITUDE.

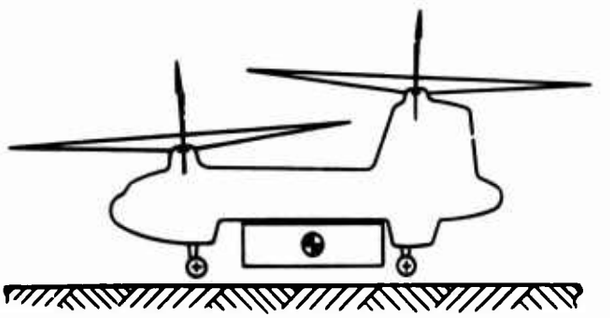

LIFT-OFF & HOVER ATTITUDE.
GROUND LEVEL HORIZONTAL.

EXTERNAL CARGO CG LOCATED AT MEAN POSITION.

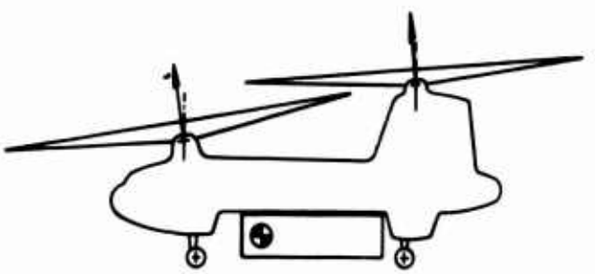

FORWARD FLIGHT ATTITUDE.

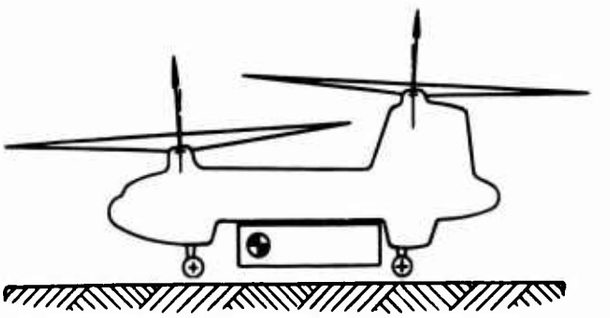

LIFT-OFF & HOVER ATTITUDE.
GROUND LEVEL HORIZONTAL.

EXTERNAL CARGO C.G LOCATED FORWARD OF MEAN POSITION.

tude Control.

B

lateral cyclic pitch. In addition to the roll moment provided by lateral thrust vector tilt, the large hub moments of each rotor add up to more than three times the control sensitivity of the articulated system. Since the articulated system provides satisfactory roll control, the semirigid rotor would probably be desensitized for good handling qualities and to provide roll control power and sensitivity compatible with the pitch control capabilities.

Directional (Yaw) Control

As with the articulated rotor, yaw control is provided through differential lateral cyclic pitch changes between the forward and aft rotors. Since hub moments are reacted internally, they produce virtually no increase in yawing moment capability. Yaw control sensitivity is, however, augmented by a higer lateral thrust rotor vector tilt per unit of lateral cyclic control. This is probably attributable to blade curvature effects.

Control Power and Sensitivity

From a control power standpoint, the semirigid rotor could be used on the heavy-lift helicopter but, using DCP control, no significant increase in pitch control power will be obtained with it. The roll control sensitivity is so high that desensitizing would probably be necessary for good handling characteristics. Although there is a small increase in yaw control sensitivity, this must be considered in the light of the obvious structural and fatigue penalties associated with the hub moments, which are higher than those observed on the articulated rotor (see Figures 110, 115, 116, 118, 123, and 124).

ANALYSIS OF STALL FLUTTER AND FLAP-LAG INSTABILITY

The maximum speed of many present and past helicopters has been limited not by power available but by increases in control loads or vibration levels, usually referred to loosely as retreating-blade stall. Recent research has shown that these phenomena are frequently due to two types of limit-cycle oscillatory motion triggered by operation with significant areas of stalled flow on the rotor blade. Neither type is divergent, but both can build up to limit-cycle amplitudes sufficient to cause high stresses or vibration. The first type is stall flutter. This can occur over a limited azimuth range in the retreating quadrants. The second is the coupled flap-lag

oscillation described in Reference 26.

The heavy-lift helicopter rotor configuration has been analyzed specifically for stall flutter and flap-lag instability characteristics. Forward and aft rotors have been analyzed for two flight configurations on the proposed operating boundary, and in one of these the effect of blade twist was evaluated by computing four different blade-twist values. It must be appreciated that the programs used for both analyses are in advanced states of preparation but are not completed. However, a correlation with CH-47A data which is under way shows sufficient agreement for both stall flutter and flap-lag instability to justify the use of these computer programs in first-order predictions of these phenomena for the heavy-lift helicopter.

The stall flutter analysis predicts pitch-link loads which show little influence from negative damping, indicating that stall flutter should not be a problem on this aircraft. The alternating pitch-link loads used for the design study were derived in the STATIC AND DYNAMIC STRUCTURAL ANALYSIS.

The flap-lag instability of the same configuration assumed lag damping nondimensionally scaled from the CH-46A and showed a well-damped response to a gust input with no indication of limit cycle 1/3 per revolution lag motion.

Stall Flutter

The pitch-link load was taken as the indicator for the presence of stall flutter, since it provides the reaction for blade torsion. While the analysis method described in the STATIC AND DYNAMIC STRUCTURAL ANALYSIS gives good agreement with test data for peak-to-peak values of pitch-link load, it can not handle the negative damping effects which promote stall flutter. Therefore, a new analysis method was developed. The method of computation was by the serial use of the separate computing programs:

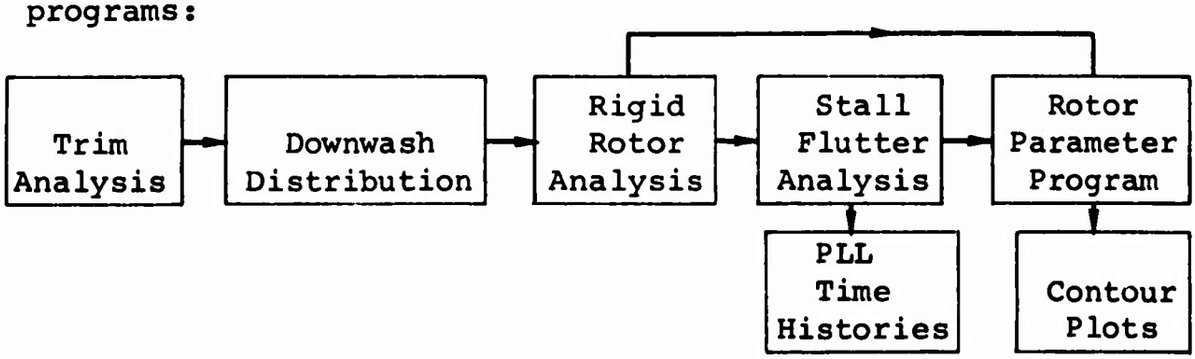

The input data used to define the heavy-lift helicopter configuration and the flight conditions are listed in Table XV.

Pitch-link loads for the 87,000-pound gross weight are shown in Figure 48; those for the 75,700-pound gross weight are shown in Figure 49. Forward and aft rotor pitch-link load time histories of blades with a twist of -10 degrees are illustrated for the following flight conditions:

1.	Gross weight	87,000 pounds (Figure 48)	75,000 pounds (Figure 49, Sheets 3 and 4)
2.	Center-of-gravity location	8 inches forward	8 inches forward
3.	Altitude	0	5000 feet
4.	True airspeed	165 knots	155 knots

The alternating loads in the fourth quadrant, where stall flutter might occur, are small compared to the advancing side of the blade, which experiences a heavy nose-down moment that dominates the peak-to-peak loading. For the forward rotor of the 75,700-pound configuration (Figure 49, except Sheet 4) some reduction of the oscillatory response with increased twist is evident; but the peak-to-peak alternating load is always dominated by the advancing blade and is practically unchanged.

All the time histories demonstrated similar behavior, and that of Figure 48, Sheet 1, was further analyzed to investigate the nature of the response. The angle-of-attack distribution is shown in Figure 50, and, since angles greater than 10 degrees can cause negative pitch damping, it is seen that most of the retreating side can be a negative damping region. The local pitching moment is shown in Figure 51, and this is seen to be dominated by large negative values in the region of the advancing blade tip (note the uneven contours). This results from an aft shift of the center of pressure caused by the relatively high Mach number (0.85) in this area. Elsewhere, the moment distribution is relatively smooth and almost entirely nose-down. The spanwise integration is plotted at the center of the diagram and also in Figure 48, Sheet 1. The distribution of aerodynamic pitch damping (Figure 52) is typically heavily positive on the advancing side and just negative over approximately 50 percent of the retreating side. The spanwise

integration is also plotted in the center of the diagram. The integrated moment represents what the pitch-link load would be if the blade was inertialess; the integrated damping is the total pitch damping that a rigid blade would experience in pitch at each azimuth. It is concluded that the total pitch-link load oscillatory response is primarily caused by the irregularities in the applied aerodynamic moment rather than negative damping. The pitch-link load would probably not be greatly different if the damping never went negative at all but just remained low and positive, indicating freedom from a stall-flutter problem.

To aid in the interpretation of the heavy-lift helicopter analysis, a high-speed CH-47A case is now illustrated by the same steps (see Figures 53 through 56). In Figure 53, a particular test case was analyzed and compared with the predicted pitch-link load and with the integrated moment. Although not closely similar to the test curve, the prediction does show similarity in the peak-to-peak load and in the nature of the curve. The CH-47A used a symmetrical airfoil rather than the drooped-nose version used on the heavy-lift helicopter, and therefore it stalls about 2 degrees earlier. The angle-of-attack contours for the CH-47A (Figure 54) show considerably more stall than those for the heavy-lift helicopter (note the opposite sense of rotation). The largest difference between the two aircraft appears in the applied moment distribution. The CH-47A with pitch axis at 19-percent chord experiences moment fluctuations all around the disc; the heavy-lift helicopter with pitch axis at 25-percent chord is relatively smooth, except that the advancing tip experiences high Mach numbers. The damping contours for the CH-47A show a larger area subject to negative damping and larger negative values, compared to the maximum positive values on the advancing side of the disc.

Flap-Lag Instability

The Flap-Lag Instability Program represents a three-bladed rotor, in which each blade is rigid and has individual flap and lag freedoms, and the hub has vertical, lateral and longitudinal freedoms. It is a modification of the helicopter stability program. It uses uniform downwash, table look-ups for aerodynamic forces, moments, and lag damper loads, and it makes no small-angle assumptions.

The cases analyzed for stall flutter were also analyzed for flap-lag instability. A 2100-foot-pound friction lag damper was used. Different effective masses were used for the three

directions in which the rotor can move; for the seven cases, these were:

1. M_x, M_y, and M_z = 1130, 760, and 1470 slugs
2. M_x, M_y, and M_z = 790, 246, and 1530 slugs
3. M_x, M_y, and M_z = 1140, 710, and 1290 slugs
4. M_x, M_y, and M_z = 1140, 710, and 1293 slugs
5. M_x, M_y, and M_z = 1140, 710, and 1299 slugs
6. M_x, M_y, and M_z = 747, 223, and 1372 slugs
7. M_x, M_y, and M_z = 1140, 710, and 1295 slugs

For the CH-47A, the 1100-foot-pound preload production lag damper was used. The effective masses were M_x, M_y, and M_z = 510, 450, and 525 slugs, respectively. The remaining input data were as for stall flutter. Figure 57 shows the flap and lag response to a gust input (Figure 58). For the first 0.5 second of the record, the steady-state response is seen. A 20-foot-per-second vertical gust is then applied for 1 second, and the mean lag angles suffer a disturbance at the rigid lag frequency. The disturbance damps rapidly, and during this time the peak-to-peak flapping does not change significantly. From Figure 59, the effect of increasing twist is seen to be slight but beneficial in that both peak-to-peak and mean lag angles are reduced. As with the stall-flutter analysis, the heavy-lift helicopter data was compared to the CH-47A case (Figure 60) subjected to the same 20-foot-per-second gust. The lag response (as a percentage of the mean angle from 0 degrees, the auto-rotation position) is significantly greater than that for the heavy-lift helicopter, and the peak-to-peak flapping almost doubles as a result of the gust. Thus, the heavy-lift helicopter is expected to be significantly more damped than the CH-47A.

Conclusions

The analysis shows that the heavy-lift helicopter rotor blade should not be critical for stall flutter when flying at maximum performance (87,000 pounds, sea level, 165 knots; or 75,700 pounds, 5000 feet, 155.5 knots). This conclusion should be reviewed in the light of further development of stall flutter technology currently being investigated.

Peak-to-peak control loads will be high on the advancing side,

due not to stall flutter but to the high Mach number at which the tip will be flying.

The rotor will be well-damped, compared to the CH-47A, with respect to flap-lag instability motions induced by gusts or other disturbances.

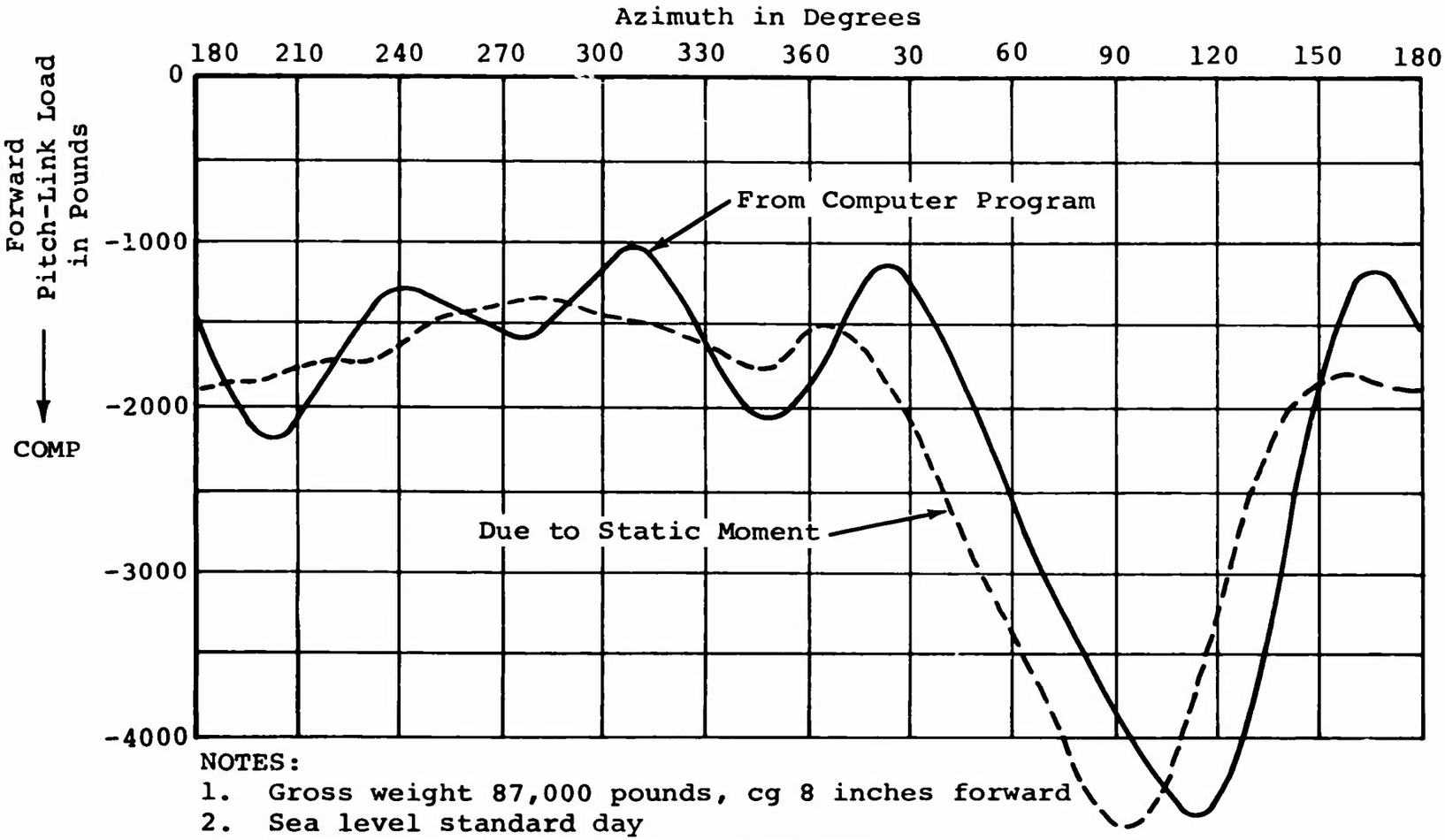

NOTES:

1. Gross weight 87,000 pounds, cg 8 inches forward
2. Sea level standard day
3. Airspeed 165 knots; 155.5 rotor rpm
4. Drooped leading edge blade
5. θ_t = -10 degrees

Figure 48. Pitch-Link Load at 87,000 Pounds Gross Weight. (Sheet 1 of 2)

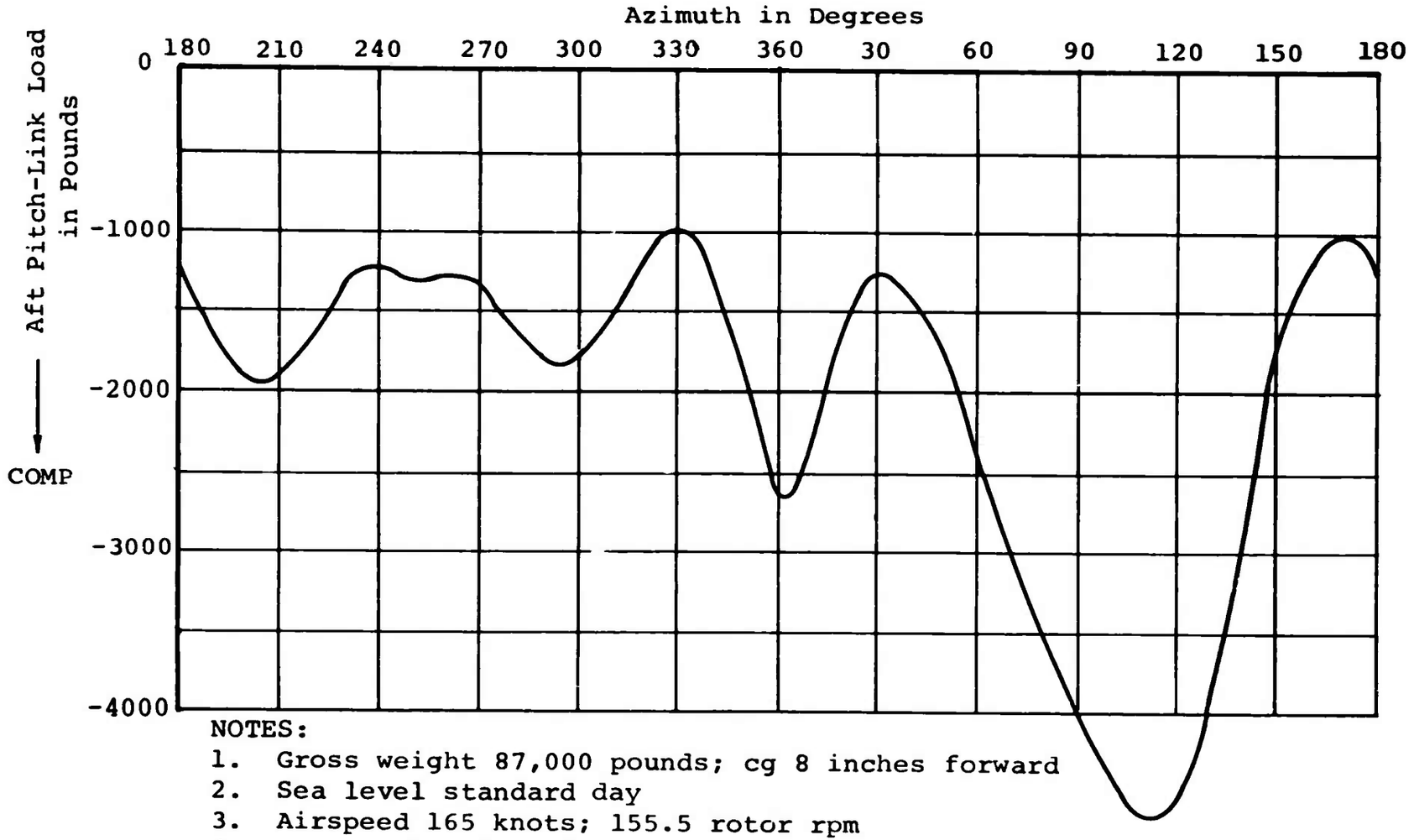

NOTES:

1. Gross weight 87,000 pounds; cg 8 inches forward
2. Sea level standard day
3. Airspeed 165 knots; 155.5 rotor rpm
4. Drooped leading-edge blade
5. θ_t = -10 degrees

Figure 48. Pitch-Link Load at 87,000 Pounds Gross Weight. (Sheet 2 of 2)

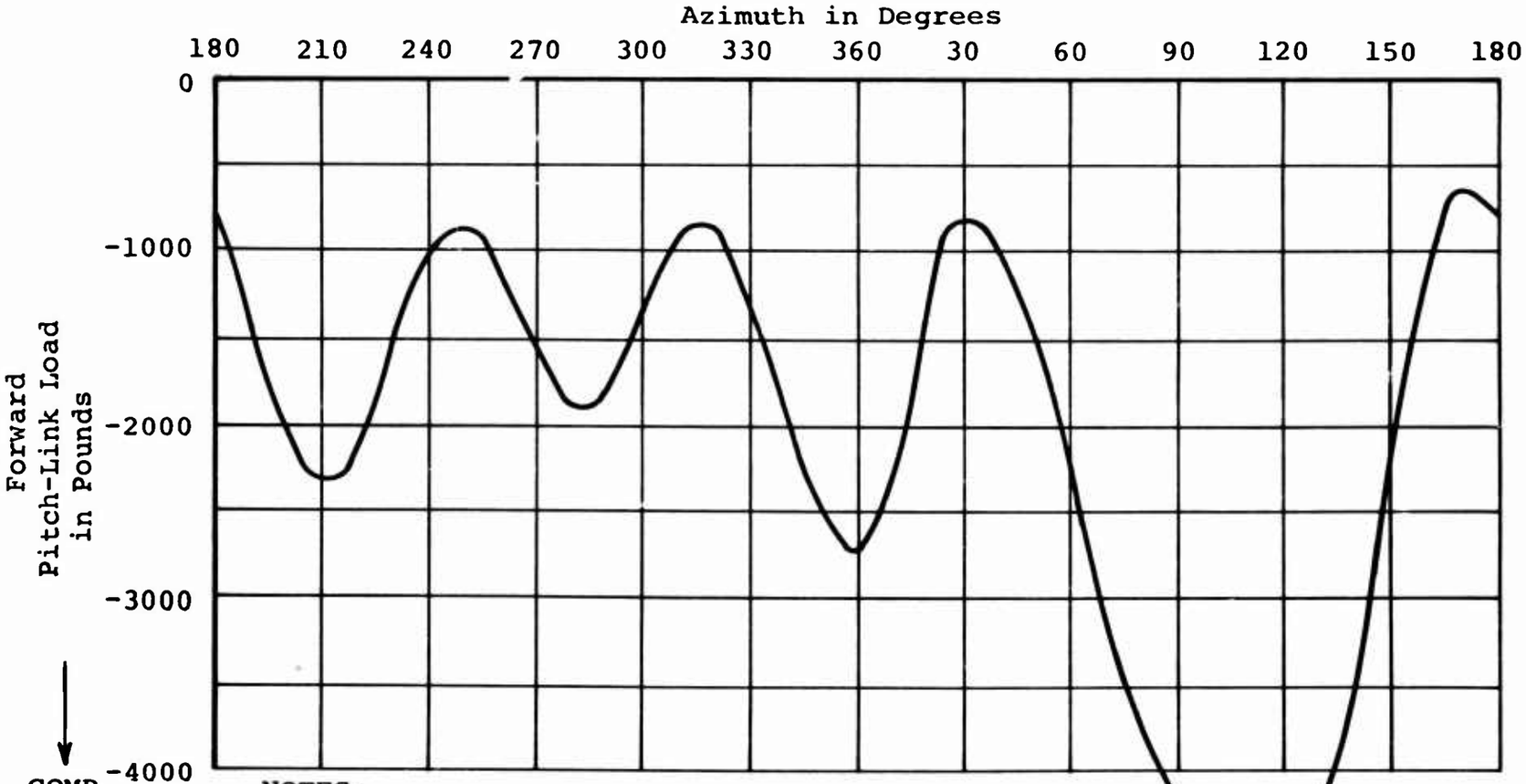

NOTES:

1. Gross weight 75,700 pounds; cg 8 inches forward
2. Altitude 5000 feet, standard
3. Airspeed 170 knots; 155.5 rotor rpm
4. Drooped leading-edge blade
5. θ_t = -6 degrees

Figure 49. Pitch-Link Load at 75,700 Pounds Gross Weight. (Sheet 1 of 5)

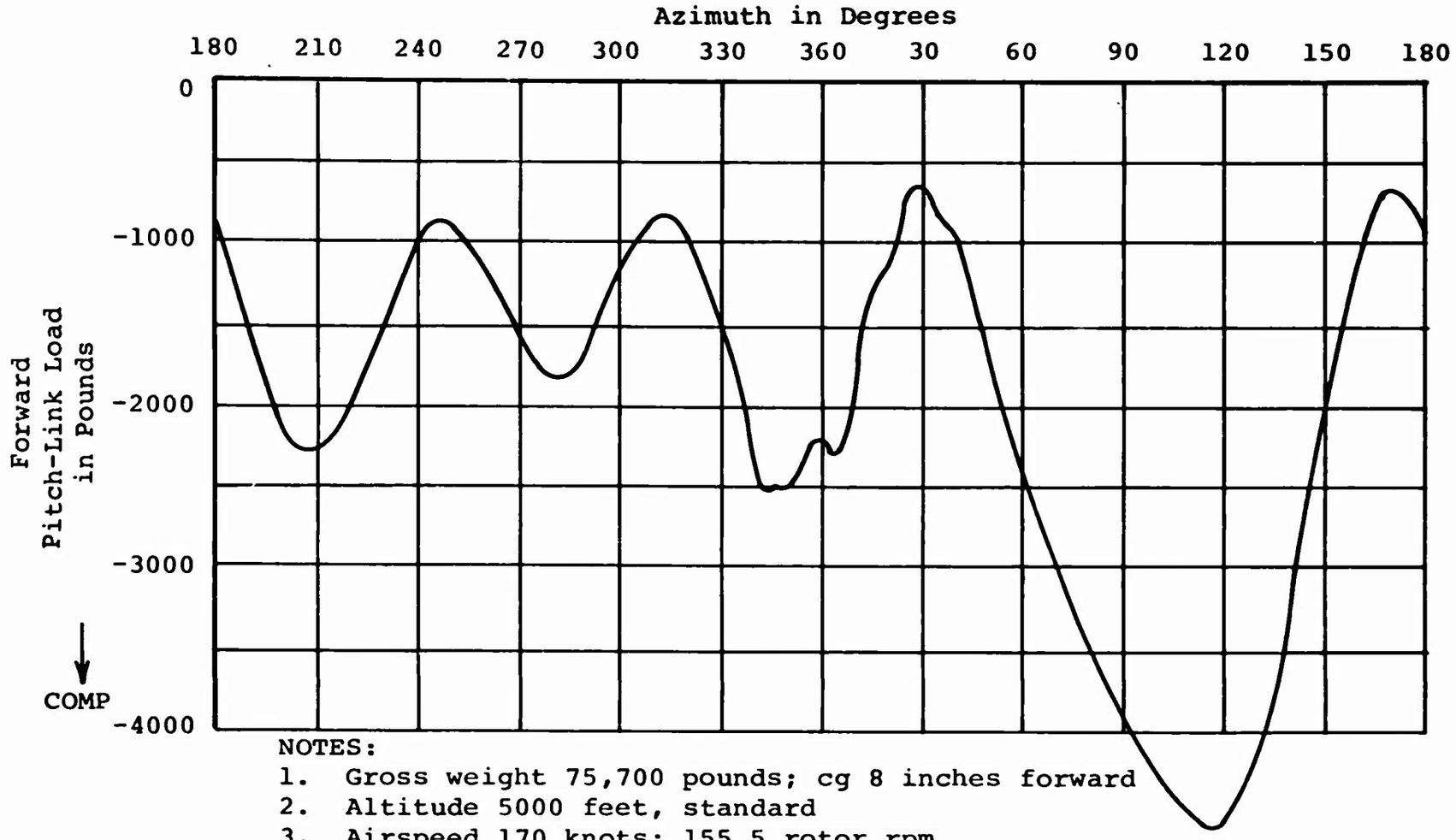

NOTES:

1. Gross weight 75,700 pounds; cg 8 inches forward
2. Altitude 5000 feet, standard
3. Airspeed 170 knots; 155.5 rotor rpm
4. Drooped leading-edge blade
5. θ_t = -8 degrees

Figure 49. Pitch-Link Load at 75,700 Pounds Gross Weight. (Sheet 2 of 5)

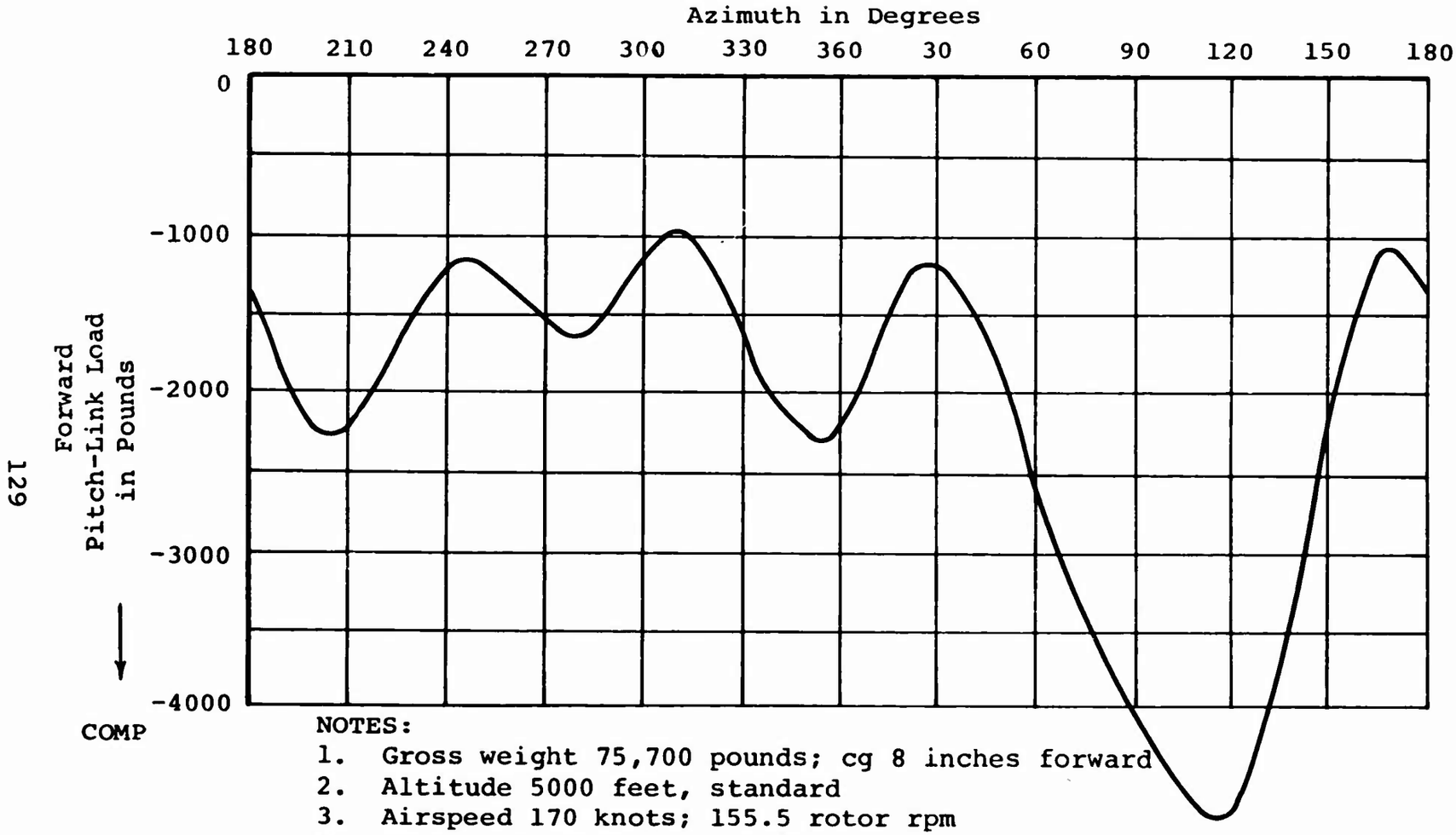

NOTES:

1. Gross weight 75,700 pounds; cg 8 inches forward
2. Altitude 5000 feet, standard
3. Airspeed 170 knots; 155.5 rotor rpm
4. Drooped leading-edge blade
5. θ_t = -10 degrees

Figure 49. Pitch-Link Load at 75,700 Pounds Gross Weight. (Sheet 3 of 5)

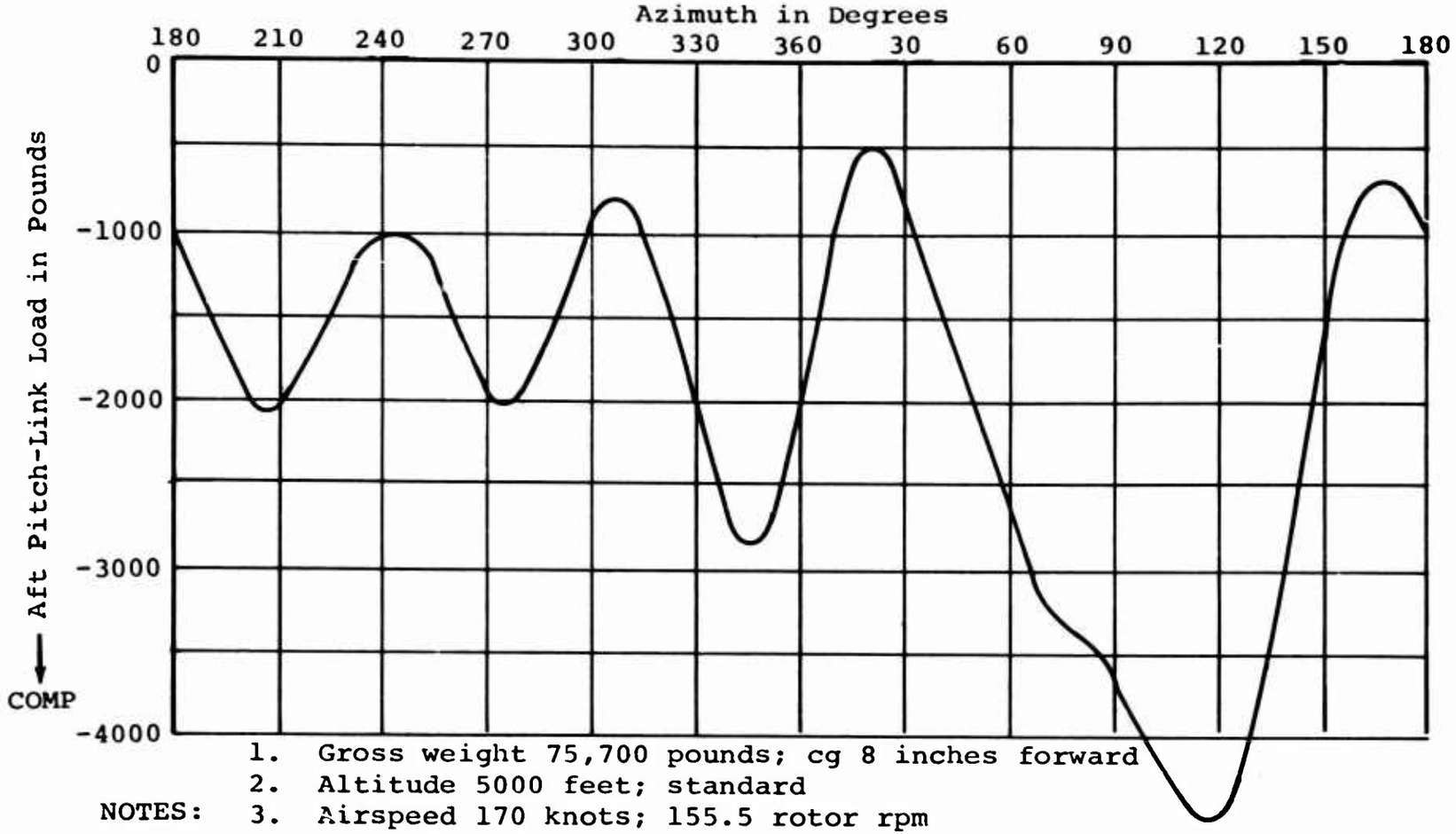

NOTES:
1. Gross weight 75,700 pounds; cg 8 inches forward
2. Altitude 5000 feet; standard
3. Airspeed 170 knots; 155.5 rotor rpm
4. Drooped leading-edge blade
5. θ_t = -10 degrees

Figure 49. Pitch-Link Load at 75,700 Pounds Gross Weight. (Sheet 4 of 5)

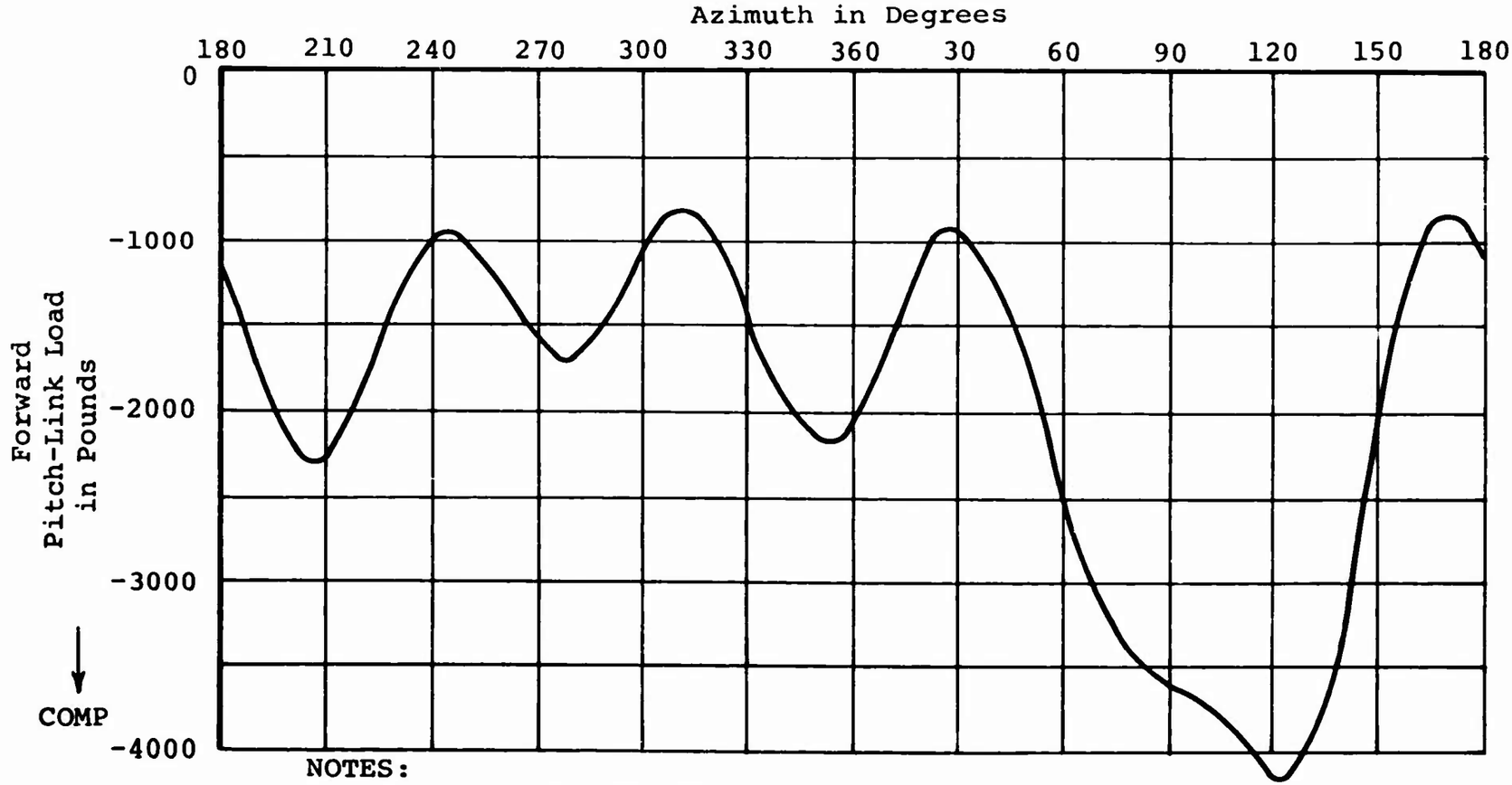

NOTES:

1. Gross weight 75,750 pounds; cg 8 inches forward
2. Altitude 5000 feet, standard
3. Airspeed 170 knots; 155.5 rotor rpm
4. Drooped leading-edge blade
5. θ_t = -12 degrees

Figure 49. Pitch-Link Load at 75,700 Pounds Gross Weight. (Sheet 5 of 5)

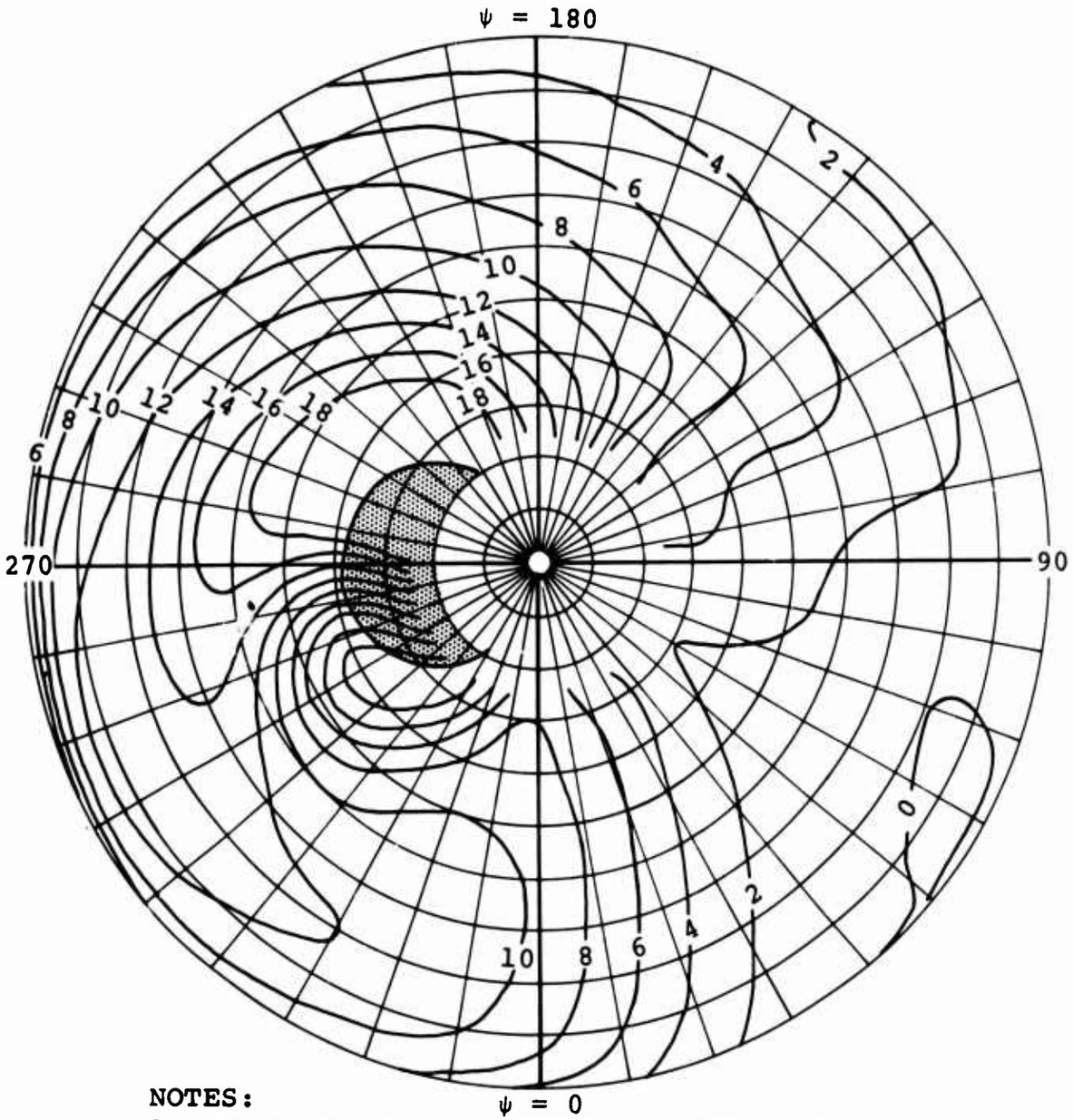

NOTES:

1. Forward rotor of heavy-lift helicopter
2. Gross weight 87,000 pounds; cg 8 inches forward
3. Airspeed 165 knots; 155 rotor rpm
4. θ_{TW} = -10 degrees ▒▒ Reverse flow region
5. $H_P = H_D = 0$

Figure 50. Forward Rotor Angle-of-Attack Contours.

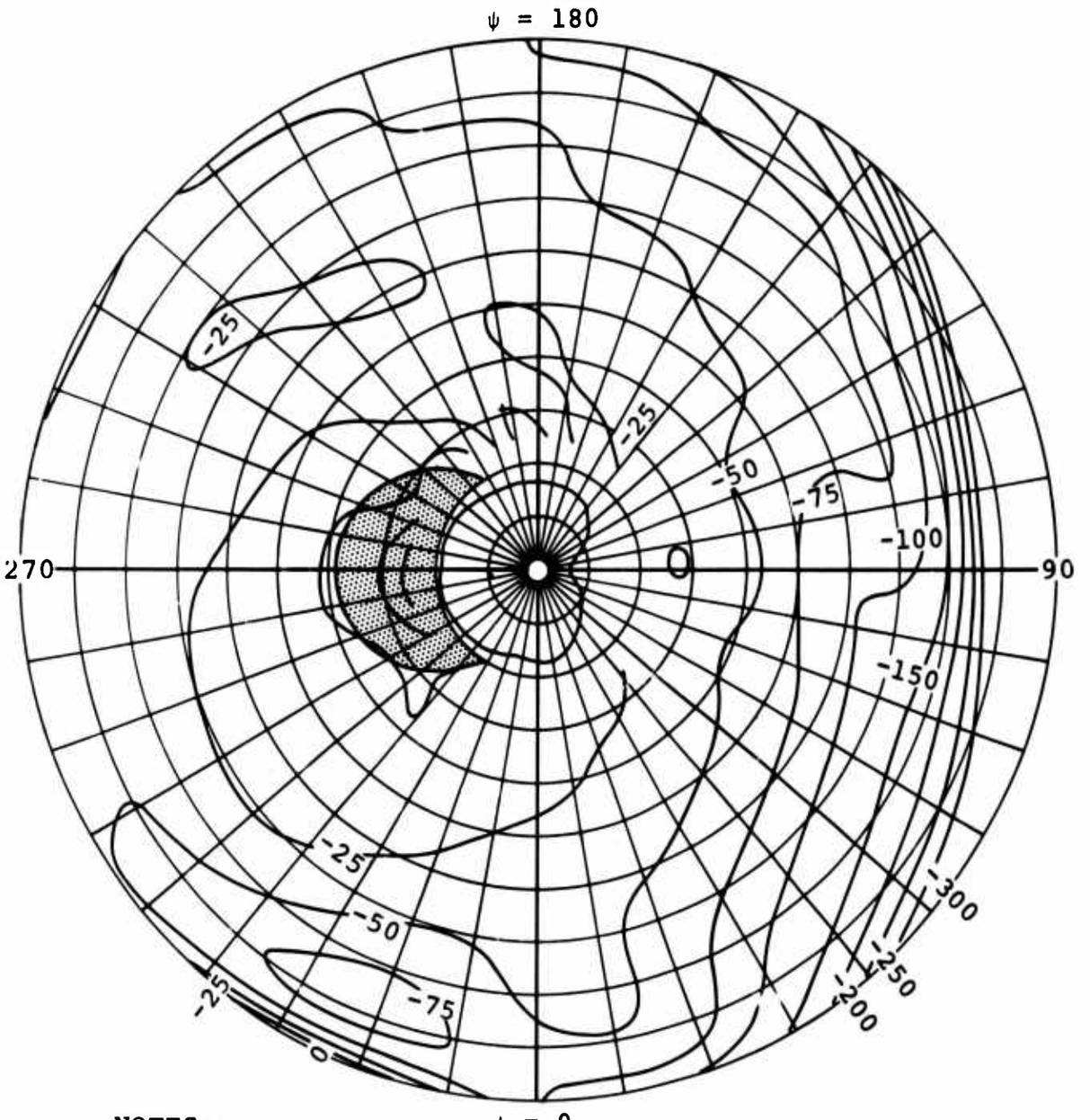

NOTES:
1. Forward rotor of heavy-lift helicopter
2. Gross weight 87,000 pounds; cg 8 inches forward
3. Airspeed 165 knots; 155 rotor rpm
4. θ_{TW} = -10 degrees ▒ Reverse flow region
5. $H_P = H_D = 0$

Figure 51. Forward Rotor Local Aerodynamic Moment Contours.

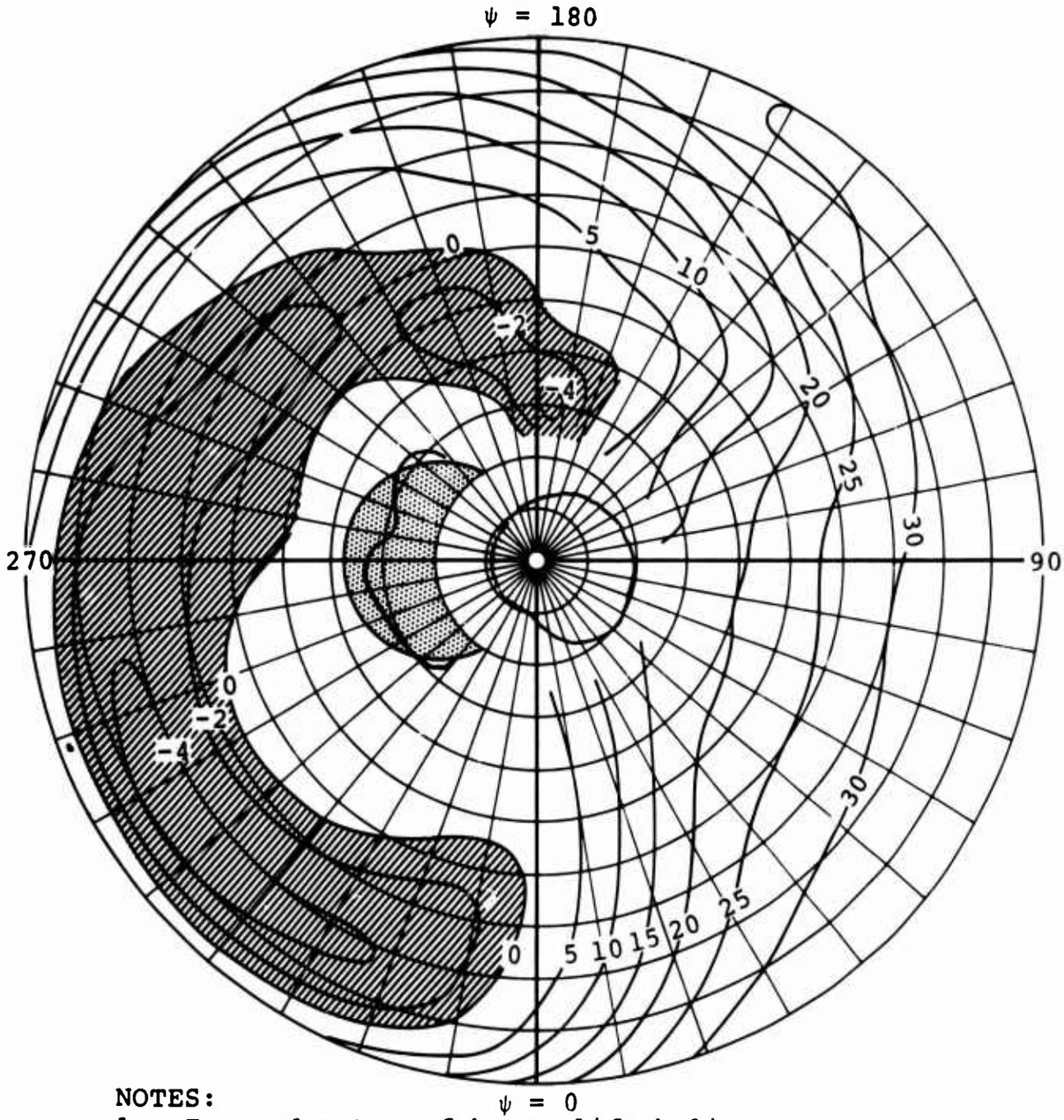

NOTES:

1. Forward rotor of heavy-lift helicopter
2. Gross weight 87,000 pounds; cg 8 inches forward
3. Airspeed 165 knots; 155 rotor rpm
4. θ_{TW} = -10 degrees
5. $H_P = H_D = 0$

Reverse flow region

Negative aerodynamic damping

Figure 52. Forward Rotor Local Aerodynamic Damping Contours.

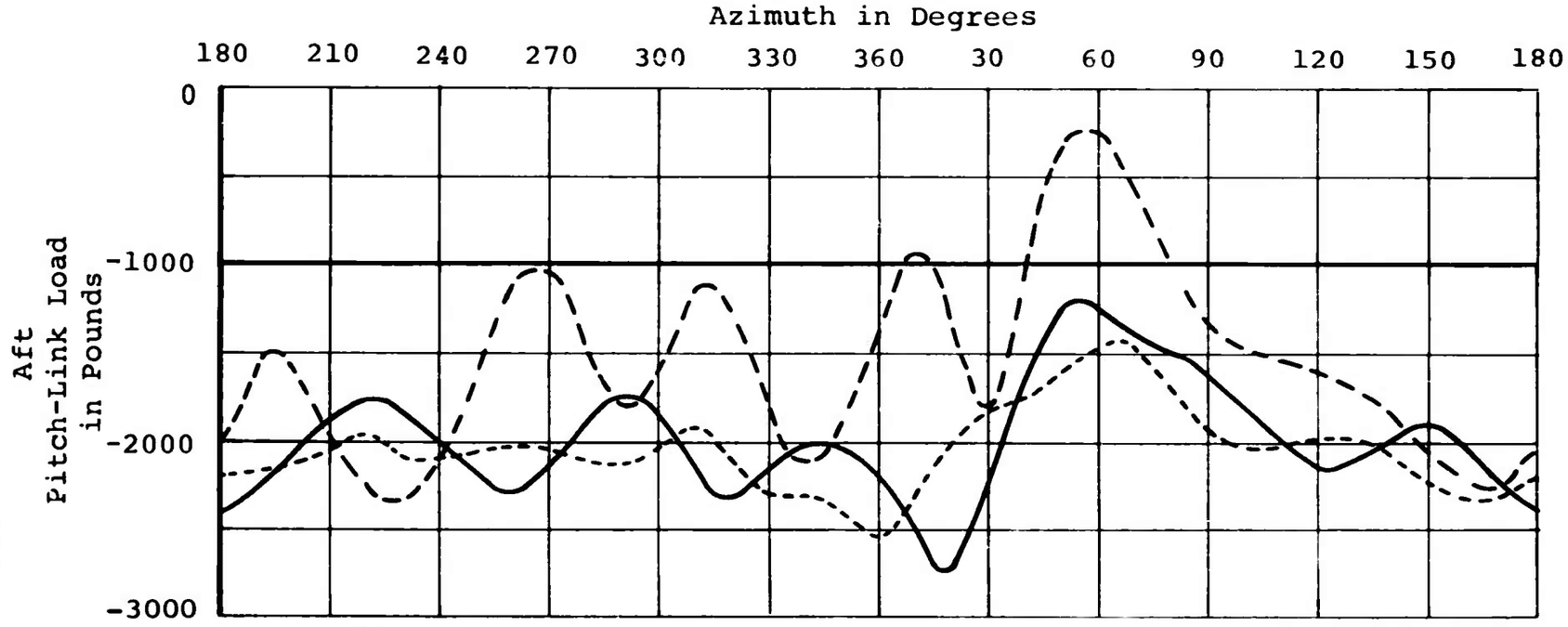

NOTES:

1. CH-47A B-5 with interim ECP 140/190 stiffness
2. Gross weight 28,240 pounds; cg 16.7 inches aft
3. Altitude 5000 feet; trim 3/5
4. Airspeed 147 knots; 230 rotor rpm
5. Symmetrical blade
6. θ_t = -9 degrees
7. Pitch-link load
   - ——— from computer program
   - - - - - - due to static moment
   - — — — from flight test (281/10)

Figure 53. CH-47A Aft Rotor Pitch-Link Load at 28,940 Pounds Gross Weight, 5000 Feet, 147 Knots.

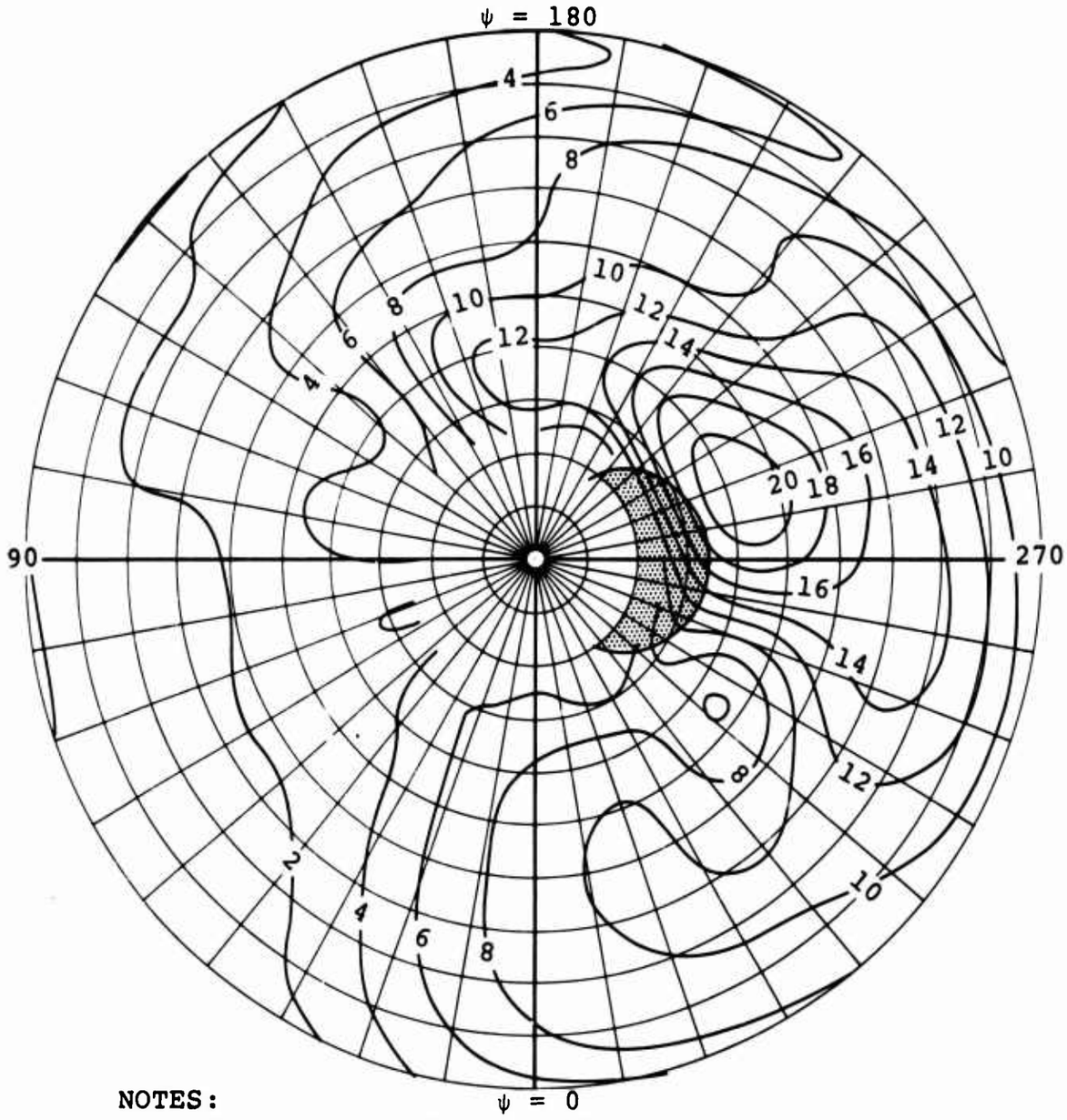

NOTES:

1. Aft rotor of CH-47A helicopter
2. Gross weight 28,240 pounds; cg 16.7 inches aft
3. Airspeed 147 knots; 230 rotor rpm
4. θ_{TW} = -9 degrees ▒▒ Reverse flow region
5. H_D = 5000 feet
6. Trim 3/5

Figure 54. CH-47A Aft Rotor Angle-of-Attack Contours.

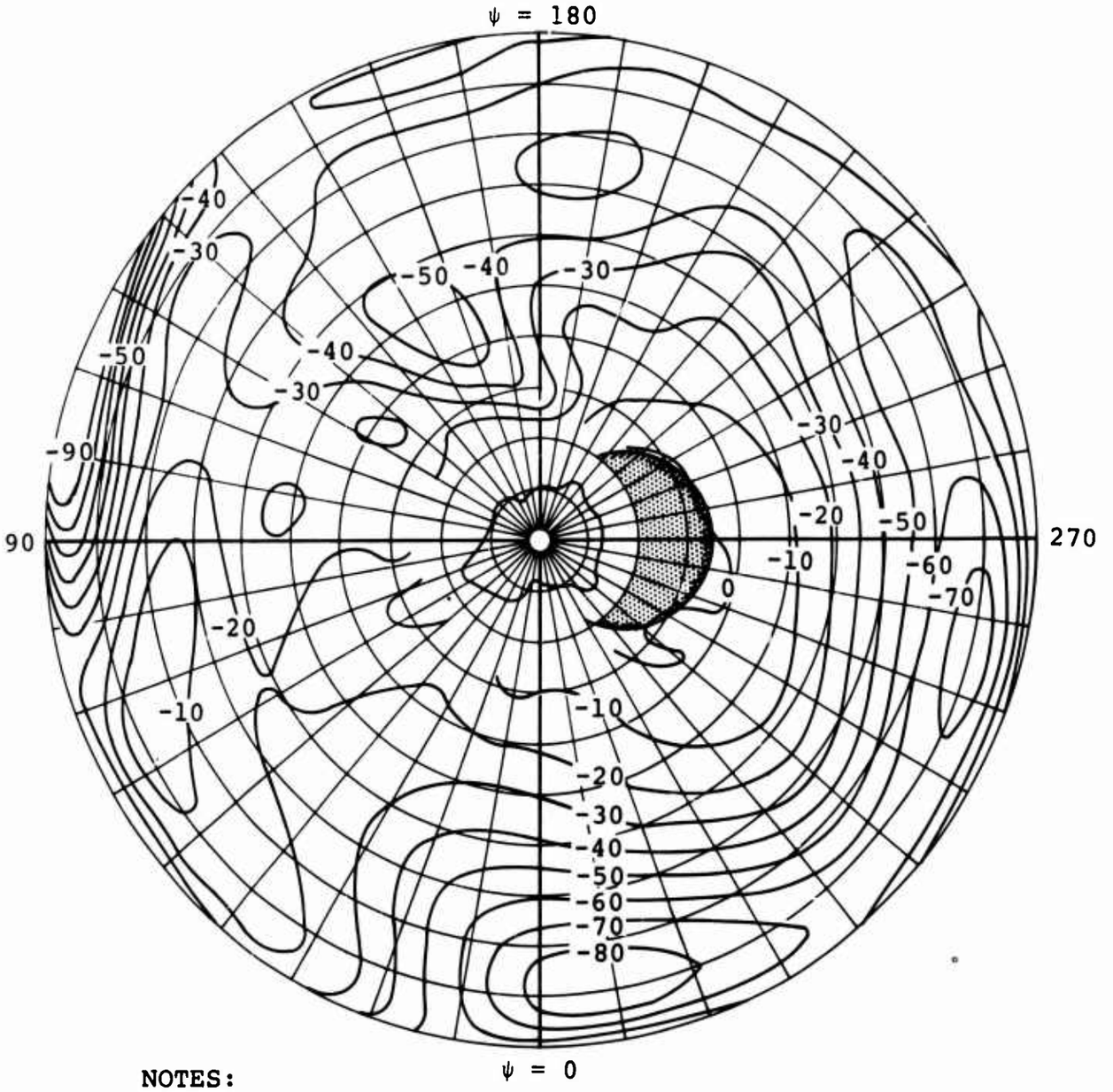

NOTES:

1. Aft rotor of CH-47A helicopter
2. Gross weight 28,240 pounds; cg 16.7 inches aft
3. Airspeed 147 knots; 230 rotor rpm
4. θ_{TW} = -9 degrees ▒▒ Reverse flow region
5. H_D = 5000 feet
6. Trim 3/5

Figure 55. CH-47A Aft Rotor Local Aerodynamic Moment Contours.

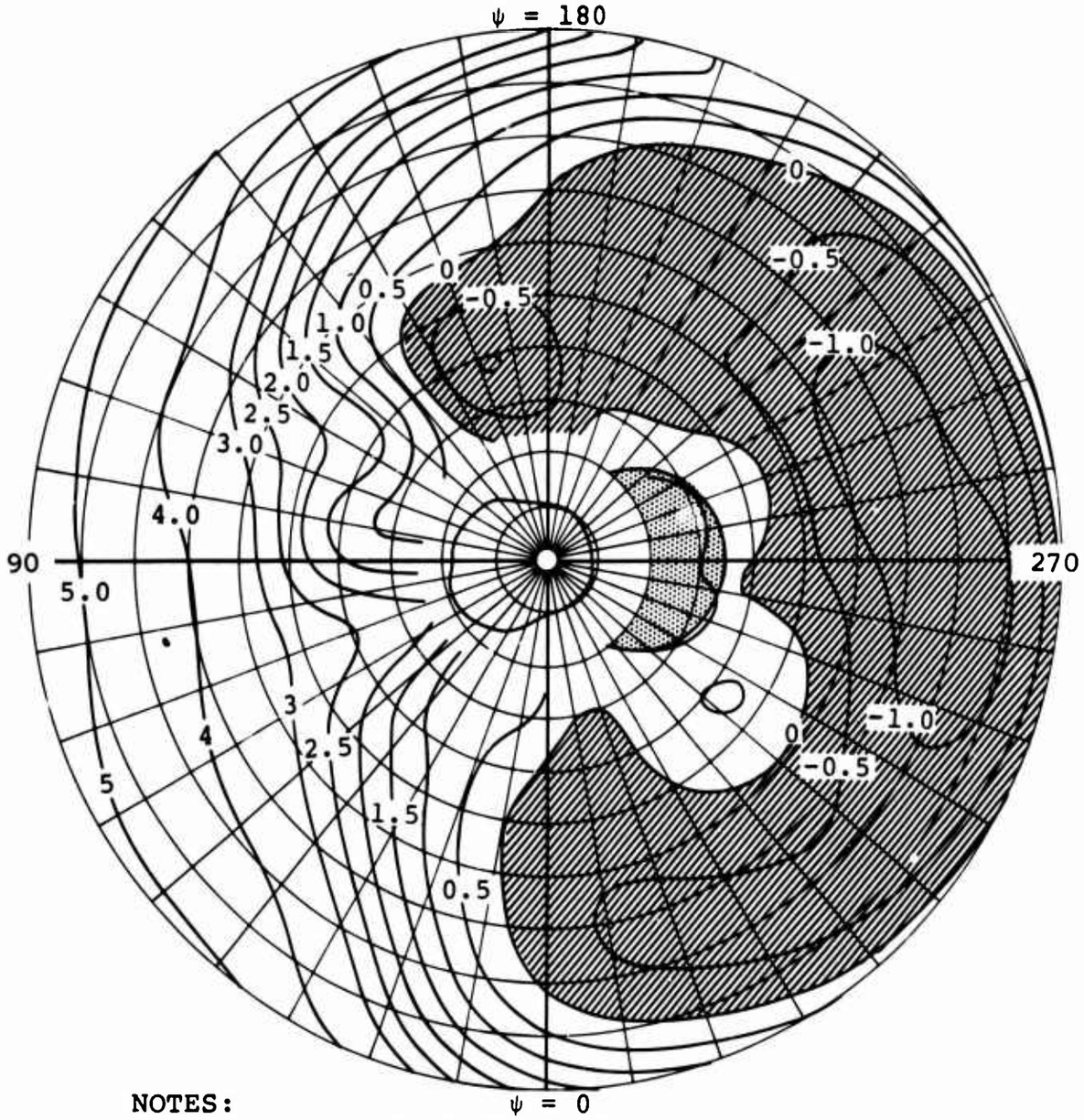

NOTES:

1. Aft rotor of CH-47A helicopter
2. Gross weight 28,240 pounds; cg 16.7 inches aft
3. Airspeed 147 knots; 230 rotor rpm
4. θ_{TW} = -9 degrees
5. H_D = 5000 feet
6. Trim 3/5

Reverse flow region

Negative aerodynamic damping

Figure 56. CH-47A Aft Rotor Local Aerodynamic Damping Contours.

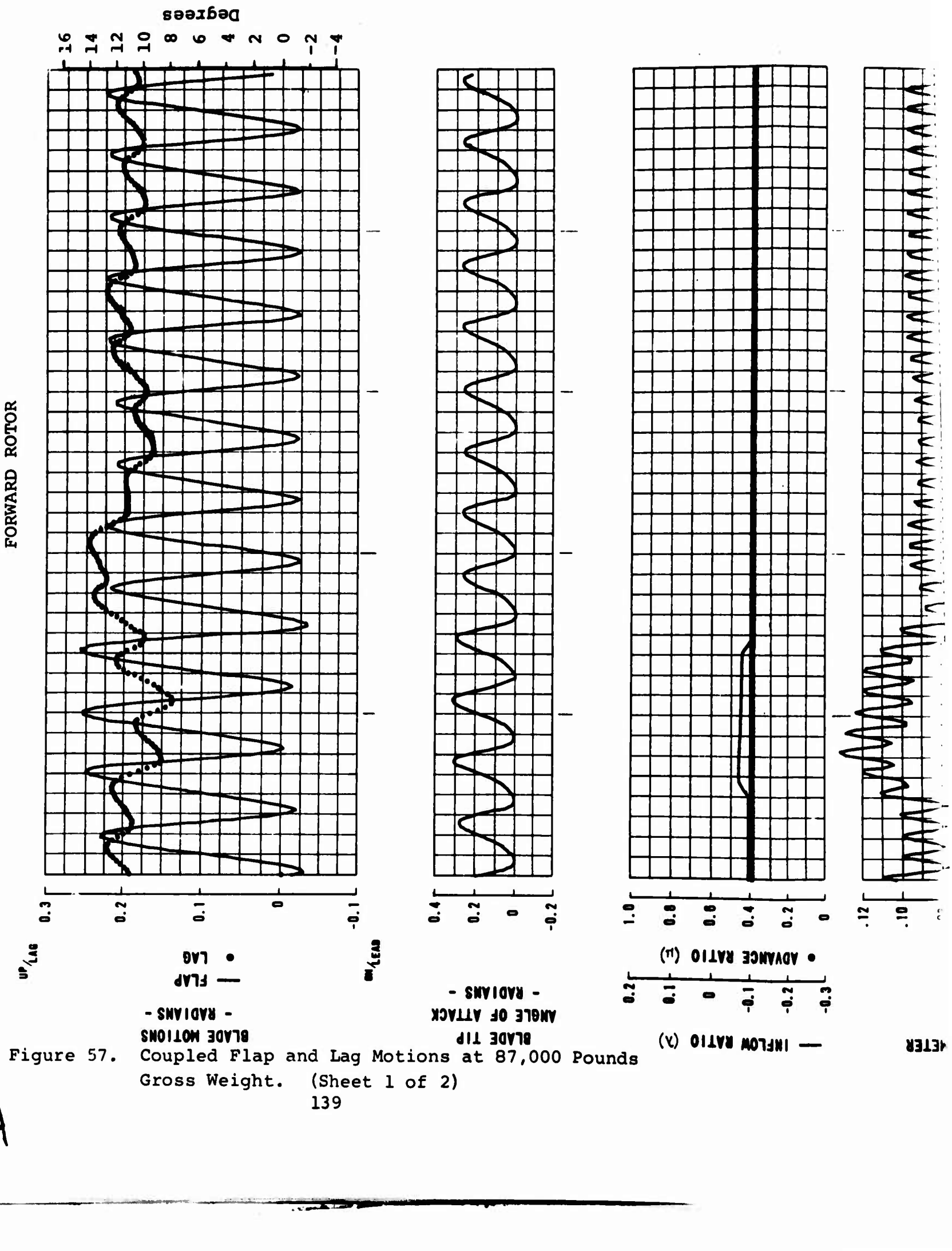

Figure 57. Coupled Flap and Lag Motions at 87,000 Pounds Gross Weight. (Sheet 1 of 2)

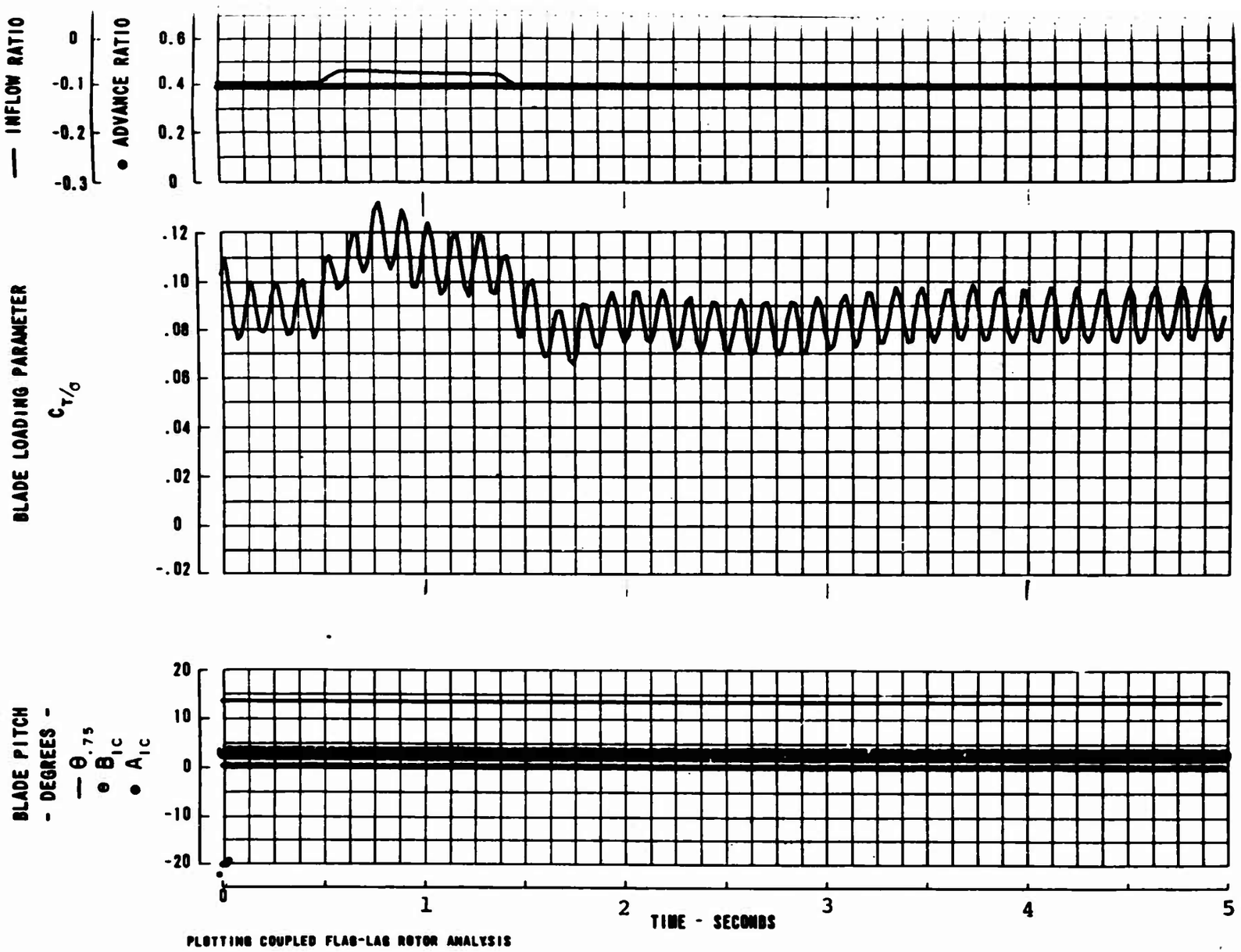

PLOTTING COUPLED FLAG-LAG ROTOR ANALYSIS

NOTES:

1. Gross Weight 87,000 pounds; cg 8 inches forward
2. $H_P = H_D = 0$
3. Airspeed 165 knots; 155 rotor rpm
4. Gust disturbance, 20 feet per second
5. $\theta_t = -10$ degrees

Figure 57. Coupled Flap and Lag Motions at 87,000 Pounds Gross Weight. (Sheet 2 of 2)

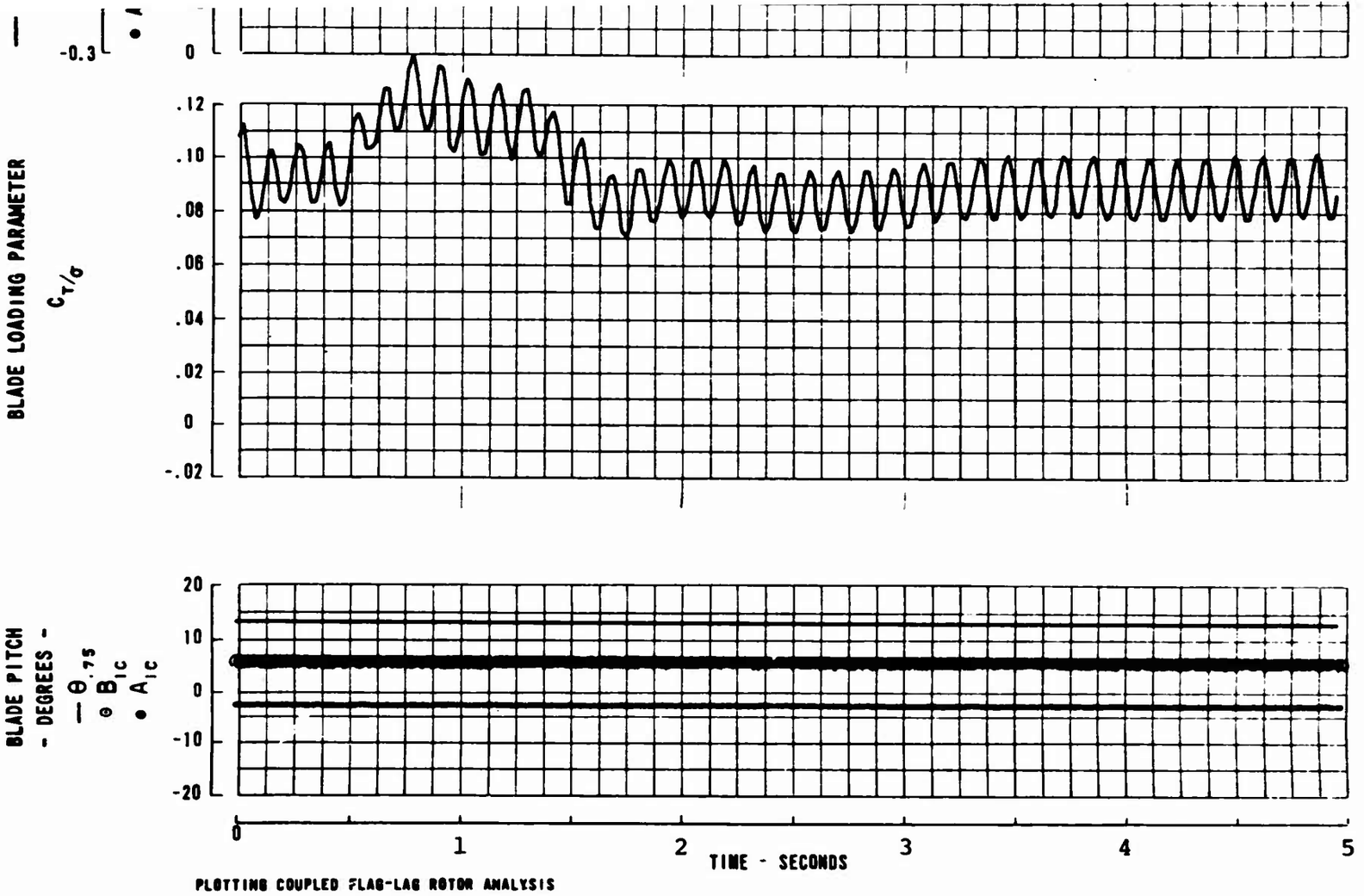

PLOTTING COUPLED FLAG-LAG ROTOR ANALYSIS

NOTES:

1. Gross weight 87,000 pounds; cg 8 inches forward
2. $H_P = H_D = 0$
3. Airspeed 165 knots; 155 rotor rpm
4. Gust disturbance, 20 feet per second
5. $\theta_t = -10$ degrees

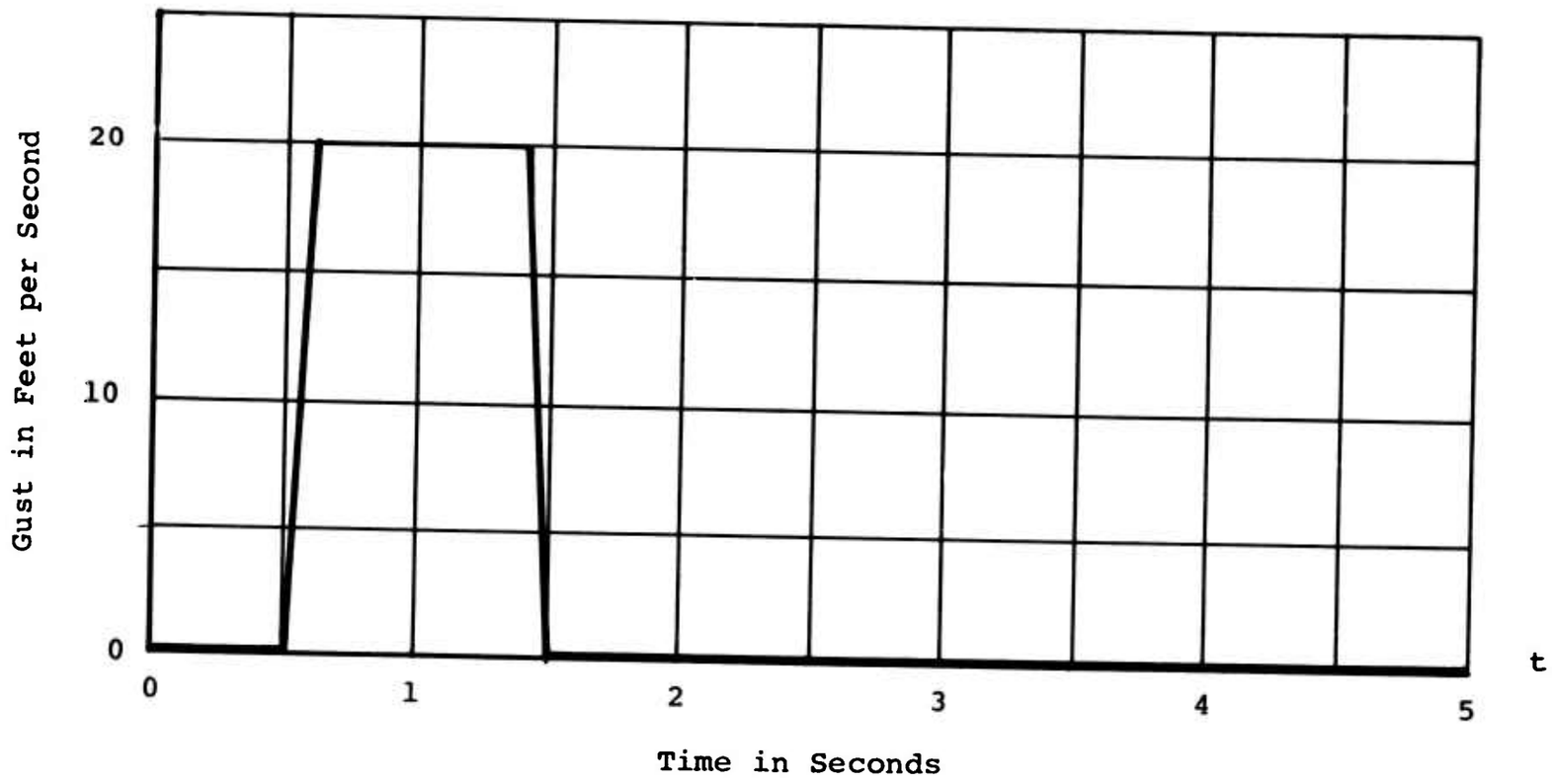

Figure 58. Gust Input Parallel to Shaft.

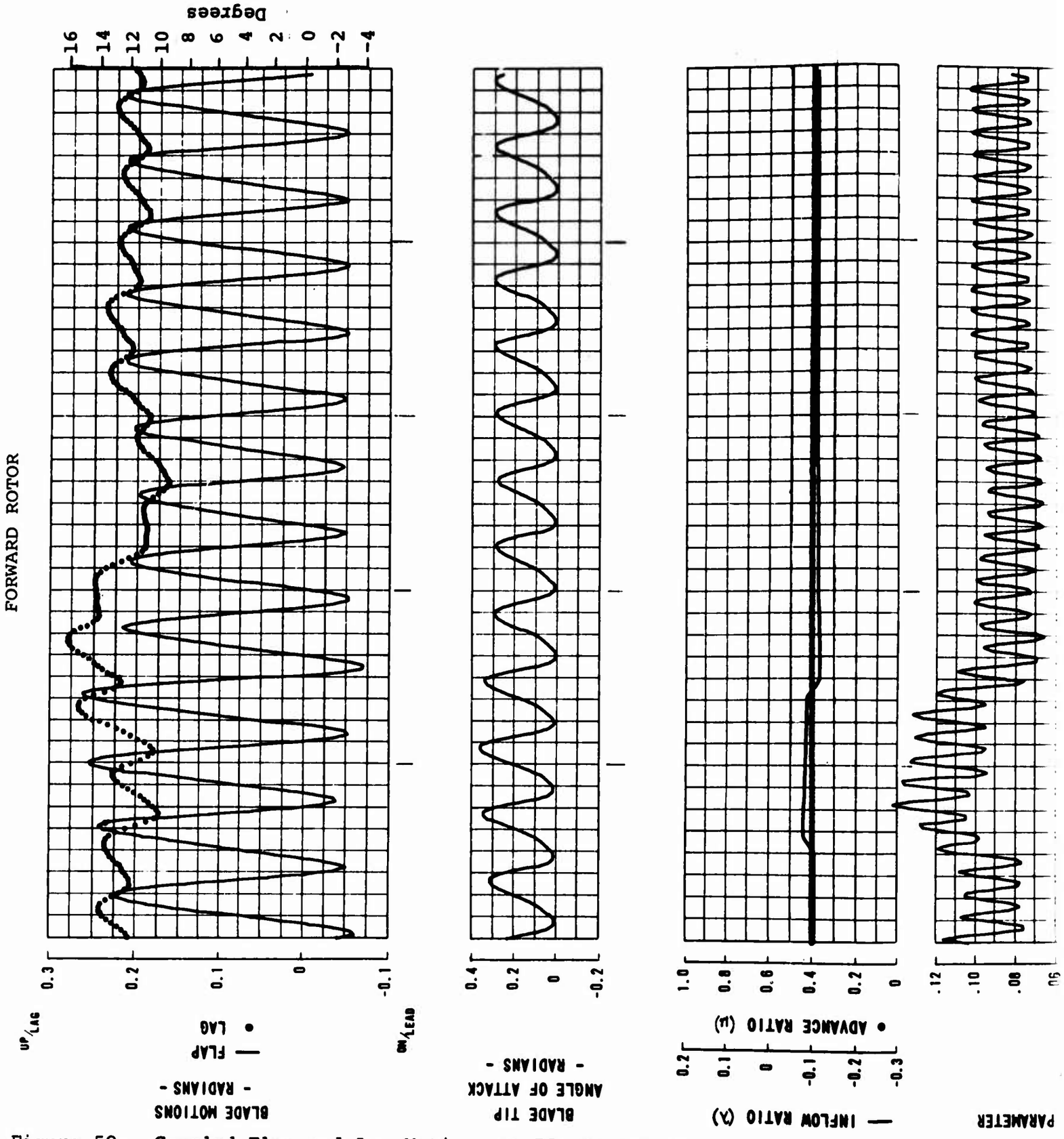

Figure 59. Coupled Flap and Lag Motions at 75,700 Pounds Gross Weight. (Sheet 1 of 5)

A

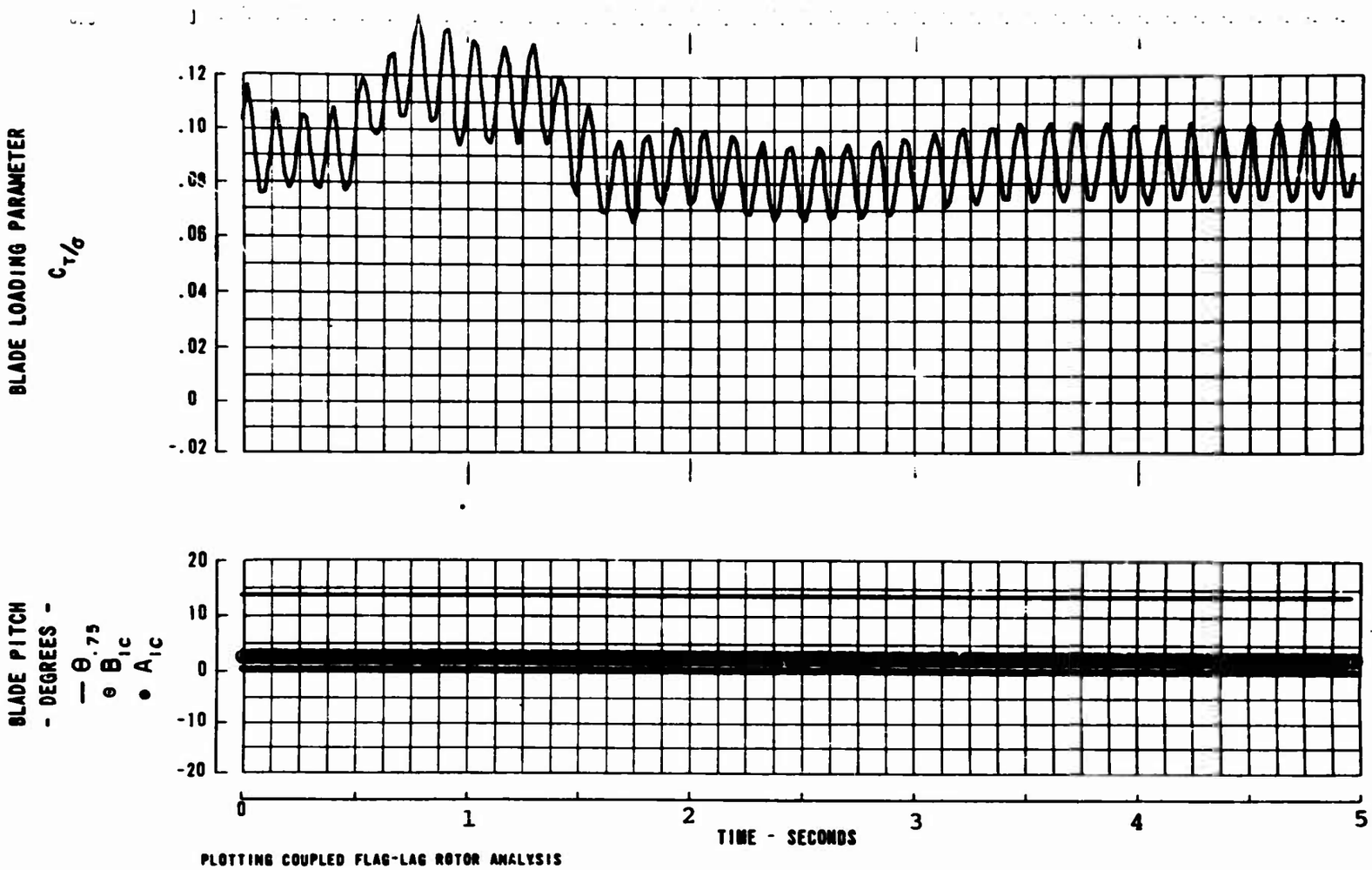

PLOTTING COUPLED FLAG-LAG ROTOR ANALYSIS

NOTES:

1. Gross weight 75,700 pounds; cg 8 inches forward
2. $H_P = H_D = 5000$ feet
3. Airspeed 170 knots; 155 rotor rpm
4. Gust disturbance, 20 feet per second
5. $\theta_t = -6$ degrees

Figure 59. Coupled Flap and Lag Motions at 75,700 Pounds Gross Weight. (Sheet 2 of 5)

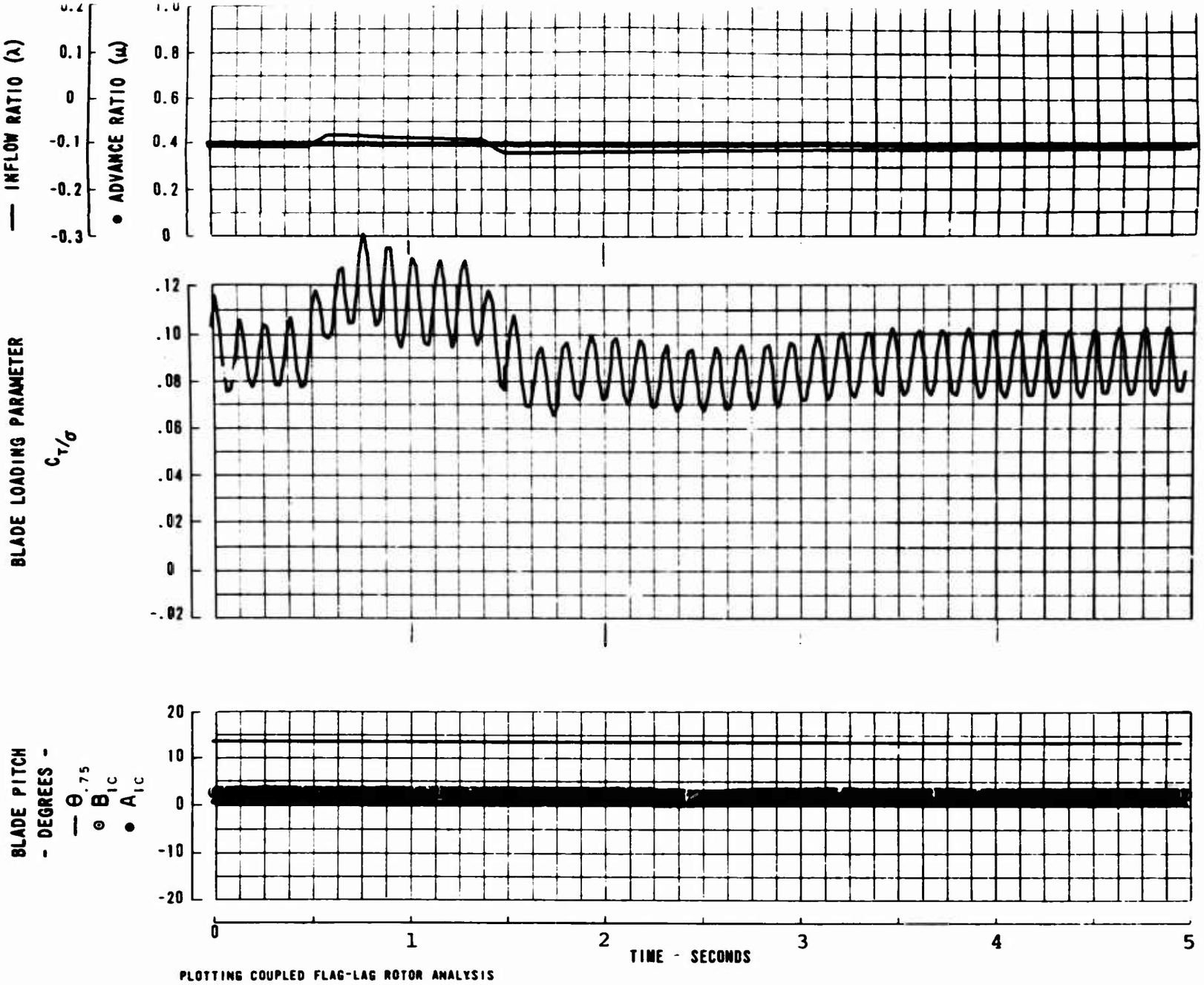

PLOTTING COUPLED FLAG-LAG ROTOR ANALYSIS

NOTES:

1. Gross weight 75,700 pounds; cg 8 inches forward
2. $H_P = H_D = 5000$ feet
3. Airspeed 170 knots; 155 rotor rpm
4. Gust disturbance, 20 feet per second
5. $\theta_t = -8$ degrees

Figure 59. Coupled Flap and Lag Motions at 75,700 Pounds Gross Weight. (Sheet 3 of 5)

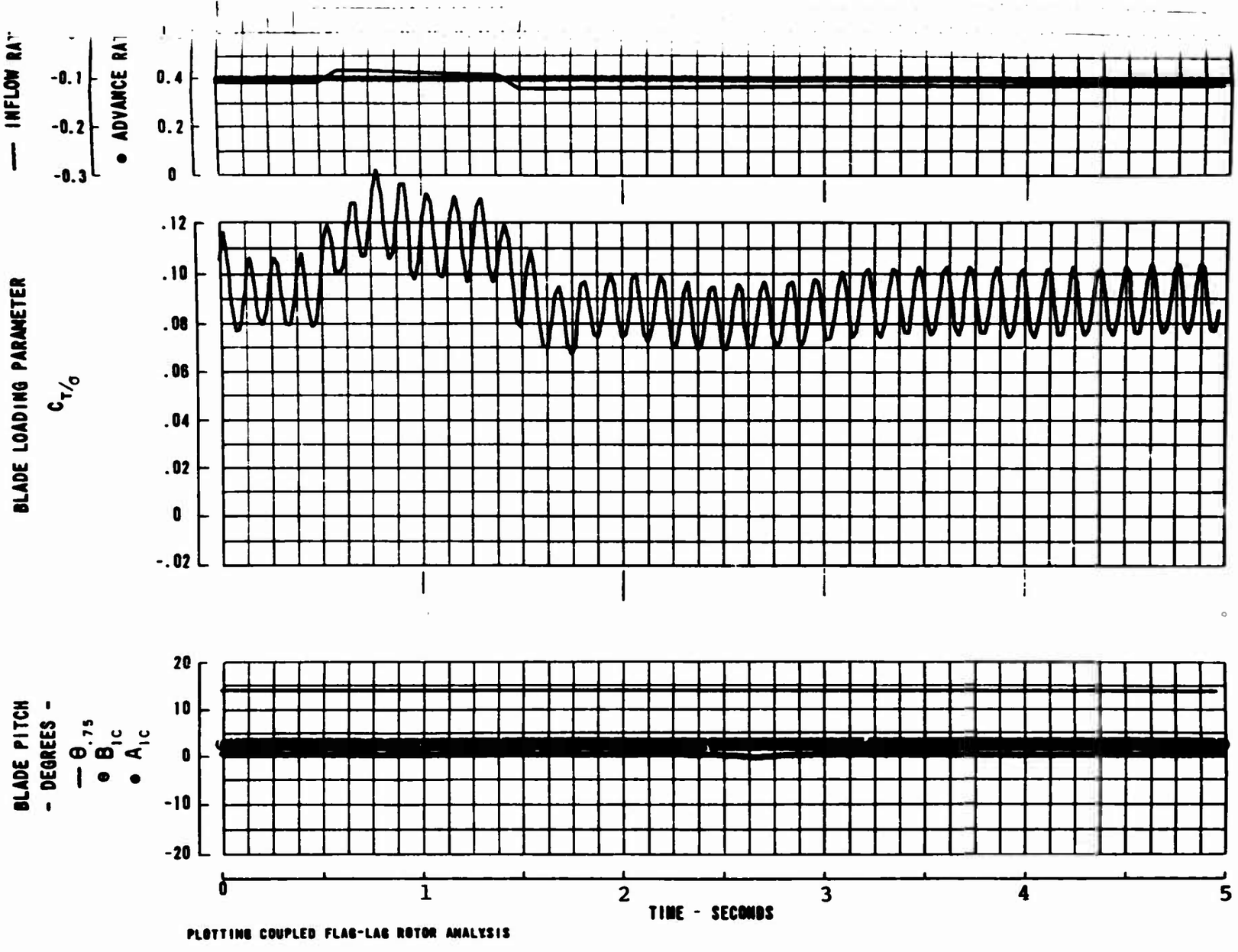

PLOTTING COUPLED FLAG-LAG ROTOR ANALYSIS

NOTES:

1. Gross weight 75,700 pounds; cg 8 inches forward
2. $H_P = H_D = 5000$ feet
3. Airspeed 170 knots; 155 rotor rpm
4. Gust disturbance, 20 feet per second
5. $\theta_t = -10$ degrees

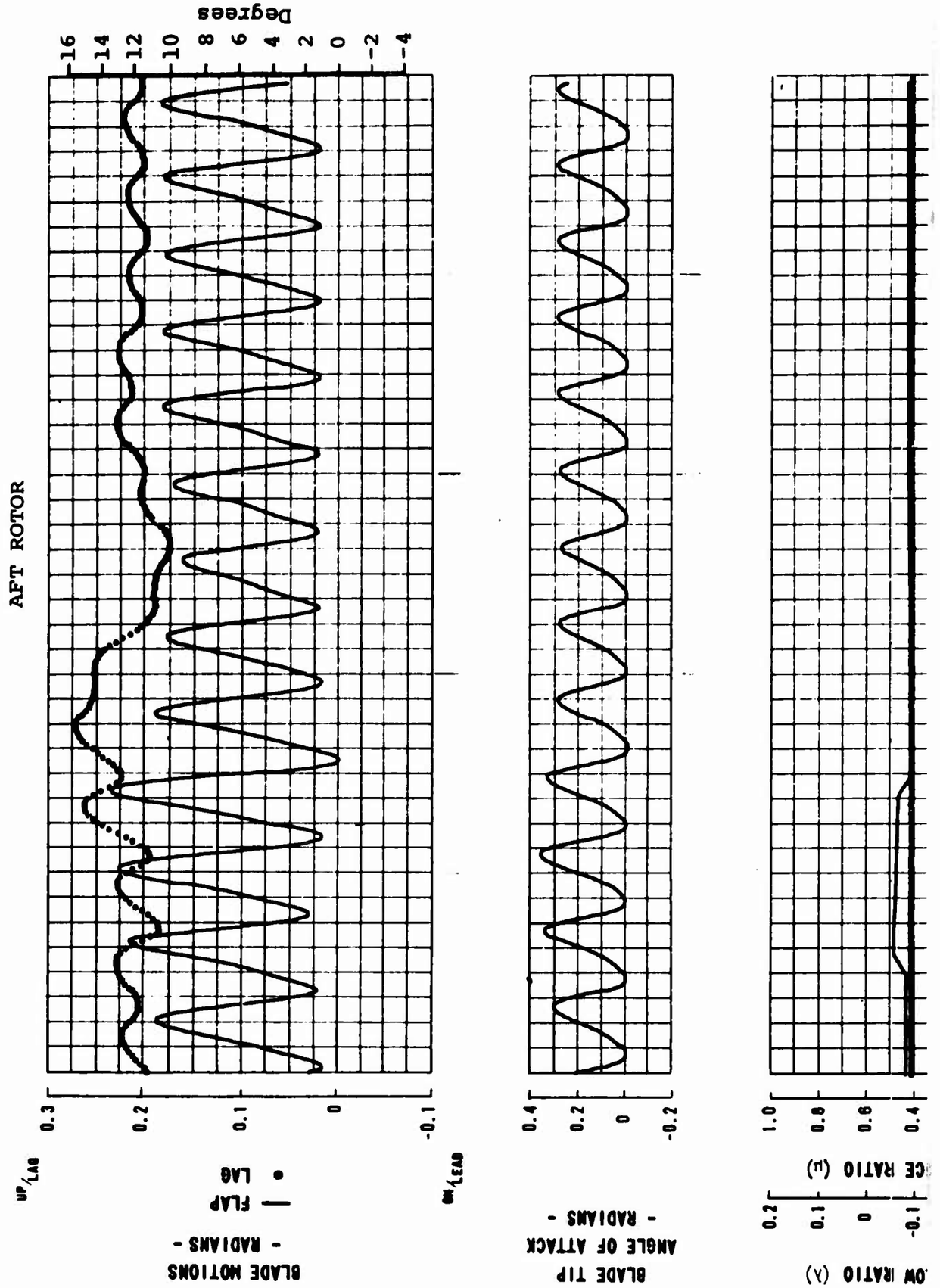

Figure 59. Coupled Flap and Lag Motions at 75,700 Pounds Gross Weight. (Sheet 4 of 5)

A

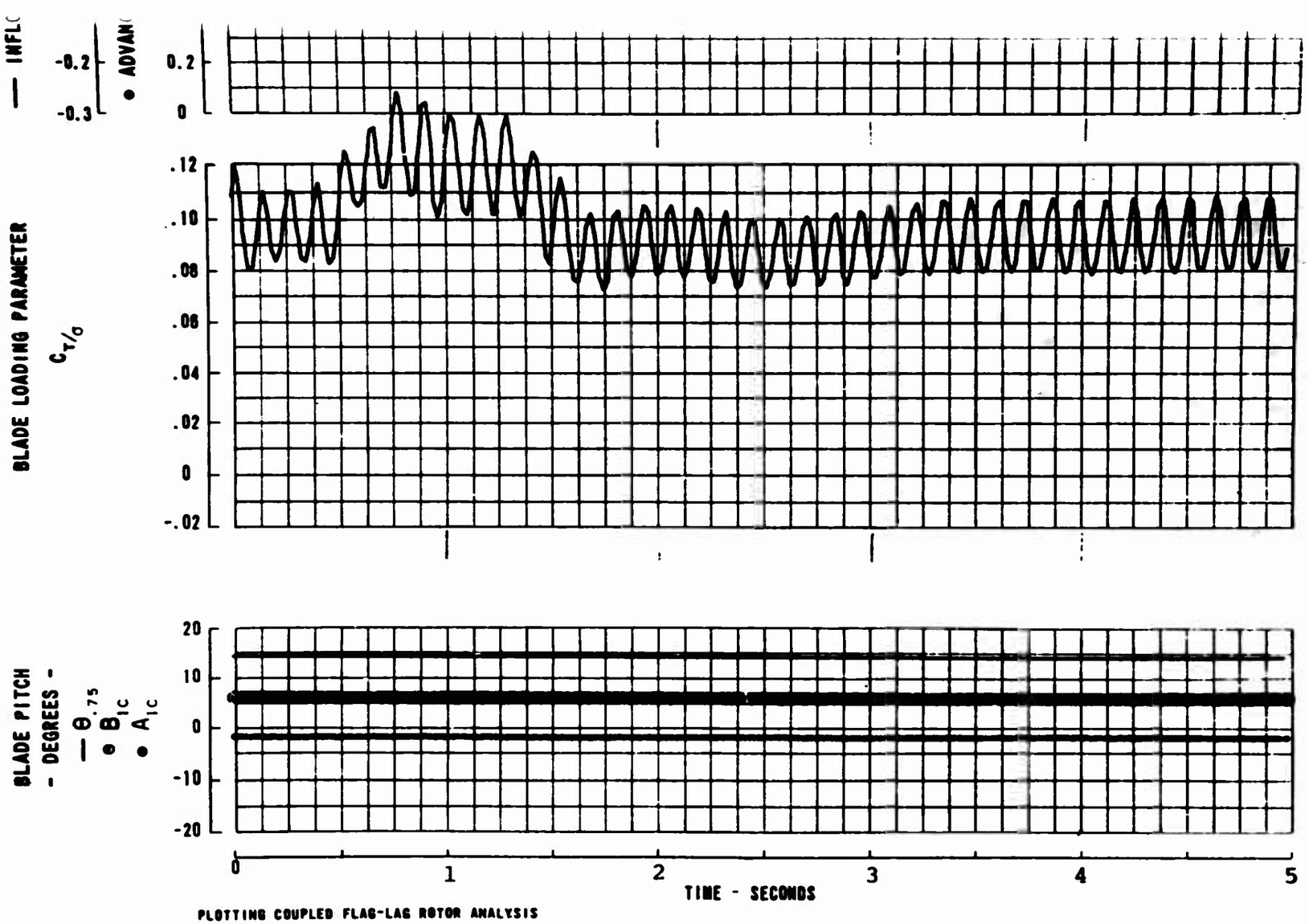

PLOTTING COUPLED FLAG-LAG ROTOR ANALYSIS

NOTES:

1. Gross weight 75,700 pounds; cg 8 inches forward
2. $H_P = H_D = 5000$ feet
3. Airspeed 170 knots; 155 rotor rpm
4. Gust disturbance, 20 feet per second
5. $\theta_t = -10$ degrees

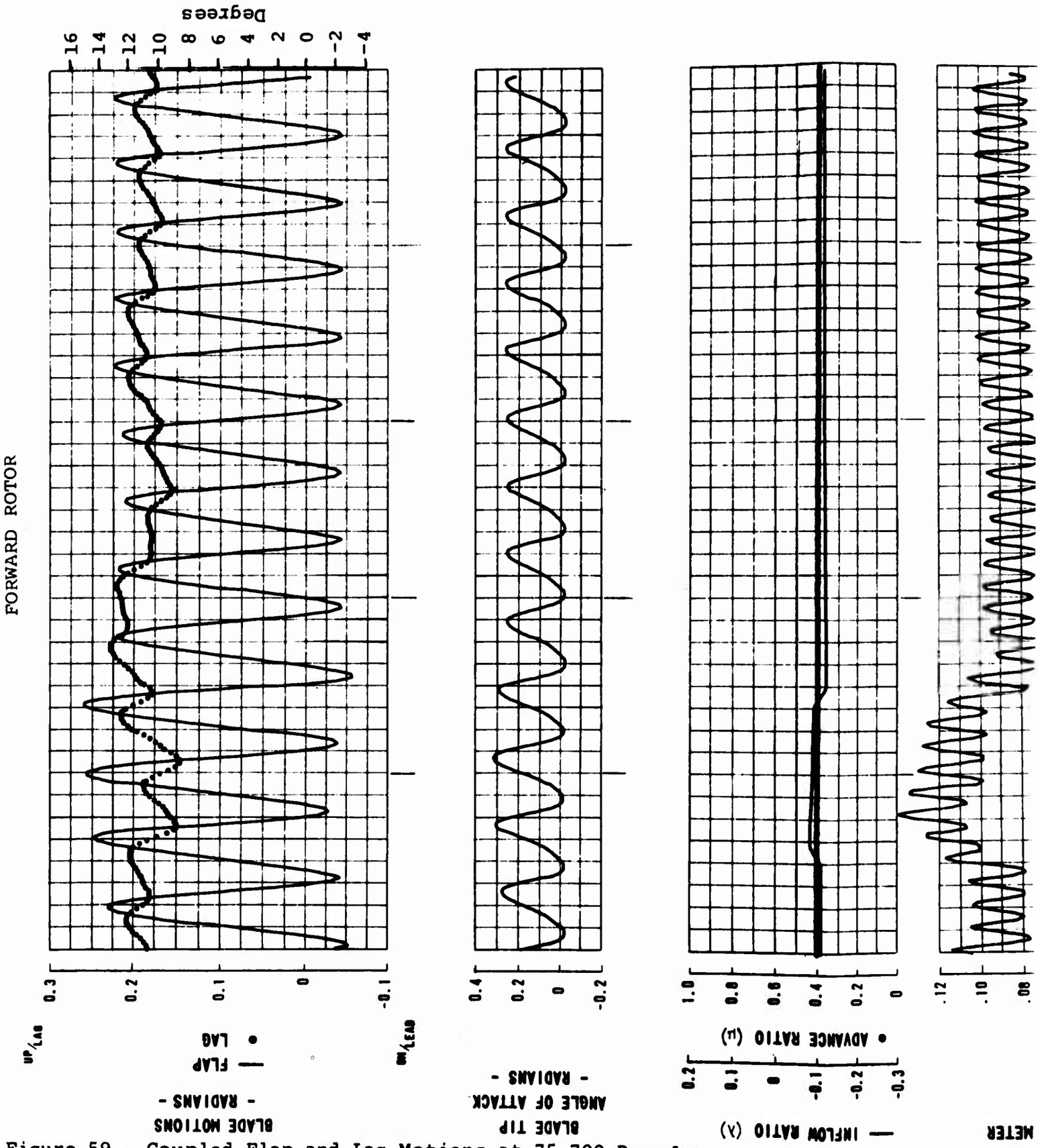

Figure 59. Coupled Flap and Lag Motions at 75,700 Pounds Gross Weight. (Sheet 5 of 5)

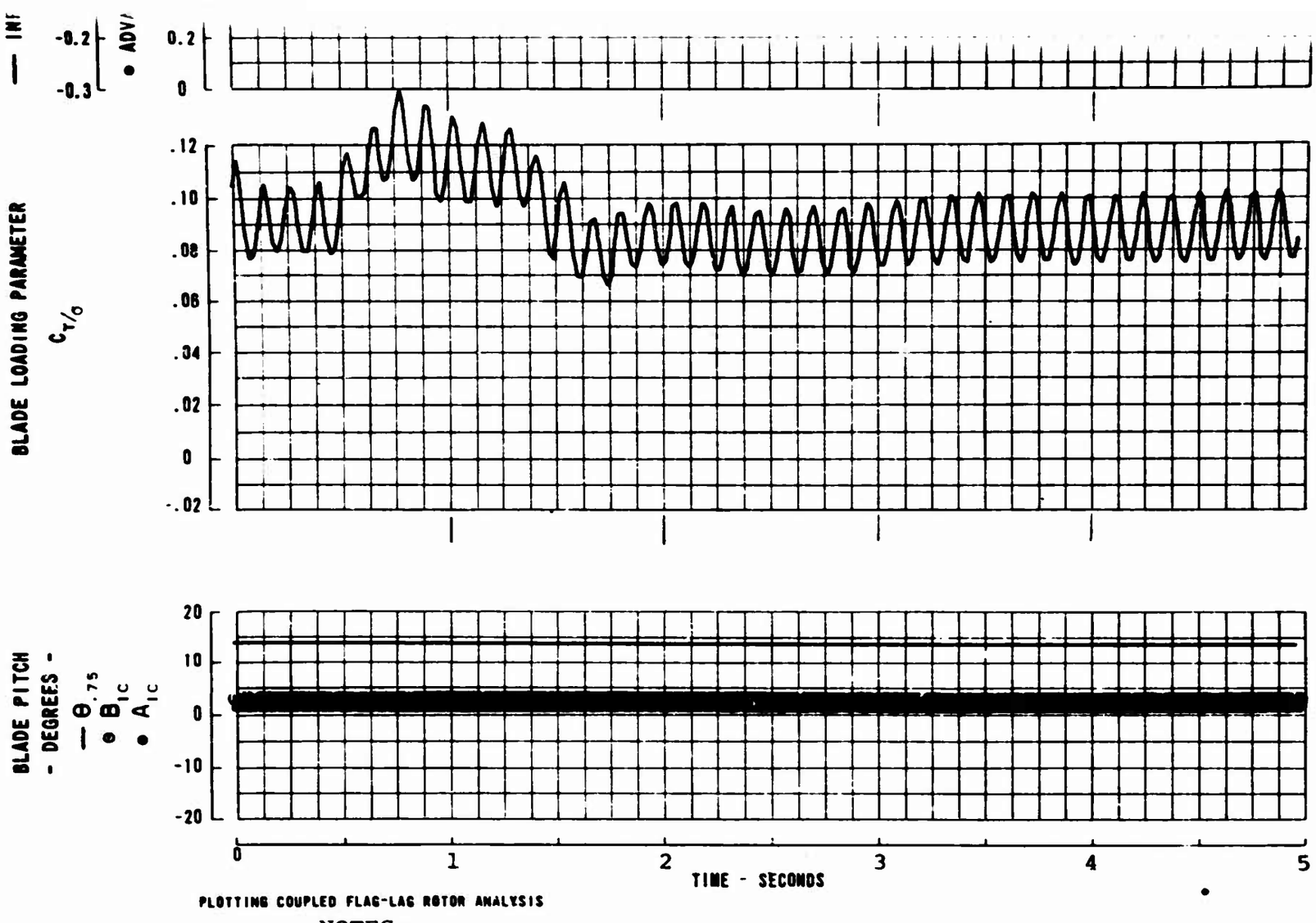

PLOTTING COUPLED FLAG-LAG ROTOR ANALYSIS

NOTES:

1. Gross Weight 75,700 pounds; cg 3 inches forward
2. $H_p = H_D = 5000$ feet
3. Airspeed 170 knots; 155 rotor rpm
4. Gust disturbance, 20 feet per second
5. $\theta_t = -12$ degrees

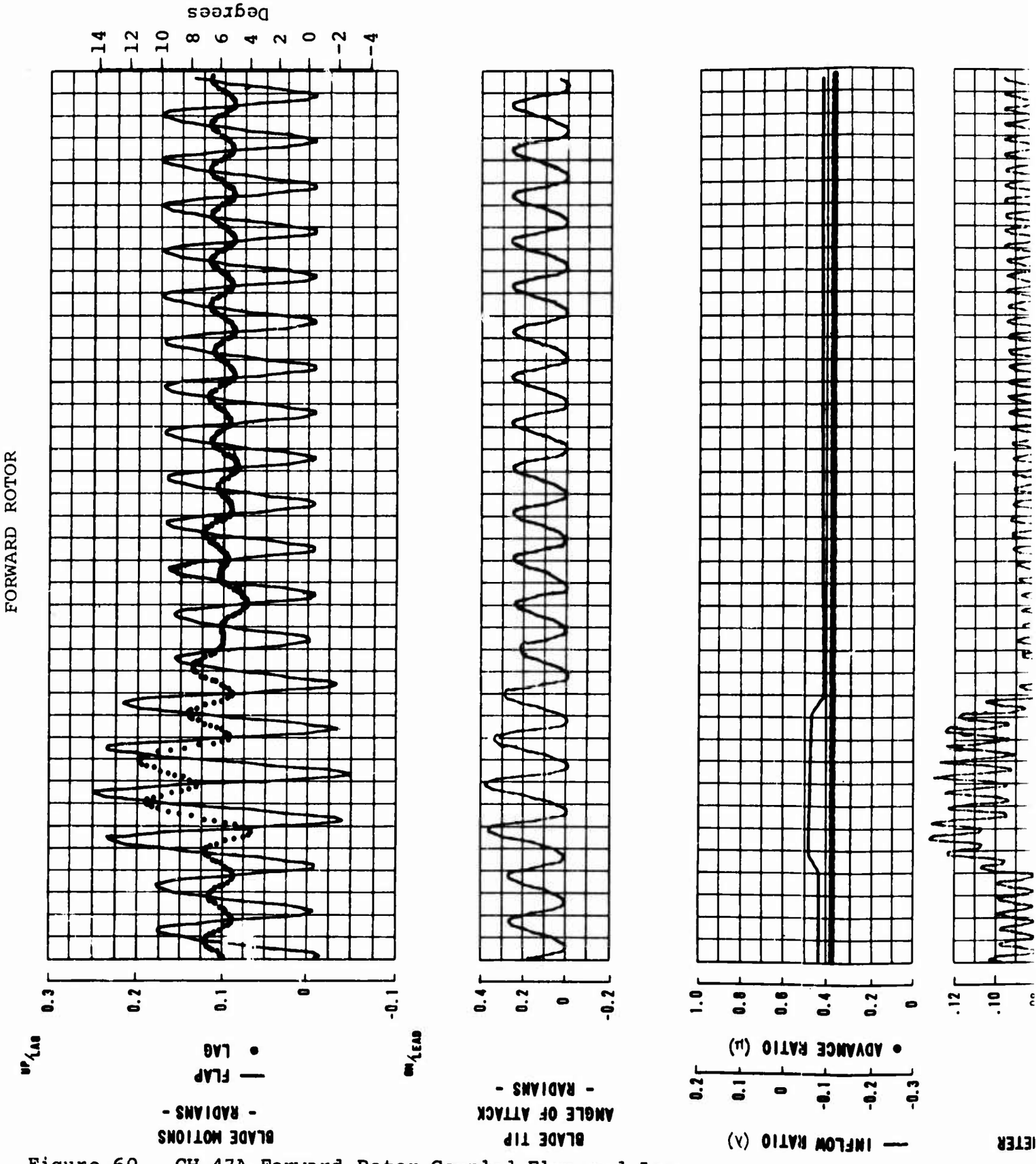

Figure 60. CH-47A Forward Rotor Coupled Flap and Lag Motions.

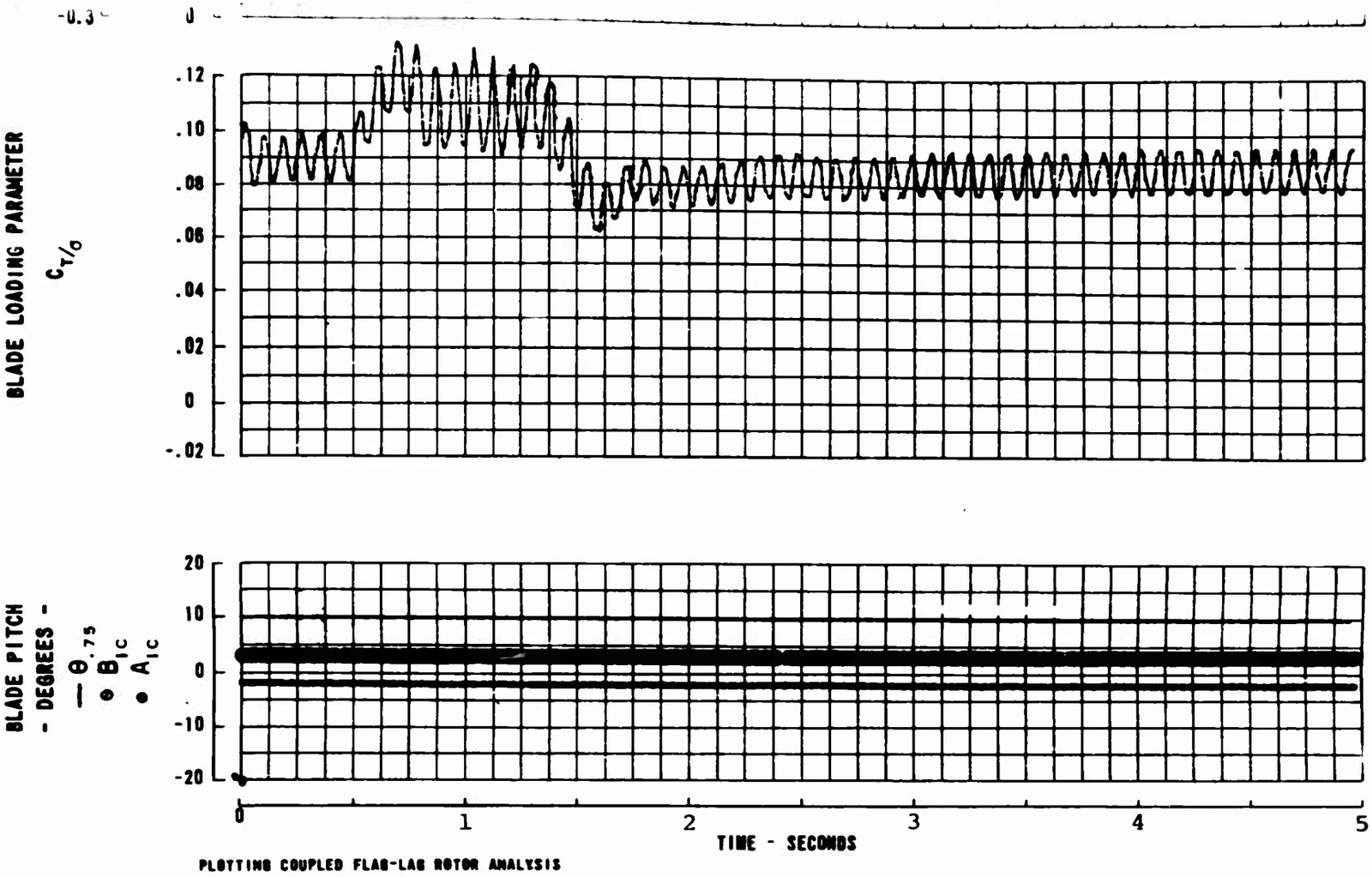

PLOTTING COUPLED FLAG-LAG ROTOR ANALYSIS

NOTES:

1. Forward rotor of CH-47A
2. Gross weight 28,940 pounds; cg 30 inches forward
3. $H_P = H_D = 4000$ feet
4. Airspeed 149 knots; 234 rotor rpm
5. Gust disturbance, 20 feet per second
6. $\theta_t = -9$ degrees

STATIC AND DYNAMIC STRUCTURAL ANALYSIS OF THE ARTICULATED ROTOR

This study of the structural integrity of the articulated rotor system includes a structural analysis of the hub, the upper controls, and three blade designs. Although the fuselage structure had not been defined, a dynamics evaluation of hub shaking forces was made and fuselage response to the forces was estimated. Projected measures to reduce vibration were reviewed. The analytical methods and justification for them are explained in the descriptions of the respective studies.

Three blades were studied for the articulated rotor: a fiberglass plastic C-spar blade, a metal D-spar high-stiffness blade, and a metal low-stiffness blade which conceivably would be a hexagonal-spar blade. The margins between allowable loads and predicted loads for these blades have been estimated. For the fiberglass plastic blade, considerable margin exists for loads in any flight regime at speeds investigated up to 165 knots. For the metal high-stiffness blade, adequate margin exists for speeds up to 140 knots. The metal low-stiffness blade has adequate margins up to 165 knots but not as large as those of the fiberglass plastic blade. The detuning of blade natural frequencies away from operating frequencies is accomplished in the plastic blade by varying strength and elasticity independently by the selective orientation of structural fibers. The metal high-stiffness blade is detuned by antinodal placement of a mass inside the D-spar; the metal low-stiffness blade is detuned by varying the height of the spar. The effect of blade twist on margins has been analyzed. The margins quoted above are based on a twist of -12 degrees; a final selection of -9 degrees for vibration reasons will give additional margins.

A possible correlation between loads and blade mean coning angles has been noted. Vertol Division anticipates a cause-and-effect relationship here, but until this is proven, historical coning angles of successful helicopters must be a basic criterion for detuned blade systems, along with static deflection and fuselage-clearance criteria. The bearing elements have been designed for 3600 hours' service life and 1200 hours between major overhauls. An analysis of the tension-torsion bar also indicates adequate margins. Comparison of blade pitching moments and allowable pitch-link loads shows

margins up to 165 knots. The swashplate lower bearing has been shown in Table V to have a B_{10} life of 2646 hours.

As is the case with many other helicopters, the cockpit vibration levels predicted for the heavy-lift helicopter do not meet specification MIL-H-8501A, but they approximate the vibration levels of existing helicopters, which indicates compliance with the state of the art. As with other helicopters using antivibration devices, or being tested to use them, the heavy-lift helicopter is expected to meet and surpass the vibration level requirements of MIL-H-8501A.

METHODOLOGY AND APPROACH TO STRESS ANALYSIS OF ROTOR BLADES

The basic methods used for rotor blade analysis are discussed here. The loading data are presented with the allowable loads so that critical areas and design airspeeds can be identified.

Centrifugal force, bending, and torsional moments acting upon the rotor blade are calculated for high-speed level flight, ground flapping, and maneuver flight. The maneuver conditions chosen are selected to represent the most critical design conditions specified in MIL-S-8698. The specific design conditions are shown in Table XVI.

The loads applied to the rotor blade during the critical conditions are calculated by the Leone-Myklestad method, and, where necessary, empirical factors are applied to these loads to ensure that they will envelop the predicted top of actual load scatter. The Leone-Myklestad method, using nonuniform downwash distribution (References 8, 9, and 10), has been developed over the years and has been shown to be in close agreement with test. The blade structure is analyzed individually for blade loadings, and then the individual stresses are superimposed (phase relationships and other factors are considered) to give a resultant critical stress at each blade section. The loadings (bending moment in flapping and chordwise planes, centrifugal force, twisting moment, transverse shear in plane of flapping moment, and local chordwise pressure loadings at critical blade stations) are investigated over a wide range of flight and ground contions, for the most adverse gross weight and center-of-gravity conditions. The blade structure is analyzed for the worst of these conditions for both the fatigue and ultimate loads.

Notes	Condition
1. For maneuver conditions, sufficient control is applied to obtain the limit load factor at the cg 2. The fatigue and limit load conditions are to be investigated for both basic design and design alternate gross weights; cg positions most forward or most aft, whichever is critical. 3. At basic design gross weight: 87,000 pounds. (Cg load factor of 2.0 at design alternate gross weight: 108,750 pounds.) 4. Minimum and maximum rotor speeds to be consistent with power-on or power-off conditions. 5. Vertical acceleration of 2.67g on the rotor blade when it is in the normal static droop position against the droop stop. 6. 1.5 times the maximum torque resulting from the following starting procedure: with the free turbine at ground idle, the rotor brake is released and the rotor brought up to ground idle speed; the throttle is then advanced to flight position, accelerating the rotors to normal rpm (N_N). 7. 1.5 times the maximum torque of the engines shall be resisted by six blades. Blade in the autorotative position. Forward speed = V_H Rotor speed = N_N 8. 2.0 times the maximum torque which can be applied by the rotor brake shall be resisted equally by six blades. Rotor speed = N_N	Limit Maneuver Condit Symmetrical dive and pullout, power on Symmetrical dive recovery from pullout, power on Symmetrical dive and pullout, autorotation Symmetrical dive recovery from pull-out, autorotation Limit Gust Condition Limit gust velocity Max. level flt. speed Fatigue Condition Refer to Table XII Special Conditions Ground flapping Starting Shock torque Rotor braking

A

TABLE XVI

ROTOR BLADE STRUCTURAL DESIGN CONDITIONS

ion	Ref. Para. in MIL-S-8698	Fwd Speed	Rotor Speed	Altitude	Load Factor at cg	Rotor Torque Distribution
euver Conditions						
al dive ut, power	3.2.2.3	V_D	N_N	Sea level	2.5 3	50/50
al dive from power on	3.2.2.3	V_D	N_N	Sea level	2.5 3	40/60
al dive ut, ion	3.2.4.1	V_D	N_{L_a}	Service ceiling	2.5 3	0
al dive from pull-rotation	3.2.4.1	V_D	N_{L_a}	Service ceiling	2.5 3	0
t Condition t velocity l flt. speed	3.2.5	V_H	N_N to N_L	Sea level	As calcu-lated	50/50
ndition Table XII	3.2.2.2	-	-	-	-	-
nditions pping	3.4.6.2	0	0	0	⑤	
	3.3.1	⑥	⑥	⑥	⑥	
ue	3.3.1	⑦	⑦	⑦	⑦	
ing	3.3.2	⑧	⑧	⑧	⑧	

Physical and Dynamic Properties

Although the properties presented are based on the preliminary design feasibility effort, the final design will optimize the following structural characteristics:

1. Blade weight
2. Centrifugal force
3. Coning angle
4. Lag angle
5. Static deflection
6. Flapwise natural frequency (0, 1, 2, 3 modes)
7. Chordwise natural frequency (0, 1, 2, 3 modes)
8. Torsional natural frequency (0, 1, 2 modes)
9. Air damping
10. Aeroelastic damped amplification factors for nine harmonics of rotor frequency
    a. Flap bending
    b. Chord bending
11. Mode shapes in a vacuum
12. Flap bending moments (Leone-Myklestad solution)
    a. Steady bending
    b. Alternating bending
    c. Root shears
    d. Pitching moments
    e. Section balance
    f. Dynamic balance

Bending Moment in Flapping and Chordwise Planes

For various blade sections along the blade span, the following structural properties are calculated for bending analysis:

1. Location of principal axis of bending.

2. Total section stiffness about their axes by elemental integration of each structural component.

3. Section effective modulus of each component at point of maximum stress. This is determined by assuming that in such a "molded" structure, the various materials will be strained equally at any one point in the structure. Stress in any material will therefore be proportional to its modulus in bending in the loading direction considered.

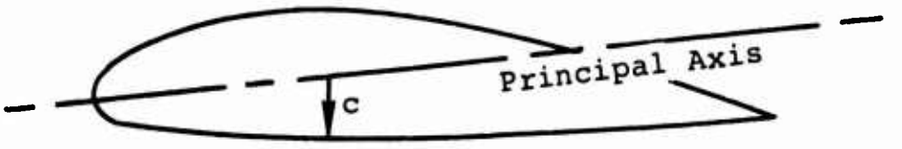

$$Z_{material} = \frac{EI_{total}}{CE_{material}}$$

Centrifugal Force Load

The centrifugal force (C_F) on the blade section is also assumed to be distributed so that it produces equal tension strains in all materials.

$$f_{C_F} = \frac{\overline{CF}\ (E)\ MAT'L}{(AE)_{TOTAL}}$$

The flapping, chordwise, and centrifugal loadings constitute all of the tension loads to which the blade is subjected. The stresses resulting from these loadings are added to give a total steady and alternating tension or compression stress at various points along a given airfoil section. The alternating components of the bending stresses are combined by considering the phase relationships of the bending moment.

Torsion

The fiberglass rotor blade is analyzed for stresses due to a torsional moment by considering a given blade section to act as a multicell structure whose webs are formed by the honeycomb cells. A cell wall is assumed to exist approximately every 10-percent chord, the effective thickness of which equals the number of honeycomb cell walls between midpoints of neighboring cells. Using the conventional-method shear flows, and using deflections of a thin-walled multicelled closed structure under torsion, the section torsional stiffness and a shear flow distribution under the applied torque are determined.

A shearing stress distribution around the airfoil in each material is then formed by dividing the shear flow by the effective skin thickness and assuming that the shear stress in a material is a function of its shear modulus.

The assumption that the blade section functions as a multicell box under torsion, with the honeycomb carrying torsional shear, has been justified by test results in which the measured values of both stiffness and stress distribution correlated excellently with theoretical values.

Flapwise Shears

Under the action of a vertical shear load, the fiberglass blade structure is again considered to act as a multicelled box in which all material is effective in carrying both bending and shear.

Using standard analysis, the redundant shear flows in each cell are determined by solving a system of simultaneous equations involving the deflection characteristics of individual dual cells. The chordwise location of the section shear center is also determined from this analysis.

Again assuming equal straining of all material at a point, the shear stress distribution in each material along the blade section is determined for a given vertical shear.

The theoretical values of shear center determined from this type of analysis compared favorably with values measured on a similarly-constructed rotor blade; this indicates that the analysis is valid.

The shear stresses due to torsion and flapwise loading are then added (phase relationships are considered) to give a net shear flow distribution around the airfoil section.

Local Pressure Loadings

Those sections of the blade, such as the blade tip, which are subjected to high pressure distributions are investigated to determine whether the aft structure is capable of transmitting the resultant bending and shear loads to the blade shear center. For this analysis, the blade is assumed to be supported as a cantilever beam at the shear center. All bending loads are conservatively assumed to be carried by the skin in differential tension, and all shear loads are assumed to be carried in the honeycomb. The critical pressure distributions are determined from wind tunnel data on similar airfoil sections under local angles of attack, defined by the improved non-uniform downwash theory.

METHODOLOGY AND APPROACH TO STRESS ANALYSIS OF THE ROTOR HUB

"Rotor hub", for purposes of this study, includes those components from the point of blade attachment at the folding hinge to the hub block at its attachment to the rotor shaft.

The loads defining these items are developed primarily from the centrifugal force considerations and flapwise, chordwise, and torsional moments established during the blade loads analysis.

All designs investigated use a tension-torsion retention system. (All current Vertol Division helicopters use this system; its simplicity and inherent redundancy have resulted in completely trouble-free operation.) Index stress levels based on current designs are used as the basis for the heavy-lift selection. Using the appropriate index allowable, data are presented as a parametric evaluation to show the interrelation of twist and length.

All articulated bearing designs shown use antifriction bearings at the horizontal pin. Since there is no purely analytical means suitable for predicting the life of an oscillating antifriction bearing, a semiempirical approach is used. Consideration is given to size effect, hub lug geometry, pin slopes and deflections, type of lubrication, and past performance.

METHODOLOGY AND APPROACH TO STRESS ANALYSIS OF ROTOR CONTROLS

The results from the Leone-Myklestad program discussed previously are used to calculate pitch-link loads. The loads, both steady and vibratory, resulting from inertia, gravity, and aerodynamic loadings are transferred to the blade effective shear center and then integrated along the blade. At the present time, this method is considered to give more reliable absolute values of peak-to-peak loads than the stall-flutter analysis used in STABILITY, CONTROL, AND FLYING QUALITIES.

Loads in the lower controls, both steady and vibratory, are then obtained by resolving the load in the pitch link, which is in the rotating system, into the stationary system. This permits evaluation of the stationary rotor control loads down to the hydraulically-operated cyclic and collective actuators that support the swashplate. The actuators are designed so that vibratory loads are not transmitted into the flight controls.

ANALYSIS METHODS--COMPARISON OF THEORY AND TEST

Since the introduction of nonuniform downwash aerodynamics, discussed in Reference 3, the correlation between theory and flight test has been excellent. An interesting phenomenon, indicated by theory and borne out by flight test, is the effect of cyclic trim and rotor overlap. This indicates that after certain forward speeds are reached, the blade and rotor control loadings reduce. Analyses are therefore conducted for a speed sweep to evaluate the critical speed at which maximum loads are obtained.

The agreement between theory and test permits such confidence in the program output that no semiempirical modification of the results is required. A comparison of theory and test is shown for the CH-47A helicopter in Figures 61 and 62.

CRITERIA FOR STRUCTURAL ANALYSIS

Basic Aircraft Data

The structural analysis is based on the basic aircraft data given in Figure 63. The fuselage geometry effects shown for the transport and crane/personnel carrier requirements have been evaluated for blade loads on the fiberglass rotor blade.

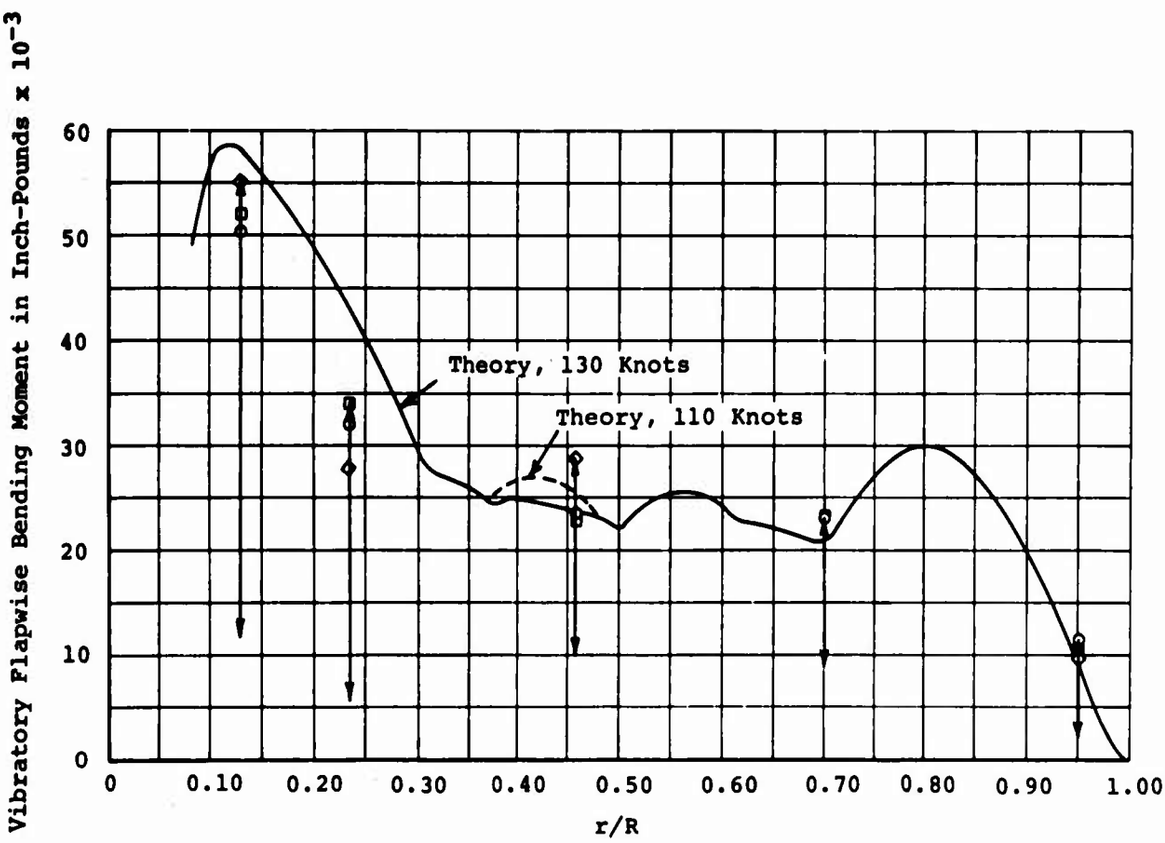

NOTES:

1. Aft rotor
2. Correlation:

	Theory	Flight-Test Data
Helicopter	CH-47A	CH-47A
Gross weight in pounds	27,500	27,400 to 29,700
CG location in inches	35.0 fwd	29.7 fwd to 18.5 aft
Altitude in feet	Sea level	Sea level to 7000
Airspeed in knots	130	105 to 155
Rotor radius in feet	29.5	29.5
Rotor rpm	230	224 to 234
Trim in degrees	3°fwd, 5°aft	3°fwd, 5°aft
Maximum measured V_H loads		⊙ = up to 100 percent ⊡ = 100 to 110 percent ◇ = greater than 110 percent

Figure 61. Correlation of Theoretical and Experimental Vibratory Flapwise Bending Moment.

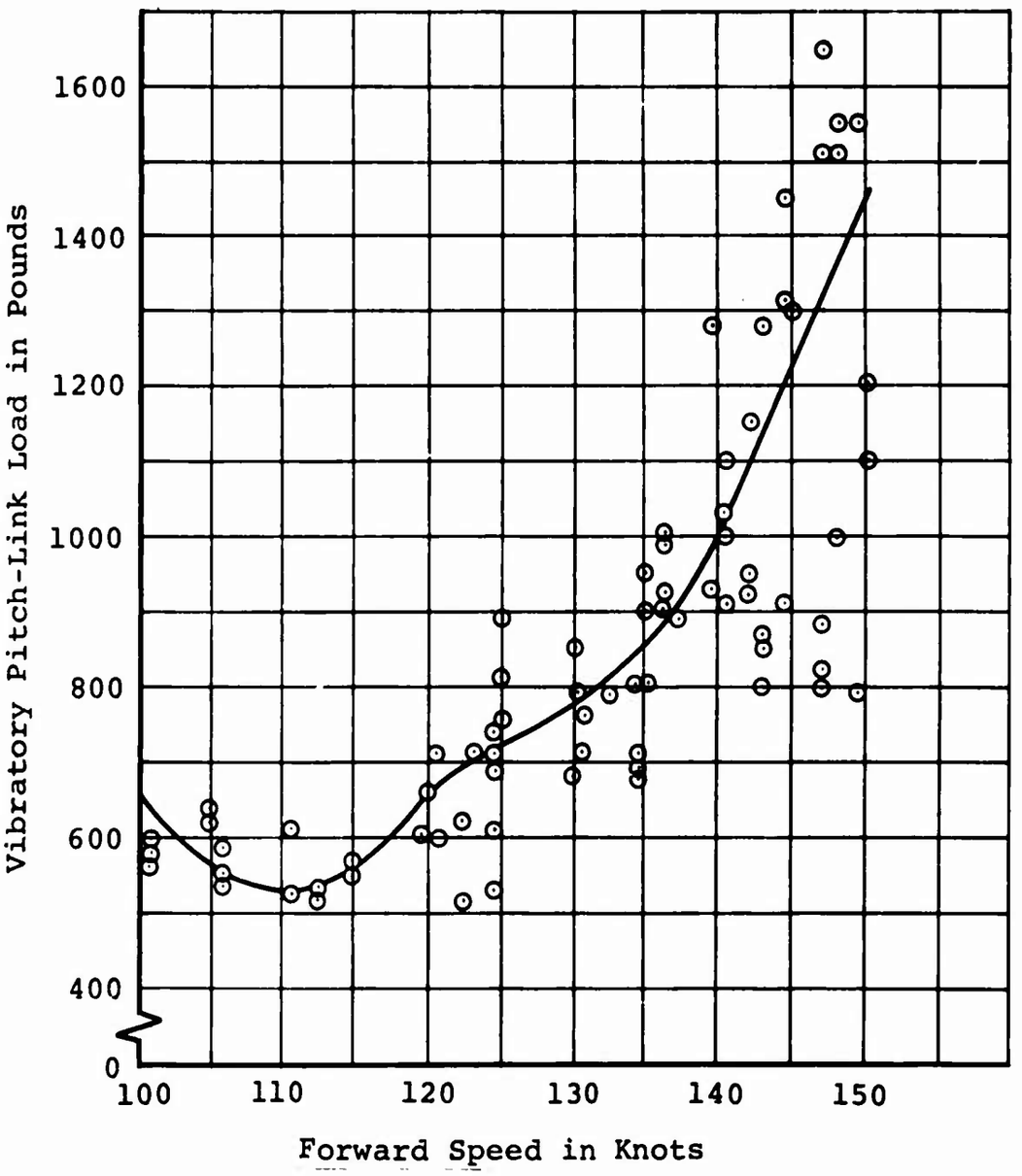

NOTES:

1. Aft rotor of CH-47A helicopter in high-speed level flight
2. Gross weight 28,550 pounds
3. cg 17 inches aft
4. Altitude 3000 feet
5. 230 rotor rpm
6. Trim 3°fwd, 5°aft
7. Experiment = ⊙ Theory = ———

Figure 62. Correlation of Theoretical and Experimental Vibratory Pitch-Link Load.

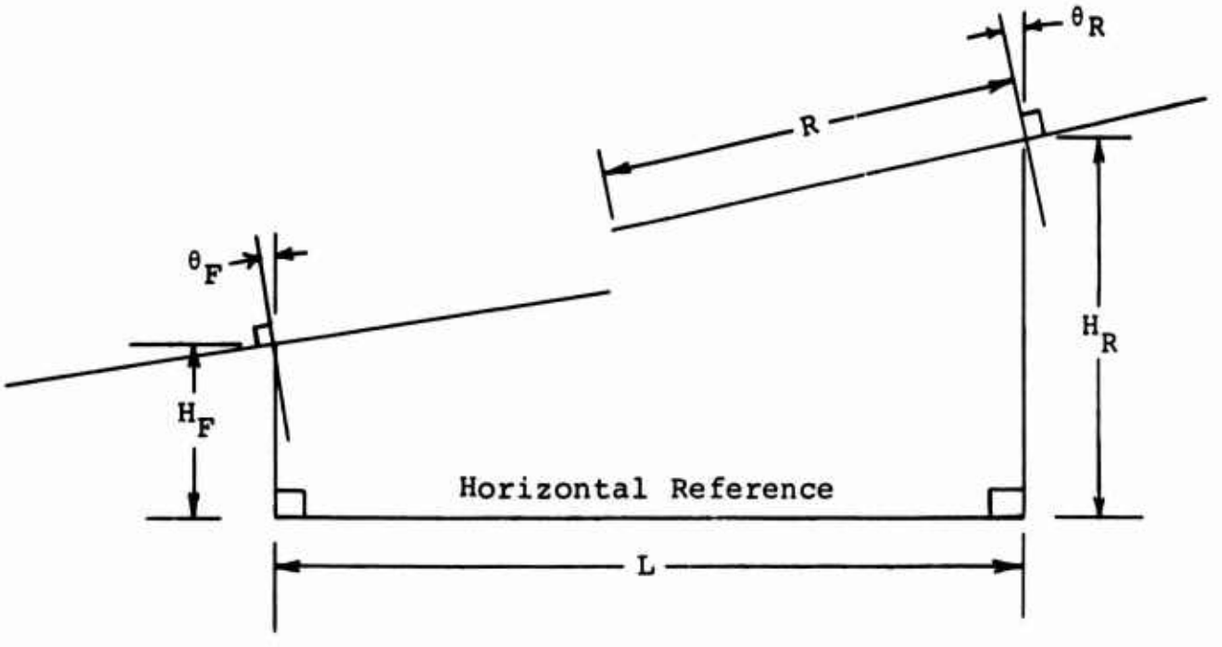

NOTES:

		Transport	Crane/Personnel Carrier
1.	Blades per rotor (b)	3	3
2.	Radius (R)	43 feet	43 feet
3.	Chord (C)	42 inches	42 inches
4.	Twist (θ_t)	-6 to -12 degrees	-6 to -12 degrees
5.	Rotor shaft inclination:		
	forward rotor (θ_F)	9 degrees	9 degrees
	aft rotor (θ_R)	4 degrees	4 degrees
6.	Horizontal distance between rotors (L)	58.20 feet	59.50 feet
7.	Height of rotor above horizontal reference		
	forward rotor (H_F)	13.25 feet	10.00 feet
	aft rotor (H_R)	24.25 feet	26.70 feet
8.	$H_R - H_F$	11.00 feet	16.70 feet

Figure 63. Summary of Tandem-Lift Rotor Helicopter Geometry.

Loading Conditions

The requirements of MIL-S-8698 have been embodied in the design loading conditions for the rotor system shown in Table XVI. These conditions which include level and maneuvering flight design requirements for a tandem helicopter are investigated for all designs. Preliminary analysis has indicated that the critical design conditions for the blades under consideration are fatigue and ground flapping.

Mission Profile

In order to evaluate the lives of the hinge and swashplate bearings, it is necessary to establish a loading spectrum that will approximate the time at each of the flight regimes. The mission profile selected (Table XVII) is based on experience with transport helicopters.

Coning

On large-diameter rotor blades, coning tends to increase if conventional blade construction and mass distribution techniques are used. Coning is approximately proportional to blade radius and inversely proportional to tip speed squared. The many questions that arise concerning an acceptable level of coning have stimulated efforts to understand its effect on vibration, lateral flapping, yaw control power, chordwise blade loads as a result of increased Coriolis forces, flap-lag stability, and so forth. A summary of coning angles in similar vehicles (Table XVIII) shows that the heavy-lift helicopter rotor blades considered in this study fall within the values for operational helicopters.

Studies are being conducted to evaluate the upper limit of coning for the effects just described. Any increase in coning will considerably reduce blade weight from the values given in this report.

Rotor Blade Deflections

On large-diameter rotor blades, static tip deflections tend to become excessive unless mass and stiffness properties are carefully optimized. The criteria established by experience at Vertol Division for clearance between the blade tip and the top of the fuselage are based on ground flapping at low collective settings and ground idle to zero rotor rpm settings.

TABLE XVII
MISSION PROFILE

Fatigue Condition	% Time	Rotor RPM	Horsepower
High-Speed Level Flight	11	155	12,000
Max. Continuous Power Climb	8	149	12,000
Cruise	54	155	9,350
Transition	11	155	7,200
Hover (OGE)	10	155	11,500
Autorotation	6	194	0

TABLE XVIII
CONING ANGLES

Criteria/Column Number

1. Blade radius (R) in feet
2. Rotor rpm
3. Weight of one rotor (W_r) in pounds
4. Flapping weight of one blade (W_f) in pounds
5. W_f/W_r
6. Flapping inertia (I_f) in foot-pound seconds squared
7. Static moment (M_β) in foot pounds
8. $I_f + (W_f/G)R^2$
9. Tip speed (V_t) in feet per second
10. Gross weight in pounds
11. Blades per aircraft (n x b)
12. (Gross weight x 0.75R) ÷ (n x b)
13. Coning angle (β) in degrees*
14. Locke number**

Model	①	②	③	④	⑤	⑥	⑦	⑧	⑨	⑩	⑪	⑫	⑬	⑭
HUP-2	17.5	273	254	70	0.275	129	392	0.195	500	5,750	6	12,500	6.5	5.0
HUP-4	17.5	273	290	89	0.306	172	514	0.201	500	7,200	6	15,600	6.2	4.0
H-21														
Wood	22.0	258	639	195	0.305	444	1,080	0.150	595	12,877 to 13,500	6	35,400 to 37,100	6.2 to 6.5	5.4
Metal	22.0	258	656	200	0.305	478	1,270	0.169	595	13,500 to 14,350	6	37,100 to 39,400	6.1 to 6.5	5.0
107-II	25.0	264	868	232	0.275	913	1,920	0.200	690	18,700 to 21,500	6	58,500 to 67,100	4.7 to 5.4	4.4
CH-46A	25.0	264	1136	315	0.276	970	2,080	0.158	690	18,700 to 21,500	6	58,500 to 67,100	4.3 to 5.1	4.1
CH-47A	29.5	230	1445	407	0.280	2,158	4,010	0.195	710	27,500 to 33,000	6	101,000 to 122,000	4.6 to 5.4	4.6
XH-16 & H-16A	41.0	137	2260	696	0.307	6,375	8,555	0.173	590	27,500 to 33,000	6	141,000 to 169,000	6.0 to 7.4	7.0
HLH														
Metal	43.0	155	4358	1226	0.280	15,900	19,200	0.225	700	87,000	6	470,000	6.2	4.3
Plastic	43.0	155	4100	1140	0.279	15,000	17,800	0.230	700	87,000	6	470,000	6.6	4.5

*Coning angle based on hover and normal cg

$$\beta = \left[\frac{0.75R\ GW/nb - \text{static moment}}{I_{flap}\ \Omega^2}\right] \quad (57.3)$$

**Locke No. $= \dfrac{\frac{1}{2}\rho a c_0 R^4}{I_{flap}}$

Adequate clearance must exist for a 3g blade loading as well as a 1g blade loading plus 7 pounds per square foot aerodynamic loading.

Component Life

All fatigue-loaded components are designed for 3600 hours' life, with allowables corresponding to mean -3 sigma (approximately 0.999 probability of nonfailure). All antifriction bearings in the rotor system (hinge bearings, swashplate bearings, and others) are designed for 1200 hours B_{10} life.

STRUCTURAL ANALYSIS OF FIBERGLASS PLASTIC ROTOR BLADES

A fiberglass plastic blade permits the freedom to orient structural fibers in order to achieve considerable mass, stiffness, and strength variations. The design shown has been iterated to achieve the desired frequencies, loads, and stresses.

Physical Properties

The significant properties defining the fiberglass blade are shown in Figures 64 through 67, which present spanwise weight, flapwise stiffness, chordwise stiffness, and torsional stiffness distributions respectively. The centrifugal force distribution is shown in Figure 68.

Static Loads and Deflections

Blade deflections and static loads due to ground flapping are shown in Figure 69. The allowable moment, based on the fiberglass compressive strength, is shown to indicate the large existing margins of safety. The blade deflections comply satisfactorily with clearance requirements.

Frequencies

It is customary at Vertol Division for all blade designs to be evaluated first from a natural frequency viewpoint before being evaluated for blade loads and stresses. The calculated frequencies are compared with experience as far as operation in the proximity of an integer frequency. Because of the use of nonuniform downwash airloads, the higher harmonic excitation loads significantly affect first, second, and third bending modes when they are amplified as the result of prox-

imity to a critical frequency. The frequencies for the fiberglass blade (see Figures 70 and 71) show satisfactory avoidance of the critical integer frequencies.

Loads and Moments

The theoretically calculated moments shown in Figures 72, 73, and 74 indicate the effects on loads due to blade twist (6 degrees and 12 degrees) and helicopter configuration (crane/personnel carrier and transport) for a speed sweep of 80, 100, 120, 140, and 160 knots.

Vibratory moments are generally higher with increased blade twist for the high-speed regime when considering the midspan portion of the blade. Moments are generally higher with decreased blade twist for the 100-knot speed regime when considering the root area of the blade.

A comparison of moments for the two configurations studied indicates in general that a transport configuration is more critical because the reduced forward-to-aft blade clearance (see Figure 63) increases blade interference effects. The interference effects excite the blade in its higher modes and cause the higher root bending moment.

Considering all variations and combinations, however, it is evident that for the fiberglass blade considerable margin exists when comparing loads in any flight regime with the blade allowables.

STRUCTURAL ANALYSIS OF METAL ROTOR BLADES

Three basic blade configurations have been evaluated. From these studies the relative merits of each design can be evaluated relative to the total weight and blade stress margins while holding frequency and coning criteria relatively constant.

An additional variable, blade twist, has also been evaluated for its effects on blade moments. The values evaluated, 6 degrees and 12 degrees, span the extremes of performance.

Physical Properties

The significant physical properties defining both the high- and low-stiffness metal blades are shown in Figures 75 through

78: spanwise weight, flapwise stiffness, chordwise stiffness, and torsional stiffness distributions, respectively. The centrifugal force distribution is shown in Figure 79.

Static Loads and Deflections

Static loads due to ground flapping and blade deflections are shown in Figure 80. The allowable moment is based on spar buckling strength. The margins are evident. Comparison of blade deflections to the clearance requirements indicates satisfactory compliance.

Frequencies

Since conventional D-spar construction methods for large-diameter blades result in an increase in stiffness that is greater than the proportional increase in blade weight, the blade natural frequencies tend to increase. If this is in a direction that approaches the nearest integer frequency then there are two basic approaches to improving the situation:

Frequency Modification by Tuning

The blade can be tuned to a lower frequency by placing a concentrated mass at an antinodal point for the bending mode under consideration. The mass is fastened by a strap to the blade root fitting so that no additional blade centrifugal stiffening occurs as a result of the additional mass. This scheme has been used successfully on the Vertol 44 helicopter. Since this approach permits the use of conventional D-spar construction methods, it is identified in the structural analysis data as the high-stiffness blade. This type of construction provides the maximum torsional stiffness.

Frequency Modification by Blade Mass Stiffness Relationships

For a given spar weight, the flapwise stiffness can be appreciably modified by changing from a D-shape to an oval or to a circle while still maintaining the same thickness ratio. The design shown utilizes a hexagonal-shaped spar that significantly reduces the stiffness-to-mass ratio. It is identified in the structural analysis data as the low-stiffness blade. Although this type of construction provides less torsional stiffness than the

high-stiffness blade, this is of little consequence since torsional frequencies are still sufficiently high.

However, it is evident that, through continued design iteration, a combination of these two approaches to tuning may result in a further-improved design. Further iteration of the D-spar blade could then achieve the desired frequencies without resorting to the use of tuning weights. The frequencies shown in Figure 81 for the metal blades indicate satisfactory avoidance of the critical integer frequencies.

Loads and Moments

The theoretically calculated moments shown in Figures 82, 83, and 84 are based on the most critical configuration and blade twist: the transport and 12 degrees twist. Moments are shown for a speed sweep of 100, 120, 140, and 160 knots. The allowable moments are shown, and they indicate an adequate margin along the entire blade from root to tip.

For 12 degrees of twist, moments at midspan for the low-stiffness blade (see Figure 82, sheet 1) are about half the moments for the high-stiffness blade. Even though moment allowables for the low-stiffness blade are lower, an adequate margin exists even at 160 knots. For the high-stiffness blade (see Figure 82, sheet 2), there is a margin only at speeds below 140 knots. A calculation for the high-stiffness blade at 160 knots with 6 degrees of twist (Figure 82, sheet 3) indicates a significant reduction in moment with the result being an adequate margin. This indicates that, for the metal blade, 6 degrees twist is more desirable than 12 degrees twist.

STRUCTURAL ANALYSIS OF ROTOR HUB

The hub components from the blade socket joint to the horizontal pin were analyzed for the most severe centrifugal, steady, and vibratory moments resulting from all the load conditions investigated. The analyses of these moments and comparisons of allowable moments versus maximum calculated loads have been described in the structural analyses of the rotor blades. They indicate adequate margins.

Cyclic and Collective Pitch Envelope

The primary blade retention concept considered is the tension-torsion strap. The design requirements for the tension-torsion

strap are determined by the most severe combinations of steady twist due to collective inputs and oscillatory twist due to cyclic inputs. Figure 34 summarizes the combinations that are attainable both from a normal operating viewpoint (for fatigue analysis) and from an infrequent maximum-displacement viewpoint (for limit analysis).

Tension-Torsion Parametric Evaluation

A parametric analysis was performed to evaluate the size and length of the tension-torsion pack, relative to the requirements of Figure 34, by the same method of analysis that has been used for this purpose on other successful helicopters. The results of this study are shown in Figure 85. The design shown is adequate when compared to the current bench-test capability of similar designs.

Flapping Hinge Bearings

Although the use of elastomeric bearings for flap, lag, and pitch motions appears extremely promising, the antifriction bearing is still the most widely used and accepted. Analysis has been performed for the conventional antifriction bearing.

Horizontal Pin Bearing Loads

In order to establish horizontal pin bearing lives, it is necessary to evaluate the load variations anticipated throughout the flight, and then to reduce these loads to an equivalent cubic mean load. The load evaluation is shown in Table XIX.

Horizontal Pin Bearing Life Calculation

An oscillating horizontal pin bearing cannot be evaluated in a manner similar to conventional bearings. The life is significantly affected by bearing proportions, angle of oscillation, and horizontal pin deflections. For this reason, a semiempirical approach is used which combines analysis with service experience. Lives calculated in this manner are shown in Table XX; they exceed the 1200-hour objective.

STRUCTURAL ANALYSIS OF ROTOR CONTROL SYSTEM

Pitch-Link Loads

Pitch-link loads are calculated concurrently with the rotor

blade loads. The pitch-link load is made up of many harmonics, depending on the proximity to critical torsional frequencies. The load is transferred from the rotating system to the stationary system. Loads are therefore established in all components down to the support actuators.

It was indicated previously that there exists a very close agreement of test with theory. The loads are shown in Figure 86 as a function of forward speed for both the crane/personnel carrier and the transport and for both the metal blade and the fiberglass plastic blade. Comparison of anticipated allowable versus expected loads shows that speeds up to 160 knots are possible in both the transport and the crane/personnel carrier.

The variation of pitch-link load throughout the blade's 360 degrees of rotation is shown in Figures 87 and 88. The effects of thrust and airspeed are compared for the fiberglass plastic blade in Figure 87 and for the high- and low-stiffness metal blades in Figure 88.

Swashplate Bearing Life

As in the case of the hinge bearings, the life of the swashplate bearings depends greatly on the flight spectrum used. The technique used to analyze the swashplate bearing is given in Reference 7. The analysis described there has been programmed on Vertol Division's computer and has been shown to give identical agreement with AFBMA (Anti-Friction Bearing Manufacturer's Association) methods when all the proper basic assumptions are made. The program goes further, however, and evaluates the effects of internal clearances, curvatures, and deflection under each loading. The loads required to calculate the life of the swashplate bearing are given in Table XXI. The results of the analysis indicate a B_{10} bearing life of 2646 hours.

DYNAMIC ANALYSIS

Of prime significance in the dynamics analysis of a large helicopter is the prediction of the vibration levels in the cockpit areas of the airframe.

The factors that contribute to the vibration level of the helicopter are many, and the manner in which these factors combine is extraordinarily complex. The rotor blade airload distribution is strongly dependent upon the characteristics of the rotor wake, and relatively minor changes in the assumptions

regarding the characteristics of that wake can have a profound influence on the predicted vibration levels. Rotor blade and fuselage dynamic characteristics are of course central to the vibration problem. Extensive analysis and development testing are devoted to these aspects.

From production testing of equivalent helicopter designs, particularly the CH-46A, the CH-47A, and the earlier H-21 helicopter, it is known that small changes in configuration associated with the arrangement of tolerances from ship to ship can cause a substantial variation in vibration characteristics. It has been concluded that the only real solution to the vibration problem lies in the development of force- or acceleration-compensating devices which will provide whatever force is required, within their stroke limitations, to cancel the vibration at the point at which it is sensed. The merits of this philosophy have been borne out by the equipping of several production helicopters with vibration absorbers.

Of course, the force requirements, and therefore the weight, of vibration-compensating devices will depend on the vibration levels of the basic aircraft. Design for acceptable vibration characteristics, and therefore minimum weight and complexity of vibration compensating devices, is undertaken to minimize the inherent vibration levels of the aircraft.

The vibration levels for the heavy-lift helicopter are predicted on the basis that no antivibration devices are installed, but devices which are under development will be available to solve any vibration problems which might arise.

The prediction of vibration levels and the hub shaking forces from which they arise is accomplished by the application of these two basic techniques.

Rotor Hub Shaking Forces

All rotor hub shaking forces described here are determined from the Rotor Analysis Digital Computer Program, a well-established proven analytical tool compiled for the study of aerodynamic, dynamic, and structural characteristics of current and advanced rotor concepts. The program has been developed from an original analysis prepared by Vertol Division for a BuWeps study of helicopter rotor hub vibratory forces (Reference 22). The effects of nonlinear aerodynamics, including nonuniform downwash and compressibility effects, are considered.

The general approach is to compute the rotor-induced velocities from each rotor and, in conjunction with classical airloading, determine the total airloading on each blade. From these airloads, Coriolis, and centrifugal forces, the dynamic response of each blade is determined. From the response in flap, pitch, and lag, the blade root shears and moments (and subsequently the hub shaking forces) are found.

To substantiate the accuracy of hub shaking forces predicted by the rotor analysis method, a comparison of calculated rotor shaking forces and test data is presented in Figure 89. The test data was recorded during the flight testing of the CH-46A for the Advanced Vibration Development Program in April 1965 (Reference 20). The excellent agreement obtained over the complete airspeed range lends a great deal of confidence to the results predicted herein.

Effects of Blade Twist on Rotor Hub Shaking Forces

The effect of blade twist on helicopter vibration levels has been investigated (References 16 and 22), with the general conclusion that decreased blade twist results in lower vibratory stress and load levels. To substantiate this effect, which is caused by the increased loading at the inboard blade sections exciting the first flexible bending mode shape of the blade, the effect of twist on the heavy-lift helicopter was investigated by considering degrees of twist at the performance envelope limits. Two flight configurations were considered:

1.	Gross weight	87,000 pounds	75,700 pounds
2.	Altitude	sea level standard day	5000 feet standard day
3.	Airspeed	165 knots	170 knots

Blade twist was considered linear with total twist values of -6, -8, -10, and -12 degrees.

The results are presented in Figure 90 as vertical shaking forces, longitudinal forces and pitching moments at three-times rotor speed for both rotors. Trends versus twist for the vertical forces and pitching moments are linear, and they

increase at a rate of approximately 2 percent per degree of twist. Although these results are for the proposed plastic blade, the metal blade shows similar trends. For longitudinal force, the trends generally decrease with twist at a rate of 0.25 percent per degree, which is for all practical purposes negligible. Longitudinal loads are small relative to the vertical loads, and the effect of twist overall will follow the trend of the vertical load.

Airspeed Trends for Rotor Hub Shaking Forces

To predict vibration level for the transport at a gross weight of 87,000 pounds, the rotor hub shaking forces were computed over a range in airspeed of 100 to 165 knots. These forces, which contribute to the vertical vibration level, are shown in Figure 91 as the longitudinal and vertical forces, and as the pitching moments for both hubs. All loads for both rotors increase with airspeed over the range in airspeed considered. To substantiate the general level of these forces, Figure 92 compares the forward rotor's nondimensional vertical force, which predominates in vibration level prediction, and the same force for the CH-47A helicopter at equivalent disc loading. This and the correlation of test and calculated shaft loads described previously illustrate the reliability of the calculated shaking forces.

Fuselage Vibration Level

For the prediction of the aircraft's response to hub shaking forces, several approaches are open.

The most common method is to represent the helicopter structure by a series of lumped masses and weightless beams with equivalent stiffness values, and to use classical methods to solve for the response. This approach has generally had limited success, particularly in the preliminary design of structures, since most helicopter structures are unsuited to representation as slender beams, and since basic structural properties are not well defined.

A better approach, when a structure is reasonably well defined, is that used for the analysis of current designs. This method is to determine first the structural stiffness using the Comprehensive Option Stiffness Matrix Organization System (COSMOS) and associated programs (Reference 18). For a given structure, this program incorporates basic flange

and spar areas, beam inertias, and effective hub and skin thicknesses, refers them to standard axes, and constructs stiffness matrices. Helicopter mass is distributed at preselected nodal locations of the complex structure, and mass matrices are constructed from them. Fuselage natural frequencies and forced response to unit or calculated hub shaking forces are then determined from the solution of the resulting dynamic matrix. This fully analytical approach to the prediction of vibration level again requires a reasonable description of the helicopter structure; and for the heavy-lift helicopter, this is not yet possible.

The third approach, more applicable in the present case where the fuselage has not yet been designed, is to scale measured response information from an existing aircraft. The geometric similarity between the CH-47A helicopter and the heavy-lift helicopter is illustrated in Figure 93. Fuselage response characteristics for the CH-47A helicopter have been determined from ground shake tests over a range in frequency from unit hub loads and moments applied to both rotor hubs. Since helicopter response level is, in general, inversely proportional to the gross weight, and since response frequency is inversely proportional to the length, the levels for the CH-47A can be scaled to yield equivalent response for the heavy-lift helicopter. From this response level, from the calculated hub shaking forces, and from the known phase relationship between the forces and response, a vector summation of the total response is obtained.

A comparison of measured helicopter vibration with that calculated by the synthetic method described above is shown in Figure 94. Vibration data are shown for the CH-47A helicopter at a gross weight of 28,000 pounds. The calculated level was determined for a 33,000-pound gross weight, since the disc loading for the CH-47A at this gross weight corresponds to a similar disc loading for the heavy-lift helicopter at 87,000 pounds gross weight. The good agreement in level and trend between the calculated value and the measured scatter is well illustrated.

The fuselage response to unit hub shaking forces (Figure 95) and the hub shaking forces predicted for 100 to 165 knots at 87,000 pounds gross weight were synthesized graphically. This synthesis for airspeeds of 100, 140, and 165 knots (Figure 96) clearly shows the importance of both amplitude and phase. Aft rotor longitudinal forces are not shown, since they have a

negligible effect on the total response.

Figure 97 represents helicopter response to hub loads in the form of cockpit vibration. This curve of heavy-lift helicopter cockpit vibrations is superimposed on similar existing helicopter vibration levels. As with existing helicopters using antivibration devices, vibration levels in the heavy-lift helicopter will be controllable to acceptable levels. Research test programs conducted by Vertol Division over the last 18 months have provided substantial insight into the nature of vibration in helicopters. Preliminary designs and feasibility tests have demonstrated the usefulness of the vibration-control devices described in the paragraphs which follow.

Blade Pendulum Flap Absorbers

The blade pendulum flap absorber is a small centrifugally-tuned pendulum which is located at the blade root retention area. A typical flap absorber is shown with its effects on blade root loads, and subsequently on vibration level, in Figure 98. These pendulums are tuned to resonance with the 3-per-revolution flapping to produce shear force which will oppose and reduce the vertical load initially generated by the blade motion and which will, in turn, reduce the vertical shaft loads. The effect of tuning on the pendulum's effectiveness is also shown.

Cockpit and Cabin Absorbers

Absorbers mounted in the fuselage are used successfully in a number of operational helicopters, such as the CH-46A, UH-2, and SH-3A. CH-46A production aircraft have two vertical absorbers and one lateral absorber under the cockpit floor. These units absorb energy which would otherwise be introduced into the aircraft structure. The amount of energy which can be absorbed depends on the size and location of the active mass. The reduction in cockpit vibration achieved with the CH-46A absorbers is shown in Figure 99.

Rotor Force Balancers

A force balancer is a device capable of producing a force in opposition to the rotor vibratory forces. Flight testing has been conducted on the CH-46A to evaluate the concept of force balancing.

A hydraulic shaker capable of producing a sinusoidal force of 800 pounds was installed under the forward transmission with its line of action in line with the rotor shaft. The purpose of this testing was to determine if this shaker, which simulated a force balancer, could reduce the predominant 3-per-revolution vertical vibration. The shaker was synchronized with rotor 3-per-revolution, and the amplitude and phase of the force output were controlled manually. An operator, using a visual display control console, monitored vibration at various fuselage locations, and then varied the amplitude and phase of the shaker force to minimize the vibration at these locations. The shaker produced a substantial reduction in vibration (see Figure 100).

Preliminary design studies have been conducted on an electromechanical device which generates force through the rotation of four eccentric weights about a common axis at three times rotor speed.

Since acceptable vibration levels and reliability are necessary conditions to be met by any aircraft configuration, recourse to the use of antivibration devices is a recognized element in product-improvement programs. Depending on the type of device, advanced versions weigh approximately 1 to 1.5 percent of design gross weight. As more refined versions become available, it is expected that the gains in human comfort and cargo protection will far offset the minor increment to weight.

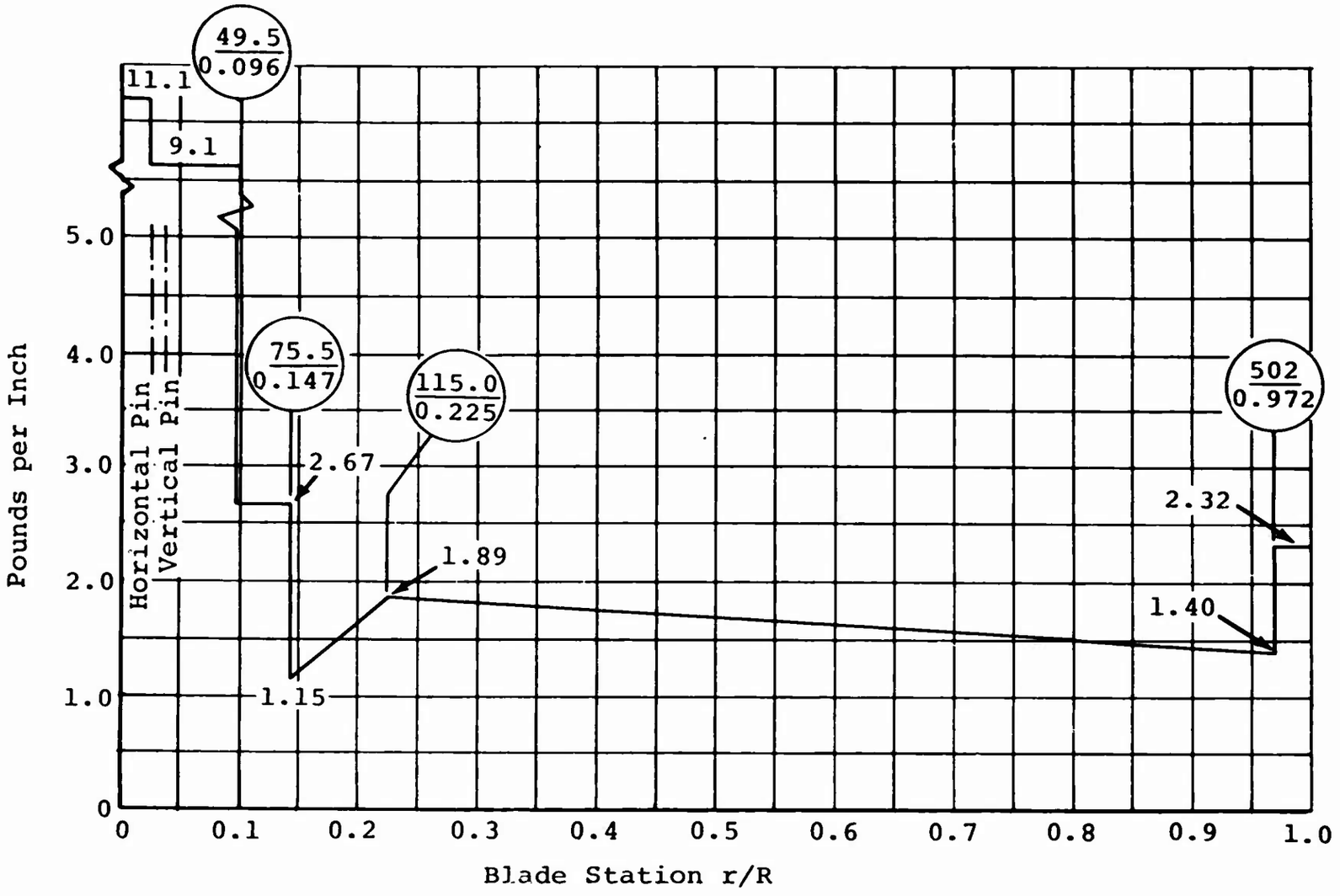

NOTE: R = 516 inches

Figure 64. Spanwise Weight Distribution of Plastic Blade.

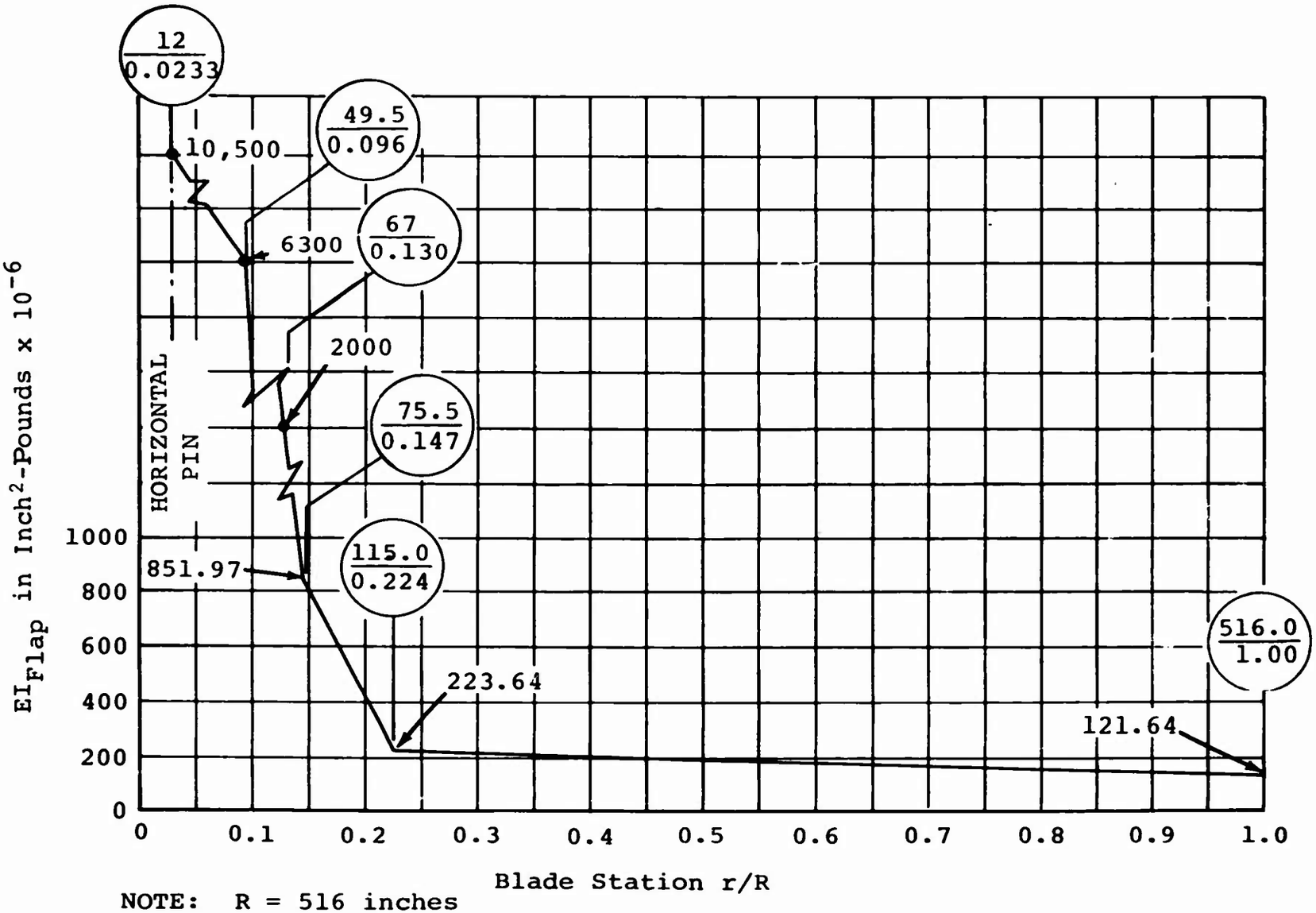

NOTE: R = 516 inches

Figure 65. Flapwise Stiffness Distribution of Plastic Blade.

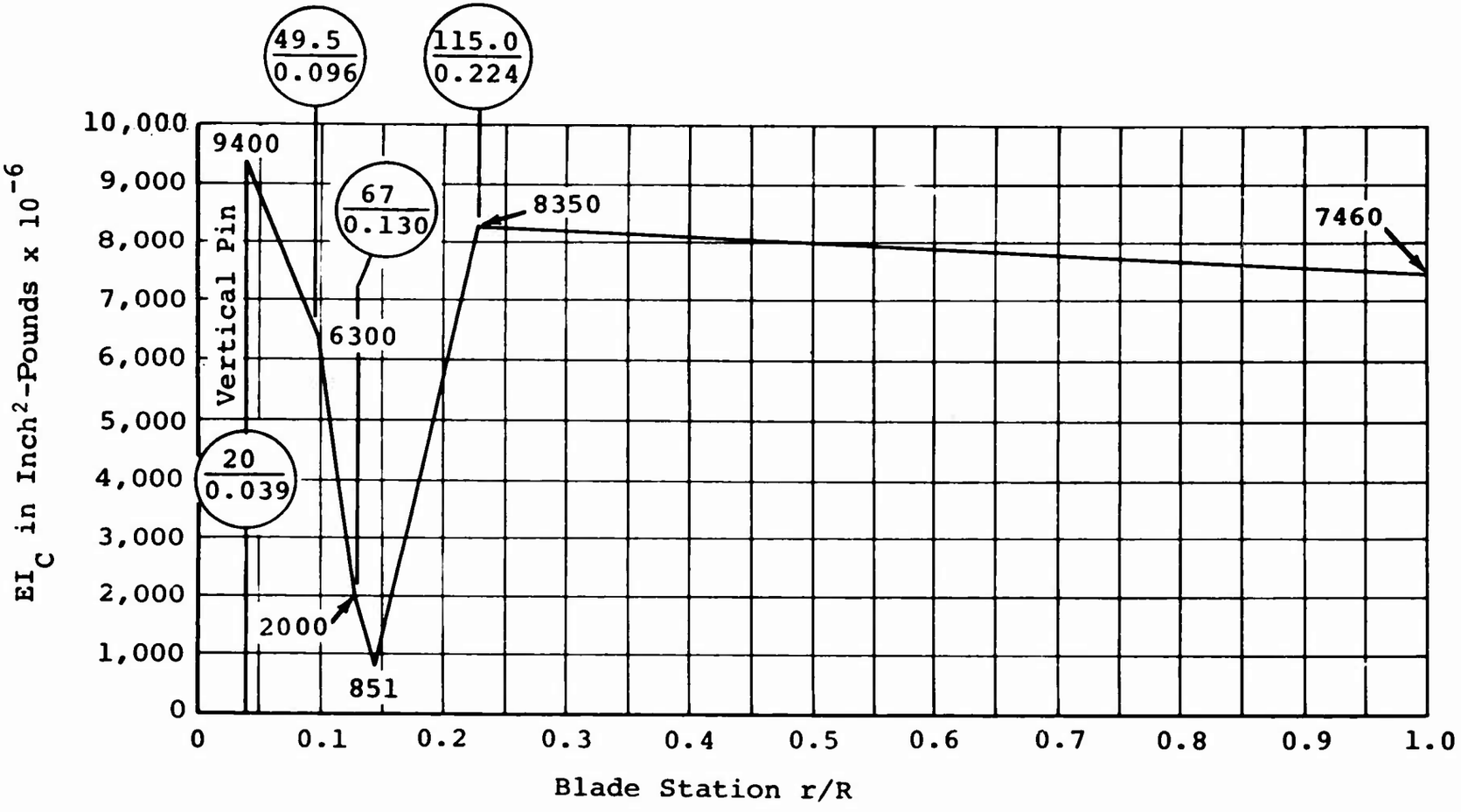

NOTE: R = 516 inches

Figure 66. Chordwise Stiffness Distribution of Plastic Blade.

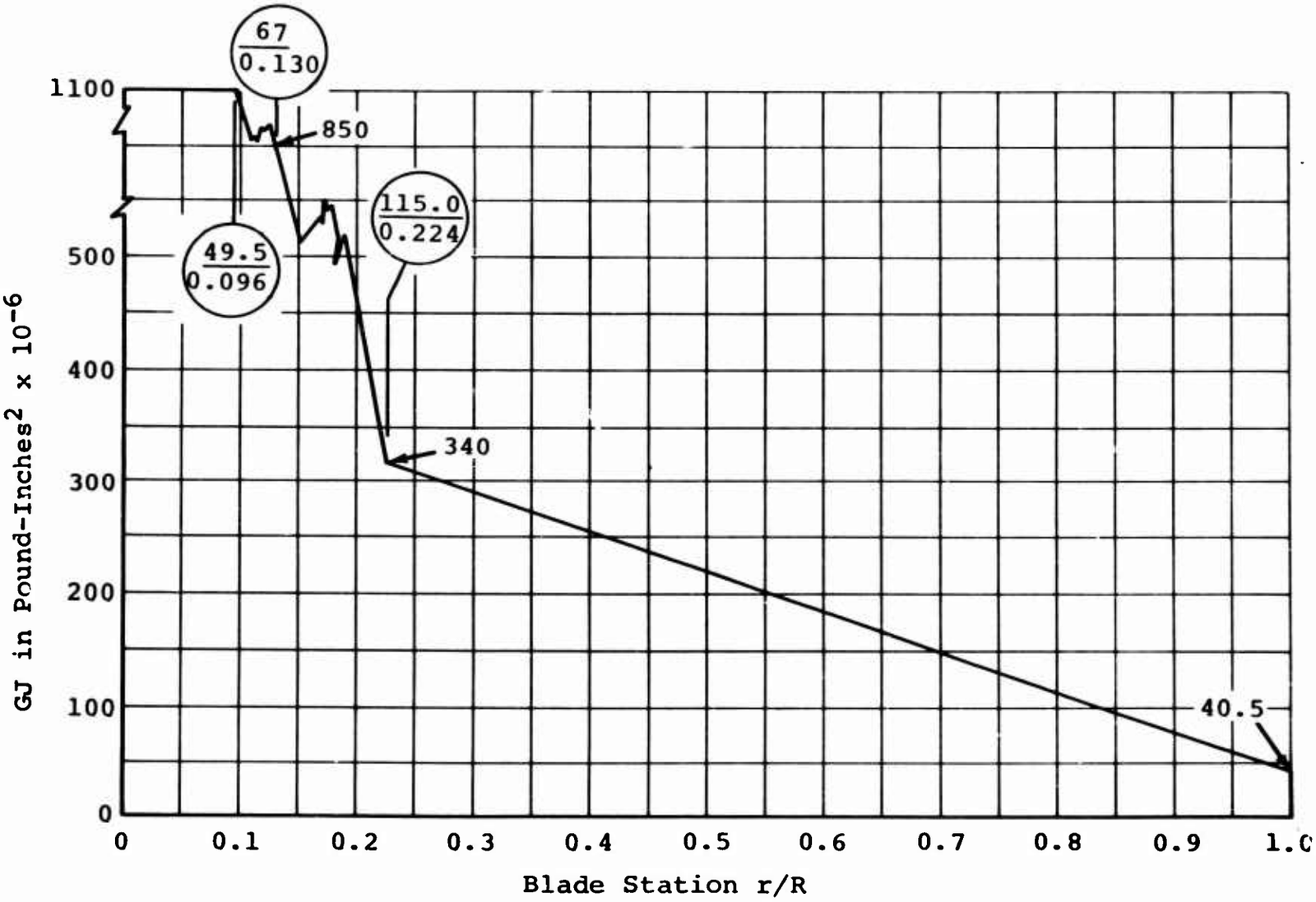

NOTE: R = 516 inches

Figure 67. Torsional Stiffness Distribution of Plastic Blade.

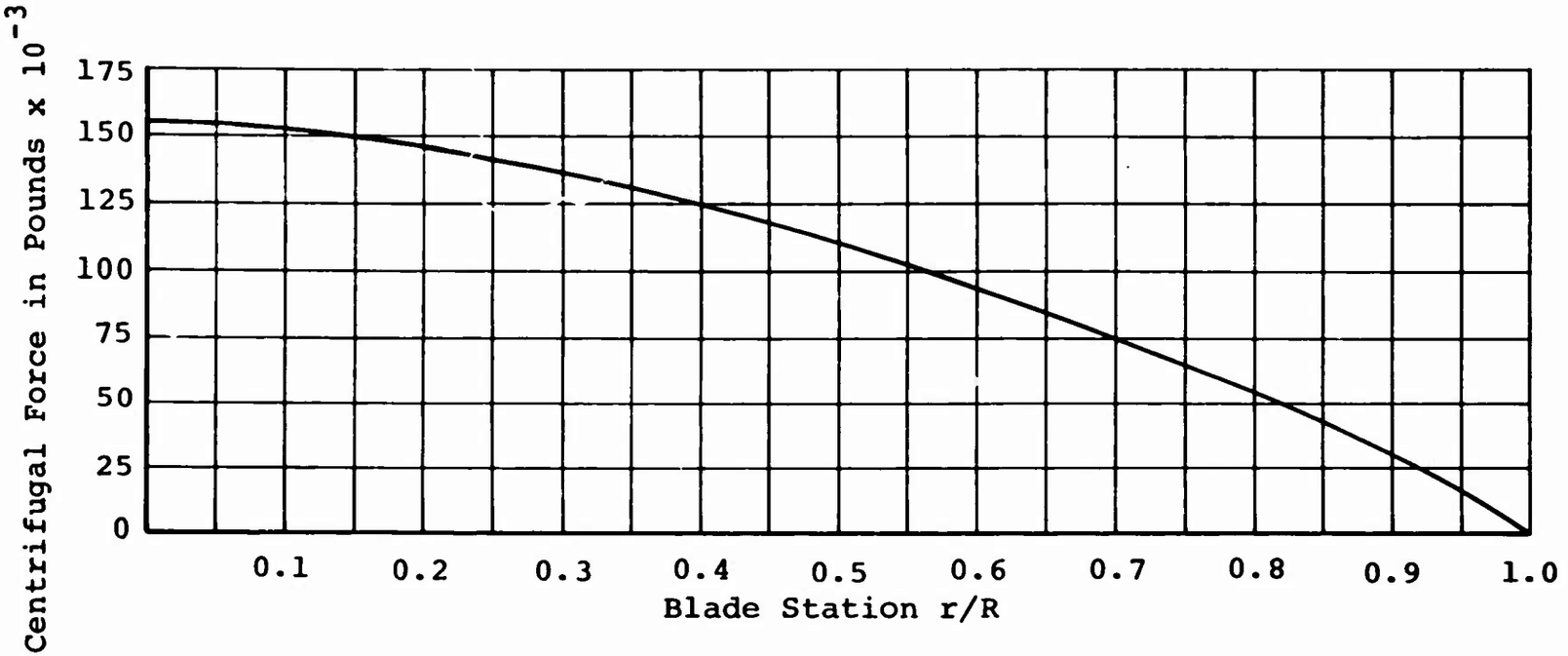

NOTE: R = 516 inches

Figure 68. Centrifugal Force Distribution of Plastic Blade.

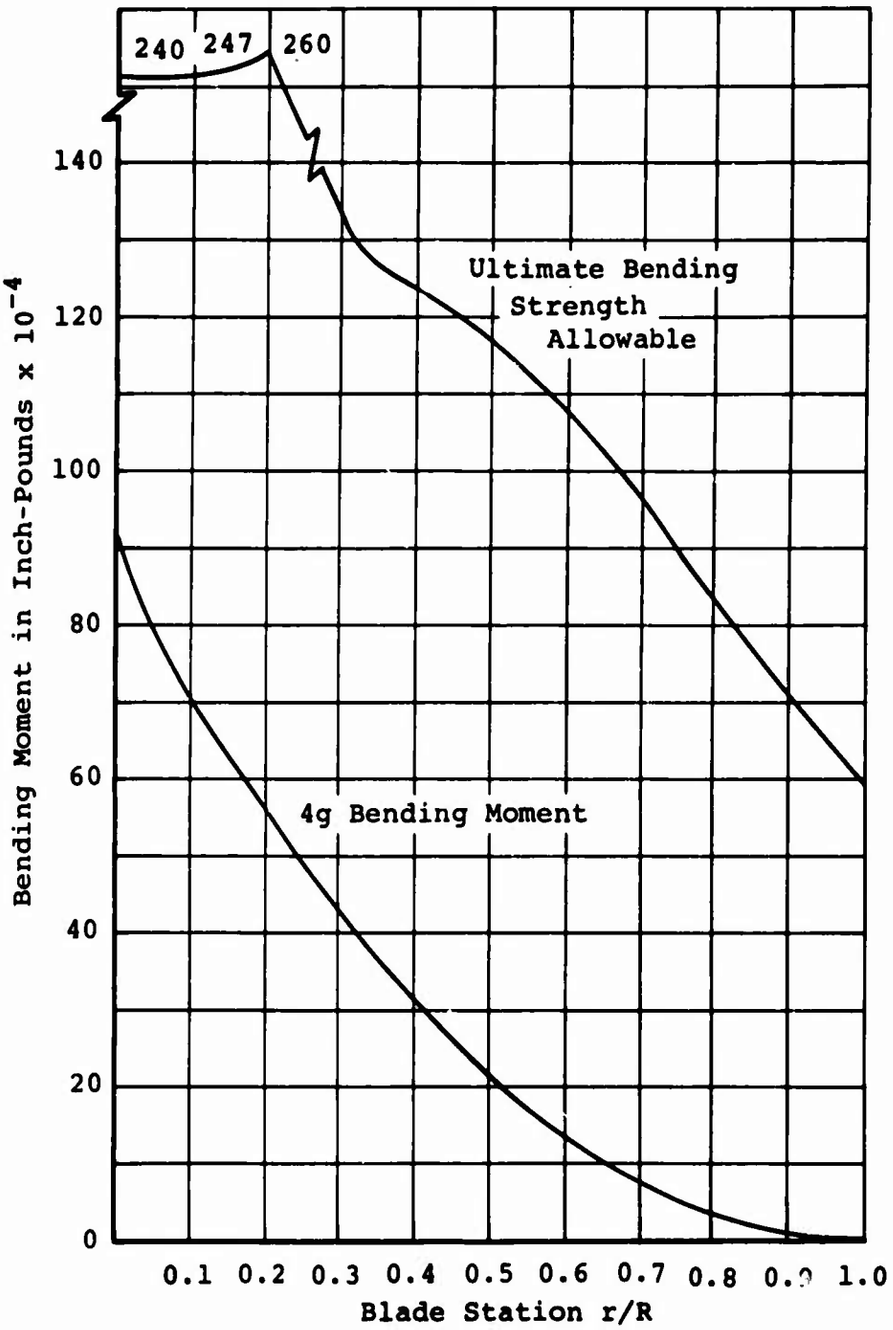

NOTES:

1. R = 516 inches
2. 3g deflection at tip is 105 inches
3. 7 pounds per square foot + 1g deflection at tip = 80 inches
4. Blade-to-fuselage clearance including 3-1/2-degree droop stop is 114 inches

Figure 69. Static Bending and Tip Deflection of Plastic Blade.

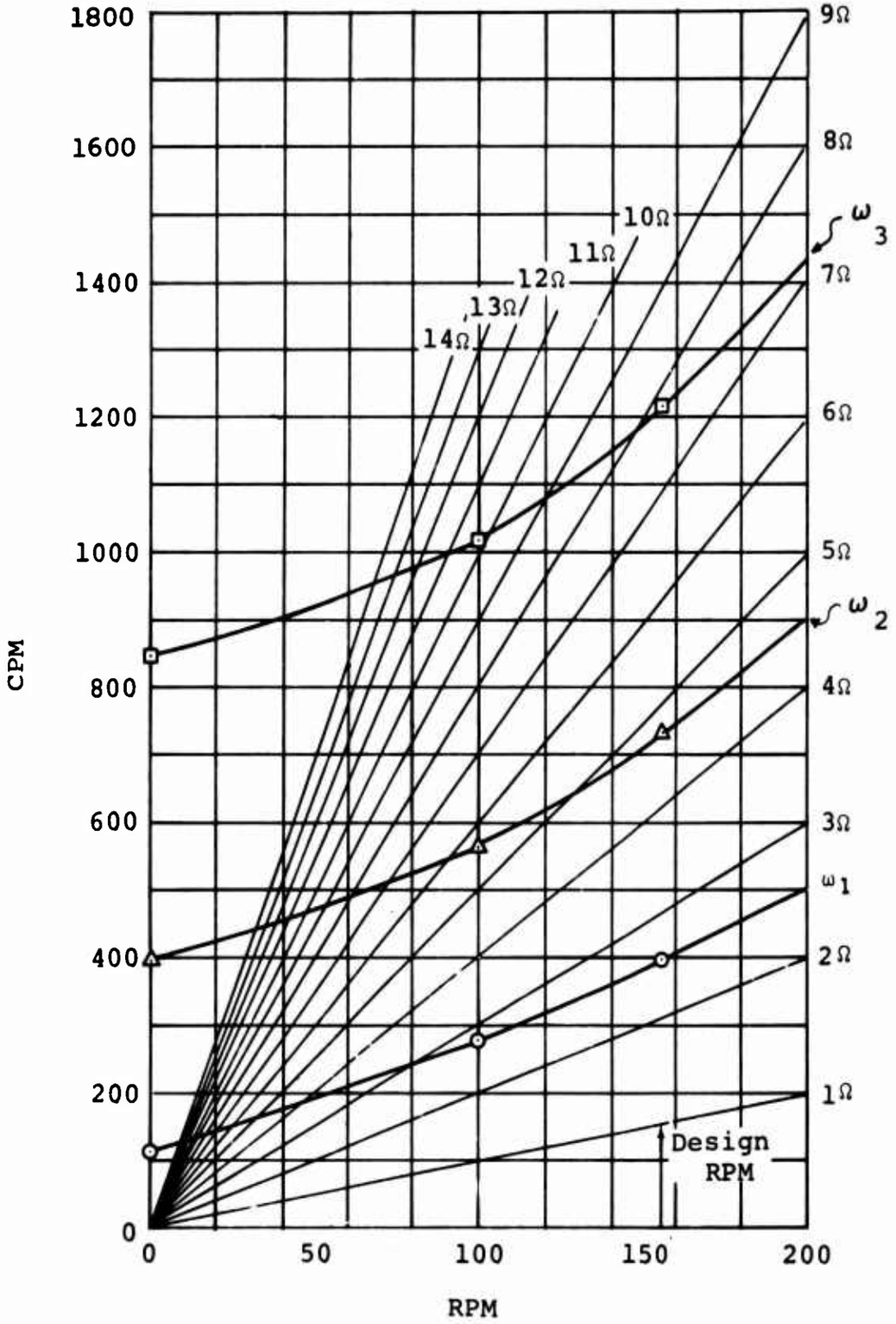

Figure 70. Flapwise Natural Frequency Spectrum of Plastic Blade.

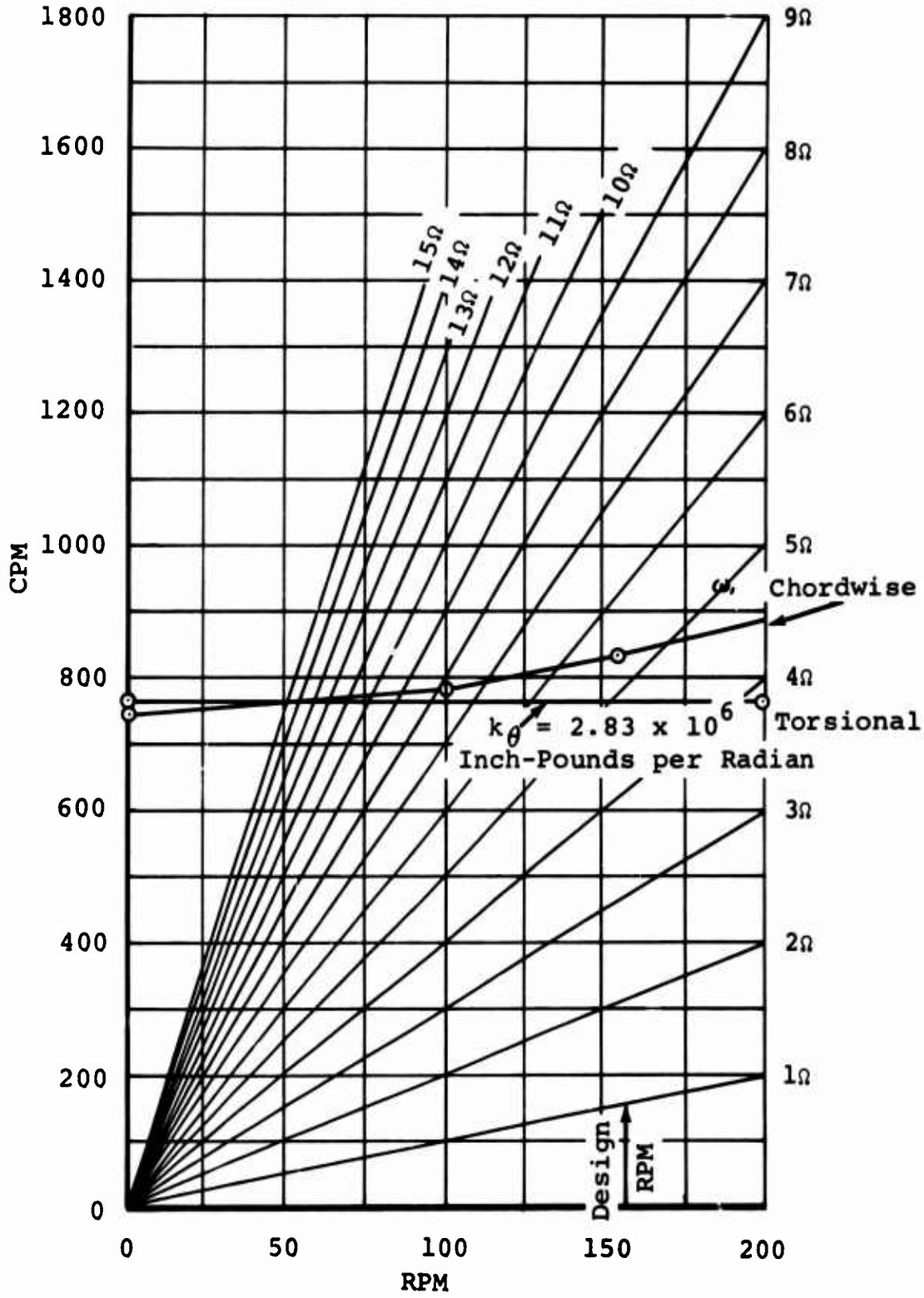

Figure 71. Chordwise and Torsional Natural Frequency Spectrum of Plastic Blade.

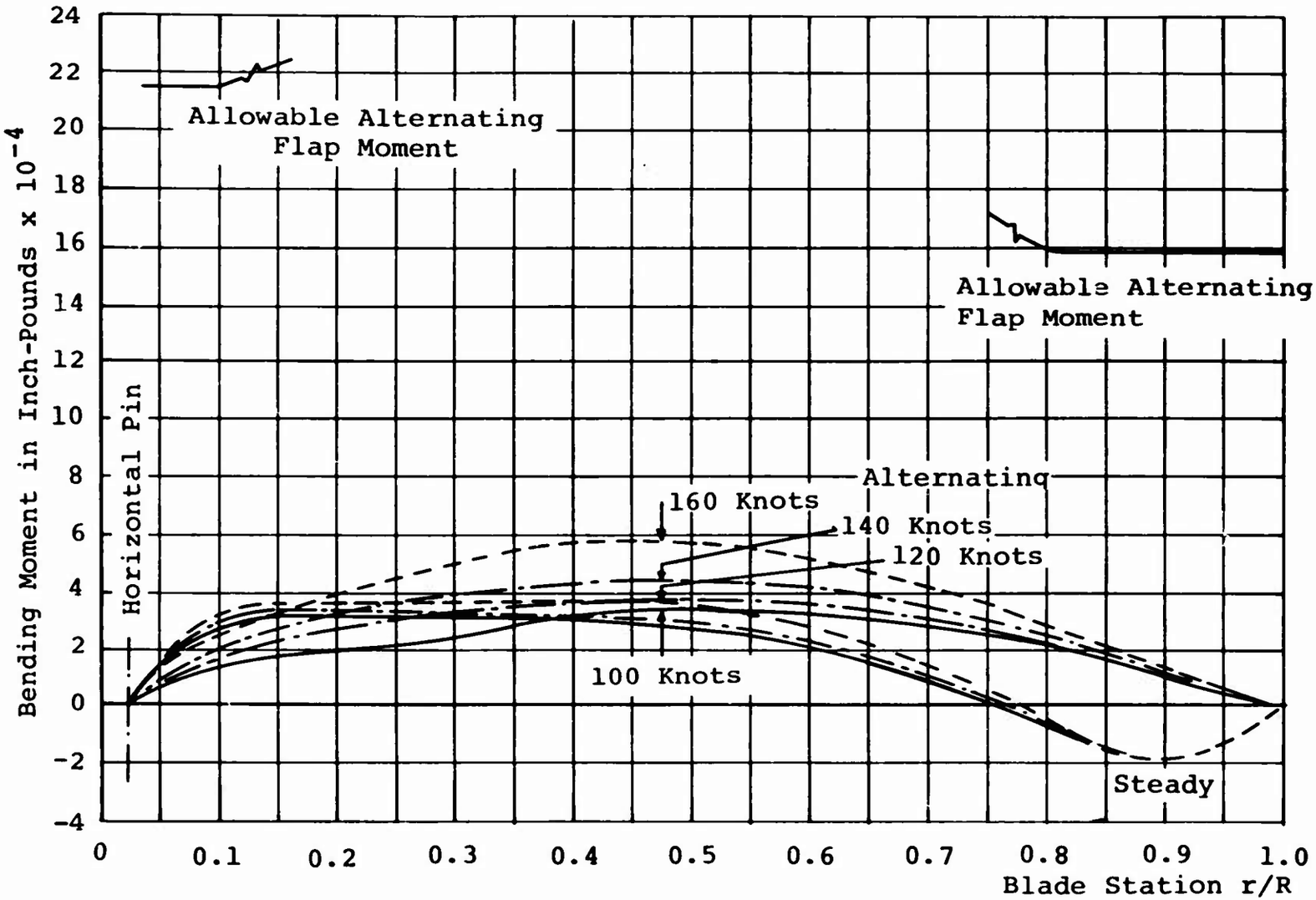

NOTES:
1. Crane/personnel carrier
2. R = 516 inches
3. θ_t = -6 degrees

Figure 72. Flapwise Bending Moments of Plastic Blade. (Sheet 1 of 4)

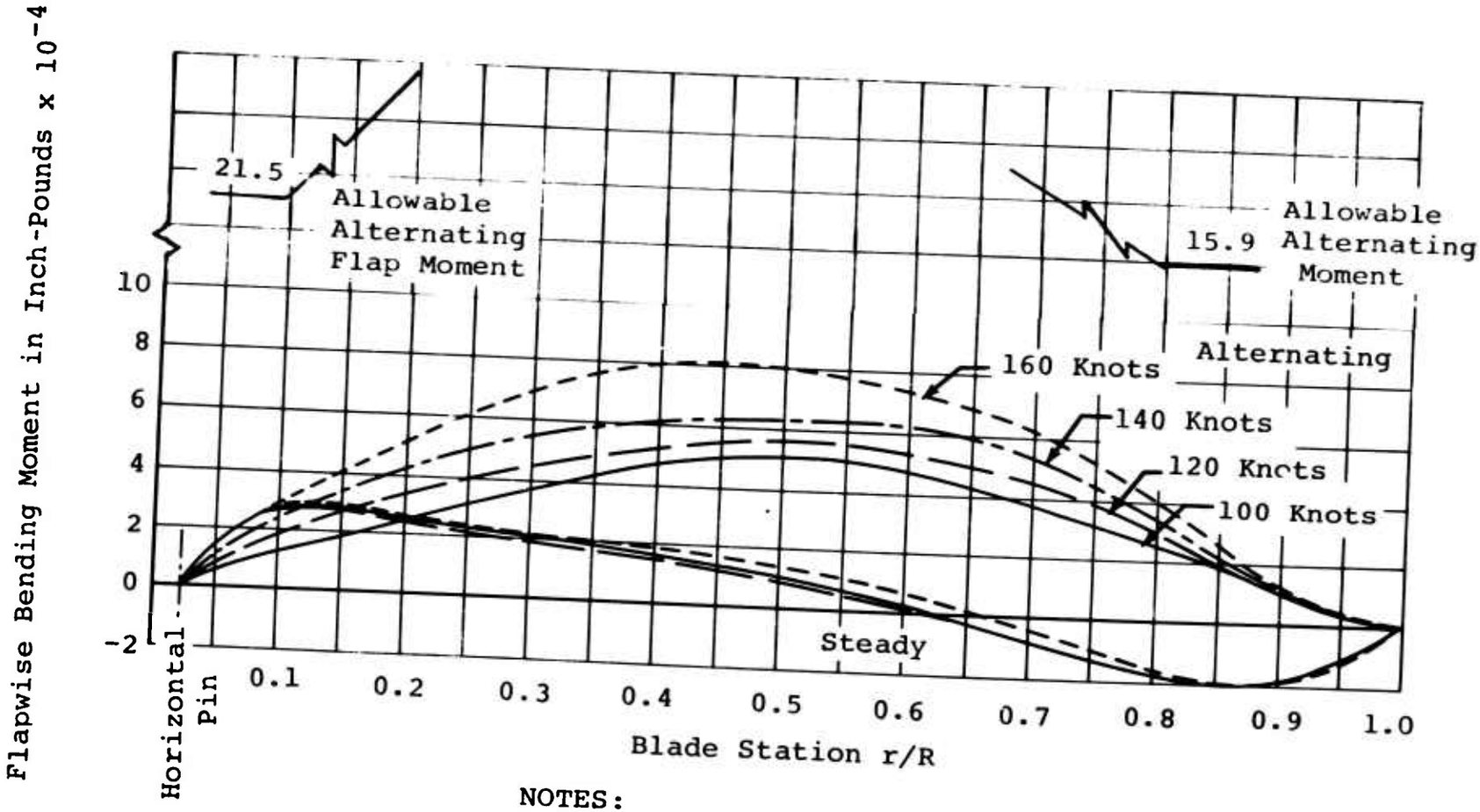

NOTES:
1. Crane/personnel carrier
2. R = 516 inches
3. θ_t = -12 degrees

Figure 72. Flapwise Bending Moments of Plastic Blade. (Sheet 2 of 4)

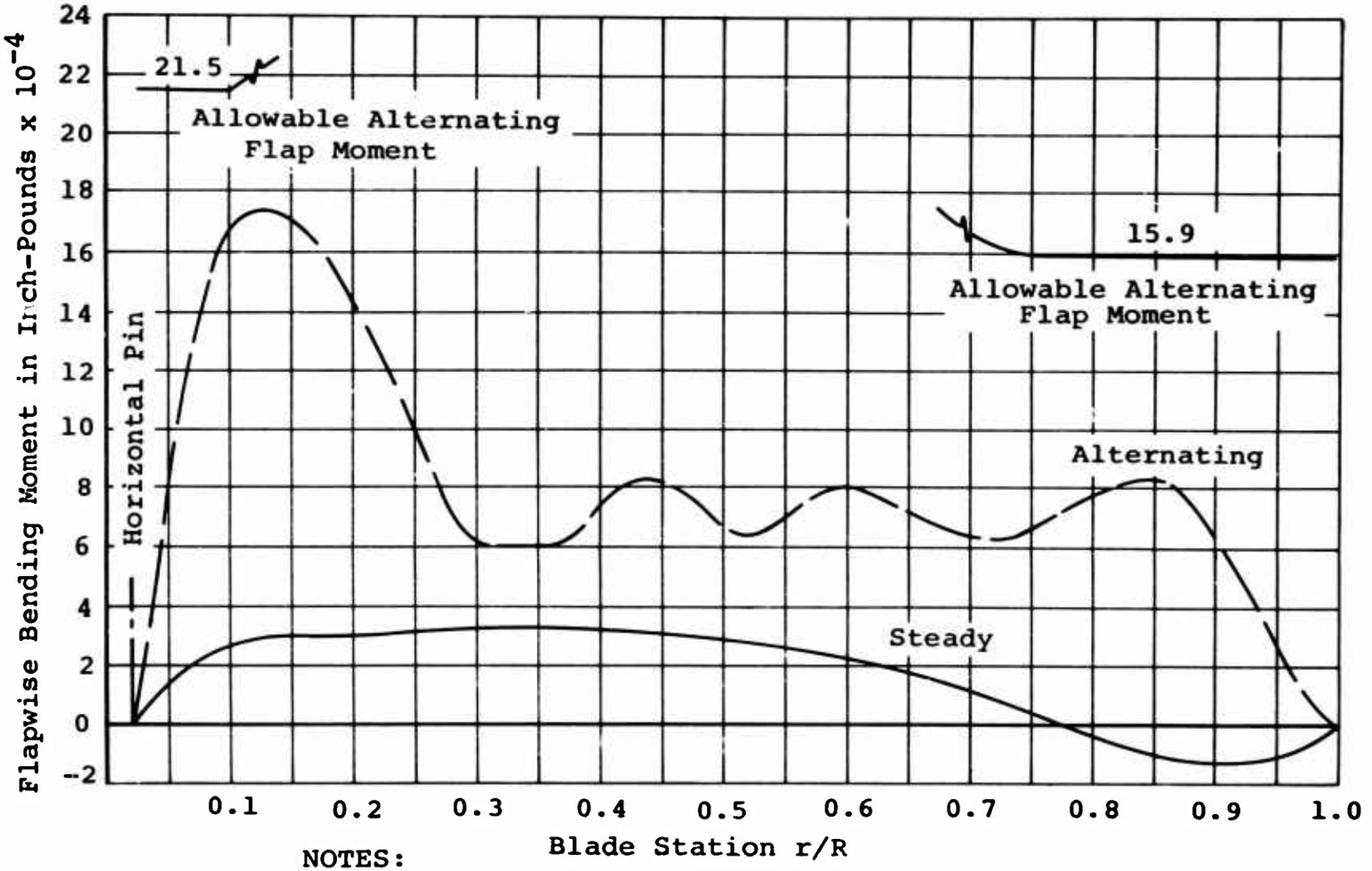

NOTES:

1. Transport
2. θ_t = -6 degrees
3. V = 100 knots
4. R = 516 inches

Figure 72. Flapwise Bending Moments of Plastic Blade. (Sheet 3 of 4)

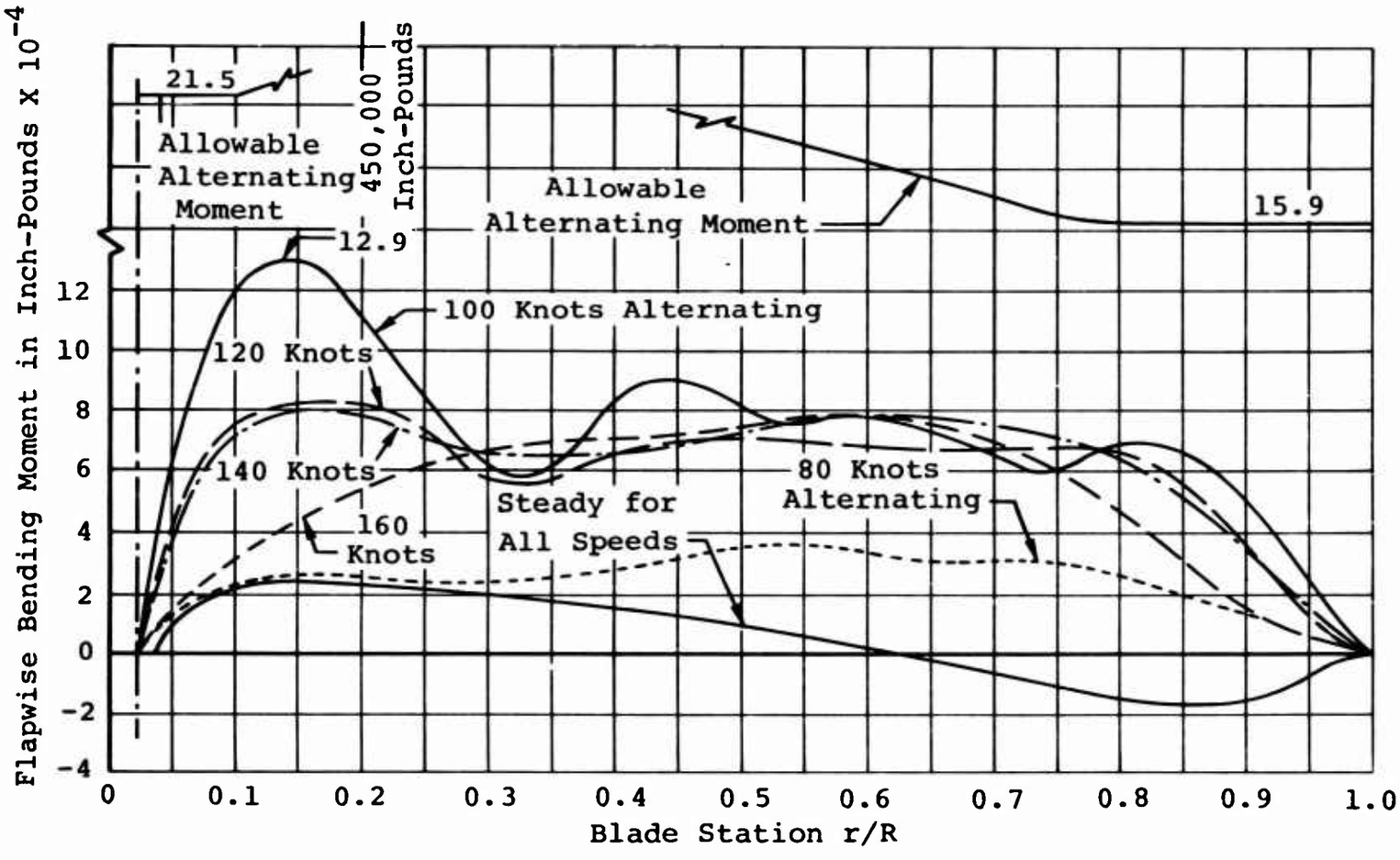

NOTES:
1. Transport
2. θ_t = -12 degrees
3. R = 516 inches

Figure 72. Flapwise Bending Moments of Plastic Blade.
(Sheet 4 of 4)

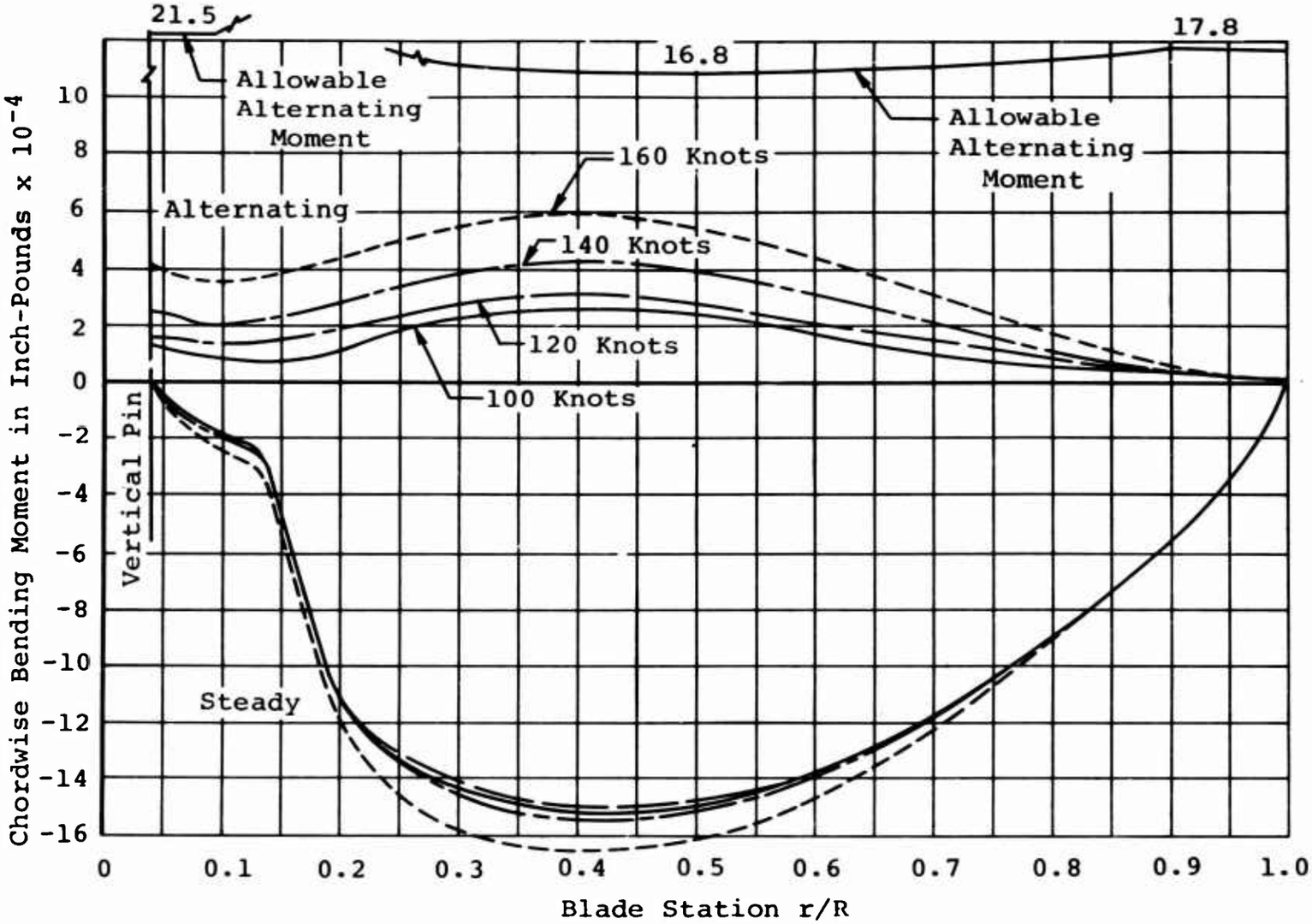

NOTES: 1. Crane/personnel carrier 2. θ_t = -6 degrees 3. R = 516 inches

Figure 73. Chordwise Bending Moments of Plastic Blade.
(Sheet 1 of 4)

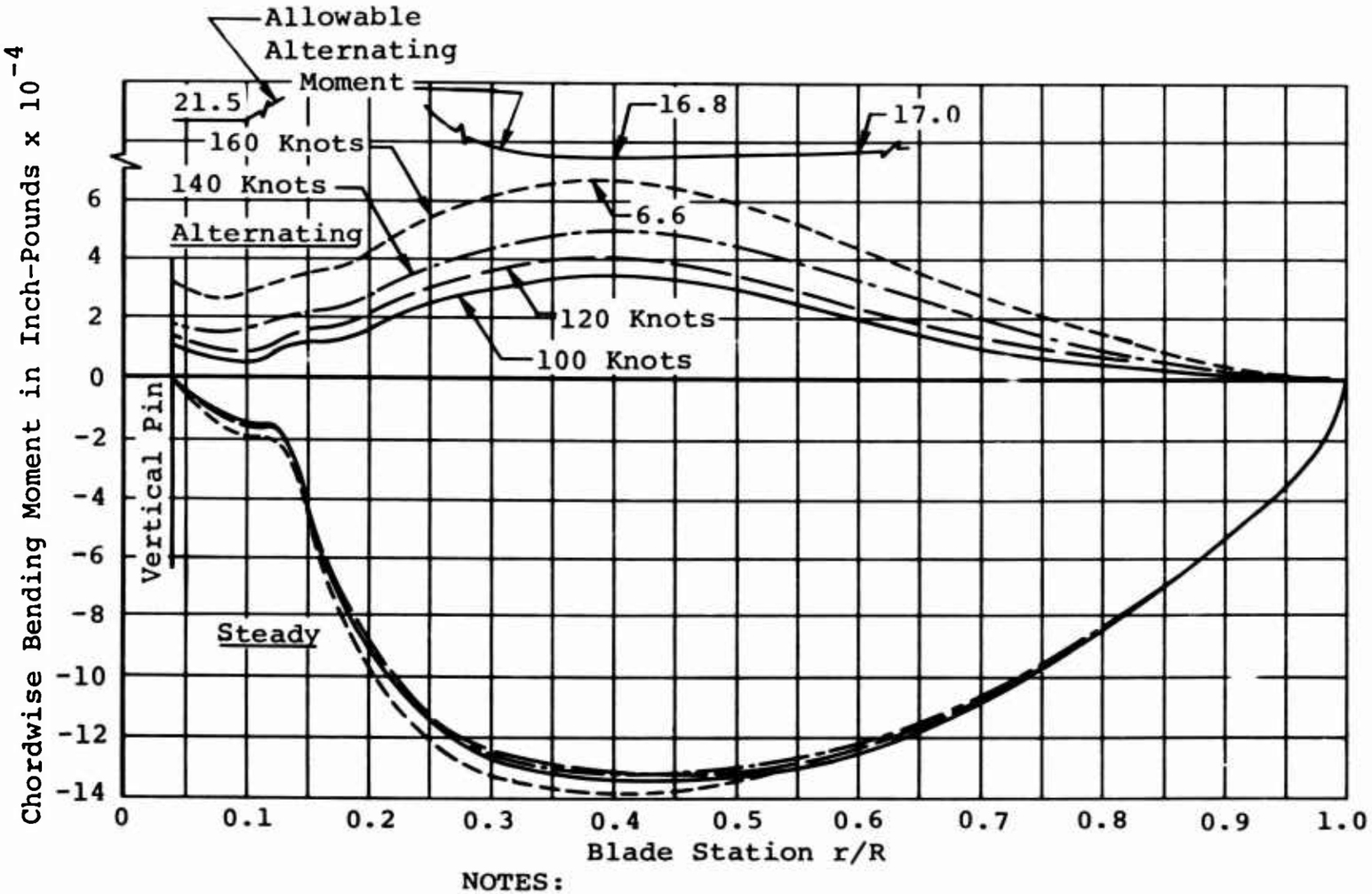

NOTES:
1. Crane/personnel carrier
2. θ_t = -12 degrees
3. R = 516 inches

Figure 73. Chordwise Bending Moments of Plastic Blade. (Sheet 2 of 4)

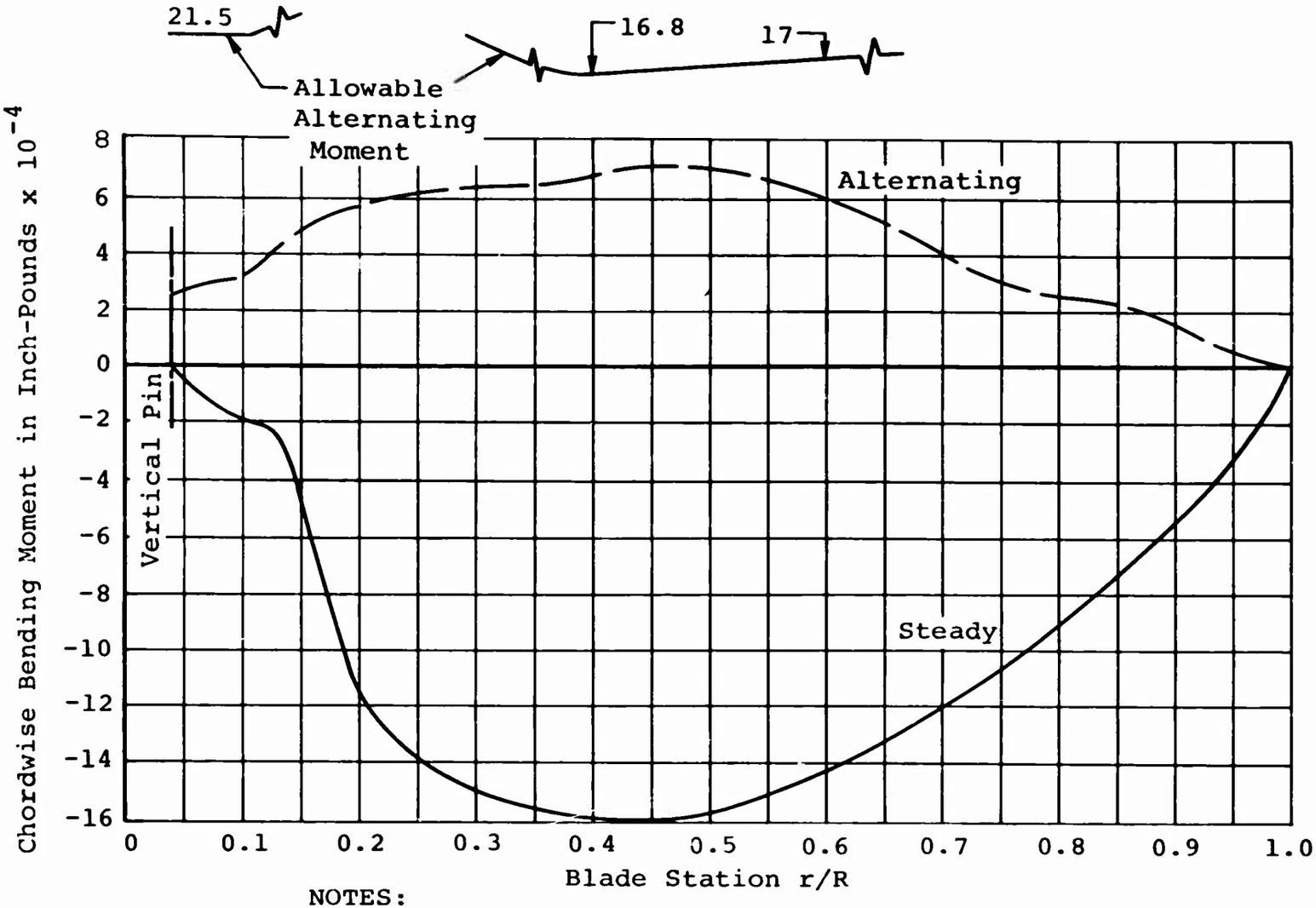

NOTES:

1. Transport
2. θ_+ = -6 degrees
3. R = 516 inches
4. V = 100 knots

Figure 73. Chordwise Bending Moments of Plastic Blade. (Sheet 3 of 4)

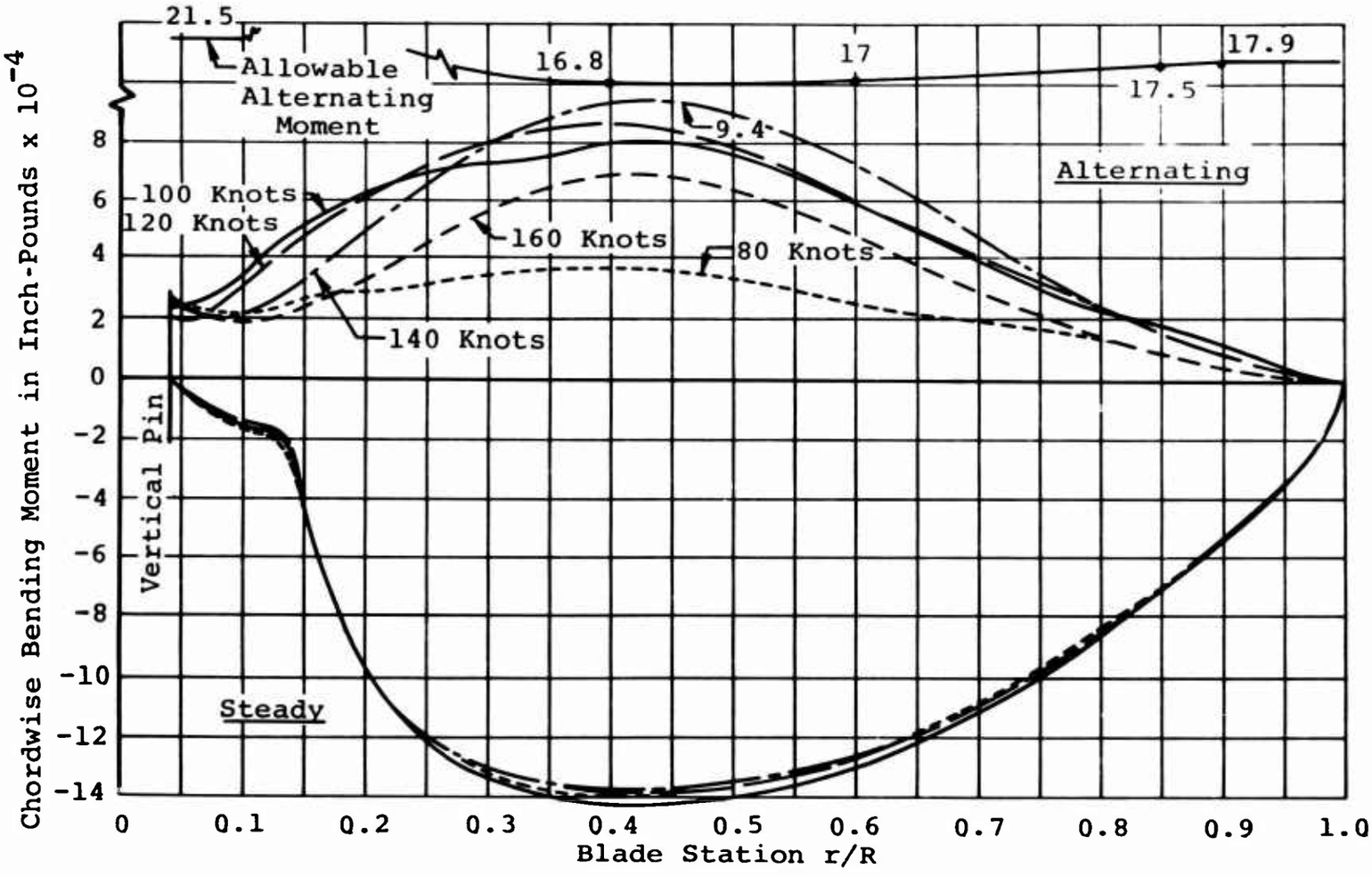

NOTES:
1. Transport
2. θ_t = -12 degrees
3. R = 516 inches

Figure 73. Chordwise Bending Moments of Plastic Blade.
(Sheet 4 of 4)

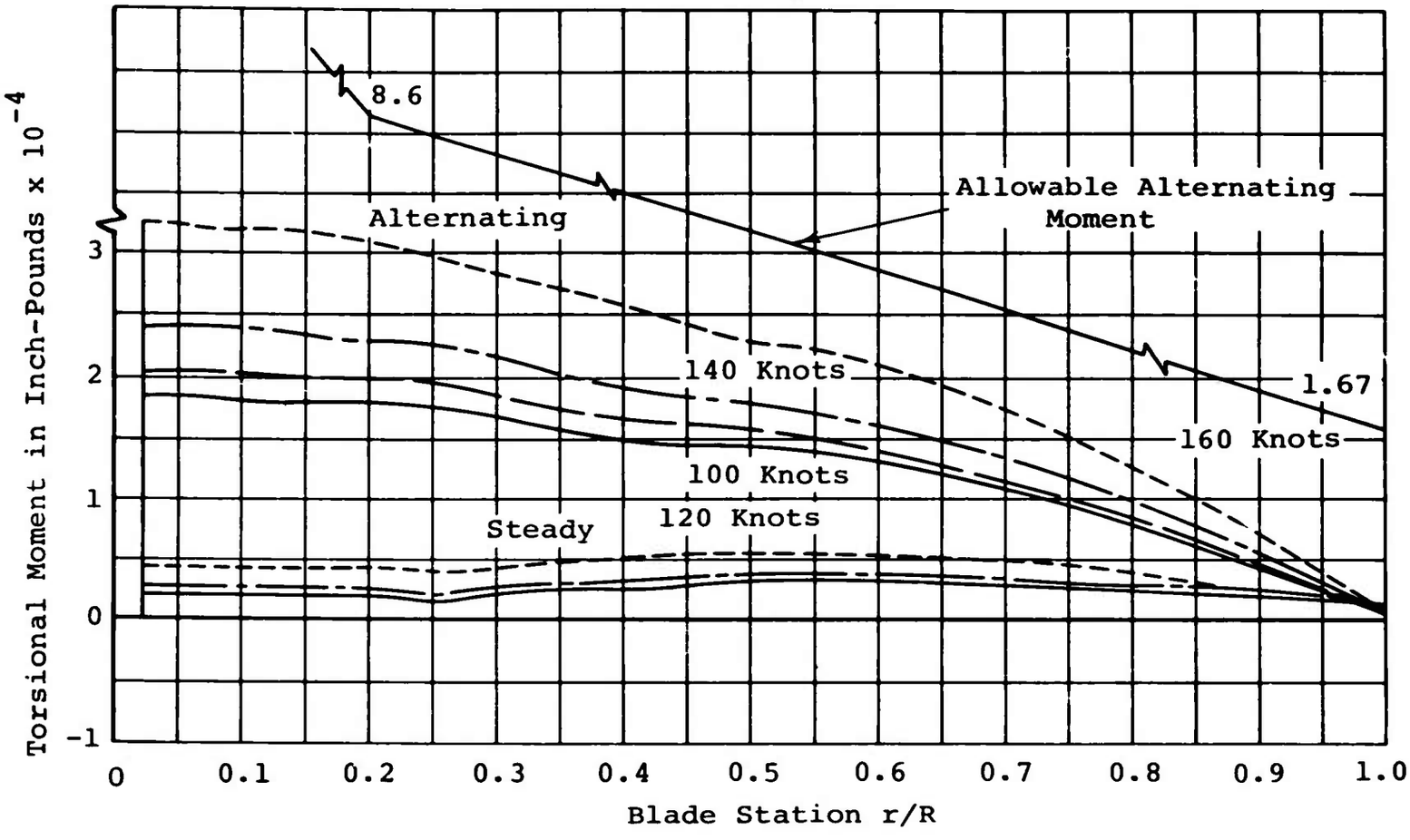

NOTES:
1. Crane/personnel carrier
2. θ_t = -6 degrees
3. R = 516 inches

Figure 74. Torsional Moments of Plastic Blade.
(Sheet 1 of 4)

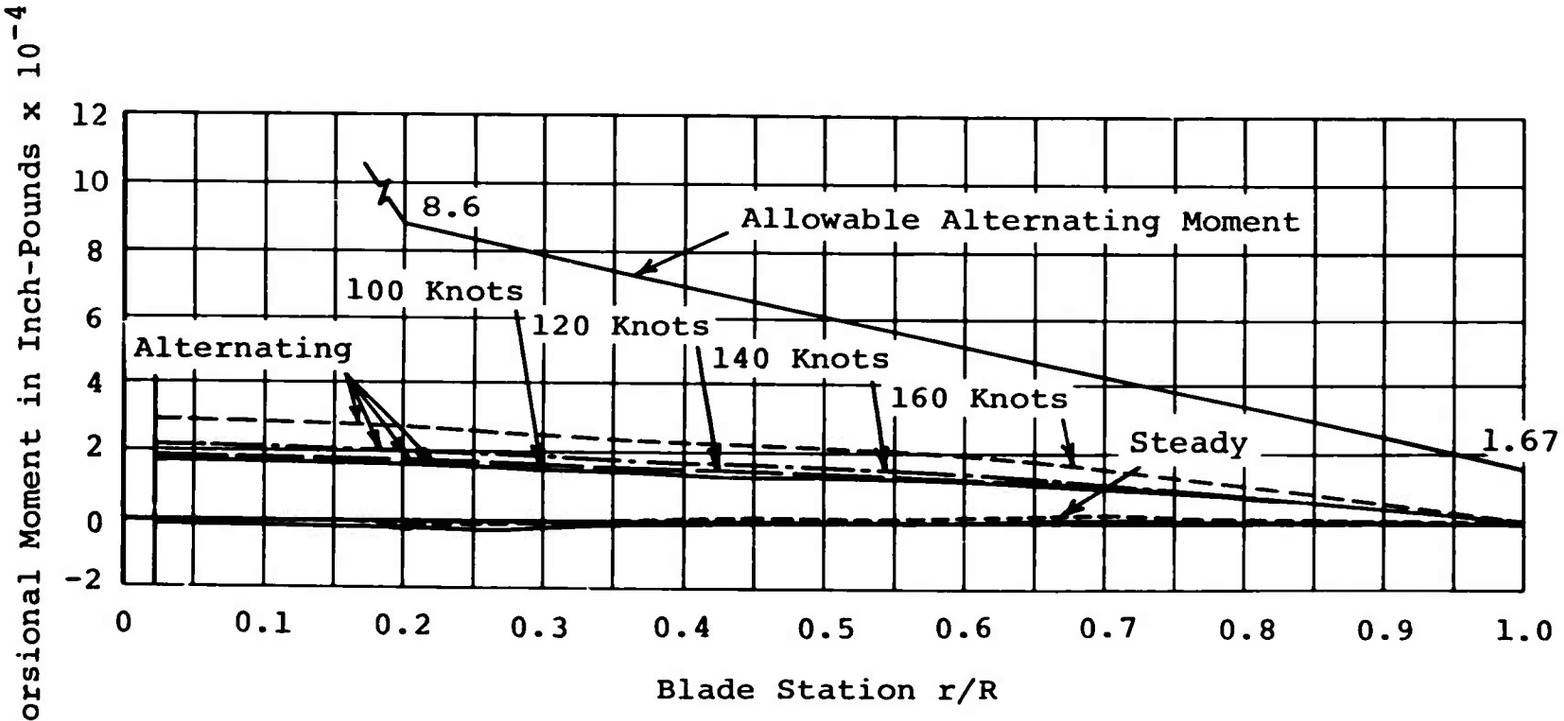

NOTES:
1. Crane/personnel carrier
2. θ_t = -12 degrees
3. R = 516 inches

Figure 74. Torsional Moments of Plastic Blade.
(Sheet 2 of 4)

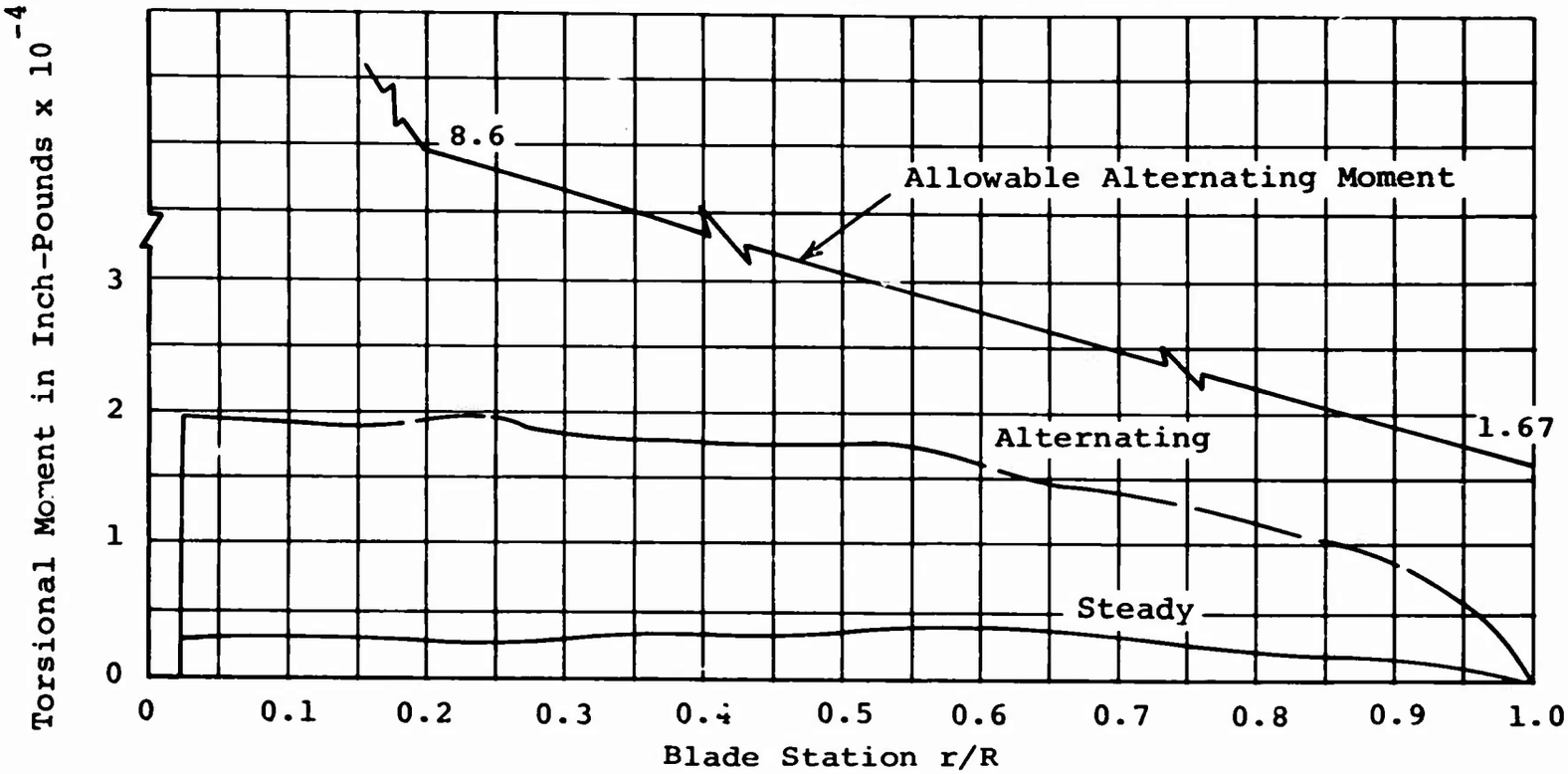

NOTES:

1. Transport
2. θ_t = -6 degrees
3. R = 516 inches
4. V = 100 knots

Figure 74. Torsional Moments of Plastic Blade.
(Sheet 3 of 4)

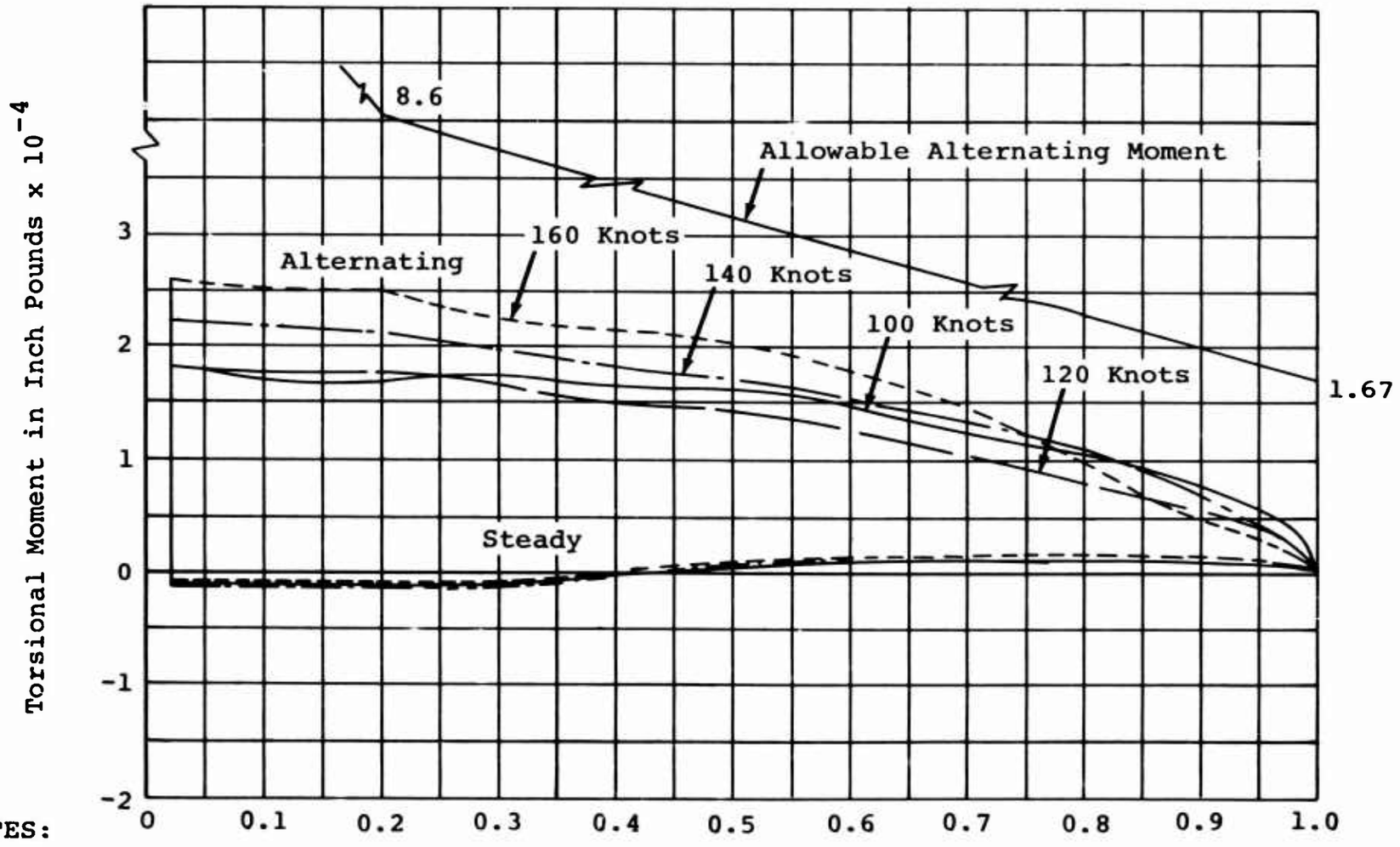

NOTES:
1. Transport
2. θ_t = -12 degrees
3. R = 516 inches

Figure 74. Torsional Moments of Plastic Blade. (Sheet 4 of 4)

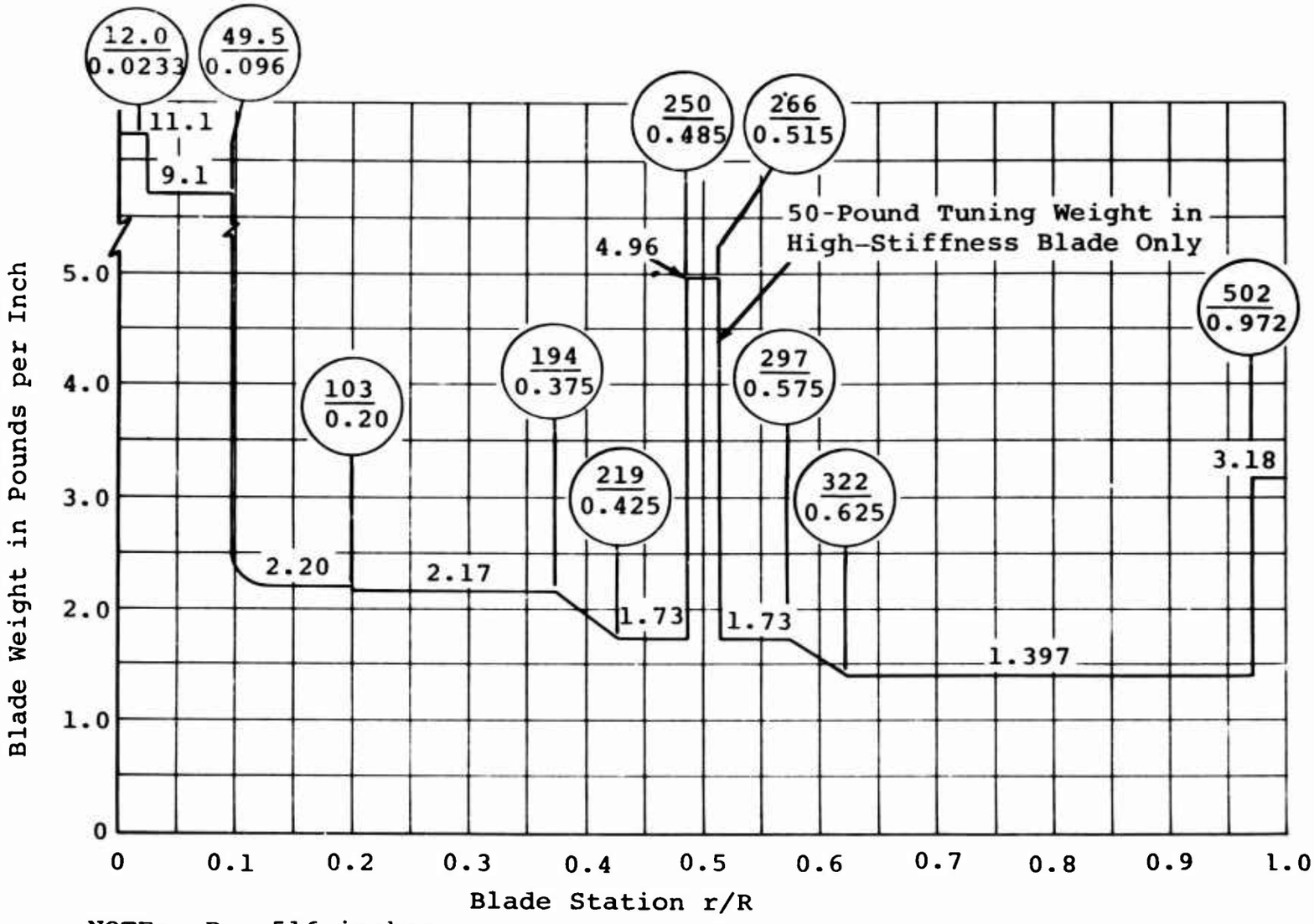

NOTE: R = 516 inches

Figure 75. Weight Distribution of Metal Blades.

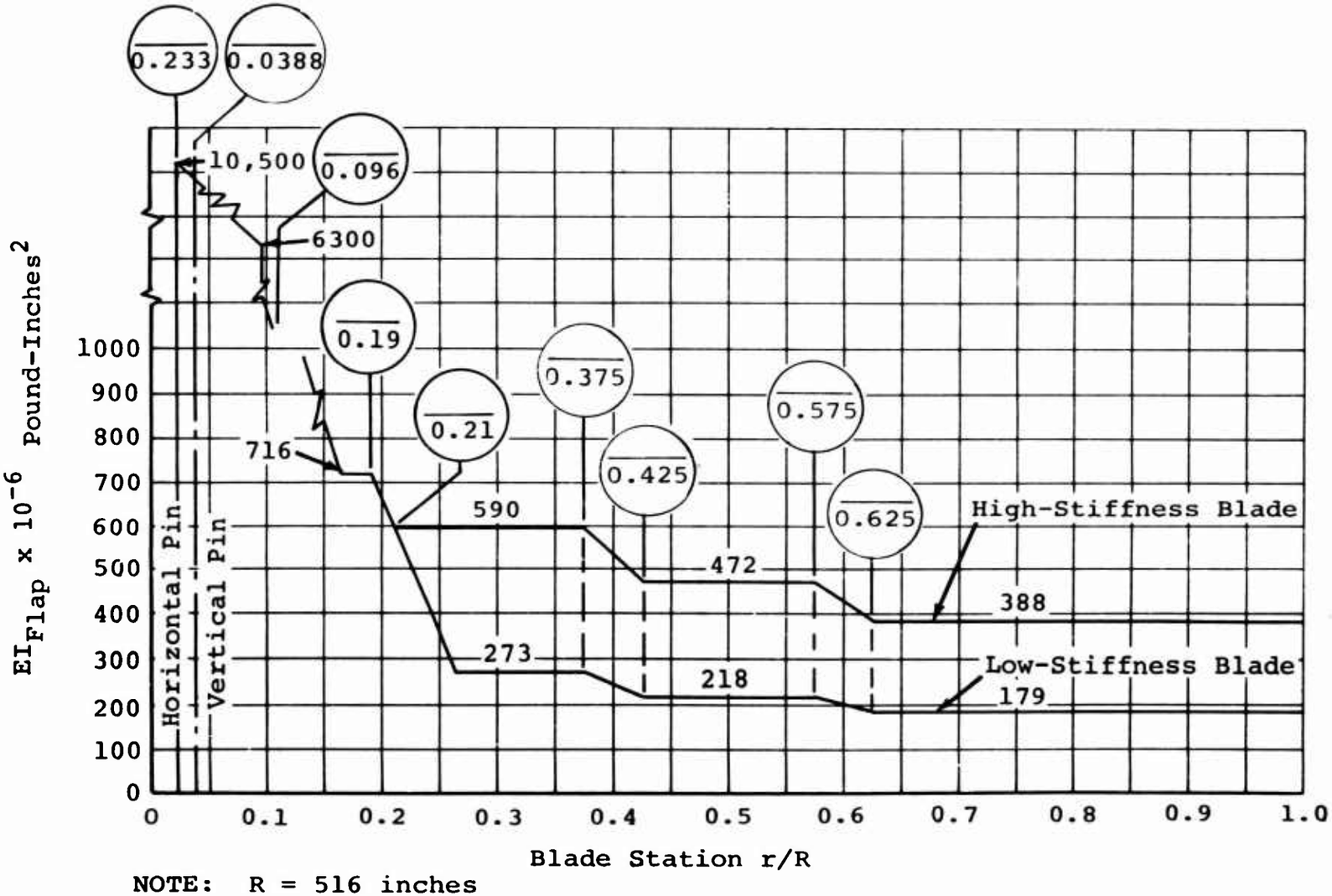

NOTE: R = 516 inches

Figure 76. Flapwise Stiffness Distribution of Metal Blades.

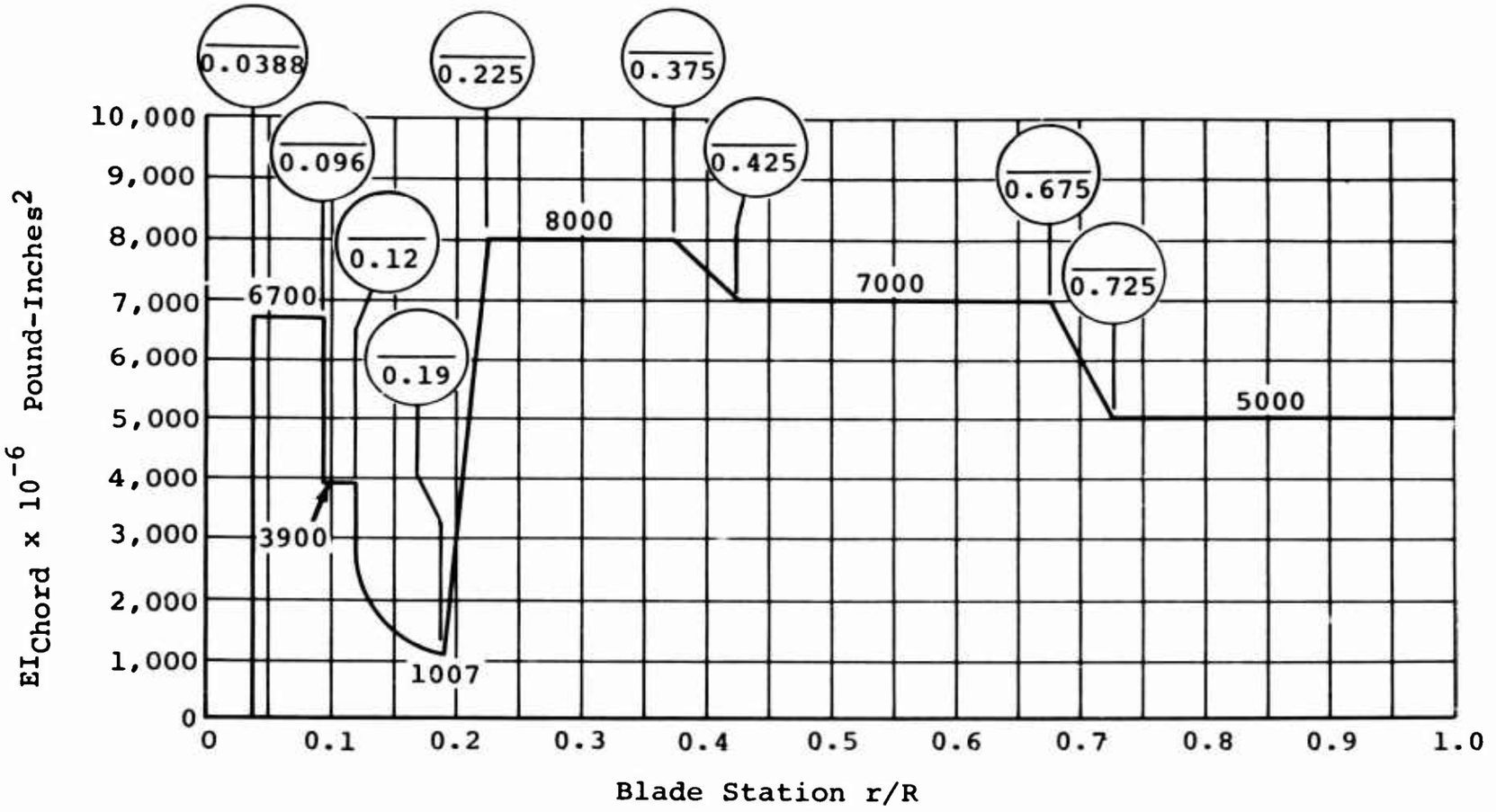

NOTE: R = 516 inches

Figure 77. Chordwise Stiffness Distribution of Metal Blades.

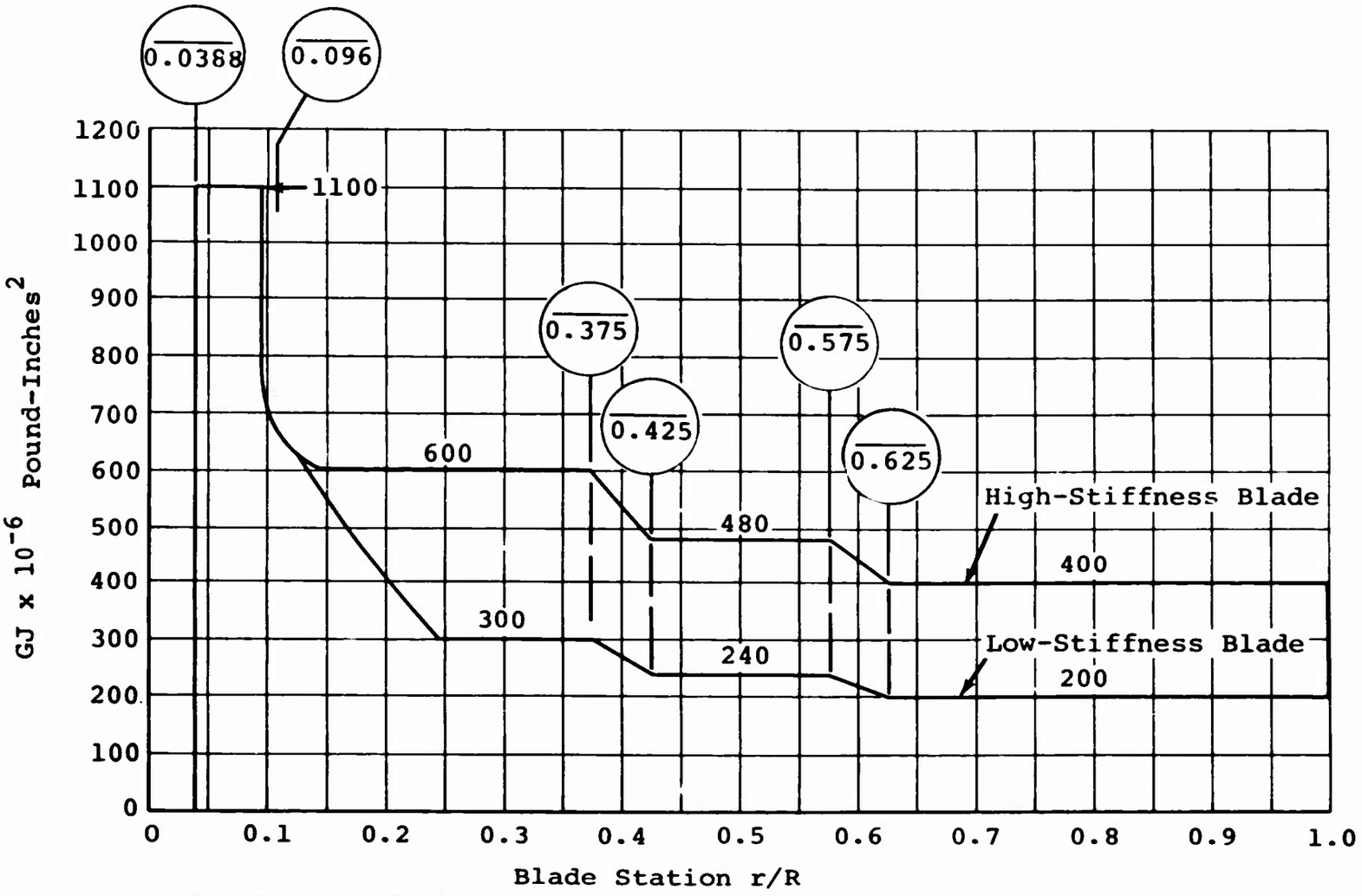

NOTE: R = 516 inches

Figure 78. Torsional Stiffness Distribution of Metal Blades.

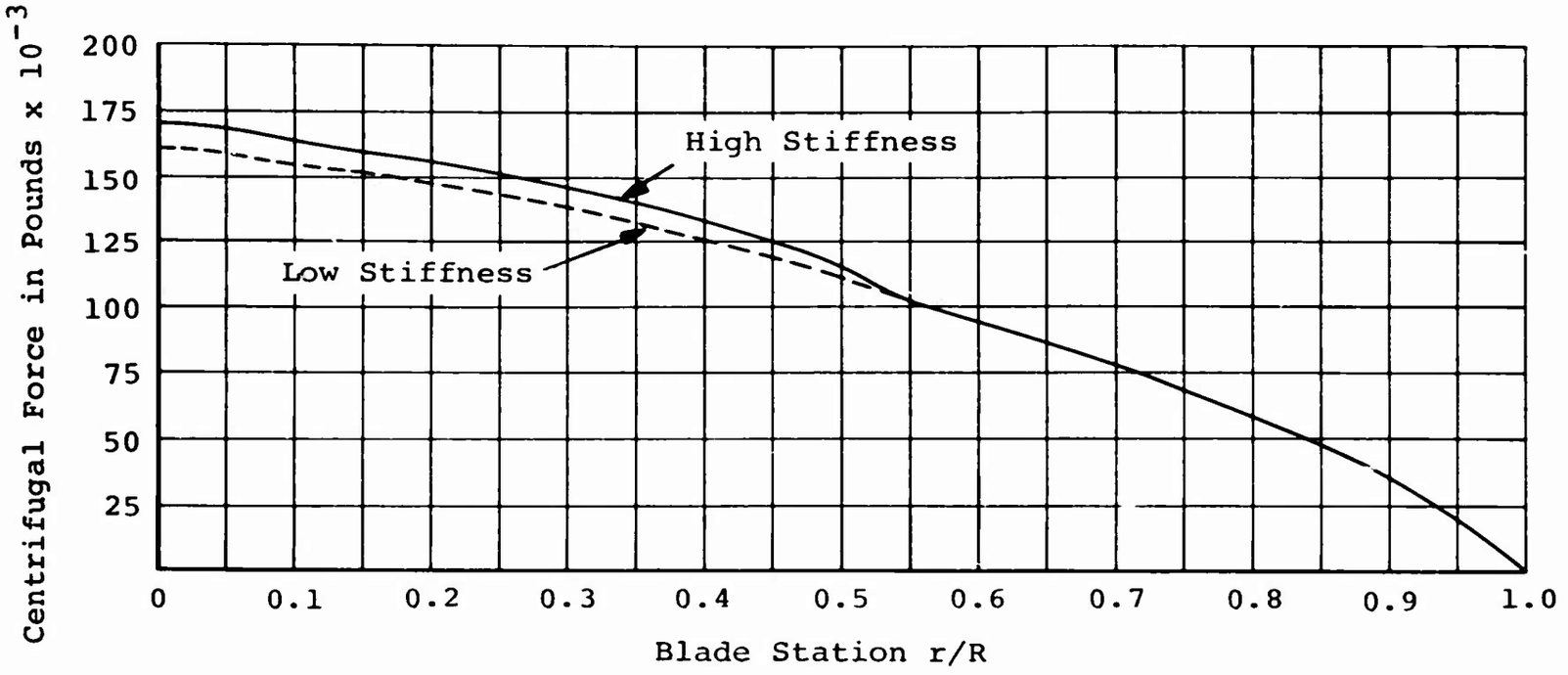

NOTES:
1. R = 516 inches
2. 155.5 rotor rpm

Figure 79. Centrifugal Force Distribution of Metal Blades.

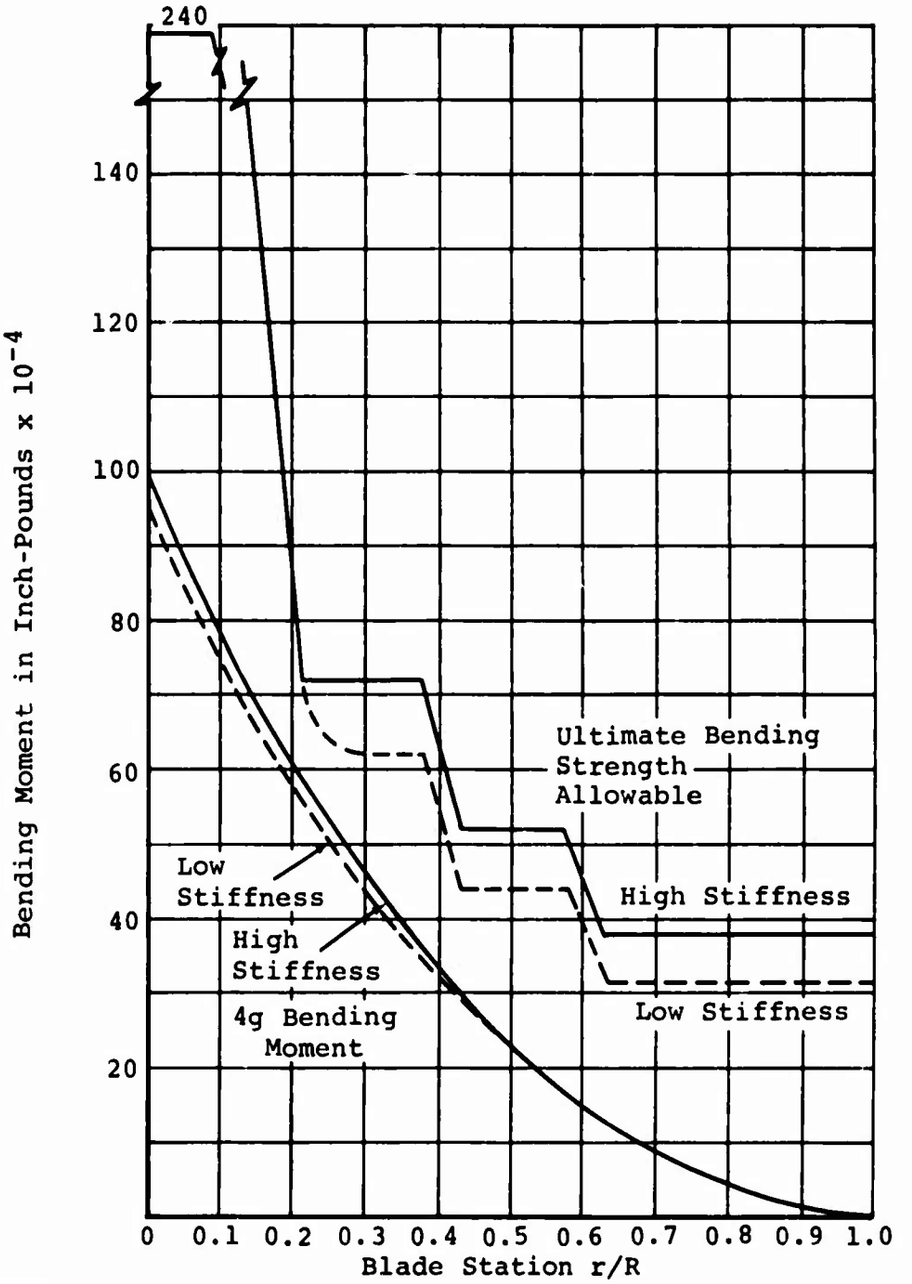

NOTES:

1. R = 516 inches
2. Tip deflection:

	Low Stiffness	High Stiffness
3g	111 inches	55 inches
7 psf + 1g	82 inches	39 inches

3. Blade-to-fuselage clearance, including 3-1/2 degrees droop stop, is 114 inches

Figure 80. Static Bending and Tip Deflection of High- and Low-Stiffness Metal Blades.

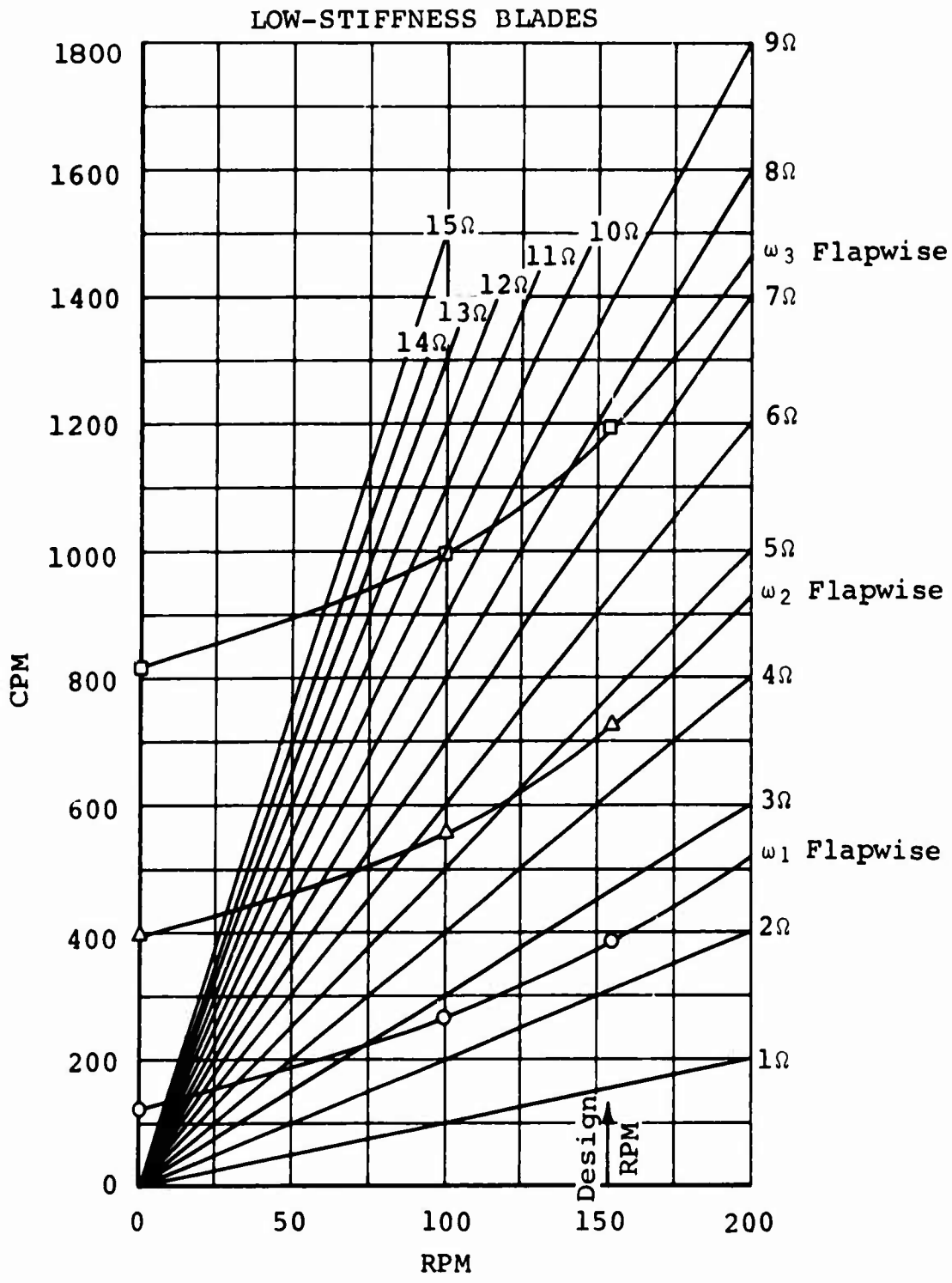

Figure 81. Natural Frequency Spectra of Metal Blades.
(Sheet 1 of 4)

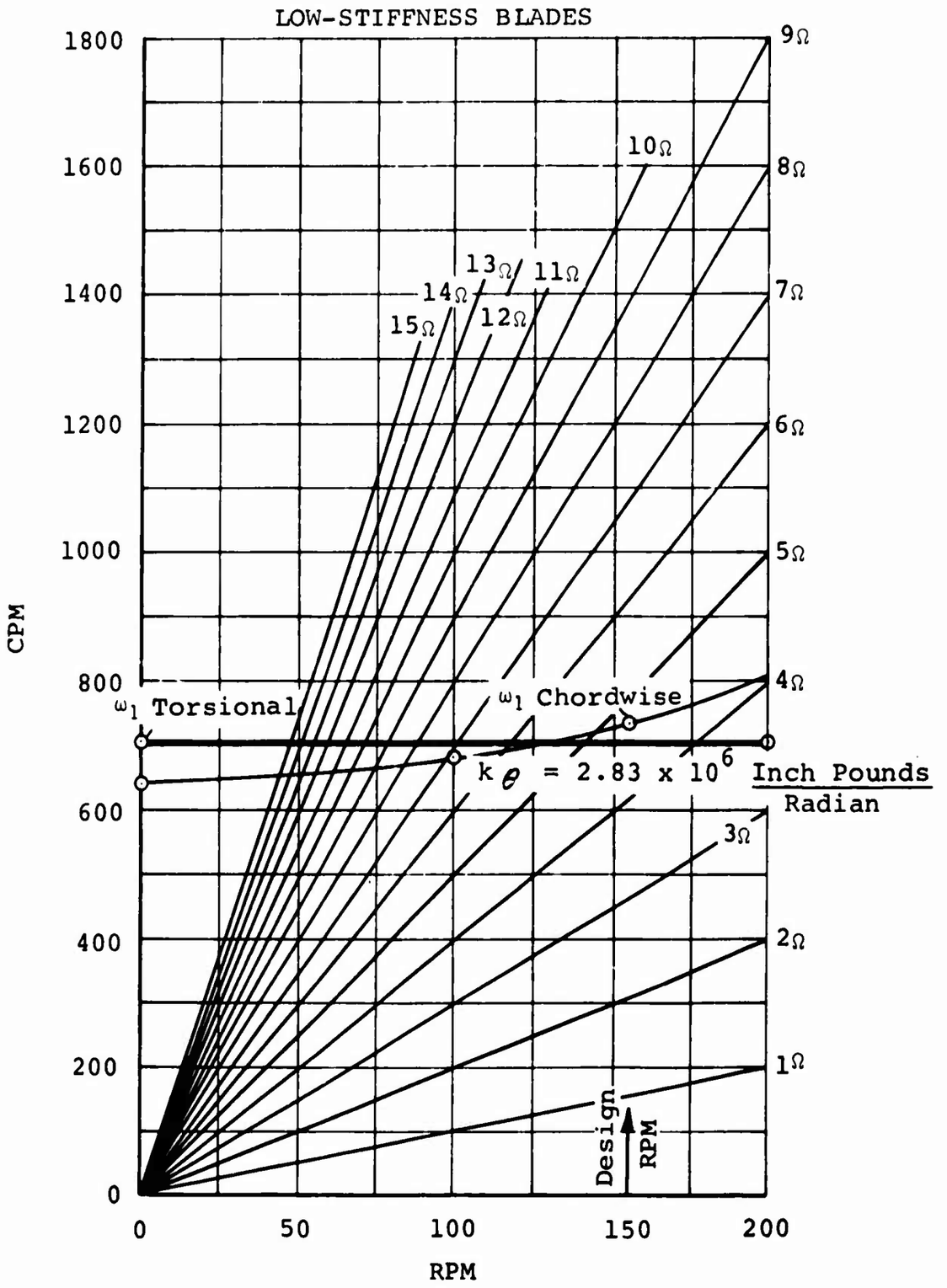

Figure 81. Natural Frequency Spectra of Metal Blades. (Sheet 2 of 4)

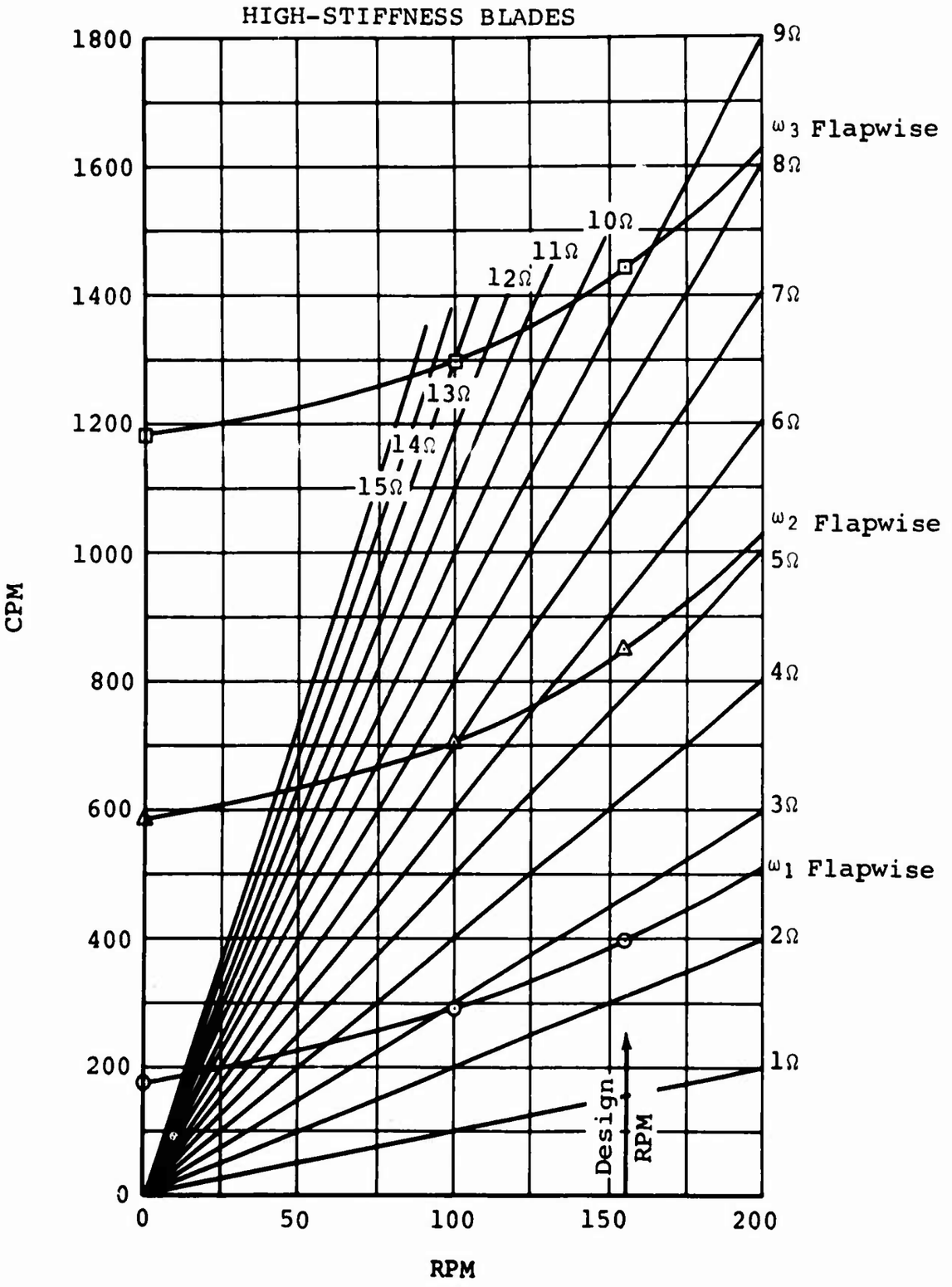

Figure 81. Natural Frequency Spectra of Metal Blades. (Sheet 3 of 4)

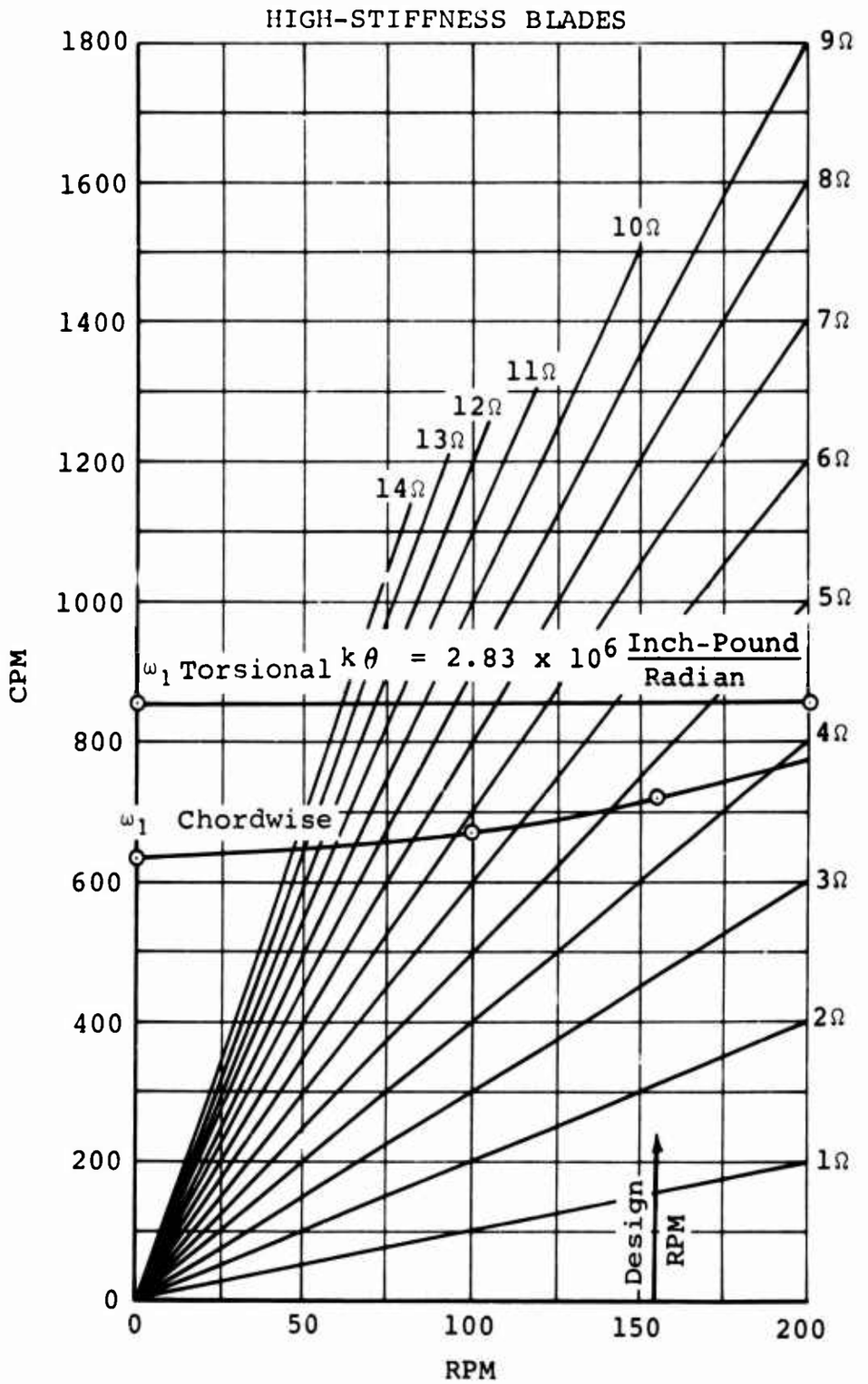

Figure 81. Natural Frequency Spectra of Metal Blades. (Sheet 4 of 4)

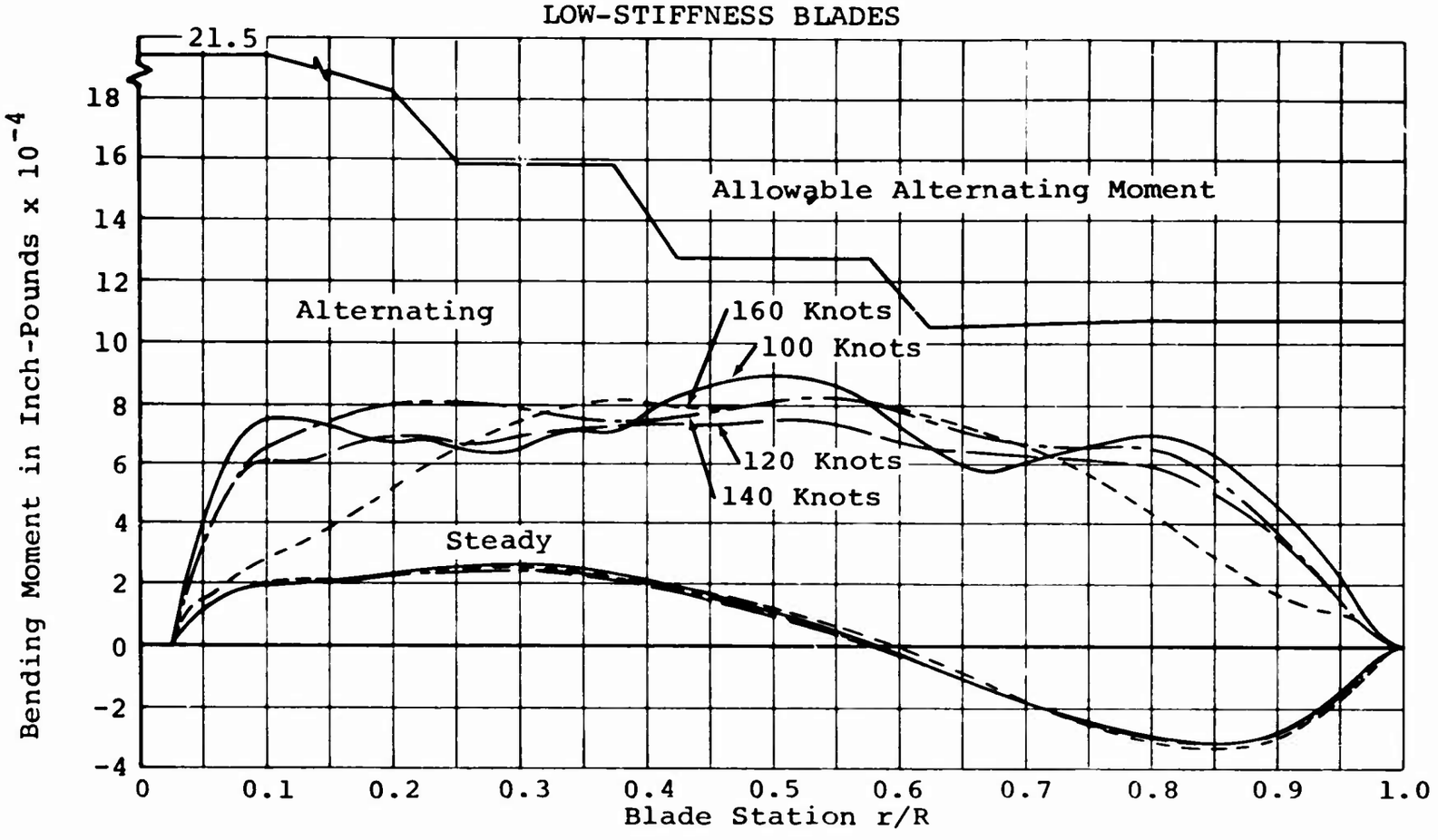

NOTES: 1. Transport
2. θ_t = -12 degrees
3. R = 516 inches

Figure 82. Flapwise Bending Moments of Metal Blades.
(Sheet 1 of 3)

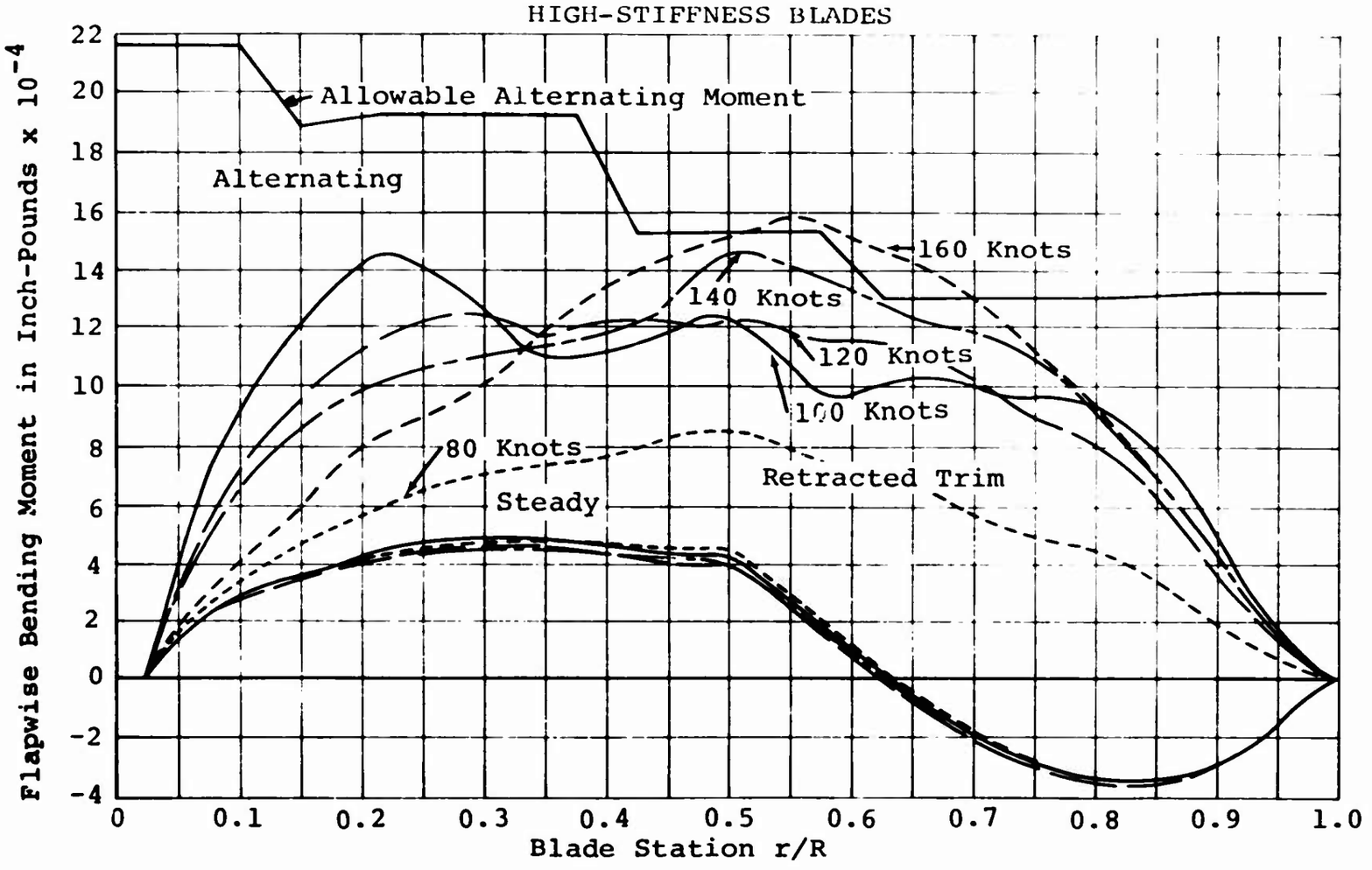

NOTES:
1. Transport
2. θ_t = -12 degrees
3. R = 516 inches

Figure 82. Flapwise Bending Moments of Metal Blades. (Sheet 2 of 3)

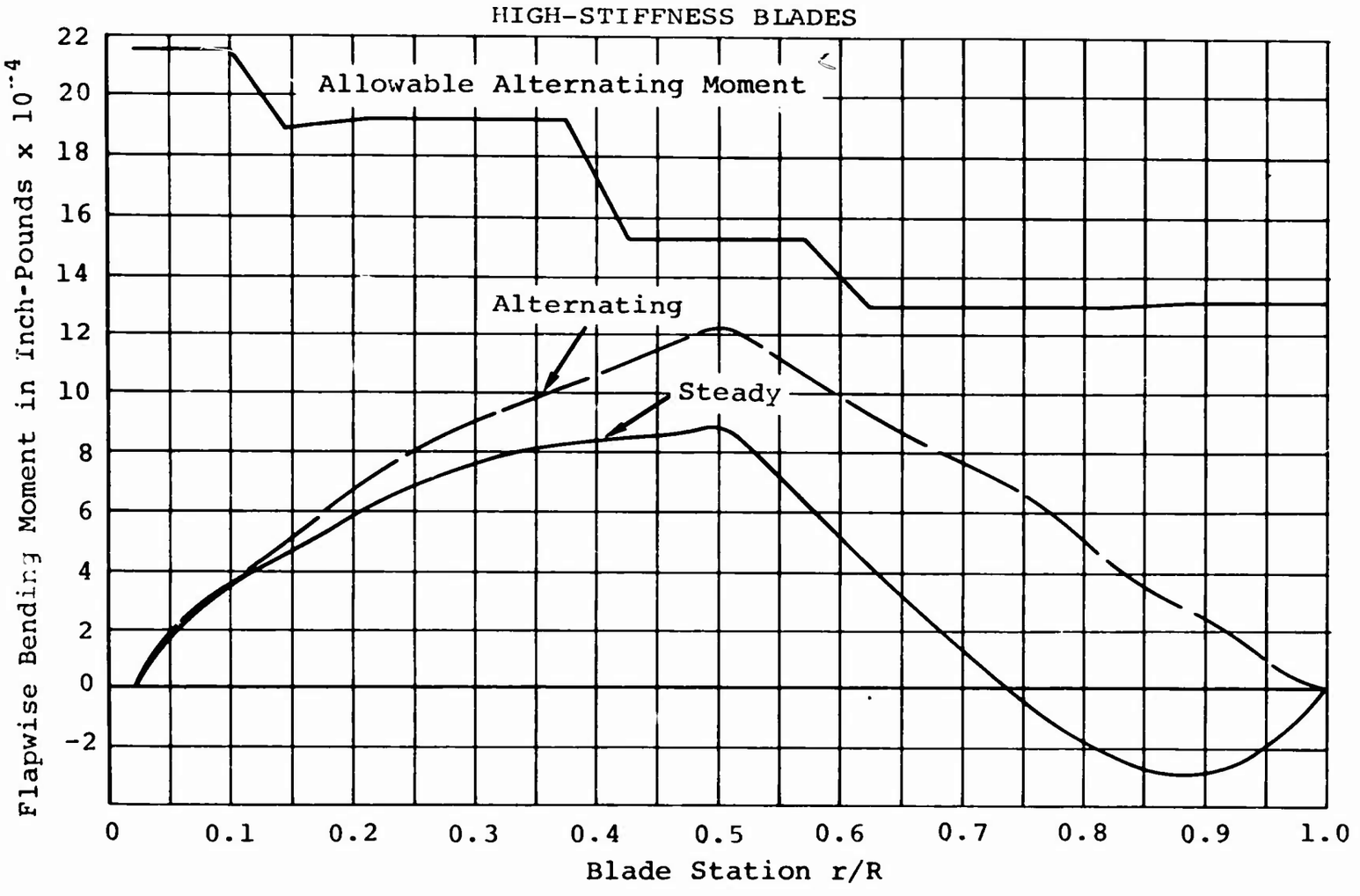

NOTES:

1. Transport
2. R = 516 inches
3. θ_t = -6 degrees
4. V = 160 Knots

Figure 32. Flapwise Bending Moments of Metal Blades. (Sheet 3 of 3)

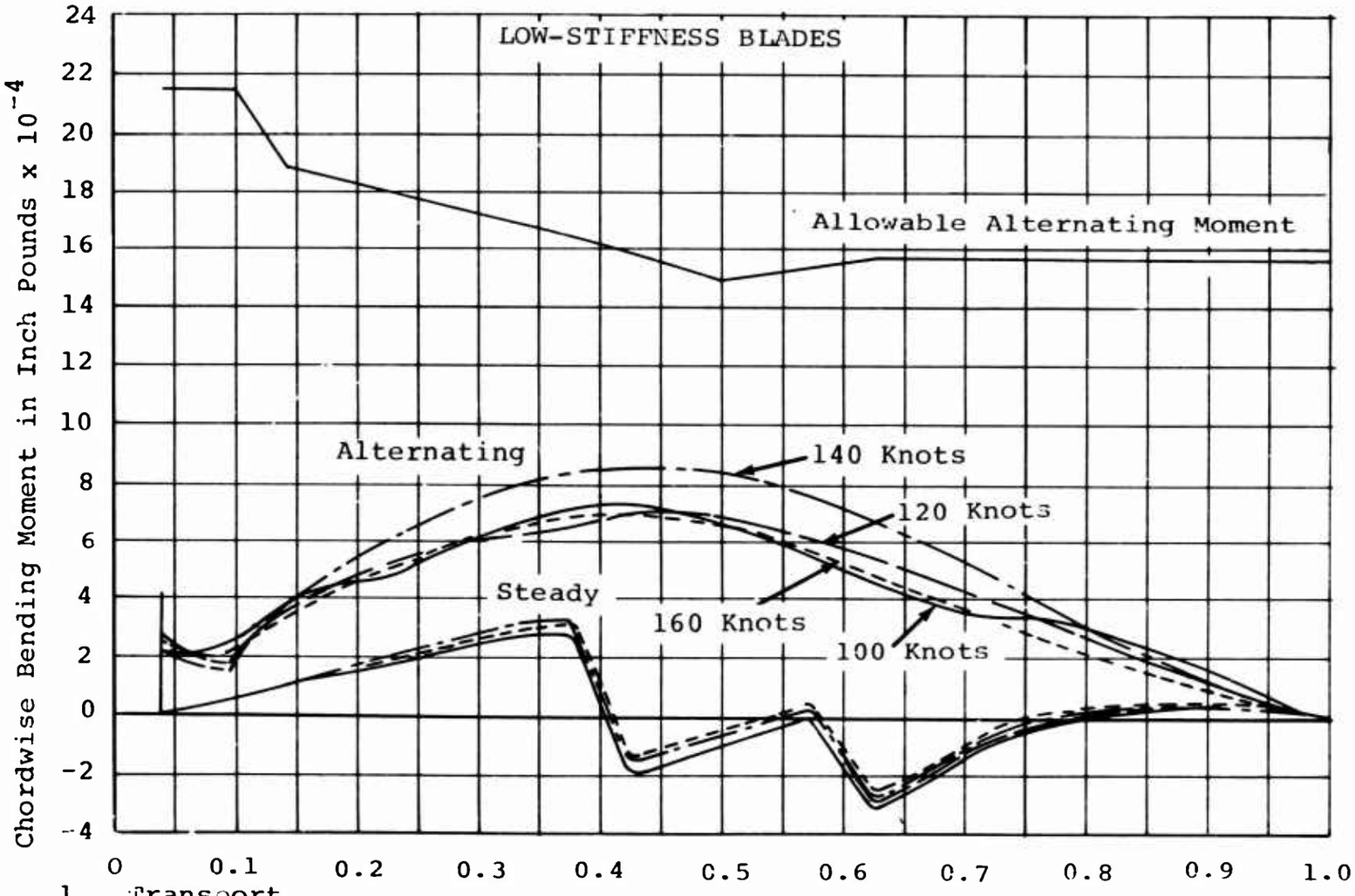

NOTES:
1. Transport
2. R = 516 inches
3. θ_t = -12 degrees

Figure 83. Chordwise Bending Moments of Metal Blades. (Sheet 1 of 3)

HIGH-STIFFNESS BLADES

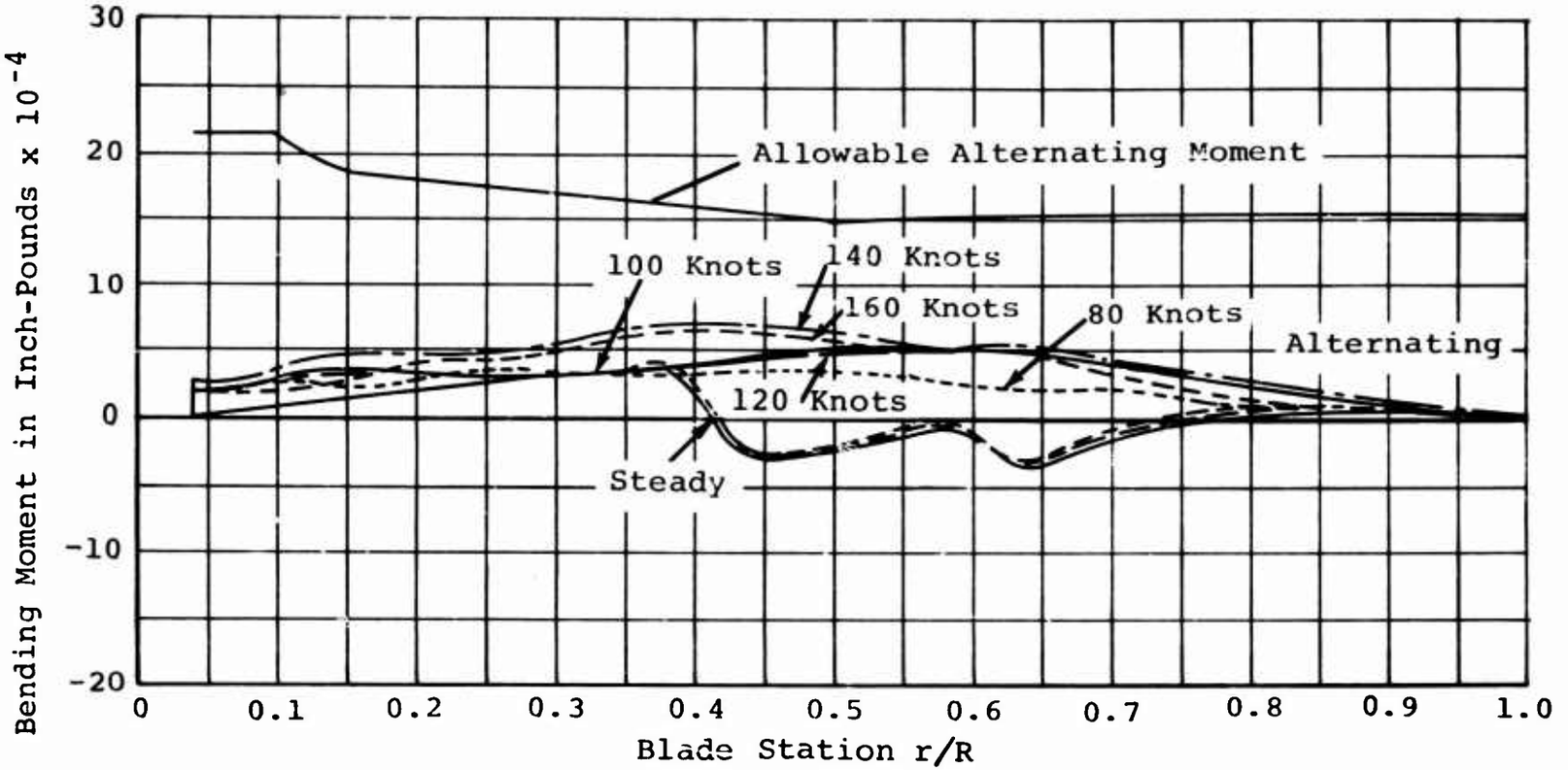

NOTES:
1. Transport
2. R = 516 inches
3. θ_t = -12 degrees

Figure 83. Chordwise Bending Moments of Metal Blades.
(Sheet 2 of 3)

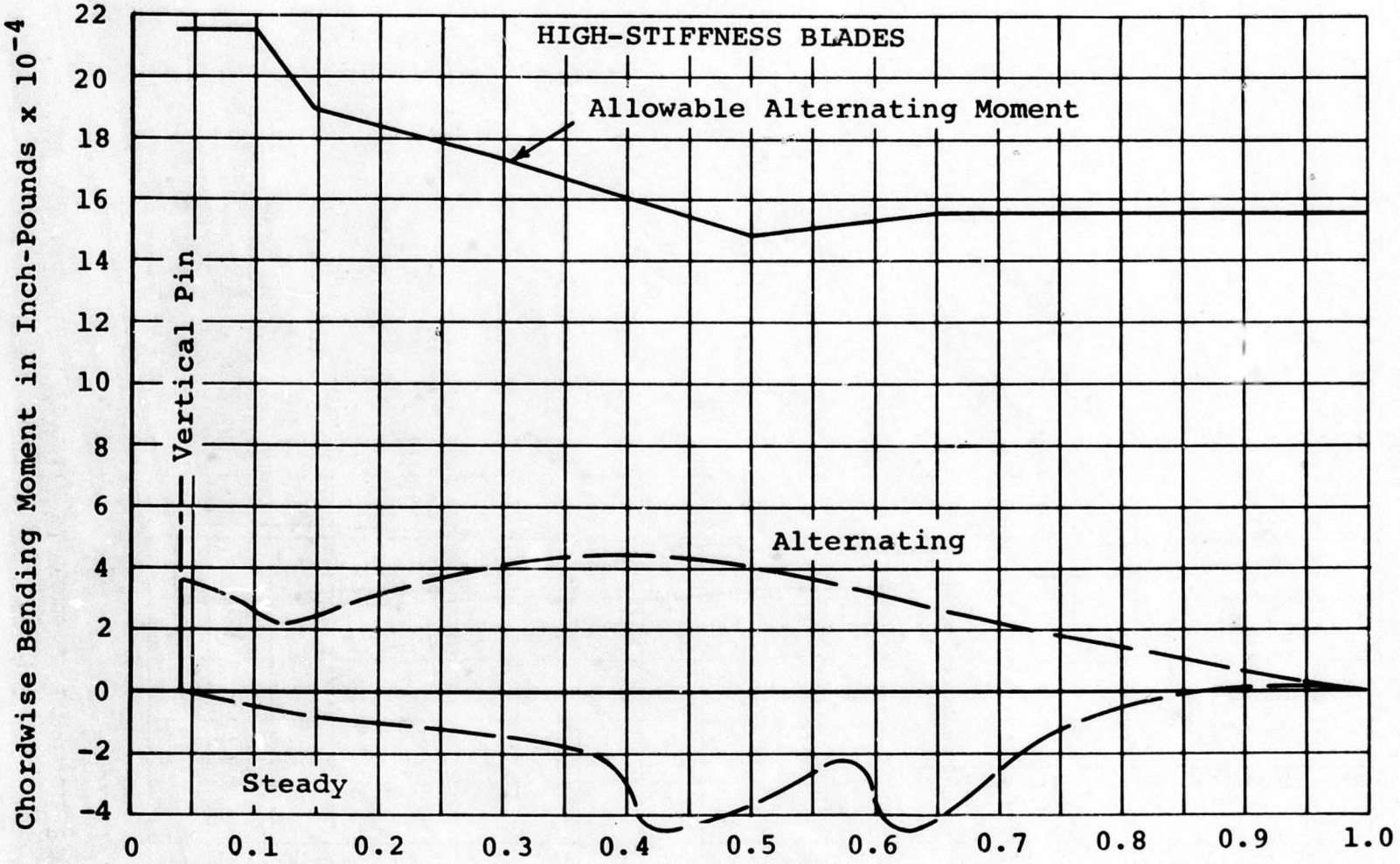

NOTES:
1. Transport
2. R = 516 inches
3. θ_t = -6 degrees
4. V_t = 160 knots

Figure 83. Chordwise Bending Moments of Metal Blades. (Sheet 3 of 3)

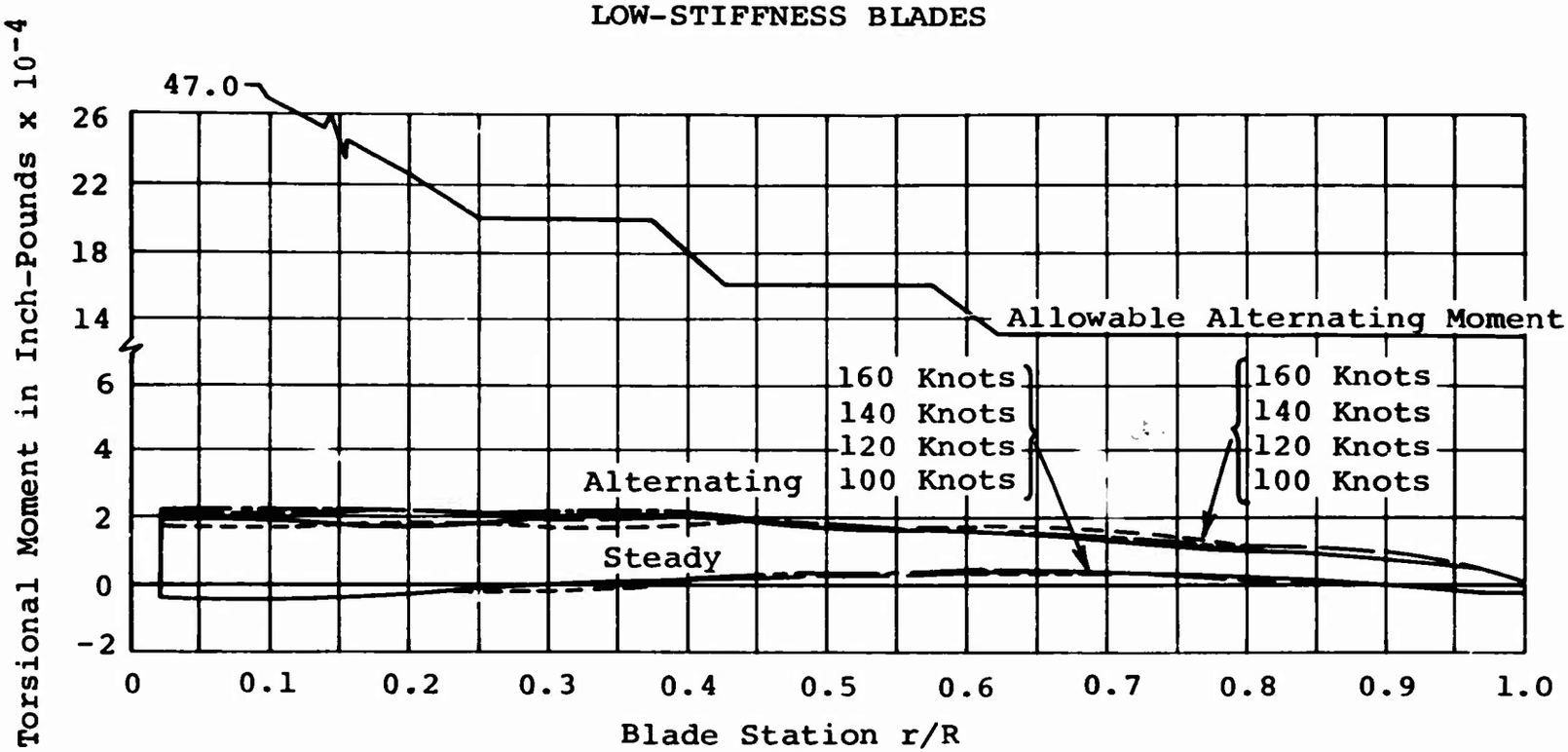

NOTES:
1. Transport
2. R = 516 inches
3. θ_t = -12 degrees

Figure 84. Torsional Moments of Metal Blades.
(Sheet 1 of 3)

HIGH-STIFFNESS BLADES

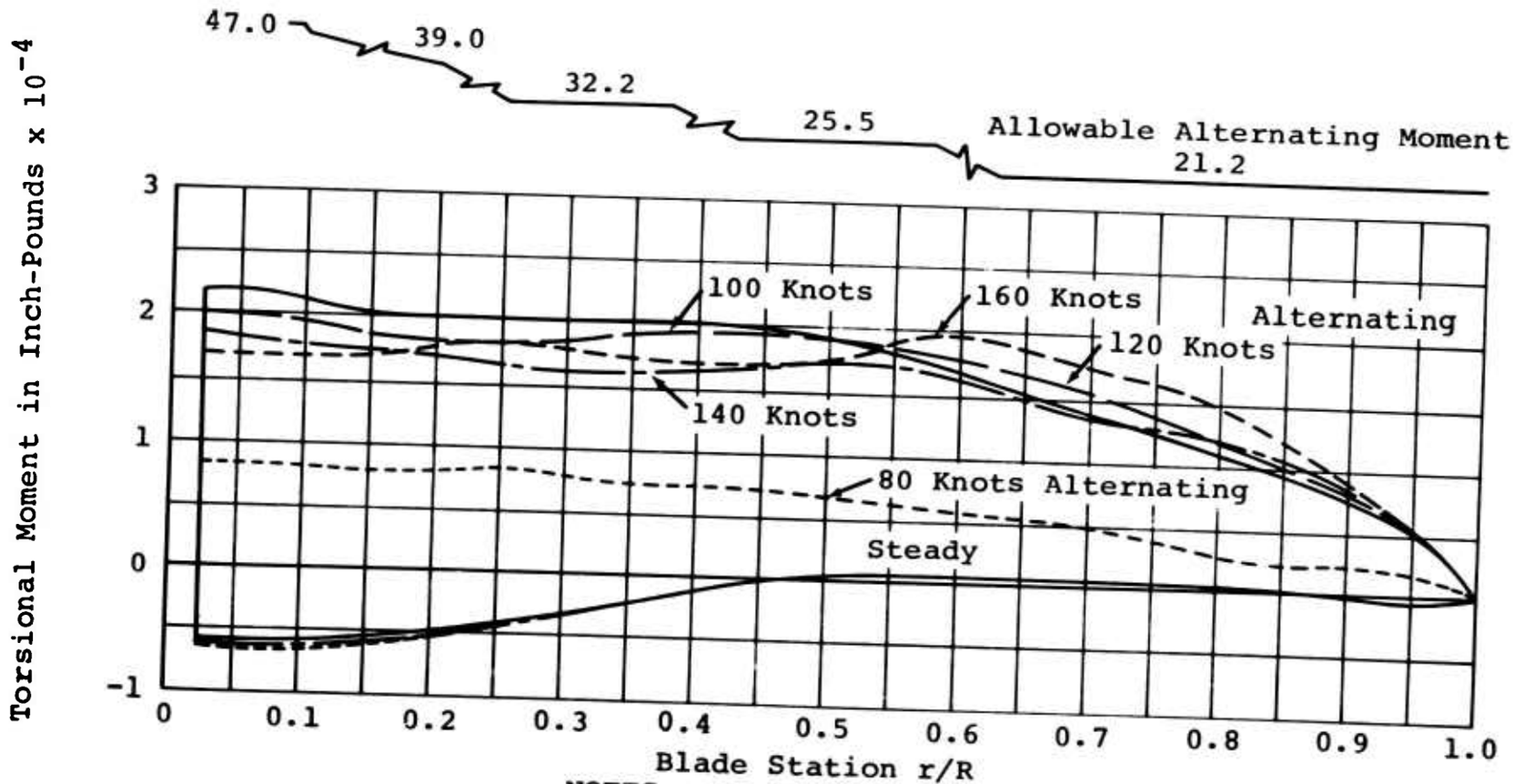

NOTES:
1. Transport
2. R = 516 inches
3. θ_t = -12 degrees

Figure 84. Torsional Moments of Metal Blades.
(Sheet 2 of 3)

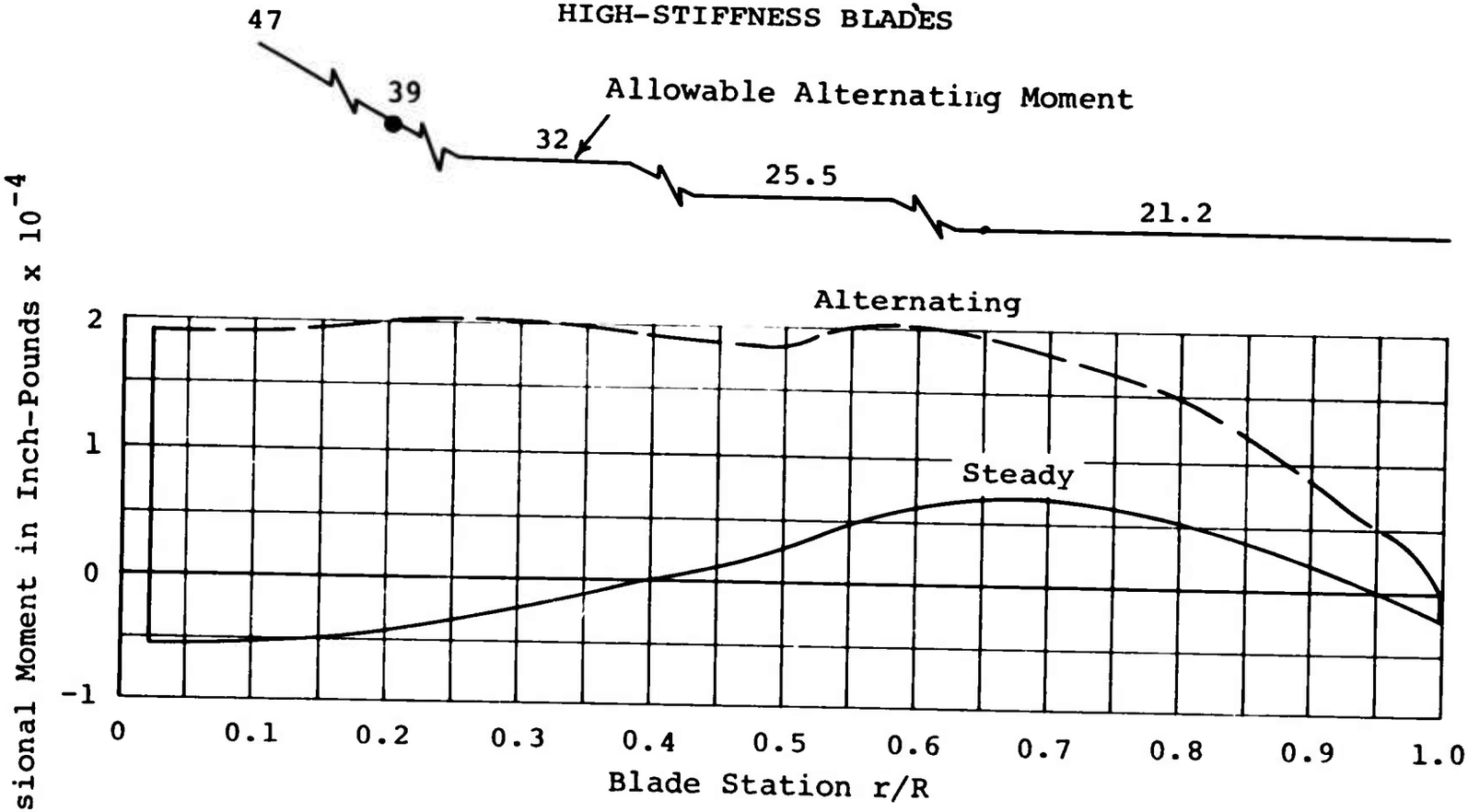

NOTES:
1. Transport
2. R = 516 inches
3. θ_t = -6 degrees
4. V = 160 knots

Figure 84. Torsional Moments of Metal Blades.
(Sheet 3 of 3)

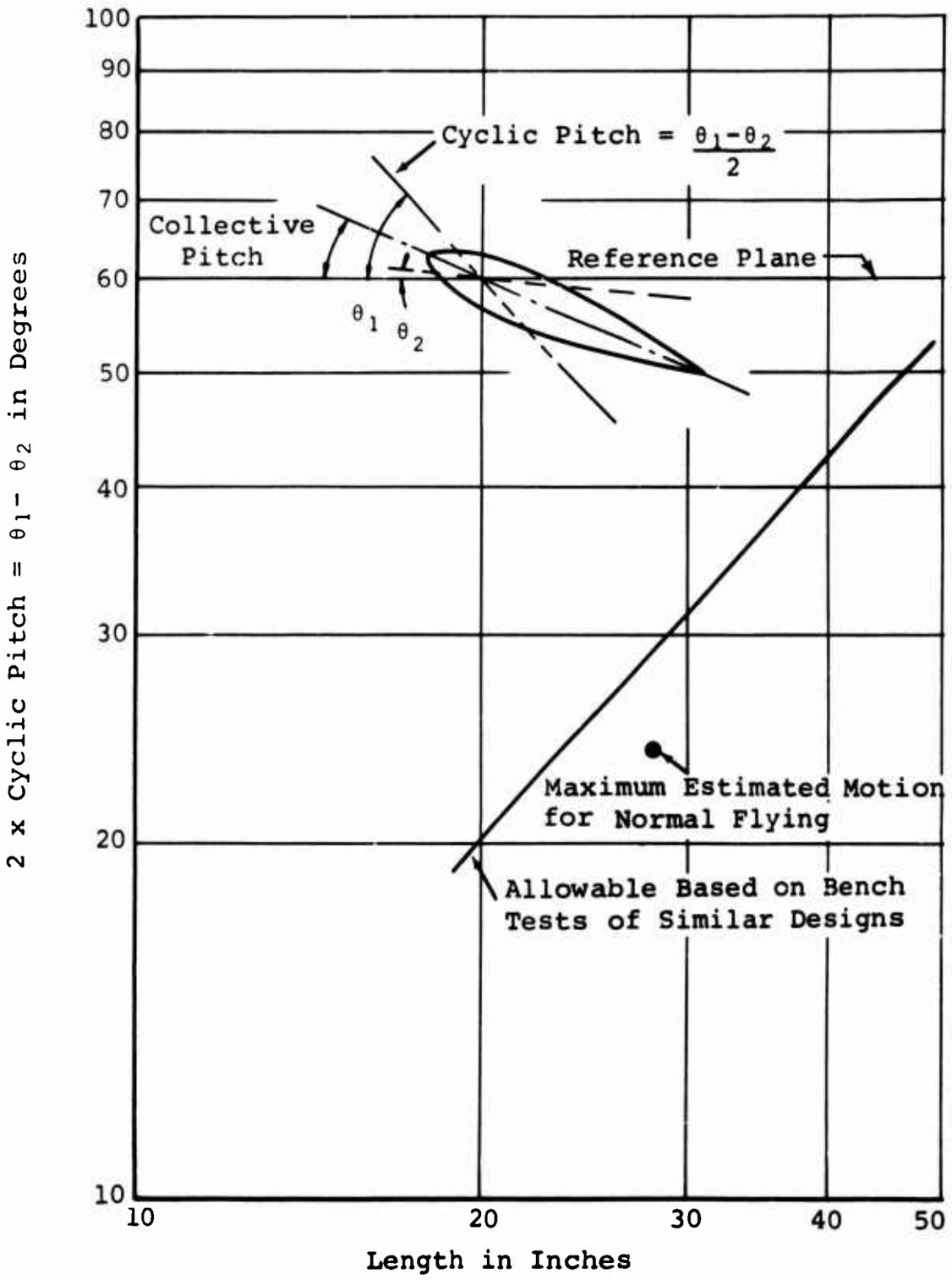

Figure 85. Parametric Evaluation of Tension-Torsion Assembly.

TABLE XIX

CUBIC MEAN LOAD ON HORIZONTAL HINGE PIN ROLLER BEARINGS

Column Number

1. Percent life
2. N (Rotor RPM)
3. OPM (Bearing Oscillations per minute)
4. P (Load in pounds; based on 788-pound blade)
5. $P_1^3 \times 10^{12}$
6. Time in hours
7. t (time in minutes)
8. (OPM) x t x 10^6
9. P^3 x (OPM) x t x 10^{21}

Flight Condition	①	②	③	④	⑤	⑥	⑦	⑧	⑨
High-speed level flight	11	155	155	85,000	614.12	132	7,920	1.2276	0.75390
Maximum power	8	149	149	78,600	485.6	96	5,760	0.8582	0.41676
Cruise	54	155	155	85,000	614.12	648	38,880	6.0264	3.70096
Transition	11	155	155	85,000	614.12	132	7,920	1.2276	0.75390
Hover	10	155	155	85,000	614.2	120	7,200	1.1160	0.68364
Autorotation	6	194	194	133,000	2352.6	72	4,320	0.8381	1.97170
	Σ 100					1200	72,000	11.2939	8.28086

$$\text{Cubic Mean Load} = \sqrt[3]{\frac{\Sigma P^3 \times (OPM) \times t}{\Sigma (OPM) \times t}} = \sqrt[3]{\frac{8.28086 \times 10^{21}}{11.2939 \times 10^6}} = 90{,}200 \text{ pounds}$$

$$\text{Mean Oscillations per Minute} = \frac{\Sigma OPM \times t}{\Sigma t} = \frac{11.2939 \times 10^6}{72{,}000} = 156.9$$

TABLE XX

B_{10} LIFE OF HORIZONTAL HINGE PIN ROLLER BEARINGS

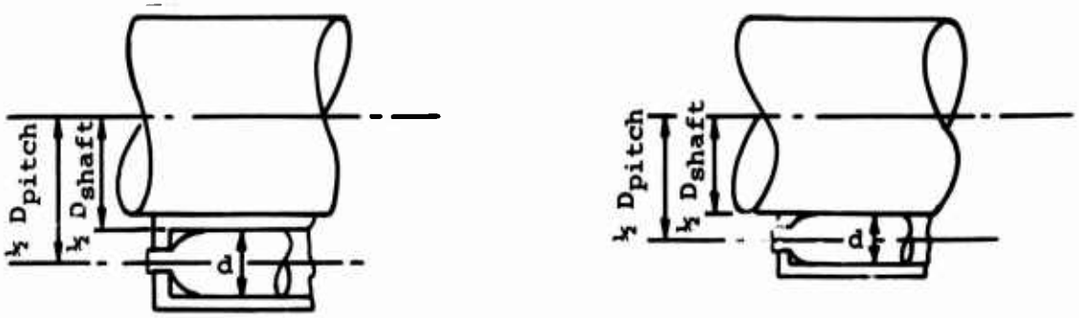

D_{shaft} = 6.0 inches

D_{pitch} = 6.9 inches

Number of rollers (N) = 40

Effective length (L_{eff}) = 2.5 inches

Roller diameter (d) = 0.5 inches

1. Static capacity of bearing = 12,000 × L_{eff} × d × (N-3) = 552,000 pounds

2. Basic oscillating capacity (C) = 0.354 × static capacity = 195,000 pounds

3. Shaft hardness factor (SHF) = 1.0
   Stationary shaft factor (SSF) = 1.0

4. $\beta = 360° \div N$
   Critical angle of oscillation = $\beta(1 + (D_{shaft} \div D_{pitch}))$ = 24°

5. Actual angle of oscillation = <24°
   Service experience factor = 1.0

6. Design oscillations per minute (OPM) = 156.9
   Size factor (SF) = 1.0

7. Cubic mean load (P) = 90,200 pounds
   Oil lubrication factor (OLF) = 1.0

8. $C \div P = 2.16$
   $(C \div P) \times SSF = 2.16$
   $((C \div P) \times SSF)^{10/3} = 13.0$

9. B_{10} Life = $((C \div P) \times SSF)^{10/3} \times (10^6 \div (60 \times OPM))$ = 1390 hours

   B_{10} Life × SF = 1390 hours

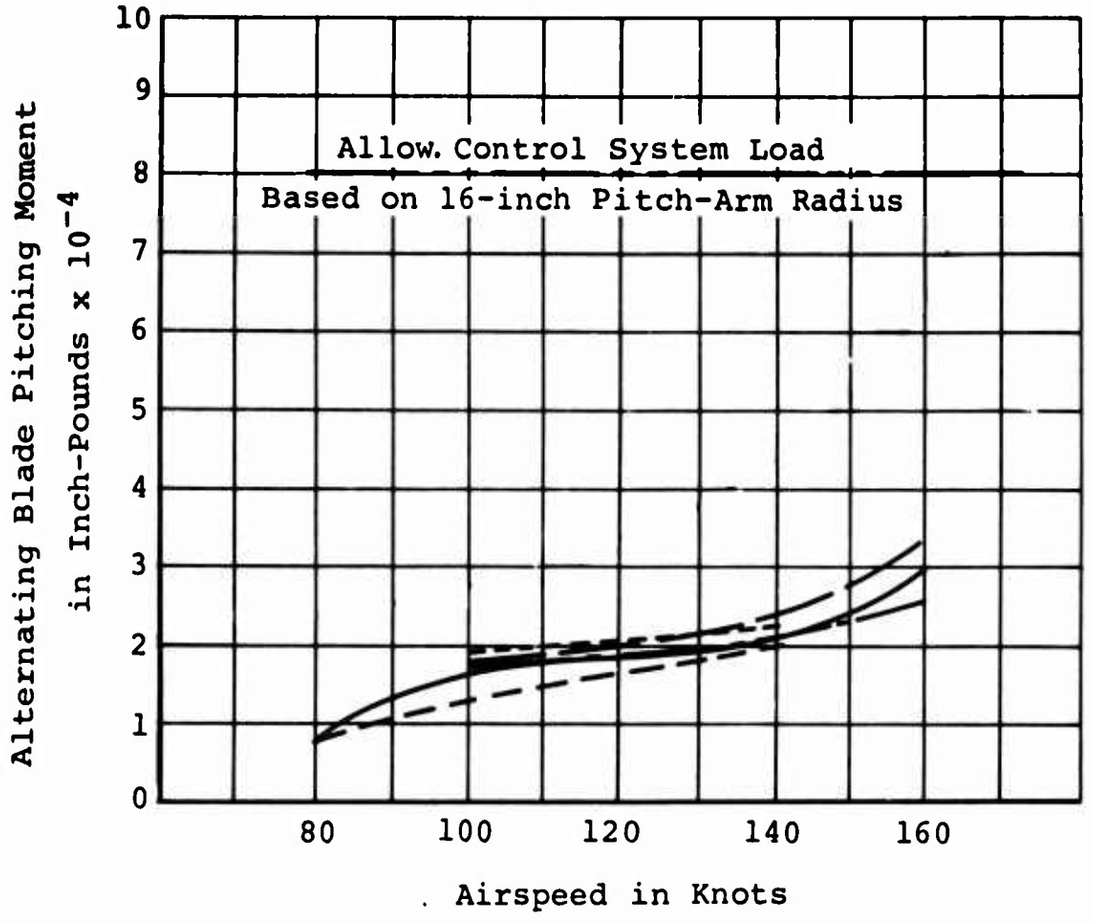

Values Predicted by Leone-Myklestad Method:

----- Low-stiffness metal blade for transport; θ_t = -12 degrees

– – – High-stiffness metal blade for transport; θ_t = -12 degrees

—·— Plastic blade for transport; θ_t = -12 degrees

——— Plastic blade for crane/personnel carrier; θ_t = -12 degrees

— — Plastic blade for crane/personnel carrier; θ_t = -6 degrees

Figure 86. Blade Pitching Moments Versus Airspeed.

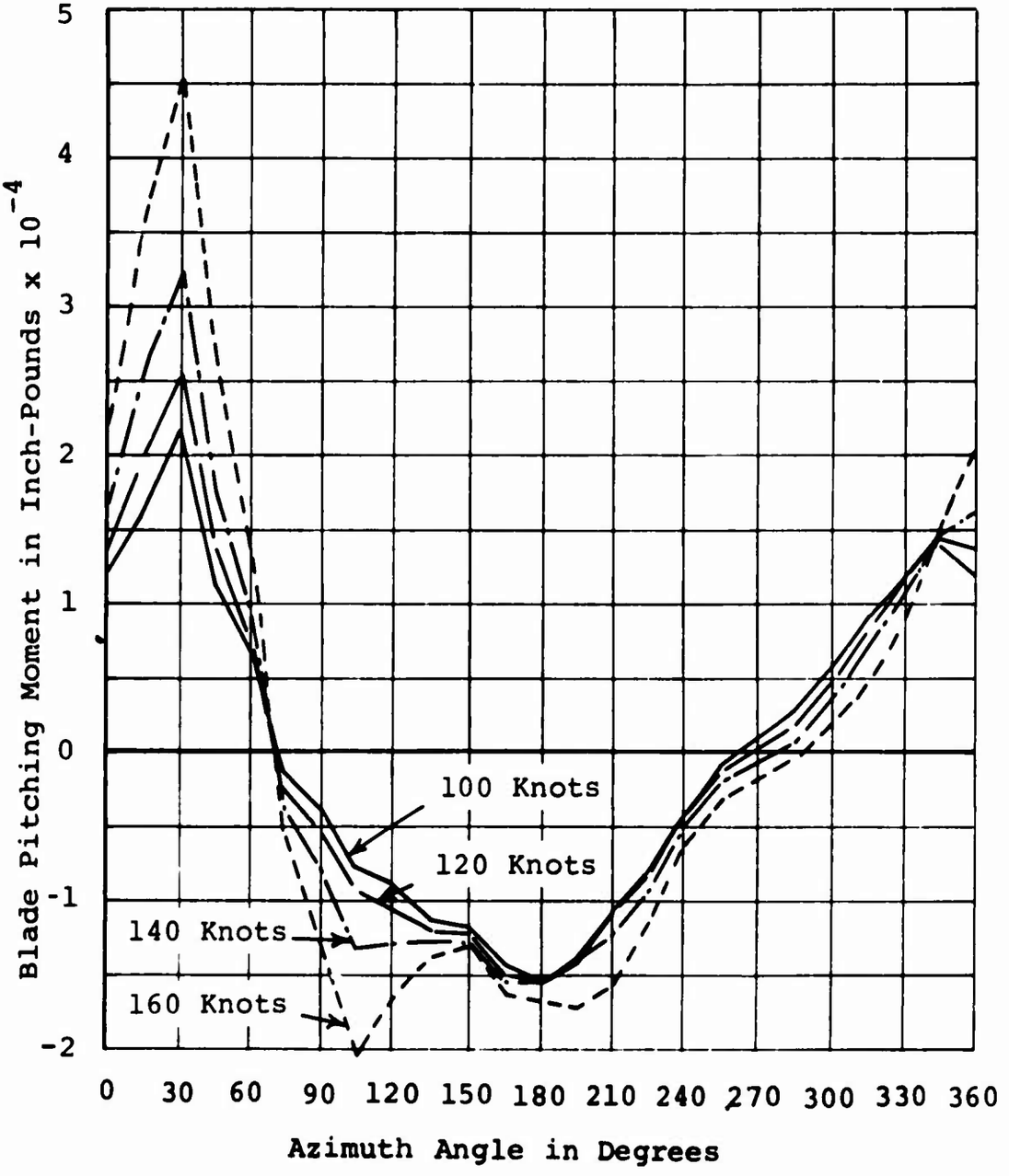

NOTES:
1. Crane
2. θt = -6 degrees

Figure 87. Blade Pitching Moments Versus Azimuth of Plastic Blade. (Sheet 1 of 3)

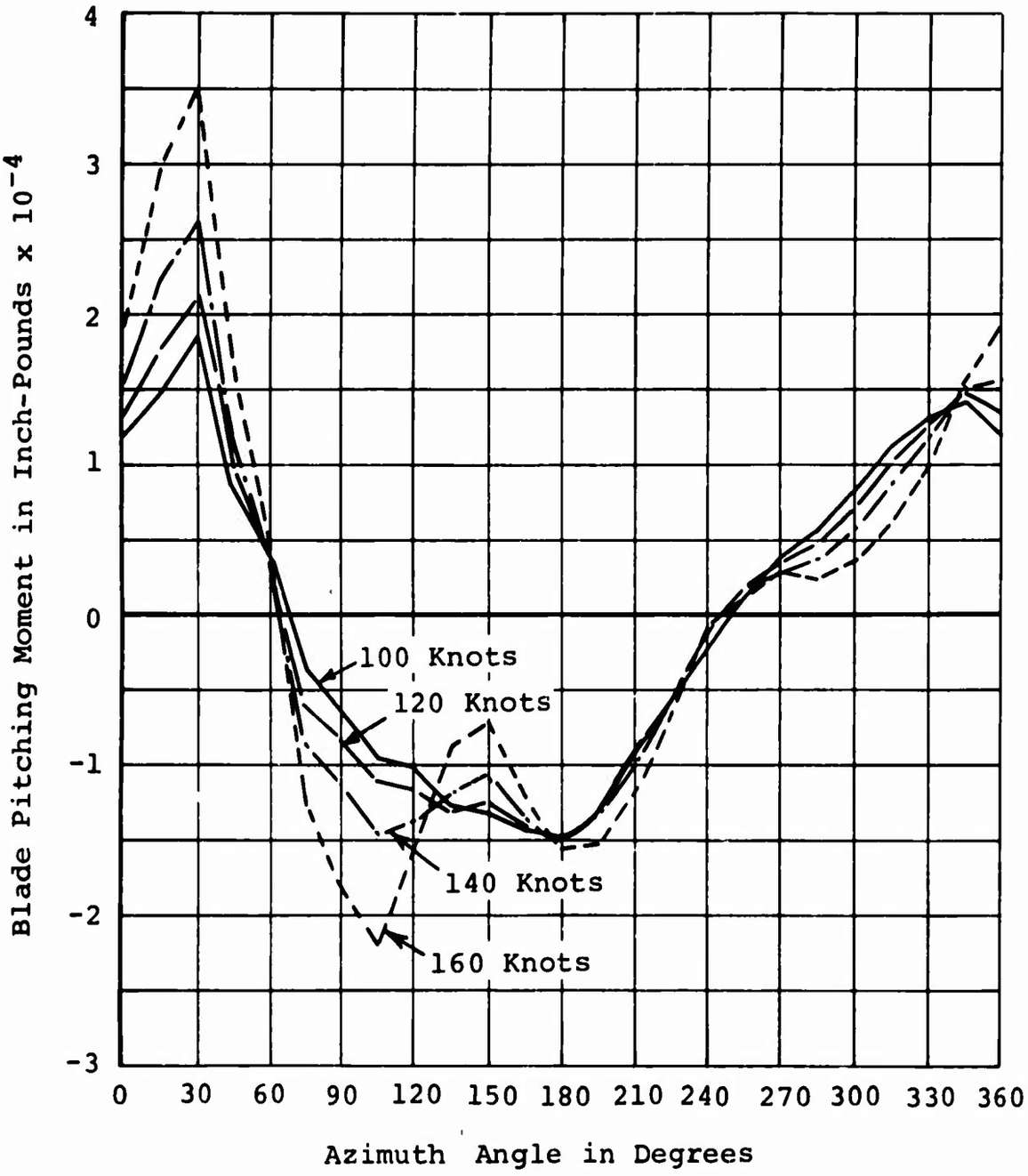

NOTES:
1. Crane
2. θ_t = -12 degrees

Figure 87. Blade Pitching Moments Versus Azimuth of Plastic Blade. (Sheet 2 of 3)

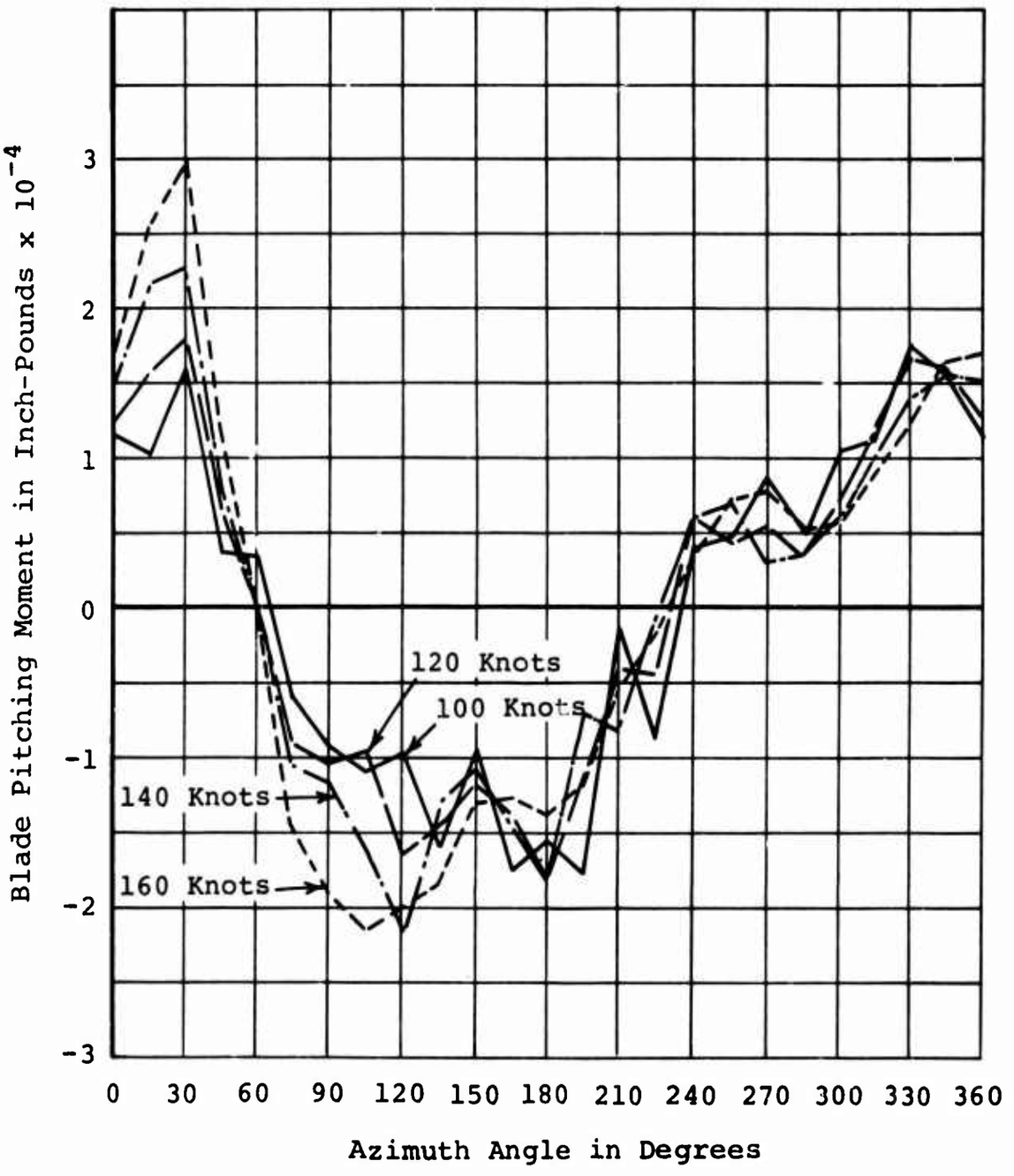

NOTES:
1. Transport
2. θ_t = -12 degrees

Figure 87. Blade Pitching Moments Versus Azimuth of Plastic Blade. (Sheet 3 of 3)

HIGH-STIFFNESS BLADES

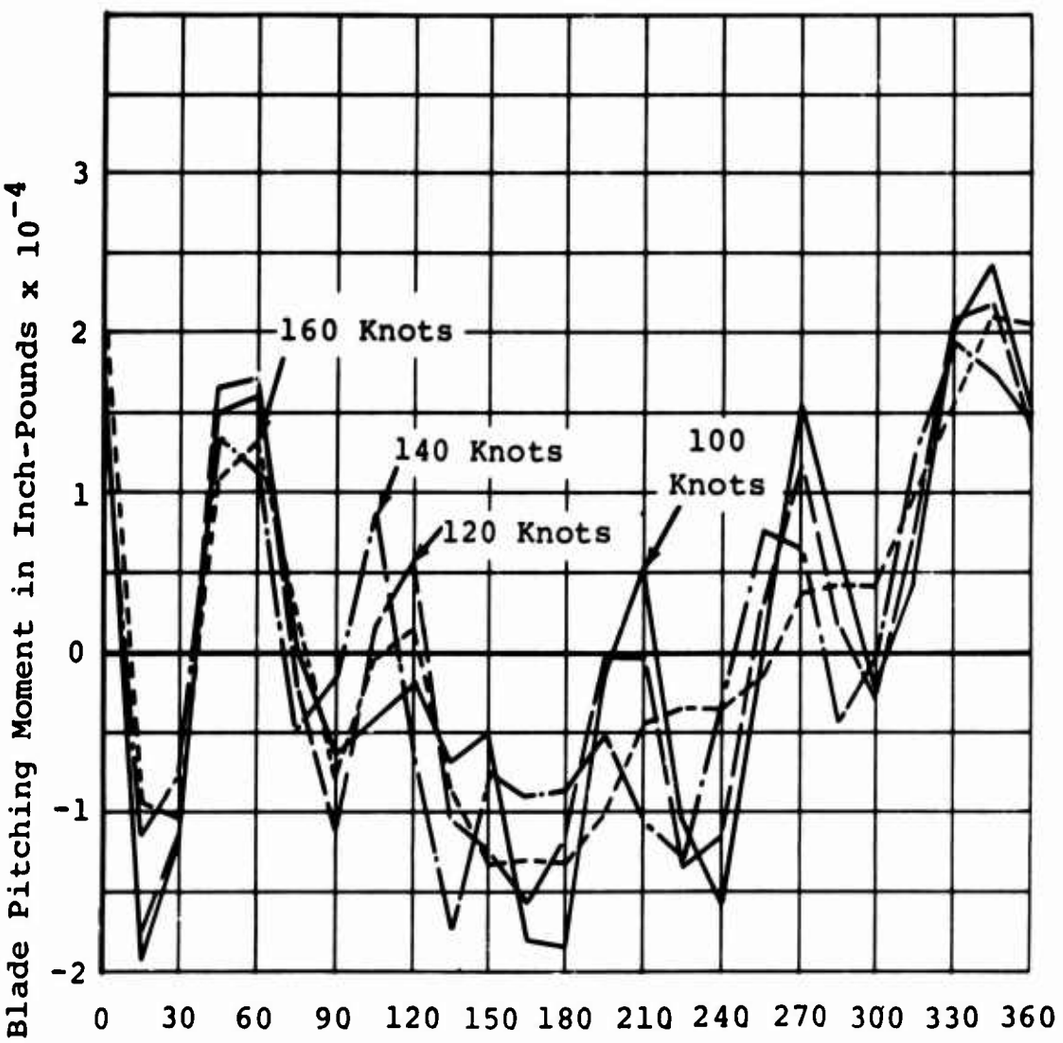

NOTES:
1. Transport
2. θ_t = -12 degrees

Figure 88. Blade Pitching Moments Versus Azimuth of Metal Blade. (Sheet 1 of 2)

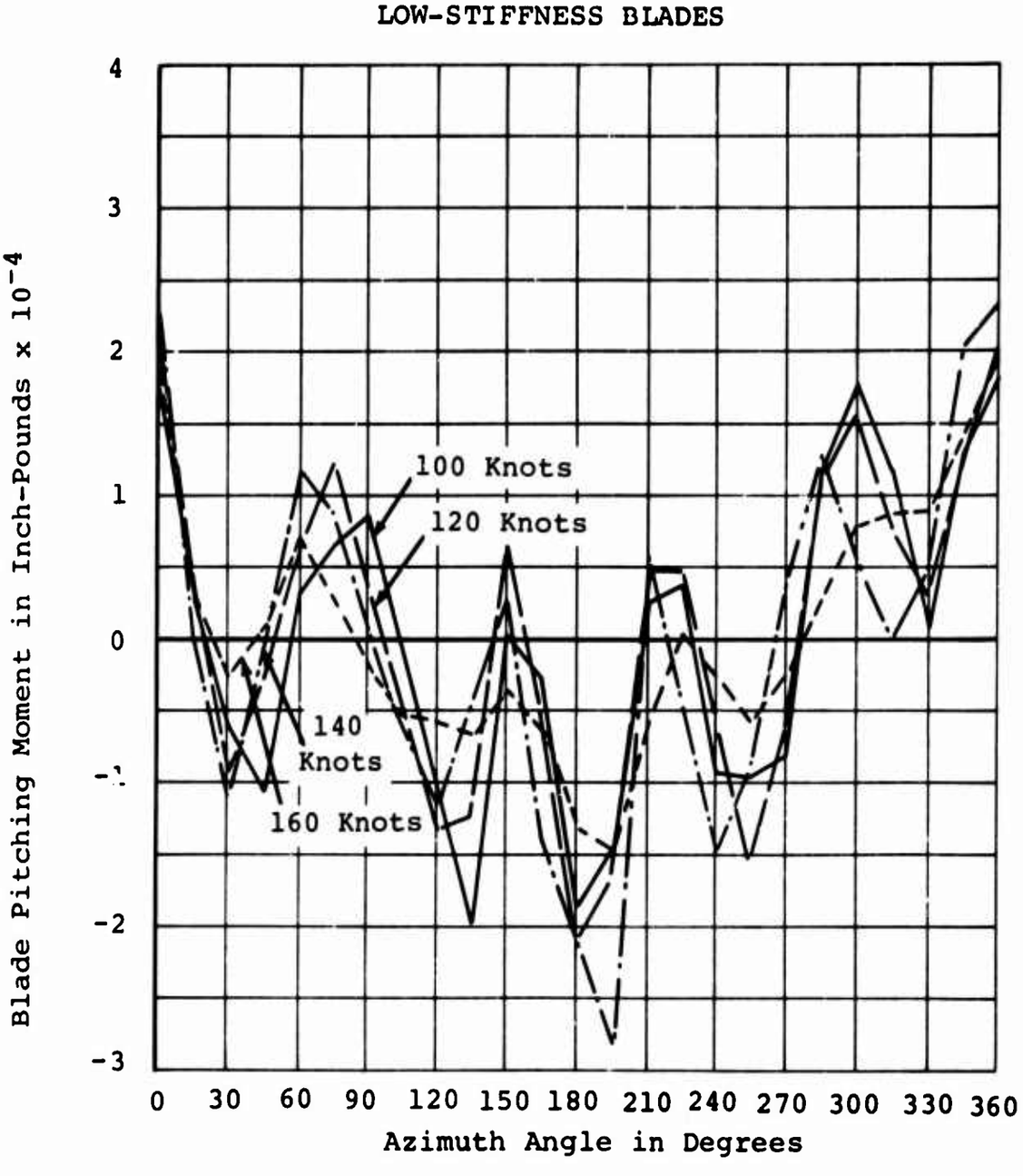

NOTES:
1. Transport
2. θ_t = -12 degrees

Figure 88. Blade Pitching Moments Versus Azimuth of Metal Blade. (Sheet 2 of 2)

TABLE XXI
BEARING LOADS AND B_{10} LIFE OF SWASHPLATE BEARINGS

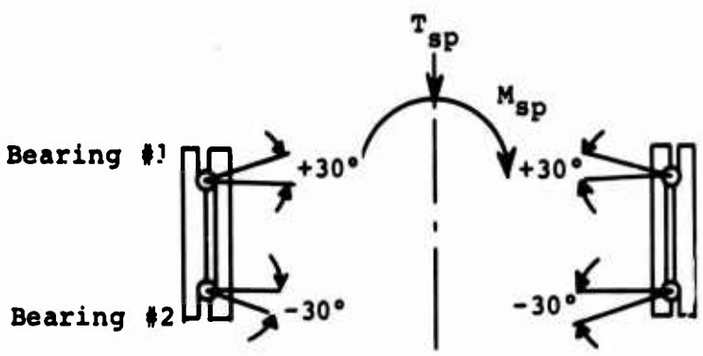

Balls per row = 139
Pitch diameter = 42.5 inches
Contact Angle = ±30°
Race curvature = 52 inches
Ball diameter = 0.6875 inch
M_{sp} = Moment, swashplate
R_{pa} = Radius, pitch arm = 16 inches
M = Pitch moment, rotor blade
P = Pitch-link load
R_{sp} = swashplate arm radius, 27.94 inches
T_{sp} = Thrust, swashplate

alt = alternating
s = steady

$$P_{alt \text{ or } s} = \frac{M}{R_{pa}}$$

$$M_{sp} = \left(\frac{3}{2}\right)\left(P_{alt}\right)\left(R_{sp}\right)$$

$$T_{sp} = 3P_s = (3)\ (0.75)P_{alt}$$

$$2.25\ P_{alt}$$

Flight Condition	% Life	P_{alt} lb	P_s lb	T_{sp} lb	MAX M_{sp} inch-lb	M inch-lb
High-Speed Level Flight	11	±5,000	3,760	11,300	2.1×10^5	80,000
Max. Power Climb	8	±4,600	3,460	10,400	1.93×10^5	73,500
Cruise	54	±3,900	2,940	8,800	1.64×10^5	62,500
Transition	11	±1,170	880	2,640	$.49 \times 10^5$	18,700
Hover	10	±1,170	880	2,640	$.49 \times 10^5$	18,700
Auto-Rot.	6	±1,420	1,070	3,220	$.597 \times 10^5$	22,600

B_{10} Life: Bearing Number 1 5650 hours
Bearing Number 2 2646 hours

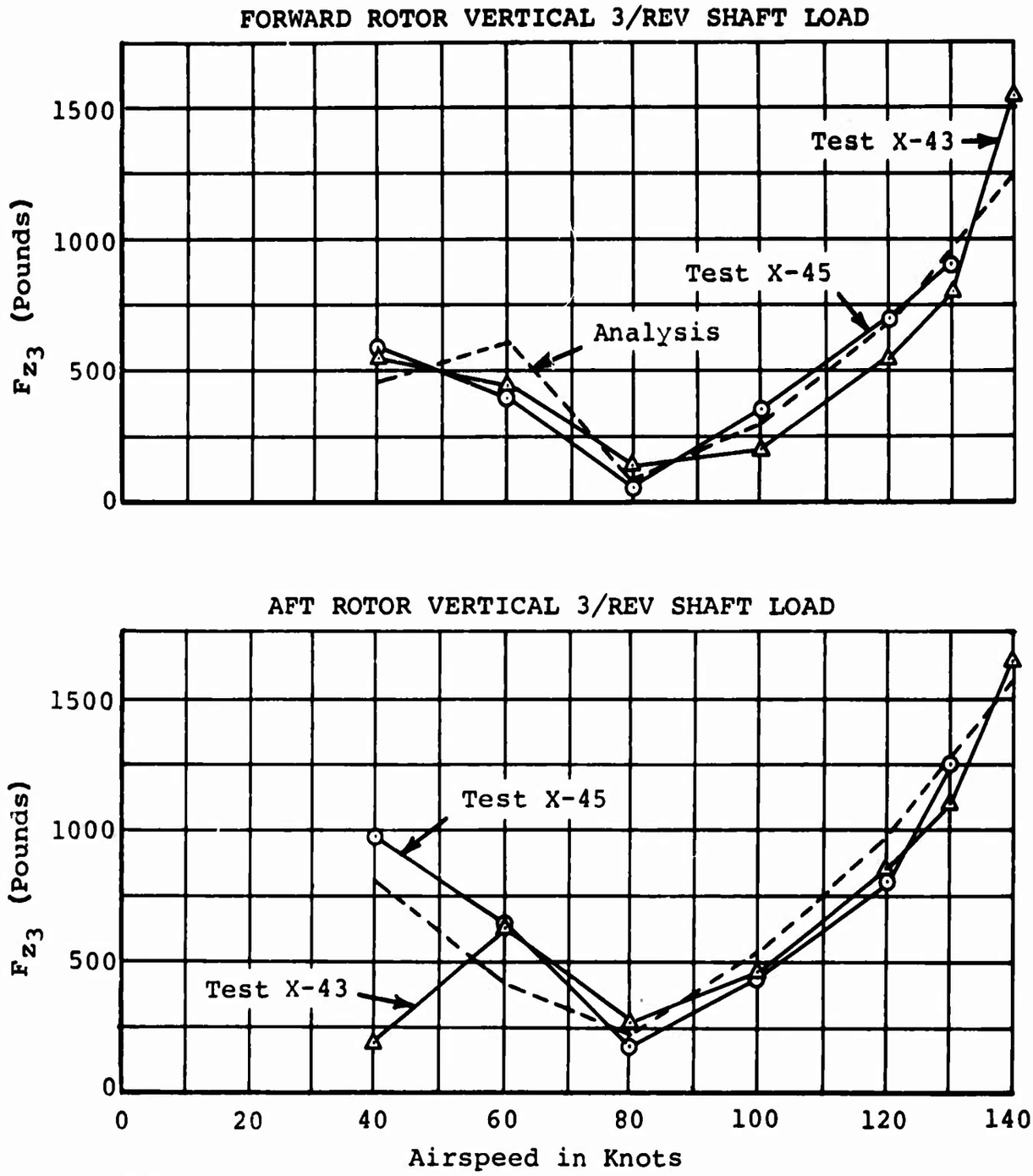

NOTES:

1. Test data from advanced vibration development (AVID) flights X-43 and X-45
2. Analysis from rotor analysis program
3. Gross weight 19,500 pounds
4. Altitude 2000 feet

Figure 89. Hub Shaking Force: Correlation of Tests and Analysis.

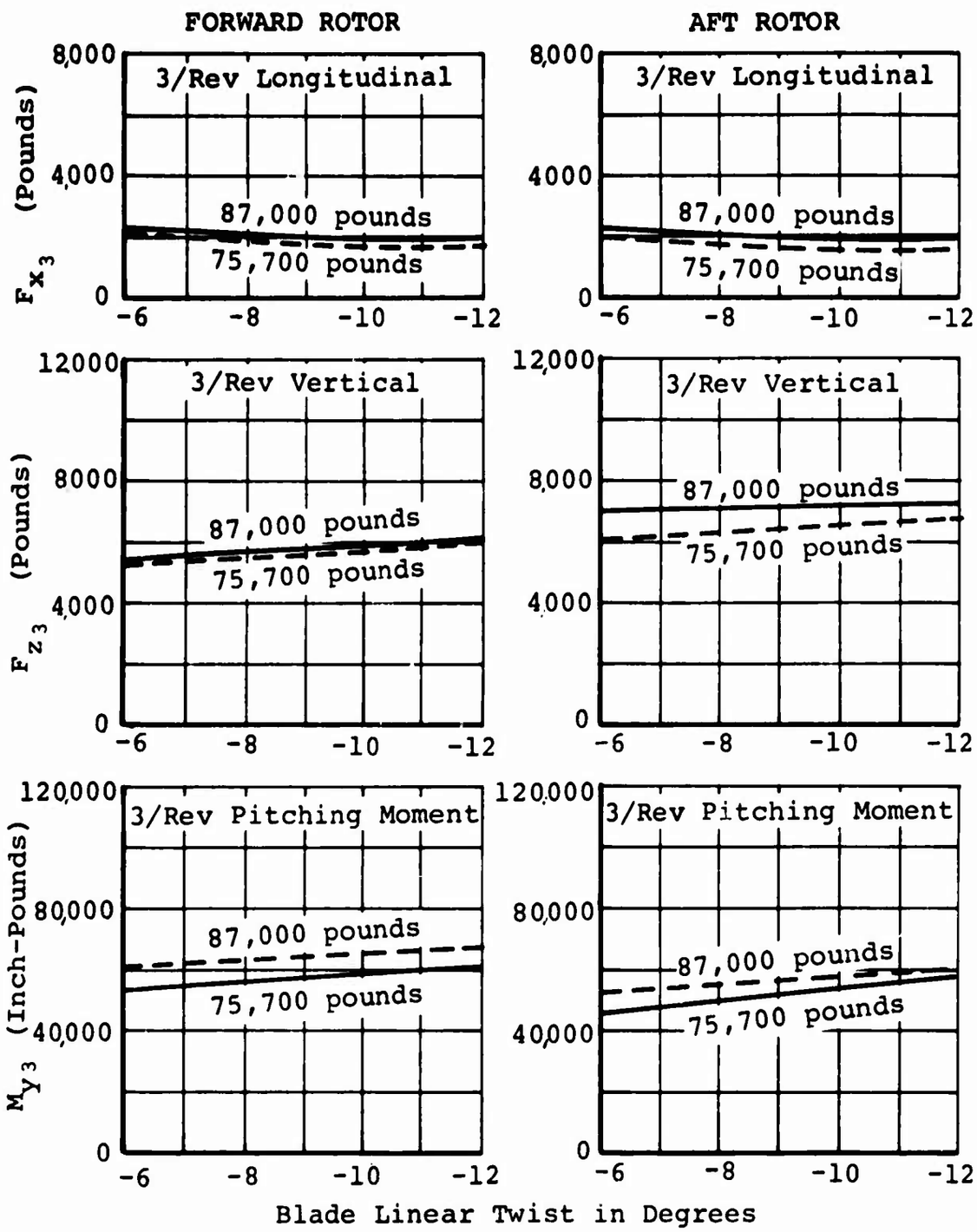

NOTES:

1. Three-bladed rotor
2. Blade radius = 43 feet
3. Chord = 42 inches
4. Rotor speed = 155 rpm
5. Tip speed = 700 feet per second
6. ____ V = 165 knots, gross weight = 87,000 pounds, sea level
   ---- V = 170 knots, gross weight = 75,700 pounds, 5000 feet

Figure 90. Effect of Twist on Hub Shaking Forces.

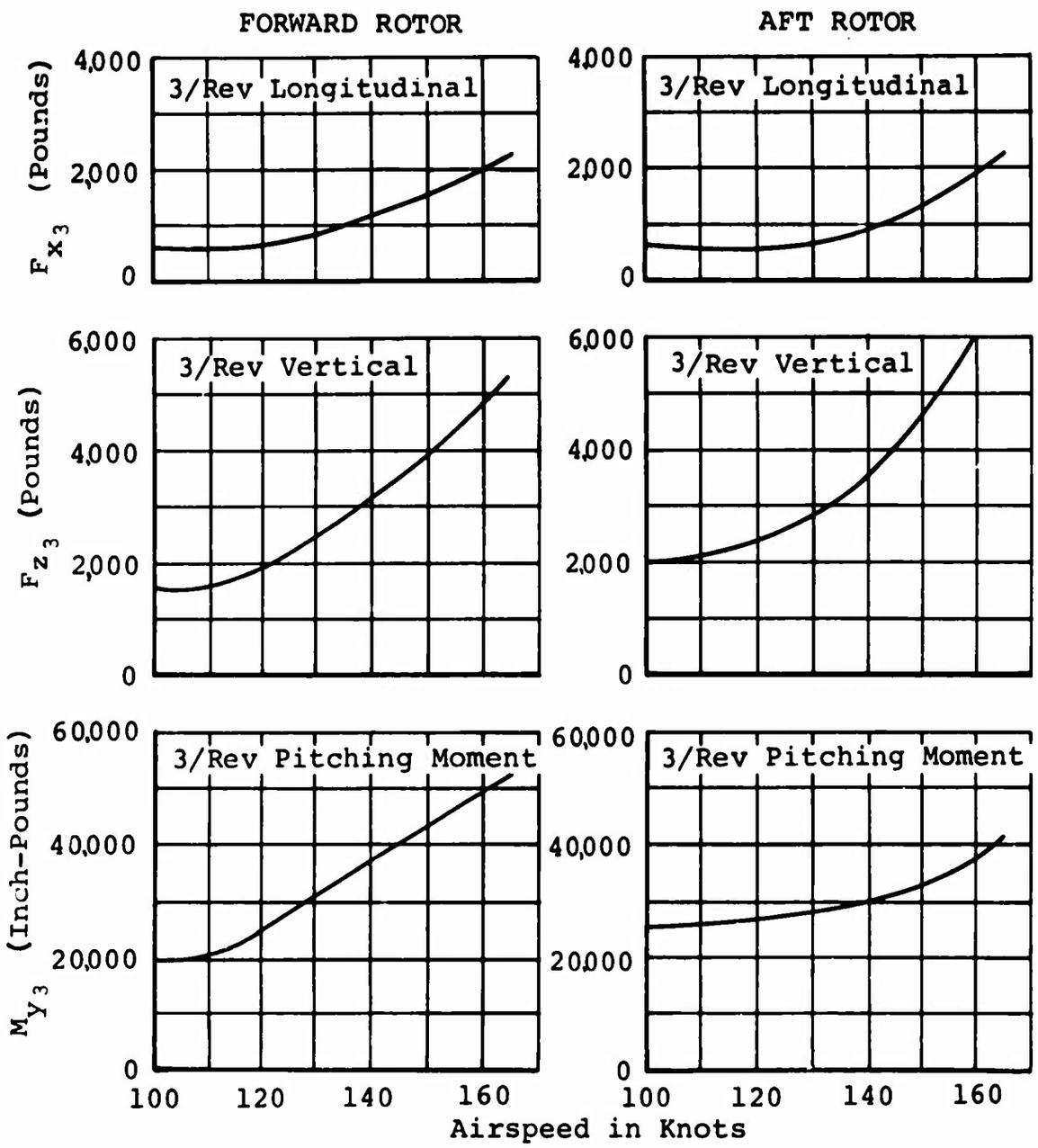

NOTES:
1. Gross weight = 87,000 pounds
2. Sea level standard day
3. Three-bladed rotor
4. Blade radius = 43 feet
5. Chord = 42 inches
6. Blade linear twist=-6 degrees
7. Rotor speed = 155 rpm
8. Tip speed = 700 feet per second

Figure 91. Effect of Airspeed on Rotor Forces.

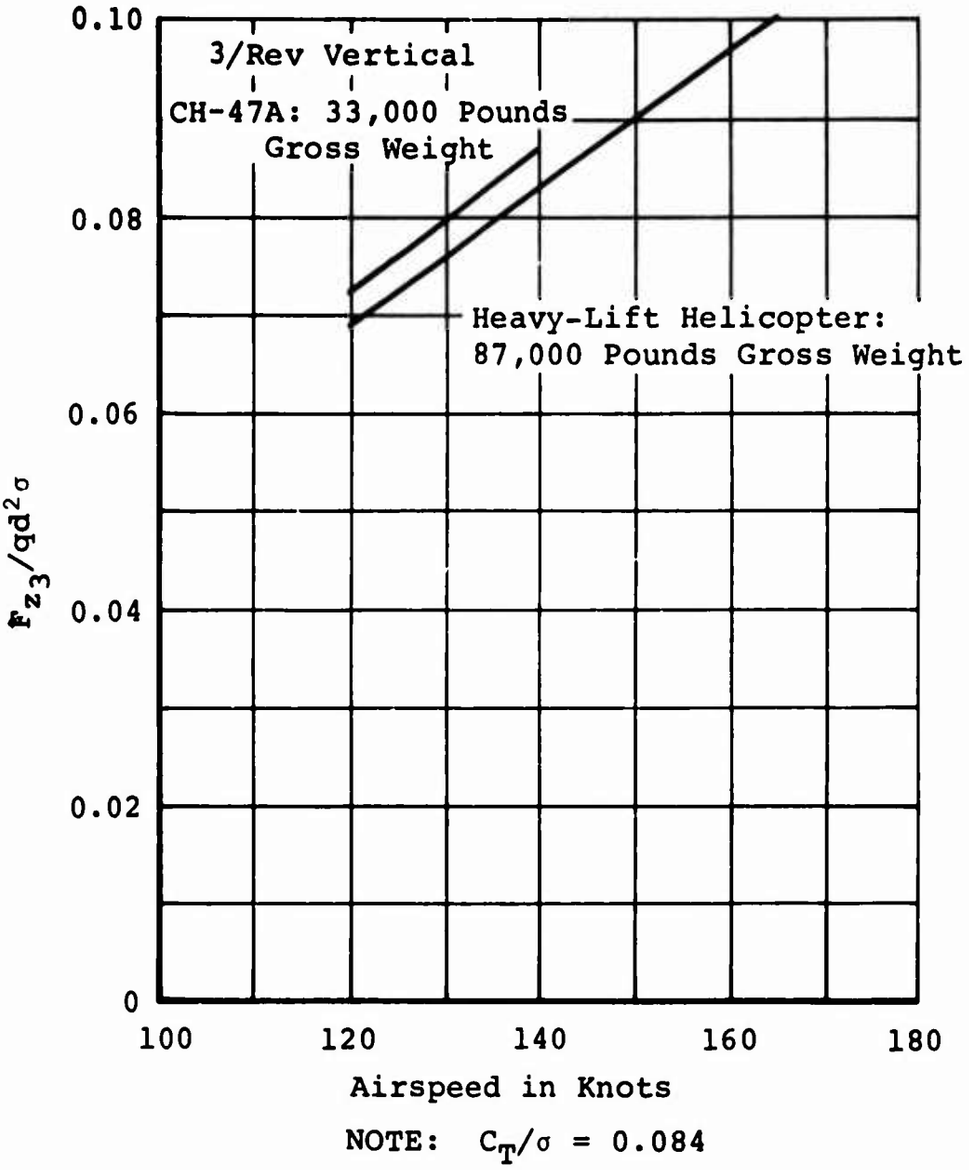

Figure 92. Nondimensional Shaking Forces.

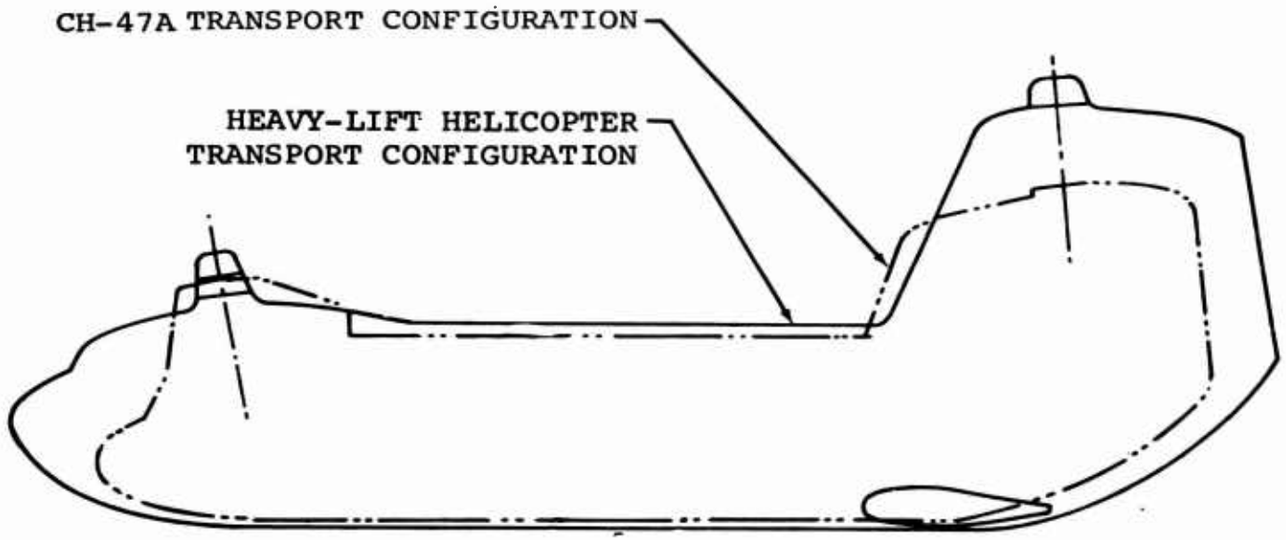

Figure 93. Geometric Similarities Between Heavy-Lift Helicopter and CH-47A.

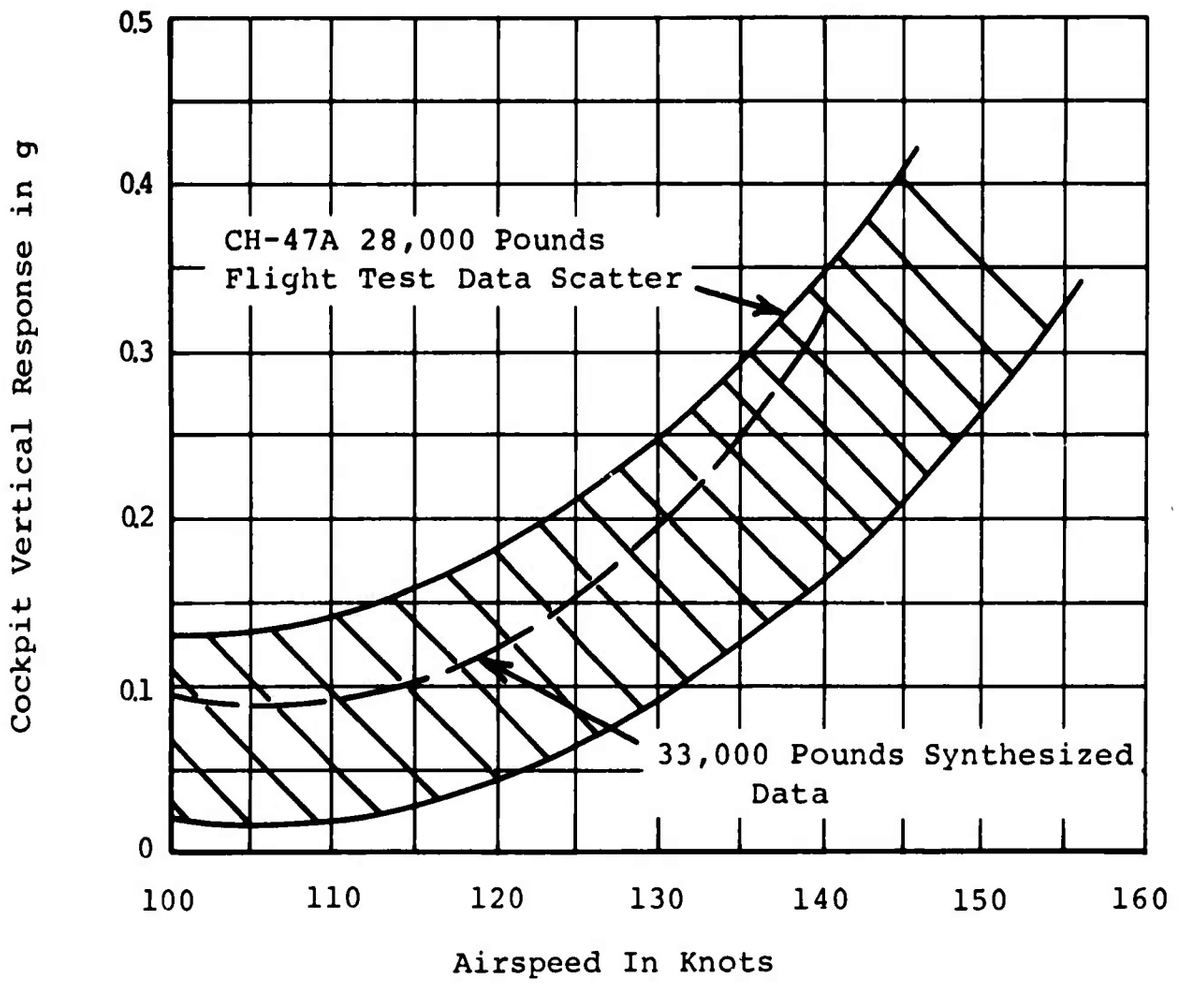

Figure 94. Vibration Level: Correlation of Tests and Analysis.

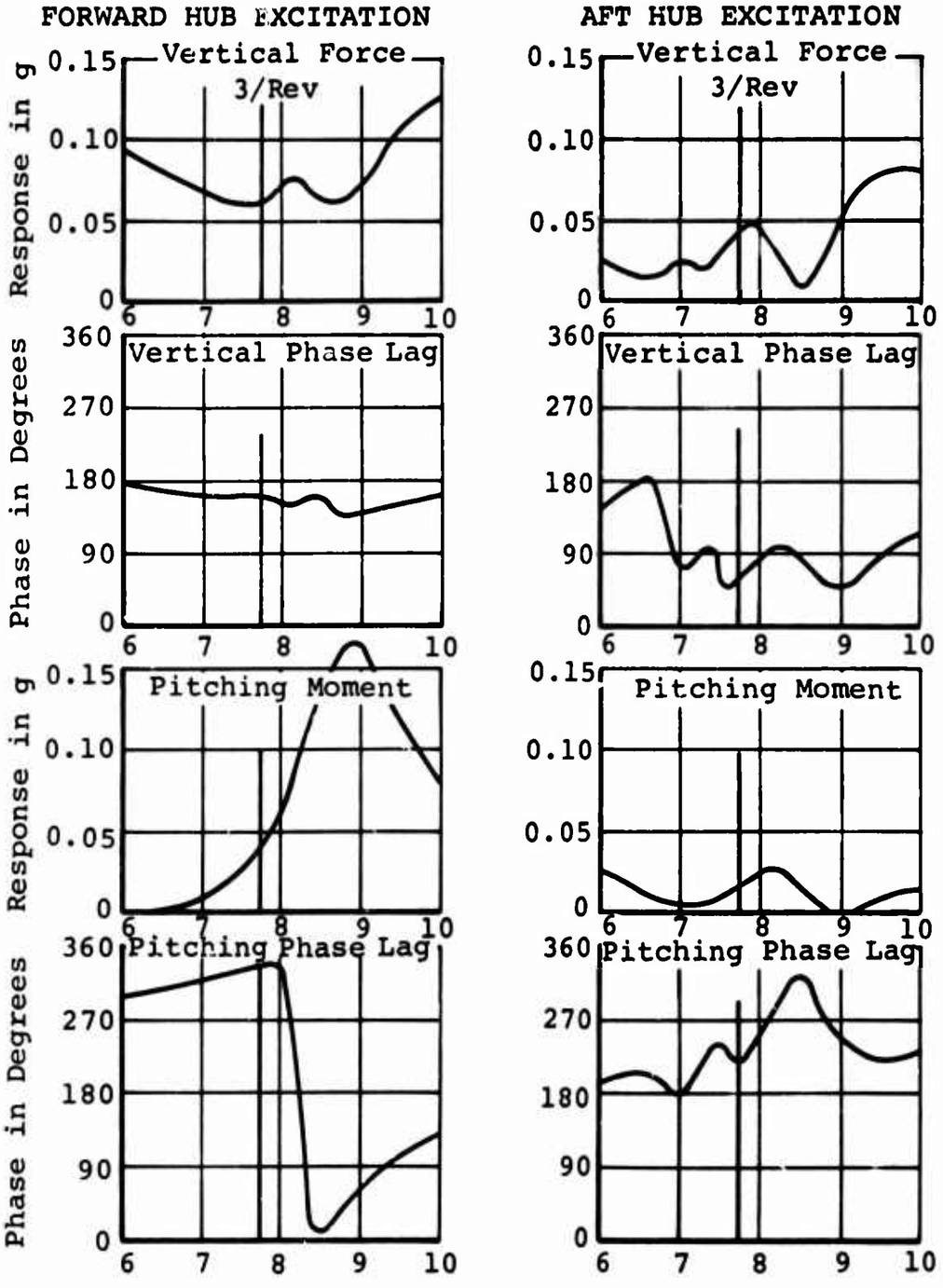

NOTES:

1. Gross weight 87,000 pounds
2. Based on CH-47A measured response data

Figure 95. Fuselage Response to Rotor Forces.

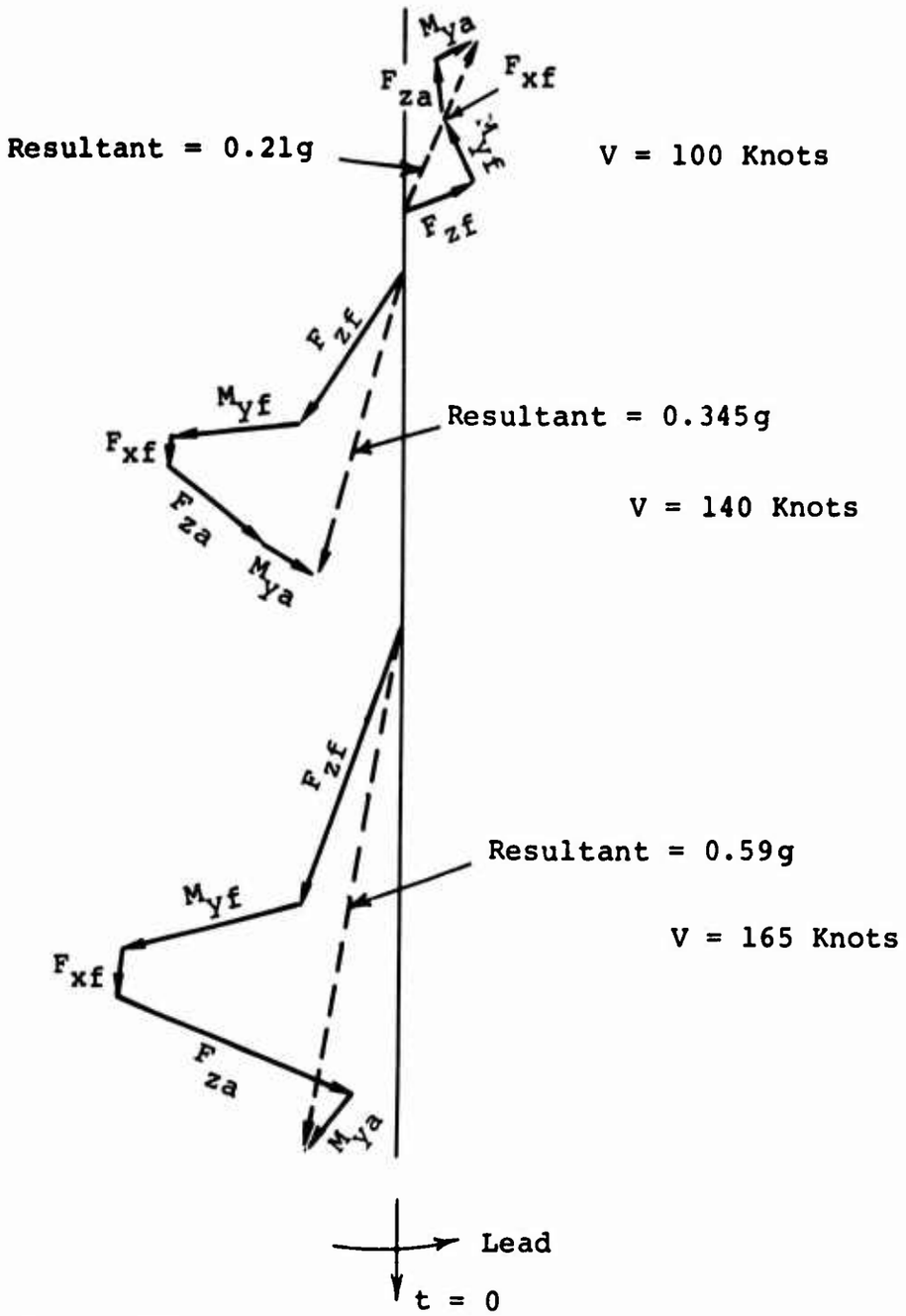

NOTES:

1. Gross weight = 87,000 pounds
2. Sea level standard day
3. Three-bladed rotor
4. Blade radius = 43 feet
5. Chord = 42 inches
6. Blade linear twist = -6 degrees
7. Rotor speed = 155.5 rpm
8. Tip speed = 700 feet per second
9. Airspeed noted
10. Response:
    - F_{zf} = forward vertical force
    - M_{xf} = forward pitching moment
    - F_{xf} = forward longitudinal force
    - F_{za} = aft vertical force
    - M_{ya} = aft pitching moment

Figure 96. Synthesized Cockpit Vibration Level.

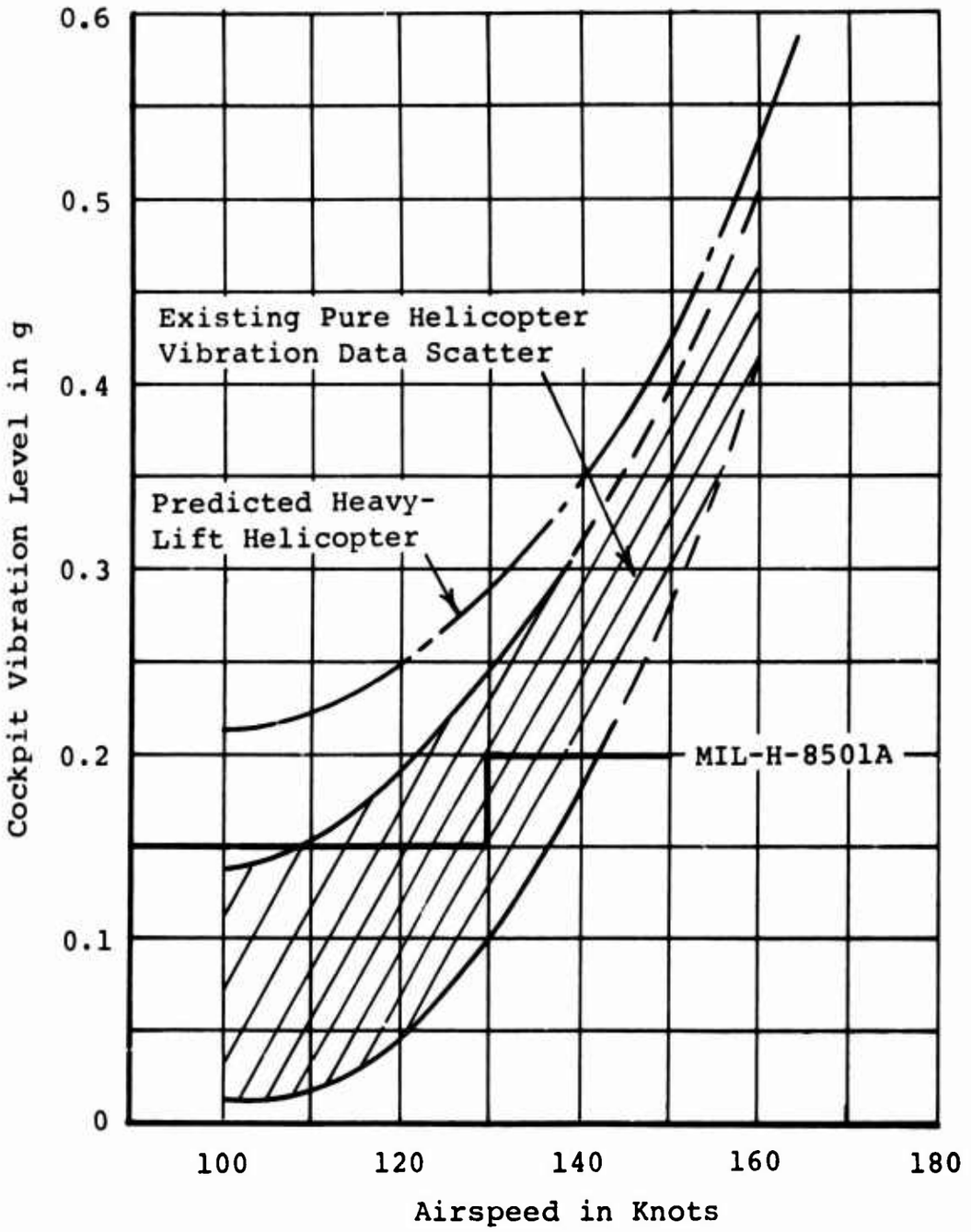

Figure 97. Predicted Cockpit Vibration Level Without Antivibration Devices.

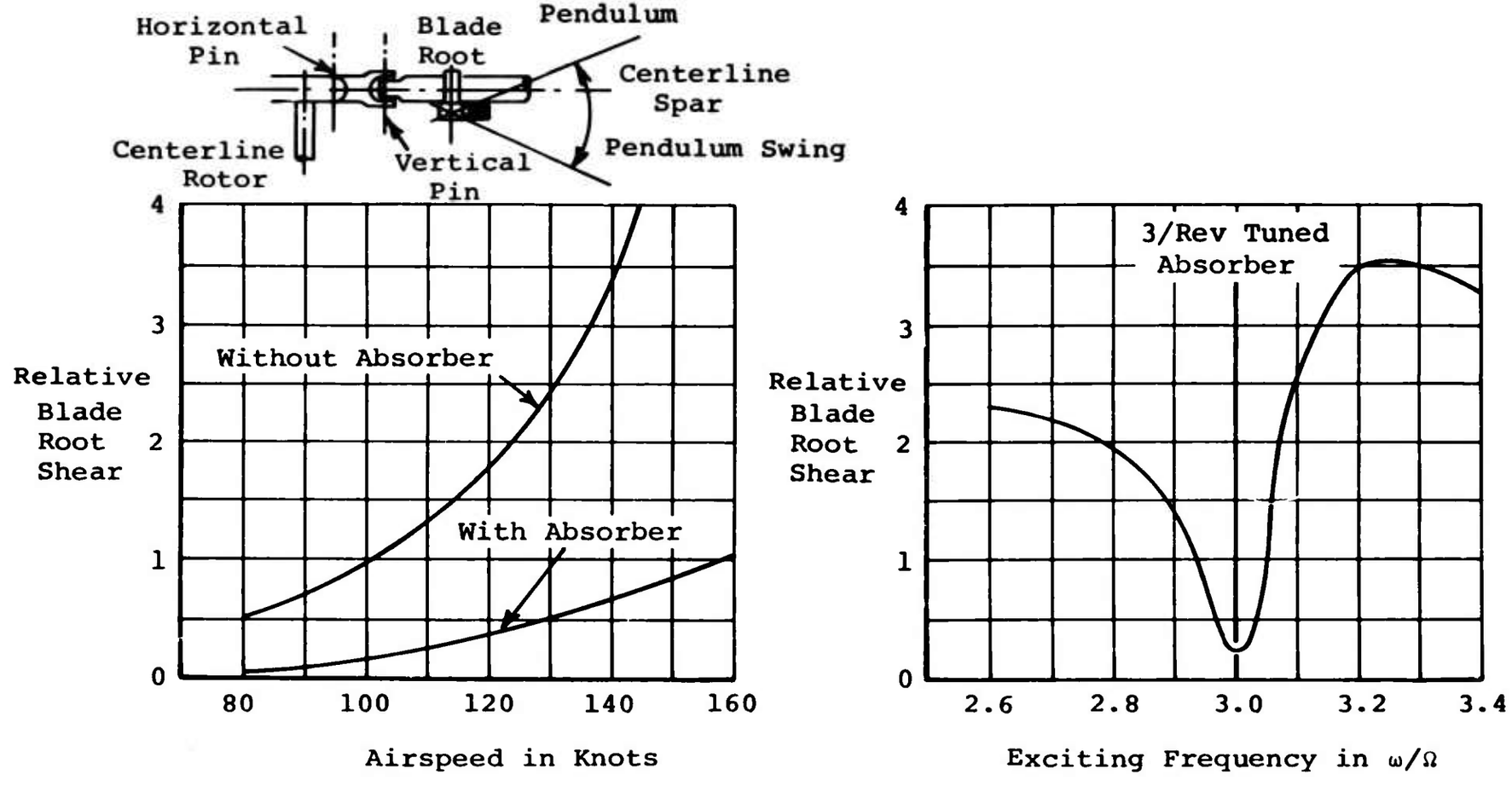

Figure 98. Blade Pendulum Absorber.

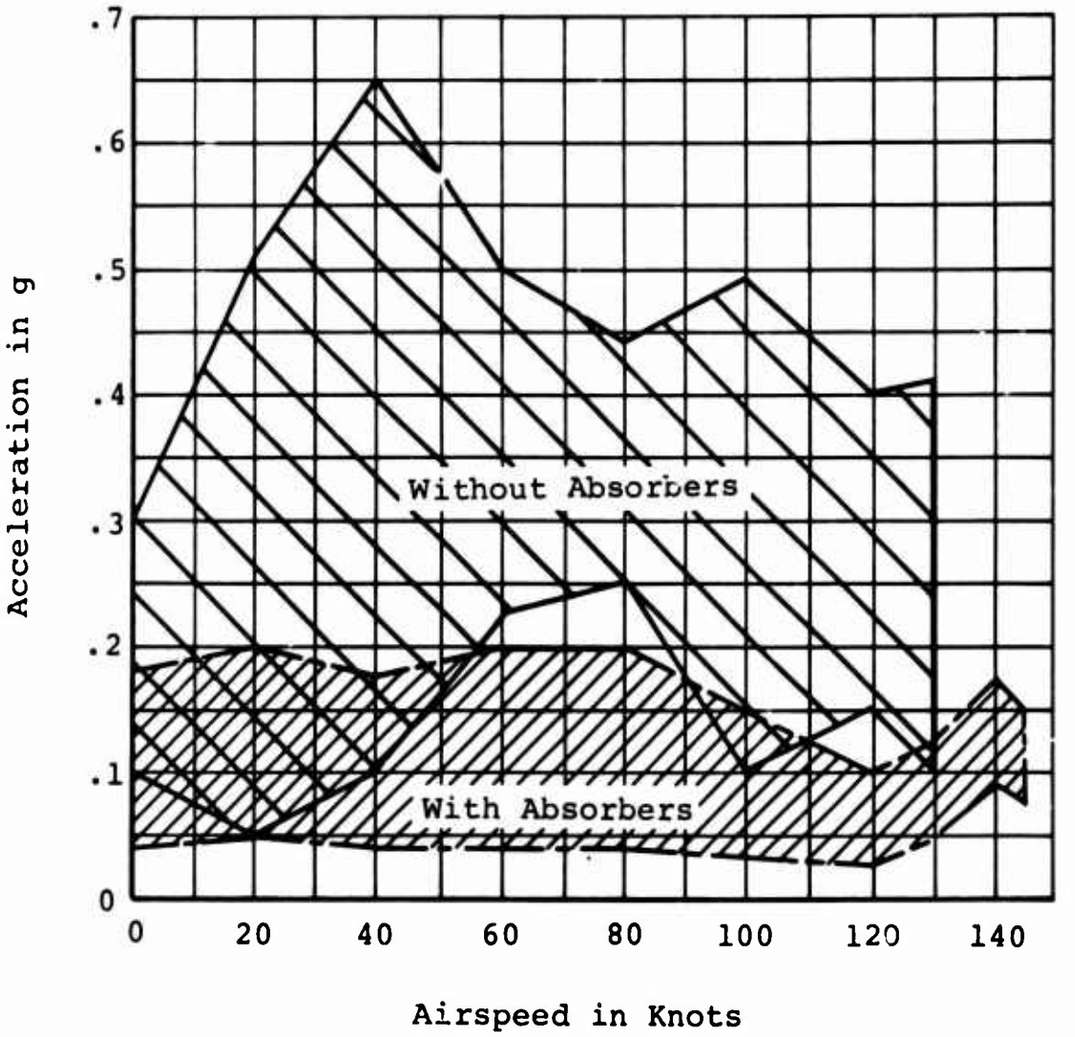

NOTE: CH-46A Flight vibration data cockpit 3Ω vertical

Figure 99. Cockpit Absorbers.

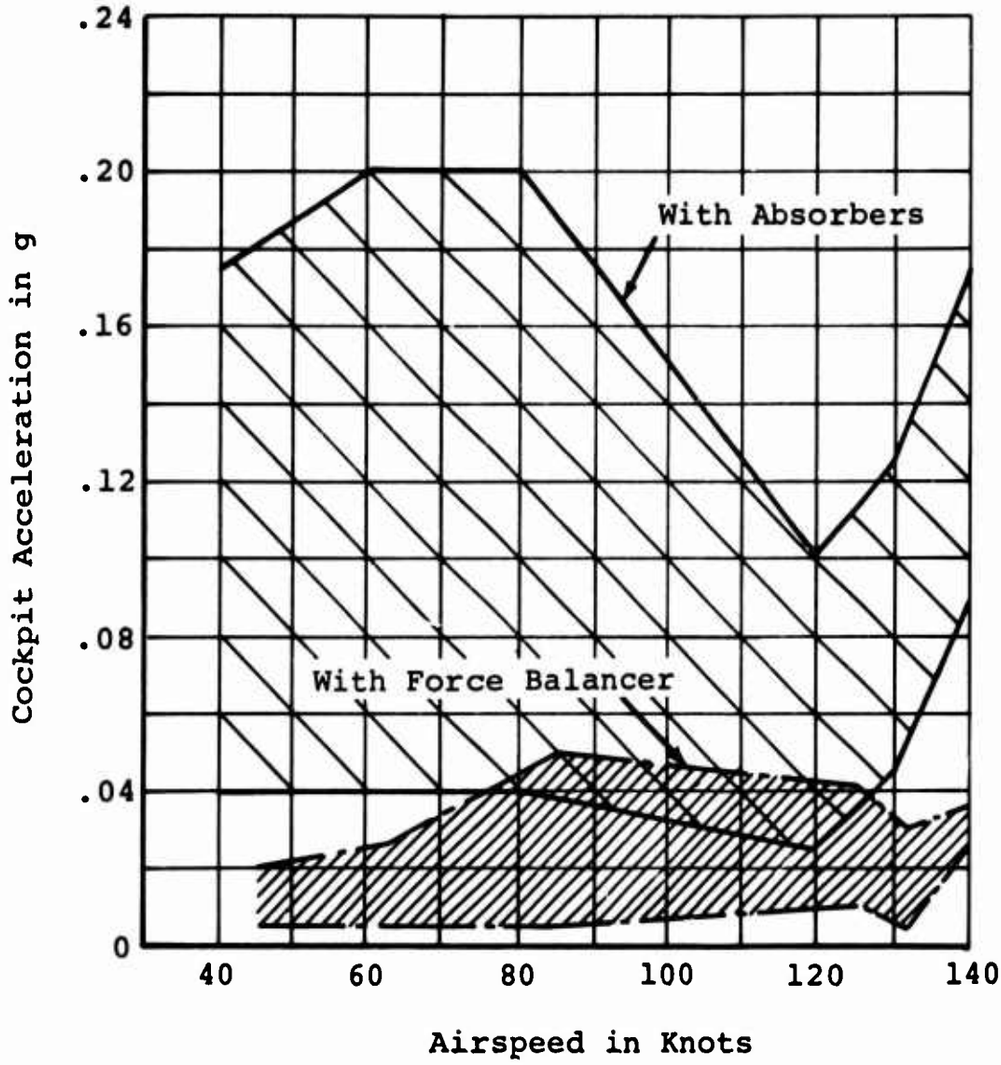

NOTE:
CH-46A flight vibration data cockpit
3/rev vertical

Figure 100. Force Balancer.

STATIC AND DYNAMIC STRUCTURAL ANALYSIS OF THE HINGELESS SEMIRIGID ROTOR

BACKGROUND

The resurgence of interest in the hingeless rotor has prompted its reevaluation as potential design for the heavy-lift helicopter. The proponents of the hingeless rotor have generally been manufacturers of single-lift/antitorque rotor helicopters, for whom the concept offers additional agility for in-flight maneuvers. It is questionable whether a tandem-lift rotor helicopter could make use of this attractive feature without incurring side effects which would offset the gains. For these reasons, a parametric study was developed to evaluate the hingeless rotor concept for use in a tandem-lift rotor system.

This study of the hingeless semirigid rotor system is limited to an exploratory parametric analysis. Although the study does not represent an optimized rotor, it does indicate the areas of risk, the possible weight increment, and areas worthy of further study. The weight penalty for a semirigid rotor in the tandem-lift rotor system is detailed in the WEIGHTS section. The weight differences between hingeless and articulated rotors with steel and titanium components can be summarized as follows:

	Articulated (lb)	Hingeless (lb)
Three rotor blades		
Steel	2396	3355
Titanium	2364	3315
Hub, hinge, and retention (total)		
Steel	2041	1705
Titanium	1529	1280
Each rotor		
Steel	4437	5060
Titanium	3893	4595
Two rotors		
Steel	8874	10120
Titaniur	7786	9190

Difference per aircraft for hingeless

Steel	+1246
Titanium	+1404

The parametric study was oriented toward establishing the boundaries which define the acceptable blade design. The boundaries investigated were those associated with the physical limitations and control power requirements of the heavy-lift helicopter.

The initial issue at hand in the study of the hingeless rotor is to demonstrate the capability for arriving at a practical blade design for a high gross weight helicopter. It was anticipated that a blade which could support the loads imposed by the gross weights involved, and simultaneously meet a minimum vibratory stress requirement, would not be competitive in weight with an articulated blade. Indeed, a further question arose of whether the so-called conventional blade or the matched-stiffness blade would be the better configuration. The trade between the two is essentially the decrease in the matched-stiffness blade's chordwise bending loads which is associated with the decoupling of the flapwise and chordwise mass-stiffness properties (Reference 11). It was therefore decided to study both types of blades to determine areas where design solutions might be evident.

If it is assumed that design solutions with sufficient strength and rigidity can be found, the question arises whether the blades will provide rotor force output characteristics which will meet control requirements of the tandem-lift rotor helicopter. It was evident from consideration of control power requirements that the lateral force vectors needed to produce yaw control would be a major concern. The added flapping restraint of the hingeless rotor was assumed to decrease lateral force output at a constant cyclic input, and subjected the structural system to greater self-equilibrating scalar moments normal to the roll axis than would have been experienced in the articulated system. It appeared that as a result of the increased moments, the hingeless rotor would not be competitive with the articulated system in tandem configurations.

The final question is, given a set of blades which meets these design requirements, whether these blades will satisfy minimum requirements for static deflection. The basic concern was static clearance between a very flexible blade and the airframe.

Although the hingeless rotor study will be limited in depth and will not attempt to represent an optimized rotor, it must examine a broad range of variables in order to identify the design solutions. Although this approach differs significantly from that used for the articulated rotor study (which assumed the articulated solution and concentrated on load acquisition and design refinement), the same analytical method was used for both, with the additional constraint imposed by locking out the flapping and lagging pins for the hingeless rotor study.

Two blades were studied: the D-spar metal blade and the matched-stiffness metal blade. Tip weights were used to meet the same coning angle criteria as the articulated rotor. To compare semirigid and articulated rotors more thoroughly, dynamic similarity should be maintained, but this was outside the scope of this study.

The following investigations would be required in a detailed study for optimization, but were excluded from the scope of this study:

1. Optimizing the portion of the blade over which most of the flexure occurs to obtain the maximum lateral force output at the minimum hub overturning moment

2. Evaluation of the most promising design configurations

3. Study of matched-frequency hingeless blades where the chordwise frequency is established by air/ ground resonance requirements

4. The effect of preconing on lateral aerodynamic force output

5. Ways of minimizing the increase in the spanwise vibratory bending moments induced by maneuvering

6. Development of the physical properties to eliminate the tip weight, and construction of blades in all categories (conventional D-spar and matched-stiffness) to be dynamically similar over the range of inboard stiffnesses.

A review of bending moments versus the allowable moments shown in Figures 112, 113, 120, and 121 indicates that optimized blades can be made for the hingeless semirigid rotor with adequate margins for the heavy-lift helicopter. Detailed conclusions for applying the hingeless rotor to the tandem-lift helicopter, and the areas of risk, are given in the ROTOR SYSTEM PARAMETRIC ANALYSIS.

CONCLUSIONS

A hingeless rotor blade and hub assembly is a feasible concept for use on a high gross weight helicopter. Such a blade system should have the following design features:

1. Preconing to reduce steady bending stresses and to improve blade-to-fuselage clearance

2. Avoidance of the use of tip weights to optimize steady aerodynamic force output

A hingeless matched-stiffness rotor has the following merits relative to an articulated rotor:

1. Reduced steady chordwise bending moments

2. More control power for a given cyclic input

The same rotor has the following disabilities:

1. Increased flap vibratory moment sensitivity due to cyclic control input during maneuvers

2. High rotor hub overturning moments

3. Susceptibility to air-ground resonance problems which must be solved outside the rotor system

In the tandem-lift rotor helicopter, rotor moment is carried as an internal circuit load and does not produce useful external forces on the helicopter, except in the roll mode. As an example, the tandem rotor helicopter normally derives its yaw control from differential lateral thrust output (see Figure 101), which relies on the magnitude of the rotor force output. Furthermore, the yaw force schematic (Figure 101) shows the typical load vector situation in which the hub moments and forces are self-equilibrating. Here, the hub moment load

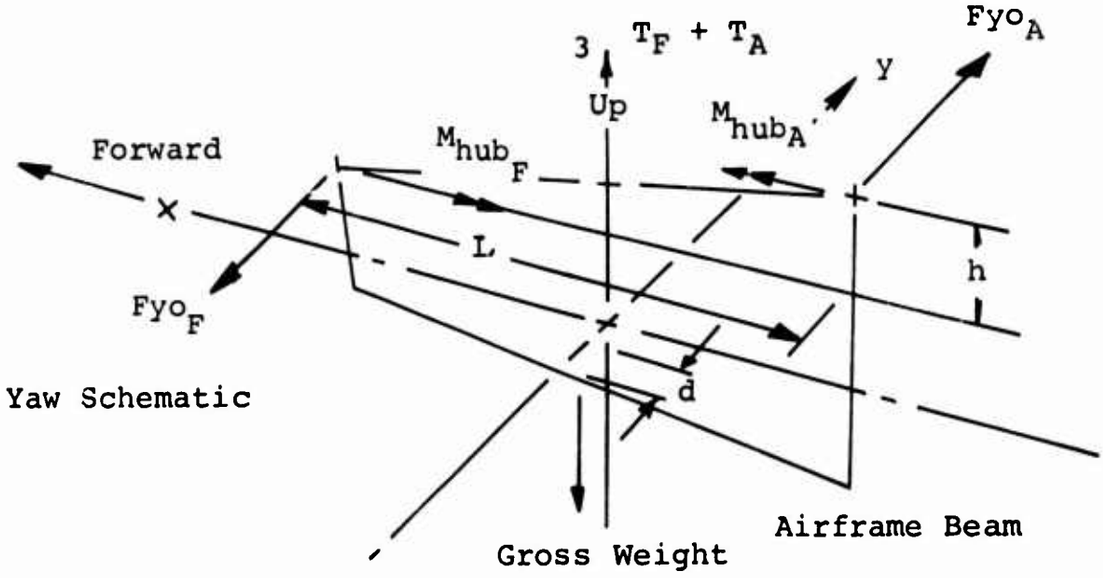

Yaw Moment = F_{y_o} x L

Roll Moment = F_{y_o} x (h) - GW x (d) - M_{hub_F} + M_{hub_A} = 0

Pitch Moment = 0

$\xi F_x = \xi F_y = \xi F_z = 0$

Figure 101. Yaw Schematic.

path is through the hub into the rotor shaft, out of the rotor shaft through the rotor support bearings, and thence to the airframe beam. Therefore, the rotor shaft and bearings must be sized for fatigue loads (rotating beam loads) which do not add to the total system capability. These fatigue loads result in a weight penalty (Δ) (see Figure 102) which is calculated as follows:

1. Assume a rotor shaft which has been sized for articulated loads.

2. Let the couple distance (h) be defined by practical limits.

3. Let Ro/R be a constant for any R chosen. Calculate the delta weight of the rotor shaft:

$$\frac{M_1}{M_2} = \frac{C_2}{I_2} \times \frac{I_1}{C_1} = \left(\frac{R_1}{R_2}\right)^3 \tag{1}$$

where

$$\frac{Ro}{R} = k = \text{constant}$$

$$\frac{R_1}{R_2} = \left(\frac{M_1}{M_2}\right)^{1/3} \tag{2}$$

$$\rho A = \omega \text{lb/in} = \rho\pi(R^2 - Ro^2) = \rho\pi R^2 \left[1 - \left(\frac{Ro}{R}\right)^2\right] \tag{3}$$

$$\frac{\omega_1}{\omega_2} = \left(\frac{R_1}{R_2}\right)^2 = \left(\frac{M_1}{M_2}\right)^{2/3} \tag{4}$$

$$\%\Delta\omega_{T\,(\text{Shaft})} = \frac{\omega_2 - \omega_1}{\omega_1} \times 100 = \left[\frac{\omega_1 \left(\frac{M_2}{M_1}\right)^{2/3}}{\omega_1} - \omega_1\right] \times 100$$

$$= \left[\left(\frac{M_2}{M_1}\right)^{2/3} - 1\right] \; 100 \tag{5}$$

In addition to the normal maneuvers just discussed, there is a trim control consideration which is unique to the tandem-lift rotor helicopter. In forward flight, the rotor blades flap up in the leading portion of the rotor disk and down in the trailing portion, which limits the helicopter's forward speed at a given forward cyclic trim. Additional trim must

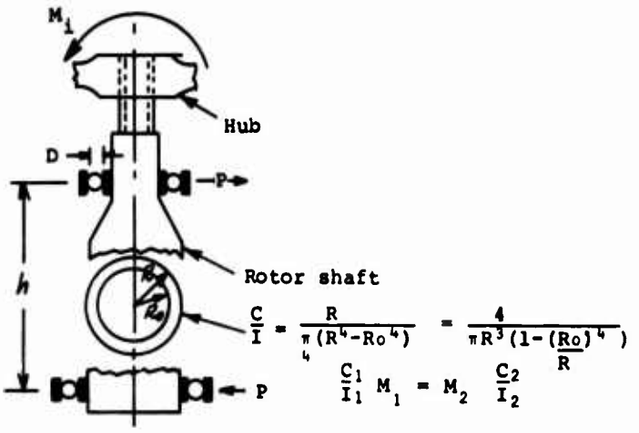

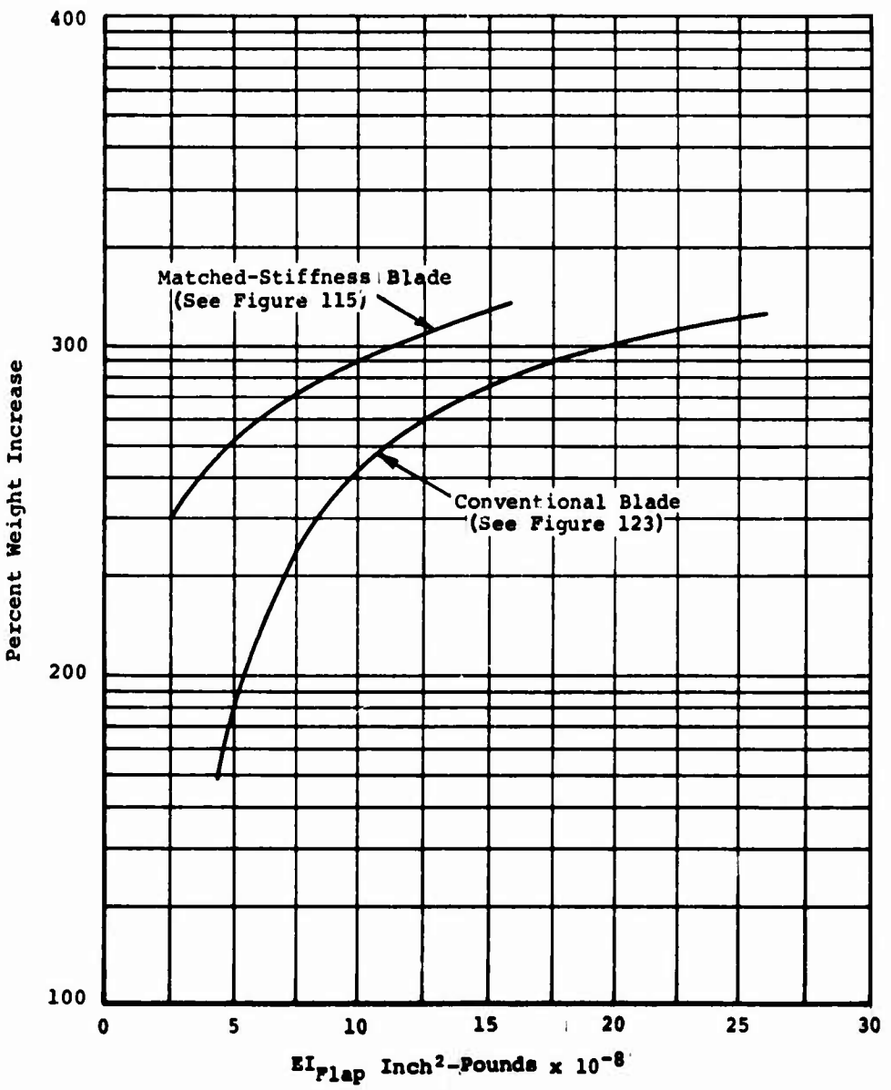

Figure 102. Delta Weight Analysis.

be supplied to suppress blade flapping above that trim which is required to obtain the thrust vector for forward flight. The incremental trim required to suppress flapping is automatically introduced through the longitudinal trim actuators, which are governed by the forward flight aerodynamic pressure. Should this trim system fail, the forward airspeed can be maintained by introducing a small amount of differential collective pitch. When the differential collective pitch is used to offset a failed trim actuator, the rotor blades are forced to operate at high flapping angles. In a hingeless tandem-lift rotor system, the fatigue damage this would cause would exceed the fatigue schedule considerably more than it would in an articulated rotor system (see Figures 115 and 123). Therefore, a proper design fatigue schedule for a hingeless rotor system should reflect a proportion of all flight time with the trim actuator inoperative. Such a fatigue schedule would manifest itself in the design as weight penalty in addition to the weight discussed previously.

CONFIGURATION

Helicopter

A crane/personnel carrier was used for this study in order to obtain the maximum variation of fuselage attitude over the speed range considered. The basic geometry of the airframe is shown in Figure 103. The operating conditions assumed were as follows:

1. Gross weight: 82,000 pounds
2. Sea level standard day
3. Center-of-gravity location: neutral
4. Equivalent flat-plate area: 238.6 square feet
5. Load factor at center of gravity: 1.0
6. Collective input: as required
7. Longitudinal cyclic input: -3 forward, -3 aft
8. Lateral cyclic input: as specified
9. Airspeed: 100 to 140 knots
10. Rotor rpm: 155.5

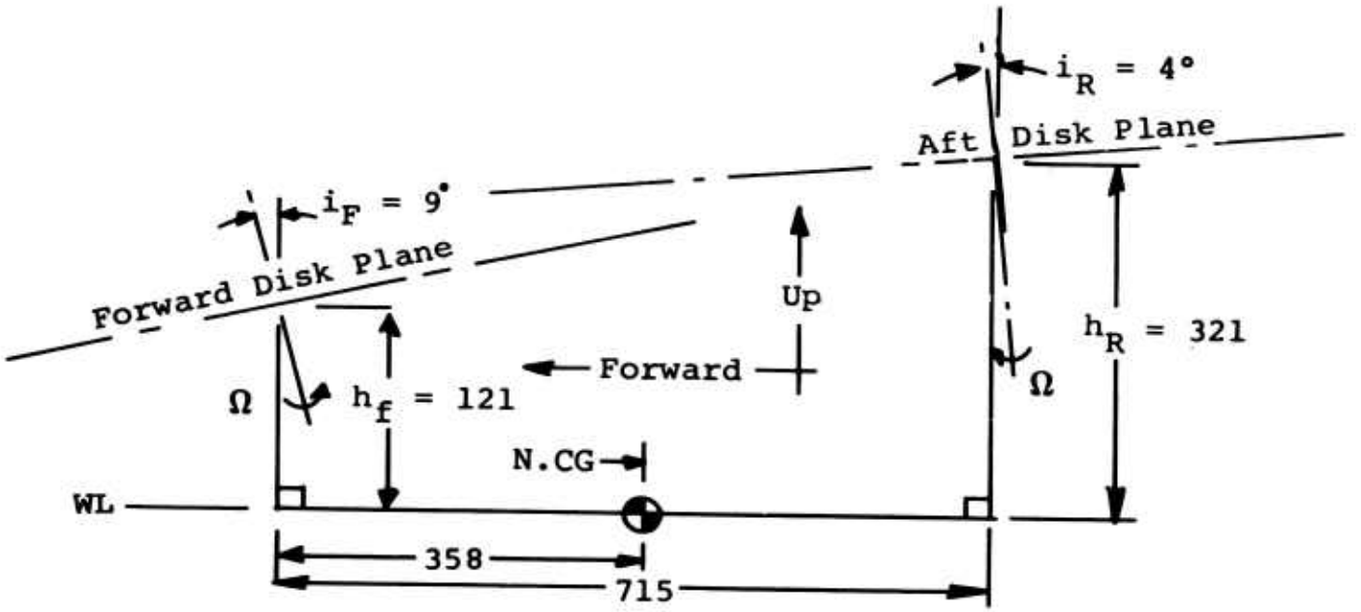

Figure 103. Basic Geometry of Airframe.

Rotor Blade

The rotor blade physical properties were synthesized by evaluating the overall rotor weight trends and developing stiffness data to meet these weight requirements. The resultant blade is qualitatively similar to the detail blade design described for the articulated rotor. In order to compare natural frequencies with those for an articulated rotor blade, an effective flapping hinge offset at 8-percent radius was used in the analysis. Two blade forms were considered: the so-called conventional blade shown in Figures 104, 105, and 106, and a matched-stiffness blade shown in Figures 107 and 108. Both blades had the following basic external geometry:

1. Radius: 43 feet

2. Chord: 3.5 feet

3. Thickness/chord ratio: 0.12

4. Airfoil cutout: 20-percent radius

The significant physical difference between the two blade forms is the acting trailing edge which is used in the conventional blade to tune the chordwise natural frequencies. It is assumed in the study that any undesirable frequency effects of the matched-stiffness blade, such as ground resonance, can be controlled by some technique other than the changing of blade physical properties.

Tip weights were used to obtain centrifugal force stiffening (a virtual change in mass stiffness, i.e., $\Sigma m/EI$). This approach permitted the study to vary the mass stiffness without obscuring the blade configuration being used. In the typical blade design, tip weights would not be used per se. Rather, the $\Sigma m/EI$ relationship would be altered to meet the design requirements with the possible addition of a tip weight for fine dynamic adjustments. Steel D-spar blades were assumed for the study, which was a conservative approach. It can be shown that for blades of equivalent $\Sigma m/EI$, a fiberglass plastic blade is roughly 3.6:1 better than a steel blade in terms of fatigue strength. The conclusion may be drawn then that a steel blade which is marginally satisfactory may be replaced by the equivalent fiberglass plastic blade which would be totally satisfactory.

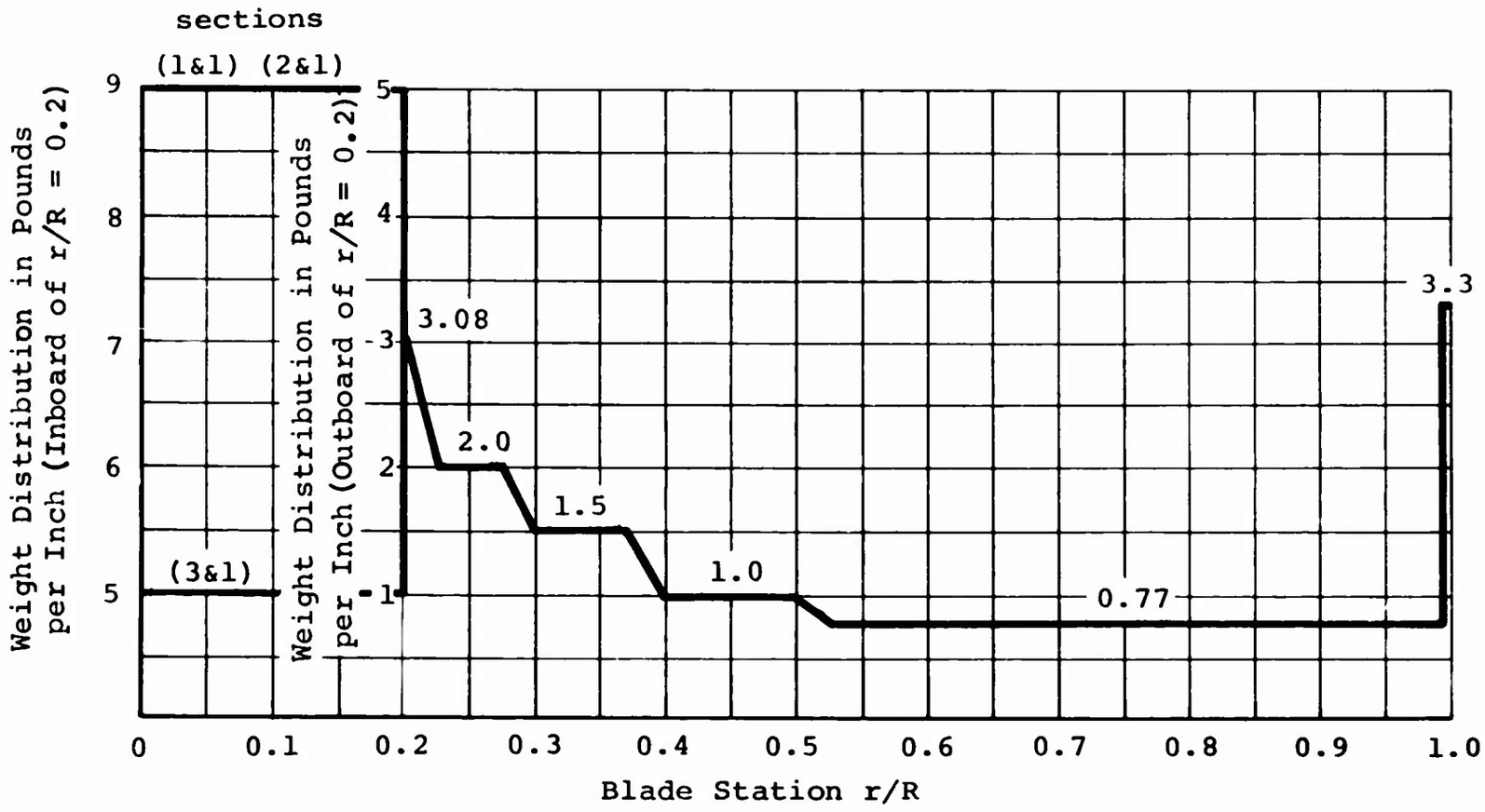

NOTES:

1. i = 1, 2, 3 flap-stiffness curves
   j = 1 chord-stiffness curve
2. Blade combinations in sets of i and j:
   1&1, 2&1, 3&1
3. R = 516 inches

Figure 104. Spanwise Weight Distribution of Conventional Blade.

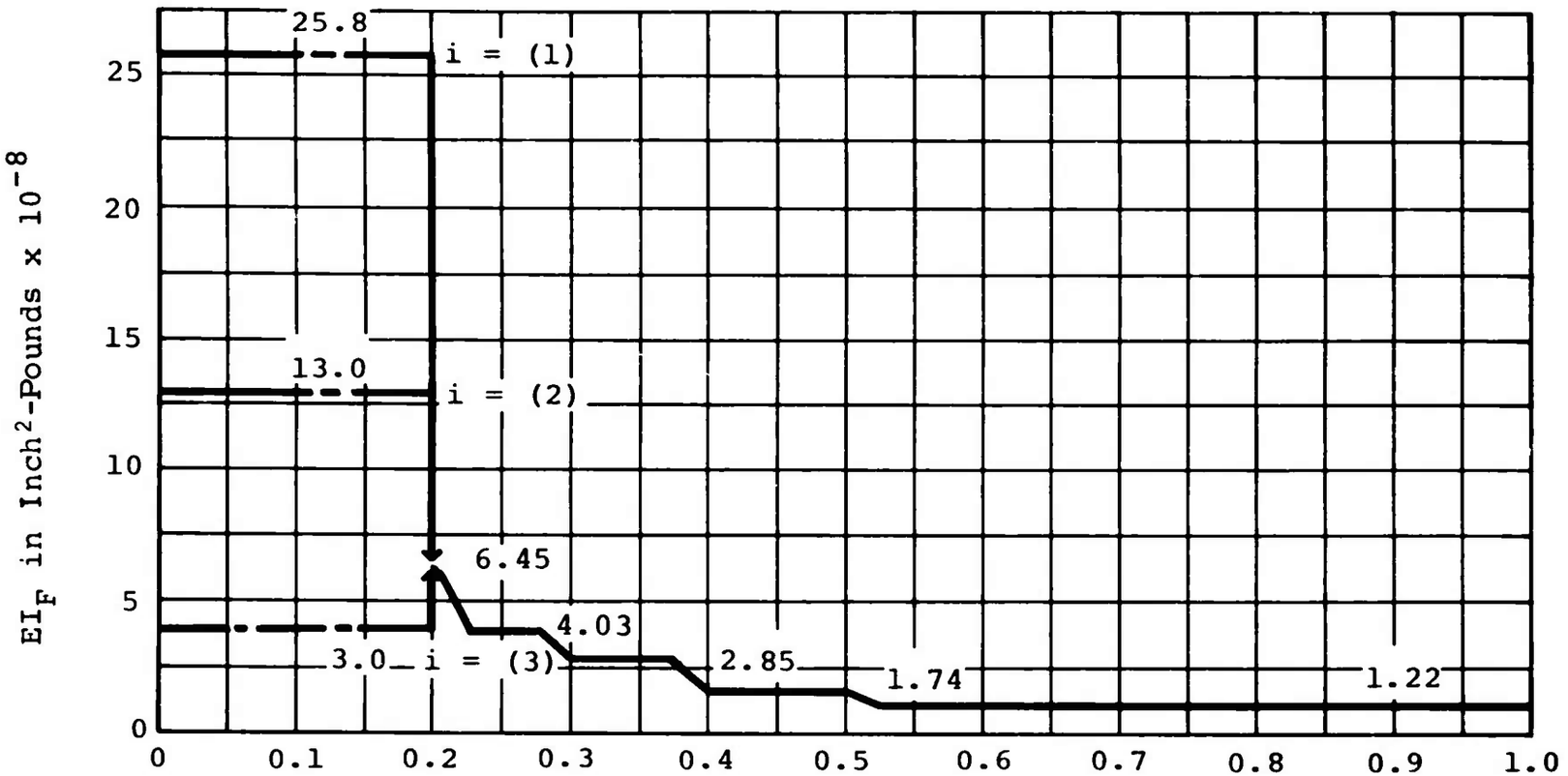

NOTES:

1. i = 1, 2, 3 flap-stiffness curves
   j = 1 chord-stiffness curve
2. Blade combinations in sets of i and j:
   1&1, 2&1, 3&1. The 2&1 combination was
   used for speed sweep.
3. R = 516 inches

Figure 105. Spanwise Stiffness Distribution of Conventional Blade.

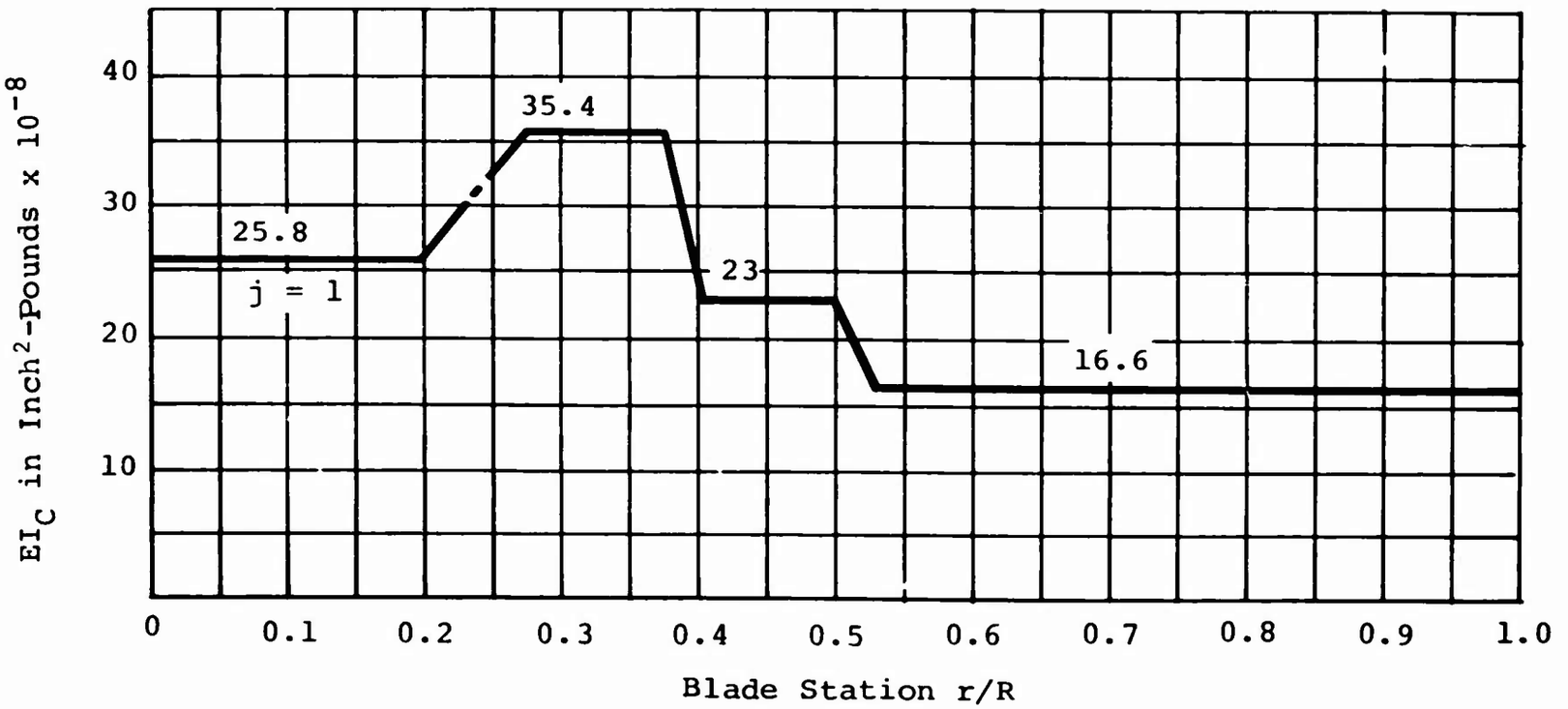

NOTES:
1. j = 1 chordwise-stiffness curve
2. R = 516 inches

Figure 106. Spanwise Chord-Stiffness Distribution of Conventional Blade.

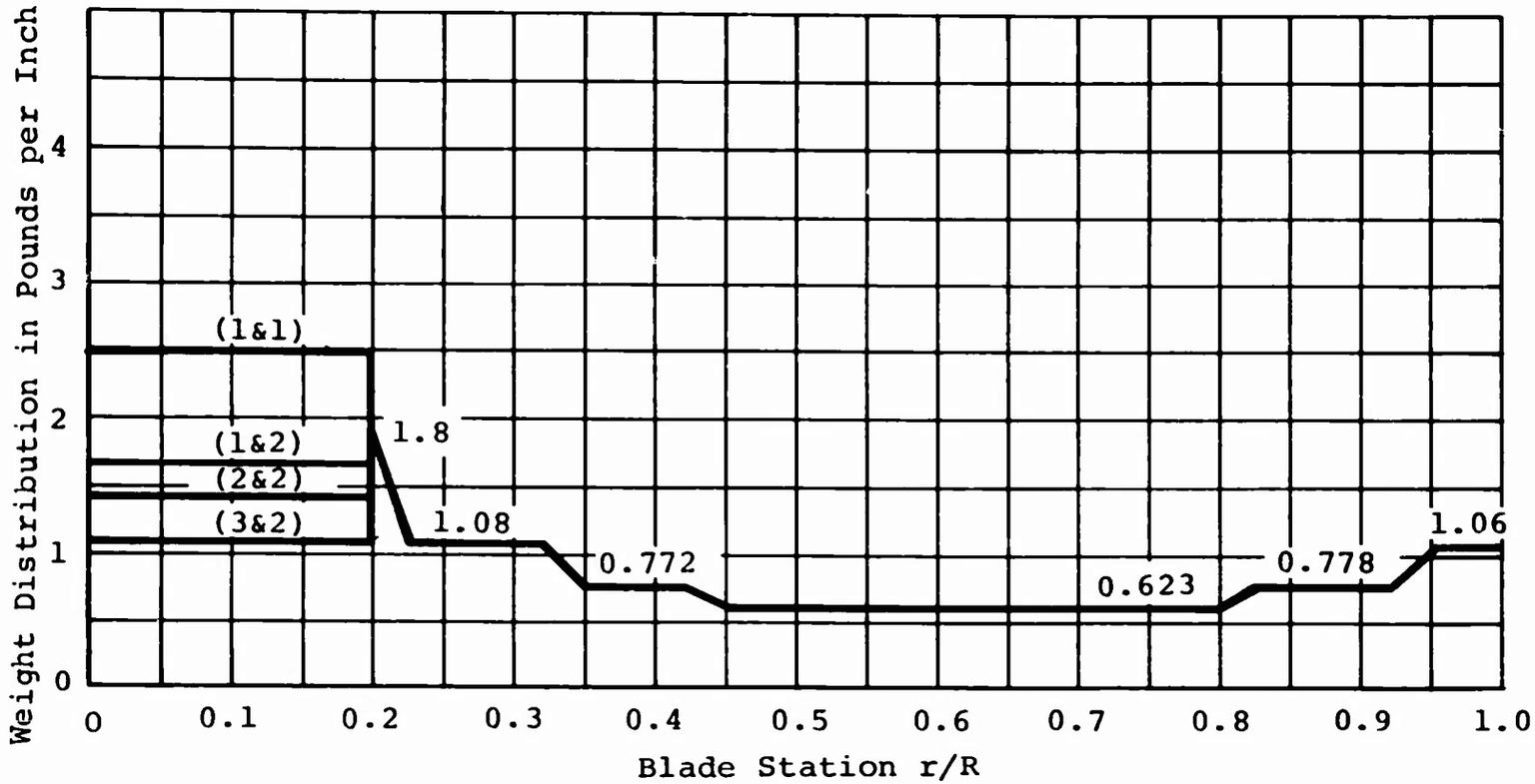

NOTES:
1. i = 1, 2, 3 flap-stiffness curves
   j = 1, 2 chord-stiffness curves
2. Blade combinations in sets of i and j:
   1&1, 1&2, 2&2, 3&2
3. R = 516 inches

Figure 107. Spanwise Weight Distribution of Matched-Stiffness Blade.

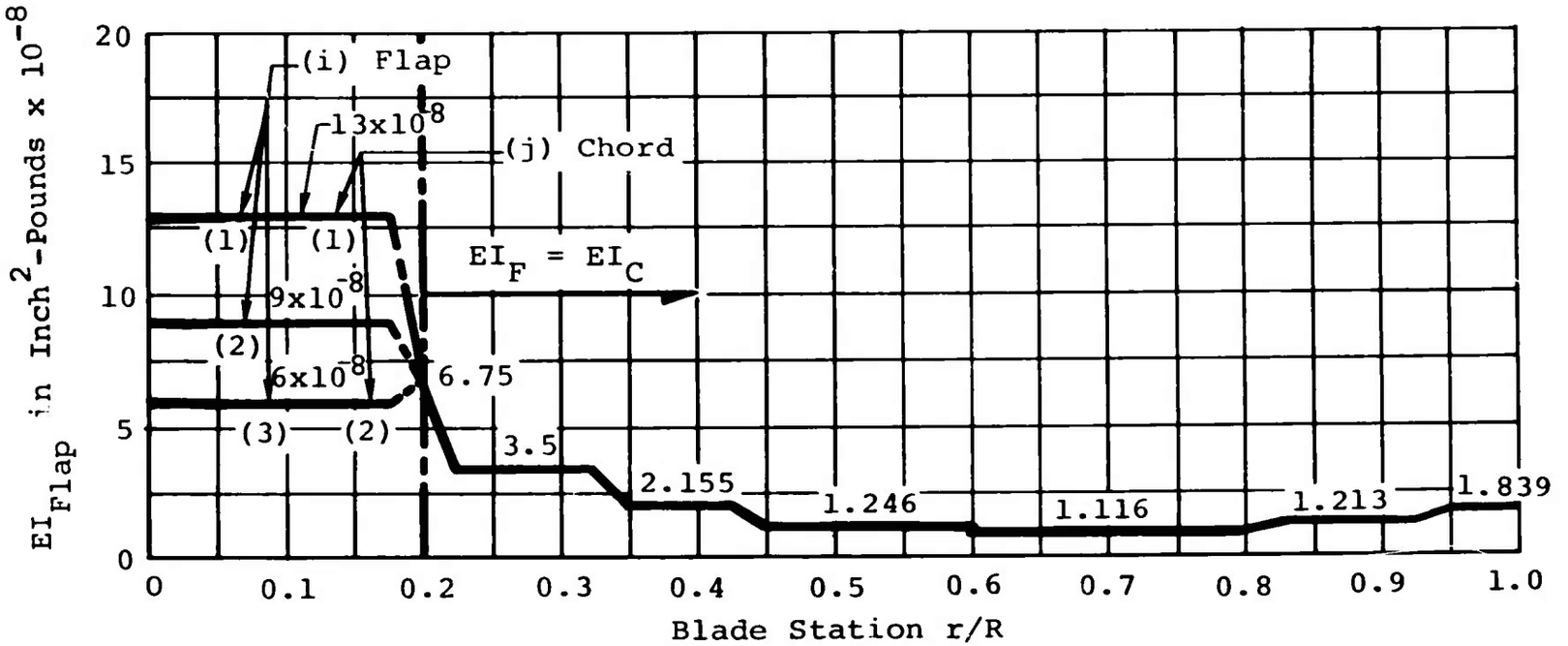

NOTES:

1. i = 1, 2, 3 flap-stiffness curves
   j = 1, 2 chord-stiffness curves
2. Blade combinations in sets of i and j:
   1&1, 1&2, 2&2, 3&2. The 3&2 combination
   was used for speed sweep.
3. R = 516 inches

Figure 108. Spanwise Stiffness Distribution of Matched-Stiffness Blade.

METHOD OF ANALYSIS

It was necessary first to establish a set of baseline blades. The blades were developed on the basis that low fatigue-stress allowables required that the blade be very flexible and therefore have low induced bending moments. Such blades tend to conform to an elastic curve established by equilibrium between blade weight centrifugal forces and blade lift. For a rotor system which uses a hub fixed to the rotating shaft, as opposed to a teetering hub, the bending load distribution induced on the rotor blade by flexing up is a function of the inboard flexibility. Thus, the initial investigation involved varying the stiffness of the inboard 20-percent radius and observing the influence over the remainder of the blade. Observations were made in terms of blade bending moment, hub overturning moment, and static deflections. The stiffness variations were done in parameters of lateral cyclic control to demonstrate the range of blade bending moment at each inboard stiffness. Data from this set of parameters were used to show the variation of steady lateral aerodynamic force output with respect to cyclic control in parameters of inboard blade stiffness. Finally, the variation in blade bending with forward velocity was checked for one moderate inboard root stiffness, which was used for both speed-sweep studies. Superimposed on these figures are data which demonstrate the parametric variation due to coning angle reduction and centrifugal-force stiffening. For comparative purposes the baseline blades were analyzed as articulated blades at points of interest in the study regime. These data points are shown as single points on the plots, except as noted.

RESULTS OF ANALYSIS

The results of the analysis appear in two sets of plots following the text: Figures 109 through 116 for the matched-stiffness blade, and Figures 117 through 124 for the conventional blade. They are arranged in parallel so that the data can readily be compared:

1. Natural frequencies
2. Vibratory bending characteristics
3. Speed sweeps at constant inboard flap stiffness
4. Flapwise and chordwise bending moments
5. Steady lateral aerodynamic force output
6. Hub overturning moments
7. Static deflection characteristics

Natural Frequencies

The following sketch defines for this report the relationships of mode numbers and associated frequencies of the hingeless and articulated rotor systems:

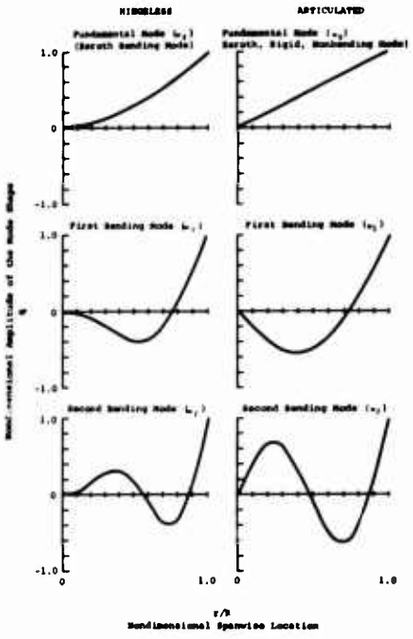

Note that both the hingeless and articulated rotor systems have fundamental modes which have no nodal points (the r/R of zero is a boundary, not a node). This establishes the numeral terminology of the natural modes, beginning with zero. The indicated subscripts of the symbol ω match the numeration of the mode, so that the frequency and mode notations correspond to the nodal indices.

Associated with the rotor blade bending mode shapes, higher than the first mode, are nonlifting flexure bending stresses which reduce the fatigue life of the rotor blade. Depending on how successfully these natural mode frequencies are avoided, the amplitude of each mode can be reduced to a minimum. Since this study was conducted at one operating speed (RPM), it was convenient to show both hinged and hingeless blades on a natural frequency diagram of nondimensional natural frequency versus rotor tip weight. Figures 109 and 117 demonstrate satisfactory avoidance of the first three natural blade frequencies relative to the forcing frequency (Ω) used in the study. Both types of matched-stiffness blades exhibit desirable natural frequency changes with the addition of tip weights.

Strength and Rigidity

Figures 110 and 118 reflect the influence of inboard root stiffness on the vibratory bending moment at selected points on the blades. The bending moments for both weighted and unweighted blades are shown with the allowable blade bending moment.

It is evident that the conventional blade is more sensitive to root stiffness variation than the matched-stiffness blades. This is particularly true in the outboard blade region, where, in addition to stiffness sensitivity, the conventional blade is strongly affected by increasing forward speed (Figures 111 and 119). However, the curves indicate a possible design solution with a conventional configuration but with a very soft inboard flapping stiffness. Of course static deflections then become large, requiring a mechanism to limit them. Also, increased root flexibility seems to satisfy the chordwise bending best. Indeed, trends indicate that a bending moment asymptote may occur at the higher inboard stiffness, and this potential should be pursued. Most notable about the matched-stiffness blade is the wide range of apparent design solutions. Once more, the most favorable design solution seems to be at the low end of the inboard stiffness scale.

Figures 112, 113, 120, and 121 are typical spanwise moments plots. These plots include the allowable moment distribution to provide a basis for comparison. These curves are intended to indicate what is happening over the remainder of the blade, with the objective of demonstrating the validity of the characteristic curves. In general, the characteristic curves are a good indication of the total blade phenomenon. It is also notable that the bending moments in the outboard 20 percent of both blade types are of the same order of magnitude.

Control Power

Control power is shown as a function of steady lateral aerodynamic force output (F_{yo}) versus lateral cyclic control input (θ_i) in Figures 114 and 122. These graphs make the significant point that the hingeless rotor has the greater yaw control power, f (F_{yo}, θ_i), which is contrary to first thoughts. However, the additional control power is not gained without exacting an equally significant debilitation in two design areas. First, the hingeless rotor blade obviously must support additional root vibratory moments at constant cyclic control

input, which is not the case for articulated rotors. Second, the hingeless rotor induces extremely large steady hub bending moments with steady cyclic control input. Once more, this is not the case for the articulated rotor. Articulated rotors do produce steady hub moments, but they are limited by the vertical shear in the rotor and by the hinge offset. The difference between the two moments is an order of magnitude as shown in Figures 115 and 123.

Rotor Hub Overturning Moment

The rotor hub overturning moment reflects the rotor shaft design requirements. Both blade types exhibit detrimental trends for this parameter as the inboard root stiffness is increased (Figures 115 and 123). Neither blade has desirable traits in this respect, but the matched-stiffness blade is the least offensive.

Static Deflection

The static deflection curves (Figures 116 and 124) establish one of the minimum root stiffness requirements. Both blade types are satisfactory for ground gust criteria, and only the matched-stiffness blade, at low inboard stiffness, is restricted at the 3g ground-flapping limit.

EVALUATION OF ANALYSIS

Table XXII is set up to evaluate the design features used in the parametric study in a quantitative way. Several important features of the parametric curves are listed and graded as desirable or not desirable. The desirability distinction is made for each option only as the option is considered. Comparison of the numerical factors identifies the best all-around design option.

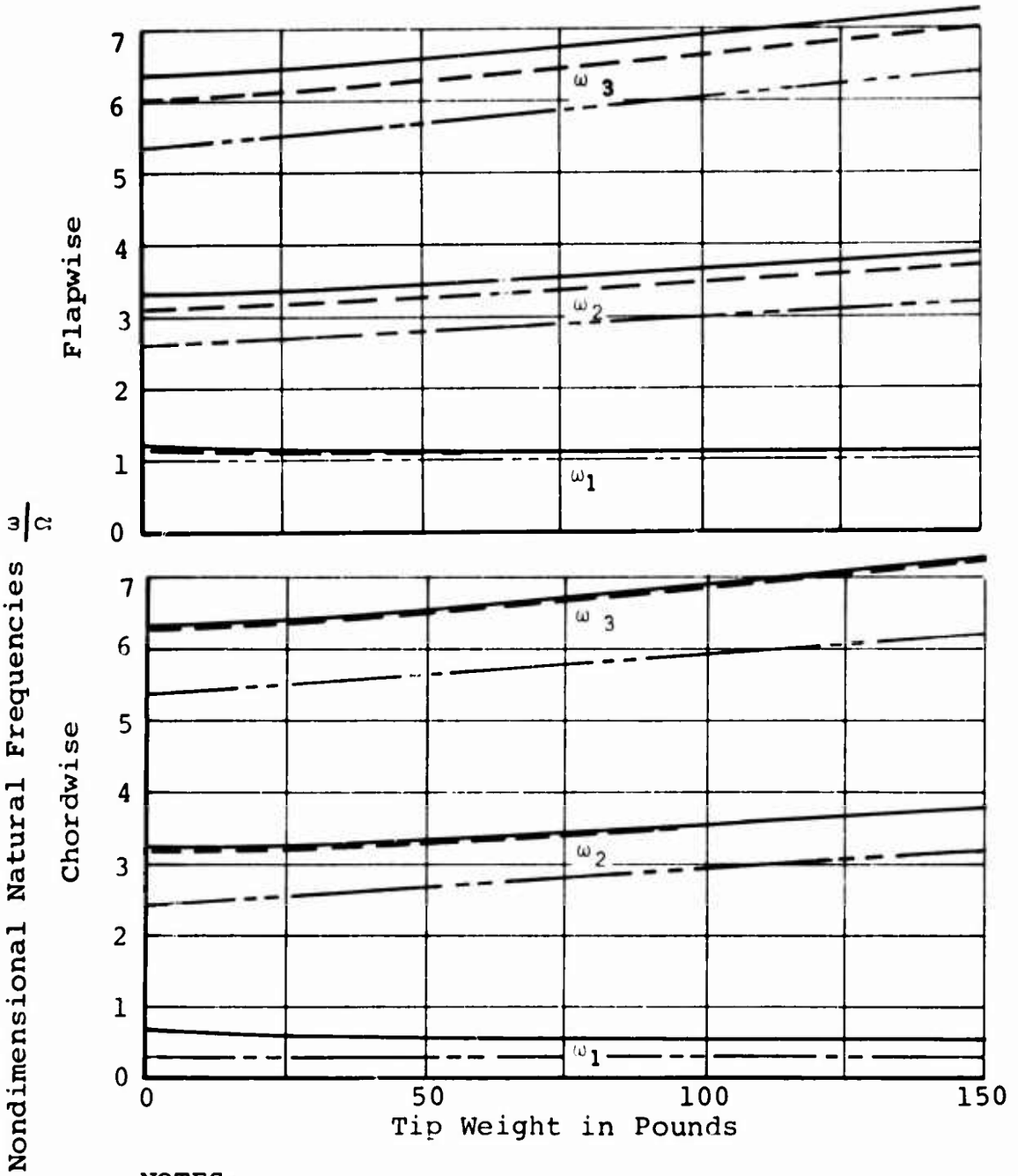

NOTES:

1. Root EI_{chord} = 13.0 x 10^{-8} inch^2-pounds
2. Ω = constant = 155 rotor rpm
3. Legend: ———— Typical high inboard stiffness
   — — — Typical low inboard stiffness
   — - - — Articulated

Figure 109. Flapwise and Chordwise Natural Frequencies of the Hingeless Rotor With Matched-Stiffness Blades.

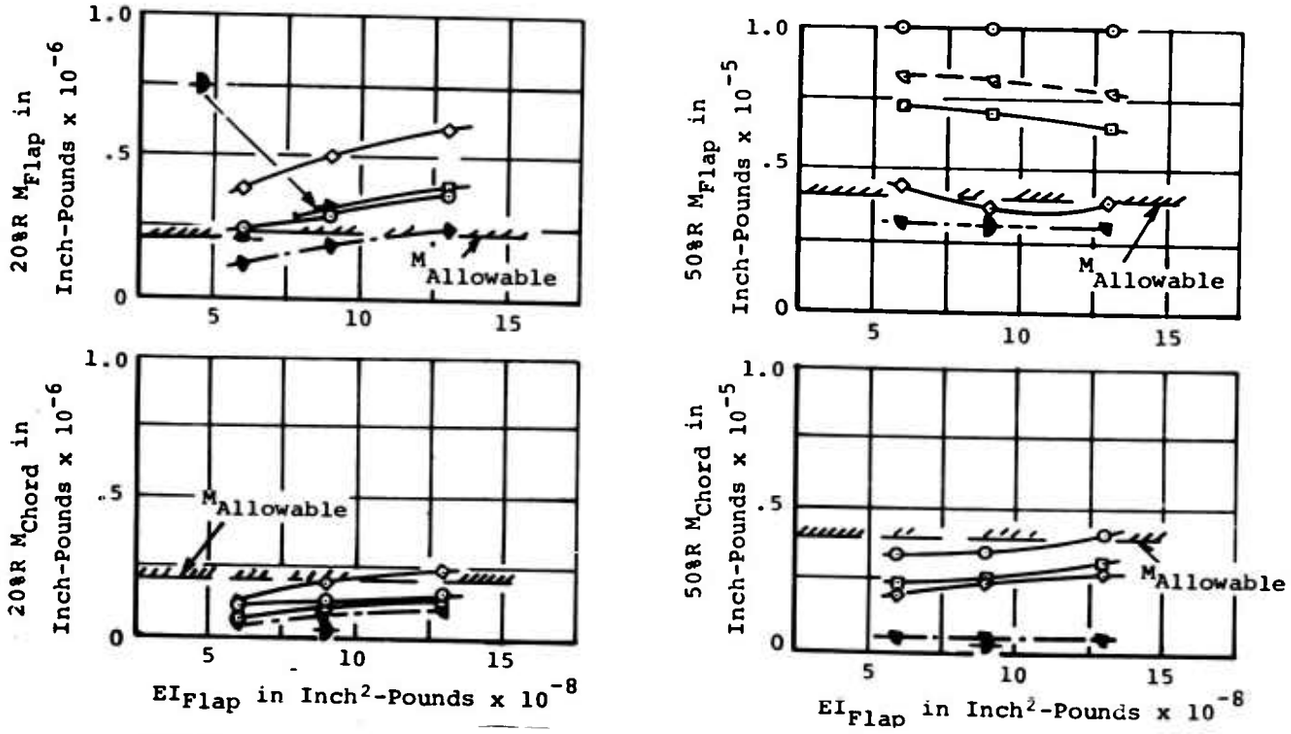

NOTES:

1. Sea level standard day
2. $V_{Forward}$ = 120 knots
3. 155 rotor rpm
4. EI_{Chord} = 6 x 10^8 inch^2-pounds
5. Lateral cyclic control input (θ_i) for untrimmed flight with unweighted blades
   - ◁ = extrapolated trim
   - ⊙ = 0 degrees
   - ⊡ = 5 degrees
   - ◇ = 10 degrees
6. Trim-weighted blade
   - ◖ = hingeless
   - ◗ = articulated

Figure 110. Vibratory Bending Characteristics of the Hingeless Rotor With Matched-Stiffness Blades.

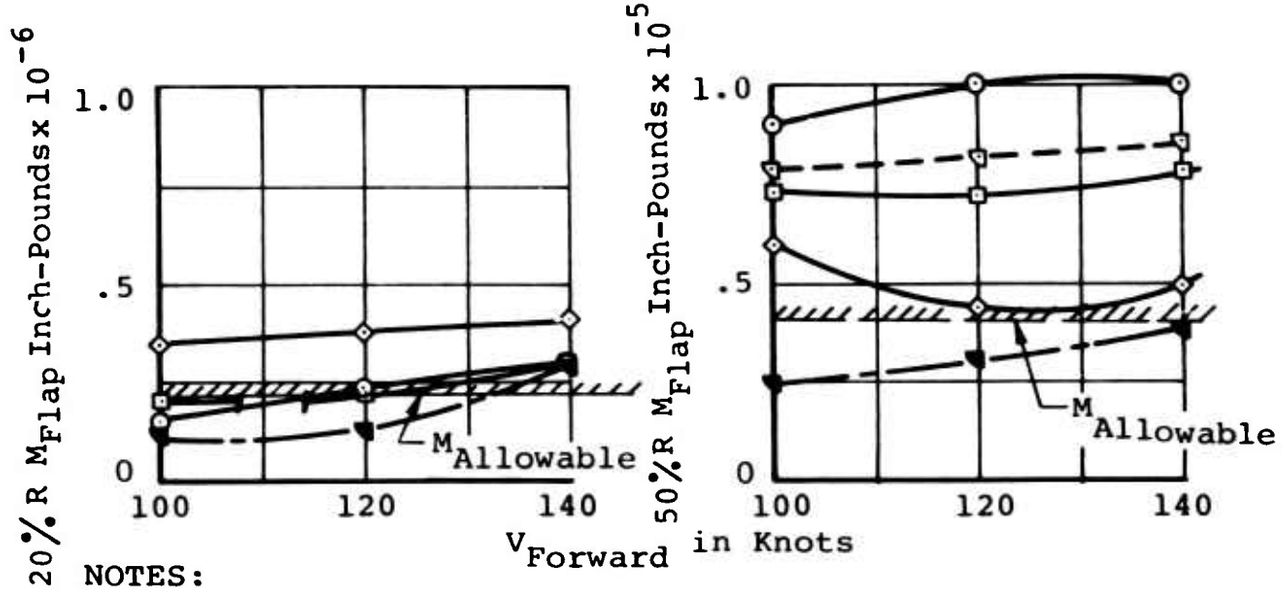

NOTES:

1. 155 rotor rpm
2. EI_{Flap} = 6.0 x 10^{-8} inch^2-pounds
3. Lateral cyclic control input (θ_1) for untrimmed flight with unweighted blades
   - ○ = 0 degrees
   - □ = 5 degrees
   - ◇ = 10 degrees
   - ▽ = extrapolated trim
4. Trim-weighted blades
   - ◖ = hingeless
   - ◗ = articulated

Figure 111. Speed Sweep at Constant Inboard Flap Stiffness for the Hingeless Rotor With Matched-Stiffness Blades.

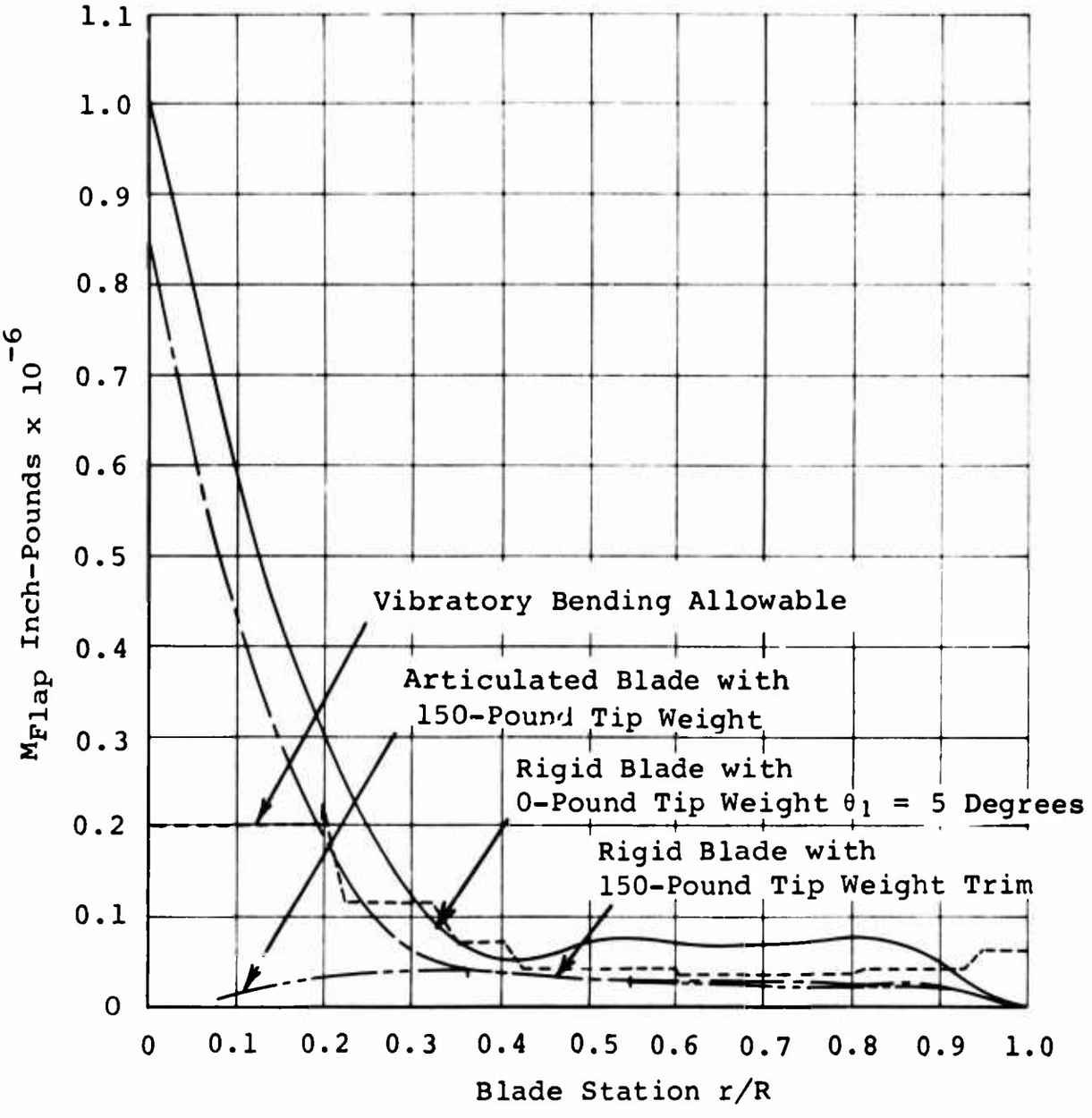

NOTES:

1. $V_{Forward}$ = 120 knots, sea level
2. Ω = 155 rotor rpm
3. Trim noted
4. EI_{Flap} = 6×10^{8} $inch^2$-pounds (inboard 20% R)
5. R = 516 inches

Figure 112. Flapwise Bending Moments of the Hingeless Rotor With Matched-Stiffness Blades.

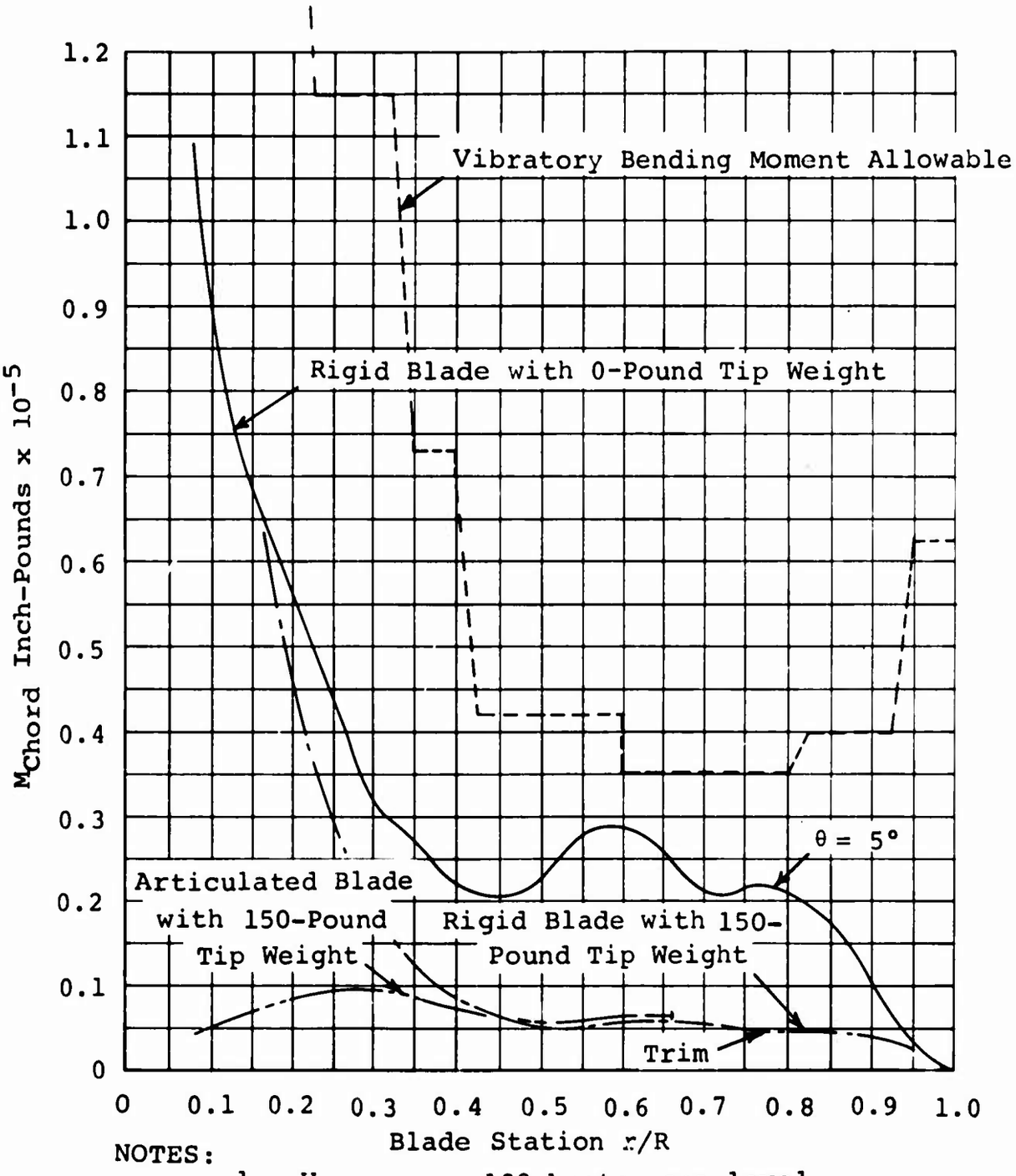

NOTES:

1. $V_{Forward}$ = 120 knots, sea level
2. Ω = 155 rotor rpm
3. Trim noted
4. EI_{Chord} = 6 x 10^{8} inch^2-pounds (inboard 20% R)
5. R = 516 inches

Figure 113. Chordwise Bending Moments of the Hingeless Rotor With Matched-Stiffness Blades.

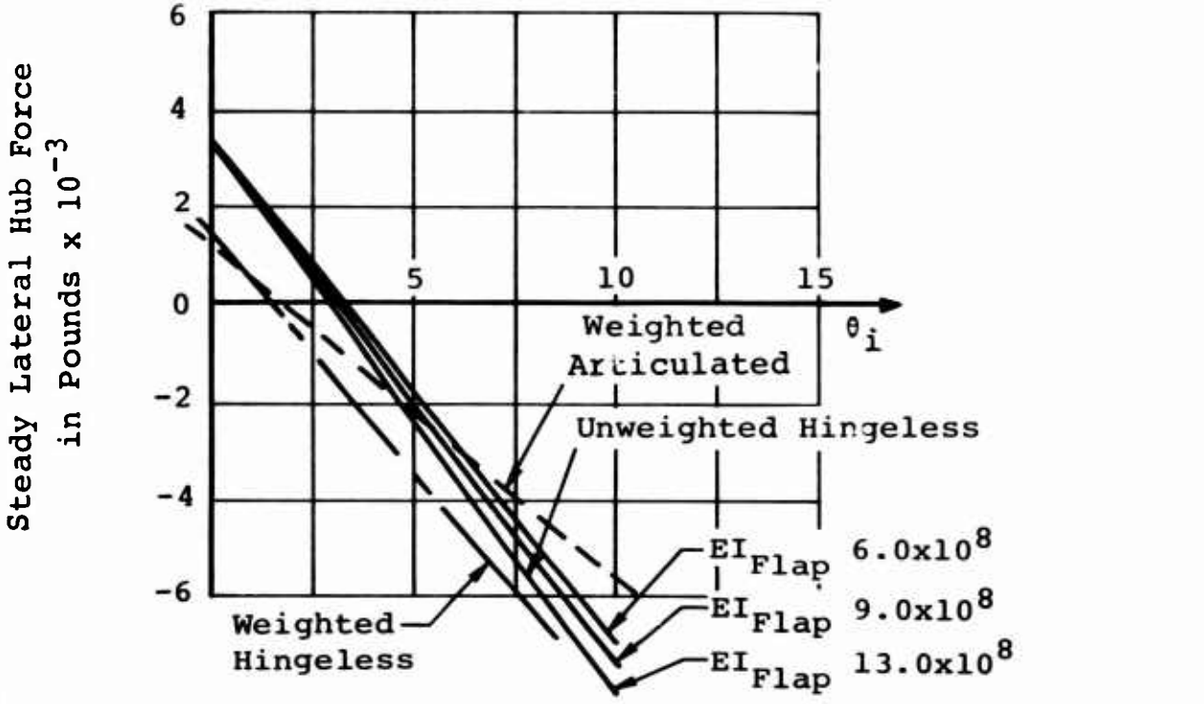

NOTES:

1. $V_{Forward}$ = 120 knots
2. 155 rotor rpm
3. Control power (F_y/θ_i) pounds per degree
   unweighted hingeless = 1080
   weighted hingeless = 980
   weighted articulated = 680

Figure 114. Steady Lateral Aerodynamic Force Output for the Hingeless Rotor With Matched-Stiffness Blades.

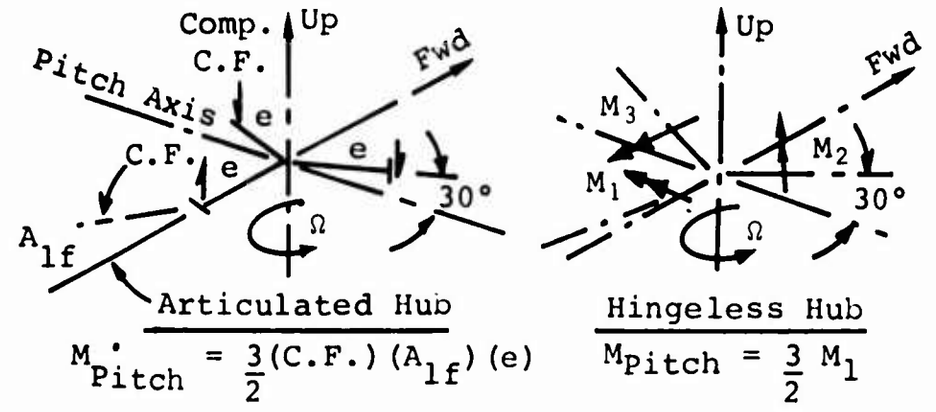

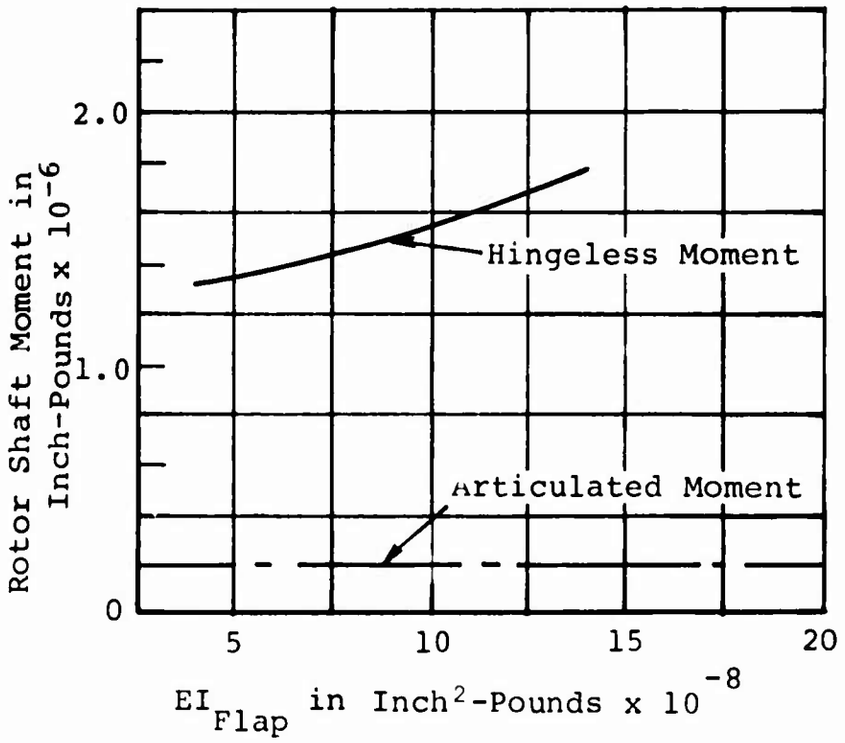

NOTE: M_1 = Average vibratory moment

Figure 115. Comparison of Hub Overturning Moments for Hingeless and Articulated Rotors With Matched-Stiffness Blades.

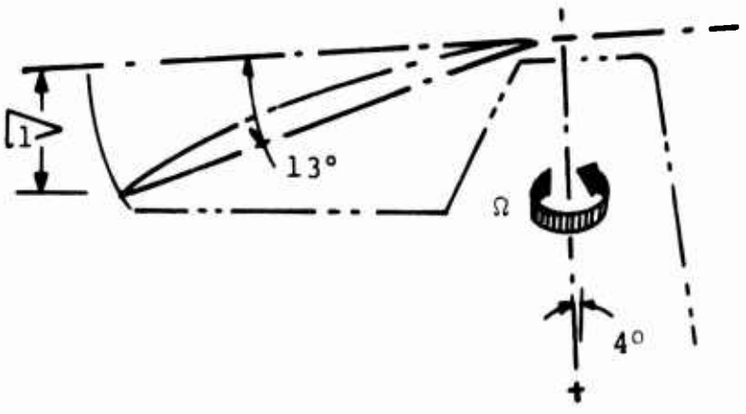

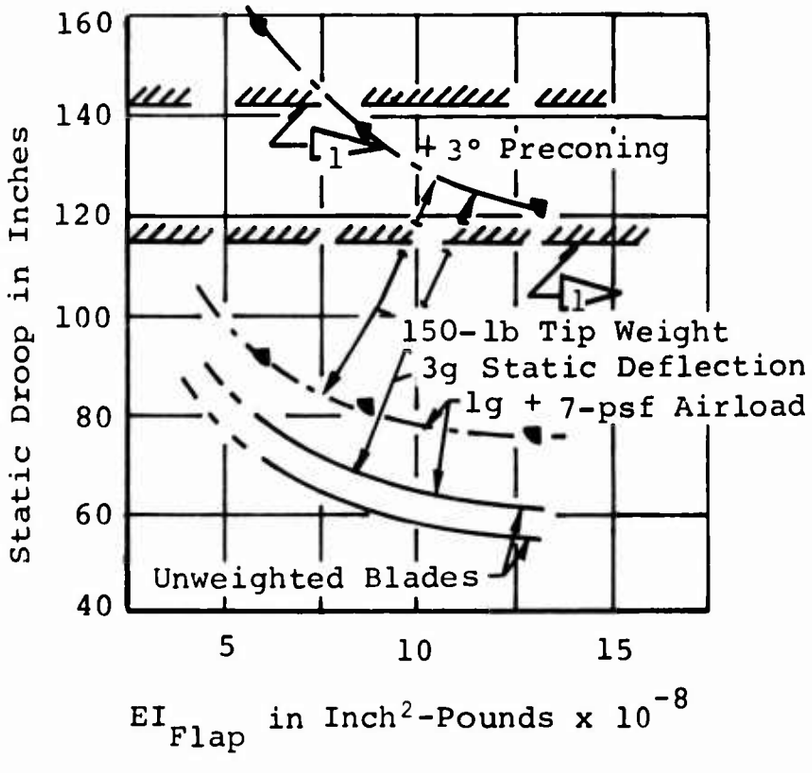

NOTE: 1 = Envelope of allowable static deflection (nonrotating)

Figure 116. Static Deflection Characteristics of the Hingeless Rotor With Matched-Stiffness Blades.

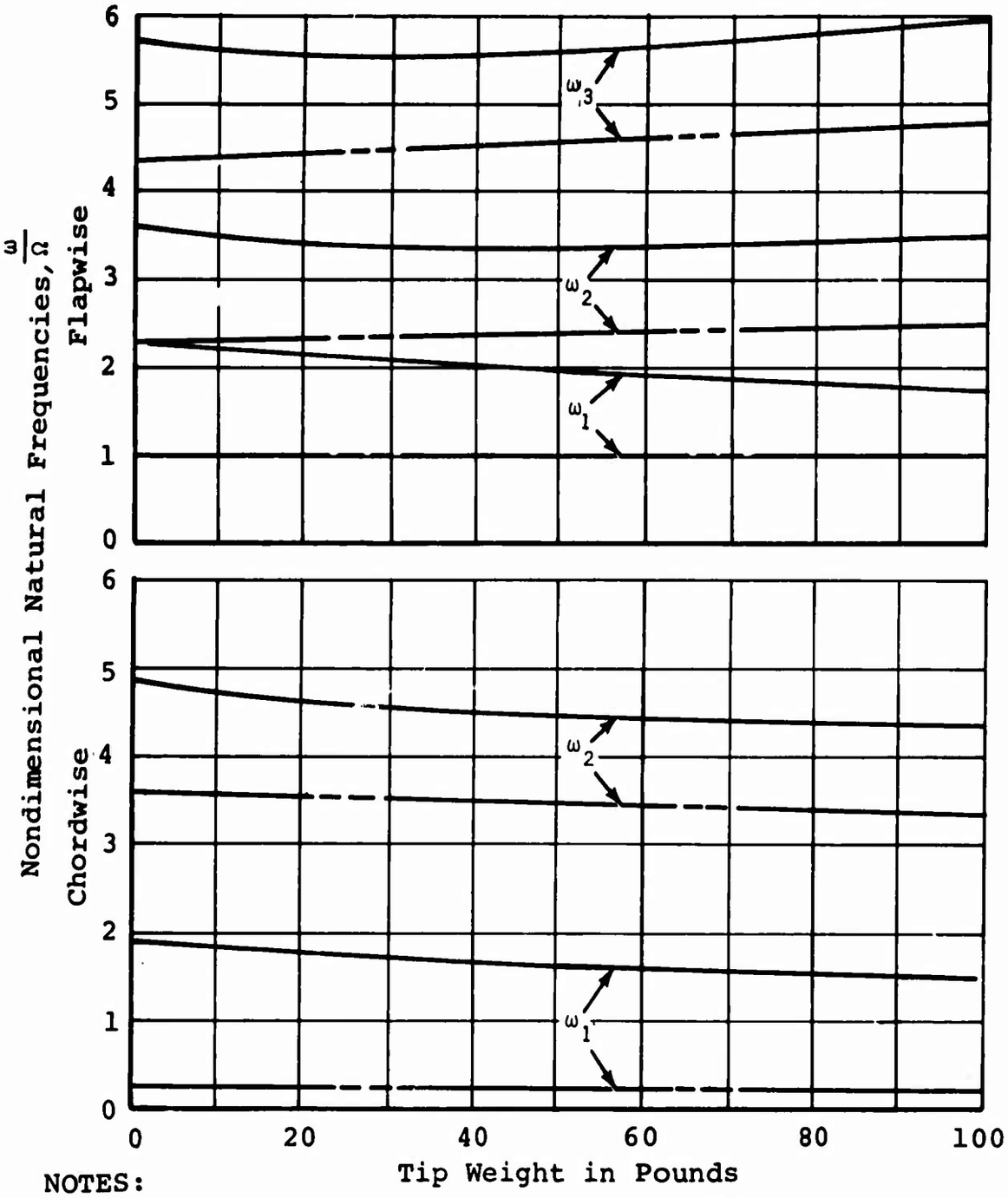

NOTES:

1. Root $EI_{flap} = EI_{chord} = 25.8 \times 10^{-8}$ inch^2-pounds
2. Ω = constant = 155 rotor rpm
3. Legend: ——— hingeless
   ——-—- articulated

Figure 117. Flapwise and Chordwise Natural Frequencies of the Hingeless Rotor With Conventional Blades.

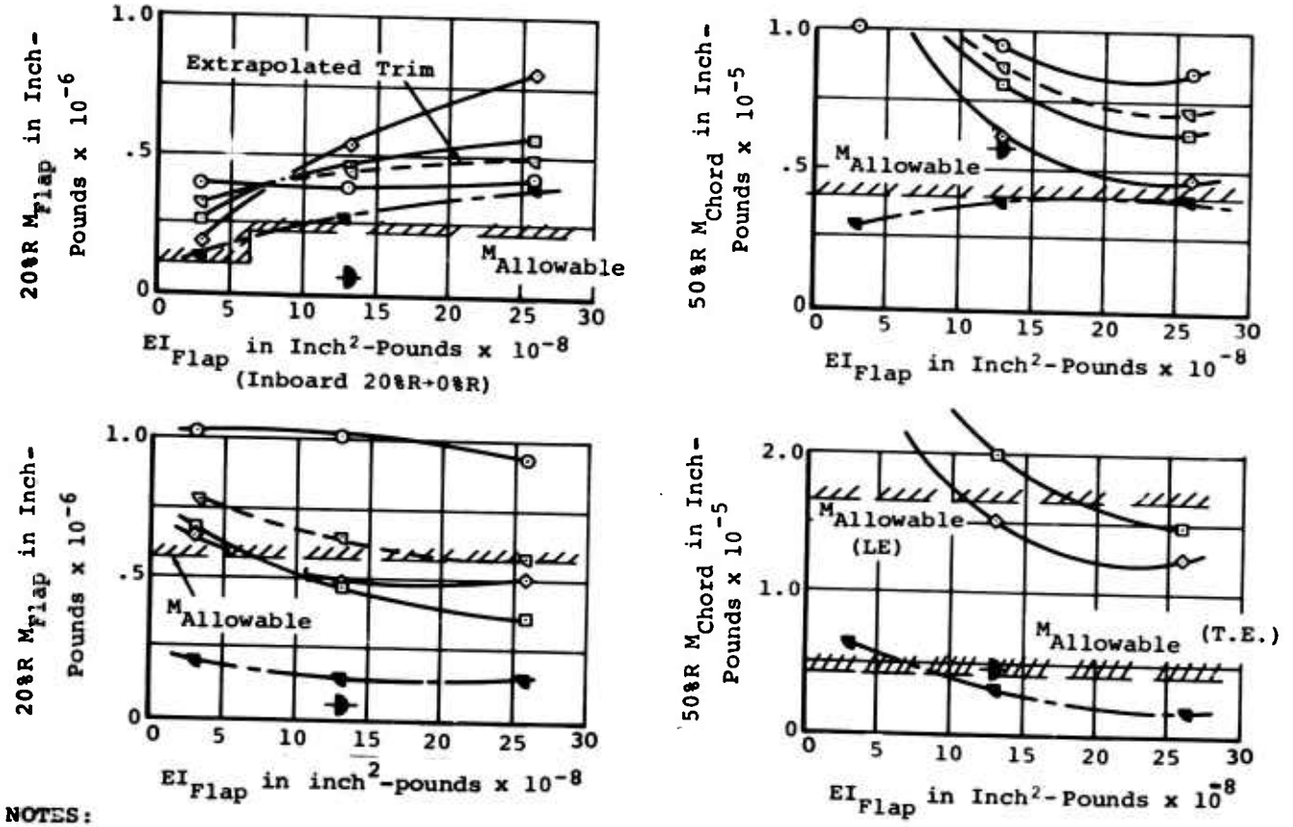

NOTES:

1. Sea level standard day
2. V_{FWD} = 120 knots
3. 155 rotor rpm
4. EI_{chord} = 25.8 x 10^9 Inch²-Pounds
5. Lateral cyclic control input (θ_i) for untrimmed flight with unweighted blades
   - ◹ = extrapolated trim
   - ⊙ = 0 degrees
   - ⊡ = 5 degrees
   - ◇ = 10 degrees
6. Trim-weighted blade
   - ● = hingeless
   - ◗ = articulated

Figure 118. Vibratory Bending Characteristics of the Hingeless Rotor With Conventional Blades.

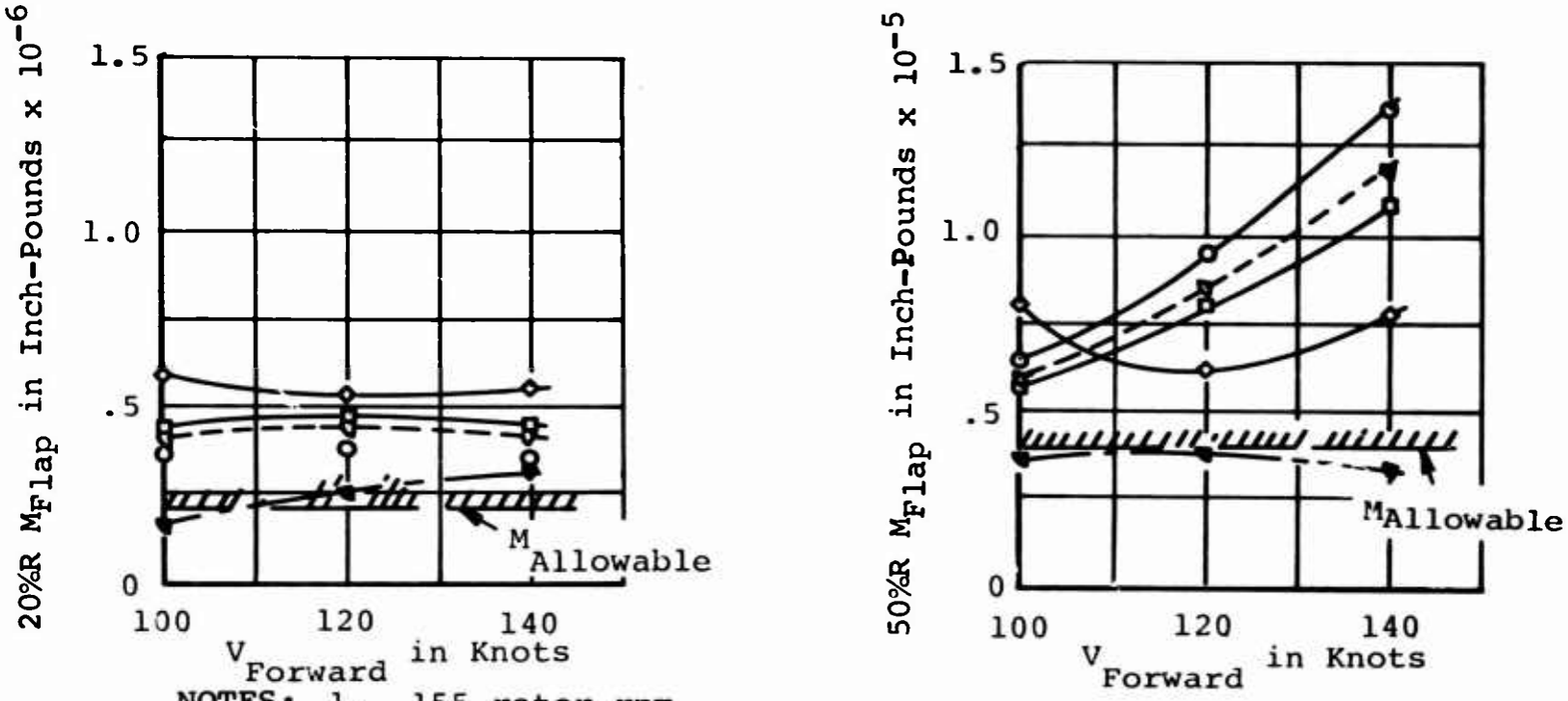

NOTES:
1. 155 rotor rpm
2. $EI_{flap} = 13.0 \times 10^8$ Inch^2-Pounds
3. Lateral cyclic control input (θ_i) for untrimmed flight with unweighted blades
   - ◪ = extrapolated trim
   - ○ = 0 degrees
   - □ = 5 degrees
   - ◇ = 10 degrees
4. Trim-weighted blade
   - ◥ = hingeless
   - ◗ = articulated

Figure 119. Speed Sweep at Constant Inboard Flap Stiffness for the Hingeless Rotor With Conventional Blades.

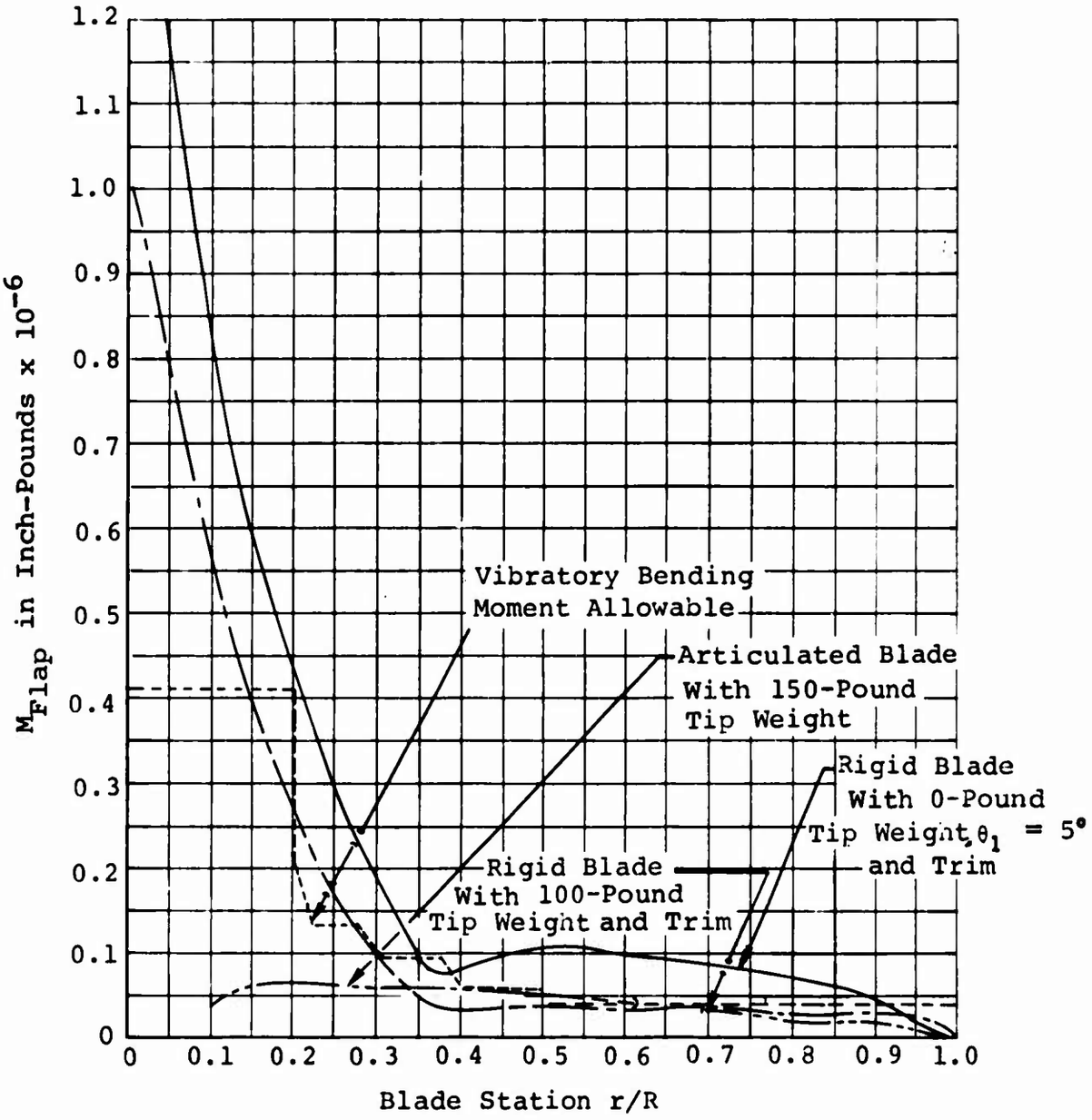

NOTES:

1. $V_{Forward}$ = 120 knots
2. Ω = 155 rotor rpm
3. Trim noted
4. EI_{Flap} = 13 x 10^{8} $inch^2$-pounds (Inboard 20%R)
5. R = 516 inches

Figure 120. Flapwise Bending Moments of the Hingeless Rotor With Conventional Blades.

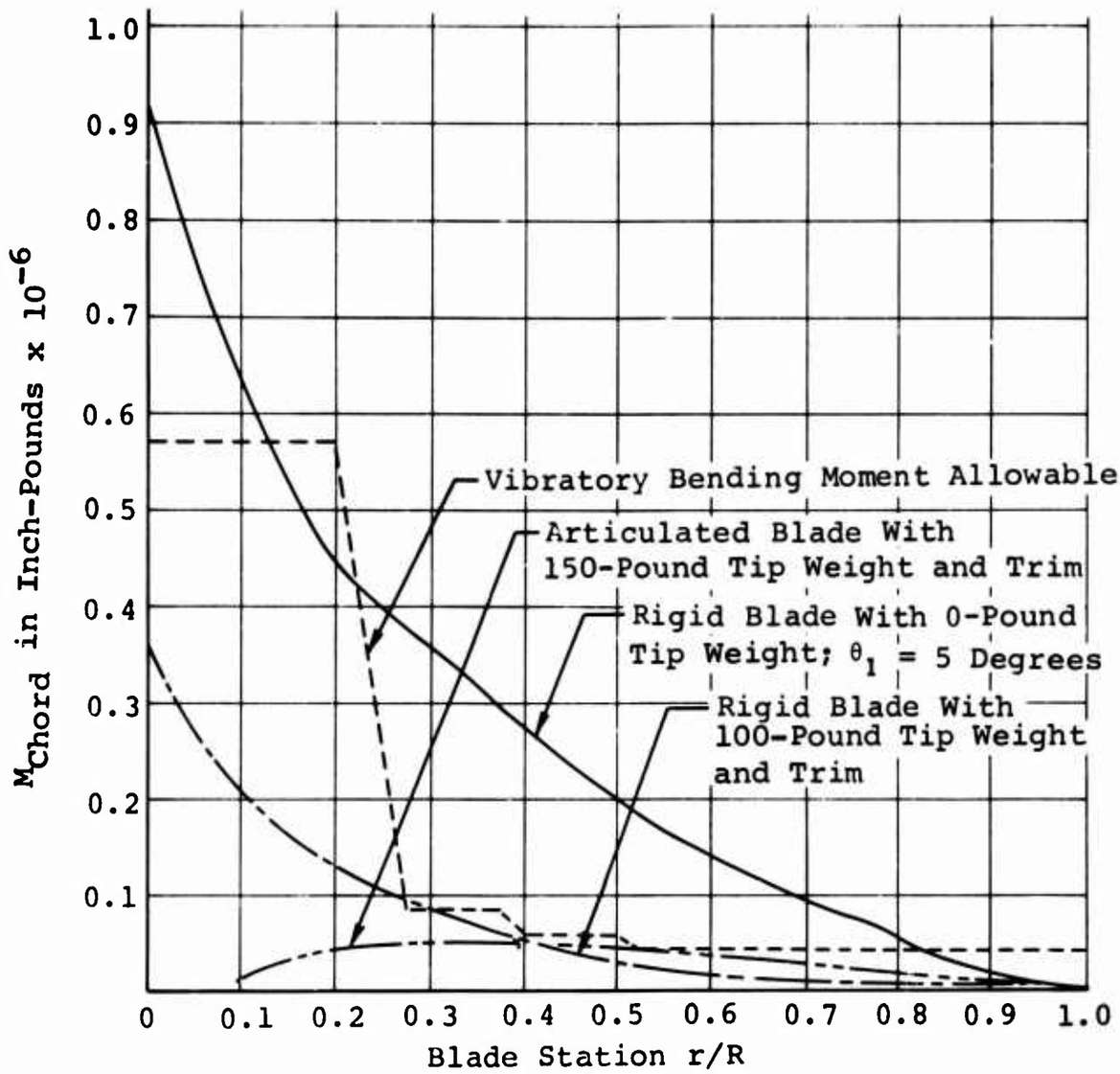

NOTES:

1. $V_{Forward}$ = 120 knots
2. Ω = 155 rotor rpm
3. Trim noted
4. EI_{Chord} = 25.8 x 10^8 inch^2-pounds (inboard 20%R)
5. R = 516 inches

Figure 121. Chordwise Bending Moments of the Hingeless Rotor With Conventional Blades.

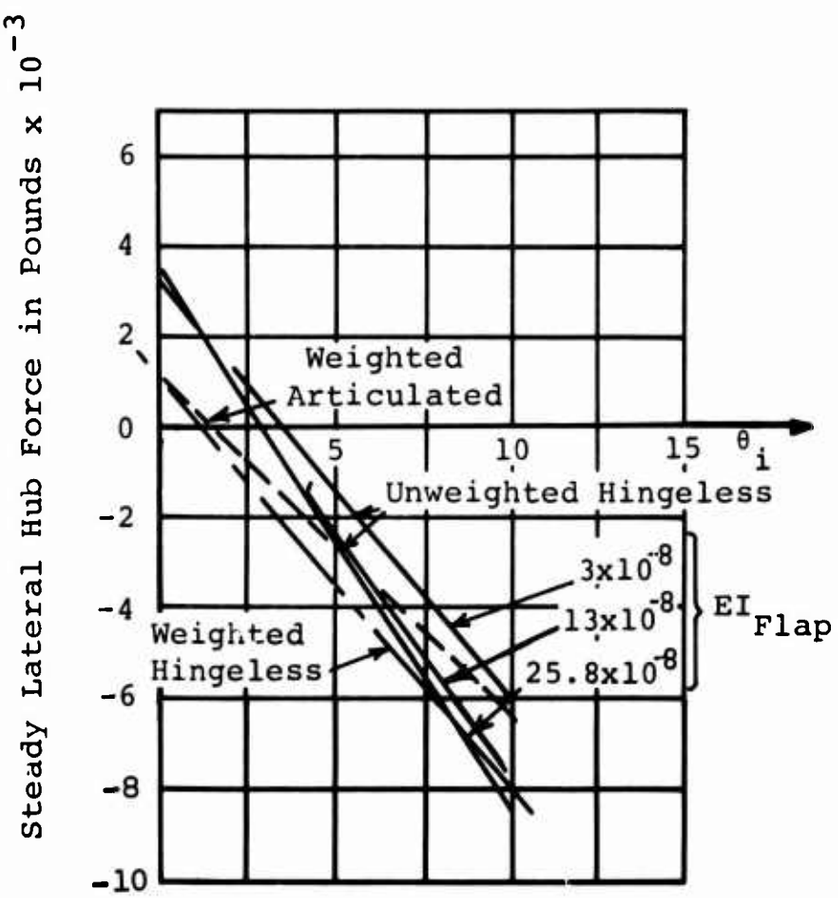

NOTES:

1. Airspeed 120 knots; 155 rotor rpm
2. Control power ($F_y/\theta_1°$) pounds per degree:
   - Unweighted hingeless = 1100
   - Weighted hingeless = 940
   - Weighted articulated = 760

Figure 122. Steady Lateral Aerodynamic Force Output for the Hingeless Rotor With Conventional Blades.

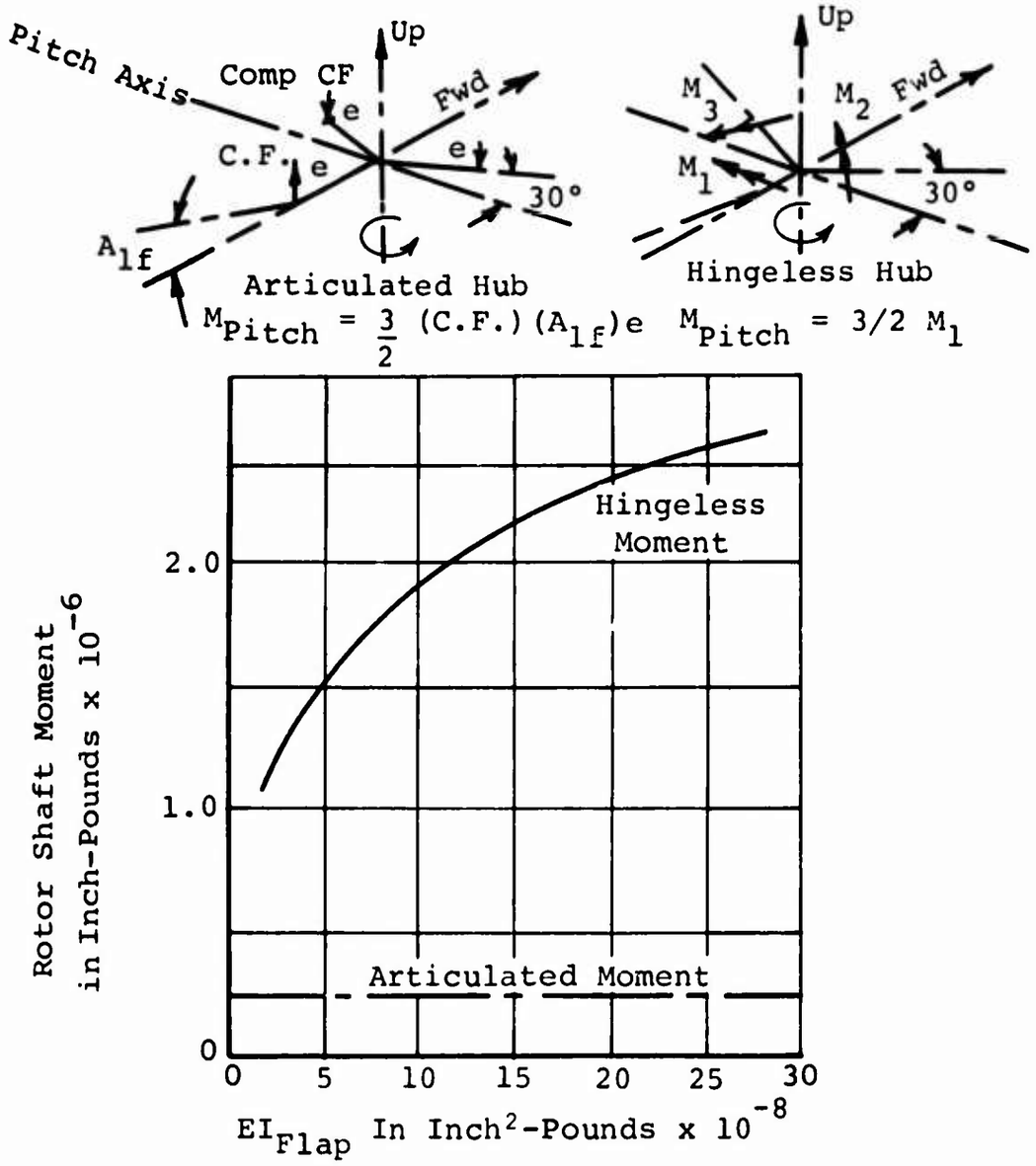

NOTE: M_1 = Average vibratory moment

Figure 123. Comparison of Hub Overturning Moments for Hingeless and Articulated Rotors With Conventional Blades.

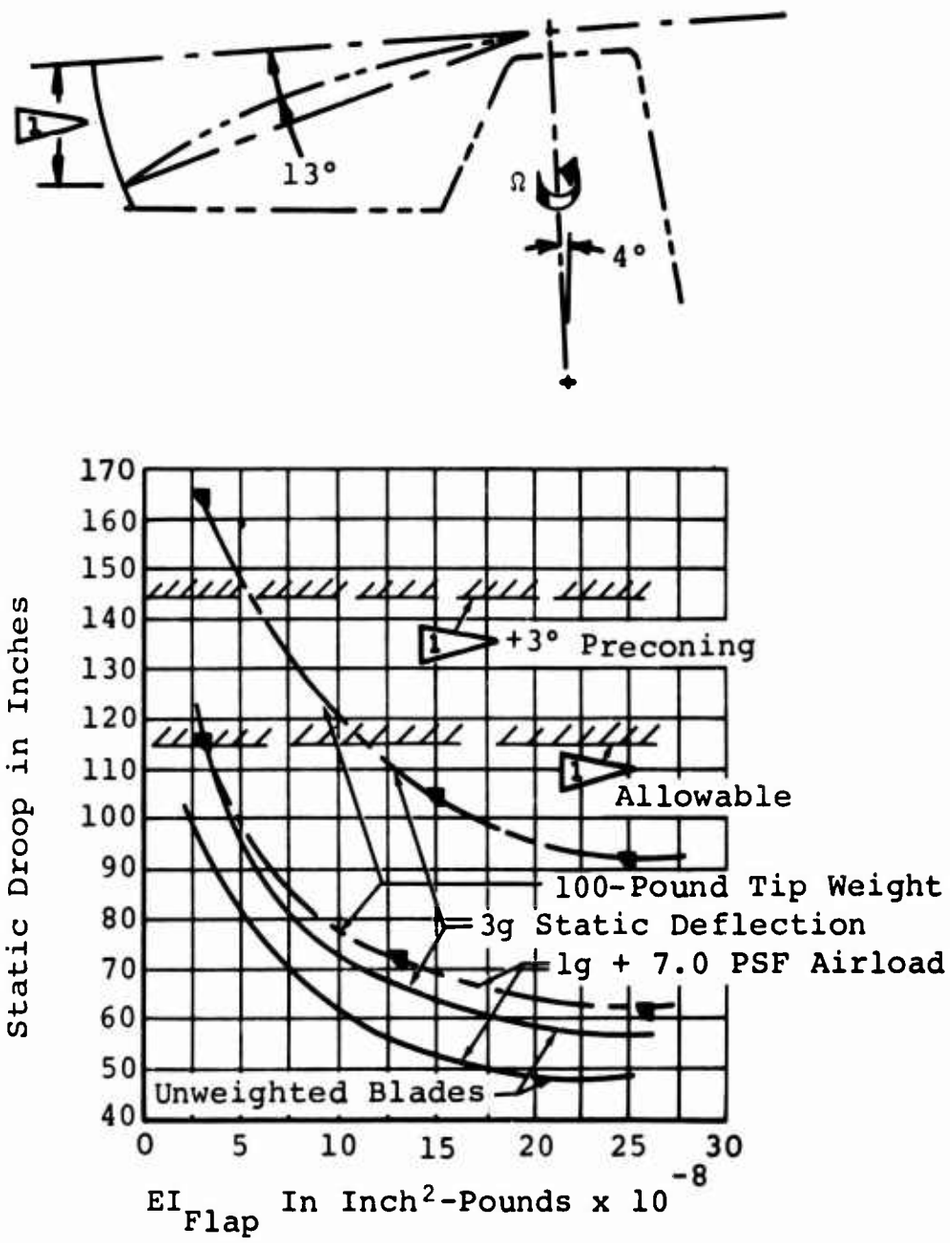

Figure 124. Static Deflection Characteristics of the Hingeless Rotor With Conventional Blades.

TABLE XXII
DESIGN FEATURES OF CONVENTIONAL AND MATCHED-STIFFNESS BLADES FOR THE HINGELESS SEMIRIGID ROTOR

Selection of Design Options	Design Features*/Column Number 1. Conventional blade, low inbd stiffness (6×10^{-8} in.^{2}-lb), no tip weight 2. Conventional blade, high inbd stiffness (25.8×10^{-8} in.^{2}-lb), no tip weight 3. Conventional blade, low inbd stiffness (6×10^{-8} in.^{2}-lb), with tip weight 4. Matched-stiffness blade, low inbd stiffness (6×10^{-8} in.^{2}-lb), no tip weight 5. Matched-stiffness blade, high inbd stiffness (13×10^{-8} in.^{2}-lb), no tip weight 6. Matched-stiffness blade, med inbd stiffness (9×10^{-8} in.^{2}-lb), with tip weight					
	(1)	(2)	(3)	(4)	(5)	(6)
Options*						
M_{Flap} INBD	+	-	+	+	-	+
M_{Flap} OUTBD	-	+	+	-	$\pm$	+
M_{Chord} INBD	-	$\pm$	+	+	+	+
M_{Chord} OUTBD	-	+	+	+	+	+
Moment scatter due to θ	-	-	$\pm$	+	+	+
Speed sweep	-	$\pm$	$\pm$	+	+	+
Steady aerodynamic force	+	+	-	+	+	-
Static deflection	+	+	-	-	+	-
Hub overturning moment	+	-	+	+	-	-
$\Sigma/9$	$+\frac{4}{9} - \frac{5}{9}$	$+\frac{6}{9} - \frac{5}{9}$	$+\frac{7}{9} - \frac{4}{9}$	$+\frac{7}{9} - \frac{2}{9}$	$+\frac{7}{9} - \frac{3}{9}$	$+\frac{7}{9} - \frac{2}{9}$
Design selection factor	$-\frac{1}{9}$	$+\frac{1}{9}$	$+\frac{3}{9}$	$+\frac{5}{9}$	$+\frac{4}{9}$	$+\frac{5}{9}$

*Options versus design features: + = desirable, - = not desirable

PRELIMINARY DESIGN LAYOUTS

The rotor pylons, the structure, the powerplant, and the drive system are shown in Figures 125 and 126 to provide a frame of reference for the design layouts discussed in this section.

ROTOR BLADES FOR AN ARTICULATED ROTOR SYSTEM

Four blade construction configurations were studied to determine the optimum blade configuration for the heavy-lift helicopter articulated rotor system: the steel D-spar, the titanium D-spar, the steel hexagonal-spar, and the fiberglass-plastic C-spar blade. Design consideration was given to alternating and steady stress levels; dynamic characteristics; static droop, buckle or rupture; and manufacturing concepts. STATIC AND DYNAMIC STRUCTURAL ANALYSIS OF THE ARTICULATED ROTOR SYSTEM is described in the section so titled.

Description of Configurations

The steel D-spar and titanium D-spar blades (Figure 127) are of similar construction except for the spar material used. The spar is formed from a constant-OD, step-tapered-ID tube to a nonsymmetrical contour following the NACA 23012 airfoil. An electrical deicing blanket and a stainless steel abrasion strip bonded to the leading edge of the spar fall within the airfoil contour. The bottom of the spar has a full-span stiffener bead formed in it to break the large flat-plate area and to help achieve the static-buckle requirements. The trailing-edge fairing is segmented fiberglass-cloth-reinforced epoxy panels laid up at a 45-degree bias over contoured honeycomb core. The fairing is bonded to the heel of the spar, and the joints are aerodynamically sealed. The trailing edges of the fairings are bonded to a continuous laminated stainless steel strip. A channel with a variable-thickness weight is bonded into the leading edge of the spar for weight and balance control. The inboard end of the spar is threaded for attachment to the socket. The socket has lugs for two-pinned attachments to the pitch housing. This two-pinned joint can be used either for blade removal or for manual blade folding. It is common to the four blades in the study.

The steel hexagonal-spar blade (Figure 128) has a spar with a hexagonal outer contour and a circular inner contour. The hexagonal contour is made by machining flats on a heavy-walled

tube which has a step-tapered ID, thus providing wall thickness variations for frequency tuning and weight savings. A stainless steel nose cap bonded to the flats machined on the spar forms the leading edge contour. An electrical deicing blanket is bonded to the outside of the nose cap and a variable-density nose block is bonded to the inside. This assembly is stabilized by an aluminum honeycomb core. The trailing-edge strip and fairings are similar to those on the D-spar. The machining of the spar washes out to a round inboard section which is threaded for root-end attachment. A drag strut between the trailing-edge strip and an A-frame on the socket is required because of low chordwise spar stiffness. Stainless steel doublers are required at the inboard end of the constant airfoil section to transfer shear loads from the drag strut to the spar.

The plastic C-spar rotor blade (Figure 129) has a spar of unidirectional continuous fiberglass filaments in an epoxy resin system wrapped inside and out with a fiberglass-crossply-reinforced epoxy skin. The trailing-edge fairing is continuous aluminum honeycomb core stabilized with a fiberglass crossply skin extending forward and bonded into the C-spar. The leading edge block is a variable-density composite bonded to the leading edge of the spar. The assembly is then wrapped with a 45-degree crossply for torsional stability and a final wrap of fiberglass cloth on a 45-degree bias. The cloth will prevent the propagation of delaminations due to foreign-object damage. A laminated stainless steel trailing-edge strip is bonded between the top and bottom skins for the full span of the constant airfoil section. A threaded conical-shaped insert is overlaid with the unidirectional filaments of the spar during lay-up, and filament winding is applied over the spar filaments for root-end retention. The structural bonding of the insert and a mechanical tie achieved by hoop tension in the filament winding over the increasing diameter of the insert will provide the required retention.

Relative Merits of Each Configuration

The D-spar requires a stiffener bead on the bottom to break the large flat-plate area and to increase the buckle strength. This configuration cannot be roll-formed; it requires a method such as pressure forming or explosion forming, which would require a development program. Rotating flapwise natural frequencies for both steel and titanium D-spar blades were above the desired range because of high stiffness-to-mass

ratios. The less-stiff titanium D-spar blade had a lower frequency. Both blade frequencies could be improved by tuning mass suspension, but at a weight penalty.

Titanium forming would require more development than steel forming because of its higher yield strength in the annealed condition at room temperature.

A large store of experience backs up the use of steel D-spars. The properties of steel under fatigue stresses are well known for both notched and unnotched conditions. On the other hand, notching and surface condition appear to have a great effect on the fatigue properties of titanium. Fatigue tests of processed spar sections in titanium will be necessary to establish component endurance limits. The use of steel for either the hexagonal or D-spars requires a corrosion-protection coating of zinc plate and a chromate surface treatment to prepare a bondable surface. Titanium is corrosion-resistant and would not require treatment for that purpose, but acid etching is required to prepare bonding surfaces.

A steel hexagonal spar has the advantage of machined bonding surfaces with dimensions held to machining tolerances, which are considerably less than rolling or pressure forming tolerances. A blade with a hexagonal spar is inherently heavier than a D-spar blade. Its center of gravity is farther aft, and the initial study showed low chordwise stiffness and natural frequency, which require trailing-edge beef-up. Leading-edge wieght increases are then required to bring the section balance forward.

The trailing edge strip begins at the inboard end of the constant airfoil section and continues to the tip of the blade, increasing chordwise stiffness along the constant section. However, inboard of the constant section, chordwise stiffness drops and requires the use of a drag strut between the trailing-edge strip and a frame on the root socket for load carrying and chordwise-frequency tuning. Doublers bonded to the outer surface of the airfoil section are required to transfer shear loads from the drag strut attachment point to the spar. Higher weight and lower stiffness account for acceptable flapwise frequencies.

The plastic blade has the inherent structural redundancy of fiber-reinforced composites, which decreases the susceptibility to catastrophic failure due to mechanical notching or battle

damage. Fiberglass composites also eliminate the danger of corrosion damage common to metallic structures.

Internal damping minimizes the response to high-frequency excitations, thus reducing stress and vibration levels. Simplification of tooling concepts can mean a reduction in tooling costs and cost per blade. The low modulus of elasticity and high strength-to-weight ratio show excellent rotating natural frequencies and low fatigue stress levels. Blade contour can be aerodynamically cleaner because the skin is laid up and cured in full-contour female molds. Other blade dimensions should also show less variation (twist, camber, trailing-edge waviness, chord, and flapwise and chordwise bow). High-envelope dimensional control would decrease the rejection rate, cut cost and time, and yield uniform aerodynamic characteristics.

Honeycomb-core-to-skin bonding can impose fabrication problems because the honeycomb is unstable in the plane perpendicular to the cell, and the bonding agent has a low viscosity at cure temperature. However, care and sequencing of operations can minimize these effects. Although material costs are higher for a plastic blade than for a metal blade, the plastic blade seems to offer a higher margin of safety, less maintenance and overhaul, and low supply costs. These features added together could all prove the plastic blade cost/effective.

The plastic blade is the most promising avenue of design and fabrication for the heavy-lift helicopter. The steel D-spar blade should also be pursued as a second selection.

ROTOR HEAD FOR AN ARTICULATED ROTOR SYSTEM

The choice of rotor head (see Figures 1 and 130) for the articulated rotor system reflects a conservative design approach which is especially appropriate. The performance of the basic configuration has been proven, so improvements substantiated by testing enjoy a high level of confidence.

Two types of fully-articulated rotor have been used by Vertol Division: the Model 107 and H-21 type, and the CH-47A and HUP type. The essential difference between them is the location of the pitch axis with respect to the lag hinge (vertical pin). The 107 and H-21 type has the pitch axis outboard of the lag hinge; the CH-47A and HUP type has the pitch axis

between the lag hinge and flap hinge (horizontal pin). The model 107 and H-21 type is best suited to the heavy-lift helicopter because flapping loads do not induce pitching moments in the system when the blades lead or lag as they do on the CH-47A and HUP type. This will:

1. Eliminate the possibility of vibrations induced from this source and permit the use of a lighter and less rigid control system.

2. Prevent parked-blade loads from feeding back through the control system.

3. Prevent excessive blade droop in parked condition which would reduce blade-to-ground and blade-to-fuselage clearances.

Although a disadvantage in the 107 and H-21 type rotor is in the carrying of the rotor weight mass farther outboard (a factor conducive to vibration), this effect has been minimized by using a substantially shorter extension link. The length of the heavy-lift helicopter link is 1.5 percent of blade radius, where the Model 107 is 3 percent. Also, the flap hinge (horizontal pin) has been moved farther outboard than on the Model 107: 2.32-percent radius for the heavy-lift helicopter versus 1.70-percent on the Model 107. This will provide the benefit of increased control power in the roll sense.

While these factors are not particularly significant in the lighter aircraft, they have an important effect on the performance of a helicopter as large as the heavy-lift helicopter.

Materials

Titanium alloy is used on all major components of the system:

1. Hub

2. Horizontal pin

3. Extension link

4. Vertical pin

5. Pitch shaft

6. Pitch housing

7. Tension-torsion strap

8. Components of the hydraulic damper

9. Blade socket and tension-torsion-strap pins

Recent tests at Vertol Division on titanium blade sockets for CH-46A helicopters yielded encouraging results. There was almost no fretting on the shot-peened faying surfaces of the highly-loaded clevis-and-lug type connections. Therefore -- contrary to expectations -- no fretting problems were encountered in titanium.

Magnesium alloy castings are used for oil reservoir tanks. Aluminum or magnesium will be used for other nonstructural applications. Steel will be used for bushings, bearings, and hardware.

Hub Retaining Plate

A hub retaining plate has several advantages over the large single nut used on the CH-47A and Model 107 types:

1. Bolts provide greater reliability than a single nut. Failure or loosening of a few bolts would not cause failure of the connection.

2. Torque wrenches for bolts are standard equipment, while the large wrench required for the nut would be bulky, expensive, and not standard equipment.

Pitch-Link Rod End Bearing

The pitch-link rod end bearing consists of a needle bearing outer element integral with a spherical dry bearing inner element. The assembly is oriented so that pitch motion occurs about the roller axis. Misalignment induced by flapping and lead-lag motion occurs about the spherical ball within the self-alignment capability of the bearing. Pitch motion will occur about the rollers rather than about the sphere because the rollers have a substantially lower coefficient of

friction than the Teflon liner. This arrangement r duces the velocity, and therefore the pressure-velocity (PV) factor, for the dry bearing element to an allowable range for this high-load application. The roller element is designed for grease-type lubrication. Lubrication is required at infrequent intervals: in the order of once every 100 to 200 hours. The bearing is lubricated or purged through the flush-type lubrication fitting on the lower body of the rod end.

This type of rod end combines the requirements of high-load and high-misalignment capability into one relatively small unit (the H-21 pitch link has nine bearings). An alternate design for this requirement might be a trunnion, but it would be heavier and more costly, and it would impose a greater maintenance burden.

Tension-Torsion Strap

The tension-torsion strap is of the same redundant design configuration used, and proven to be reliable, on all present Vertol Division helicopters. For the heavy-lift helicopter, however, it is made of laminations of titanium plate rather than steel plate. The titanium strap weighs approximately 198 pounds per helicopter, compared to 276 pounds per helicopter for a structurally equivalent steel strap.

A new and promising concept for tension-torsion straps is being tested and developed at the present time. It consists of strands of wire wrapped longitudinally over end connections, with a polyurethane matrix and a circumferential wire jacket to contain the wires and keep them properly oriented during tie bar operation. The more efficient load distribution inherent in this strap makes possible lower weight and longer life than the laminated plate counterpart. A wire-wound strap of the same length as the 28-inch laminated titanium strap shown would weigh approximately 159 pounds per helicopter, 29 pounds less than the titanium strap. Although preliminary testing of the wire-wound strap has been successful, it is not the primary choice because it does not have the performance-proven experience record of the laminated type.

Blade Connection

The blade connection is similar to that used on the Model 107, but it is improved in detail design features. It consists of two vertical pins installed through multiple lugs on the pitch

housing and blade socket. The multiple lug design offers the fail-safe feature of additional limited service life in the event of the failure of the outer lugs (those at top and bottom of the connection, most distant from the pitch axis), and it also serves as a hinge for manual blade folding.

When the blades are to be removed, both pins are withdrawn. When the blades are to be folded, one of the pins is withdrawn (either one, depending on the direction of folding required for that blade), and the blade is rotated about the remaining pin.

On the Model 107, tapered pins are used to eliminate play and possible hole elongation from pounding. Experience has shown that this type of pin is difficult to remove in the field, and the joint is subject to fretting and galling when blades are removed or folded. The design presented here is intended to correct these conditions. It employs close-tolerance straight pins fitted with a small positive clearance to facilitate removal. The pin geometry is arranged to prevent load reversals at the pins and thus to prevent hole elongation from pounding. Dry bearings are installed in the pitch housing lugs to prevent pin fretting during folding. A pitch lock pin is provided for orientation and lockout of blade pitch during this operation.

Bearings

Because of the significantly lower cost, weight, and maintenance associated with dry bearings, every effort has been made to make as widespread use of them on this rotor hub assembly as our experience and testing permit.

Dry bearings made of Teflon fabric are used on the vertical pin, blade disconnect fittings, and in part on the pitch link. The basic limitation for this type of bearing is the pressure-times-velocity (PV) factor. PV may vary with type of motion, load distribution, temperature, mating surface finish, and fit. Moreover, if the diameter is increased to reduce the area loading, the velocity increases adversely (for a given angular velocity of motion). Dry bearings can be used on the vertical pin because the oscillating angle is relatively small and the unit pressure can be reduced by the use of multiple lugs, rather than by a diameter increase. Full-scale bearings of this type have been successfully tested for the CH-47A helicopter. For the heavy-lift helicopter, the Teflon fabric

bearings in the multilug lag hinge will operate at a PV of 25,000. This bearing is 3 inches in diameter, which is within the range of presently tested bearings under lag hinge conditions. Based on our experience with life and environmental testing of bearings of this size under rotor hinge conditions, the Teflon fabric lag hinge will not only contribute to low initial cost, but will also provide maintenance-free service between rotor overhauls.

The other two hinges (horizontal and pitch) are designed for oil bath needle bearings. However, the tests of dry bearings now in progress will continue. The rotor hub is designed to accept dry bearings in these hinges with a minimum of modification.

ROTOR CONTROLS FOR AN ARTICULATED ROTOR SYSTEM

The rotor controls system shown in Figures 1, 131, and 132 represents a partially integrated concept of transmission, controls, and rotor hub which minimizes the space and weight requirement of the system.

The transmission case has been extended so that the upper rotor shaft support bearing is inside the swashplate slider guide.

The spherical ball-slider swashplate gimbal design with dry-lubricant Teflon fabric bearings is similar to that used in the CH-47A helicopter and has given maintenance-free service while permitting a degree of compactness not present in previous rotor control systems.

The stationary swashplate ring is supported by three control actuators to provide collective, longitudinal, and lateral cyclic swashplate motion. An antitorque scissors permits mounting the actuators in spherical bearings and eliminates any possibility of the actuators' carrying side loads.

The collective-pitch bungee (Figure 133) is most effectively located in the lower control system. However, the ball-slider arrangement cannot transmit the bungee loads. Either an alternate linkage must be developed to operate the base of the actuators through the collective system, or the ball-slider must be abandoned in favor of a less compact and more complex gimbal ring.

The swashplate bearing is a double-row angular-contact bearing

of conventional design. The oil lubrication system provides dependable, maintenance-free operation as experienced by the CH-47A. The design of this bearing and related components is backed up by operational experience and considerable component testing. Dry-lubricant bearings have been considered for the swashplate bearing, but the design requirements exceed the capability of any dry lubricant bearings tested so far by Vertol Division.

The rainshield has been eliminated to make the rotor system more compact. Experience with the CH-46A indicates that the aerodynamic drag of an unfaired swashplate assembly will be less than that of a completely faired pylon.

With the exception of the swashplate bearing, all of the upper control bearings are dry-lubricant bearings made of Teflon fabric. Dry-lubricant bearings of this type have had extensive environmental testing, and they are operating satisfactorily exposed to the weather in the upper pitch links and lag dampers of the CH-46A and CH-47A. The environmental protection provided by a rainshield is not needed for these components.

Both the CH-46A and CH-47A helicopters use oil-lubricated bearings in the rotor hub hinges, which are constantly exposed to the weather, with no adverse effect. No further development of design technology will be required to ensure satisfactory performance of the oil-lubricated swashplate assembly under the same conditions of exposure. Adequate drainage is provided to prevent entrapment of water which could cause icing or penetrate the seals.

HINGELESS ROTOR HUB AND PLASTIC BLADE

The hingeless rotor hub is shown in Figure 134. The plastic blade designed for the hingeless rotor is shown in Figure 135.

ELASTOMERIC ROTOR HUB

A rotor hub with one elastomeric bearing per blade to provide articulation in flap, lag, and pitch offers very great potential for a compact, lightweight, maintenance-free rotor hub (see Figure 136). A design study comparing this elastomeric bearing hub with a CH-46A-type hub, where the loads are known, showed the following major advantages for the elastomeric design:

1. A 60-percent reduction in the number of major components

2. A 25-percent reduction in weight

3. The resultant reductions in cost due to the weight and parts savings

4. A 17-percent reduction in drag

These factors suggest a breakthrough in rotor hub design. The concept seems so promising that elastomeric rotor hubs are being designed for growth versions of the CH-46 helicopter. Full-scale hubs will be built, and all components will be qualified for flight testing. However, the elastomeric rotor hub should be investigated in more depth before it is chosen as the primary concept for the heavy-lift helicopter. When design of the growth CH-46 hub has been completed, a better comparison can be made of the elastomeric hub and the conventional articulated hub. At that point, accurate projections can be made for the heavy-lift helicopter (the concept is not size-limited). In the meantime, the conventional articulated hub is used for weight and performance predictions, without relying on advances in the state of the art.

SECTION A.A.

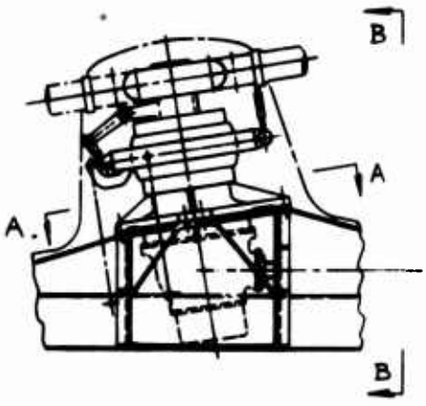

ASSEMBLY OF ROTOR TO STRUCTURE.
- FORWARD ROTOR.
SCALE :- 1/20

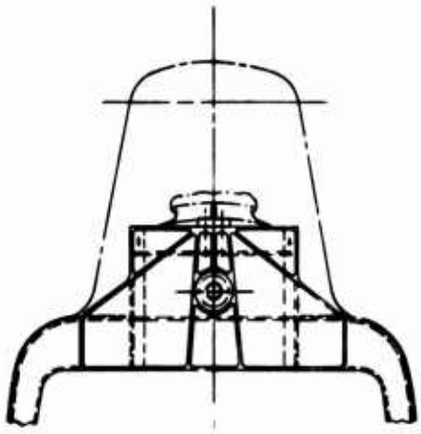

SECTION B.B.

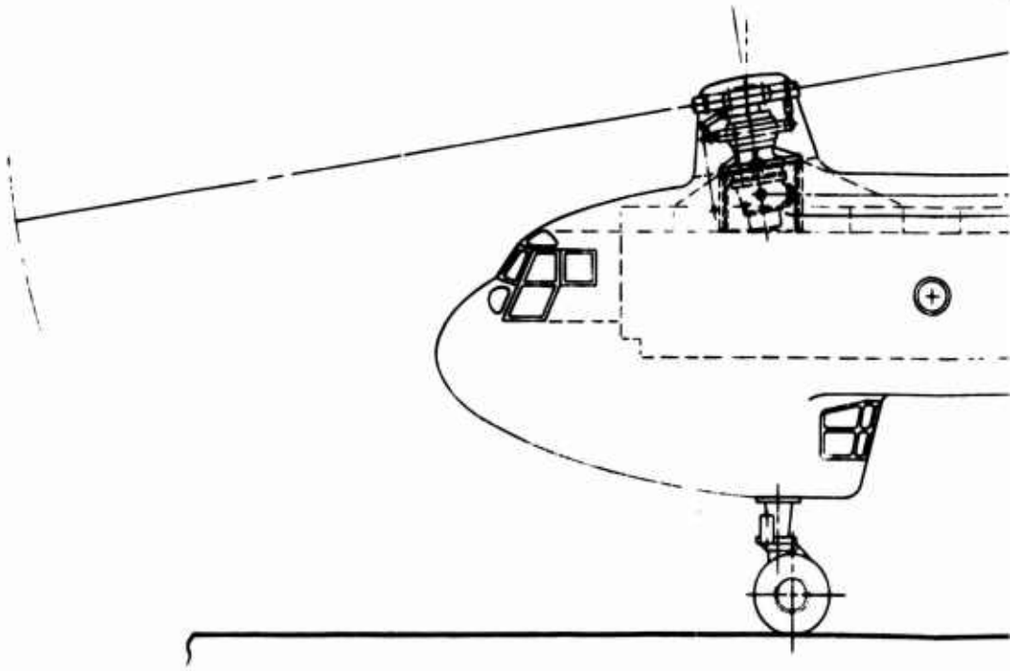

Figure 125. Pylon Structure for Forward and Aft Rotors.

A

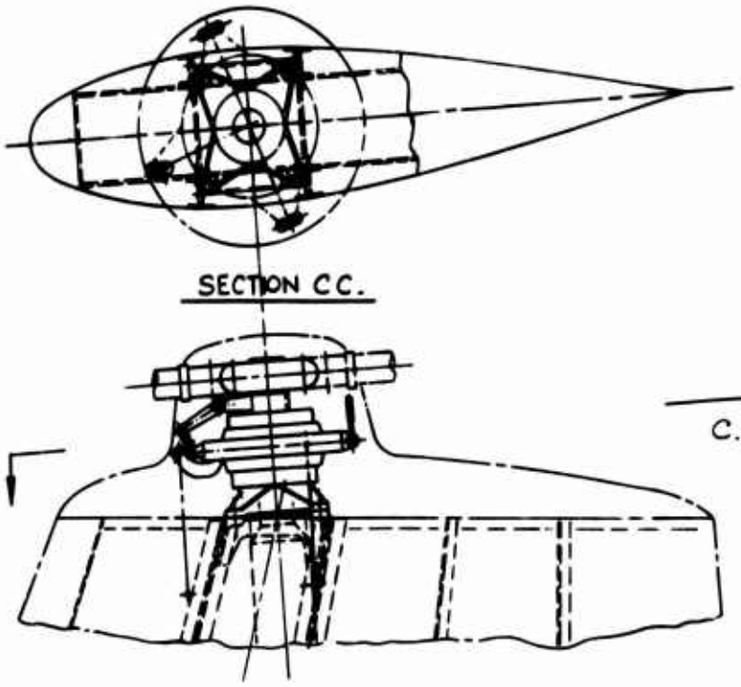

SECTION CC.

ASSEMBLY OF ROTOR TO STRUCTURE.

— REAR ROTOR. —

SCALE: 1/20.

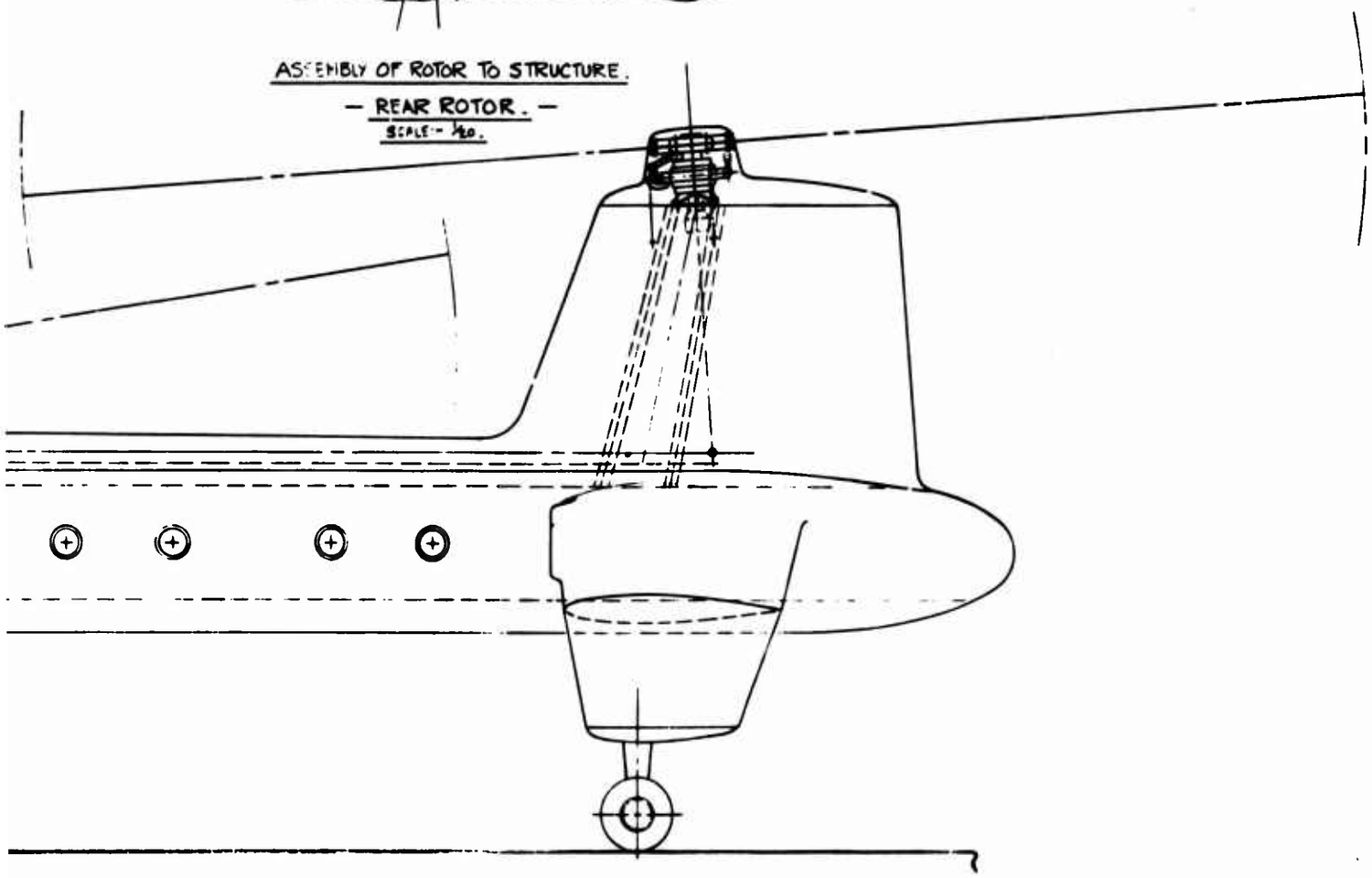

B

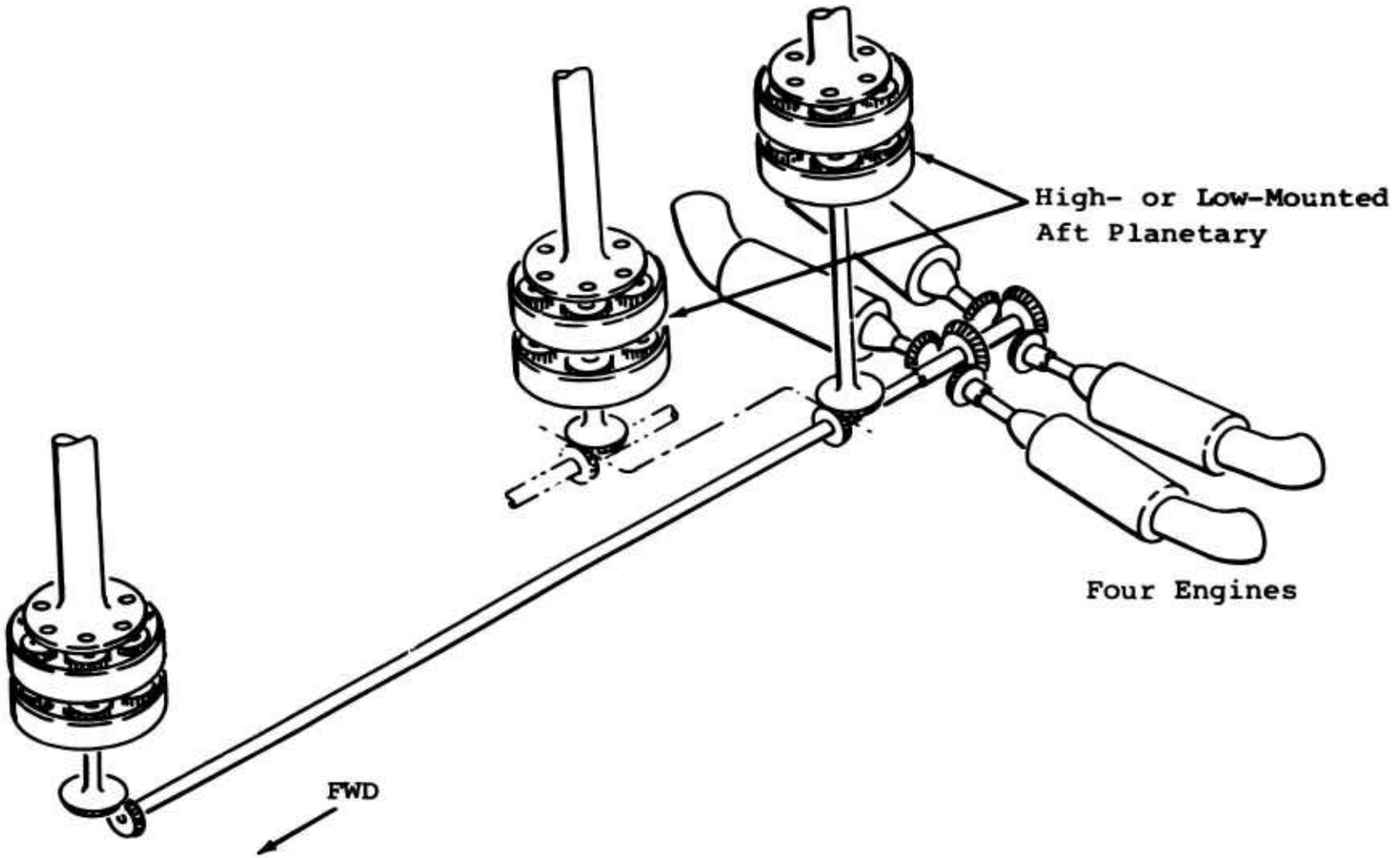

Figure 126. Powerplant and Drive System.

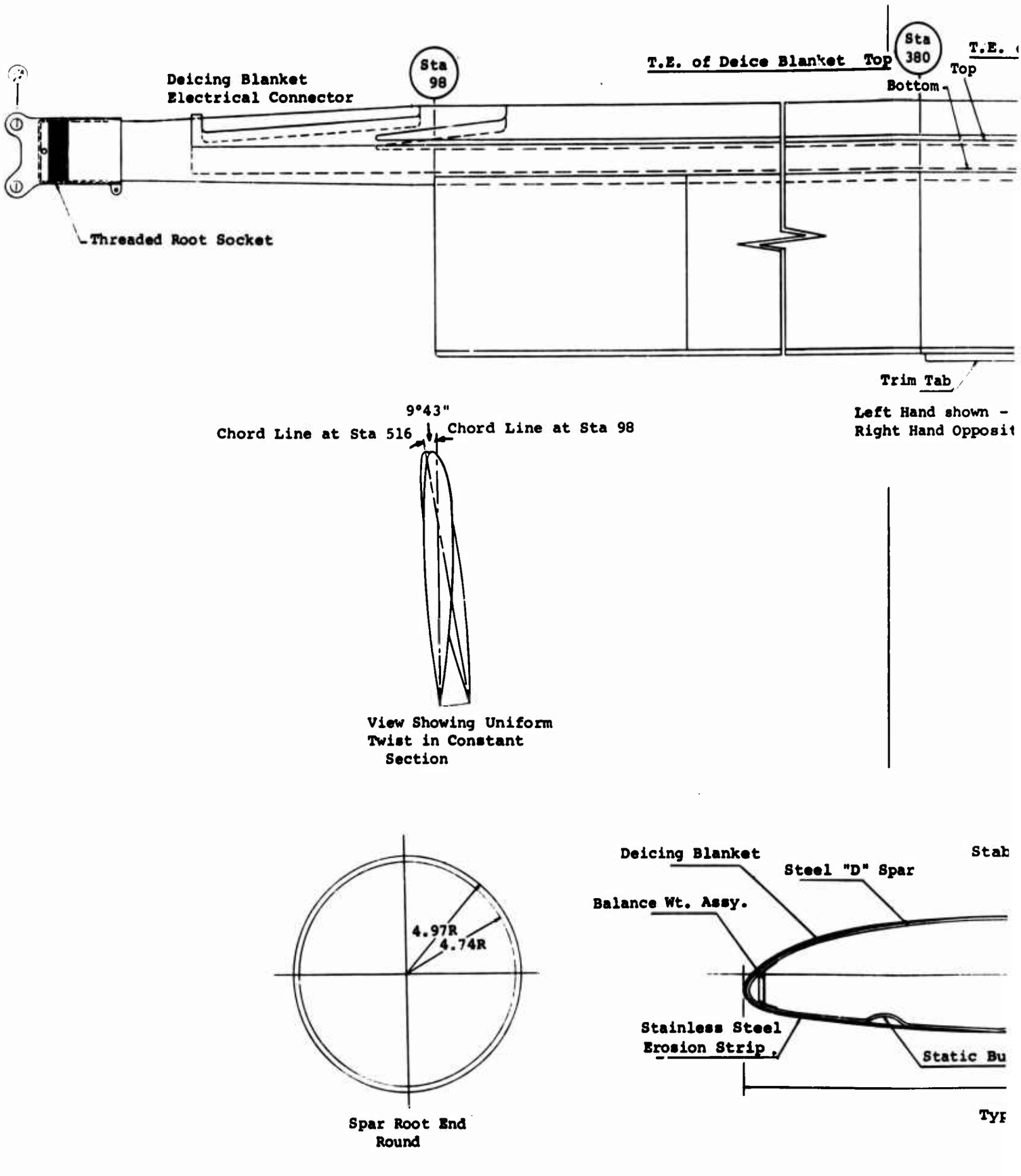

Figure 127. Metal D-Spar Nonsymmetrical Rotor Blade.

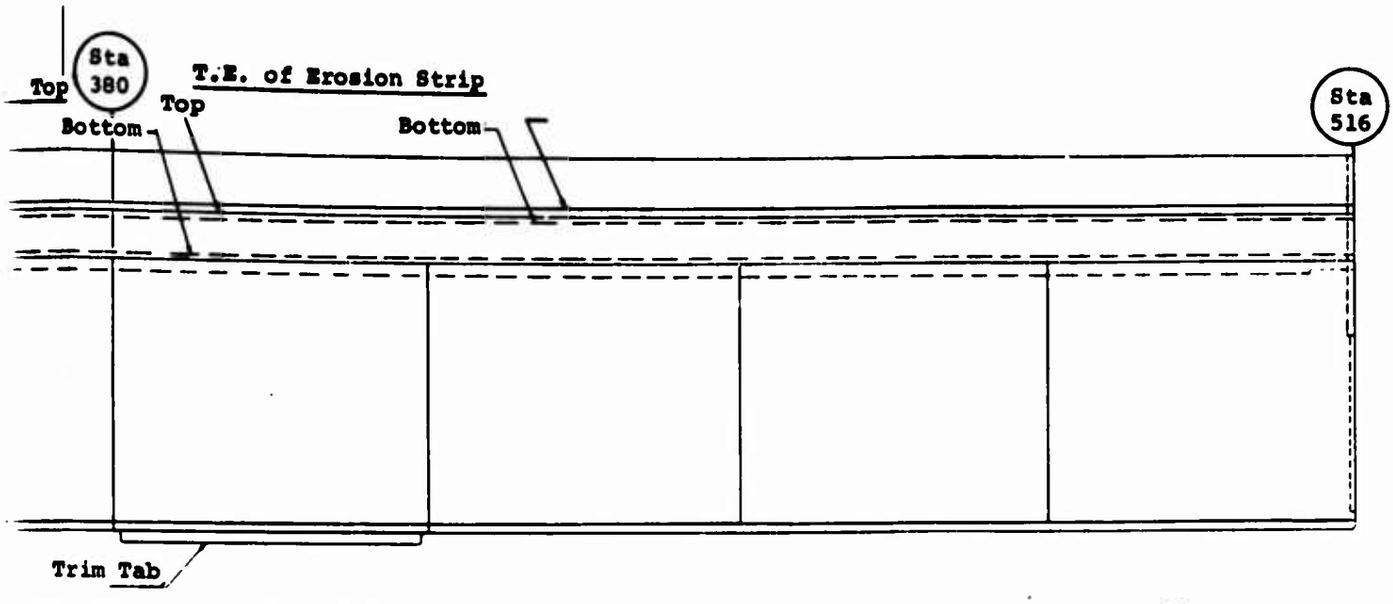

Left Hand shown - Fwd Blade
Right Hand Opposite - Aft Blade Scale: ½

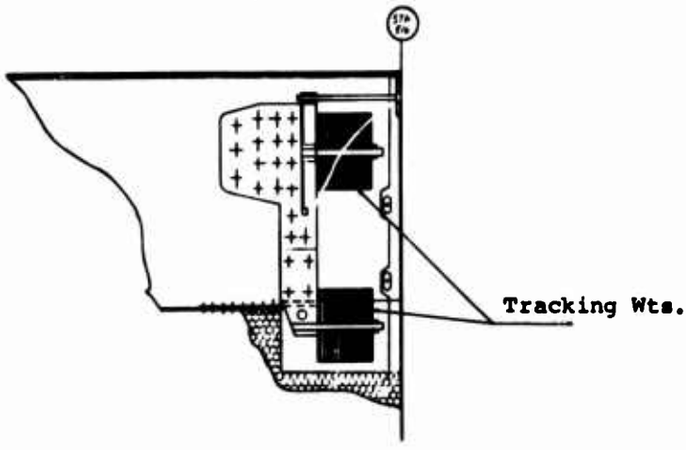

Section Thru Chord ℄ at Tip
Scale: ½

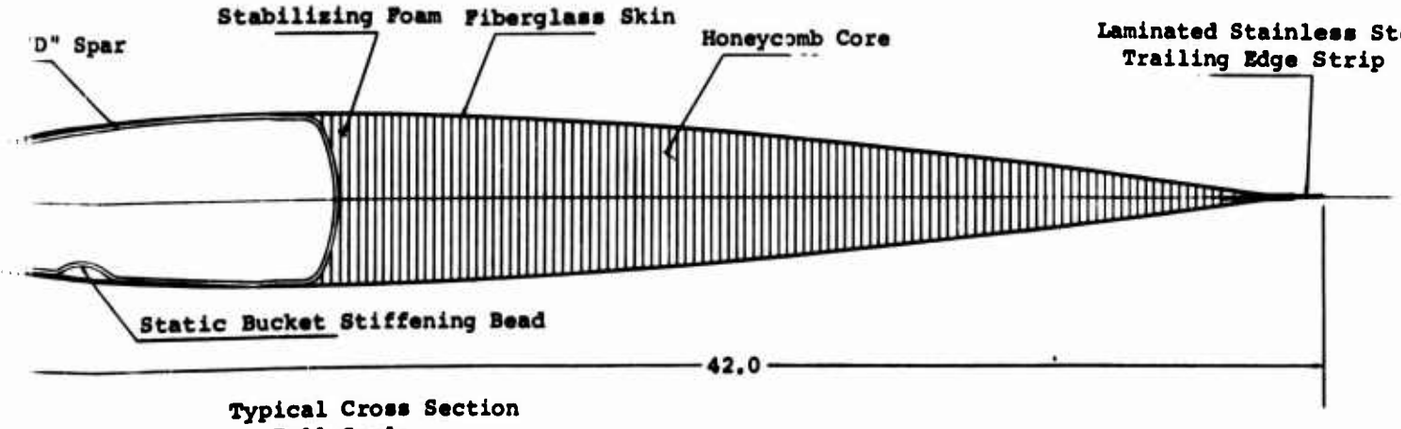

Typical Cross Section
Full Scale

B

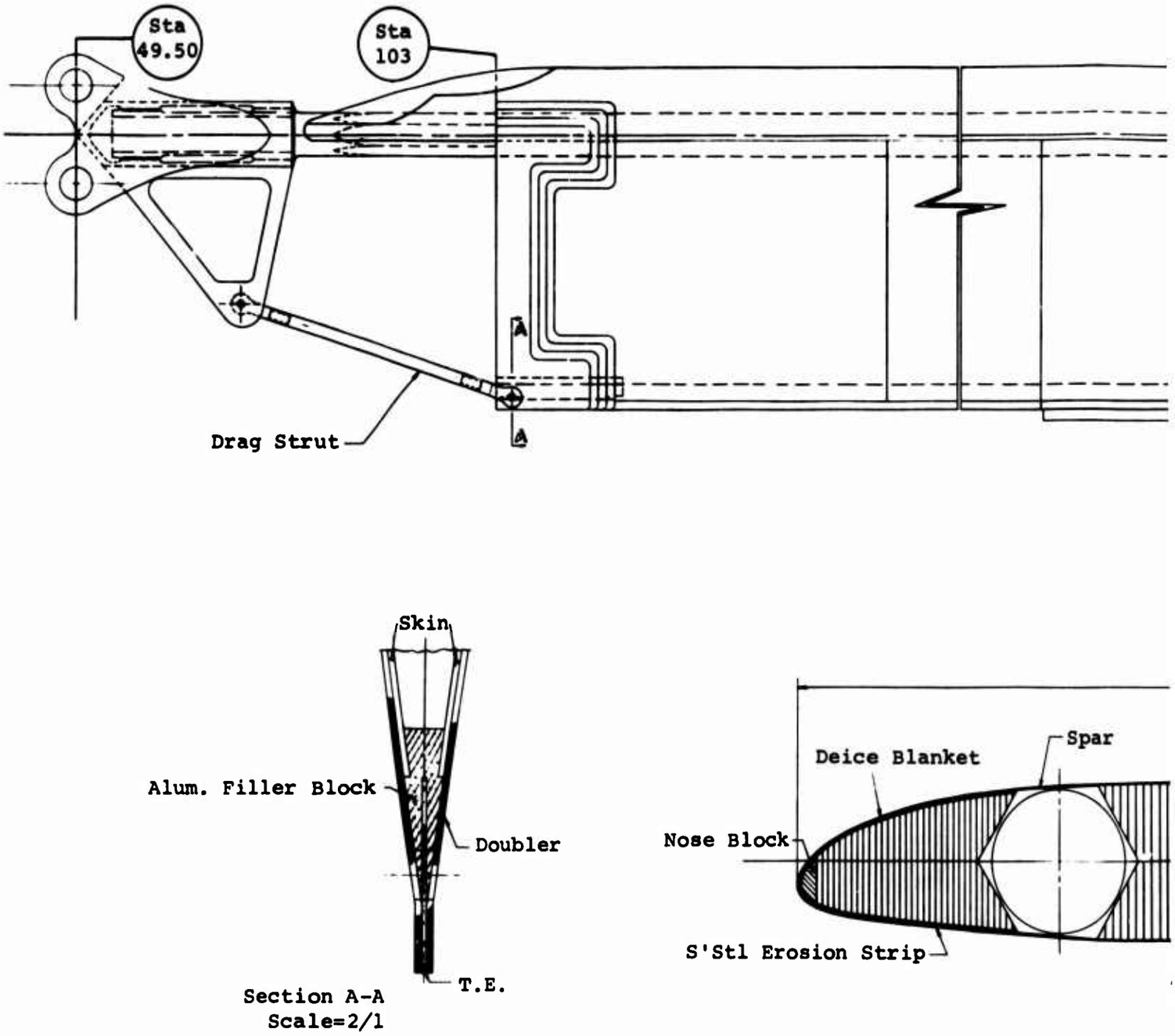

Figure 128. Steel Hexagonal-Spar Rotor Blade.

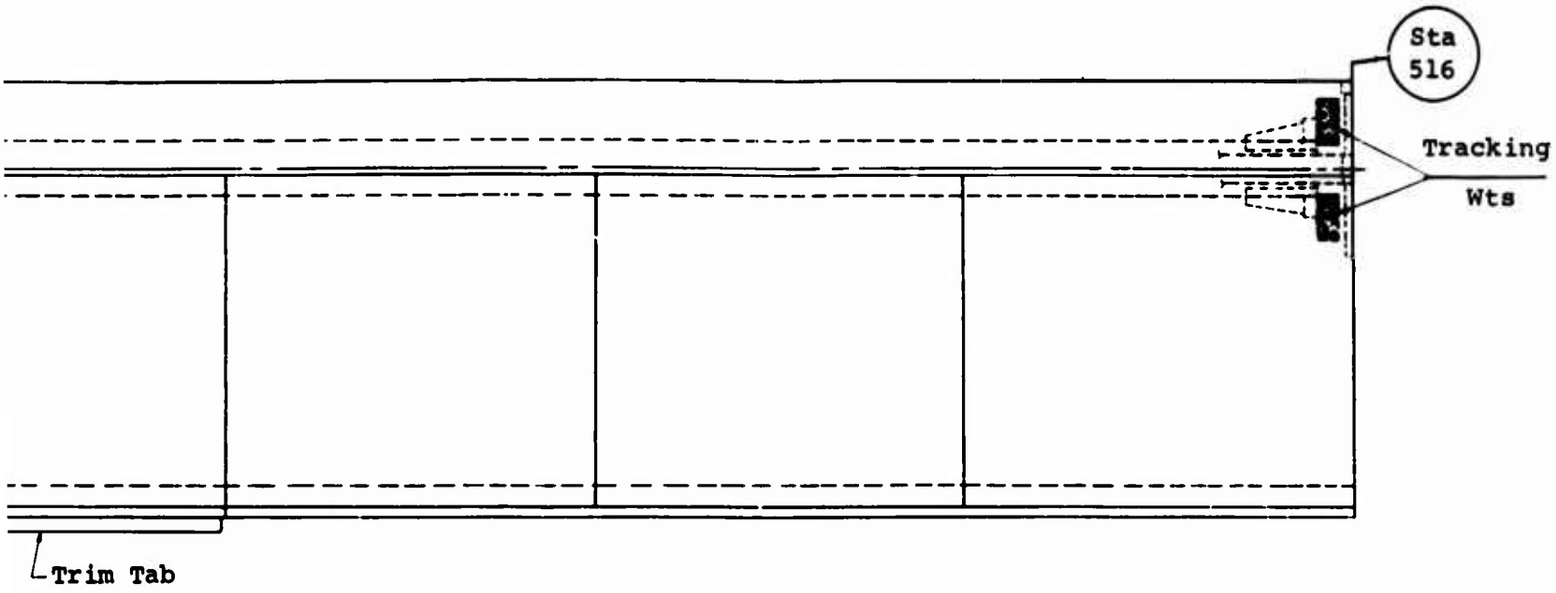

Plain View-Blade Assy
L.H. Shown R.H. Opp.
Twist Omitted for Clarity
Scale-1/4

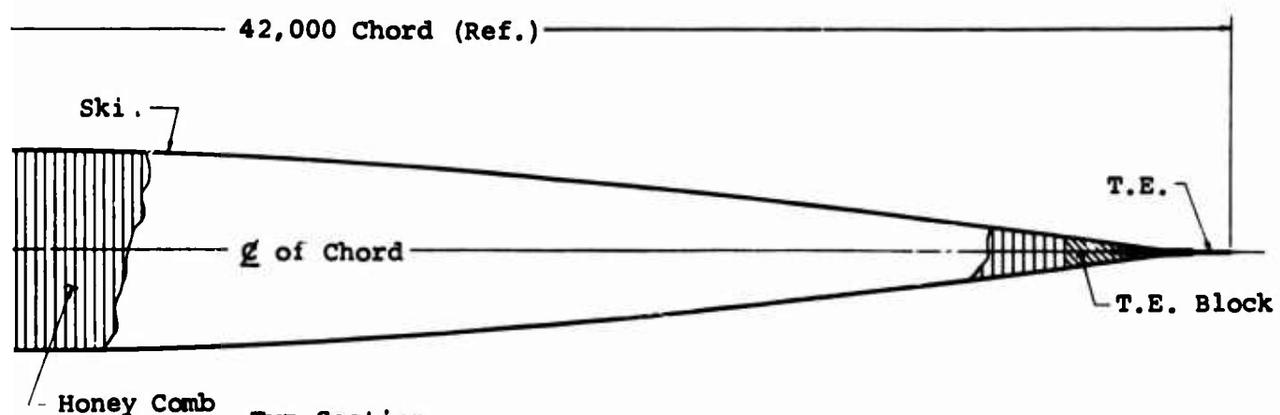

Typ Section
Rotated 90° C'Clk. W.

B

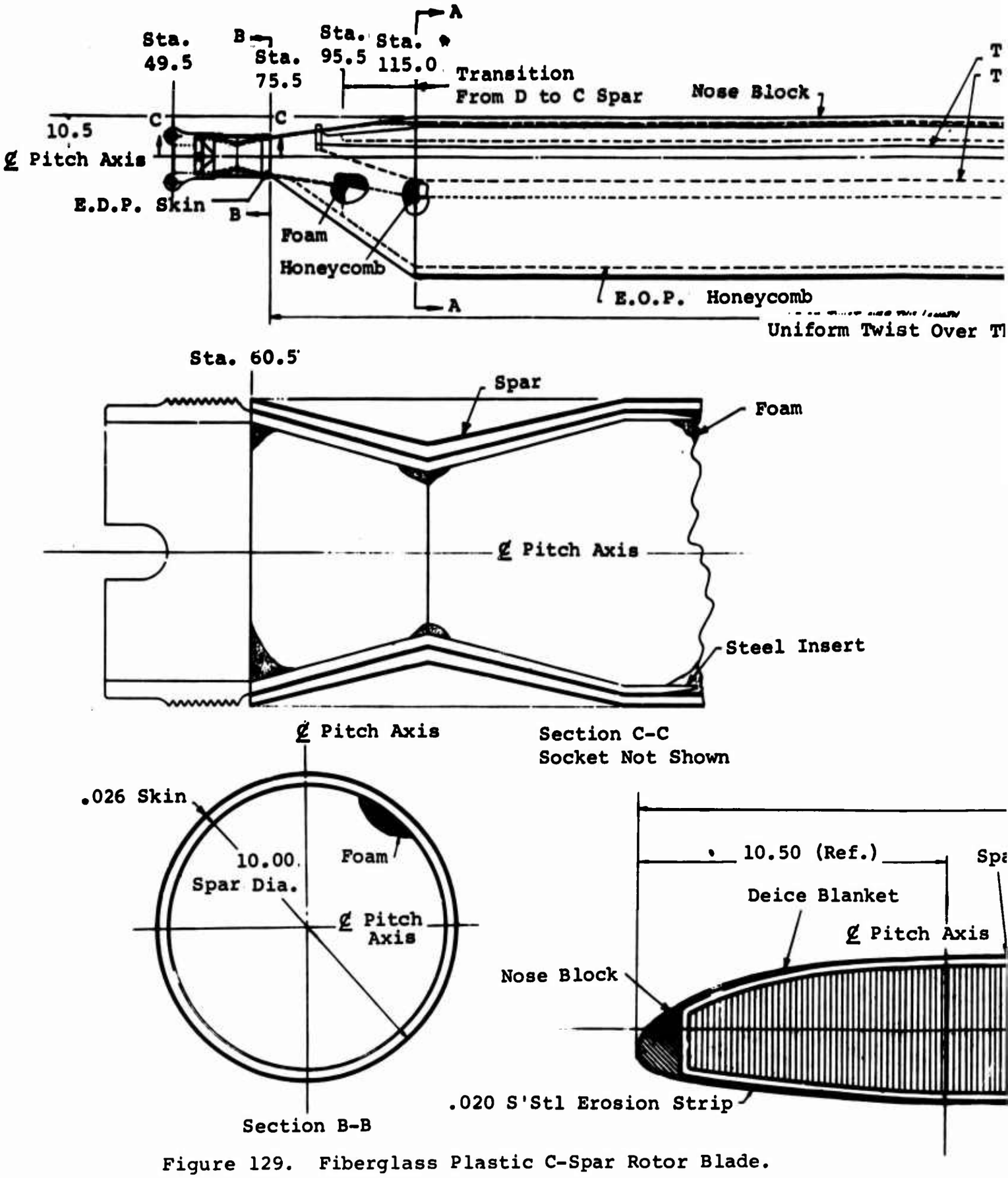

Figure 129. Fiberglass Plastic C-Spar Rotor Blade.

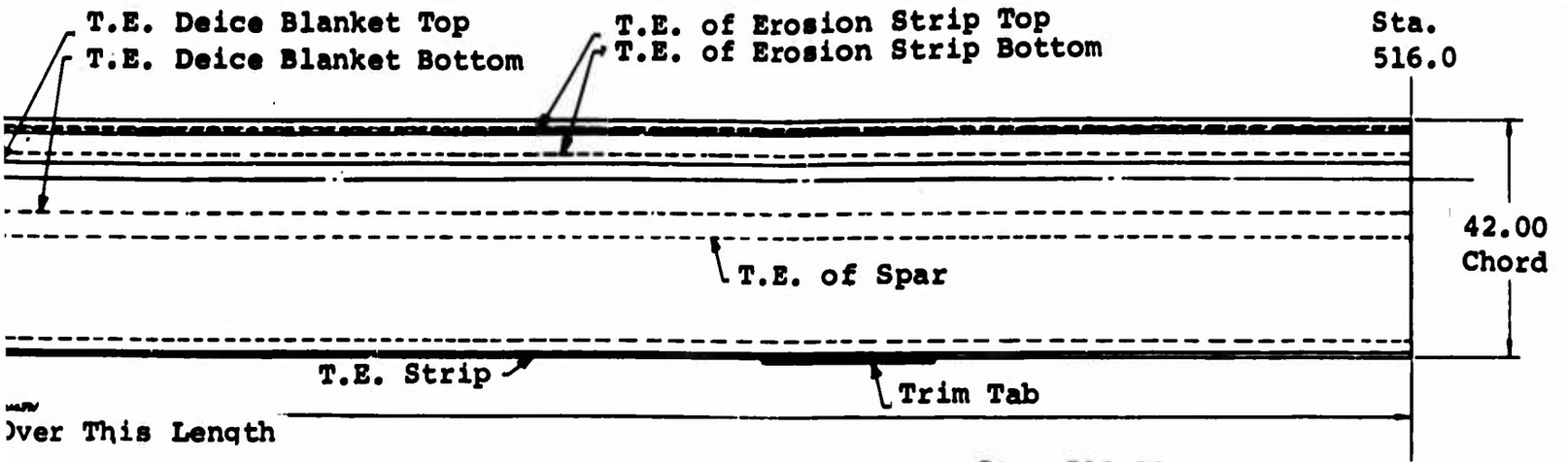

Plan View - Blade Assembly
L.H. Shown R.H. Opp.
(Twist Omitted for Clarity)
Scale: 1/8

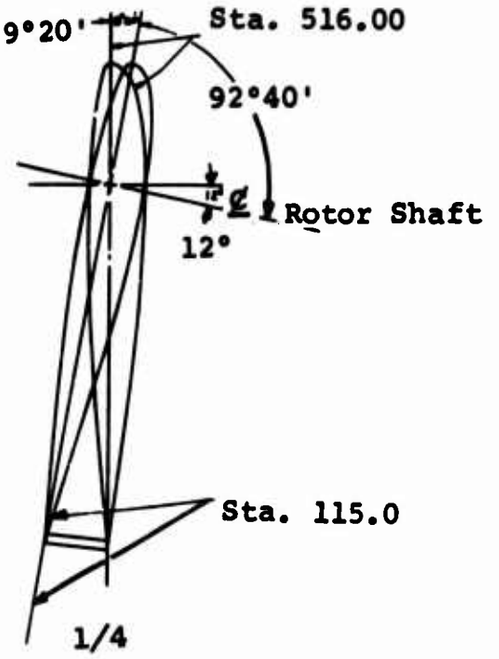

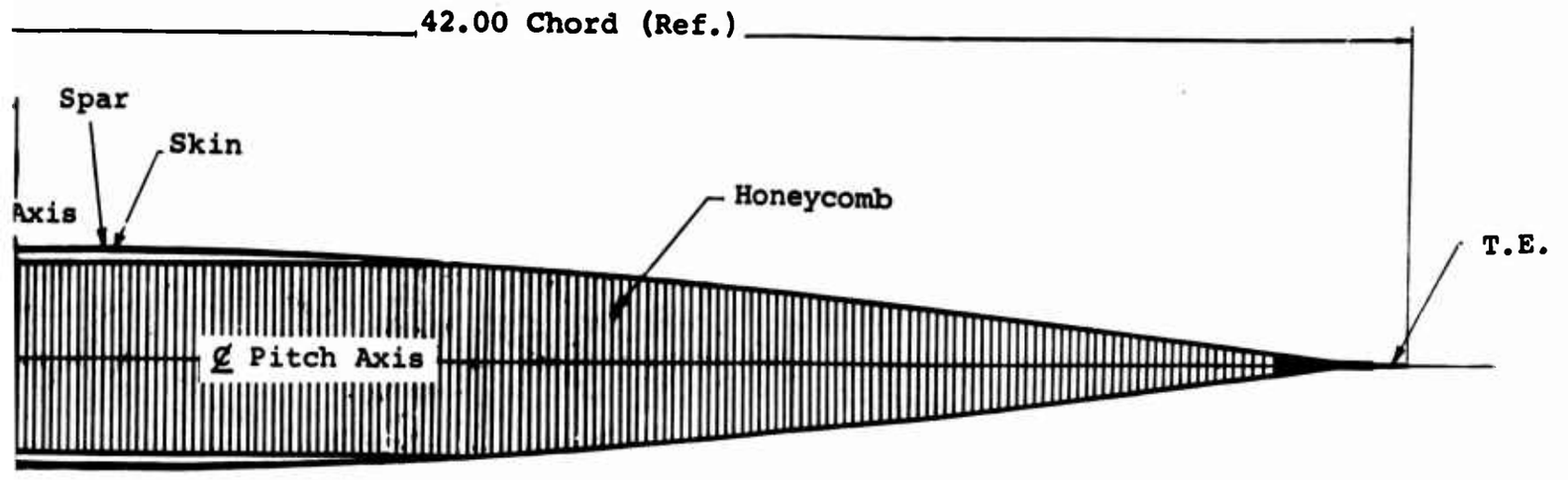

Section A-A
Rotated 90° C'Clk

B

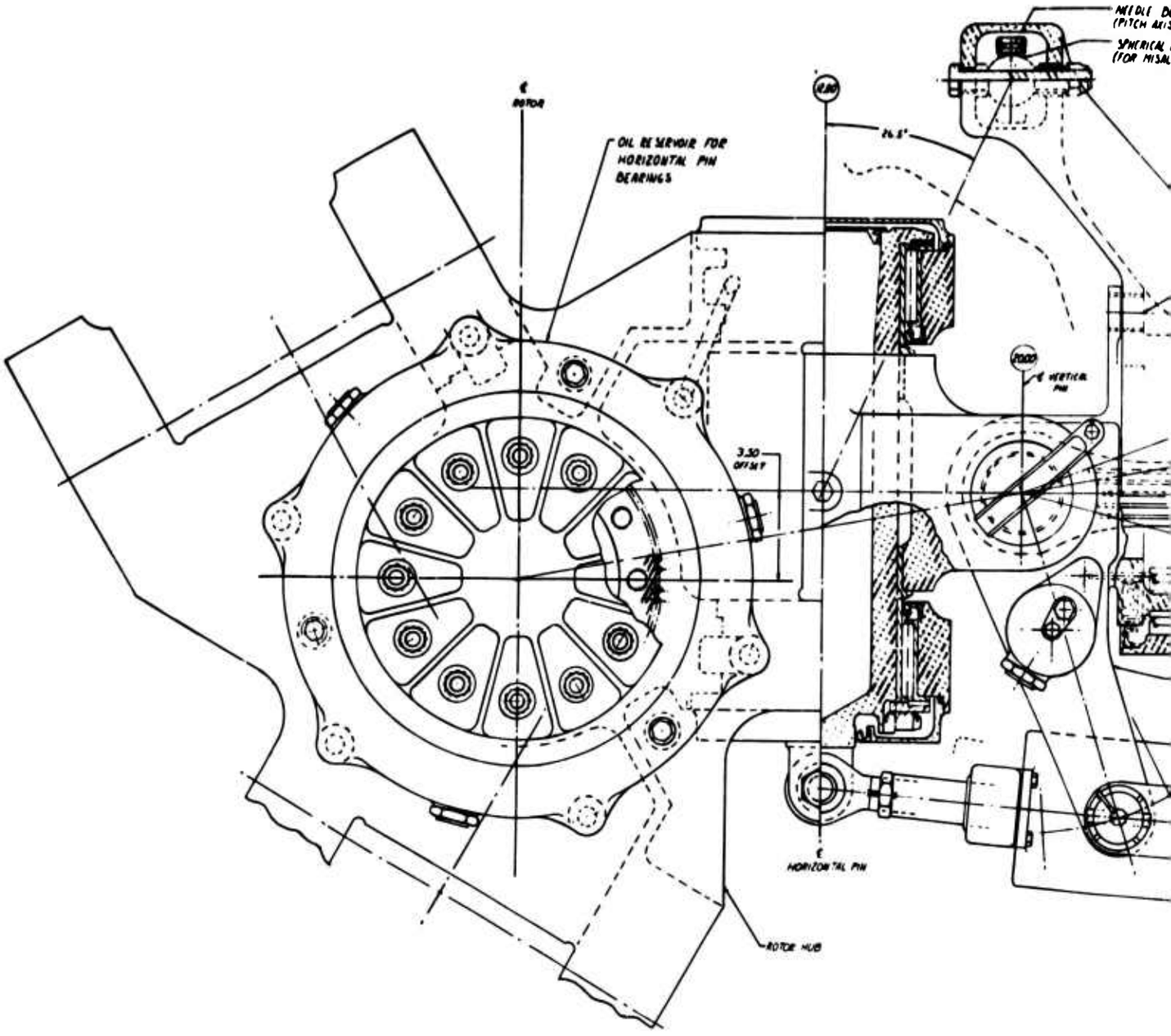

Figure 130. Articulated Forward Rotor Hub. (Sheet 1 of 2)

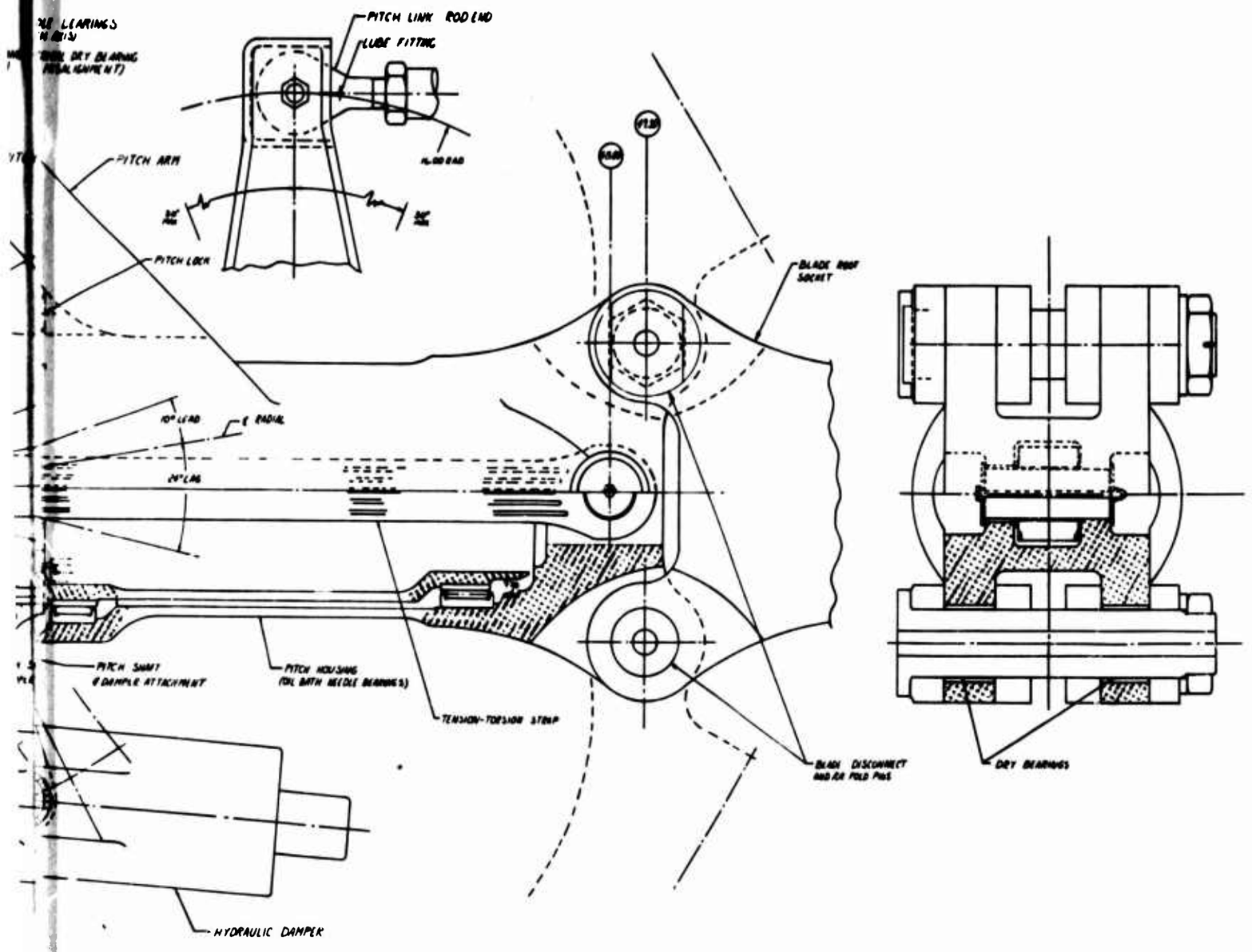
PITCH LINK ROD END
LUBE FITTING
PITCH ARM
PITCH LOCK
BLADE ROOT SOCKET
10° LEAD
E RADIAL
24° LAG
PITCH SHAFT & DAMPER ATTACHMENT
PITCH HOUSING (OIL BATH NEEDLE BEARINGS)
TENSION-TORSION STRAP
BLADE DISCONNECT AND AIR FOLD PINS
DRY BEARINGS
HYDRAULIC DAMPER

B

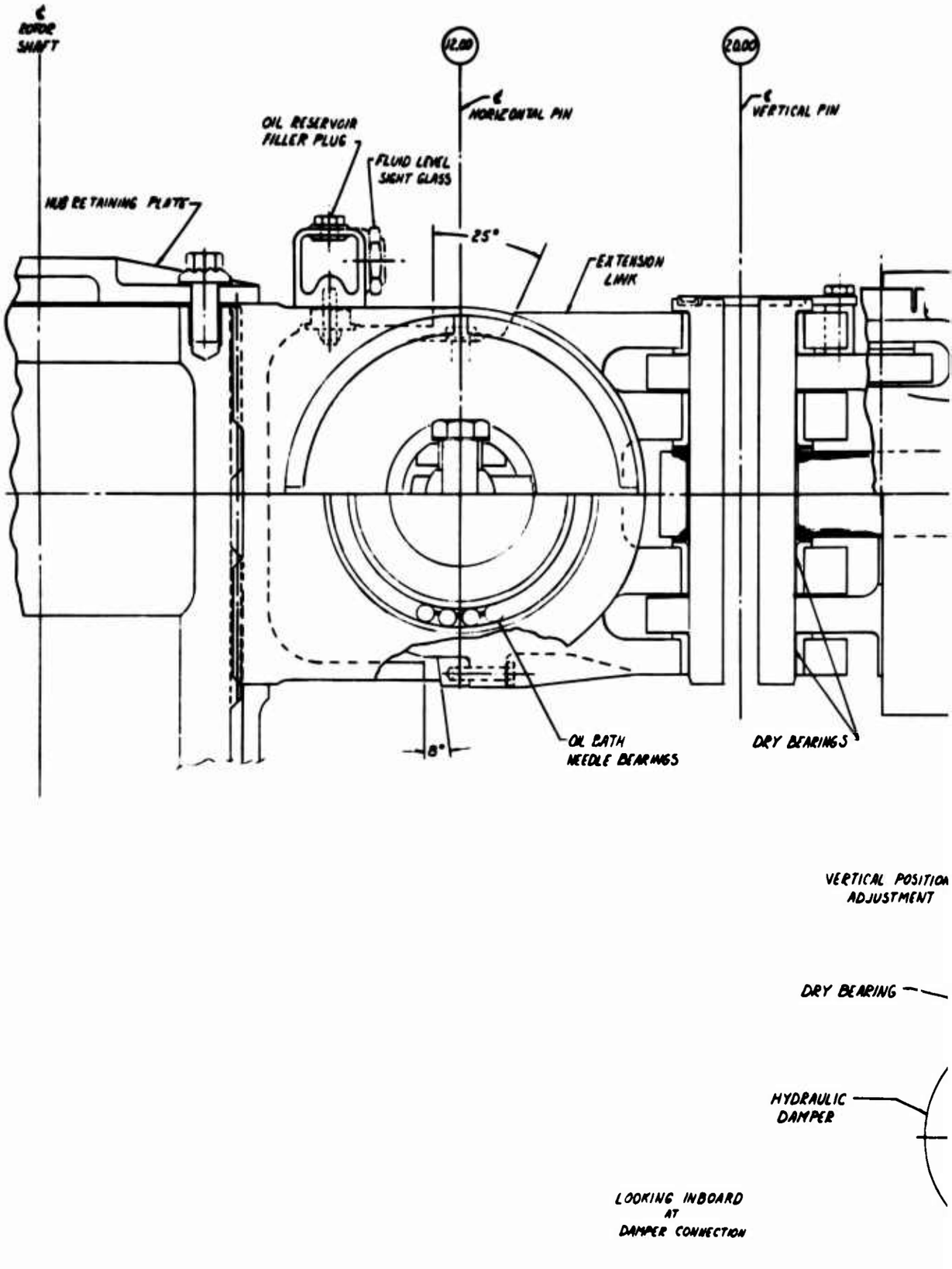

Figure 130. Articulated Forward Rotor Hub. (Sheet 2 of 2)

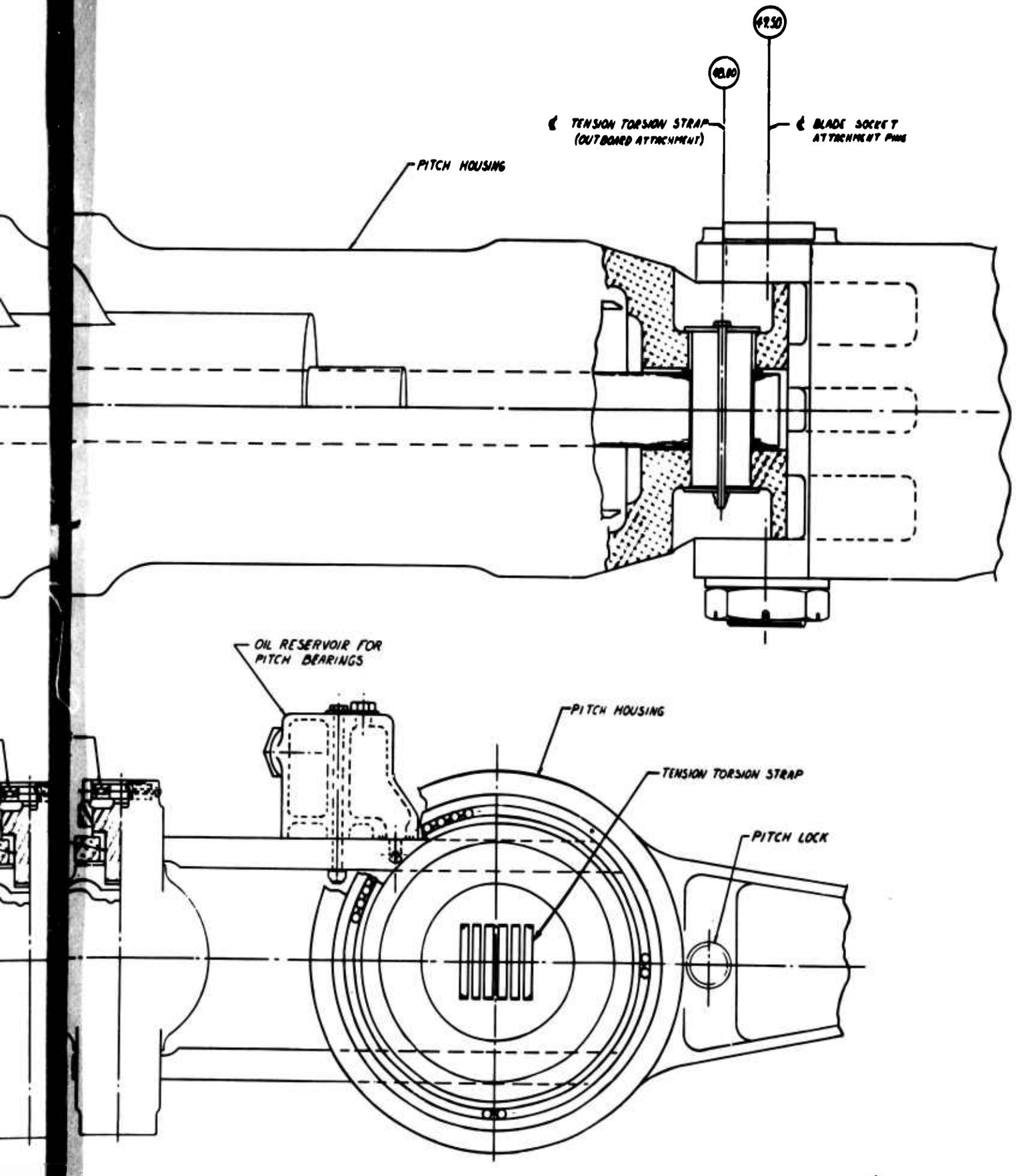
42.50
40.00
℄ TENSION TORSION STRAP (OUTBOARD ATTACHMENT)
℄ BLADE SOCKET ATTACHMENT PINS
PITCH HOUSING
OIL RESERVOIR FOR PITCH BEARINGS
PITCH HOUSING
TENSION TORSION STRAP
PITCH LOCK

B

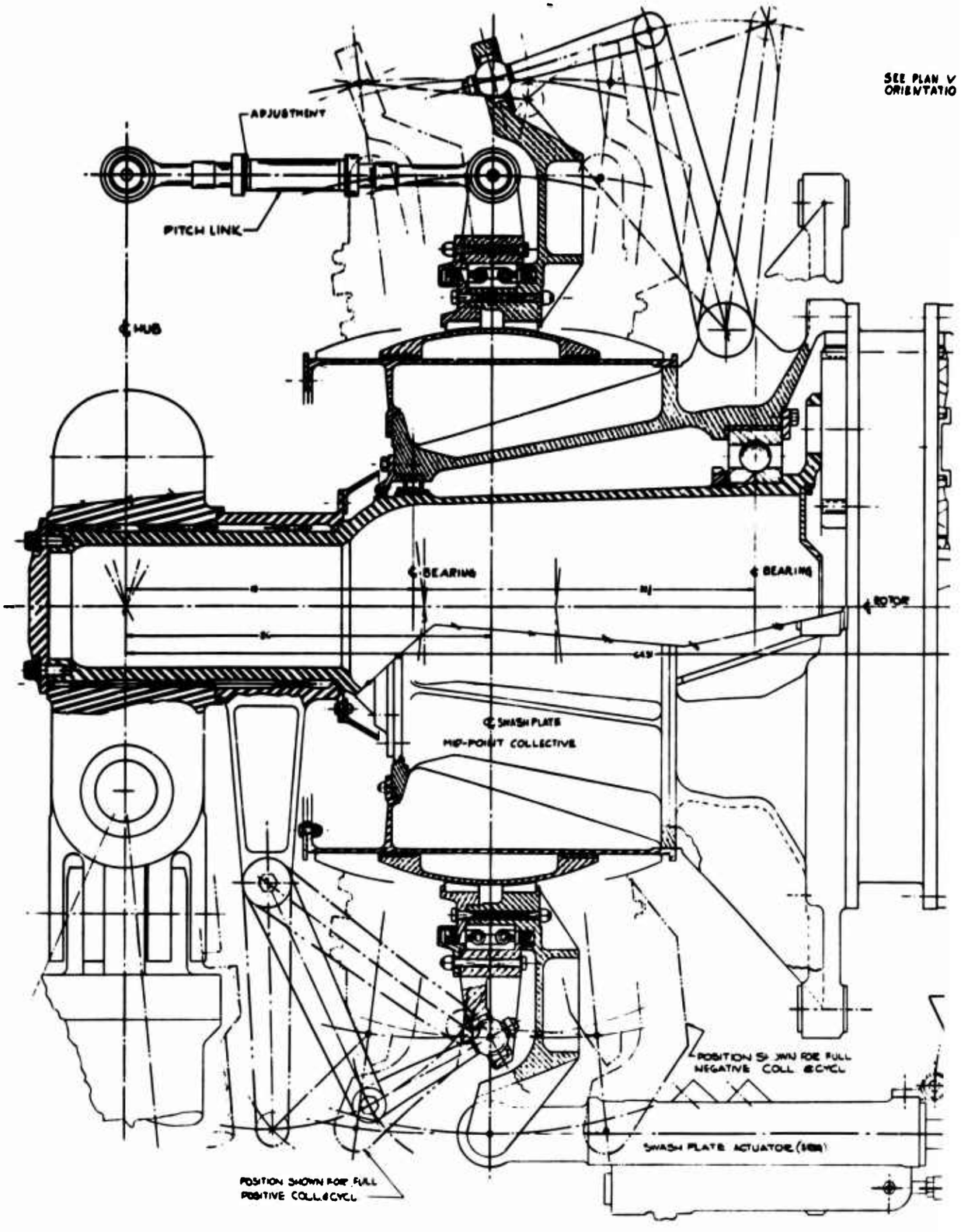

Figure 131. Forward Rotor Upper Controls. (Sheet 1 of 2)

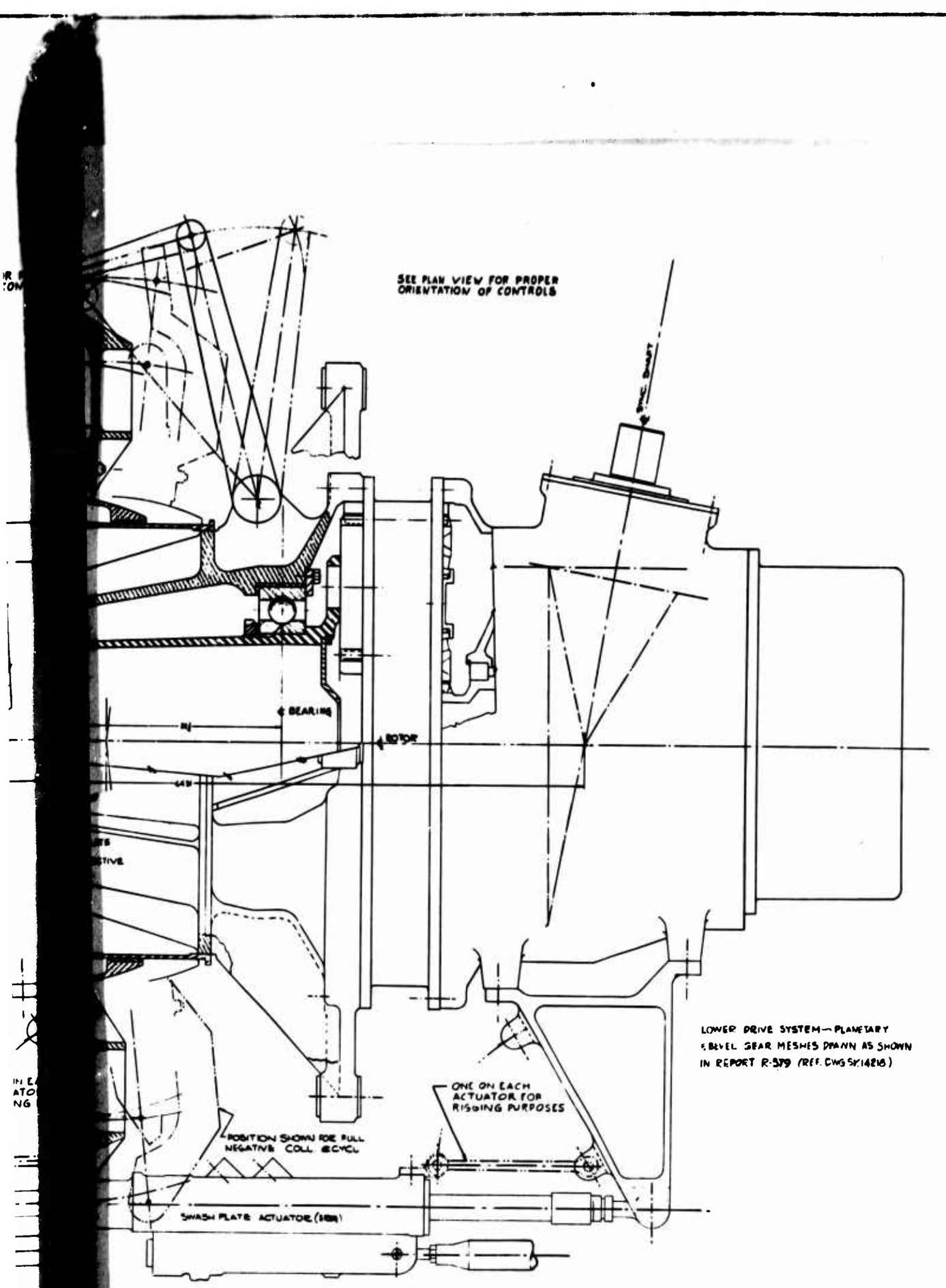

rols. (Sheet 1 of 2)

B

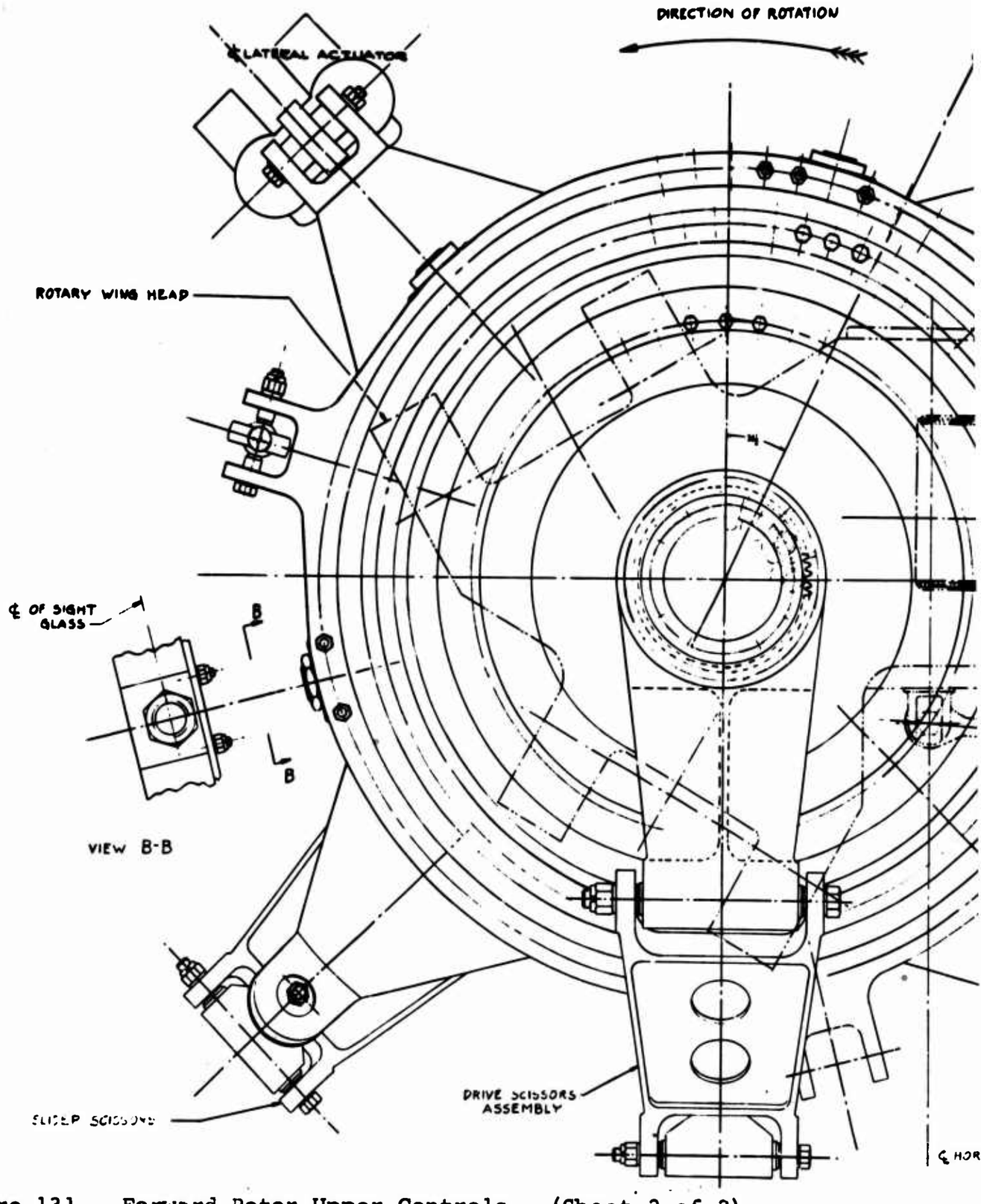

Figure 131. Forward Rotor Upper Controls. (Sheet 2 of 2)

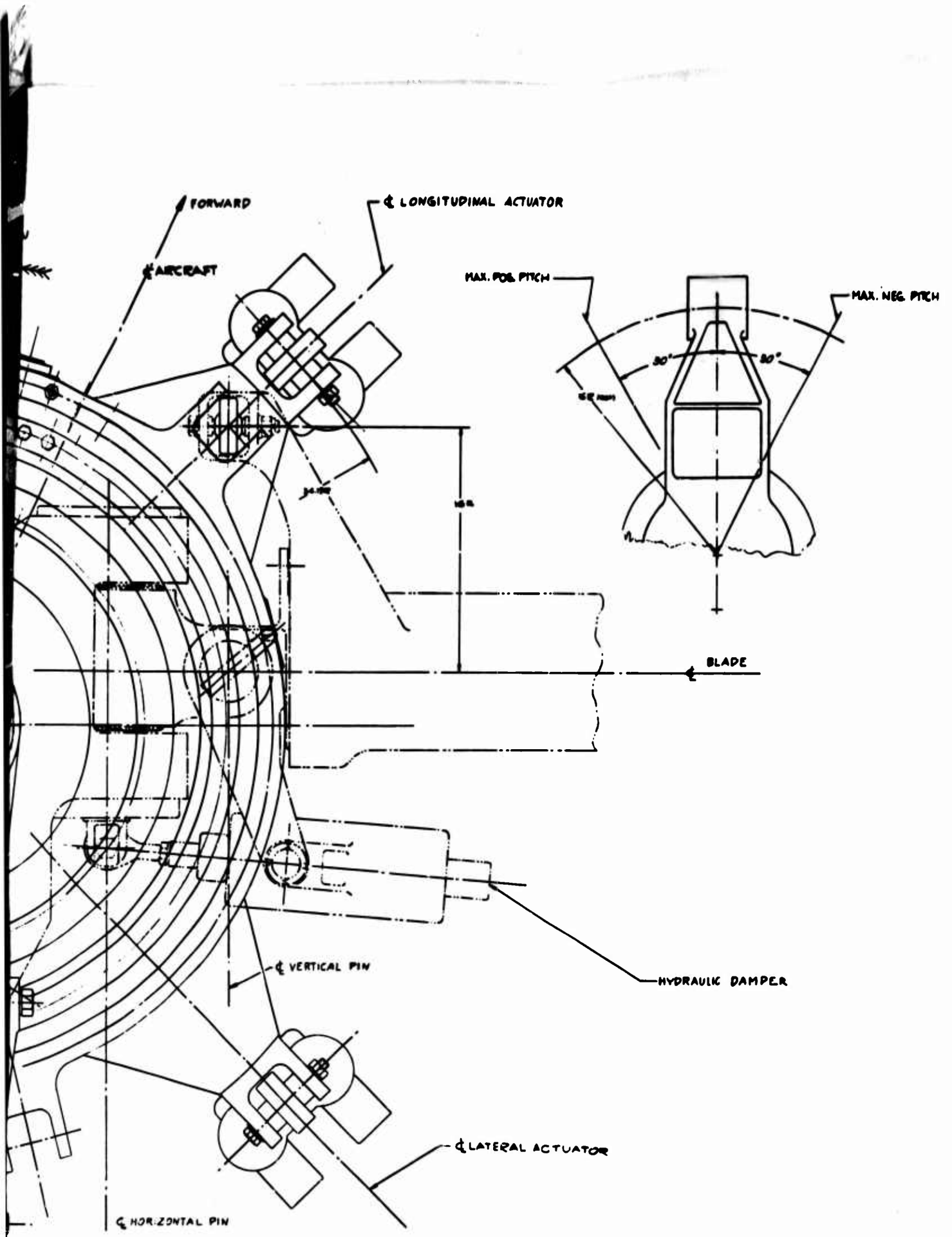
FORWARD
℄ LONGITUDINAL ACTUATOR
℄ AIRCRAFT
MAX. POS. PITCH
MAX. NEG. PITCH
30°
30°
BLADE
℄ VERTICAL PIN
HYDRAULIC DAMPER
℄ LATERAL ACTUATOR
℄ HORIZONTAL PIN

B

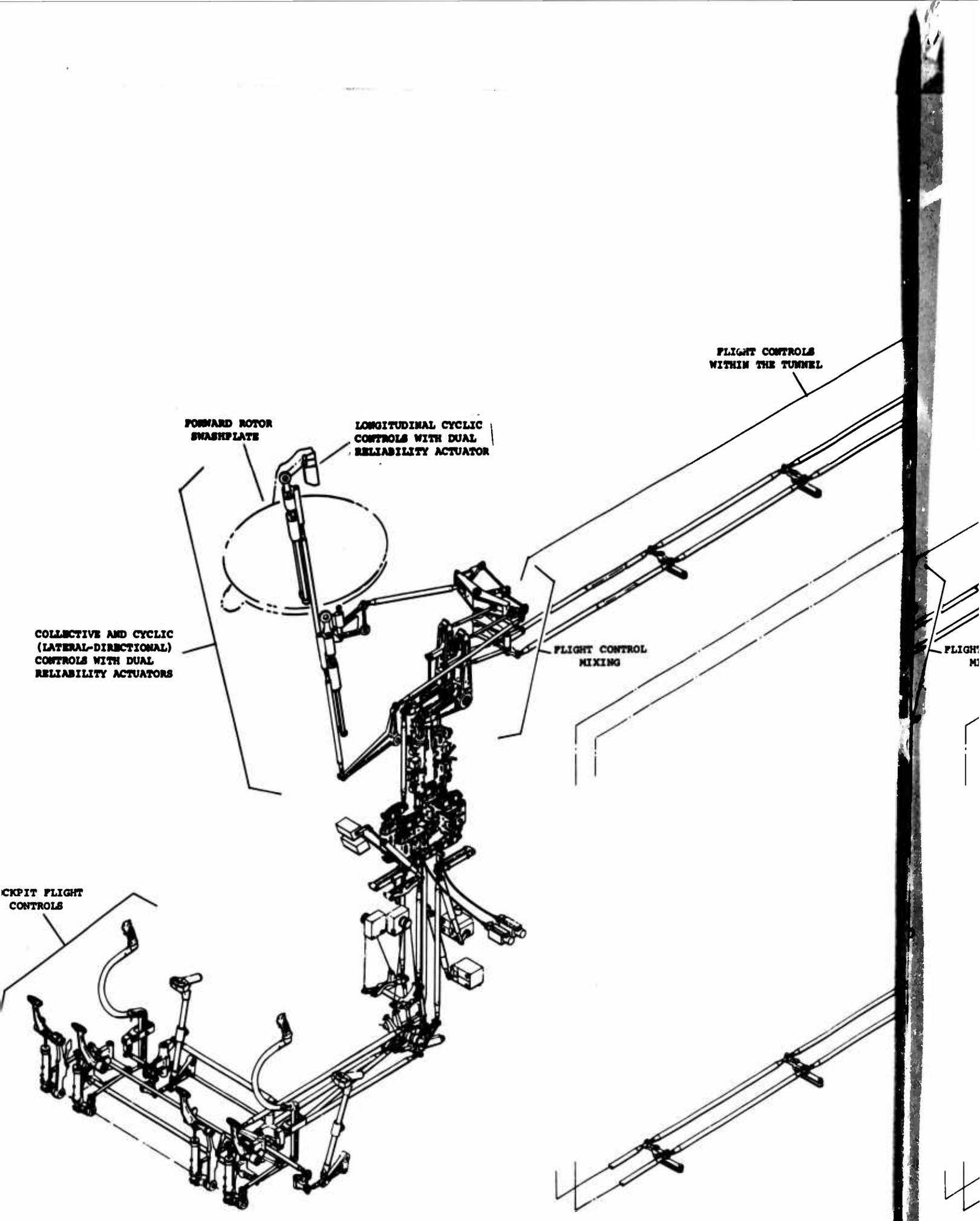

Figure 132. Flight Controls.

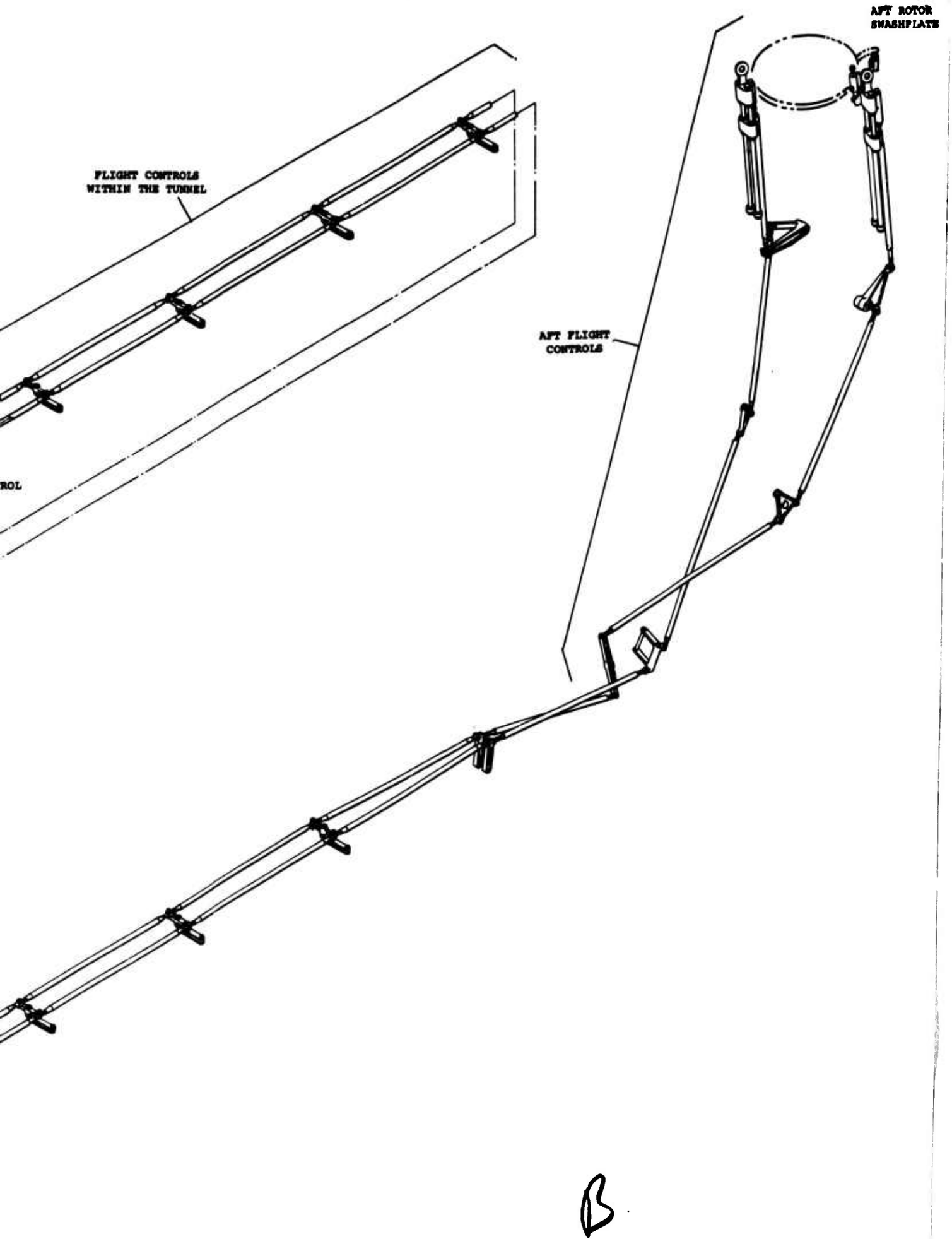
AFT ROTOR
SWASHPLATE
FLIGHT CONTROLS
WITHIN THE TUNNEL
AFT FLIGHT
CONTROLS
ROL

B

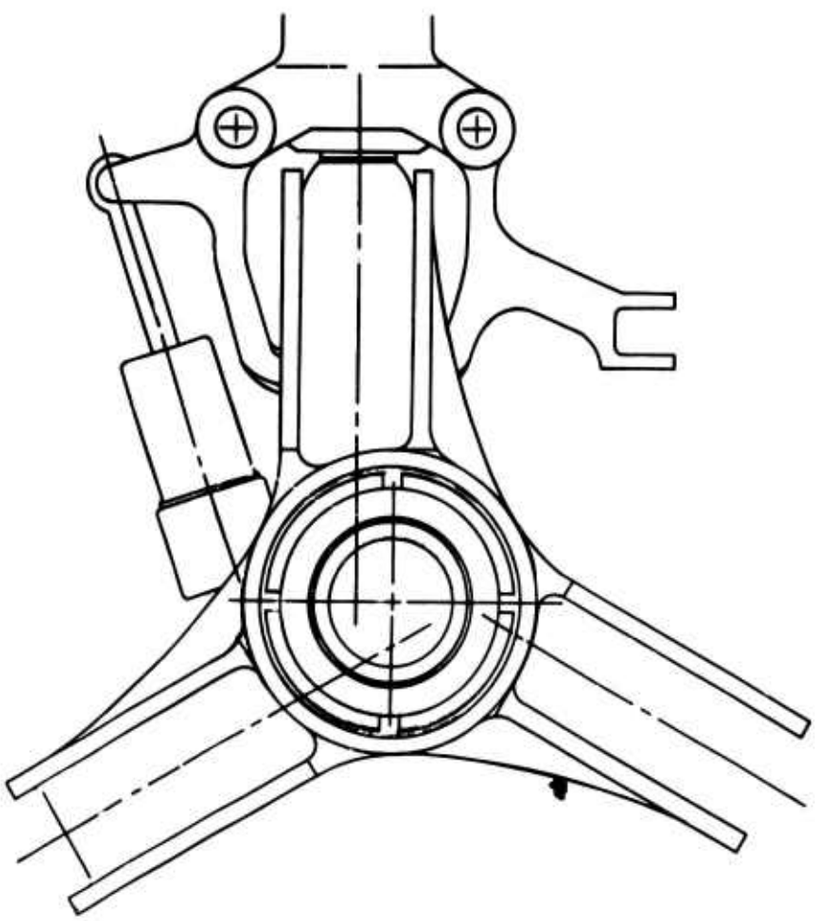

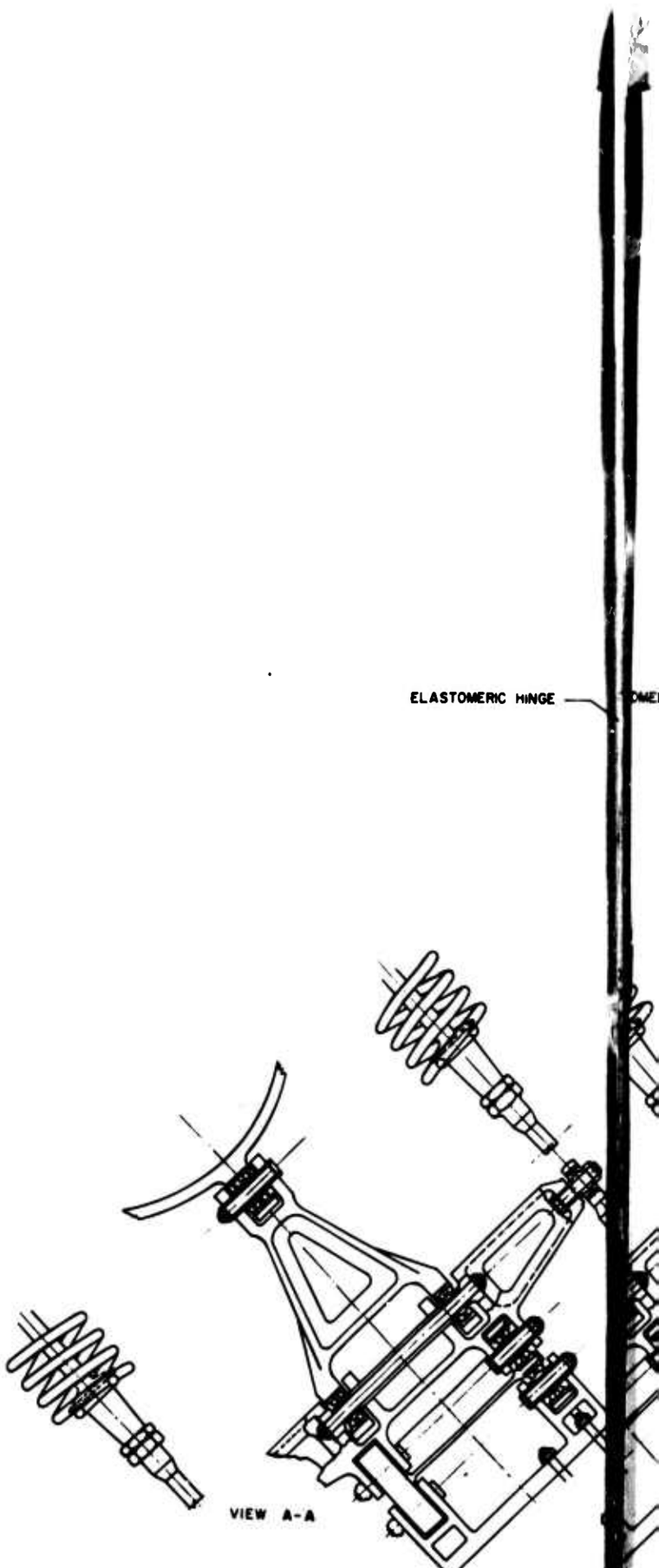

Figure 133. Collective-Pitch Bungee.

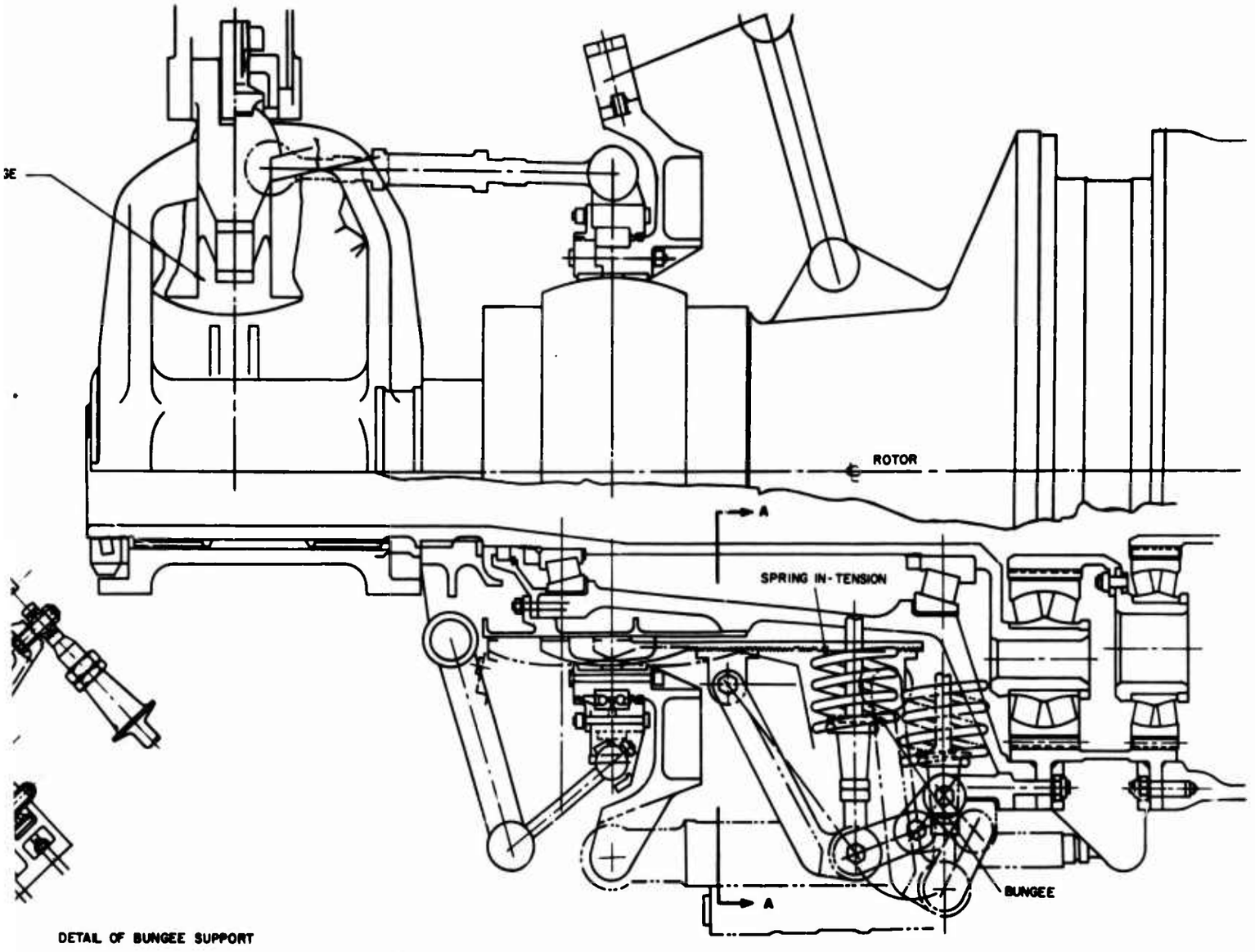

DETAIL OF BUNGEE SUPPORT

B

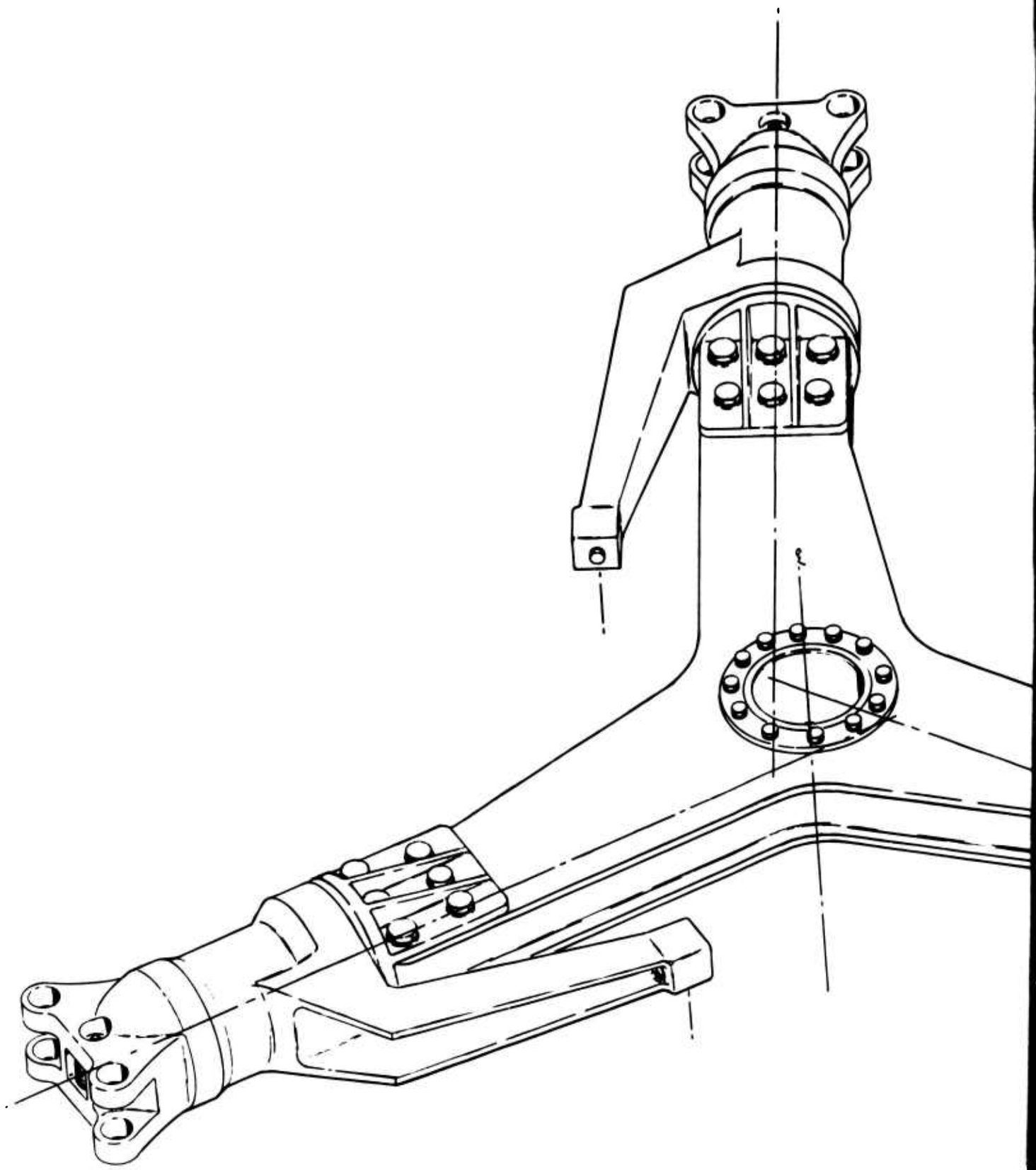

Figure 134. Hingeless Forward Rotor Hub.

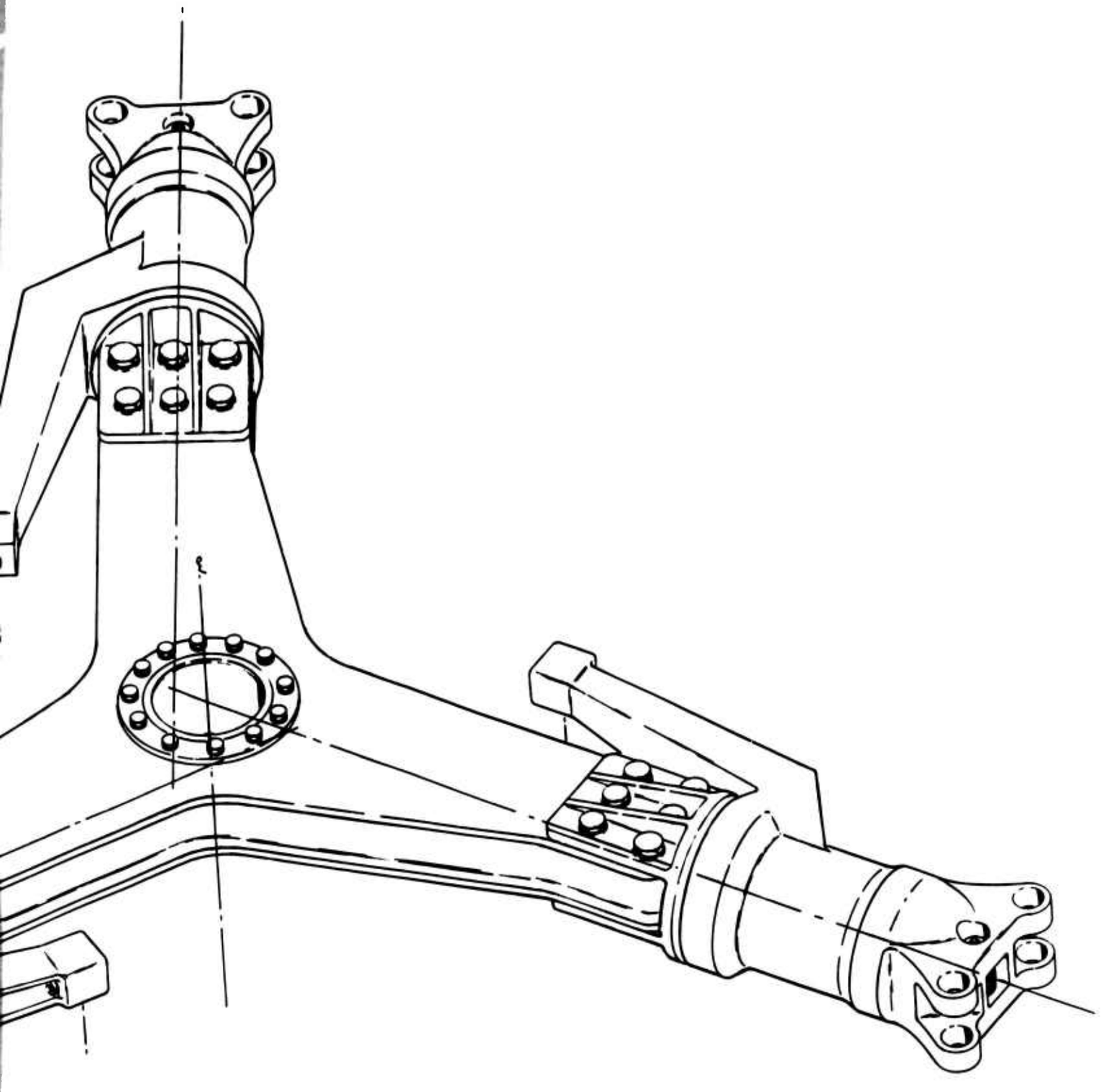

Rotor Hub.

B

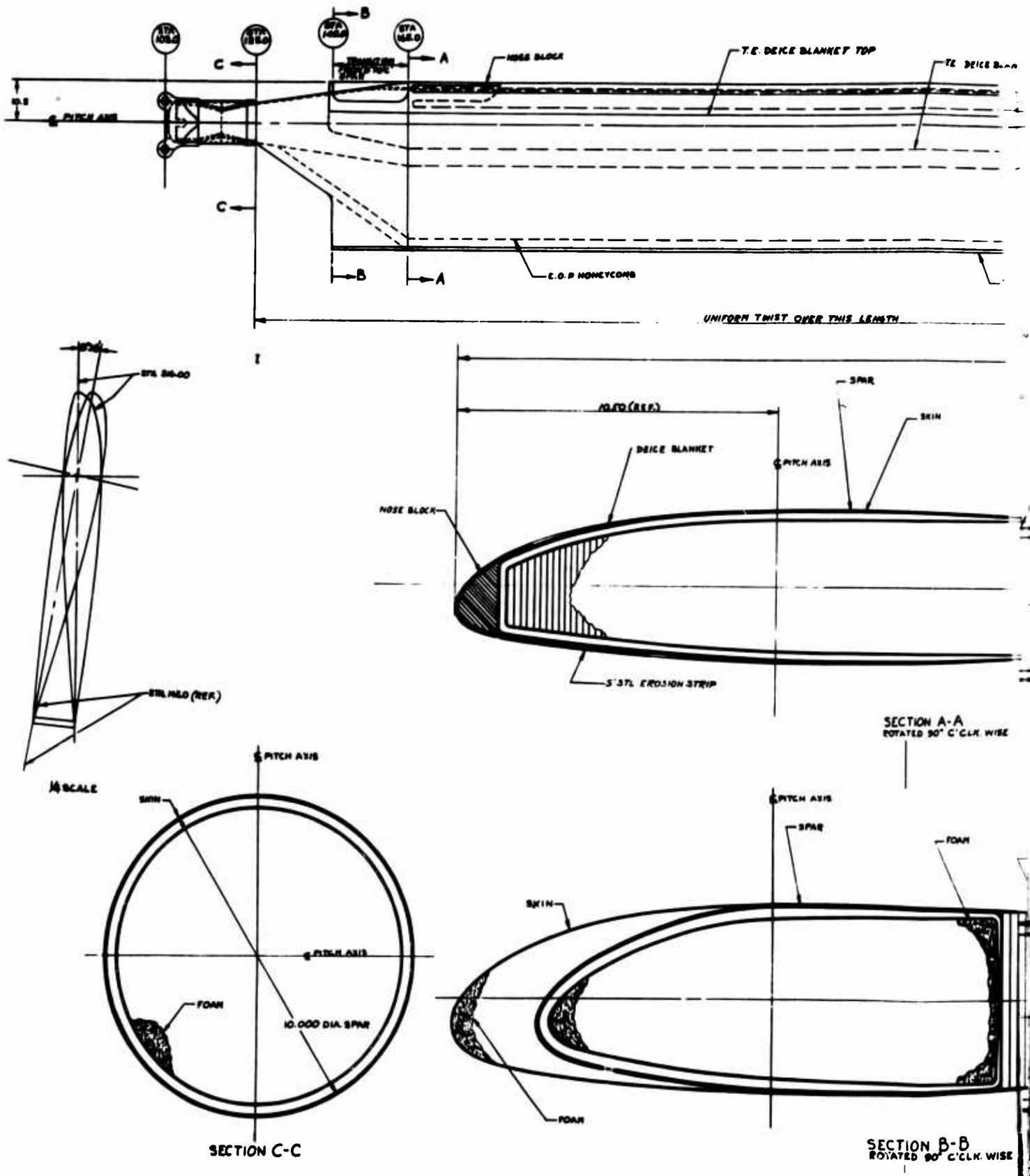

Figure 135. Plastic Rotor Blade for Hingeless Rotor.

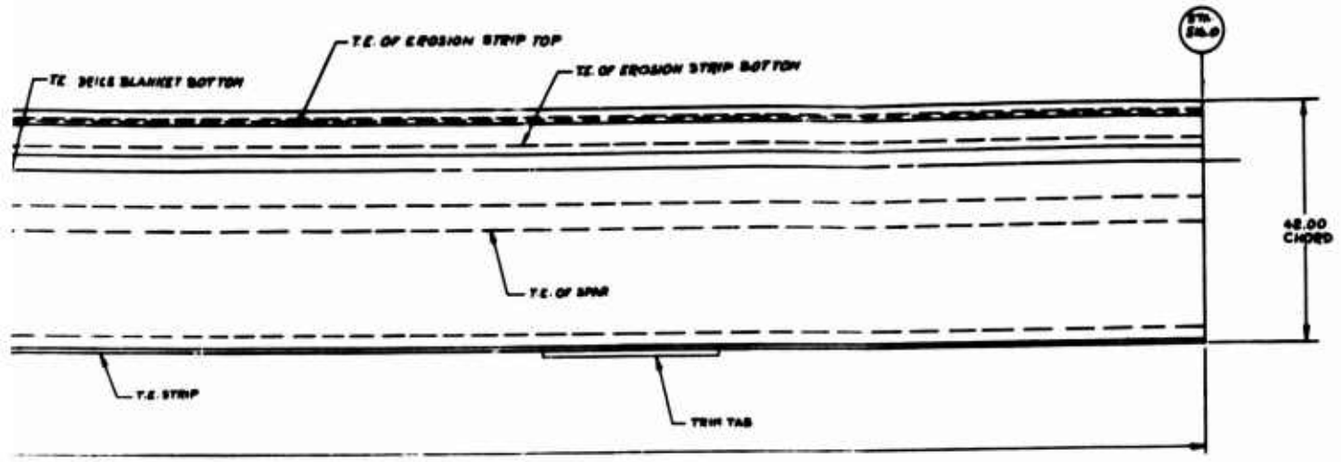

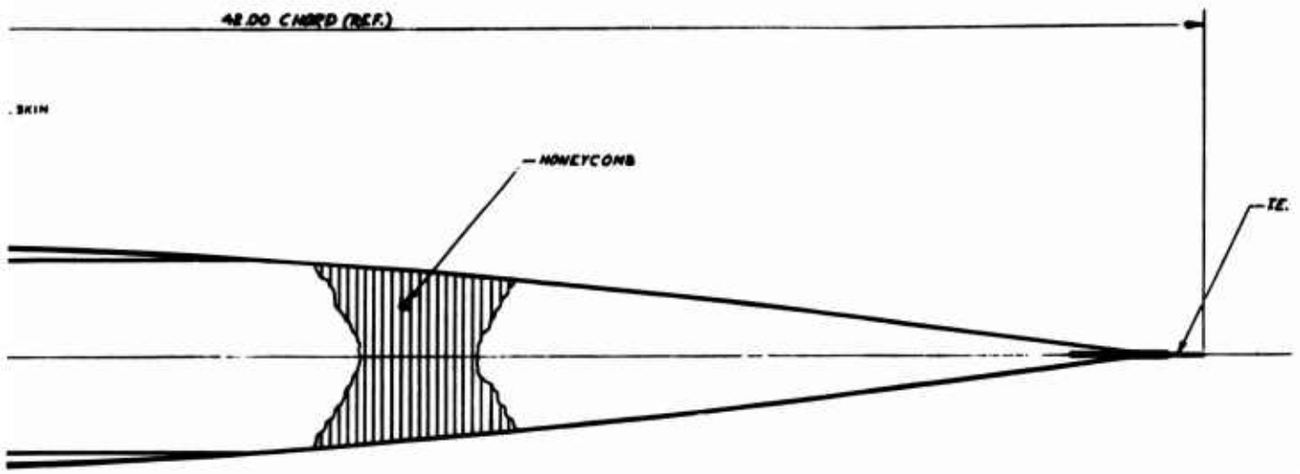

'ION A-A
ED 90° C'CLK. WISE

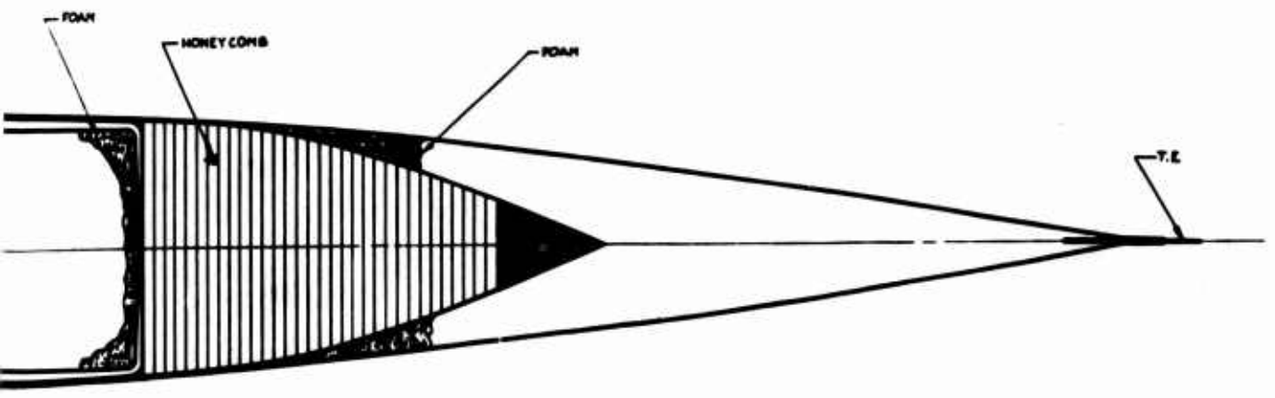

ION B-B
ED 90° C'CLK. WISE

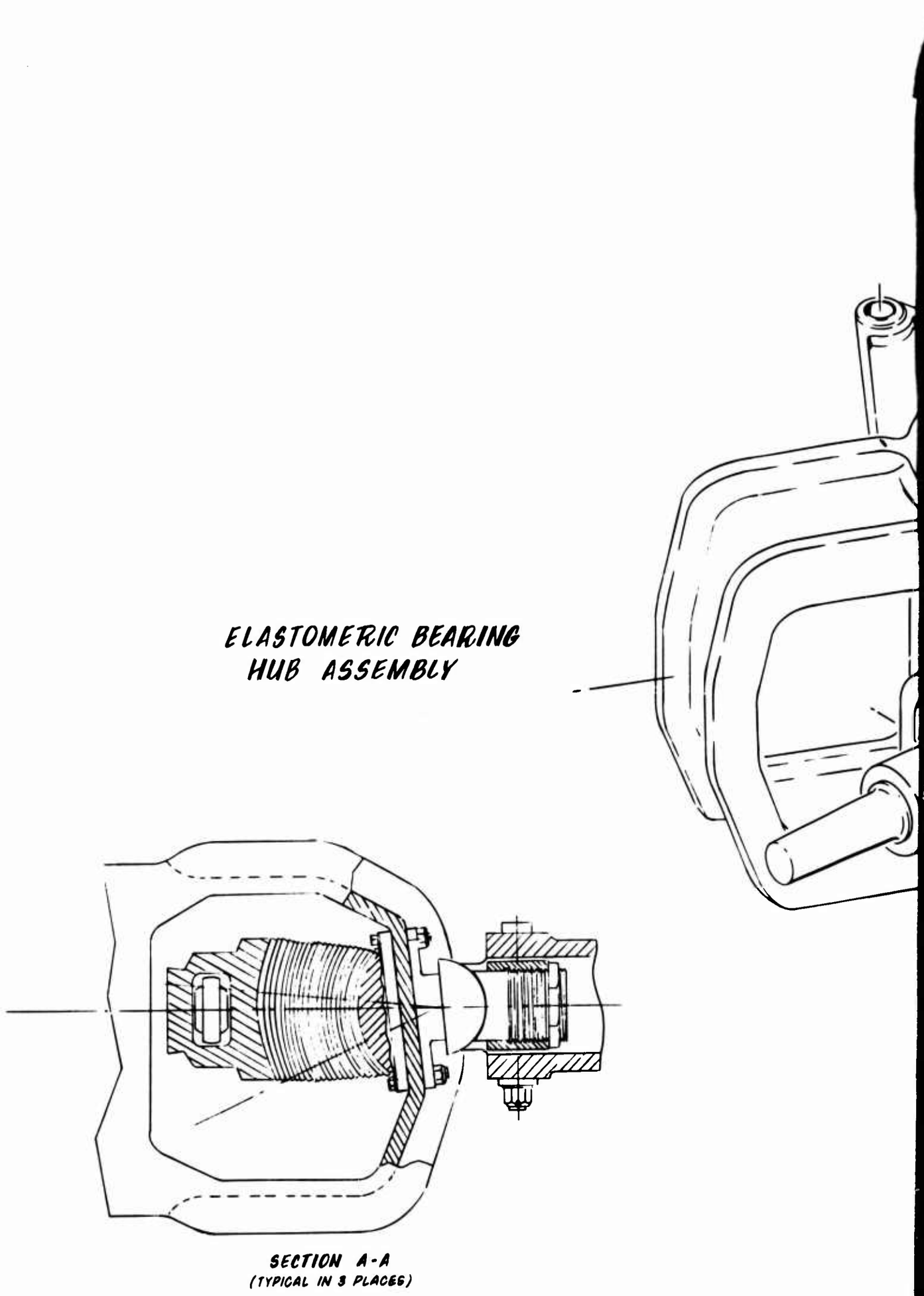

Figure 136. Coincident-Hinge Elastomeric Bearing Rotor Hub. (Sheet 1 of 2)

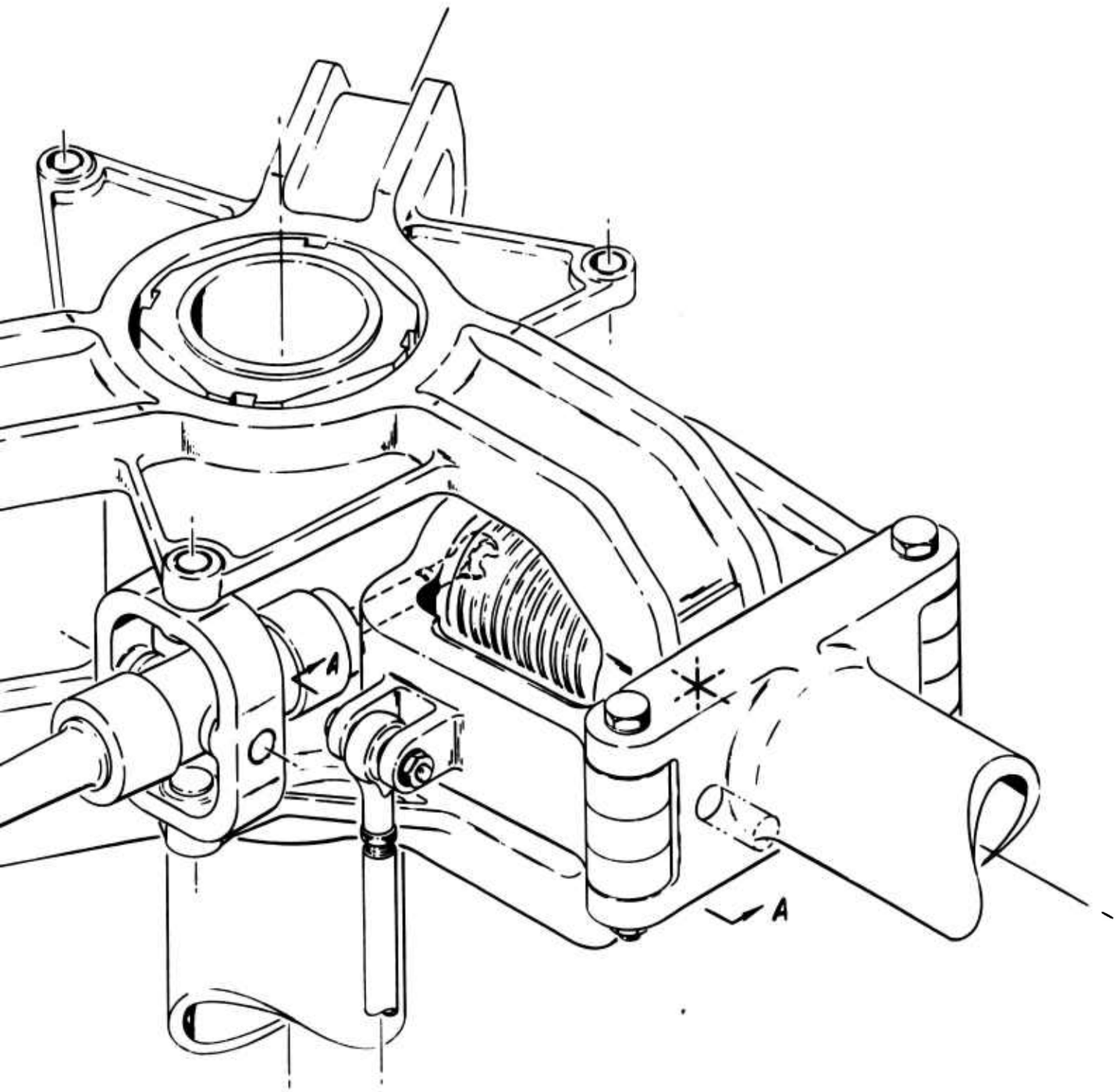

B

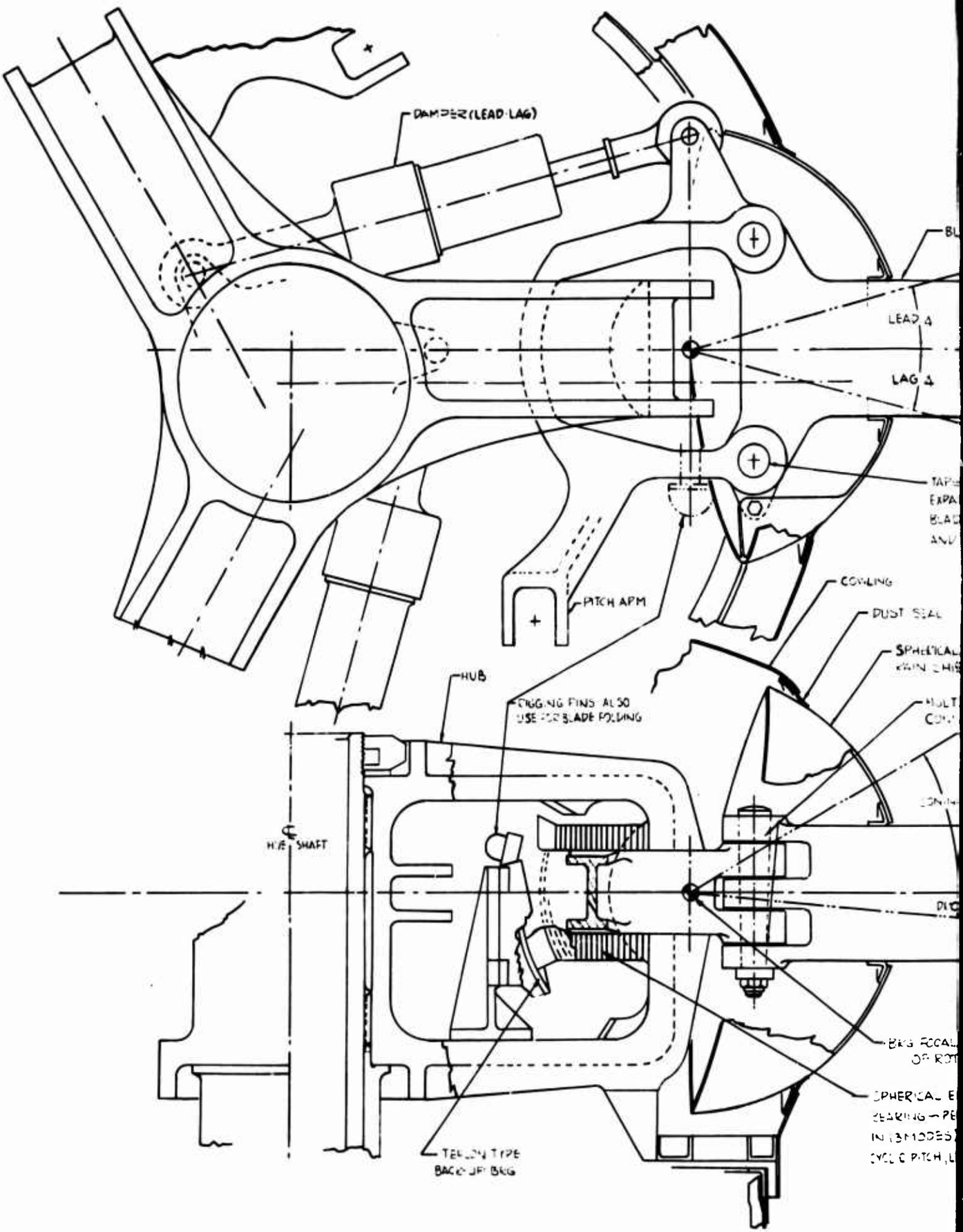

Figure 136. Coincident-Hinge Elastomeric Bearing Rotor Hub. (Sheet 2 of 2)

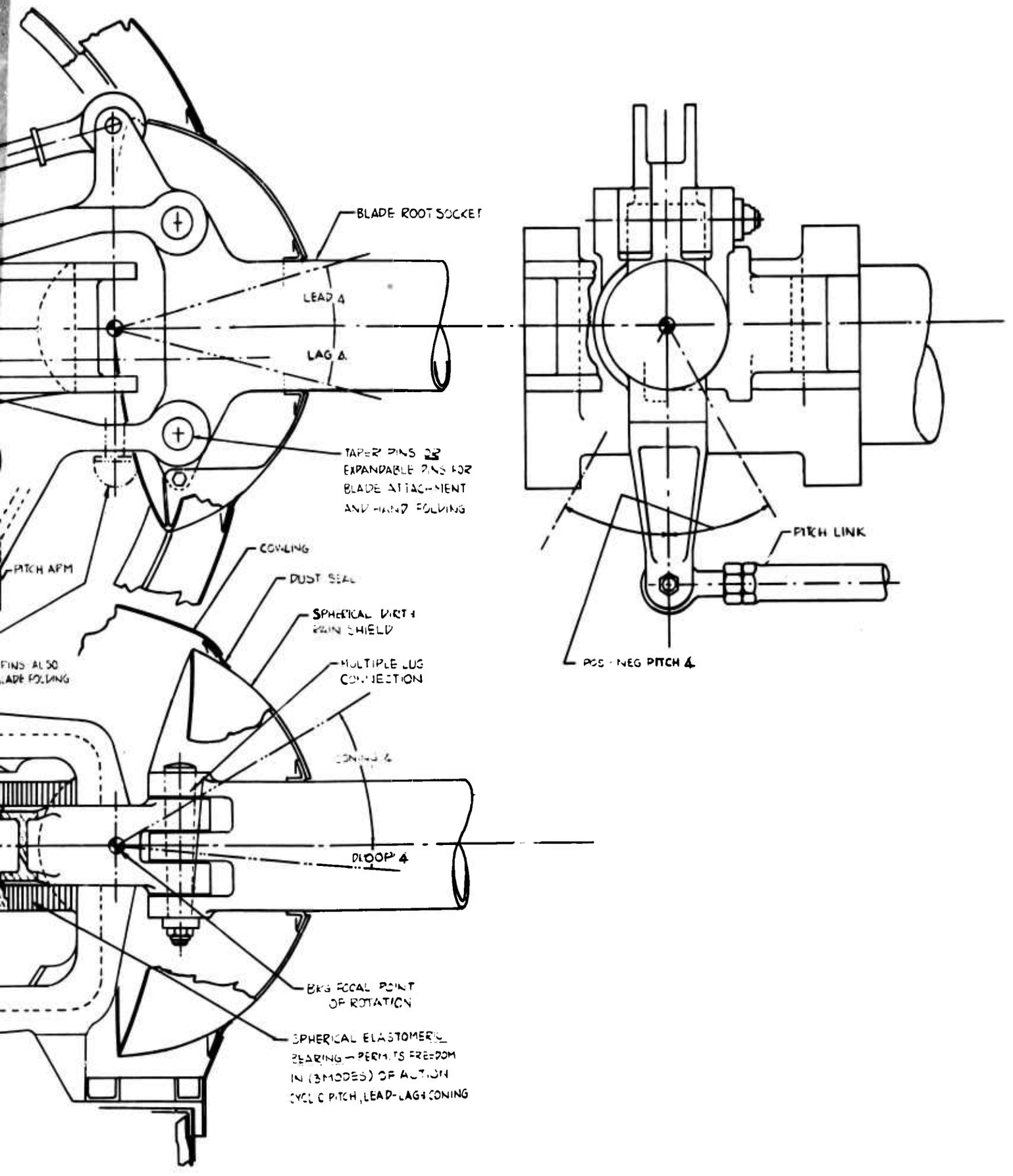

Bearing Rotor Hub.

WEIGHTS

The weights shown in this section have been derived from weight trends developed by Vertol Division, statistical data from existing aircraft, preliminary layouts and stress data, and vendors. The weights of the various groups were first calculated by these standard methods reflecting the existing state of the art. The group weights were then optimized by use of advanced materials and technologies, representative of the 1968-to-1972 state of the art.

Four Summary Weight Statements (MIL-STD-451, Part I) are shown for the following heavy-lift helicopter configurations:

1. Tandem-lift rotor transport
2. Tandem-lift rotor crane/personnel carrier
3. Single-lift/antitorque rotor transport
4. Single-lift/antitorque rotor crane/personnel carrier

MAIN ROTOR GROUP (ARTICULATED)

Derivation of Trend Weight

The weight of the rotor group was derived from the Vertol Division Rotor Group Weight Trend and the following parameters:

1. Total rotor group weight (W_R) in pounds
2. Weight of rotor group per rotor (W_r) in pounds
3. Rotor radius (R) in feet
4. Number of blades per rotor (b)
5. Blade chord (C) in feet
6. Horsepower required (HP_r)
7. Design limit tip speed (V_{t_ℓ}) in feet per second

8. Distance from centerline of rotation to point of blade attachment (r)

9. Nondimensional blade droop factor (kd)

10. Number of rotors (n_r)

11. $F(R, b, C, HP_r, V_{tl}, kd) = K$

12. $W = AK^X$; $W_R = W_r \times n_r$

After the rotor weight was determined by this trend, weight optimization criteria were applied to reflect the rotor weight representing the 1968-to-1972 state of the art. Blade weight was reduced 5 percent by using advanced structural materials and techniques. Hub weight was reduced 9.2 percent for the reduction of centrifugal-force loads imposed on the hub by the lighter blades, and for the use of titanium and higher strength steel alloys. The total weight saving realized when these criteria were used was approximately 11.5 percent of the rotor group weight. By comparison, present production aircraft using titanium with existing technologies realize a 6-percent reduction in rotor group weight.

Derivation of Design Weight

The rotor group design weight is based on calculated layout weights for the hub, hinge, and blade-retention components. It has been used to corroborate the trend weight from the "CONFIGURATION PARAMETRIC ANALYSIS" and, subsequently, to replace the rotor trend weights in the summary weights. The blade weight for the preliminary design study is obtained from the weight distribution curve (Figure 64). This curve is an output from the STATIC AND DYNAMIC STRUCTURAL ANALYSIS.

Design Weight of Tandem-Lift Rotor System

The detail design studies reveal high coning angles when the rotor trend weight is used. Since the coning angle requires further study, for the present, the coning-angle limit has been set at 6.6 degrees. This is based on satisfactory experience with such coning angles on Vertol Division helicopters. The 6.6-degree limit increases blade weight by 150 pounds per blade. With steel components, the resultant centrifugal force loads cause an increase of approximately 326 pounds per rotor in the hub, hinge, and blade-retention

system. The weight saving realized by substituting titanium for steel, where feasible, is 543 pounds per rotor over the steel component weight, as shown below.

Weight Increase (Δ) of Design Weight Above Trend Weight for Tandem-Lift Rotor System

1. Δ Blade weight (steel root-end fitting)
   = +150 pounds x 3 = +450 pounds per rotor

   Δ Weight of hub, hinge, blade retention (steel components) = +326 pounds

   Total Δ weight for steel = +776 pounds per rotor

2. Δ Blade weight (titanium root-end fitting)
   = +140 pounds x 3 = +420 pounds per rotor

   Δ Weight of hub, hinge, blade retention (titanium components) = -187 pounds

   Total Δ weight for titanium components
   = +233 pounds per rotor

With steel components, design weight exceeds trend weight by 1552 pounds per aircraft. Although the use of titanium does not completely offset the weight increase, when the steel is replaced with titanium at 80 percent of its allowable stress, the design weight is only 466 pounds per aircraft greater than trend weight.

Design Weight of Single-Lift/Antitorque Rotor System

An investigation using the trend weight reveals coning angles which exceed those of the tandem-lift rotor blades by two to three degrees.

With the same coning angle limit criteria as for the tandem-lift rotor helicopters, the weight of the lift-rotor blade weight increases by 379 pounds per blade. The increased centrifugal-force load causes the weight of the hub, hinge, and blade-retention system to increase by approximately 1582 pounds.

With steel components, the total effect of the coning angle criteria is an increase of 3477 pounds in the rotor group weight. Substituting titanium for steel, where feasible, results in a reduction of 1424 pounds. The overall effect of the coning-angle criteria and titanium substitution is an

increase in the weight of the lift-rotor group of 2053 pounds over the trend weight.

Weight Increase (Δ) of Design Weight above Trend Weight for Single-Lift/Antitorque Rotor System

1. Δ Blade weight (steel root-end fitting) = +379 pounds x 5 = +1895 pounds per rotor

   Δ Weight of hub, hinge, blade retention (steel components) = +1582 pounds

   Total Δ weight for steel components = +3477 pounds per rotor

2. Δ Blade weight (titanium root end fitting) = +350 x 5 = +1750 pounds per rotor

   Δ Weight of hub, hinge, blade retention (titanium components) = +303 pounds

   Total Δ weight for titanium components = +2053 pounds per rotor

The increase of 3477 pounds in the single-lift/antitorque rotor configuration seems to be out of proportion when compared (steel versus steel component) to the 776-pound increase in the tandem-lift rotor configuration. It should be noted, however, that the design gross weights and rotor speeds (rpm) differ between the two configurations:

1. Rotor radius: 43 feet for tandem, 48 feet for single

2. Design gross weight: 87,000 pounds for tandem, 91,600 pounds for single

3. Rotor speed: 155.5 rpm for tandem, 139 rpm for single

Restricting the maximum coning angle to 6.6 degrees, the blade weight required to produce this limit can be determined by the following:

$$\beta \text{ (radians)} = \left| \frac{0.75R\left(GW/n_r \times b\right) - M}{I_f \Omega^2} \right| \qquad (6)$$

where

β is coning angle in radians

R is blade radius in feet

GW is design gross weight in pounds

n_r is number of rotors

b is number of blades per rotor

M is static moment in foot-pounds or $W_f \times \bar{R}$

W_f is blade flapping weight in pounds

$\bar{R}$ is radial blade center of gravity from centerline of flapping hinge in feet

I_f is blade flapping inertia in foot-pound-seconds squared, or $k(W_f/g)L^2$

k is blade flapping inertia proportionality factor

L is length of flapping portion of blade in feet, or R-d

d is flapping hinge offset in feet

Ω is rotor speed in radians per second

Substituting the known parameters for both the tandem-lift and single-lift/antitorque rotor configurations into the above equation results in the following:

1. For the tandem-lift rotor system

$$\beta = 6.6 \text{ degrees} = 0.1152 \text{ radian} = 0.795 \left\{ \frac{0.75\ (43)(87{,}000/2x3) - W_f \bar{R}}{0.19\ (W_f/g)L^2 \times [0.105(156 \text{ rpm})]^2} \right\} \quad (7)$$

2. For the single-lift/antitorque rotor system

$$\beta = 6.6 \text{ degrees} = 0.1152 \text{ radian} = 0.795 \left\{ \frac{0.75\ (48)\ (91{,}600/1x5) - W_f \bar{R}}{0.19\ (W_f/g)L^2 \times [0.105\ (139 \text{ rpm})]^2} \right\} \quad (8)$$

Comparing both expressions, it can be seen that the expression for the single-lift/antitorque rotor system will always result in a higher blade weight. Substituting the design gross weight and rotor rpm of the tandem-lift rotor system into the coning-angle expression for the single-lift/antitorque rotor system would result in a weight of 973 pounds per blade. This represents an increase of 100 pounds per blade over the trend weight used in the ROTOR SYSTEM PARAMETRIC ANALYSIS for the single-lift/antitorque rotor system. The net effect of this parameter substitution would be an increase

of 878 pounds over the lift-rotor group weight shown in the ROTOR SYSTEM PARAMETRIC ANALYSIS. This weight increase, compared with the 776-pound increase for the tandem-lift rotor system, seems reasonable.

Returning to the original increase of 3477 pounds for the single-lift/antitorque rotor system, the following reasoning explains the discrepancy between the two rotor group weight increases:

1. Basic Δ weight due to coning angle +2911 pounds

   Δ Weight based on substitution of tandem's gross weight and rotor rpm in single's expression is +878 pounds

   Δ Weight required for proper centrifugal force level to attain the coning-angle limit, due to lower rpm of the single-lift/antitorque rotor system is +2033 pounds

2. Δ Weight penalty due to higher gross weight is + 566 pounds

3. Net Δ weight is +3477 pounds

Pending the results of additional coning-angle studies, the coning angle limit has been set at 6.6 degrees. If the results of these studies indicate that the precise coning angle requirement can be greater than 6.6 degrees, the weights of rotor group components will be reduced.

TAIL GROUP (SINGLE-LIFT/ANTITORQUE ROTOR HELICOPTERS)

The weight of the tail group consists of the tail rotor weight and the weight of the horizontal stabilizer. The tail rotor weight is derived using the Vertol Division rotor group trend with a modified multiplying constant, and with the non-dimensional blade droop factor eliminated. The weight of the horizontal stabilizer is a function of the stabilizer area and a standard unit stabilizer weight in pounds per square foot.

BODY GROUP

The weight of the body group has been derived using the Vertol Division body group trend. The transport's weight was obtained by use of the body group trend for transport-type helicopters. The crane/personnel carrier's weight was derived from the basic structure weight trend plus the built-up weight of secondary structure, and by the addition of specific weight penalties for special design features.

The following parameters were used in deriving the body group trends:

1. Weight of body group (W_{BG}) in pounds = AK^x
2. Weight of basic structure (W_{BS}) in pounds = BK^x
3. Design gross weight (Wg) in pounds
4. Ultimate load factor (n)
5. Wetted area (including pylons) (S_f) in square feet
6. Cabin length (from nose to aft end of cabin floor) (l_c) in feet
7. Ramp well length (l_{rw}) in feet
8. Allowable cg travel (CG) in feet
9. Maximum forward flight speed (V_{max}) in knots
10. Body group weight factor (K) = f(Wg, n, S_f, l_c, l_{rw}, ΔCG, V_{max})
11. Total body group weight constant (A)
12. Basic structure weight constant (B)
13. Exponential power factor for K (x)

After determining the body group weight, the structural weight was reduced by 5 percent to reflect the use of advanced technologies available in the 1968-to-1972 time span. This resulted in a total reduction of approximately 4 percent of the body group weight.

ALIGHTING GEAR GROUP

The weight of the alighting gear group was derived by use of a standard percentage of design gross weight for structure, a fixed constant for controls, and the latest vendor weights for the high-flotation (low UCI, CBR = 1.5) rolling components.

FLIGHT CONTROLS GROUP

The weight of the flight controls group was derived from the current Vertol Division weight trend for the flight controls subsystems, plus a fixed constant weight for the dual stability augmentation system (SAS) and hover controls for the loadmaster's flight station.

1. Total flight controls weight (W_{FC}) in pounds
   $= W_{cc} + W_{uc} + W_{sc} + W_{SAS} + W_{LC}$
   $= f\ (Wg) + g\ (W_r) + h\ (W_r) + 80 + 55$
   $= f\ (Wg) + g\ (W_r) + h\ (W_r) + 135$

2. Weight of cockpit controls (W_{cc}) in pounds
   $= f\ (Wg)$

3. Weight of upper controls (W_{uc}) in pounds
   $= g\ (W_r)$

4. Weight of system controls (including hydraulic boost system) (W_{sc}) in pounds
   $= h\ (W_r)$

5. Weight of stability augmentation system (W_{SAS})
   = 80 pounds

6. Weight of loadmaster's hover controls (W_{LC})
   = 55 pounds

7. Design gross weight (Wg) in pounds

8. Rotor group weight factor (W_r)

ENGINE SECTION OR NACELLE GROUP

The weight of the engine section is a function of engine weight and size. The weight of the engine mounts is a function of engine weight, crash load factor, and number of engines per aircraft.

PROPULSION GROUP

Engine

Engine weights are taken from the current engine specification for the engines specified for each configuration.

Engine Installation and Fuel System, Excluding Tanks

Standard installation weights, similar to the T55-L-7 installation in the CH-47A, were used for air induction and exhaust, cooling, lubrication, engine controls, and starting systems. In addition, the fuel system weight, excluding the fuel tanks, is similar to the CH-47A installation.

Fuel Tanks

Fuel tanks are derived using a standard value in pounds per gallon for 50-percent self-sealing cells, protected against .30-caliber (7.62mm) projectiles.

Drive System Trend Weights

The ROTOR SYSTEM PARAMETRIC ANALYSIS used the drive system weight trends modified to reflect the results of the "Heavy-Lift Transmission Study" (Reference 27), done under Contract DA 44-177-AMC-241(T).

Drive System Design Weight

The drive system design weight was derived from the Vertol-developed building-block method which analyzes each section or stage of the drive system. (It is more accurate than the overall drive system trend.) The multiplying constant for the overall trend was then adjusted to obtain the results of the building-block analysis. The following is the overall trend expression for the drive system:

1. Total drive system weight (W_{DS}) in pounds
   Standard Trend $W_{DS} = AK^{Y}$
   Advanced Trend $W_{DS} = BK^{Y}$

2. Transmission design horsepower (HPx)

3. Rotor hover rpm (N_r)

4. Drive system weight factor (K)
   = f (HPx, N_r)
   y = Exponential power factor for K

5. Multiplying constant for standard trend (A)

6. Multiplying constant for advanced-technology trend (B)

DERIVATION OF WEIGHTS FOR FIXED EQUIPMENT

The following group weights have been determined from statistical analysis of existing aircraft and from preliminary requirements specified in the original QMDO issued by the Army. These group weights will vary depending on the configuration, but the variation will be small when comparing similar types of aircraft, such as two transports: a single-lift/antitorque rotor transport versus a tandem-lift rotor transport.

AUXILIARY POWERPLANT

Estimated weight for a 125-horsepower system is 130 pounds.

INSTRUMENT GROUP

$$W = 180 + 17\ N_E, \tag{9}$$

where
N_E is number of engines

HYDRAULIC AND PNEUMATIC GROUP

Estimated weight is 300 pounds.

ELECTRICAL GROUP

Estimated weight is 995 pounds.

ELECTRONICS GROUP

Communications Systems

1.	UHF radio	15 pounds
2.	VHF/FM radio with homer	35 pounds
3.	FM auxiliary radio	6 pounds
4.	Crew intercom	25 pounds

5. Loudspeaker system	58 pounds
6. Total	139 pounds

Navigation Systems

1. ADF-LF/MF	27 pounds
2. VOR/DME/LOC	50 pounds
3. Marker beacon	9 pounds
4. Total	86 pounds

Identification (IFF)

Total	35 pounds

Common Avionics Installation

Shelves, Racks, etc.	20 pounds
Total Electronics Group	280 pounds

FURNISHING AND EQUIPMENT GROUP

Personnel Accommodations

Personnel accommodations include crew seat installations, relief tubes, and provisions for troop seats and litters.

$$W_{PA} = 130 + 2.4\ N_T + 0.5\ N_L \qquad (10)$$

where

130 is constant weight of crew accommodations

2.4 N_T is provisions for troop seats

N_T is number of troops

0.5 N_L is provisions for litters

N_L is number of litters

Miscellaneous Equipment

Miscellaneous equipment includes data cases, windshield wipers, checklists, rearview mirrors, instrument boards, and consoles. In the transport configuration, the weight of cargo tiedown fittings is added as a function of cargo floor area.

Transport

$$W_{ME} = 60 + f(L_1 \times W_1) \tag{11}$$

where

L_1 is length of cargo floor in feet

W_1 is weight of cargo floor in feet

Crane/Personnel Carrier

W_{ME} is constant = 60 pounds

Furnishings

The weight of soundproofing and insulation in the cockpit area is shown for this subsystem.

W_F is constant = 60 pounds

Emergency Equipment

This subgroup includes the weight of portable fire extinguishers, first aid kits, and the weight of engine fire detectors and extinguisher systems as a function of the number of engines.

$$W_{EE} = 42 + 14\ N_E \tag{12}$$

where

N_E is number of engines

Air Conditioning and Anti-icing Group

This group includes the weights for the cockpit heating and ventilation system (heat exchange type), windshield deicing, and engine air inlet deicing. The cabin heating and ventilation system and the rotor blade deicing system are optional kit items and are not included in this group weight.

$$W_A/\bar{C} = 80 + 12\ N_E \qquad (13)$$

where
80 is weight of cockpit heating and ventilation system (70 pounds, plus weight of windshield deicing system, 10 pounds)

N_E is number of engines

Auxiliary Gear Group

The weight shown for this group represents 32 pounds of aircraft handling gear (tiedown, jacking, towing, hoisting, etc.) and 2518 pounds of load handling gear. This 2518 pounds is comprised of the following components:

Cargo Hooks

1. 20-ton capacity (1 required)	150 pounds
2. 15-ton capacity (4 required at 75 pounds each)	300 pounds

Cargo Winch and Cable

1. 20-ton capacity (1 required)	457 pounds
2. 15-ton capacity (4 required at 344 pounds each)	1376 pounds
Equipment Supports	235 pounds

FIXED USEFUL LOAD

Fixed useful load consists of four crew members (pilot, copilot, crew chief, and loadmaster), trapped liquids, and engine oil.

$$W_{FUL} = 4 \times 200 + 20 + 15\ N_E \qquad (14)$$

where
N_E is number of engines

$$W_{FUL} = 820 + 15\ N_E \qquad (15)$$

COMPARISON STUDY

Weights of the articulated and the hingeless semirigid rotor systems have been compared. The 6.6-degree coning angle is held constant regardless of rotor system configuration.

Articulated Rotor System

The weight analysis for the articulated system has been described previously.

Hingeless Semirigid Rotor System

The weight for the tandem hingeless semirigid rotor system is based on the trend curve relationships of the Vertol Division rotor trend. A trend line drawn through the lightest semirigid rotor points, and parallel to the articulated rotor trend, shows that, for equal size and power, the semirigid and rigid rotor systems are at least 1.25 times heavier than Vertol Division articulated rotors. The weight of semirigid and rigid rotor blades ranges from 50 to 65 percent of the weight of the rotor. When 55 percent was used as a realistic estimate for blade weight, and the hub, hinge, and retention were reduced by 25 percent for weight reductions assumed to occur on this design, the weights given in Table XXIII were derived.

It should be noted that the factor of 1.25 was applied to the basic articulated rotor before the addition of blade weight, which, as previously discussed, was necessary to reduce coning to the 6.6 degrees considered to be desirable. Thus, the weight for the hingeless semirigid rotor system is realistic, even though it is less than 90 percent of the weight of all other semirigid and rigid rotors for which we have data. Since the blades of the hingeless rotor are heavier than those of the articulated rotor, the coning angle should be less than 6.6 degrees.

Although the hingeless semirigid rotor can be applied to the tandem-lift rotor system, it produces high pure hub-fuselage twisting moments when yaw control is applied, which are detrimental to the configuration. These hub overturning moments are on the order of five times the moment present in the articulated system (see Figures 115 and 118). This increased moment results in weight increases in the body group and drive system. Table XXIV lists these required weight increases. The overall effect of replacing an articulated

rotor with a hingeless semirigid rotor in a tandem-lift rotor system is a net weight-empty penalty of 6614 pounds. This weight penalty represents approximately 6 percent of the design gross weight, and is inherent in a tandem-lift rotor helicopter because of the closed structural circuit requirements for this type aircraft.

TABLE XXIII
WEIGHT COMPARISON OF THE HINGELESS MATCHED-STIFFNESS ROTOR SYSTEM AND THE ARTICULATED ROTOR SYSTEM

Component	Articulated		Hingeless	
	Steel (lb)	Titanium (lb)	Steel (lb)	Titanium (lb)
Three rotor blades	2396	2364	3355	3315
Hub, hinge, and retention	2041	1529	1705	1280
Each rotor	4437	3893	5060	4595
Two rotors	8874	7786	10120	9190
Increase (Δ) per aircraft			+1246	+1404

TABLE XXIV
WEIGHT INCREASES (Δ) IN BODY GROUP AND DRIVE SYSTEM REQUIRED BY INCREASED OVERTURNING MOMENT IN HINGELESS HUB

Group	Articulated	Hingeless	Increase (Δ)	
Rotor Group				
Refer to Table XXIII	7786	9190	+	+1404
Body Group				
Estimated weight penalty in forward frames due to rotor and transmission loads	205	460	+ 255	
Aft pylon primary structure	510	1145	+ 635	
Δ Torsional material between rotors	--	900	+ 900	
Total	715	2505	+1790	+1790
Drive Group				
Rotor shafts and bearings	1605	3875	+2270	
Main-transmission housings	1080	1380	+ 300	
Transmission supports	425	1275	+ 850	
Total	3110	6530	+3420	+3420
Total Rotor, Body, and Drive Groups				+6614

MIL-STD-451, Part I
NAME J. F. Biglin, Jr.
DATE

PAGE
MODEL HLH
REPORT

SUMMARY WEIGHT STATEMENT
ROTORCRAFT ONLY
ESTIMATED - [redacted]
(Cross out those not applicable)
for
Tandem-Lift Rotor Transport

CONTRACT
ROTORCRAFT, GOVERNMENT NUMBER
ROTORCRAFT, CONTRACTOR NUMBER
MANUFACTURED BY Boeing Company-Vertol Division

		Main	Auxiliary
Engine	Manufactured by	Lycoming	
	Model	LTC4B-11	
	Number	4	
Propeller	Manufactured by		
	Model		
	Number		

MIL-STD-451 PART 1 ROTORCRAFT PAGE
NAME SUMMARY WEIGHT STATEMENT MODEL
DATE WEIGHT EMPTY REPORT

1							
2	ROTOR GROUP						7786
3	BLADE ASSEMBLY					4728	
4	HUB					678	
5	HINGE AND BLADE RETENTION					2380	
6		FLAPPING					
7		LEAD LAG					
8		PITCH					
9		FOLDING					
10	WING GROUP						
11	WING PANELS-BASIC STRUCTURE						
12	CENTER SECTION-BASIC STRUCTURE						
13	INTERMEDIATE PANEL-BASIC STRUCTURE						
14	OUTER PANEL-BASIC STRUCTURE-INCL TIPS			LBS			
15	SECONDARY STRUCT-INCL FOLD MECH			LBS			
16	AILERONS - INCL BALANCE WTS			LBS			
17	FLAPS						
18	-TRAILING EDGE						
19	-LEADING EDGE						
20	SLATS						
21	SPOILERS						
22							
23	TAIL GROUP						
24	TAIL ROTOR						
25	- BLADES						
26	- HUB						
27	STABILIZER - BASIC STRUCTURE						
28	FINS - BASIC STRUCTURE - INCL DORSAL			LBS			
29	SECONDARY STRUCTURE - STABILIZER AND FINS						
30	ELEVATOR - INCL BALANCE WEIGHT			LBS			
31	RUDDER - INCL BALANCE WEIGHT			LBS			
32							
33	BODY GROUP						11700
34	FUSELAGE OR HULL - BASIC STRUCTURE						
35	BOOMS - BASIC STRUCTURE						
36	SECONDARY STRUCTURE - FUSELAGE OR HULL						
37	- BOOMS						
38	- DOORS, PANELS & MISC						
39							
40							
41	ALIGHTING GEAR - LAND TYPE	Tri-Cycle					3384
42	LOCATION	*ROLLING	STRUCT	CONTROLS		Totals	
43		ASSEMBLY					
44	Fuselage - Nose (Aux.)	338	360	65		763	
45	L.G. Stub - Aft (Main)	816	1765	40		2621	
46							
47							
48							
49							
50	ALIGHTING GEAR GROUP - WATER TYPE						
51	LOCATION	FLOATS	STRUTS	CONTROLS			
52							
53							
54							
55							
56							
57							

* WHEELS, BRAKES, TIRES, TUBES AND AIR

MIL-STD-451 PART 1 ROTORCRAFT PAGE
NAME SUMMARY WEIGHT STATEMENT MODEL
DATE WEIGHT EMPTY REPORT

1							
2	FLIGHT CONTROLS GROUP						2755
3	COCKPIT CONTROLS					163	
4	AUTOMATIC STABILIZATION					80	
5	SYSTEM CONTROLS - ROTOR	NON ROTATING				1290	
6		ROTATING				1167	
7	- FIXED	WING					
8	Loadmaster's Controls					55	
9							
10	ENGINE SECTION OR NACELLE	GROUP					420
11	INBOARD						
12	CENTER						
13	OUTBOARD						
14	DOORS, PANELS AND MISC						
15							
16	PROPULSION GROUP						10765
17			X	AUXILIARY	XX	MAIN	X
18	ENGINE INSTALLATION					2580	
19	ENGINE				2580		
20	TIP BURNERS				-		
21	LOAD COMPRESSOR				-		
22	REDUCTION GEAR BOX, ETC				-		
23	ACCESSORY GEAR BOXES AND	DRIVES				-	
24	SUPERCHARGER-FOR TURBOS					-	
25	AIR INDUCTION SYSTEM					20	
26	EXHAUST SYSTEM					60	
27	COOLING SYSTEM					10	
28	LUBRICATING SYSTEM					30	
29	TANKS				-		
30	BACKING BD, TANK SUP &	PADDING			-		
31	COOLING INSTALLATION				-		
32	PLUMBING, ETC				30		
33	FUEL SYSTEM					500	
34	TANKS - UNPROTECTED				-		
35	- PROTECTED				340		
36	BACKING BD, TANK SUP &	PADDING			-		
37	PLUMBING, ETC				160		
38	WATER INJECTION SYSTEM					-	
39	ENGINE CONTROLS					80	
40	STARTING SYSTEM					180	
41	PROPELLER INSTALLATION					-	
42	DRIVE SYSTEM					7305	
43	GEAR BOXES				4973		
44	LUBE SYSTEM (Incl. Oil)				746		
45	CLUTCH AND MISC				-		
46	TRANSMISSION DRIVE				569		
47	ROTOR SHAFT (Aft)				835		
48	JET DRIVE				-		
49	Rotor Brake				182		
50							
51							
52	AUXILIARY POWER PLANT GROUP						130
53							
54							
55							
56							
57							

-03-

MIL-STD-451 PART 1	ROTORCRAFT	PAGE
NAME	SUMMARY WEIGHT STATEMENT	MODEL
DATE	WEIGHT EMPTY	REPORT

1							
2							
3							
4	INSTRUMENT AND NAVIGATIONAL EQUIPMENT GROUP						248
5	INSTRUMENTS					248	
6	NAVIGATIONAL EQUIPMENT					-	
7							
8							
9	HYDRAULIC AND PNEUMATIC GROUP						300
10	HYDRAULIC					300	
11	PNEUMATIC					-	
12							
13							
14	ELECTRICAL GROUP						995
15	A C SYSTEM					737	
16	D C SYSTEM					258	
17							
18							
19	ELECTRONICS GROUP						280
20	EQUIPMENT					188	
21	INSTALLATION					92	
22							
23							
24	ARMAMENT GROUP - INCL GUNFIRE PROTECTION				LBS		-
25							
26	FURNISHINGS AND EQUIPMENT GROUP						783
27	ACCOMMODATIONS FOR PERSONNEL					466	
28	MISCELLANEOUS EQUIPMENT X INCL			LBS	BALLASTX	181	
29	FURNISHINGS					60	
30	EMERGENCY EQUIPMENT					76	
31							
32							
33							
34	AIR CONDITIONING AND ANTI-ICING EQUIPMENT						128
35	AIR CONDITIONING					70	
36	ANTI-ICING					58	
37							
38							
39	PHOTOGRAPHIC GROUP						-
40	EQUIPMENT						
41	INSTALLATION						
42							
43	AUXILIARY GEAR GROUP						2550
44	AIRCRAFT HANDLING GEAR					32	
45	LOAD HANDLING GEAR					2518	
46	ATO GEAR					-	
47							
48							
49							
50							
51							
52							
53							
54	MANUFACTURING VARIATION						-
55							
56							
57	TOTAL-WEIGHT EMPTY - PAGES 2, 3 AND 4						42224

-04-

MIL-STD-491 PART 1 SUMMARY WEIGHT STATEMENT PAGE
NAME USEFUL LOAD GROSS WEIGHT MODEL
DATE REPORT

LOAD CONDITION				MISSION		
				12 Ton	20 Ton	Ferry
CREW - NO. 4				800	800	800
PASSENGERS - NO.				-	-	-
FUEL LOCATION	TYPE	GALS		-	-	-
UNUSABLE Fuse.	JP-5			8	8	8
INTERNAL - Main - Fuse.	JP-5	1345/600/1345		8750	3900	8750
- Aux.	JP-5	8014		-	-	52088
EXTERNAL						
BOMB BAY						
Aux. Fuel System (incl. tanks)				-	-	4808
OIL						
UNUSABLE				12	12	12
ENGINE				60	60	60
BAGGAGE						
CARGO/Payload				24000	40000	-
ARMAMENT						
GUNS-LOCATION	TYPE**	QUANTITY	CALIBER			
AMM						
BOMB INSTL*						
BOMBS						
TORPEDO INSTL*						
TORPEDOES						
ROCKET INSTL*						
ROCKETS						
EQUIPMENT-PYROTECHNICS						
-PHOTOGRAPHIC						
-*OXYGEN						
-MISCELLANEOUS						
USEFUL LOAD				33630	44780	66526
Weight Empty - Page 4				42224	42224	42224
GROSS WEIGHTS - PAGES 2-5				75854	87004	108750

* IF NOT SPECIFIED AS WEIGHT EMPTY ** FIXED, FLEXIBLE, ETC.

MIL-STD-451 PART 1 SUMMARY WEIGHT STATEMENT PAGE
NAME DIMENSIONAL STRUCTURAL DATA MODEL
DATE ROTORCRAFT REPORT

1	LENGTH - OVERALL - Feet		143.67	X BLADES FOLDED	89.0		
2	GENERAL DATA			BOOM	FUS	NAC	CABIN
3	LENGTH - MAXIMUM FEET				89.0		57.5
4	DEPTH - MAXIMUM FEET				13.15		10.0
5	WIDTH - MAXIMUM FEET				14.60		12.0
6	WETTED AREA TOTAL - Sq. Feet				5030.0		-
7	WETTED AREA GLASS				-		-
8	WING TAIL & FLOOR DATA			WING	H TAIL	V TAIL	FLOOR
9	GROSS AREA - SQUARE FEET						
10	WEIGHT/GROSS AREA - POUNDS PER SQUARE FEET						
11	SPAN - FEET						
12	FOLDED SPAN - FEET						
13	*THEORETICAL ROOT CHORD - INCHES						
14	MAXIMUM THICKNESS - INCHES						
15	CHORD AT PLANFORM BREAK INCHES						
16	MAXIMUM THICKNESS - INCHES						
17	THEORETICAL TIP CHORD - INCHES						
18	MAXIMUM THICKNESS - INCHES						
19	DORSAL AREA INCLUDED IN FUSELAGE			SQ FT	TAIL		SQ FT
20	TAIL LENGTH 25% MAC WING TO 25% MAC HORIZONTAL TAIL					FEET	
21	AREA - SQ FT PER ROTORCRAFT FLAPS			AILERONS		SPOILERS	
22	SLATS			WING LE		WING TE	
23	**ROTOR DATA - TYPE - ARTICULATING		FLAPPING - FEATHERING			RIGID	
24	X MAIN ROTOR			XX	TAIL ROTOR		X
25	FROM CL ROTATION - INCHES 115.0		ROOT 516.0	TIP	ROOT		TIP
26	CHORD - INCHES		42.00	42.00			
27	THICKNESS - INCHES		4.86	4.86			
28					MAIN-FWD	MAIN-AFT	TAIL
29	BLADE RADIUS - FEET				43.0	43.0	-
30	NUMBER BLADES				3	3	-
31	BLADE AREA-TOTAL-~~OUTBOARD~~	Sq. Ft.	~~INCHES×RADIUS~~		451.5	451.5	-
32	DISC AREA - TOTAL SWEPT	11618	SQUARE FEET - OVERLAP			SQUARE FEET	
33	TIP SPEED AT DESIGN LIMIT	ROTOR-SPEED-POWER-FT/SEC			*****	12000 HP-875 fps	
34	DESIGN FACTOR USED BY CONTRACTOR.	1.25 x Hover Tip Speed (700 fps)					
35	LOCATION FROM HORIZONTAL REF DATUM	INCHES			180	876	
36	PRESSURE JET % BLADE SECTION AREA	FOR DUCT					
37	TIP JET THRUST						GEAR***
38	POWER TRANSMISSION DATA				HP	RPM	RATIO
39	MAX POWER - TAKE-OFF				12000	15600	100:1
40	ALIGHT GEAR TYPE** ~~BICYCLE~~-TRICYCLE	~~QUADRICYCLE~~-SKID-~~OUTRIGGER~~				MAIN-AFT	AUX-FWD
41	GEAR LENGTH - OLEO EXTND CL AXLE TO CL TRUNNION						
42	OLEO TRAVEL - FULL EXTENDED TO COMPRESSED		INCHES			(4)	(2)
43	WHEEL SIZE AND NUMBER REQUIRED					17.00-16	17.00-16
44	FUEL AND OIL SYSTEM		LOCATION	NO. TANKS	****GALS	NO. TANKS	****GALS
45					UNPRTCTD		PROTECTD
46	FUEL - BUILT IN (50% Self Seal.)	Fuse.				2	1345
47	FUEL - EXTERNAL						
48	LUBRICATING SYSTEM (Engine-Self Contained)						
49	HYDRAULIC SYSTEM						
50	STRUCTURAL DATA - CONDITION			FUEL IN WINGS-LB	DESIGN GROSS WT	STRESS GROSS WT	ULT LF
52	FLIGHT			0	87000	87000	3.75
53	LANDING			0	87000	87000	
54	% DESIGN LOAD	WING	% FWD RTR		60%	AFT RTR	60%
56	*TYPE OF POWER TRANSMISSION - GEARED - ~~BELT-CHAIN-FRICTION-HYDRAULIC~~						

* PARALLEL TO CL @ CL ROTORCRAFT *** GEAR RATIO-ENG TO ROTOR
** CROSS OUT NON-APPLICABLE TYPE **** TOTAL USEABLE CAPACITY
***** REFER TO PARA. 5.1.1.3-ITEMS 6-33 & 6-34

MIL-STD-451, Part I
NAME J. F. Biglin, Jr.
DATE

PAGE
MODEL HLH
REPORT

SUMMARY WEIGHT STATEMENT
ROTORCRAFT ONLY
ESTIMATED - [redacted]
(Cross out those not applicable)

for

Tandem-Lift Rotor Crane/Personnel Carrier

CONTRACT
ROTORCRAFT, GOVERNMENT NUMBER
ROTORCRAFT, CONTRACTOR NUMBER
MANUFACTURED BY Boeing Company - Vertol Division

		Main	Auxiliary
Engine	Manufactured by	Lycoming	
	Model	LTC4B-11	
	Number	4	
Propeller	Manufactured by		
	Model		
	Number		

MIL-STD-451 PART 1 ROTORCRAFT PAGE
NAME SUMMARY WEIGHT STATEMENT MODEL
DATE WEIGHT EMPTY REPORT

1							
2	ROTOR GROUP						7786
3	BLADE ASSEMBLY					4728	
4	HUB					678	
5	HINGE AND BLADE RETENTION					2380	
6		FLAPPING					
7		LEAD LAG					
8		PITCH					
9		FOLDING					
10	WING GROUP						
11	WING PANELS-BASIC STRUCTURE						
12	CENTER SECTION-BASIC STRUCTURE						
13	INTERMEDIATE PANEL-BASIC STRUCTURE						
14	OUTER PANEL-BASIC STRUCTURE-INCL TIPS			LBS			
15	SECONDARY STRUCT-INCL FOLD MECH			LBS			
16	AILERONS - INCL BALANCE WTS			LBS			
17	FLAPS						
18	-TRAILING EDGE						
19	-LEADING EDGE						
20	SLATS						
21	SPOILERS						
22							
23	TAIL GROUP						
24	TAIL ROTOR						
25	- BLADES						
26	- HUB						
27	STABILIZER - BASIC STRUCTURE						
28	FINS - BASIC STRUCTURE - INCL DORSAL			LBS			
29	SECONDARY STRUCTURE - STABILIZER AND FINS						
30	ELEVATOR - INCL BALANCE WEIGHT			LBS			
31	RUDDER - INCL BALANCE WEIGHT			LBS			
32							
33	BODY GROUP						9090
34	FUSELAGE OR HULL - BASIC STRUCTURE					6275	
35	BOOMS - BASIC STRUCTURE						
36	SECONDARY STRUCTURE - FUSELAGE OR HULL					1050	
37	- BOOMS						
38	- DOORS, PANELS & MISC					1765	
39							
40							
41	ALIGHTING GEAR - LAND TYPE - Tri-Cycle						3919
42	LOCATION	*ROLLING	STRUCT	CONTROLS		Totals	
43		ASSEMBLY					
44	Fuselage - Nose (Aux)	338	385	65		788	
45	L.G. Stub - Aft (Main)	816	2275	40		3131	
46							
47							
48							
49							
50	ALIGHTING GEAR GROUP - WATER TYPE						
51	LOCATION	FLOATS	STRUTS	CONTROLS			
52							
53							
54							
55							
56							
57							

* WHEELS, BRAKES, TIRES, TUBES AND AIR

-02-

MIL-STD-451 PART 1 ROTORCRAFT PAGE
NAME SUMMARY WEIGHT STATEMENT MODEL
DATE WEIGHT EMPTY REPORT

1							
2	FLIGHT CONTROLS GROUP						2755
3	COCKPIT CONTROLS					163	
4	AUTOMATIC STABILIZATION					80	
5	SYSTEM CONTROLS - ROTOR	NON ROTATING				1290	
6		ROTATING				1167	
7	- FIXED WING					-	
8	Loadmaster's Controls					55	
9							
10	ENGINE SECTION OR NACELLE GROUP						185
11	INBOARD						
12	CENTER						
13	OUTBOARD						
14	DOORS, PANELS AND MISC						
15							
16	PROPULSION GROUP						10825
17			X AUXILIARY XX		MAIN X		
18	ENGINE INSTALLATION					2580	
19	ENGINE				2580		
20	TIP BURNERS				-		
21	LOAD COMPRESSOR				-		
22	REDUCTION GEAR BOX, ETC				-		
23	ACCESSORY GEAR BOXES AND DRIVES					-	
24	SUPERCHARGER-FOR TURBOS					-	
25	AIR INDUCTION SYSTEM					30	
26	EXHAUST SYSTEM					60	
27	COOLING SYSTEM					10	
28	LUBRICATING SYSTEM					30	
29	TANKS				-		
30	BACKING BD, TANK SUP & PADDING				-		
31	COOLING INSTALLATION				-		
32	PLUMBING, ETC				30		
33	FUEL SYSTEM					550	
34	TANKS - UNPROTECTED				-		
35	- PROTECTED				390		
36	BACKING BD, TANK SUP & PADDING				-		
37	PLUMBING, ETC				160		
38	WATER INJECTION SYSTEM					-	
39	ENGINE CONTROLS					80	
40	STARTING SYSTEM					180	
41	PROPELLER INSTALLATION					-	
42	DRIVE SYSTEM					7305	
43	GEAR BOXES				4973		
44	LUBE SYSTEM				746		
45	CLUTCH AND MISC				-		
46	TRANSMISSION DRIVE				569		
47	ROTOR SHAFT (Aft)				835		
48	JET DRIVE				-		
49	Rotor Brake				182		
50							
51							
52	AUXILIARY POWER PLANT GROUP						130
53							
54							
55							
56							
57							

MIL-STD-451 PART 1 ROTORCRAFT PAGE
NAME SUMMARY WEIGHT STATEMENT MODEL
DATE WEIGHT EMPTY REPORT

1							
2							
3							
4	INSTRUMENT AND NAVIGATIONAL EQUIPMENT GROUP						248
5	INSTRUMENTS					248	
6	NAVIGATIONAL EQUIPMENT					-	
7							
8							
9	HYDRAULIC AND PNEUMATIC GROUP						300
10	HYDRAULIC					300	
11	PNEUMATIC					-	
12							
13							
14	ELECTRICAL GROUP						995
15	A C SYSTEM					737	
16	D C SYSTEM					258	
17							
18							
19	ELECTRONICS GROUP						280
20	EQUIPMENT					188	
21	INSTALLATION					92	
22							
23							
24	ARMAMENT GROUP - INCL GUNFIRE PROTECTION				LBS		-
25							
26	FURNISHINGS AND EQUIPMENT GROUP						578
27	ACCOMMODATIONS FOR PERSONNEL					382	
28	MISCELLANEOUS EQUIPMENT X INCL			LBS	BALLASTX	60	
29	FURNISHINGS					60	
30	EMERGENCY EQUIPMENT					76	
31							
32							
33							
34	AIR CONDITIONING AND ANTI-ICING EQUIPMENT						128
35	AIR CONDITIONING					70	
36	ANTI-ICING					58	
37							
38							
39	PHOTOGRAPHIC GROUP						-
40	EQUIPMENT						
41	INSTALLATION						
42							
43	AUXILIARY GEAR GROUP						2550
44	AIRCRAFT HANDLING GEAR					32	
45	LOAD HANDLING GEAR					2518	
46	ATO GEAR					-	
47							
48							
49							
50							
51							
52							
53							
54	MANUFACTURING VARIATION						
55							
56							
57	TOTAL-WEIGHT EMPTY - PAGES 2, 3 AND 4						39769

-04-

MIL-STD-451 PART 1 SUMMARY WEIGHT STATEMENT PAGE
NAME USEFUL LOAD GROSS WEIGHT MODEL
DATE REPORT

					MISSION		
1	LOAD CONDITION				12 Ton	20 Ton	Ferry
2							
3	CREW - NO. 4				800	800	800
4	PASSENGERS - NO.				-	-	-
5	FUEL LOCATION	TYPE	GALS		-	-	-
6	UNUSABLE Fuse.	JP-5			8	8	8
7	INTERNAL - Main - Fuse.	JP-5	1477/619/1477		9600	4020	9600
8	- Aux.	JP-5	8240		-	-	53557
9							
10							
11	EXTERNAL						
12							
13							
14							
15	BOMB BAY						
16							
17	Aux. Fuel System (incl. tanks)				-	-	4944
18							
19	OIL						
20	UNUSABLE				12	12	12
21	ENGINE				60	60	60
22							
23							
24							
25	BAGGAGE						
26	CARGO /Payload				24000	40000	-
27							
28	ARMAMENT						
29	GUNS-LOCATION TYPE**	QUANTITY	CALIBER				
30							
31							
32							
33							
34	AMM						
35							
36							
37							
38	BOMB INSTL*						
39	BOMBS						
40							
41	TORPEDO INSTL*						
42	TORPEDOES						
43							
44	ROCKET INSTL*						
45	ROCKETS						
46							
47	EQUIPMENT-PYROTECHNICS						
48	-PHOTOGRAPHIC						
49							
50	-*OXYGEN						
51							
52	-MISCELLANEOUS						
53							
54							
55	USEFUL LOAD				34480	44900	68981
56	Weight Empty - Page 4				39769	39769	39769
57	GROSS WEIGHTS - PAGES 2-5				74249	84669	108750

* IF NOT SPECIFIED AS WEIGHT EMPTY ** FIXED, FLEXIBLE, ETC.

-05-

MIL-STD-451 PART 1 SUMMARY WEIGHT STATEMENT PAGE
NAME DIMENSIONAL STRUCTURAL DATA MODEL
DATE ROTORCRAFT REPORT

1	LENGTH - OVERALL - Feet	143.50	X BLADES FOLDED	96.7			
2	GENERAL DATA		BOOM	FUS	NAC	CABIN	
3	LENGTH - MAXIMUM FEET			96.7		45.00	
4	DEPTH - MAXIMUM FEET			12.25		7.00	
5	WIDTH - MAXIMUM FEET			12.00		10.00	
6	WETTED AREA TOTAL - Sq. Ft.			4650.0		-	
7	WETTED AREA GLASS			-		-	
8	WING TAIL & FLOOR DATA		WING	H TAIL	V TAIL	FLOOR	
9	GROSS AREA - SQUARE FEET						
10	WEIGHT/GROSS AREA - POUNDS PER SQUARE FEET						
11	SPAN - FEET						
12	FOLDED SPAN - FEET						
13	*THEORETICAL ROOT CHORD - INCHES						
14	MAXIMUM THICKNESS - INCHES						
15	CHORD AT PLANFORM BREAK INCHES						
16	MAXIMUM THICKNESS - INCHES						
17	THEORETICAL TIP CHORD - INCHES						
18	MAXIMUM THICKNESS - INCHES						
19	DORSAL AREA INCLUDED IN FUSELAGE		SQ FT	TAIL		SQ FT	
20	TAIL LENGTH 25% MAC WING TO 25% MAC HORIZONTAL TAIL				FEET		
21	AREA - SQ FT PER ROTORCRAFT FLAPS		AILERONS		SPOILERS		
22	SLATS		WING LE		WING TE		
23	**ROTOR DATA - TYPE - ARTICULATING PLANING - TEETERING				RIGID		
24	X MAIN ROTOR		XX	TAIL ROTOR		X	
25	FROM CL ROTATION - INCHES 115.0	ROOT 516.0	TIP	ROOT		TIP	
26	CHORD - INCHES	42.00	42.00				
27	THICKNESS - INCHES	4.86	4.86				
28				MAIN-FWD	MAIN-AFT	TAIL	
29	BLADE RADIUS - FEET			43.0	43.0	-	
30	NUMBER BLADES			3	3	-	
31	BLADE AREA-TOTAL-OUTBOARD Sq. Ft.	INCHES RADIUS		451.5	451.5	-	
32	DISC AREA - TOTAL SWEPT 11,618	SQUARE FEET - OVERLAP			SQUARE FEET		
33	TIP SPEED AT DESIGN LIMIT ROTOR-SPEED-POWER-FT/SEC			*****12000 HP -		875 fps	
34	DESIGN FACTOR USED BY CONTRACTOR.	1.25 X Hover Tip Speed		(700 fps)			
35	LOCATION FROM HORIZONTAL REF DATUM	INCHES		215	910		
36	PRESSURE JET % BLADE SECTION AREA	FOR DUCT					
37	TIP JET THRUST					GEAR***	
38	POWER TRANSMISSION DATA			HP	RPM	RATIO	
39	MAX POWER - TAKE-OFF			12000	15600	100:1	
40	ALIGHT GEAR TYPE**BICYCLE-TRICYCLE QUADRICYCLE-SKID OUTRIGGER				MAIN-AFT	AUX-FWD	
41	GEAR LENGTH - OLEO EXTND CL AXLE TO CL TRUNNION						
42	OLEO TRAVEL - FULL EXTENDED TO COMPRESSED	INCHES			(4)	(2)	
43	WHEEL SIZE AND NUMBER REQUIRED				17.00-16	17.00-16	
44	FUEL AND OIL SYSTEM	LOCATION	NO. TANKS	****GALS	NO. TANKS	****GALS	
45				UNPRTCTD		PROTECTD	
46	FUEL - BUILT IN -(50% Self-Seal)	Fuse			2	1475	
47	FUEL - EXTERNAL						
48	LUBRICATING SYSTEM (Engine-Self	Contrined)					
49	HYDRAULIC SYSTEM						
50	STRUCTURAL DATA - CONDITION		FUEL IN	DESIGN	STRESS		
51			WINGS-LB	GROSS WT	GROSS WT	ULT LF	
52	FLIGHT		0	87,000	87,000	3.75	
53	LANDING		0	87,000	87,000	-	
54	% DESIGN LOAD WING	- % FWD RTR		60 % AFT RTR		60 %	
55							
56	**TYPE OF POWER TRANSMISSION - GEARED -						
57							

* PARALLEL TO CL @ CL ROTORCRAFT *** GEAR RATIO-ENG TO ROTOR
** CROSS OUT NON-APPLICABLE TYPE **** TOTAL USEABLE CAPACITY
***** REFER TO PARA. 5.1.1.3-ITEMS 6-33 & 6-34

-06-

MIL-STD-451, Part I
NAME J.F. Biglin, Jr.
DATE

PAGE
MODEL HLH
REPORT

SUMMARY WEIGHT STATEMENT
ROTORCRAFT ONLY
ESTIMATED - ~~UNDERSTATED~~ - ~~ACTUAL~~
(Cross out those not applicable)
for
Single-Lift/Antitorque Rotor Transport

CONTRACT
ROTORCRAFT, GOVERNMENT NUMBER
ROTORCRAFT, CONTRACTOR NUMBER
MANUFACTURED BY Boeing Company - Vertol Division

		Main	Auxiliary
Engine	Manufactured by	Allison	
	Model	501-M26	
	Number	4	
Propeller	Manufactured by		
	Model		
	Number		

MIL-STD-451 PART 1 ROTORCRAFT PAGE
NAME SUMMARY WEIGHT STATEMENT MODEL
DATE WEIGHT EMPTY REPORT

1							
2	ROTOR GROUP						9160
3	BLADE ASSEMBLY					5430	
4	HUB					445	
5	HINGE AND BLADE RETENTION					3285	
6		FLAPPING					
7		LEAD LAG					
8		PITCH					
9		FOLDING					
10	WING GROUP						
11	WING PANELS-BASIC STRUCTURE						
12	CENTER SECTION-BASIC STRUCTURE						
13	INTERMEDIATE PANEL-BASIC STRUCTURE						
14	OUTER PANEL-BASIC STRUCTURE-INCL TIPS			LBS			
15	SECONDARY STRUCT-INCL FOLD MECH			LBS			
16	AILERONS - INCL BALANCE WTS			LBS			
17	FLAPS						
18	-TRAILING EDGE						
19	-LEADING EDGE						
20	SLATS						
21	SPOILERS						
22							
23	TAIL GROUP						1110
24	TAIL ROTOR					930	
25	- BLADES						
26	- HUB						
27	STABILIZER - BASIC STRUCTURE					180	
28	FINS - BASIC STRUCTURE - INCL DORSAL			LBS			
29	SECONDARY STRUCTURE - STABILIZER AND FINS						
30	ELEVATOR - INCL BALANCE WEIGHT			LBS			
31	RUDDER - INCL BALANCE WEIGHT			LBS			
32							
33	BODY GROUP						10600
34	FUSELAGE OR HULL - BASIC STRUCTURE						
35	BOOMS - BASIC STRUCTURE						
36	SECONDARY STRUCTURE - FUSELAGE OR HULL						
37	- BOOMS						
38	- DOORS, PANELS & MISC						
39							
40							
41	ALIGHTING GEAR - LAND TYPE Tri-Cycle						3544
42	LOCATION	*ROLLING	STRUCT	CONTROLS		Totals	
43		ASSEMBLY					
44	Fuselage - Nose (Aux.)	338	400	65		803	
45	L.G. Stubs - Aft (Main)	816	1885	40		2741	
46							
47							
48							
49							
50	ALIGHTING GEAR GROUP - WATER TYPE						
51	LOCATION	FLOATS	STRUTS	CONTROLS			
52							
53							
54							
55							
56							
57							

* WHEELS, BRAKES, TIRES, TUBES AND AIR

-02-

MIL-STD-451 PART 1 ROTORCRAFT PAGE
NAME SUMMARY WEIGHT STATEMENT MODEL
DATE WEIGHT EMPTY REPORT

1							
2	FLIGHT CONTROLS GROUP						3010
3	COCKPIT CONTROLS					165	
4	AUTOMATIC STABILIZATION					80	
5	SYSTEM CONTROLS - ROTOR	NON ROTATING				1335	
6		ROTATING				1375	
7	- FIXED	WING				-	
8	Load Master's Controls					55	
9							
10	ENGINE SECTION OR NACELLE	GROUP					575
11	INBOARD						
12	CENTER						
13	OUTBOARD						
14	DOORS, PANELS AND MISC						
15							
16	PROPULSION GROUP						
17			X AUXILIARY	XX	MAIN	X	13760
18	ENGINE INSTALLATION					4140	
19	ENGINE				4140		
20	TIP BURNERS				-		
21	LOAD COMPRESSOR				-		
22	REDUCTION GEAR BOX, ETC				-		
23	ACCESSORY GEAR BOXES AND	DRIVES				-	
24	SUPERCHARGER-FOR TURBOS					-	
25	AIR INDUCTION SYSTEM					20	
26	EXHAUST SYSTEM					60	
27	COOLING SYSTEM					20	
28	LUBRICATING SYSTEM					30	
29	TANKS				-		
30	BACKING BD, TANK SUP &	PADDING			-		
31	COOLING INSTALLATION				-		
32	PLUMBING, ETC				30		
33	FUEL SYSTEM					560	
34	TANKS - UNPROTECTED				-		
35	- PROTECTED				400		
36	BACKING BD, TANK SUP &	PADDING			-		
37	PLUMBING, ETC				160		
38	WATER INJECTION SYSTEM					-	
39	ENGINE CONTROLS					80	
40	STARTING SYSTEM					200	
41	PROPELLER INSTALLATION					-	
42	DRIVE SYSTEM					8650	
43	GEAR BOXES						
44	LUBE SYSTEM						
45	CLUTCH AND MISC						
46	TRANSMISSION DRIVE						
47	ROTOR SHAFT						
48	JET DRIVE						
49							
50							
51							
52	AUXILIARY POWER PLANT GROUP						130
53							
54							
55							
56							
57							

-03-

MIL-STD-451 PART 1 ROTORCRAFT PAGE
NAME SUMMARY WEIGHT STATEMENT MODEL
DATE WEIGHT EMPTY REPORT

1							
2							
3							
4	INSTRUMENT AND NAVIGATIONAL EQUIPMENT GROUP						248
5	INSTRUMENTS					248	
6	NAVIGATIONAL EQUIPMENT					-	
7							
8							
9	HYDRAULIC AND PNEUMATIC GROUP						300
10	HYDRAULIC					300	
11	PNEUMATIC					-	
12							
13							
14	ELECTRICAL GROUP						995
15	A C SYSTEM					737	
16	D C SYSTEM					258	
17							
18							
19	ELECTRONICS GROUP						280
20	EQUIPMENT					188	
21	INSTALLATION					92	
22							
23							
24	ARMAMENT GROUP - INCL GUNFIRE PROTECTION				LBS		-
25							
26	FURNISHINGS AND EQUIPMENT GROUP						783
27	ACCOMMODATIONS FOR PERSONNEL					466	
28	MISCELLANEOUS EQUIPMENT X INCL			LBS	BALLASTX	181	
29	FURNISHINGS					60	
30	EMERGENCY EQUIPMENT					76	
31							
32							
33							
34	AIR CONDITIONING AND ANTI-ICING EQUIPMENT						128
35	AIR CONDITIONING					70	
36	ANTI-ICING					58	
37							
38							
39	PHOTOGRAPHIC GROUP						-
40	EQUIPMENT						
41	INSTALLATION						
42							
43	AUXILIARY GEAR GROUP						2550
44	AIRCRAFT HANDLING GEAR					32	
45	LOAD HANDLING GEAR					2518	
46	ATO GEAR					-	
47							
48							
49							
50							
51							
52							
53							
54	MANUFACTURING VARIATION						-
55							
56							
57	TOTAL-WEIGHT EMPTY - PAGES 2, 3 AND 4						47173

-04-

MIL-STD-451 PART 1 SUMMARY WEIGHT STATEMENT PAGE
NAME USEFUL LOAD GROSS WEIGHT MODEL
DATE REPORT

					MISSIONS		
1	LOAD CONDITION				12 Ton	20 Ton	Ferry
2							
3	CREW - NO. 4				800	800	800
4	PASSENGERS - NO.				-	-	-
5	FUEL LOCATION	TYPE	GALS		8	8	8
6	UNUSABLE	JP-5					
7	INTERNAL - Main	JP-5	1520/720/1520		9890	4670	9890
8	- Aux.	JP-5	7966		-	-	51778
9							
10							
11	EXTERNAL						
12							
13							
14							
15	BOMB BAY						
16							
17	Aux. Fuel System (incl. tanks)				-	-	4779
18							
19	OIL						
20	UNUSABLE				12	12	12
21	ENGINE				60	60	60
22							
23							
24							
25	BAGGAGE						
26	CARGO/Payload				24000	40000	-
27							
28	ARMAMENT						
29	GUNS-LOCATION TYPE**	QUANTITY	CALIBER				
30							
31							
32							
33							
34	AMM						
35							
36							
37							
38	BOMB INSTL*						
39	BOMBS						
40							
41	TORPEDO INSTL*						
42	TORPEDOES						
43							
44	ROCKET INSTL*						
45	ROCKETS						
46							
47	EQUIPMENT-PYROTECHNICS						
48	-PHOTOGRAPHIC						
49							
50	-*OXYGEN						
51							
52	-MISCELLANEOUS						
53							
54							
55	USEFUL LOAD				34770	45550	67327
56	Weight Empty - Page 4				47173	47173	47173
57	GROSS WEIGHTS - PAGES 2-5				81943	92723	114500

* IF NOT SPECIFIED AS WEIGHT EMPTY ** FIXED, FLEXIBLE, ETC.

-09-

MIL-STD-451 PART 1 SUMMARY WEIGHT STATEMENT PAGE
NAME DIMENSIONAL STRUCTURAL DATA MODEL
DATE ROTORCRAFT REPORT

1	LENGTH - OVERALL		122.75	X BLADES FOLDED	107.5		
2	GENERAL DATA			BOOM	FUS	NAC	CABIN
3	LENGTH - MAXIMUM FEET			17.00	105.00		56.67
4	DEPTH - MAXIMUM FEET			3.33	13.83		9.00
5	WIDTH - MAXIMUM FEET		(Avg.)	7.50	14.67		12.00
6	WETTED AREA TOTAL			-	4482.0		-
7	WETTED AREA GLASS						
8	WING TAIL & FLOOR DATA			WING	H TAIL	V TAIL	FLOOR
9	GROSS AREA - SQUARE FEET						
10	WEIGHT/GROSS AREA - POUNDS PER SQUARE FEET						
11	SPAN - FEET						
12	FOLDED SPAN - FEET						
13	*THEORETICAL ROOT CHORD - INCHES						
14	MAXIMUM THICKNESS - INCHES						
15	CHORD AT PLANFORM BREAK INCHES						
16	MAXIMUM THICKNESS - INCHES						
17	THEORETICAL TIP CHORD - INCHES						
18	MAXIMUM THICKNESS - INCHES						
19	DORSAL AREA INCLUDED IN FUSELAGE			SQ FT	TAIL		SQ FT
20	TAIL LENGTH 25% MAC WING TO 25% MAC HORIZONTAL TAIL					FEET	
21	AREA - SQ FT PER ROTORCRAFT FLAPS			AILERONS		SPOILERS	
22	SLATS			WING LE		WING TE	
23	**ROTOR DATA - TYPE - ARTICULATING						
24	X MAIN ROTOR			XX TAIL ROTOR			X
25	FROM CL ROTATION - INCHES		ROOT	TIP	ROOT		TIP
26	CHORD - INCHES		48.00	48.00		13.20	13.20
27	THICKNESS - INCHES		5.76	5.76		1.58	1.58
28					MAIN-FWD	AFT	TAIL
29	BLADE RADIUS - FEET				48.0		12.5
30	NUMBER BLADES				5		6
31	BLADE AREA-TOTAL Sq. Ft.		INCHES RADIUS		960.0		82.5
32	DISC AREA - TOTAL SWEPT 7238		SQUARE FEET - OVERLAP			SQUARE FEET	
33	TIP SPEED AT DESIGN LIMIT ROTOR-SPEED-POWER-FT/SEC				***** 15500 HP 875 fps.		
34	DESIGN FACTOR USED BY CONTRACTOR.		1.25 X Hover Tip Speed		(700 fps)		
35	LOCATION FROM HORIZONTAL REF DATUM		INCHES		538		1290
36	PRESSURE JET % BLADE SECTION AREA FOR DUCT						
37	TIP JET THRUST						GEAR***
38	POWER TRANSMISSION DATA				HP	RPM	RATIO
39	MAX POWER - TAKE-OFF				15500	15600	112.2:1
40	ALIGHT GEAR TYPE** BICYCLE-TRICYCLE					MAIN-AFT	AUX-FWD
41	GEAR LENGTH - OLEO EXTND CL AXLE TO CL TRUNNION						
42	OLEO TRAVEL - FULL EXTENDED TO COMPRESSED		INCHES			(2)	(4)
43	WHEEL SIZE AND NUMBER REQUIRED					17.00-16	17.00-16
44	FUEL AND OIL SYSTEM		LOCATION	NO. TANKS	****GALS	NO. TANKS	****GALS
45					UNPRTCTD		PROTECTD
46	FUEL - BUILT IN (50% Self-Seal)		Fuse.			2	1520
47	FUEL - EXTERNAL						
48	LUBRICATING SYSTEM - Integral with engine						
49	HYDRAULIC SYSTEM						
50	STRUCTURAL DATA - CONDITION			FUEL IN	DESIGN	STRESS	
51				WINGS-LB	GROSS WT	GROSS WT	ULT LF
52	FLIGHT			0	91600	91600	3.75
53	LANDING			0	91600	91600	
54	% DESIGN LOAD	WING	%	FWD RTR	100%	AFT RTR	- %
55							
56	**TYPE OF POWER TRANSMISSION - GEARED						
57							

* PARALLEL TO CL @ CL ROTORCRAFT *** GEAR RATIO-ENG TO ROTOR
** CROSS OUT NON-APPLICABLE TYPE **** TOTAL USEABLE CAPACITY
***** REFER TO PARA. 5.1.1.3-ITEMS 6-33 & 6-34 -06-

MIL-STD-451, Part I
NAME J. F. Biglin, Jr.
DATE

PAGE
MODEL HLH
REPORT

SUMMARY WEIGHT STATEMENT
ROTORCRAFT ONLY
ESTIMATED - [redacted]
(Cross out those not applicable)

for

Single-Lift/Antitorque Rotor Crane/Personnel Carrier

CONTRACT
ROTORCRAFT, GOVERNMENT NUMBER
ROTORCRAFT, CONTRACTOR NUMBER
MANUFACTURED BY Boeing Company - Vertol Division

		Main	Auxiliary
Engine	Manufactured by	Allison	
	Model	501-M26	
	Number	4	
Propeller	Manufactured by		
	Model		
	Number		

MIL-STD-451 PART 1 | ROTORCRAFT | PAGE
NAME | SUMMARY WEIGHT STATEMENT | MODEL
DATE | WEIGHT EMPTY | REPORT

1							
2	ROTOR GROUP						9160
3	BLADE ASSEMBLY					5430	
4	HUB					445	
5	HINGE AND BLADE RETENTION					3285	
6		FLAPPING					
7		LEAD LAG					
8		PITCH					
9		FOLDING					
10	WING GROUP						
11	WING PANELS-BASIC STRUCTURE						
12	CENTER SECTION-BASIC STRUCTURE						
13	INTERMEDIATE PANEL-BASIC STRUCTURE						
14	OUTER PANEL-BASIC STRUCTURE-INCL TIPS			LBS			
15	SECONDARY STRUCT-INCL FOLD MECH			LBS			
16	AILERONS - INCL BALANCE WTS			LBS			
17	FLAPS						
18	-TRAILING EDGE						
19	-LEADING EDGE						
20	SLATS						
21	SPOILERS						
22							
23	TAIL GROUP						1110
24	TAIL ROTOR					930	
25	- BLADES						
26	- HUB						
27	STABILIZER - BASIC STRUCTURE					180	
28	FINS - BASIC STRUCTURE - INCL DORSAL			LBS			
29	SECONDARY STRUCTURE - STABILIZER AND FINS						
30	ELEVATOR - INCL BALANCE WEIGHT			LBS			
31	RUDDER - INCL BALANCE WEIGHT			LBS			
32							
33	BODY GROUP						8950
34	FUSELAGE OR HULL - BASIC STRUCTURE					6125	
35	BOOMS - BASIC STRUCTURE						
36	SECONDARY STRUCTURE - FUSELAGE OR HULL					1050	
37	- BOOMS						
38	- DOORS, PANELS & MISC					1775	
39							
40							
41	ALIGHTING GEAR - LAND TYPE Tri-Cycle						4125
42	LOCATION	*ROLLING ASSEMBLY	STRUCT	CONTROLS		Totals	
43							
44	Fuselage - Nose (Aux.)	338	422	65		825	
45	L.G. Stub - Aft (Main)	816	2444	40		3300	
46							
47							
48							
49							
50	ALIGHTING GEAR GROUP - WATER TYPE						
51	LOCATION	FLOATS	STRUTS	CONTROLS			
52							
53							
54							
55							
56							
57							

* WHEELS, BRAKES, TIRES, TUBES AND AIR

-02-

MIL-STD-451 PART 1 ROTORCRAFT PAGE
NAME SUMMARY WEIGHT STATEMENT MODEL
DATE WEIGHT EMPTY REPORT

1							
2	FLIGHT CONTROLS GROUP						3010
3	COCKPIT CONTROLS					165	
4	AUTOMATIC STABILIZATION					80	
5	SYSTEM CONTROLS - ROTOR	NON ROTATING				1335	
6		ROTATING				1375	
7	- FIXED	WING				-	
8	LOADMASTER'S CONTROLS					55	
9							
10	ENGINE SECTION OR NACELLE	GROUP					575
11	INBOARD						
12	CENTER						
13	OUTBOARD						
14	DOORS, PANELS AND MISC						
15							
16	PROPULSION GROUP						
17			X AUXILIARY	XX	MAIN	X	13810
18	ENGINE INSTALLATION					4140	
19	ENGINE				4140		
20	TIP BURNERS				-		
21	LOAD COMPRESSOR				-		
22	REDUCTION GEAR BOX, ETC				-		
23	ACCESSORY GEAR BOXES AND	DRIVES				-	
24	SUPERCHARGER-FOR TURBOS					-	
25	AIR INDUCTION SYSTEM					30	
26	EXHAUST SYSTEM					60	
27	COOLING SYSTEM					20	
28	LUBRICATING SYSTEM					30	
29	TANKS				-		
30	BACKING BD, TANK SUP &	PADDING			-		
31	COOLING INSTALLATION				-		
32	PLUMBING, ETC				30		
33	FUEL SYSTEM					600	
34	TANKS - UNPROTECTED				-		
35	- PROTECTED				440		
36	BACKING BD, TANK SUP &	PADDING			-		
37	PLUMBING, ETC				160		
38	WATER INJECTION SYSTEM					-	
39	ENGINE CONTROLS					80	
40	STARTING SYSTEM					200	
41	PROPELLER INSTALLATION					-	
42	DRIVE SYSTEM					8650	
43	GEAR BOXES						
44	LUBE SYSTEM						
45	CLUTCH AND MISC						
46	TRANSMISSION DRIVE						
47	ROTOR SHAFT						
48	JET DRIVE						
49							
50							
51							
52	AUXILIARY POWER PLANT GROUP						130
53							
54							
55							
56							
57							

-03-

MIL-STD-451 PART 1 | ROTORCRAFT | PAGE
NAME | SUMMARY WEIGHT STATEMENT | MODEL
DATE | WEIGHT EMPTY | REPORT

1							
2							
3							
4	INSTRUMENT AND NAVIGATIONAL EQUIPMENT GROUP						248
5	INSTRUMENTS					248	
6	NAVIGATIONAL EQUIPMENT					-	
7							
8							
9	HYDRAULIC AND PNEUMATIC GROUP						300
10	HYDRAULIC					300	
11	PNEUMATIC					-	
12							
13							
14	ELECTRICAL GROUP						995
15	A C SYSTEM					737	
16	D C SYSTEM					258	
17							
18							
19	ELECTRONICS GROUP						280
20	EQUIPMENT					188	
21	INSTALLATION					92	
22							
23							
24	ARMAMENT GROUP - INCL GUNFIRE PROTECTION				LBS		-
25							
26	FURNISHINGS AND EQUIPMENT GROUP						578
27	ACCOMMODATIONS FOR PERSONNEL					382	
28	MISCELLANEOUS EQUIPMENT X INCL			LBS	BALLASTX	60	
29	FURNISHINGS					60	
30	EMERGENCY EQUIPMENT					76	
31							
32							
33							
34	AIR CONDITIONING AND ANTI-ICING EQUIPMENT						128
35	AIR CONDITIONING					70	
36	ANTI-ICING					58	
37							
38							
39	PHOTOGRAPHIC GROUP						-
40	EQUIPMENT						
41	INSTALLATION						
42							
43	AUXILIARY GEAR GROUP						2550
44	AIRCRAFT HANDLING GEAR					32	
45	LOAD HANDLING GEAR					2518	
46	ATO GEAR					-	
47							
48							
49							
50							
51							
52							
53							
54	MANUFACTURING VARIATION						-
55							
56							
57	TOTAL-WEIGHT EMPTY - PAGES 2, 3 AND 4						45949

-04-

MIL-STD-451 PART 1 SUMMARY WEIGHT STATEMENT PAGE
NAME USEFUL LOAD GROSS WEIGHT MODEL
DATE REPORT

					MISSIONS		
1	LOAD CONDITION						
2					12 Ton	20 Ton	Ferry
3	CREW - NO. 4				800	800	800
4	PASSENGERS - NO.				-		
5	FUEL LOCATION	TYPE	GALS		-		
6	UNUSABLE Fuse.	JP-5			8	8	8
7	INTERNAL Fuse.	JP-5	1665/730/1665		10816	4735	10816
8							
9							
10							
11	EXTERNAL - Aux. Fuel	JP-5	8008		-	-	52050
12	-Aux. Fuel System	-	-	-	-	-	4805
13							
14							
15	BOMB BAY						
16							
17							
18							
19	OIL						
20	UNUSABLE				12	12	12
21	ENGINE				60	60	60
22							
23							
24							
25	BAGGAGE						
26	CARGO/Payload				24000	40000	-
27							
28	ARMAMENT						
29	GUNS-LOCATION TYPE**	QUANTITY	CALIBER				
30							
31							
32							
33							
34	AMM						
35							
36							
37							
38	BOMB INSTL*						
39	BOMBS						
40							
41	TORPEDO INSTL*						
42	TORPEDOES						
43							
44	ROCKET INSTL*						
45	ROCKETS						
46							
47	EQUIPMENT-PYROTECHNICS						
48	-PHOTOGRAPHIC						
49							
50	-*OXYGEN						
51							
52	-MISCELLANEOUS						
53							
54							
55	USEFUL LOAD				35696	45687	68551
56	Weight Empty - Page 4				45949	45949	45949
57	GROSS WEIGHTS - PAGES 2-5				81645	91636	114500

* IF NOT SPECIFIED AS WEIGHT EMPTY ** FIXED, FLEXIBLE, ETC.

-09-

MIL-STD-451 PART 1 SUMMARY WEIGHT STATEMENT PAGE
NAME DIMENSIONAL STRUCTURAL DATA MODEL
DATE ROTORCRAFT REPORT

1	LENGTH - OVERALL Feet		122.75	X BLADES FOLDED		107.5	
2	GENERAL DATA			BOOM	FUS	MAC	CABIN
3	LENGTH - MAXIMUM FEET			17.00	105.00		46.25
4	DEPTH - MAXIMUM FEET			5.50	10.00		6.50
5	WIDTH - MAXIMUM FEET			7.00	12.50		10.00
6	WETTED AREA TOTAL			-	4155.0		-
7	WETTED AREA GLASS						
8	WING TAIL & FLOOR DATA			WING	H TAIL	V TAIL	FLOOR
9	GROSS AREA - SQUARE FEET						
10	WEIGHT/GROSS AREA - POUNDS PER SQUARE FEET						
11	SPAN - FEET						
12	FOLDED SPAN - FEET						
13	*THEORETICAL ROOT CHORD - INCHES						
14	MAXIMUM THICKNESS - INCHES						
15	CHORD AT PLANFORM BREAK INCHES						
16	MAXIMUM THICKNESS - INCHES						
17	THEORETICAL TIP CHORD - INCHES						
18	MAXIMUM THICKNESS - INCHES						
19	DORSAL AREA INCLUDED IN FUSELAGE			SQ FT	TAIL		SQ FT
20	TAIL LENGTH 25% MAC WING TO 25% MAC HORIZONTAL TAIL					FEET	
21	AREA - SQ FT PER ROTORCRAFT FLAPS			AILERONS		SPOILERS	
22	SLATS			WING LE		WING TE	
23	**ROTOR DATA - TYPE - ARTICULATING			[illegible]		[illegible]	
24	X MAIN ROTOR			XX	TAIL ROTOR		X
25	FROM CL ROTATION - INCHES		ROOT	TIP		ROOT	TIP
26	CHORD - INCHES		48.00	48.00		13.20	13.20
27	THICKNESS - INCHES		5.76	5.76		1.58	1.58
28					MAIN-[illegible]		TAIL
29	BLADE RADIUS - FEET				48.0		12.5
30	NUMBER BLADES				5		6
31	BLADE AREA-TOTAL-[illegible]	Sq. Ft.	[illegible]		960.0		82.5
32	DISC AREA - TOTAL SWEPT	7238	SQUARE FEET - OVERLAP				SQUARE FEET
33	TIP SPEED AT DESIGN LIMIT	ROTOR-SPEED-POWER-FT/SEC			***** 15500 HP 875 fps		
34	DESIGN FACTOR USED BY CONTRACTOR.	1.25 X Hover Tip Speed			(700 fps)		
35	LOCATION FROM HORIZONTAL REF DATUM	INCHES			564		1374
36	PRESSURE JET % BLADE SECTION AREA	FOR DUCT					
37	TIP JET THRUST						GEAR***
38	POWER TRANSMISSION DATA				HP	RPM	RATIO
39	MAX POWER - TAKE-OFF				15500	15600	112.2:1
40	ALIGHT GEAR TYPE**[illegible]	TRICYCLE	[illegible]			MAIN-AFT	AUX-FWD
41	GEAR LENGTH - OLEO EXTND CL AXLE TO CL TRUNNION						
42	OLEO TRAVEL - FULL EXTENDED TO COMPRESSED			INCHES		(4)	(2)
43	WHEEL SIZE AND NUMBER REQUIRED					17.00-16	17.00-16
44	FUEL AND OIL SYSTEM		LOCATION	NO. TANKS	****GALS UNPRTCTD	NO. TANKS	****GALS PROTECTD
45							
46	FUEL - BUILT IN (50% Self-Seal)		Fuse.			2	1665
47	FUEL - EXTERNAL						
48	LUBRICATING SYSTEM Integral with engine						
49	HYDRAULIC SYSTEM						
50	STRUCTURAL DATA - CONDITION			FUEL IN WINGS-LB	DESIGN GROSS WT	STRESS GROSS WT	ULT LF
51							
52	FLIGHT			0	91600	91600	3.75
53	LANDING			0	91600	91600	
54	% DESIGN LOAD	WING	0 %	FWD RTR	%	AFT RTR	- %
55							
56	**TYPE OF POWER TRANSMISSION - GEARED - [illegible]						
57							

* PARALLEL TO CL @ CL ROTORCRAFT *** GEAR RATIO-ENG TO ROTOR
** CROSS OUT NON-APPLICABLE TYPE **** TOTAL USEABLE CAPACITY
***** REFER TO PARA. 5.1.1.3-ITEMS 6-33 & 6-34

RELIABILITY

The term reliability can be resolved into three categories: system reliability, mission reliability, and flight-safety reliability.

SYSTEM RELIABILITY

System reliability is the probability of performing a defined mission of specified duration without incurring a primary malfunction requiring unscheduled maintenance before the next periodic inspection.

A primary malfunction is one occurring during the useful life of the component that is not caused by faulty maintenance, handling, or operator techniques, or by failure of related parts.

The system reliability requirement for the heavy-lift helicopter, including avionics, navigation equipment, and GFE, is expected to be 65 percent for the heavy-lift mission.

MISSION RELIABILITY

Mission reliability is the probability of performing a defined mission of specified duration without incurring a mission-affecting primary malfunction.

A mission-affecting primary malfunction is defined as any primary malfunction which would cause the aircraft to abort the mission.

The mission reliability requirement for the heavy-lift helicopter is expected to be 95 percent for the heavy-lift mission.

FLIGHT-SAFETY RELIABILITY

Flight-safety reliability is the probability of performing a defined mission of specified duration without incurring a primary malfunction that results in loss or severe damage to the aircraft.

The flight-safety reliability requirement for the heavy-lift helicopter is expected to be 99.992 percent for the heavy-lift mission.

Aircraft flight-safety characteristics are generally not subject to tradeoff because of the value placed on human life. In the conceptual design phase it is therefore important to identify and select aircraft configurations that provide the maximum inherent flight safety. In order to establish a configuration for the heavy-lift helicopter, Vertol Division conducted an evaluation of typical single-lift/antitorque rotor and tandem-lift rotor helicopters. One of the objectives of the evaluation was to determine the safety-of-flight characteristics of the two configurations. This evaluation was performed by comparing the number of dynamic system components which can degrade flight safety, and by comparing helicopter catastrophic failure rates demonstrated by dynamic system components.

Safety-of-Flight Components

Safety-of-flight components are those components whose failure can cause a catastrophe. A catastrophe is any event which results in serious injury or death to an occupant of the aircraft, major damage to the aircraft, or loss of the aircraft. The number of safety-of-flight components in the indicated subsystems for typical helicopters now in production is as follows:

	Single-Lift Antitorque (S-61)	Tandem-Lift (CH-47A)
Rotor Blade	25	18
Rotor Head and Controls	130	80
Drive	30	67
Total	185	165

Catastrophes per 1000 Flight Hours

Another measure of helicopter safety is the frequency with which safety-of-flight components have failed, resulting in catastrophes. This is a better indication of helicopter safety than the critical-parts-count, since it is based on experience.

Recorded data from U.S. military helicopter catastrophes during the 3-year period from 1959 through 1961 was reviewed

for safety-of-flight experience demonstrated by dynamic systems of helicopters during typical utilization. The catastrophic failure rate per 1000 flight hours experienced by single-lift/antitorque rotor helicopters (0.0309) was 48 percent higher than that of tandem-lift rotor helicopters (0.0209). Although the reliability figures favor a tandem-lift rotor helicopter, the difference is not great. It can therefore be concluded that with reliability as a goal (and every helicopter manufacturer adopts the building of a reliable aircraft as his goal), neither tandem-lift nor single-lift/antitorque rotor designs can claim a decisive advantage.

BIBLIOGRAPHY

1. Biglin, J. F., Heavy-Lift Helicopter Weight Estimating Methods for the Rotor Configuration Parametric Study, Document D8-0239, Vertol Division, The Boeing Company, Morton, Pennsylvania, November 1965.

2. Curry, Major Paul R., Matthews, James T., Jr., of U.S. Army Transportation Research Command,* "Advanced Rotary-Wing Handling Qualities," Proceedings of the American Helicopter Society Twentieth Annual National Forum, Washington, D.C., May 1964.

3. Davenport, Franklyn J., "A Method for Computation of the Induced Velocity Field of a Rotor in Forward Flight, Suitable for Applications to Tandem Rotor Configurations," Journal of the American Helicopter Society, Volume 9, Number 3, July 1964.

4. Foulke, W. K., Exploration of High-Speed Flight with the XH-51A Rigid Rotor Helicopter, AD 617966, USAAVLABS Technical Report 65-25, U.S. Army Aviation Materiel Laboratories, Fort Eustis, Virginia, June 1965.

5. Garren, John F., Jr., Kelly, James R., Reeder, John P., Effects of Gross Changes in Static Directional Stability on V/STOL Handling Characteristics Based on a Flight Investigation, NASA TND-2477, October 1964.

6. Garren, John F., Jr., Kelly, James R., Reeder, John P., A Visual Flight Investigation of Hovering and Low-Speed VTOL Control Requirements, NASA TND-2788, October 1965.

7. Jones, A. B., "Ball and Roller Bearing Analysis Program S-33" based on A General Theory for Elastically Constrained Ball and Radial Roller Bearings Under Arbitrary Load and Speed Conditions, Paper 59 Lub-10, American Society of Mechanical Engineers.

8. Leone, Peter F., "Theoretical and Experimental Study of the Coupled Flap Bending and Torsion Aeroelastic Vibrations of a Helicopter Rotor Blade," Proceedings of the American Helicopter Society Thirteenth Annual National Forum, May 1957.

*Now U.S. Army Aviation Materiel Laboratories

9. Leone, Peter F., "Theory of Rotor Blade Uncoupled Flap Bending Aeroelastic Vibrations," Proceedings of the American Helicopter Society Tenth Annual National Forum, May 1954.

10. Leone, Peter F., "Theory of Rotor Blade Uncoupled Lag Bending Aeroelastic Vibrations," Proceedings of the American Helicopter Society Eleventh Annual National Forum, April 1955.

11. Lockheed-California Company, Investigation of Elastic Coupling Phenomena of High Speed Rigid Rotor Systems, TRECOM Technical Report 63-75, U.S. Army Transportation Research Command,* Fort Eustis, Virginia, June 1964.

12. MIL-HDBK-5, Strength of Metal Aircraft Elements.

13. MIL-H-8501A, General Requirements for Helicopter Flying and Ground Handling Qualities.

14. Rasch, N., Report of Test on Flight Evaluation of External Cargo Loads YCH-47A, Report 114-T-113.13, Vertol Division, The Boeing Company, Morton, Pennsylvania, June 1963.

15. Salmirs, Seymour, Tapscott, The Effects of Various Combinations of Damping and Control Power on Helicopter Handling Qualities During Both Instrument and Visual Flight, NASA TND-58, 1959.

16. Sikorsky Aircraft, Division of United Aircraft Corporation, Parametric Investigation of the Aerodynamic and Aeroelastic Characteristics of Articulated and Rigid (Hingeless) Helicopter Rotor Systems, TRECOM Technical Report 64-15, U.S. Army Transportation Research Command,* Fort Eustis, Virginia, April 1964.

17. Tapscott, Robert J., "Review of Helicopter Handling Qualities Criteria and Summary of Recent Flight Handling Qualities Studies," Proceedings of the American Helicopter Society Twentieth Annual National Forum, Washington, D.C. May 1964.

18. Turner, M.J., Clough, R.W., Martin, H.C., Topp, L.J., "Stiffness and Deflection Analysis of Complex Structures," Journal of the Aeronautical Sciences, Volume 23, September 1956

*Idem

19. High Performance Helicopter Progress Summary Report, TRECOM Technical Report 64-61, AD 607344, U.S. Army Transportation Research Command,* Fort Eustis, Virginia, Oct. 1964.

20. Advanced Vibration Development (AVID), Document 107-M-D-09, Vertol Division, The Boeing Company, Morton, Pennsylvania, April 1965.

21. Flight Evaluation of Redesigned External Cargo Sling for H-21 Helicopter, TRECOM Technical Report 61-33, Vertol Division, The Boeing Company, U.S. Army Transportation Research Command,* Fort Eustis, Virginia, January 1961.

22. Helicopter Rotor Hub Vibratory Forces, Technical Report R-244, Vertol Division, The Boeing Company, Morton, Pennsylvania, May 1961.

23. Structural Design Manual, Vertol Division, The Boeing Company, Morton, Pennsylvania, current.

24. Curry, Paul R., Matthews, James T., Jr., Suggested Requirements for V/STOL Flying Qualities, USAAVLABS Technical Report 65-45 RTM 37, U.S. Army Aviation Materiel Laboratories, Fort Eustis, Virginia, June 1965.

25. Whitfield, A. A., Blackburn, W. E., UH-2 Helicopter High-Speed Flight Research Program Utilizing Jet Thrust Augmentation, USAAVLABS Technical Report 65-14, AD 616104, U.S. Army Aviation Materiel Laboratories, Fort Eustis, Virginia, March 1965.

26. Young, M., "A Theory of Rotor Blade Motion in Powered Flight," Journal of the American Helicopter Society, July 1964.

27. Mack, J., Transmission Study for Tandem-Rotor Shaft-Driven Heavy-Lift Helicopters, USSAAVLABS Technical Report 65-56, Technical Report R-379, Vertol Division, The Boeing Company, U.S. Army Aviation Materiel Laboratories, Fort Eustis, Virginia, September 1965.

*Idem

DISTRIBUTION

US Army Materiel Command	5
US Army Aviation Materiel Command	6
Chief of R&D, DA	1
US Army Aviation Materiel Laboratories	28
US Army R&D Group (Europe)	2
US Army Engineer R&D Laboratories	2
US Army Limited War Laboratory	1
US Army Human Engineering Laboratories	1
US Army Research Office-Durham	1
US Army Test and Evaluation Command	1
Plastics Technical Evaluation Center	1
US Army Medical R&D Command	1
US Army Engineer Waterways Experiment Station	1
US Army Combat Developments Command, Fort Belvoir	2
US Army Combat Developments Command Experimentation Command	3
US Army War College	1
US Army Command and General Staff College	1
US Army Aviation School	1
US Army Tank-Automotive Center	2
US Army Armor and Engineer Board	1
US Army Electronics Command	2
US Army Aviation Test Activity, Edwards AFB	2
Air Force Flight Test Center, Edwards AFB	2
US Army Field Office, Andrews AFB	1
Systems Engineering Groups, Wright-Patterson AFB	3
Air Force Flight Dynamics Laboratory, Wright-Patterson AFB	1
Air Force Aero Propulsion Laboratory, Wright-Patterson AFB	1
Air Proving Ground Center, Eglin AFB	1
Naval Ship Engineering Center	1
Naval Air Systems Command	17
Chief of Naval Research	5
US Naval Research Laboratory	1
Commandant of the Marine Corps	1
Marine Corps Liaison Officer, US Army Transporta ion School	1
Ames Research Center, NASA	1
Lewis Research Center, NASA	1
Manned Spacecraft Center, NASA	1
NASA Scientific and Technical Information Facility	2
NAFEC Library (FAA)	2
National Tillage Machinery Laboratory	1
US Army Aviation Human Research Unit	2
US Army Board for Aviation Accident Research	1
Bureau of Safety, Civil Aeronautics Board	2

US Naval Aviation Safety Center, Norfolk	2
Federal Aviation Agency, Washington, D. C.	2
Civil Aeromedical Research Institute, FAA	2
Defense Documentation Center	20

APPENDIX: WEIGHT ESTIMATION METHODS

This appendix summarizes the weight estimation methods which were used to establish the weights for the heavy-lift helicopter. The methods used to establish the weight estimates for the heavy-lift helicopter are based on standard procedures and weight trends developed by Vertol Division's Weights Group.

The estimation methods include the use of trend curves, weights based on results of preliminary stress analysis, vendor sources, and preliminary equipment requirements specified in the original QMDO issued by the Army.

The trend curves and the required fixed weights were programmed as part of the Mission Analysis Program (A-88). Reiteration of the program for convergence on design gross weight and mission performance produced optimized design parameters.

Using these design parameters, a complete manual analysis was performed to derive the group weights for the MIL-STD-451 format, (the Mission Analysis Program does not have this format) and to provide a final check of the program's weight section.

The weight data generated for the preliminary design study was done manually; it was based on the finalized results from the rotor system parametric analysis. With the exception of the rotor group, all trends used in the preliminary design study are the same as those used for the rotor system parametric analysis.

ROTOR GROUP--DISCUSSION

The Rotor Group Trend was used to establish the weight for the rotor system parametric analysis. This trend predicts the rotor group weight per rotor based on existing technology. The parameters used in deriving the trend K-factor reflect the effect on rotor weight of blade area, power required, design-limit tip speed, point of blade attachment, and static droop criteria. The Rotor Group Trend (Figure 137) is a plot of rotor group weight per rotor versus the trend K-factor. Historically, the Rotor Group Trend has always predicted the rotor group weight to a high degree of accuracy for standard-size helicopters.

The rotor sizes, and gross weights associated with the heavy-lift helicopter have an adverse effect on blade coning angle. This can be seen from the following equation:

$$\beta = \left\{ \frac{0.75R \left(\frac{GW}{N_r \times b} \right) - M}{I_f \Omega^2} \right\} \tag{16}$$

where

- β is blade coning angle in radians
- R is rotor radius in feet
- GW is design gross weight in pounds
- n_r is number of rotors
- b is number of blades per rotor
- M is blade static moment in foot-pounds, or $W_f \bar{R}$
- W_f is blade flapping weight in pounds
- $\bar{R}$ is distance from centerline of flapping hinge to blade center of gravity in feet
- I_f is blade flapping inertia in foot-pound-seconds^2, or $k \left(\frac{W_f}{g} \right) L^2$
- L is R-d
- d is flapping-hinge offset
- k is blade flapping inertia proportionality factor
- Ω is rotor speed in radians per second

Substituting W_f, L, and R in the static moment and inertia expressions, the equation becomes

$$\beta = \left\{ \frac{0.75R \left(\frac{GW}{N_r \times b} \right) - W_f \bar{R}}{k \left(\frac{W_b}{g} \right) L^2 \Omega^2} \right\} \tag{17}$$

As gross weight and radius increase, holding blade weight and tip speed constant, rotor speed decreases and the coning angle increases. If the coning angle is set at a given value, the blade weight required to produce this angle can be determined for any combination of gross weight, blade radius, and rotor speed.

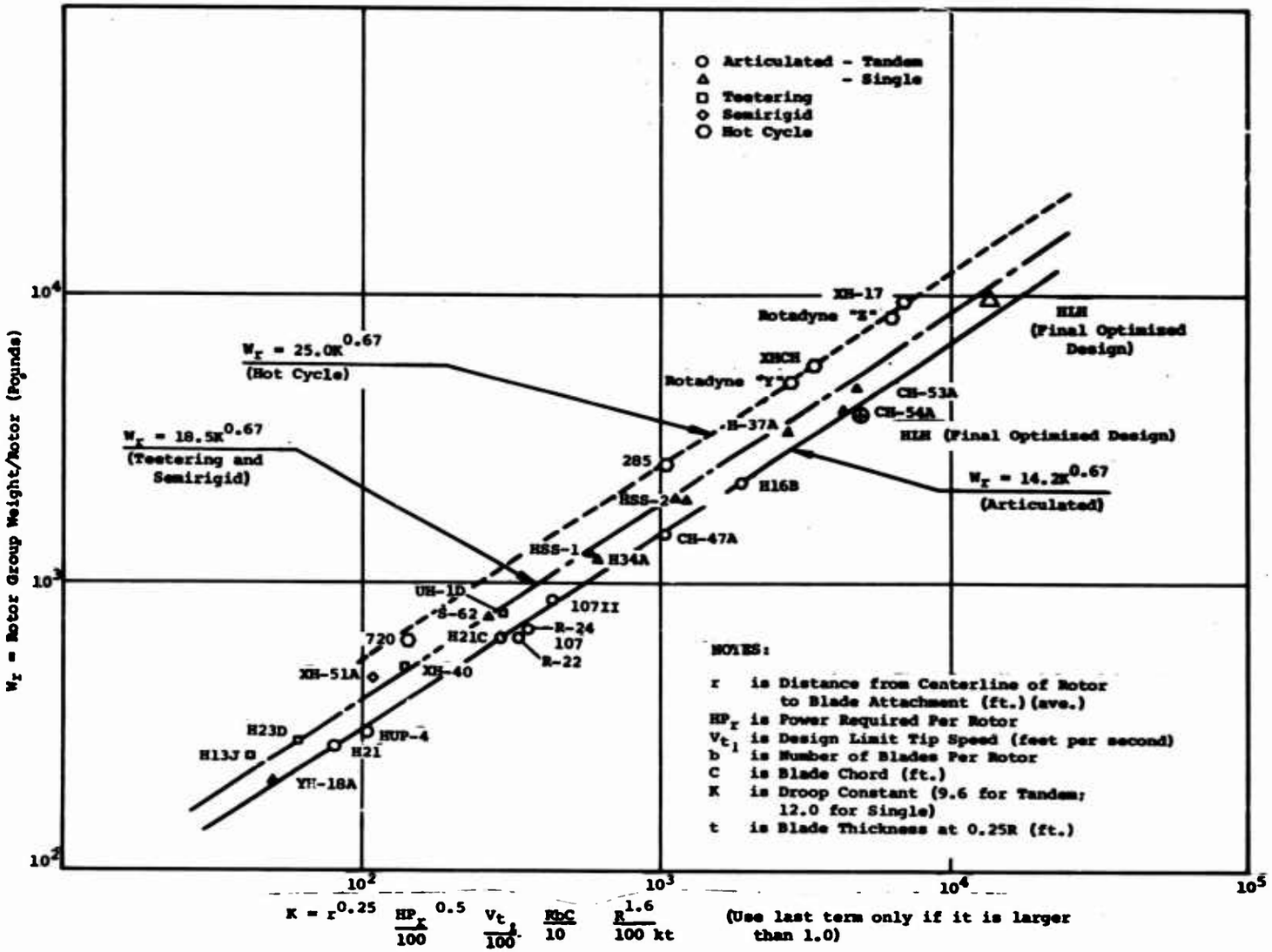

Figure 137. Rotor Group Weight Trend.

The preliminary design study revealed the occurrence of high coning angles when rotor weights derived by the standard trend were used. Since this existing trend does not reflect blade coning angle, it could not be used for the preliminary design study.

The following are the detail weight analyses for preliminary design of the tandem-lift and single-lift/antitorque rotor systems based on this procedure.

ROTOR GROUP--TANDEM-LIFT ROTOR SYSTEM

The rotor group weight is obtained by using the blade weight distribution curve (Figure 64) to establish the weight of the blade, and by calculated weights based on preliminary stress analysis and layouts for the hub, hinge, and blade retention system.

Blades

Using the blade weight distribution curve (Figure 64) for the P-6 fiberglass blade, the following blade weight is established:

Station 49.5-75.5:	26.0 x 2.67 lb/in.	= 69.4
Station 75.5-115.0 1/2	(39.5)(1.15 + 1.89) lb/in.	= 60.0
Station 115.0-502.0: 1/2	(387.0)(1.89 + 1.40) lb/in.	= 636.6
Station 502.0-516.0:	14.0 x 2.32 lb/in.	= 32.5
Total weight in pounds per blade (steel root-end fitting)		= 798.5

The weight of the steel root-end fitting (station 49.5-75.5) is 26.0 (2.67-1.15) lb/in = 39.5. Substituting titanium at 80-percent allowable stress value results in a weight saving of 10.5 pounds per blade. Weight of titanium fitting is 39.5 pounds x 0.735 = 29.0.

Total weight in pounds per blade (titanium root-end fitting)	= 788.0

Rotor Hub Assembly

Based on preliminary stress analysis for sizes, and the preliminary layout for the rotor head, the following weights for the hub components have been calculated:

1.	Hub block - Steel	443
	- Titanium	316
2.	Hub retaining plate - Steel	17
	- Titanium	12
3.	Hub oil reservoir - Magnesium	7
4.	Hub lubricating oil (0.534 gallons x 7.5 pounds per gallon	4

Total hub weight in pounds per rotor

steel components	471
titanium components	39

Hinge and Blade Retention System

The following table shows the weight breakdown calculated for the hinge and blade retention system. These weights are based on sizes established by stress analysis of the preliminary rotor hub layout.

Component	No. Per Rotor	Steel Unit Weight (lb)	Steel Weight Rotor (lb)	Titanium Unit Weight (lb)	Titanium Weight Rotor (lb)
Horizontal Pin	3	72.0	216.0	51.5	154.5
-Retainer cap	3	4.5	13.5	3.2	9.6
-Retainer cap	3	3.8	11.4	2.7	8.1
-Retainer	3	1.9	5.7	1.4	4.2
-Retainer nut	3	2.5	7.5	1.8	5.4
-Seals*	6	0.5	3.0	0.5	3.0
-Bushings	6	2.2	13.2	1.6	9.6
-Bearings assy*	6	18.5	111.0	18.5	111.0
Extension link	3	78.5	235.5	56.0	168.0
Tension-torsion strap	3	46.0	138.0	33.0	99.0
Tension-torsion pin	3	6.0	18.0	4.3	12.9
Vertical pin	3	28.0	84.0	20.0	60.0
Pitch housing	3	128.0	384.0	91.0	273.0
Pitch shaft					
Inbd brg assy*	3	27.0	81.0	27.0	81.0
Obd brg assy*	3	14.0	42.0	14.0	42.0
Oil reservoir*	3	1.0	3.0	1.0	3.0
Lubricating Oil	-	1.0	3.0	1.0	3.0
Total Weight per Rotor			1570.8		1190.7
Use			1570		1190

*The following components are not affected by substituting titanium for steel:
Horizontal pin seals are aluminum.
Bearing assemblies must be steel.
Pitch shaft oil reservoir is magnesium.

Rotor Group Weight Summary

The results of the rotor group weight analysis are summarized in the following table.

ROTOR COMPONENTS	WEIGHT PER ROTOR STEEL (lb)	WEIGHT PER ROTOR TITANIUM (lb)
Blades (3/rotor)	2395.5	2364.0
Hub	471.0	339.0
Hinge and blade retention	1570.0	1190.0
Total weight per rotor (W_r)	4436.5	3893.0
Number of Rotors (n_r)	x 2	x 2
Total Rotor Group Weight (W_R)	8873.0	7786.0

The substitution of titanium for steel in these rotor system components is feasible within existing technology. Therefore, the rotor group weight for the preliminary design study is 7786 pounds per aircraft.

ROTOR GROUP--SINGLE-LIFT/ANTITORQUE ROTOR SYSTEM

The group weight for the single-lift/antitorque rotor system is obtained as described below.

Blades

The same coning angle criteria established for the tandem-lift rotor system is applied to the single-lift/antitorque rotor system. Restricting the coning angle to a maximum of 6.6 degrees, the blade weight required to produce this limit can be determined by using equation 18.

$$\beta(\text{radians}) = \frac{0.75\ R\ \dfrac{GW}{N_r \times b} - M}{I_f \Omega^2} \qquad (18)$$

where

β is coning angle in radians
R is rotor radius in feet
GW is design gross weight in pounds
N_r is number of rotors
b is number of blades per rotor
M is blade static moment in foot-pounds, or $W_f \bar{R}$
W_f is blade flapping weight in pounds
$\bar{R}$ is distance from centerline of flapping hinge to blade center of gravity in feet
I_f is blade flapping inertia in foot-pound-seconds squared, or $k \frac{W_f}{g} L^2$
k is 0.19
L is R-d, or 48 - 1.5 = 46.5
d is hinge offset
Ω is rotor speed in radians per second

Substituting the known parameters in the equation results in the following:

$$\beta = 6.6° = 0.1152 \text{ radians} = \frac{0.75(48.0)\left(\frac{91,600}{1 \times 5}\right) - W_f \bar{R}}{0.19\left(\frac{W_f}{g}\right) L^2 \times [0.105(139 \text{ rpm})]^2} \quad (19)$$

Based on a blade weight distribution, the blade center of gravity was determined to be at 40 percent of the rotor radius. The flapping hinge offset (distance from centerline of rotation to centerline of flapping hinge) for the single-lift/antitorque rotor system is 1.5 feet. Therefore, the value of $\bar{R}$ is

$$\bar{R} = 0.40\ (48.0) - 1.5 = 17.7 \text{ feet}$$

$$\beta = 0.1152 = \frac{0.75\ (48.0)\left(\frac{91,600}{1 \times 5}\right) - W_f\ (17.7)}{0.19\left(\frac{W_f}{32.2}\right)\ (46.5)^2\ [0.105\ (139 \text{ rpm})]^2} \quad (20)$$

Solving for W_f, the required blade flapping weight is 2003 pounds per blade.

The ratio of blade weight to blade flapping weight is:

$$\frac{W_b}{W_f} = 0.600. \tag{21}$$

Therefore, the blade weight is:

$$W_b = 0.6\ (2003) = 1202 \text{ pounds per blade} \tag{22}$$

Rotor Hub Assembly

The weight of a steel hub assembly is estimated to be 20 percent of the total blade weight (0.20 W_b):

$$W_h = 0.20\Sigma W_b$$
$$= 0.20\ (1202 \times 5) = 1202 \text{ pounds} \tag{23}$$

Hinge and Blade Retention System

The weight of the hinge and blade retention system is obtained by subtracting the blade weight (W_b) from the blade flapping weight (W_f).

$$W_H = W_f - W_b = 2003 - 1202$$

$$= 801 \text{ pounds per blade} \times 5 = 4005 \text{ pounds} \tag{24}$$

This weight is again based on steel components.

Rotor Group Weight Optimization

The total rotor group weight derived in the preceding paragraphs is 11,217 pounds. In order to reflect the technology advances available in 1968 to 1972, the rotor group weight will be optimized using the same criteria used for the tandem-lift rotor system. This optimization is obtained by substituting titanium, at 80 percent of allowable stress, for steel components wherever feasible.

Blades

The steel root-end fitting accounts for 9 percent of the blade weight.

$$W_F \text{ (Steel)} = 0.09(1202) = 108 \text{ pounds per blade} \tag{25}$$

W_F (Titanium) = 108 (0.735) = 79 pounds per blade (26)

Total weight saving = 5 (29 pounds per blade) = 145 pounds. (27)

Hub Assembly

Substituting titanium for steel in the hub results in a weight reduction of 318 pounds.

Hinge and Blade-Retention System

The weight of the hinge and blade-retention system is 4005 pounds using steel components. Since some of these components (bearings, bushings, etc.) must remain steel, only 84.5 percent of the total system weight can be considered for titanium substitution. The titanium reduction factor of 0.735 is increased to 0.716 based on the more detailed analysis performed on the tandem-lift rotor.

W_H = 4005 x 0.845 = 3384 pounds available for titanium substitution. (28)

W_H (Titanium) = 3384 x 0.716 = 2423 pounds

W_H (Steel) = 4005 x 3384 = 621 pounds

Total W_H using titanium = 3044 pounds

This is a weight saving of 961 pounds.

Rotor Group Weight Summary

The following table summarizes the weights for blades, hub, hinge and blade retention system for the single-lift/antitorque rotor system.

Rotor Group	Std Steel (lb)	Opt'zed Ti (lb)
Blades (5 required)	6,010	5,865
Hub	1,202	884
Hinge and blade retention	4,005	3,044
Total rotor group weight	11,217	9,793

The weight of the optimized rotor group is used in this report.

TAIL GROUP--SINGLE-LIFT/ANTITORQUE ROTOR SYSTEM ONLY

The weight of the horizontal stablizer is estimated using a unit weight of 2.73 pounds per square foot multiplied by the stabilizer area in square feet.

The tail rotor weight is obtained using the standard rotor group trend modified by changing the multiplying constant from 14.2 to 16.05.

BODY GROUP

Vertol Division has developed two weight trends for use in determining helicopter fuselage weights. The overall Body Group Trend (Figure 138) is used to derive the weights for the transport. The weights for the crane are developed by using the Body Group Basic Structure Trend (Figure 139) to obtain the basic structure weights, and adding the built-up weight of secondary structure and penalties for specific design features. The K-factor for both trends is identical and reflects the effect of the following parameters on body weight: design gross weight (Wg), ultimate load factor (n), fuselage wetted area (S_f), cabin length (l_c), ramp well length (l_{rw}), allowable center of gravity travel (ΔCG), and maximum forward flight velocity (V_{max}).

While the body group trend gives excellent correlation for transport helicopters, the basic structure trend is applicable to almost all helicopter configurations. The basic structure approach was used for the crane configurations because of the significantly smaller amount of secondary structure in this type aircraft.

ALIGHTING GEAR GROUP

The weights for this group are derived using a standard percentage of design gross weight for structure, a fixed constant for controls which is based on existing installations, and the latest vendor weights for the high-flotation (low unit construction index) rolling gear.

The detail weight breakdowns for the tandem-lift rotor and the single-lift/antitorque rotor helicopters cover both the rotor system parametric analysis and preliminary design study.

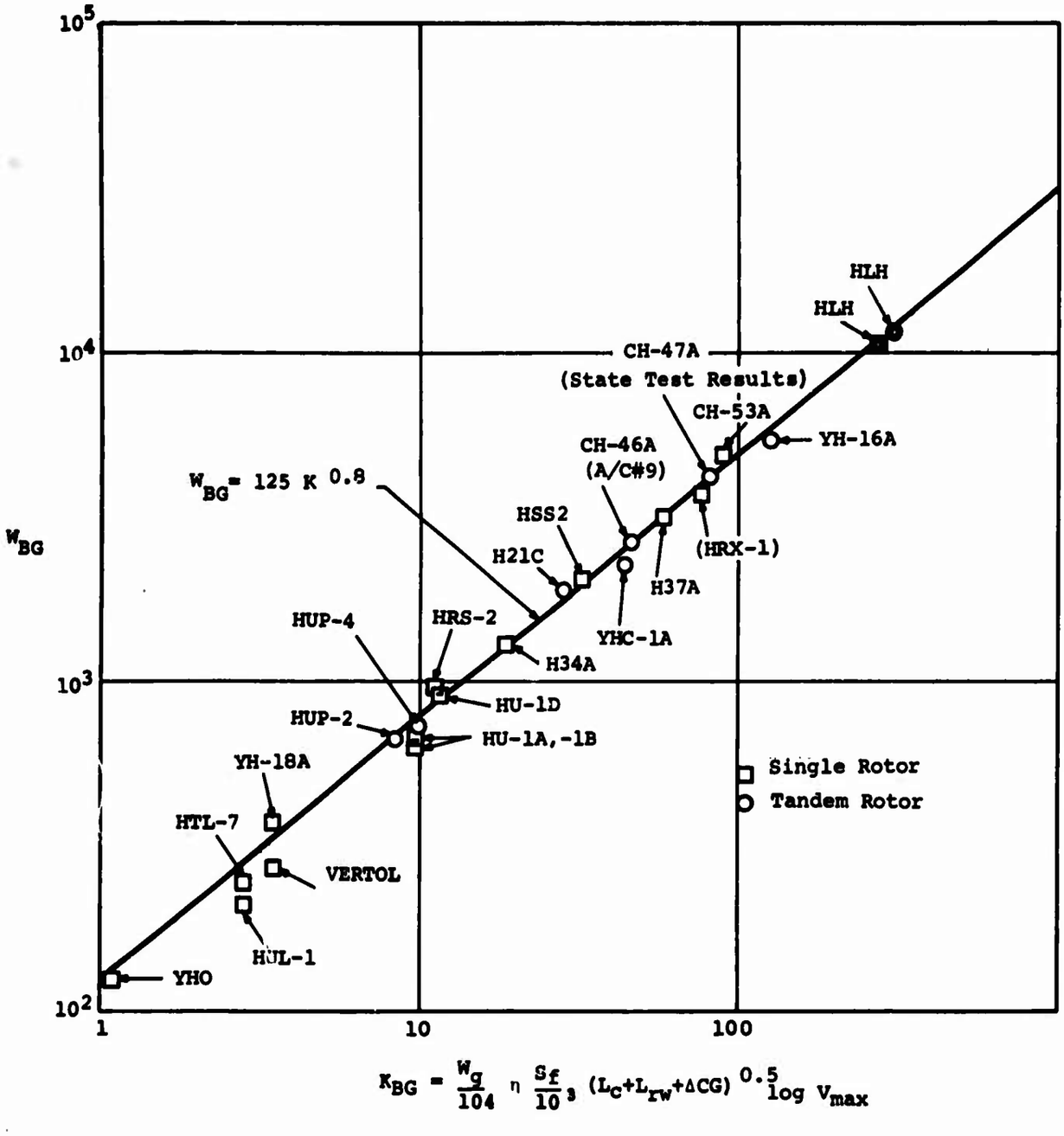

Figure 138. Body Group - Transport Helicopters.

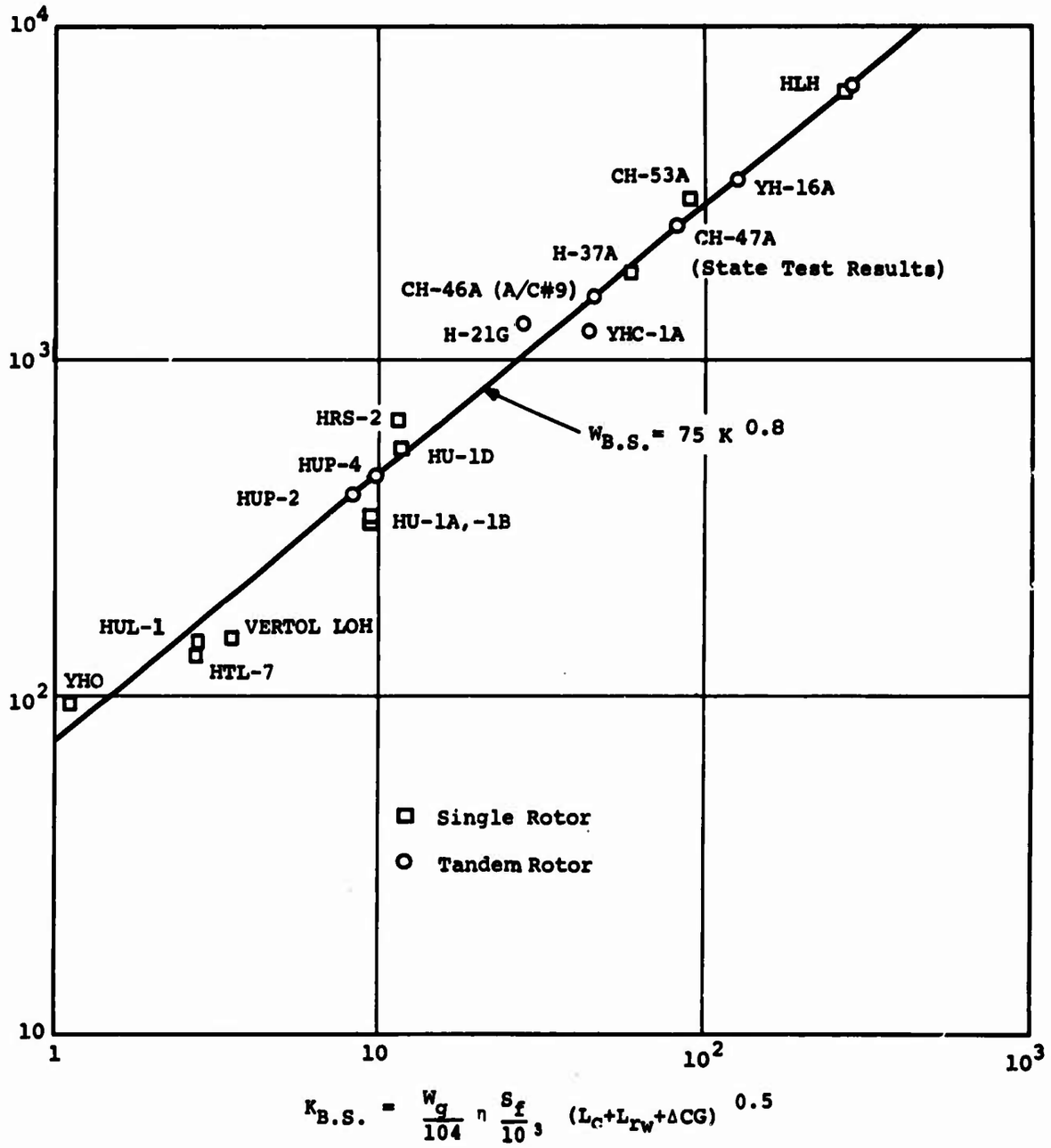

Figure 139. Body Group - Basic Structure.

Parametric Analysis of Tandem-Lift Rotor Transport

This configuration uses a standard fixed tricycle gear arrangement with quad-bogie mounted wheels on all three gears. The following is the weight derivation for this helicopter:

Rolling Gear			1322 pounds
Forward (Auxiliary) Gear:			
(4) 17.00-16 Wheel Assemblies (at 169 pounds each)	676		
Aft (Main) Gear:			
(8) 11.00-12 Wheel Assemblies (including brakes)	646		
Controls and Supports: (Estimated Weights)			55 pounds
Forward Gear	15		
Aft Gear	40		
Power Steering - Forward Gear Only (Estimated Weights)			50 pounds
Structure			2600 pounds
Forward Gear: 0.5 percent Wg = 0.005 (87,000)	435		
Aft Gear: 1.55 percent Wg = 0.155 (87,000)	1350		
Wheel Bogies	480		
Forward: 1/3 x 0.55 percent Wg = 1/3(0.55 percent) (87,000)		160	
Aft: 2/3 x 0.55 percent Wg = 2/3(0.55 percent)(87,000)		320	
Aft Landing Gear Stubs 11.2 ft x 5.0 ft x 3.0 ps x 2 required	335	335	
Total Existing Technology Alighting Gear Group			4027 pounds

Advanced technology weight optimization reduces the weight of structure by 5 percent:

Structure: 2600 pounds x 0.95	2470 pounds
Add:	
Rolling Gear	1322
Controls and Supports	55
Power Steering	50
Total Advanced Technology Alighting Gear Group	3897 pounds

Parametric Analysis of Tandem-Lift Rotor Crane/Personnel Carrier

The crane/personnel carrier configuration uses a fixed tricycle gear arrangement with quad-bogie mounted wheels on all three gears. The aft (main) gear is mounted on long struts to accommodate load clearances and to provide for straddling of external loads. The weight derivation for this aircraft is as follows:

Rolling Gear		1322 pounds
Forward (Auxiliary) Gear: (4) 17.00-16 Wheel Assemblies (at 169 pounds each)	676	
Aft (Main) Gear: (8) 11.00-12 Wheel Assemblies (including brakes)	646	
Controls and Supports (Estimated Weights)		55 pounds
Forward Gear	15	
Aft Gear	40	
Power Steering - Forward Gear Only (Estimated Weights)		50 pounds
Structure (Tall Aft Gear)		3872 pounds
Forward Gear: 0.5 percent W_g = 0.005 (87,000 pounds)	435	
Aft Gear: 3.6 percent W_g = 0.036 (87,000 pounds)	3132	
Wheel Bogies:	305	

Forward: 1/3 x 0.35 percent (87,000)	102	
Aft: 2/3 x 0.35 percent (87,000)	203	
Total Alighting Gear Group (Existing Technology)		5299 pounds

Using a 5-percent weight reduction factor, to reflect the 1968-1972 technology advances, reduces the weight of alighting gear structure.

Structure: 3872 pounds x 0.95		3678 pounds
Add:		
Rolling Gear		1322
Controls and Supports		55
Power Steering		50
Total Advanced Technology Alighting Gear Group		5105 pounds

Preliminary Design Study of Tandem-Lift Rotor Transport

This configuration uses a standard fixed tricycle gear arrangement with dual wheels on all three gears. The following is the weight derivation for this configuration:

Forward (Auxiliary) Gear		763 pounds
Rolling Gear	338	
Tires: 17.00-16 (2 at 124 pounds each)	248	
Tubes: 17.00-16 (2 at 19 pounds each)	38	
Wheels: 17.00-16 (2 at 24 pounds each)	48	
Air: Estimated at 2.0 pounds per tire	4	
Controls and Supports (Estimated)		15 pounds
Power Steering (Estimated)		50 pounds
Structure		360 pounds

The estimated weight for the forward landing gear structure is equal to 25 percent (Wg x 3.5 percent) minus the weight of rolling gear controls and supports, and power steering.

Ws = 0.25 (87,000 pound x 3.5 percent)
= 763 pounds - 403 pounds (29)

Aft (Main) Gear		2621 pounds
Rolling Gear	816	
Tires: 17.00-16 (4 at 124 pounds each)	496	
Tubes: 17.00-16 (4 at 19 pounds each)	76	
Wheels: 17.00-16 (4 at 24 pounds each)	96	
Brakes: (4 at 35 pounds each) (KECap.= 1.9 x 10^6 foot-pound)	140	
Air: Estimated at 2.0 pounds per tire	8	
Controls and Supports (Estimated)		40
Structure		
Ws = 0.75 (87,000 x 3.5 percent) = 2286 - 856 pounds		1430 (30)
Add: Main Gear Stubs: 56 feet squared per side x 3.0 psf x 2 = 235 pounds		____
Total Alighting Gear Group		3384 pounds

Preliminary Desig.. Study of Tandem-Lift Rotor Crane/Personnel Carrier

The alighting gear is a fixed, tricycle, dual-wheel arrangement with tall aft (main) gear to accommodate load clearances and straddling capability. The total group weight is approximately 4-1/2 percent of the design gross weight, with a 20/80 percent group weight distribution between the auxiliary and main gear respectively.

Forward (Auxiliary) Gear			788 pounds
Rolling Gear		338	
Tires: 17.00-16 (2 at 124 pound	248		
Tubes: 17.00-16 (2 at 19 pound	38		
Wheels: 17.00-16 (2 at 24 pound	48		
Air: Estimated at 2.0 pound	4		
Controls and Supports		15	
Power Steering		50	
Structure		385	
Ws = 0.20 (87,000 x 4.5 percent) = 788-403 pounds			(31)
Aft (Main) Gear			3131 pounds
Rolling Gear		816	
Tires: 17.00-16 (4 at 124 pounds each)	496		
Tubes: 17.00-16 (4 at 19 pounds each)	76		
Wheels: 17.00-16 (4 at 24 pounds each)	96		
Brakes: (4 at 35 pounds each) (KE Cap = 1.9 x 10^6 foot-pounds)	140		
Air: Estimated at 2.0 pounds per tire	8		
Controls and Supports		40	
Structure		2275	
Ws = 0.80 (87,000 x 4.5 percent) = 3131-856 pounds			(32)
Total Alighting Gear Group			3919 pounds

Parametric Analysis of Single-Lift/Antitorque Rotor Transport

This configuration uses a standard fixed tricycle gear arrangement with quad bogie-mounted wheels on all three gears.

Rolling Gear		1322 pounds
Forward (Auxiliary) Gear: (4) 17.00-16 Wheel Assembly (at 169 pounds each)	676	
Aft (Main) Gear: (8) 11.00-12 Wheel Assembly (at 80.75 pounds each including brakes)	646	
Controls and Supports (Estimated)		55 pounds
Forward Gear	15	
Aft Gear	40	
Power Steering - Forward Gear Only (Estimated)		50 pounds
Structure		2873 pounds
Forward Gear: 1/3 (2.22 percent) (91,600 pounds)	678	
Aft Gear: 2/3 (2.22 percent) (91,600 pounds)	1356	
Wheel Bogies:	504	
Forward: 1/3 (0.55 percent) (91,600 pounds)	168	
Aft: 2/3 (0.55 percent) (91,600 pounds)	336	
Main Landing Gear Stubs	335	
56 feet squared per side x 3.0 pounds per square foot x 2	335	

Reducing the structure weight by 5 percent for the 1968-1972 advanced technology:

Structure 2873 pounds x 0.95	2729
Rolling Gear	1322
Controls and Supports	55

Power Steering	50	
Total Alighting Gear Group (Advanced Technology)		4156 pounds

Parametric Analysis of Single Rotor Crane/Personnel Carrier

The crane/personnel carrier uses the same gear arrangement as the transport. The major difference between configurations is the tall aft (main) gear struts to provide for clearances and straddling of large external loads.

Rolling Gear	Same as Transport	1322 pounds
Controls and Supports	Same as Transport	55 pounds
Power Steering	Same as Transport	50 pounds
	Subtotal	1427 pounds
Structure (with Tall Aft Gear)		4066 pounds
Forward Gear: 0.4 percent (91,500 pounds)	366	
Aft Gear: 3.7 percent (91,500 pounds)	3380	
Wheel Bogies: 0.35 percent (91,500 pounds)	320	
	Total	5493 pounds

Using a 1968-1972 advanced technology weight reduction factor of 5 percent results in an alighting gear group weight of:

Structure	4066 pounds x 0.95	3860
Rolling Gear		1322
Controls and Supports		55
Power Steering		50
Total Alighting Gear Group		5287 pounds

Preliminary Design Study of Single-Lift/Antitorque Rotor Transport

This configuration uses a standard fixed tricycle gear arrangement with dual wheels on all three gears. The following is the weight derivation for this helicopter.

Forward (Auxiliary) Gear			803 pounds
Rolling Gear		338	
Tires: 17.00-16 (2 at 124 pounds each)	248		
Tubes: 17.00-16 (2 at 19 pounds each)	38		
Wheels: 17.00-16 (2 at 24 pounds each)	48		
Air: Estimated at 2.0 pounds per tire	4		
Controls and Supports (Estimated)		15	
Power Steering (Estimated)		50	
Structure		400	

The estimated weight for the forward landing gear structure is equal to 25 percent (Wg x 3.5 percent) minus the weight of rolling gear, controls and supports, and power steering.

Ws = 0.25 (91,600 pounds x 3.5 percent
= 803-403 pounds = 400 pounds (33)

Aft (Main) Gear			2741 pounds
Rolling Gear		816	
Tires: 17.00-16 (4 at 124 pounds each)	496		
Tubes: 17.00-16 (4 at 19 pounds each)	76		
Wheels: 17.00-16 (4 at 24 pounds each)	96		
Brakes: (4 at 35 pounds each) KE Cap. = 1.9 x 10^6 foot-pounds)	140		

Air: Estimated at 2.0 pounds per tire	8	
Controls and Supports (Estimated Weight)		40
Structure		1885
Ws = 0.75 (91,600 pounds x 3.5 percent) = 2406-856 pounds		1550
Add: Main Gear Stubs: 45 feet squared per side x 3.0 psf x 2		335
Total Alighting Gear Group		3544 pounds

Preliminary Design Study of Single-Lift/Antitorque Rotor Crane/ Personnel Carrier

The alighting gear for this configuration is a fixed, tricycle, dual-wheel arrangement with tall aft (main) gear to accommodate load clearances and straddling capability. The total group weight is approximately 4-1/2 percent of the design gross weight, with a 20/80 percent group weight distribution between the auxiliary and main gear respectively.

Forward (Auxiliary) Gear		825 pounds
Rolling Gear		338
Tires: 17.00-16 (2 at 124 pounds each)	248	
Tubes: 17.00-16 (2 at 19 pounds each)	38	
Wheels: 17.00-16 (2 at 24 pounds each)	48	
Air: Estimated at 2.0 pounds per tire	4	
Controls and Supports		15
Power Steering		50
Structure		422
Ws = 0.20 (91,600 x 4.5 percent) = 825-403 pounds		

(34)

Aft (Main) Gear		3300 pounds
Rolling Gear	816	
Tires: 17.00-16 (4 at 124 pounds each)	496	
Tubes: 17.00-16 (4 at 19 pounds each)	76	
Wheels: 17.00-16 (4 at 24 pounds each)	96	
Brakes: (4 at 35 pounds each) (KE Cap = 1.9 x 10^6 foot-pounds)	140	
Air: Estimated at 2.0 pounds per tire	8	
Controls and Supports	40	
Structures	2444	
Ws = 0.80 (91,600 x 4.5 percent) = 3300-856 pounds		____ (35)
Total Alighting Gear Group		4125 pounds

FLIGHT CONTROLS GROUP

The weights for cockpit, upper, and system controls have been derived using the trend curves (Figures 140, 141, and 142). Estimated weights are used for the stability augmentation system (S.A.S.), and the loadmaster's hover controls.

The weight of cockpit controls is obtained from equation 36:

$$W_{CC} = 26\left(\frac{W_g}{10^3}\right)^{0.41} \qquad (36)$$

where
W_g is design gross weight

The trend expressions for upper controls are:

$$W_{UC} = n_r \times 0.15\ W_r \qquad (37)$$

where
n_r is number of rotors
W_r is rotor group weight per rotor

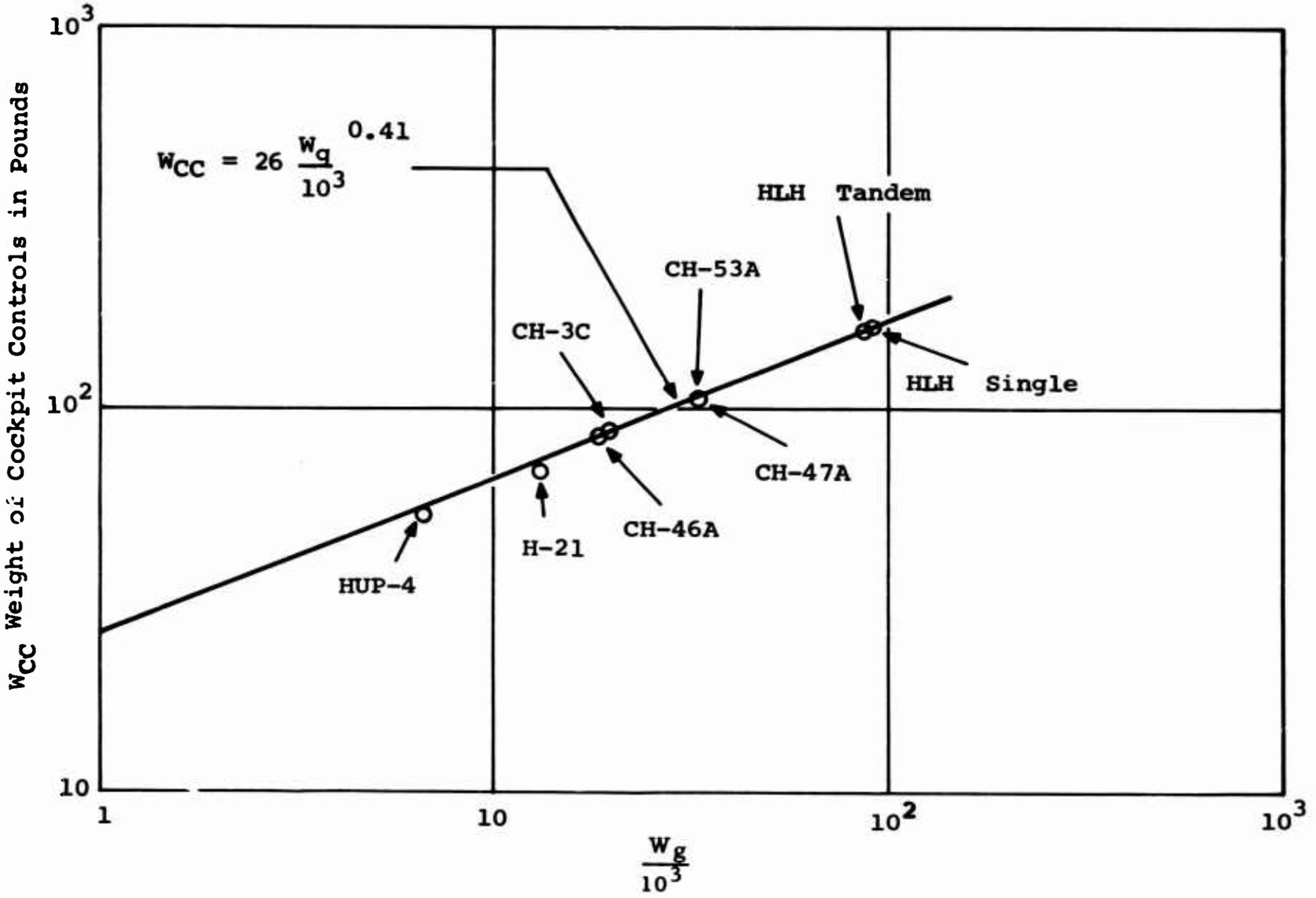

Figure 140. Flight Controls Group-Cockpit Controls Weight Trend (for Helicopter Dual Cockpit Controls).

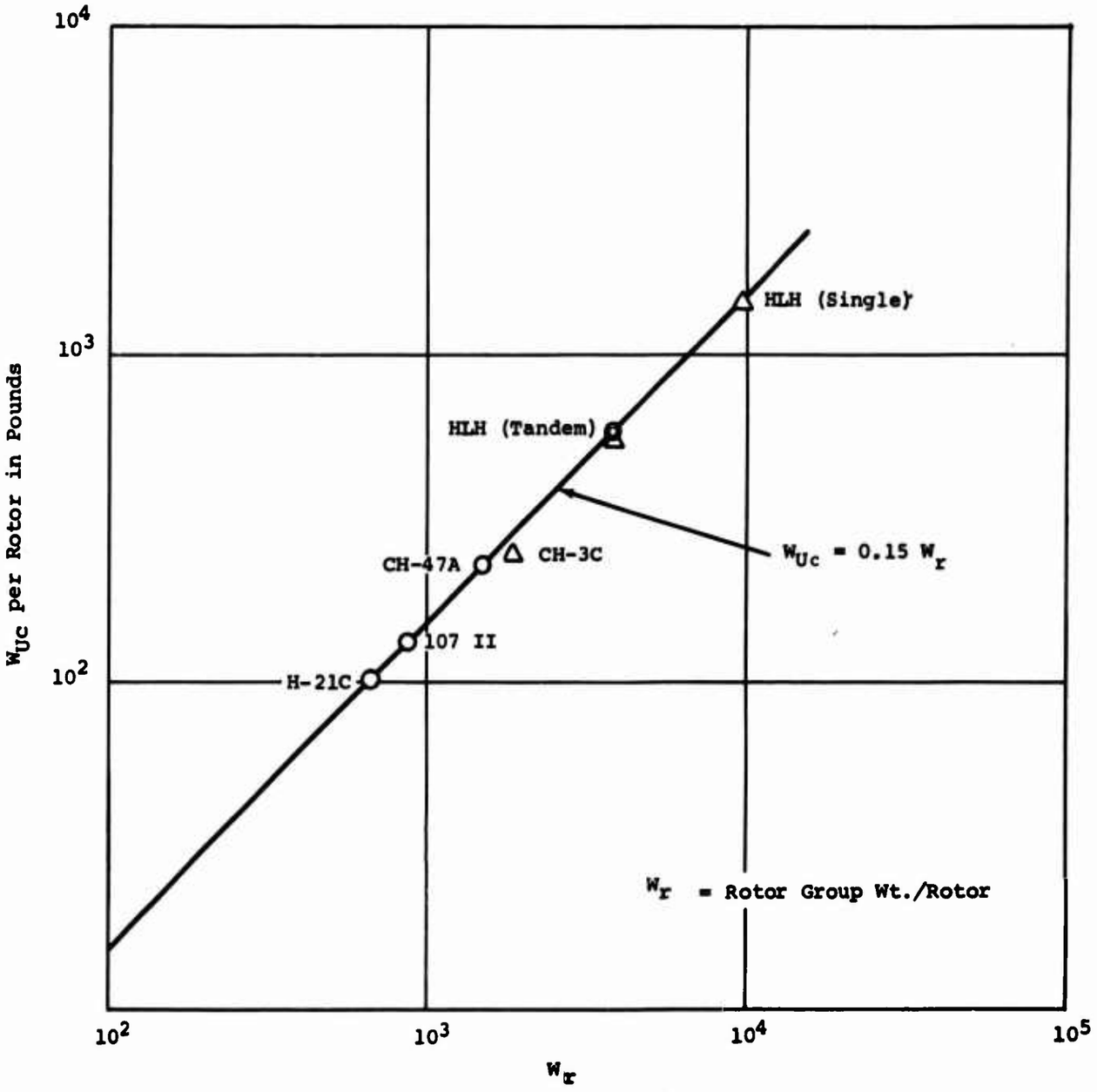

Figure 141. Flight Controls Group Upper Controls Weight Trend, Including Upper Boost Actuators.

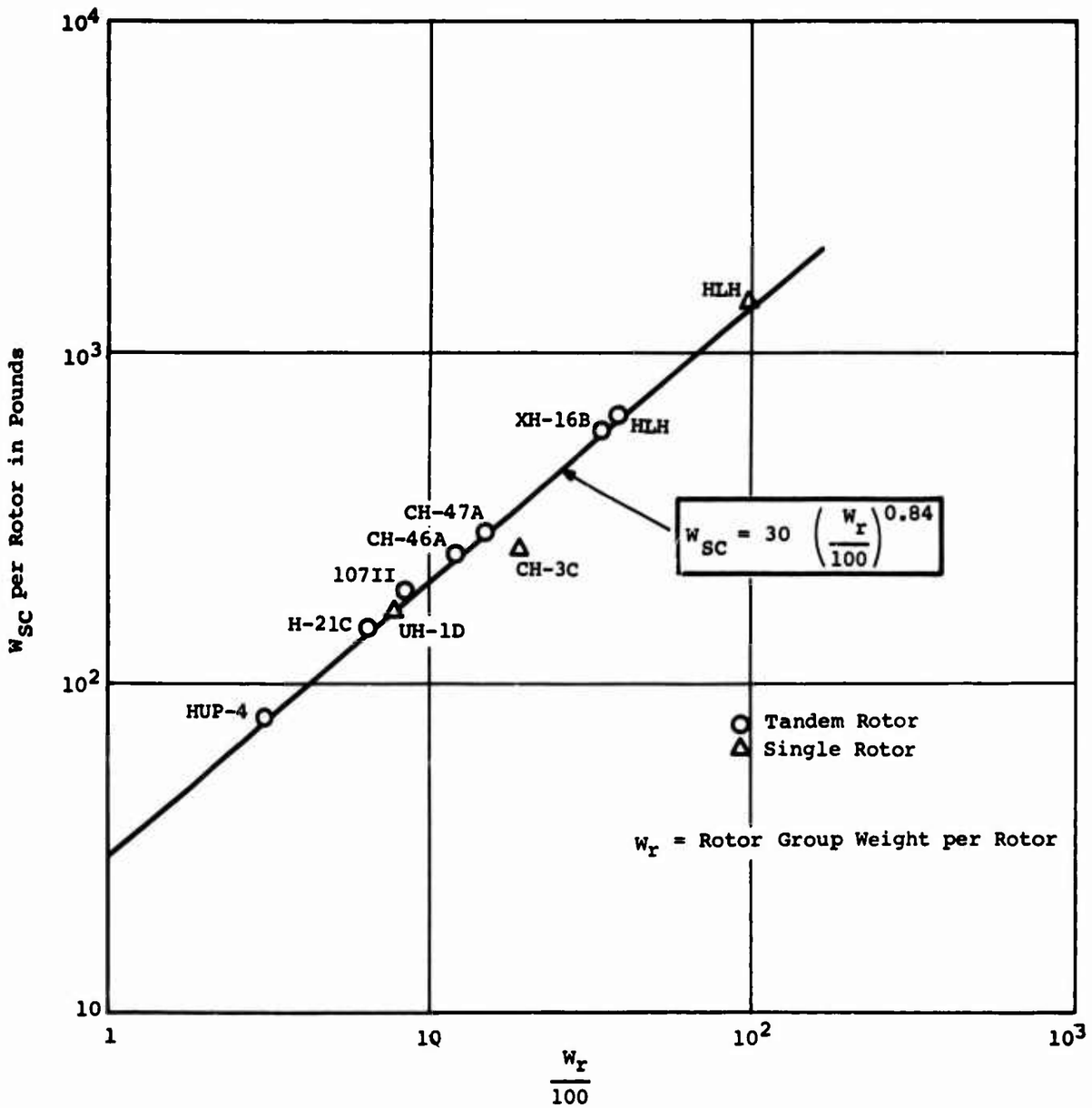

Figure 142. Flight Controls Group System Controls Weight Trend.

ENGINE SECTION OR NACELLE GROUP

Parametric Analysis of Tandem-Lift Rotor System

The engine section weight is assumed to be identical in both tandem-lift rotor configurations. The weight estimate is based on a similar installation in the CH-47A. For purposes of the parametric study, the engine section weight has been reduced to a function of the number of engines. The following is the weight estimate for the LTC4B-11 type engine installation.

$$W_{ES} = 90 \times N_E = 90 \times 4 = 360 \text{ pounds} \quad (38)$$

where
N_E is number of engines

Reducing this weight by 5 percent to reflect the 1968-1972 advanced technology results in an engine section weight of

$$(W_{ES})_A = 360 \times 0.95 = 342 \text{ pounds} \quad (39)$$

Parametric Analysis of Single-Lift/Antitorque Rotor System

The engine section weight is assumed to be the same for both single-lift/antitorque rotor configurations. For purposes of the parametric study, the weight of the engine section has been reduced to a function of the number of engines, and is based on similar single-lift/antitorque rotor engine installations. The following is the weight estimate for the 501-M26 engines.

$$W_{ES} = 152\ N_E = 152 \times 4 = 608 \text{ pounds} \quad (40)$$

where
N_E is number of engines

Reducing this weight by 5 percent for advanced technology results in a weight saving of 33 pounds.

$$(W_{ES})_A = 608 - 33 = 575 \text{ pounds} \quad (41)$$

Preliminary Design Study of Tandem-Lift Rotor Transport

The engine section weight is a function of engine size and weight. Engine mount weight is a function of engine weight and

crash load factor. Standard unit weights in pounds per square foot are used to determine firewall and nacelle structure weights.

The engines in the transport configuration are installed in a stub-wing type structure, and each pair of engines is separated by a structural firewall.

Engine Mount

$$W_M = (We \times \eta_{CR})^{0.41} \times N_E = \quad 140 \text{ pounds} \quad (42)$$

where
We is engine weight
η_{CR} is crash load factor
N_E is number of engines

$$W_M = (645 \times 8.0)^{0.41} \times 4 = \quad 140 \text{ pounds} \quad (43)$$

Structural Firewall — 30 pounds

12.5 feet squared per side x 1.2 psf
x 2 required = 30 pounds

Nacelle Structure — 270 pounds

226 feet squared per side x 0.6 psf
= 135 pounds per side x 2 = 270 pounds

Total Nacelle Group - Existing Technology — 440 pounds

Advanced technology weight optimization factor — x 0.95

Total Nacelle Group - Advanced Technology — 420 pounds

Preliminary Design Study of Tandem-Lift Rotor Crane/Personnel Carrier

The engines in both crane configurations are installed in the aft landing gear support struts and are separated by a structural firewall. The weight for nacelle structure is included in the landing gear group weight for aft gear structure.

Engine Mounts — Same as Transport — 140 pounds

Structural Firewall — 54 pounds

22.5 squared feet per side x 1.2 pounds per square foot

x 2 required = 54 pounds ____

Total Nacelle Group - Existing Technology 194 pounds
Advanced technology weight optimization factor x 0.95

Total Nacelle Group - Advanced Technology 185 pounds

Preliminary Design of Single-Lift/Antitorque Rotor Aircraft

The engine section weight is a function of engine size and weight. The weight of engine mounts is a function of engine weight and crash load factor. The crash load factor has been increased from 8g to 20g on the single-lift/antitorque rotor system because of the location of the engines above the cabin.

Engine Mount

$$W_M = We(n_{CR})^{0.41} \times N_E \qquad (44)$$ 232 pounds

where
We is engine weight = 1030 pounds
n_{CR} is crash load factor = 20
N_E is number of engines = 4

W_M is $\left[1030(20)\right]^{0.41} \times 4 = 232$ pounds

Nacelle Structure and Firewall 343 pounds

Nacelle wetted area 45 square feet
at 1.91 pounds per square foot x 4 = 343 pounds

Total Nacelle Group - Advanced Technology 575 pounds

PROPULSION GROUP (EXCLUDING DRIVE SYSTEM)

The engine weights are taken from manufacturers' specifications. The weights of propulsion subsystems are based on similar installations from existing aircraft.

Fuel tank weights are obtained using a unit weight of 0.2625 pounds per gallon multiplied by the total usable capacity in gallons. This unit weight represents a tank with 50-percent self-sealing cells protected against 7.62mm (.30 cal.) projectiles.

DRIVE SYSTEM

The drive system weight for the rotor system parametric analysis was obtained using the "overall" trend, modified to reflect the results of the Heavy-Lift Transmission Study (Reference 27). The standard trend expression (Figure 143) is

$$W_D = 260 \left(\frac{k \, HP_x}{Nr} \right)^{0.8} \tag{45}$$

where

HP_x is transmission design horsepower
N_r is rotor speed (rpm)
k is 1.0 for single-lift/antitorque rotor system
or 1.2 for tandem-lift rotor system

The modified trend equation is

$$W_D = 196 \left(\frac{1.2 \, HP_x}{n_r} \right)^{0.8} \quad \text{for tandem-lift rotor} \tag{46}$$

and

$$W_D = 200 \left(\frac{1.0 \, HP_x}{n_r} \right)^{0.8} \quad \text{for single-lift/antitorque rotor} \tag{47}$$

The drive system weights for the preliminary design study were estimated using the following equations:

$$W_D = 195 \left(\frac{1.2 \, HP_x}{n_r} \right)^{0.8} \quad \text{for tandem-lift rotor} \tag{48}$$

and

$$W_D = 200 \left(\frac{1.0 \, HP_x}{n_r} \right)^{0.8} \quad \text{for single-lift/antitorque rotor} \tag{49}$$

NOTE: The small adjustment in the constant of the tandem-lift rotor equation used for the preliminary design study resulted from a detailed item-by-item review of the drive system using proprietary estimating methods.

FIXED EQUIPMENT GROUPS

The following group weights have been determined from statistical analysis of existing aircraft and from preliminary requirements specified in the original QMDO issued by the Army. These group weights will vary depending on the configuration, but the variation will be small when comparing similar type aircraft; i.e., single-lift/antitorque rotor versus tandem-lift rotor transports.

Auxiliary Powerplant Group	
(125 HP System)	**130**
CH-47A unit (80 HP) = 67 pounds = 0.84 pounds per horsepower; HLH unit (125 HP) = 125 horsepower x 0.84 pounds per horsepower	105
Air induction system	3
Exhaust system	1
Fuel system: pump (3 pounds) + plumbing (5 pounds)	8
Controls	10
Supports and miscellaneous	3

Instruments Group — **248**

$$W_I = 180 + 17\ N_E \qquad (50)$$

where

180 is weight (pounds) of flight, fuel, quantity, drive hydraulic and miscellaneous instrument installations

17 is weight (pounds) of engine instruments per engine

N_E is number of engines

$$W_I = 180 + 17\ (4) = 248 \text{ pounds} \qquad (51$$

Hydraulics Group	**300**
Motors, pumps and supports	55
Reservoirs and accumulators	38
Filters, pressure regulators, and valves	30
Circuitry	4
Plumbing	98
Fluid	40
Cooler installation	27
System Supports	8

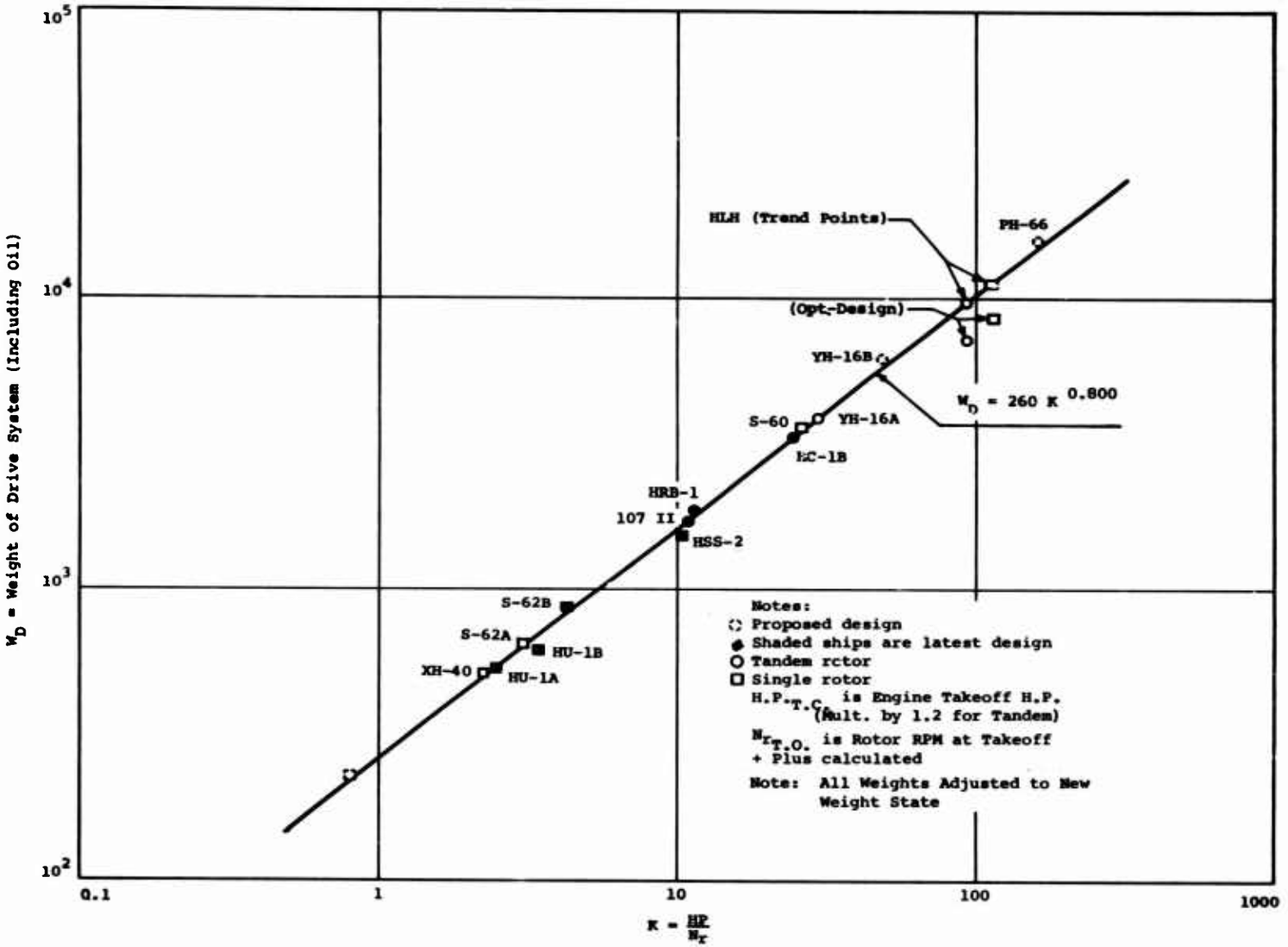

Figure 143. Drive System Weight Trend for Turbine-Powered Helicopters

Electrical Group			**995**
AC System			737
Power supply		275	
Generators (3) 40 KVA	231		
Cooling ducts	2		
APP (1) 15 KVA	42		
Power conversion		49	
Transformers	24		
Rectifiers	25		
Power distribution and control		384	
Generator control boxes	43		
Supervisory panels	20		
Meters, switches, and circuit breakers	16		
Junction, fuse, and distribution boxes	41		
Relays	6		
Wiring and plugs	258		
Lights and signal devices		9	
Equipment supports		20	
DC System			258
Power Supply - 22 ampere-hour battery and supports		57	
Power conversion - (2) static inverters		32	
Power distribution and control		152	
Supervisory panels	14		
Switches and circuit breakers	24		
Junction, fuse, and distribution boxes	17		
Relays	4		
Wiring and plugs	93		
Lights and signal devices		14	
Equipment supports		3	
Electronics Group			**280**

	Government Furnished	Contractor Furnished	Instal-lation
Communications	56	40	43
UHF radio	10	-	5
VHF/FM radio (with homing)	27	-	8
FM auxiliary radio	4	-	2
Crew intercom (ICS)	15	-	10
Loudspeaker system	-	40	18

	Government Furnished	Contractor Furnished	Installation
Navigation	62	-	24
ADF-LF/MF	18	-	9
VOR/DME/LOX	40	-	10
Marker beacon	4	-	5
Identification (IFF)	30	-	5
Common Avionics Instruments	-	-	20
	148	40	92
Total Electronics Group			280
Furnishings and Equipment Group: Transport Configuration			783
Personnel Accommodations			466
Pilot and copilot seats (2 at 48 pounds each)		96	
Crew seats (2 at 9 pounds each)		18	
Miscellaneous Accommodations and oxygen provisions		16	
Troop seat provisions 2.4 x 120 troops		288	
Litter provisions 0.5 x 96 litters		48	
Miscellaneous Equipment			181
Map and data cases		2	
Windshield wiper installation		10	
Rearview mirror installation		13	
Consoles, panels, C/B panels, etc.		35	
Cargo tiedown fittings 45 feet long x 12 feet wide x 0.224 psf		121	
Furnishings			60
Soundproofing and insulation in cockpit area			
Emergency Equipment			76
Portable fire extinguisher (2 at 8 pounds each)		16	
First-aid kits (2 at 2 pounds each)		4	

Engine fire detection system (3 pounds per engine)	12	
Engine fire extinguishing system (11 pounds per engine)	44	
Furnishings and Equipment Group: Crane/Personnel Carrier		**578**
Personnel Accommodations		**382**
Pilot and copilot seats (2 at 48 pounds)	96	
Crew seats (2 at 9 pounds each)	18	
Miscellaneous accommodations and oxygen provisions	16	
Troop seat provisions: 2.4 x 90 troops	216	
Litter provisions: 0.5 x 72 litters	36	
Miscellaneous Equipment		**60**
Map and data cases	2	
Windshield wiper installation	10	
Rearview mirror installation	13	
Consoles, panels, C/B panels, etc.	35	
Furnishings (Same as transport)		**60**
Emergency Equipment (Same as transport)		**76**
Air Conditioning and Anti-icing Group		**128**
Air Conditioning		**70**
Cockpit heating and ventilation system	70	
Fans	6	
Heat exchange (bleed air type)	15	
Ducting - cockpit area	20	
- bleed air	15	
Controls	5	
Valves, mufflers, and supports	9	
Anti-icing		**58**
Windshield deicing (electrical)	10	
Engine inlet anti-icing (bleed-air) (12 pounds per engine x 4 = 48 pounds)	48	

Auxiliary Gear Group		2550
Aircraft handling gear		32
Provisions for jacking	10	
Provisions for hoisting	15	
Aircraft tiedown provisions	7	
Load handling gear (5-winch system)		2518
Cargo Hook - 20-ton capacity (1 required)	150	
- 15-ton capacity (4 at 75 pounds each)	300	
Winch - 20-ton capacity (1 required)	457*	
- 15-ton capacity (4 at 344 pounds each)	1376**	
Equipment supports	235	

NOTE: * Weight includes 75 feet of 7/8-inch diameter cable (MIL-C-5424)

** Weight includes 75 feet of 3/4-inch diameter cable (MIL-C-5424)

UNCLASSIFIED

Security Classification

DOCUMENT CONTROL DATA - R&D

(Security classification of title, body of abstract and indexing annotation must be entered when the overall report is classified)

1 ORIGINATING ACTIVITY (Corporate author) Vertol Division The Boeing Company Morton, Pennsylvania	2a REPORT SECURITY CLASSIFICATION Unclassified 2b GROUP N/A

3. REPORT TITLE

STUDY OF THE HEAVY-LIFT HELICOPTER ROTOR CONFIGURATION

4. DESCRIPTIVE NOTES (Type of report and inclusive dates)

Final

5. AUTHOR(S) (Last name, first name, initial)

Wax, Charles M., and Tocci, Rocco C.

6. REPORT DATE	7a. TOTAL NO. OF PAGES	7b. NO. OF REFS
November 1966	404	27

8a. CONTRACT OR GRANT NO. DA44-177-AMC-206(T) b. PROJECT NO. Task 1P125901A14203 c. d.	9a. ORIGINATOR'S REPORT NUMBER(S) USAAVLABS Technical Report 66-61 9b. OTHER REPORT NO(S) (Any other numbers that may be assigned this report) R-445

10. AVAILABILITY/LIMITATION NOTICES

Distribution of this document is unlimited.

11. SUPPLEMENTARY NOTES	12. SPONSORING MILITARY ACTIVITY
	U.S. Army Aviation Materiel Laboratories, Fort Eustis, Virginia 23604

13. ABSTRACT

A two-part parametric analysis and design study was conducted to define the optimum shaft-driven rotor system for the heavy-lift helicopter.

A parametric analysis was made for the tandem-lift rotor system and the single-lift/antitorque rotor system; mathematical models were programmed for derivation by large digital computers.

The preliminary design study used the rotor geometry determined by the rotor system parametric analysis. Attention was given primarily to the articulated rotor. Study of the hingeless semirigid rotor was limited to an exploratory parametric analysis which, however, covers the areas of risk, the weight increment, and the areas worthy of further study. The preliminary design study specifically covers stall flutter, flap-lag instability, rotor hub shaking forces, and fuselage response.

DD FORM 1 JAN 64 1473

UNCLASSIFIED

Security Classification

14. KEY WORDS	LINK A		LINK B		LINK C	
	ROLE	WT	ROLE	WT	ROLE	WT
Heavy-Lift helicopter						
Helicopter rotor						
Rotor systems						
Transport helicopter						
Crane/personnel carrier helicopter						
Articulated rotor system						
Hingeless rotor system						

INSTRUCTIONS

1. ORIGINATING ACTIVITY: Enter the name and address of the contractor, subcontractor, grantee, Department of Defense activity or other organization *(corporate author)* issuing the report.

2a. REPORT SECURITY CLASSIFICATION: Enter the overall security classification of the report. Indicate whether "Restricted Data" is included. Marking is to be in accordance with appropriate security regulations.

2b. GROUP: Automatic downgrading is specified in DoD Directive 5200.10 and Armed Forces Industrial Manual. Enter the group number. Also, when applicable, show that optional markings have been used for Group 3 and Group 4 as authorized.

3. REPORT TITLE: Enter the complete report title in all capital letters. Titles in all cases should be unclassified. If a meaningful title cannot be selected without classification, show title classification in all capitals in parenthesis immediately following the title.

4. DESCRIPTIVE NOTES: If appropriate, enter the type of report, e.g., interim, progress, summary, annual, or final. Give the inclusive dates when a specific reporting period is covered.

5. AUTHOR(S): Enter the name(s) of author(s) as shown on or in the report. Enter last name, first name, middle initial. If military, show rank and branch of service. The name of the principal author is an absolute minimum requirement.

6. REPORT DATE: Enter the date of the report as day, month, year; or month, year. If more than one date appears on the report, use date of publication.

7a. TOTAL NUMBER OF PAGES: The total page count should follow normal pagination procedures, i.e., enter the number of pages containing information.

7b. NUMBER OF REFERENCES: Enter the total number of references cited in the report.

8a. CONTRACT OR GRANT NUMBER: If appropriate, enter the applicable number of the contract or grant under which the report was written.

8b, 8c, & 8d. PROJECT NUMBER: Enter the appropriate military department identification, such as project number, subproject number, system numbers, task number, etc.

9a. ORIGINATOR'S REPORT NUMBER(S): Enter the official report number by which the document will be identified and controlled by the originating activity. This number must be unique to this report.

9b. OTHER REPORT NUMBER(S): If the report has been assigned any other report numbers *(either by the originator or by the sponsor)*, also enter this number(s).

10. AVAILABILITY/LIMITATION NOTICES: Enter any limitations on further dissemination of the report, other than those imposed by security classification, using standard statements such as:

(1) "Qualified requesters may obtain copies of this report from DDC."

(2) "Foreign announcement and dissemination of this report by DDC is not authorized."

(3) "U. S. Government agencies may obtain copies of this report directly from DDC. Other qualified DDC users shall request through _____."

(4) "U. S. military agencies may obtain copies of this report directly from DDC. Other qualified users shall request through _____."

(5) "All distribution of this report is controlled. Qualified DDC users shall request through _____."

If the report has been furnished to the Office of Technical Services, Department of Commerce, for sale to the public, indicate this fact and enter the price, if known.

11. SUPPLEMENTARY NOTES: Use for additional explanatory notes.

12. SPONSORING MILITARY ACTIVITY: Enter the name of the departmental project office or laboratory sponsoring *(paying for)* the research and development. Include address.

13. ABSTRACT: Enter an abstract giving a brief and factual summary of the document indicative of the report, even though it may also appear elsewhere in the body of the technical report. If additional space is required, a continuation sheet shall be attached.

It is highly desirable that the abstract of classified reports be unclassified. Each paragraph of the abstract shall end with an indication of the military security classification of the information in the paragraph, represented as *(TS)*, *(S)*, *(C)*, or *(U)*.

There is no limitation on the length of the abstract. However, the suggested length is from 150 to 225 words.

14. KEY WORDS: Key words are technically meaningful terms or short phrases that characterize a report and may be used as index entries for cataloging the report. Key words must be selected so that no security classification is required. Identifiers, such as equipment model designation, trade name, military project code name, geographic location, may be used as key words but will be followed by an indication of technical context. The assignment of links, rules, and weights is optional.